WILD IMMUNOLOGY – THE ANSWERS ARE OUT THERE

EDITED BY: Gregory M. Woods and Andrew S. Flies
PUBLISHED IN: Frontiers in Immunology

frontiers Research Topics

ISSN 1664-8714
ISBN 978-2-88945-809-7
DOI 10.3389/978-2-88945-809-7

About Frontiers

Frontiers is more than just an open-access publisher of scholarly articles: it is a pioneering approach to the world of academia, radically improving the way scholarly research is managed. The grand vision of Frontiers is a world where all people have an equal opportunity to seek, share and generate knowledge. Frontiers provides immediate and permanent online open access to all its publications, but this alone is not enough to realize our grand goals.

Frontiers Journal Series

The Frontiers Journal Series is a multi-tier and interdisciplinary set of open-access, online journals, promising a paradigm shift from the current review, selection and dissemination processes in academic publishing. All Frontiers journals are driven by researchers for researchers; therefore, they constitute a service to the scholarly community. At the same time, the Frontiers Journal Series operates on a revolutionary invention, the tiered publishing system, initially addressing specific communities of scholars, and gradually climbing up to broader public understanding, thus serving the interests of the lay society, too.

Dedication to Quality

Each Frontiers article is a landmark of the highest quality, thanks to genuinely collaborative interactions between authors and review editors, who include some of the world's best academicians. Research must be certified by peers before entering a stream of knowledge that may eventually reach the public - and shape society; therefore, Frontiers only applies the most rigorous and unbiased reviews.
Frontiers revolutionizes research publishing by freely delivering the most outstanding research, evaluated with no bias from both the academic and social point of view. By applying the most advanced information technologies, Frontiers is catapulting scholarly publishing into a new generation.

What are Frontiers Research Topics?

Frontiers Research Topics are very popular trademarks of the Frontiers Journals Series: they are collections of at least ten articles, all centered on a particular subject. With their unique mix of varied contributions from Original Research to Review Articles, Frontiers Research Topics unify the most influential researchers, the latest key findings and historical advances in a hot research area! Find out more on how to host your own Frontiers Research Topic or contribute to one as an author by contacting the Frontiers Editorial Office: researchtopics@frontiersin.org

WILD IMMUNOLOGY – THE ANSWERS ARE OUT THERE

Topic Editors:
Gregory M. Woods, University of Tasmania, Australia
Andrew S. Flies, University of Tasmania, Australia

Looking for "The answers are out there, somewhere".
Image credit: Andrew S. Flies.

"Go into partnership with nature; she does more than half the work and asks none of the fee." – Martin H. Fisher.

Nature has undertaken an immense amount of work throughout evolution. The evolutionary process has provided a power of information that can address key questions such as – Which immune molecules and pathways are conserved across species? Which molecules and pathways are exploited by pathogens to cause disease? What methods can be broadly used or readily adapted for wild immunology? How does co-infection and exposure to a dynamic environment affect immunity?

Section 1 addresses these questions through an evolutionary approach. Laboratory mice have been instrumental in dissecting the nuances of the immune system. The first paper investigates the immunology of wild mice and reviews how evolution and

ecology sculpt differences in the immune responses of wild mice and laboratory mice. A better understanding of wild immunology is required and sets the scene for the subsequent papers.

Although nature doesn't ask for a fee, it is appropriate that nature is repaid in one form or another. The translational theme of the second section incorporates papers that translate wild immunology back to nature. But any non-human, non-laboratory mouse research environment is hindered by a lack of research tools, hence the underlying theme throughout the second section.

Physiological resource allocation is carefully balanced according to the most important needs of the body. Tissue homeostasis can involve trade-offs between energy requirements of the host and compensatory mechanisms to respond to infection. The third section comprises a collection of papers that employ novel strategies to understand how the immune system is compensated under challenging physiological situations.

Technology has provided substantial advances in understanding the immune system at cellular and molecular levels. The specificity of these tools (e.g. monoclonal antibodies) often limits the study to a specific species or strain. A consequence of similar genetic sequences or cross-reactivity is that the technology can be adapted to wild species. Section 4 provides two examples of probing wild immunology by adapting technology developed for laboratory species.

Citation: Woods, G. M., Flies, A. S., eds. (2019). Wild Immunology – The Answers Are Out There. Lausanne: Frontiers Media. doi: 10.3389/978-2-88945-809-7

Table of Contents

SECTION 3

BALANCING IMMUNITY WITH TISSUE HOMEOSTASIS

SECTION 4

NOVEL AND CLASSICAL APPROACHES TO INVESTIGATING IMMUNE FUNCTION

frontiers in Immunology

EDITORIAL
published: 30 January 2019
doi: 10.3389/fimmu.2019.00126

Editorial: Wild Immunology—The Answers Are Out There

Andrew S. Flies[1]* *and Gregory M. Woods*[1,2]

[1] Menzies Institute for Medical Research, University of Tasmania, Hobart, TAS, Australia, [2] School of Medicine, University of Tasmania, Hobart, TAS, Australia

Keywords: natural disease model, host-pathogen, bats, tasmanian devil, out-of-the-box, re-wild, IgE, comparative immunology

Editorial on the Research Topic

Wild Immunology—The Answers Are Out There

Laboratory mice have been the workhorse of immunology research. Well-characterized, inbred mice raised in controlled environments have fostered an understanding of precise immunological mechanisms. Experimental variation has been minimized, but results rarely translate into successful therapies for humans or other animals (1, 2). Simple experimental modifications such as co-housing a pet shop mouse with laboratory mice can alter the immunophenotype of standard mouse strains (3). Considering the limitations of traditional laboratory immunology, intrepid researchers have delved into the nascent field of wild immunology. This "Wild Immunology—the answers are out there" Research Topic has collected original research articles, perspectives, and hypotheses. Capitalizing on wild immunology will help steer future research toward productive translational outcomes and fill knowledge gaps left by the standard immunology models.

Taking laboratory mice out of the box and re-wilding them in an outdoor enclosure is a simple approach to building on the vast amount of laboratory mouse immunology available. A DNA metabarcoding approach was used to quantify variation in feeding habits in a semi-natural environment, rather than the traditional approach of eliminating variation in the laboratory Budischak et al. Dietary quality and infection with *Trichuris muris* affected immune parameters (e.g., IgG1, IL-13) in the re-wilded mice, but did not reduce parasite load. This study also found that mice on the low-protein diet spent more time foraging, which could result in increased exposure to pathogens. Future re-wilding studies that incorporate disease models and experimental treatments should produce steady progress toward translational outputs by addressing natural variation from the outset, rather than only in clinical trials.

The emergence of various "omics" techniques (e.g., RNA transcriptomics) has opened new research pathways for non-model organisms. Transcriptomics were used for wild wood mice (*Apodemus sylvaticus*) to show that both "immune" and "non-immune" genes can be strong predictors of parasite burden Babayan et al. In this case the balance of protective immunity and tissue homeostasis resulted in relatively stable parasite loads and immune profiles. A significant negative association was found between worm burden and cytokine receptors (IL-5RA, IL-17RA). By contrast there were no significant positive or negative associations with cytokines, highlighting potential problems of serological assays focused on soluble cytokines that don't account for receptor expression.

The above two original studies using wild and re-wilded rodents were complemented by a thorough review of wild rodent immunological studies Viney and Riley. This immunology of wild rodents review is an excellent starting point for any researcher looking to venture into wild immunology. It shows how the study of wild rodents in a natural environment helps understand how immune responses contribute to fitness in the wild.

OPEN ACCESS

Edited by:
Armin Saalmueller, Veterinärmedizinische Universität Wien, Austria

Reviewed by:
Martin Faldyna, Veterinary Research Institute (VRI), Czechia

***Correspondence:**
Andrew S. Flies
andy.flies@utas.edu.au

Specialty section:
This article was submitted to Comparative Immunology, a section of the journal Frontiers in Immunology

Received: *13 July 2018*
Accepted: *15 January 2019*
Published: *30 January 2019*

Citation:
Flies AS and Woods GM (2019) Editorial: Wild Immunology—The Answers Are Out There. Front. Immunol. 10:126. doi: 10.3389/fimmu.2019.00126

The prevalence of allergy is increasing in industrialized nations and is associated with dysregulated IgE effector functions. Hellman et al. found that dogs and Scandinavian wolves (*Canis lupus*) have serum IgE concentrations up to 200 times higher than non-allergic humans and laboratory rodents. Similar patterns have been observed in other wild species. A primary function of IgE is to induce degranulation of mast cells and basophils that rapidly amplify inflammatory responses upon initial infection by parasites Hellman et al. The reduced exposure to parasites in industrialized nations and the striking differences in IgE levels across species and environments suggests that immunological investigations of animals in natural settings could shed light on the growing allergy problem in humans. Importantly, Hellman et al. also provide thorough analysis and review of Fc receptors, which are necessary for most antibody-mediated effector functions, but are often overlooked in antibody-focused studies.

In addition to the rise in urban-associated diseases in humans, pathogens from wild animal populations can spillover into human and domestic animals. Bats (*Chiroptera*) are the second largest order of mammals and are host to a plethora of pathogens with the potential for cross-species transmission. A thought-provoking Hypothesis and Theory article describing unique aspects of the bat immune system proposed that two key features of the bat immune system might account for their ability to harbor pathogenic viruses Schountz et al. First, the IFN locus of the Australian black flying fox (*Pteropus alecto*) has fewer type I IFN genes than other mammals examined at that time, but that antiviral IFN-α mRNA is constitutively expressed at high levels (4). Second, the diversity of naive antibody repertoires in bats exceeds the diversity in other species studied to date [Schountz et al.; (5)]. The authors hypothesize that the combined "always on" IFN-α and diverse antibody repertoire allows bats to control infections at early stages, and thus minimize pathogenicity from virus and immunopathology Schountz et al. The long-life span of many bat species presents an opportunity to investigate changes in immunity across life history, which is limited in short-lived laboratory rodents.

Longitudinal studies of natural disease models can also fill gaps in our understanding of immunity and host-pathogen coevolution. A novel *Mycoplasma gallisepticum* pathogen emerged in wild house finches (*Haemorhous mexicanus*) and led to a 60% decrease in the wild finch population Vinkler et al. Comparison of pathogenicity of the original (1994) and more recent (2006) strains revealed that the increased virulence observed across this time scale has been driven in part by the host's pro-inflammatory response and incomplete host immunity [Vinkler et al.; (6)]. A similar pattern occurred with the myxoma virus used for rabbit (*Oryctolagus cuniculus*) control that began in the 1950s. An evolved 1990 myxoma virus strain became highly virulent because it induced septic shock like inflammatory response that led to immune collapse (7).

Simple and cost-effective disease surveillance tools and immunological reagents adaptable for a range of species are required to address issues of pathogen spillover, host-pathogen evolution, and immunity in natural settings. Glidden et al. assessed non-specific markers of inflammation in response to foot-and-mouth disease virus in African buffalo (*Syncerus caffer*). The buffalo were monitored for non-specific markers of inflammation every 2–3 months over 2 years. Serum haptoglobin was found to be a reliable surveillance marker of recent infection.

A cost-effective version of RNAseq (TagSeq) was used to fill the species-specific reagent void in a natural host-parasite system of threespine sticklebacks (*Gasterosteus aculeatus*) and native cestode parasites (*Schistocephalus solidus*) Lohman et al. Previous studies have shown that two geographically-isolated populations of sticklebacks are equally susceptible to infection, but that one population can suppress parasite growth substantially more than the other (8). The TagSeq analysis suggests that the parasite-resistant population had a dynamic gene expression profile, whereas the less-resistant population has a more static gene expression profile.

Wild immunology studies have value in understanding the evolution of the immune system. A review on melanomacrophage centers (MMC) highlighted that these aggregates of pigmented phagocytes can be found in vertebrates Steinel and Bolnick. As MMC share similarities with mammalian germinal centers it is tantalizing to suggest that MMC in fish have an immunological role and could be the evolutionary precursors of germinal centers. However, the authors caution that further genetic and functional studies are required before solid conclusions can be drawn.

The Tasmanian devil facial tumor disease (DFTD) has provided a rare opportunity to scrutinize the interplay between cancer and the immune system on a large scale in a natural tumor model. A vaccinate-and-release study of Tasmanian devils demonstrated that tumor-specific antibodies can be generated and represents a step forward in the search for a prophylactic vaccines Pye et al. This is a direct demonstration that wild immunology studies can have direct application to conservation and emerging disease solutions. The true test to evaluate any vaccine approach must occur in the wild, or in real-world contexts.

As functional experimental studies require significant resource investment (e.g., labor, reagents), using *in silico* analysis prior to embarking on wet lab studies and reagent development can yield more efficient use of limited resources. A comparative analysis of immune checkpoint molecules in two marsupials (*metatheria*) and seven placental species (*eutherians*) Flies et al. revealed that many key motifs and binding domains are conserved across more than 160 million years of evolution. The strong selective pressure to maintain immune checkpoints across species and environments suggests these checkpoints could offer stable therapeutic and vaccine targets for human disease and DFTD.

In summary, wildlife studies, particularly long-term monitoring studies, have begun addressing long-standing questions in immunology. Taking animals out of the lab and into more natural environments has yielded surprising results that are likely to help fill major knowledge gaps regarding the evolution and development of immunity in a wide range of species. We have only scratched the surface of the potential for wild immunology and look forward to finding more answers in the wild in the coming decades.

AUTHOR CONTRIBUTIONS

All authors listed have made a substantial, direct and intellectual contribution to the work, and approved it for publication.

FUNDING

This work was supported by ARC DECRA grant #DE180100484, ARC Linkage grant #LP0989727, ARC Discovery grant #DP130100715, University of Tasmania Foundation Dr. Eric Guiler Tasmanian Devil Research Grants through funds raised by the Save the Tasmanian Devil Appeal (2017, 2018).

ACKNOWLEDGMENTS

We thank all contributors to this Research Topic and members of our research team for their collective insight.

REFERENCES

1. Brody H. Animal health. *Nature* (2017) 543:S41. doi: 10.1038/543S41a
2. Willyard C. Squeaky clean mice could be ruining research. *Nature* (2018) 556:16–18. doi: 10.1038/d41586-018-03916-9
3. Beura LK, Hamilton SE, Bi K, Schenkel JM, Odumade OA, Casey KA, et al. Normalizing the environment ecapitulates adult human immune traits in laboratory mice. *Nature* (2016) 532:512–6. doi: 10.1038/nature17655
4. Zhou P, Tachedjian M, Wynne JW, Boyd V, Cui J, Smith I, et al. Contraction of the type I IFN locus and unusual constitutive expression of IFN-α in bats. *Proc Natl Acad Sci USA*. (2016) 113:2696–2701. doi: 10.1073/pnas.1518240113
5. Baker ML, Tachedjian M, Wang LF. Immunoglobulin heavy chain diversity in Pteropid bats: Evidence for a diverse and highly specific antigen binding repertoire. *Immunogenetics* (2010) 62:173–84. doi: 10.1007/s00251-010-0425-4
6. Fleming-Davies AE, Williams PD, Dhondt AA, Dobson AP, Hochachka WM, Leon AE, et al. Incomplete host immunity favors the evolution of virulence in an emergent pathogen. *Science* (2018) 359:1030–3. doi: 10.1126/science.aao2140
7. Kerr PJ, Cattadori IM, Liu J, Sim DG, Dodds JW, Brooks JW, et al. Next step in the ongoing arms race between myxoma virus and wild rabbits in Australia is a novel disease phenotype. *Proc Natl Acad Sci USA*. (2017) 114:201710336. doi: 10.1073/pnas.1710336114
8. Weber JN, Steinel NC, Shim KC, Bolnick DI. Recent evolution of extreme cestode growth suppression by a vertebrate host. *Proc Natl Acad Sci USA*. (2017) 114:6575–80. doi: 10.1073/pnas.1620095114

Conflict of Interest Statement: The authors declare that the research was conducted in the absence of any commercial or financial relationships that could be construed as a potential conflict of interest.

frontiers in Immunology

REVIEW
published: 14 November 2017
doi: 10.3389/fimmu.2017.01481

The Immunology of Wild Rodents: Current Status and Future Prospects

Mark Viney[1] and Eleanor M. Riley[2†]*

[1] School of Biological Sciences, University of Bristol, Bristol, United Kingdom, [2] Department of Immunology and Infection, London School of Hygiene and Tropical Medicine, London, United Kingdom

Wild animals' immune responses contribute to their evolutionary fitness. These responses are moulded by selection to be appropriate to the actual antigenic environment in which the animals live, but without imposing an excessive energetic demand which compromises other component of fitness. But, exactly what these responses are, and how they compare with those of laboratory animals, has been little studied. Here, we review the very small number of published studies of immune responses of wild rodents, finding general agreement that their humoral (antibody) responses are highly elevated when compared with those of laboratory animals, and that wild rodents' cellular immune system reveals extensive antigenic exposure. In contrast, proliferative and cytokine responses of *ex vivo*-stimulated immune cells of wild rodents are typically depressed compared with those of laboratory animals. Collectively, these responses are appropriate to wild animals' lives, because the elevated responses reflect the cumulative exposure to infection, while the depressed proliferative and cytokine responses are indicative of effective immune homeostasis that minimizes immunopathology. A more comprehensive understanding of the immune ecology of wild animals requires (i) understanding the antigenic load to which wild animals are exposed, and identification of any key antigens that mould the immune repertoire, (ii) identifying immunoregulatory processes of wild animals and the events that induce them, and (iii) understanding the actual resource state of wild animals, and the immunological consequences that flow from this. Together, by extending studies of wild rodents, particularly addressing these questions (while drawing on our immunological understanding of laboratory animals), we will be better able to understand how rodents' immune responses contribute to their fitness in the wild.

Keywords: mouse, rat, vole, rodent, immune, immunology, wild

OPEN ACCESS

Edited by:
Andrew Steven Flies, University of Tasmania, Australia

Reviewed by:
Beatriz Novoa, Consejo Superior de Investigaciones Científicas (CSIC), Spain
Joachim Kurtz, Universität Münster, Germany
Stephen Christopher Jameson, University of Minnesota, United States

****Correspondence:***
Mark Viney
mark.viney@bristol.ac.uk

†Present address:
Eleanor M. Riley, The Roslin Institute and Royal (Dick) School of Veterinary Studies, University of Edinburgh, Midlothian EH25 9RG, United Kingdom

Specialty section:
This article was submitted to Comparative Immunology, a section of the journal Frontiers in Immunology

Received: *30 August 2017*
Accepted: *23 October 2017*
Published: *14 November 2017*

Citation:
Viney M and Riley EM (2017) The Immunology of Wild Rodents: Current Status and Future Prospects. Front. Immunol. 8:1481. doi: 10.3389/fimmu.2017.01481

ON FINDING THAT YOUR EXPERIMENTAL MODEL IS WRONG

Model experimental systems—*E. coli*, yeast, *Drosophila*, *C. elegans*, mice—are a bedrock of modern experimental biology. Enormous investment has been made in these models, and they underpin large, international research efforts. Choosing to work with the right model can make or break an academic career.

One of us (Mark Viney) has used a simple laboratory model—infecting laboratory rats (*Rattus norvegicus)* with the nematode parasite *Strongyloides ratti* (1–4). Moreover, the model had a purity: in the wild *S. ratti* infects *R. norvegicus*, so the model was simply moving parasites from wild rats into laboratory rats. Experiments using this elegantly simple model had discovered how the

parasite's life cycle was controlled by a range of environmental effects, including the host immune response (1). This was a fascinating discovery, illuminating an association of such intimacy, where a parasite used the host to control its life cycle decisions.

But there was a gnawing problem. Each rat that was infected became immune to *S. ratti* after about 5 weeks, expelling the worms and becoming resistant to reinfection (5). Because of this, parasites were maintained by continually infecting parasite-naïve rats. In contrast, in the wild, almost two-thirds of rats were infected with *S. ratti* (6), suggesting that wild animals were not becoming immune to *S. ratti*, as their lab cousins so readily were. If the immunology of lab rats infected with *S. ratti* was so different to that of wild rats, then what had this lab model really revealed about how the host immune response actually controlled the parasite's life cycle in the wild? Intuitively, we reasoned that laboratory and wild rats were immunologically different: wild animals were leading stressful, resource-limited lives, and so were making low-level, insufficient immune responses against parasites, and that was why *S. ratti* infections were so common in the wild.

Intuition is one thing; what did the literature say? The answer—remarkably little. We could find almost no studies of the immune systems of wild rodents, and the little evidence that existed did not obviously support the hypothesis that wild rodents' immune responses were impaired or impoverished. There were rather more studies of laboratory animals, livestock, as well as some wild animals (mainly birds), generally supporting the idea that immune resources were energetically and resource costly (7), and so one could argue that there were likely to be some resource-based constraints on wild rodents' immune responses. But, overall, there was not any clear information on what immune responses wild rodents were making or how this might explain why *S. ratti* infections were so much more common in the wild than laboratory studies predicted that they would be. This disconnect from the lab to the wild in this hitherto, elegantly simple model—and that so little was known about wild animal immunology in general—spurred our determined look into wild rodents' immune responses.

KEY CONCEPTS IN ECO-IMMUNOLOGY

Eco-immunology is the study of the immune responses of wild animals in ecologically relevant settings. The broader rationale for studying the immune responses of wild animals is that these responses contribute to wild animals' evolutionary fitness (7). Immune systems respond to antigenic stimuli received by an animal and so different individuals within a population, different populations of a species, and different species, will each have qualitatively and quantitatively different exposure to antigens. Mammalian immune systems are adaptable and will respond, in one way or another, to any antigen they encounter. However, selection will act to optimize the form and nature of these immune responses to maximize fitness, in the context of other selection pressures to which animals are subject (8, 9). This leads to the first key concept of eco-immunology: immunoheterogeneity, so that different species, different populations within species, or different individuals within populations may differ in the immune responses that they make. These differences will be seen (i) in the resting status of the immune system, observed as the standing immune response, but also (ii) when animals are compared for their responses to a standard antigenic challenge, for example to vaccination. Animals will differ in these regards for both intrinsic reasons (e.g., genetically) and for extrinsic, contextual reasons, for example their different exposure to infection, and other challenges during their lives. It is appropriate that immunoheterogeneity is the first key concept of eco-immunology, because understanding both the ultimate and proximate causes of this heterogeneity, and its consequences, is arguably the central question in eco-immunology.

Making immune responses is just one aspect of an animal's physiological demands. In addition, animals have to grow, seek, and compete for food and mates, and reproduce. All of these processes require energy. It is clear that immune responses are energetically demanding (7), as too is growing, foraging, and reproducing. Therefore, with the assumption that many wild animals are energy limited, then these limited resources have to be deployed among these competing physiological and life-history processes in such a way as to maximize evolutionary fitness. This means that the immune responses of wild animals may be sub-maximal because of energy limitation. This is the second key concept of eco-immunology: that individuals' immune responses may be constrained by resource availability, and more generally that immune responses can be affected by an animal's wider physiological state. Further, variation among individuals in the quantities of resource they have and in how they allocate these resources to immune function (or not) importantly contributes to immunoheterogeneity (key concept 1, above).

Animals are exposed to and infected with a myriad of organisms—viruses, bacteria, fungi, protozoa, and metazoa, both internally and externally (7). The vast majority of these are usually harmless commensals which the immune system has to learn to ignore, but a small proportion are potentially dangerous pathogens that need to be recognized and, if possible, eliminated. Being infected with these organisms is a normal part of animal life, and animals and their immune systems have evolved in their presence. All of these organisms are sources of antigenic stimulus for the immune system, though the nature and degree of this stimulation varies among different types of organisms, their number, and their location in, or on, their host. This is the third key concept of eco-immunology: that animals have a potentially very large and diverse antigenic load. This antigenic load will differ among individuals within populations, among populations within species, and among species, and so also contribute to immunoheterogeneity (key concept 1, above).

Applying these three key concepts to laboratory and wild animals reveals substantial differences between them. In laboratory animals, immunoheterogeneity (key concept 1) among individuals within a species is minimized, if not extinguished, while in wild animals it exists in abundance. Laboratory animals are rarely resource limited (key concept 2), suggesting that their immune responses are maximal, while in wild animals we presume that resource limitation is widespread and so that immune responses may be sub-maximal (though they may be optimal) (10). Laboratory animals are usually maintained with a much reduced burden of infection (key concept 3), while wild animals have infections in abundance. Therefore, fully understanding the immune

responses of animals and how they contribute to their fitness absolutely requires that they are studied in wild populations—this is the *raison d'être* of eco-immunology. However, the enormously detailed understanding of mammalian immune systems that has come from the extensive study of laboratory animals will play a central role in this endeavour, giving eco-immunologists both the tools to probe the immune systems of wild animals and some founding concepts from which to interpret data from these studies.

IMMUNE FUNCTION IN WILD RODENTS

There are notably few studies of the immune systems of wild rodents, whereas immunological studies of laboratory rodents abound. Specifically, a Web of Knowledge search for publications whose titles and abstracts mention "mouse/mice" and "immun-" finds 19,997 papers in 2016 alone (and 187,154 between 2006 and 2016, inclusive). By contrast, we are aware of only 26 published studies of the immunology of wild rodents. A predominance *per se* of studies of laboratory models over wild systems is not necessarily problematic but, as discussed above, extrapolation from laboratory models to wild animals is unlikely to be straightforward so that the underrepresentation of the immunological study of wild animals is worrying.

The published studies of wild rodent immunology are summarized in **Table 1** (11–36). The criterion for inclusion was (i) that the animals had to directly originate from the wild (though we include studies that use pet shop-acquired animals too) and (ii) that some immunological parameter was measured. Here, we review these studies.

Comparisons of Wild and Laboratory Rodent Immune Responses

There are seven published studies of mice, *Mus musculus*, that explicitly compared wild and laboratory animals. Two of these studies were experimental, where wild-caught mice were immunized—either with sheep red blood cells (SRBC) or with keyhole limpet haemocyanin (KLH)—and the effect compared with the same immunization of laboratory mice (11, 13). In both cases, the immune responses of the wild mice were greater than those of laboratory mice, seen as higher anti-KLH antibody titres and greater antibody avidity (13) and greater SRBC lytic effect (11).

The remaining five studies of mice were observational, and measured and compared, various immune parameters between wild and laboratory mice. Comparisons of spleen cell populations in wild and laboratory *M. musculus* (13, 14) showed that wild mice had proportionately more $CD4^+$ T cells and greater numbers of activated $CD4^+$ T cells than laboratory mice and that their B cells, dendritic cells (DCs), macrophages, and natural killer (NK) cells had a more activated phenotype. However, spleen cells from wild and laboratory mice produced similar amounts of interferon-γ (IFN-γ) after *in vitro* restimulation with the T cell mitogen concanavalin A (Con A) (13). In a separate study, *in vitro* restimulation of splenocytes with exogenous cytokines resulted in more rapid expression of the high affinity IL-2 receptor (CD25) by NK cells of wild mice compared to laboratory mice and these cells were more likely to produce IFN-γ (14). A more detailed comparison of wild, pet shop-derived mice (in some way a halfway-house between

TABLE 1 | A summary of studies of the immunology of wild rodents, (A) where wild and laboratory animals have been compared and (B) where wild animals only have been studied.

Author	Species	Sample Size	Reference
(A)			
Lochmiller et al. (1991)	*Mus musculus*	1 wild; 6 laboratory	(11)
Devalapalli et al. (2006)	Mice	10 wild; 24 laboratory	(12)
Abolins et al. (2011)	*Mus musculus domesticus*	33 wild; 32 laboratory	(13)
Boysen et al. (2011)	*M. musculus*	22 wild; 31 laboratory	(14)
Beura et al. (2016)	*M. musculus*	10 wild; 6 pet shop; 9 laboratory	(15)
Abolins et al. (2017)	*M. musculus domesticus*	460 wild; 181 wild compared with 64 laboratory	(16)
Japp et al. (2017)	*M. musculus*	Unspecified pet shop; unspecified laboratory	(17)
Lochmiller et al. (1993)	*Sigmodon hispidus*	47 wild; 67 captive	(18)
Devalapalli et al. (2006)	Rat	58 wild; 15 laboratory	(12)
Lesher et al. (2006)	*Rattus norvegicus*	54 wild; unspecified laboratory	(19)
Kataranovski et al. (2009)	*R. norvegicus*	48 wild; 48 laboratory	(20)
Kataranovski et al. (2009)	*R. norvegicus*	48 wild; 48 laboratory	(21)
Trama et al. (2012)	*R. norvegicus*	8 wild; 7 laboratory	(22)
Beldomenico et al. (2008)	*Microtus agrestis*	1,574 wild; 186 captive	(23)
(B)			
Lochmiller et al. (1992)	*S. hispidus*	108	(24)
Vestey et al. (1993)	*S. hispidus*	131 captive and wild caught	(25)
Lochmiller et al. (1994)	*S. hispidus*	310	(26)
Davis et al. (1979)	*R. norvegicus*	39	(27)
Shonnard et al. (1979)	*R. norvegicus*	48	(28)
Andrianaivoarimanana et al. (2012)	*Rattus rattus*	425	(29)
Beldomenico et al. (2008)	*M. agrestis*	771	(30)
Jackson et al. (2011)	*M. agrestis*	307	(31)
Beldomenico et al. (2008)	*M. agrestis*	1,574	(23)
Arriero et al. (2017)	*M. agrestis*	60	(32)
Sinclair and Lochmiller (2000)	*Microtus ochrogaster*	140	(33)
Lochmiller et al. (1991)	*Microtus pinetorum*	7	(11)
Lochmiller et al. (1991)	*Peromyscus leucopus*	29	(11)
Schwanz et al. (2011)	*P. leucopus*	49	(34)
Lehmer et al. (2010)	*Peromyscus maniculatus*	633	(35)
Lochmiller et al. (1991)	*Neotoma floridana*	4	(11)
Lochmiller et al. (1991)	*Onychomys leucogaster*	2	(11)
Lochmiller et al. (1991)	*Perognathus hispidus*	7	(11)
Jackson et al. (2009)	*Apodemus sylvaticus*	100	(36)

wild and laboratory animals) and laboratory mice (15) showed that the non-laboratory mice had higher frequencies of antigen-experienced, terminal effector and tissue-resident $CD8^+$ cells compared with laboratory mice (15).

In our own recent work with wild *Mus musculus domesticus*, we undertook a systematic, immune-system wide analysis using a large sample of mice from different populations across the southern UK (16). This analysis also found that, by many measures, the immune systems of wild mice were more activated, or more antigen-experienced, than those of laboratory mice. This was seen as significantly higher concentrations of serum immunoglobulins (IgG, IgE) and acute phase proteins (serum amyloid P and haptoglobin), and as the wild mice splenocytes having proportionately more T cells, higher T cell: B cell and higher $CD4^+$:$CD8^+$ cell ratios, and more $CD11b^+$ myeloid cells (16). These data were consistent with earlier work which found wild mice to have higher IgG and IgE titres than laboratory mice, although no difference in IgM titres (12). Significantly, the status that the $CD4^+$ and $CD8^+$ cells were markedly different between wild and laboratory mice, with wild mouse cells being comparatively more likely to be effector or effector memory cells than naïve cells, while the opposite was the case for the laboratory mice (16). There was very marked interindividual heterogeneity in almost all immune measures of wild mice, which was much more extensive than among the laboratory mice (16). Wild mouse NK cells were also found to be in a comparatively highly activated state (16), also supporting previous observations (14). Among myeloid cells, wild mice were found to have a sub-population of these cells—which we have called hypergranulocytic myeloid cells—that appear not to have been described from laboratory mice (16).

In notable contrast to these many signatures of activation of the immune responses in wild mice, the production of nine cytokines (IFN-γ, IL-1β, IL-4, IL-6, IL-10, IL-12p40, IL-12p70, IL-13, and MIP-2α) from wild mouse splenocytes following *in vitro* stimulation with four pathogen-associated ligands tended to be much lower than from cells of laboratory mice (16). Specifically, among 45 comparisons (5 culture conditions and 9 cytokines) there were 16 significant differences in cytokine concentrations between wild and laboratory mice, of which 13 were lower in the wild mice, compared with the laboratory mice. The only exception to this trend was that some cytokine responses (IFN-γ, IL-4, and MIP-2α) to a T cell mitogen were significantly higher among wild than lab mice (16). One interpretation of these data is that in wild mice there are substantial antigen-specific responses, but innate immune responses to pathogen ligands are highly constrained (possibly a homeostatic mechanism to prevent overwhelming inflammation in the face of continued pathogen challenge).

Detailed cytometric comparison of pet shop mice with laboratory mice [specific pathogen free (SPF), non-SPF, or quarantine mice] (17) showed differences among the groups, with pet shop mice having higher frequencies of innate immune cells, particularly NK cells (17), again a finding consistent with other studies (14). Pet shop mice also had notably more granulocytes, monocytes, and DCs; higher frequencies of antigen-experienced B cells and plasma cells; more effector and memory $CD4^+$ and $CD8^+$ cells, all consistent with their likely greater exposure to infection when compared with the laboratory mice (17). After polyclonal stimulation (with phorbol-myristate-acetate and ionomycin), pet shop mouse splenic $CD4^+$ and $CD8^+$ T cells produced more IFN-γ and IL-17A than the laboratory mice, but less TNF-α, among seven cytokines assayed in total (17).

Collectively, these seven studies of *Mus* show a broadly consistent picture: that the immune systems of wild mice are more activated and show evidence of greater antigen exposure (higher antibody titres, greater antibody avidity, proportionally more effector cells, and a higher activation state of those cells) than the immune systems of laboratory mice. This is commensurate with the *a priori* expectation that wild mice, presumably, are continually and repeatedly exposed to a diverse repertoire of commensal and pathogenic organisms. Interestingly, co-housing of laboratory mice with pet shop mice results in a rather rapid expansion of antigen-experienced ($CD44^{hi}$) $CD8^+$ T cells in laboratory mice, suggesting indeed that exposure of laboratory mice to infections from wild mice drives the immune system toward the immunological phenotype of wild mice (15). Somewhat surprisingly, there is a consistent finding that innate immune function (as measured by cytokine production) tends to be depressed in wild mice compared to laboratory mice, whereas the antigen-experienced T cells of wild mice are activated.

Beyond mice, studies have also compared the immune systems of wild and laboratory rats, *R. norvegicus*. Overall, peripheral thymic and spleen cell populations of wild and laboratory rats tended to be rather similar, though wild rat spleens had proportionally fewer $CD4^+$ T cells and more $CD8^+$ T cells (22) than laboratory rats. Also, the proportion of peripheral T cells expressing CD62L was lower, and the proportion expressing major histocompatibility (MHC) Class II was higher, in wild rats compared to laboratory rats, consistent with higher proportions of antigen-experienced effector memory T cells among wild rats (22). However, the picture of T cell maturation was complicated, with wild rats having higher proportions of immature $CD4^+CD8^+$ double-positive peripheral T cells, but lower proportions of immature $CD90^+CD4^+$ T cells, and higher proportions of $CD59^+CD8^+$ cells (a marker involved in complement regulation) (22). Two other studies showed relatively small differences in the composition of peripheral (21) and splenic (19) mononuclear cells among wild and laboratory rats. Similarly, concentrations of circulating cytokines and chemokines were, overall, not different between wild and laboratory rats and for those that did differ (5 of 23 measured), the laboratory rats had higher cytokine concentrations than the wild rats (22). However, as for studies of wild mice, many measures of immune status were much more variable among wild rats than among laboratory rats (20, 22). Other studies found that wild rat spleens were larger (as a proportion of body mass) than those of laboratory rats, and that their splenocytes proliferated less, and their T cells did not upregulate expression of CD25 or CD134 and produced less IL-2 and TNF-α, but significantly more IL-4, in response to *in vitro* Con A stimulation (19, 20). Finally, both of these studies observed lower circulating concentrations of TNF-α in wild rats compared with laboratory rats (19, 22). For measures of humoral immunity, wild rats antibody titres (IgE, G, and M) were higher than those of laboratory rats, consistent with the likely greater antigen exposure of

wild animals (12, 19). Increased exposure to infection was also indicated by the high prevalence of chronic, inflammatory lung (among 33% of animals), and kidney (among 25% of animals) disease, commonly accompanied by increased numbers of peripheral leukocytes, in wild rats that was not seen in laboratory rats (21).

Similarly, a study comparing wild and laboratory-maintained cotton rats, *Sigmodon hispidus,* also found larger spleens (both absolutely and as a proportion of total body mass) containing more cells, but lower proliferative responses to pokeweed mitogen (PWM) and Con A in wild rats compared with laboratory animals (18).

All told, these six studies of two species of rats tend to show rather subtle differences between wild and laboratory animals, which cannot easily be classified as one population being either more or less immunologically active than the other. However, as observed for wild mice, wild rats tend to have higher antibody titres but their generic (i.e., mitogen driven) spleen cell proliferative capacity and cytokine production is lower than that of laboratory animals.

A comparison of haematological parameters between wild and wild-caught, but captive, voles, *Microtus agrestis* showed that captive animals had comparatively higher erythrocyte, lymphocyte and monocyte densities, with a notable decline in lymphocyte density in both males and females when reproduction began (23).

Collectively, these 14 studies of mice, rats and voles show that wild rodents' immune systems are generally in a highly antigen-experienced state (seen as comparatively more mature, effector lymphocyte populations and higher antibody titres) consistent with these wild animals being subject to sustained antigenic exposure. *In vitro* functional responses (to mitogens and microbial products) show a more mixed picture, with often fewer differences between wild and laboratory animals and often lower responses in wild animals. Critically, highly elevated proliferative or cytokine responses—putatively commensurate with the elevation of other aspects of the immune response—are not seen. While we could speculate about the reasons for this apparent disconnect between past immune experience and current immune function, there are currently too few studies, and these studies are too limited in scope, to allow robust conclusions to be drawn.

Other Studies of Immune Responses of Wild Rodents

There have been other observational studies of the immune status of wild (or near wild) rodents, but with no explicit comparison to laboratory animals, which we will now review.

For wild *S. hispidus, in vitro* splenocyte proliferative responses to PWM were greater than to Con A, but both responses varied in a similar pattern across seasons, but mitogen-induced responses tended to vary inversely with spontaneous proliferation (reflecting the *in vivo* activation state of the cells) (26). In wild-caught cotton rats (or their first-generation captive offspring) the size of Peyer's patches increased with animals' age as did the number of large intestine lymphoid follicles (24). Experimental manipulation of animals' diet (both wild caught, but then captive maintained, but also including some captive colony animals) affected investment in lymphoid tissue, with the total mass of Peyer's patches being smaller in animals fed a low (4%) protein diet, compared with those fed a 16% protein diet, though Peyer's patches were a significantly greater a proportion of body mass in low protein diet (24). In animals (wild caught and from an outbred captive colony) fed low protein diets, their spleen, thymus, and packed cell volumes were generally lower, compared with those fed the high protein diet (25). These diets also had functional effects, with low protein diet-fed animals having comparatively lower serum complement activity but higher delayed type hypersensitivity (DTH) responses (25).

There have been three immunization studies of brown rats, *R. norvegicus*. This found that antibody titres varied widely among rats immunized with a polymeric peptide, with their responsiveness linked to their MHC haplotype (27, 29). Similarly, wild rats (*R. rattus*) infected with the plague bacterium (*Yersinia pestis*) developed long-lasting IgG and IgM responses, though there was heterogeneity of responses among animals from different locations (28).

There have been a number of studies of wild voles, *Microtus* spp. A longitudinal survey of wild *M. agrestis* populations found that erythrocyte density declined in the spring, peaking in the autumn; lymphocyte density was greatest in summer and autumn, and tended to decline in older animals; neutrophil density peaked in spring, and monocytes behaved similarly, though slightly later (23). There were some sex effects, with neutrophil and erythrocyte densities being higher in males, with reproduction also affecting many measures, but often in complex ways connected with prior animal density (23).

Longitudinal studies of *M. agrestis* revealed that anaemia (as an indicator of poor body condition) predisposed individuals to monocytosis (indicative of infection), whereas the effect of lymphocyte density with regard to monocytosis varied with animal density, and that monocytosis preceded a decline in lymphocyte numbers and erythrocyte density (30).

Also in *M. agrestis*, transcriptional analysis of genes coding for cytokines (TGF-β1, IL-1β, IL-10, and IFN-γ) in response to toll-like receptor (TLR)-2 and TLR-9 agonists, and expression of transcription factors related to immunological function (FoxP3, Tbet, Gata3, and IRF5) in PHA-stimulated splenocytes, showed strong seasonal effects (31). Specifically, pro-inflammatory responses were elevated in late winter and early spring, declining thereafter, whereas anti-inflammatory responses, generally, declined as day length increased, though there was heterogeneity among individual anti-inflammatory markers (31). Markers of anti-inflammatory responses also tended to decline as animals moved from non-mating status, to mating, then gravid status, while markers of inflammation were negatively associated with body condition (32). In *M. agrestis*, longitudinal analysis of the expression of genes coding for IFN-γ, Gata3, and IL-10, showed that individuals consistently differ in their expression of IFN-γ, with some evidence showing that the other two genes were also consistently expressed differently (32). In *M. ochrogaster*, complement-dependent haemolysis and IL-2-dependent splenocyte proliferation both varied temporally, though without a clear, repeatable annual pattern (33). Females' reproduction reduced

their haemolysis responses and affected splenocyte proliferation (33). Together these studies of *Microtus* spp. have shown that a range of immunological parameters can be measured, and that these are often affected in complex ways by animals' state and their environment, which includes demographic characteristics of the relevant populations, as well as infection.

There has also been immunological study of deer mice, *Peromyscus* spp. and field mice, *Apodemus sylvaticus*. Oral immunization of wild *P. leucopus* with a *Borrelia burgdorferi* antigen induced dose-dependent IgG responses, as well as increases in the density of peripheral neutrophils and eosinophils (34). In *P. maniculatus*, anti-Sin Nombre virus IgG titres were higher in males, compared with females, and males' antibody titre was positively related to body mass (35). In *A. sylvaticus*, *in vitro* splenocyte stimulation with TLR-2 and TLR-9 agonists induced high levels of TNF-α secretion and these responses (summarized as principal components) were negatively correlated to infection with a helminth and an ectoparasite (suggestive of pathogen-induced immunomodulation), but were not related to animals' size, mass, or life-history state (36). Primary immune responses to SRBC immunization *P. leucopus*, *M. pinetorum*, *Neotoma floridana*, *Onychomys leucogaster*, and *Perognathus hispidus* have been induced and were all heterogeneous among the individual animals studied (11).

These 15 diverse studies (**Table 1**) of other wild rodents, where there is no explicit comparison to laboratory animals, shows that immune responses differ among individuals, that effects of season and other aspects of animals' environments are important, as too is age, though there are often no reported sex differences, though reproduction can be a significant immunological event. These studies also show that infections are important in affecting an animal's immune status.

UNDERSTANDING THE IMMUNE RESPONSES OF WILD RODENTS—A SYNTHESIS AND QUESTIONS FOR THE FUTURE

Taken together, a coherent picture of wild rodent immune responses begins to emerge from these 26 studies. Specifically, that the humoral, and adaptive and innate cellular compartments of their immune systems are highly active—and more so than those of laboratory animals—with this immune phenotype entirely consistent with high level and continuous antigenic challenge (especially compared with laboratory animals). But functional cellular responses of wild rodents—in particular, proliferative and cytokine responses to broad spectrum stimuli such as mitogens or TLR agonists—are lower than those observed in laboratory animals. There is therefore a disconnect between different aspects of the immune biology of wild animals when judged against the accepted paradigms derived from studies of laboratory animals. Specifically, in wild rodents, despite evidence of extensive prior and current exposure to immunological challenges (i.e., high antibody titres, highly differentiated lymphocyte populations expressing markers of recent or current activation and immune memory) their ability to respond appropriately to an additional immunological stimulus is lower than one might expect given data from laboratory animals. Although data are limited, there is some evidence that antigen-specific T cell responses of wild rodents may be similar to (or higher than) those of laboratory mice (16), such that lower-than-expected immune function may be limited to innate immune responses—but much more work is required to determine whether this is indeed true.

Notwithstanding this current unknown, an important question is: which of these situations is "normal" and which is "abnormal"? Are wild animal responses abnormally low, or are laboratory animal responses abnormally high? Perhaps the most parsimonious explanation to this paradox is that, in the face of persistent or repeated infectious challenge, high-level proliferative and cytokine responses can cause severe tissue pathology, and to avoid this, functional immune responses of wild rodents are moderated so that individuals are adequately protected from infection while avoiding immune-mediated damage. This explanation has to be understood with the context that wild animals are exposed to a very large and diverse antigenic load (key concept 3, above). By comparison, laboratory animals have a very low antigenic burden, and thus their resting level of immune activation is much lower, and they may, therefore, be able to sustain higher proliferative and cytokine responses to any individual stimulus without causing immunopathology. In support of this hypothesis, immune responses of laboratory mice share many features of the neonatal human immune response (15). If true, this idea implies that the constrained cellular immune responses of wild rodents are both mechanistically and evolutionarily appropriate. In contrast, immune responses of laboratory rodents are more typical of those of a naïve, antigen-inexperienced animal. If so, then the initial immune response of any animal (in the lab, animals entering an experiment; in the wild, newly born animals) are high, but that these then decline with continued antigenic exposure (which is the natural life course in wild animals, if they survive, but which rarely happens in laboratory experiments).

It is also important to remember that these functional immune responses are, at least in part, measures of the influence of immunoregulatory processes. There is evidence from studies in humans that immunoregulatory mechanisms accrue over the life course and in response to microbial exposure, for example, by the accumulation of regulatory T cells (37, 38), though the relevance of age-dependent effects in laboratory rodents to those of wild rodents which are typically short lived (16, 32) remains unclear. We therefore need to be mindful that while one can measure many immune parameters, these represent different, discrete aspects of the functioning immune system, ranging from frontline effector responses against a pathogen, to back-room regulatory processes. The immunoregulatory processes and the homeostatic state of wild rodents' immune systems will be appropriate to the nature and degree of antigenic stimulation to which these animals are exposed (and so will vary among individuals within populations, among populations within species, and among species). In one sense, this is self evident—the immune system responds in a regulated way to antigenic stimulation. The immunoregulatory processes of laboratory animals may be qualitatively or quantitatively different, given the very different environments in which these animals live.

This analysis generates two important research priorities for future studies of wild rodent populations. First, to discover and quantify the totality of infections—and so antigenic exposure—to which wild animals are exposed. While we are confident in asserting that wild animals have very heavy, extensive, high-level infections, there is actually rather little substantive evidence of this. While certain infections (particularly protozoan and metazoan parasites, together with some named viruses) are quite well characterized, the microbiota and pathogen load of wild animals is poorly characterized (both qualitatively and quantitatively) (39), despite this likely being the dominant source of antigenic challenge for wild rodents. The second research priority is to understand the immunoregulatory processes of wild rodents. These processes are the proximate mechanism by which the magnitude of many effector immune responses is determined. Linking these two questions together makes it interesting to ask: what is the quantitative relationship between antigenic load, immunoregulation, and effector outputs? A quantitative understanding of the action and interaction of components of the mammalian immune system is, arguably, woefully lacking, but such quantitative understanding is likely to be necessary to understand the relationship between infection and immune responses in wild animals. Ultimately, this level of understanding is necessary to be able to make predictions about which immune responses will be induced in response to particular infections given the overall antigen load, something that is not generally possible even in laboratory animals.

Other important ideas arise from these 26 studies—that there can be strong seasonal effects on the immune system [a pattern that is commonly seen among animals more generally (40)], and that these can also be affected by aspects of animals' state (for example, their age, reproductive status, etc.), and the infections that they have. Interpreting an immune measure of a wild animal critically depends on understanding how, and under what scenarios, the immune measures of interest change. Interpretation of single immune measures without a broader context is likely to be very difficult and unreliable. Moreover, given the immunoheterogeneity that exists among individuals, both substantial sample sizes and, ideally, longitudinal measures of immune parameters are needed to properly study the immunology of wild rodents.

The energetic costs of immune responses are well established in studies of laboratory animals and of some wild animals, particularly birds, though this has actually been rather little studied in wild rodents (7). Notably, many of the studies reviewed above have sought relationships between measures of body condition and immune responses, but very often fail to find them. As noted above, manipulation of the diet of captive wild-caught cotton rats (24, 25) affected their investment in lymphoid tissue and some immune reactions. We assume that many wild animals are resource limited, and so expect that immune responses may be submaximal. However, in truth, high levels of immune responsiveness are, in general, seen in wild rodents. There are two aspects to resolving this conundrum. The first is that resource availability will vary among individual wild animals, so that some will be well resourced, while others will be poorly resourced. The second is that animals' immune responses will have evolved in the actual resource context of those animals, so that if animals are normally resource limited, then the optimal immune response that can be achieved under those conditions will be selected for. Showing that enhancing an animal's diet can further increase measures of immune responses does not invalidate this view, but just shows that resource availability can alter immune responses. This, therefore, raises a third key question for future studies, which is to better understand the actual resource state of wild animals and its temporal variation, and so understand how this impacts, if at all, on animals' immune responses.

The focus of most of these studies of wild rodents is on measures of aspects of the immune response. While this is perfectly reasonable, it is also important to bear in mind that the ultimate functional effect of these immune responses is what really matters. Understanding this is much harder, especially given the high level and heterogeneous infectious challenge that we presume wild animals are exposed to. There is substantial interest in understanding the factors that affect the zoonotic spill-over of pathogens from wild animals, including from rodents (41, 42). The immune responses that wild animals make against their infections and the effect that these have on those infections is likely to be a critical factor affecting the potential for such zoonotic spill-over. This, therefore, emphasizes the applied relevance of understanding the immune responses of wild rodents in the context of the infections that these animals harbour, especially since many of these species (*Mus, Rattus*) live commensally with humans, especially in population-dense urban areas.

ON FINDING THAT YOUR EXPERIMENTAL MODEL IS WRONG—PART 2

The intuition—that wild rats with their stress-filled, resource-limited lives were making very poor immune responses against the nematode *S. ratti* and so making it more common in the wild, than would be predicted from the behaviour of infections in laboratory animals—is likely wrong. From the review of the available literature (**Table 1**), it seems clear that wild rats' immune systems are probably making very high-level responses to *S. ratti,* as well as to their myriad other infections. Studies of laboratory rats show that while there are a number of different effector processes acting against *S. ratti* parasites (both infective stages migrating through the host toward the gut, and adult parasites in the gut), clearance of adult stages from the host gut is achieved by an intestinal mucosal mast cell response that depends on IL-3, among other cytokines (43–45). Wild animals' cytokine responses to antigenic stimulation are often depressed, compared with those of laboratory animals, and it is this that may underlie the apparent failure of wild rats to eliminate *S. ratti* infections. To put it formally, we can hypothesize that in wild rats infected with *S. ratti* the resultant antigenic stimulation is insufficient to generate an IL-3 response (and response of other cytokines) that is able to drive an effective mast cell response in the rat gut mucosa, with the consequence that the *S. ratti* parasites survive. Under this hypothesis the non-response could be due to ineffective (i) presentation of *S. ratti* antigen

and/or (ii) subsequent induction of cytokine responses in wild rats.

CONCLUSION

The immune system and its responses play a critical role in the lives of wild animals, but these responses are very often poorly understood. Immune processes are a key factor affecting the ecology of wild animals, and to fully understand the ecology of animals, these immune processes must be brought to the fore. The current small number of studies on wild rodents shows that such studies are possible, and the emerging picture of wild rodent immunology suggests some of the next research questions that the field should address.

AUTHOR CONTRIBUTIONS

The authors co-wrote the paper and approved it for publication.

FUNDING

This work was supported by grant number NE/I022892/1 from NERC, UK.

REFERENCES

1. Harvey SC, Gemmill AW, Read AF, Viney ME. The control of morph development in the parasitic nematode *Strongyloides ratti*. *Proc Biol Sci* (2000) 267:2057–63. doi:10.1098/rspb.2000.1249
2. Paterson S, Viney ME. Host immune responses are necessary for density-dependence in nematode infections. *Parasitology* (2002) 125:283–92. doi:10.1017/S0031182002002056
3. Viney ME, Lok JB. *Strongyloides* spp. *The C. elegans Research Community*. WormBook (2007). Available from: http://www.wormbook.org
4. Viney ME, Kikuchi T. *Strongyloides ratti* and *S. venezuelensis* – rodent models of *Strongyloides* infection. *Parasitology* (2017) 144:285–94. doi:10.1017/S0031182016000020
5. Wilkes CP, Bleay C, Paterson S, Viney ME. The immune response during a *Strongyloides ratti* infection of rats. *Parasite Immunol* (2007) 29:339–46. doi:10.1111/j.1365-3024.2007.00945.x
6. Fisher MC, Viney ME. The population genetic structure of the facultatively sexual parasitic nematode *Strongyloides ratti* in wild rats. *Proc Biol Sci* (1998) 265:703–9. doi:10.1098/rspb.1998.0350
7. Viney ME, Riley EM. From immunology to eco-immunology: more than a new name. In: Malagoli D, Ottaviani E, editors. *Eco-Immunology: Evolutive Aspects and Future Perspectives*. UK: Springer (2014). p. 1–19.
8. Graham AL. Optimal immunity meets natural variation: the evolutionary biology of host defence. *Parasite Immunol* (2013) 35:315–7. doi:10.1111/pim.12073
9. Boots M, Donnelly R, White A. Optimal immune defence in the light of variation in lifespan. *Parasite Immunol* (2013) 35:331–8. doi:10.1111/pim.12055
10. Viney ME, Riley EM, Buchanan KL. Optimal immune responses: immunocompetence revisited. *Trends Ecol Evol* (2005) 20:665–9. doi:10.1016/j.tree.2005.10.003
11. Lochmiller RL, Vestey MR, McMurry ST. Primary immune responses of selected small mammal species to heterologous erythrocytes. *Comp Biochem Physiol A Comp Physiol* (1991) 100:139–43. doi:10.1016/0300-9629(91)90196-J
12. Devalapalli AP, Lesher A, Shieh K, Solow JS, Everett ML, Edala AS, et al. Increased levels of IgE and autoreactive, polyreactive IgG in wild rodents: implications for the hygiene hypothesis. *Scand J Immunol* (2006) 64:125–36. doi:10.1111/j.1365-3083.2006.01785.x
13. Abolins SR, Pocock MJO, Hafalla JCR, Riley EM, Viney ME. Measures of immune function of wild mice, *Mus musculus*. *Mol Ecol* (2011) 20:881–92. doi:10.1111/j.1365-294X.2010.04910.x
14. Boysen P, Eide DM, Storset AK. Natural killer cells in free-living *Mus musculus* have a primed phenotype. *Mol Ecol* (2011) 20:5103–10. doi:10.1111/j.1365-294X.2011.05269.x
15. Beura LK, Hamilton SE, Bi K, Schenkel JM, Odumade OA, Casey KA, et al. Normalizing the environment recapitulates adult human immune traits in laboratory mice. *Nature* (2016) 532:512–6. doi:10.1038/nature17655
16. Abolins S, King E, Lazarou L, Weldon L, Hughes L, Drescher P, et al. The comparative immunology of wild and laboratory mice *Mus musculus domesticus*. *Nat Commun* (2017) 8:14811. doi:10.1038/ncomms14811
17. Japp AS, Hoffmann K, Schlickeiser S, Glauben R, Nikolaou C, Maecker HT, et al. Wild immunology assessed by multidimensional mass cytometry. *Cytometry A* (2017) 91A:85–95. doi:10.1002/cyto.a.22906
18. Lochmiller RL, Vestey MR, McMurry ST. Phenotypic variation in lymphoproliferative responsiveness to mitogenic stimulation in cotton rats. *J Mammol* (1993) 74:189–97. doi:10.2307/1381920
19. Lesher A, Li B, Whitt P, Newton N, Devalapalli AP, Shieh K, et al. Increased IL-4 production and attenuated proliferative pro-inflammatory responses of splenocytes from wild-caught rats (*Rattus norvegicus*). *Immunol Cell Biol* (2006) 84:374–82. doi:10.1111/j.1440-1711.2006.01440.x
20. Kataranovski M, Mirkov I, Zolotarevski L, Popov A, Belij S, Stošič J, et al. Basic indices of spleen immune activity in natural populations of Norway rats (*Rattus norvegicus* Berkenhout, 1769) in Serbia. *Arch Biol Sci* (2009) 61:723–32. doi:10.2298/ABS0902213K
21. Kataranovski MV, Radović DL, Zolotarevski LD, Popov AD, Kataranovski DS. Immune-related health-relevant changes in natural publications of Norway rats (*Rattus norvegicus* Berkenhout, 1769): white blood cell counts, leukocyte activity, and peripheral organ infiltration. *Arch Biol Sci* (2009) 61:213–23. doi:10.2298/ABS0902213K
22. Trama AM, Holzknecht ZE, Thomas AD, Su K-Y, Lee SM, Foltz EE, et al. Lymphocyte phenotypes in the wild-caught rats suggest potential mechanisms underlying increased immune sensitivity in post-industrial environments. *Cell Mol Immunol* (2012) 9:163–74. doi:10.1038/cmi.2011.61
23. Beldomenico PM, Telfer S, Gebert S, Lukomski L, Bennett M, Begon M. The dynamics of health in wild field vole populations: a haematological perspective. *J Anim Ecol* (2008) 77:984–97. doi:10.1111/j.1365-2656.2008.01413.x
24. Lochmiller RL, Vestey MR, McMurry ST. Gut associated lymphoid tissue in the cotton rat (*Sigmodon hispidus*) and its response to protein restriction. *J Wildl Dis* (1992) 28:1–9. doi:10.7589/0090-3558-28.1.1
25. Vestey MR, McMurry ST, Lochmiller RL. Influence of dietary protein on selected measures of humoral and cellular immunity in the cotton rat *Sigmodon hispidus*. *Can J Zool* (1993) 71:579–86. doi:10.1139/z93-079
26. Lochmiller RL, Vestey MR, McMurry ST. Temporal variation in humoral and cell-mediated immune response in a *Sigmodon hispidus* population. *Ecology* (1994) 75:236–45. doi:10.2307/1939397
27. Davis BK, Shonnard JW, Crammer DV, Lobel SA. The immune response to poly(Glu^{52}Lys^{33}Tyr^{15}) in inbred and wild rats. *Transplant Proc* (1979) 11:1593–7.
28. Shonnard JW, Davis BK, Crammer DV, Radka FSF, Gill TJ. The association of immune responsiveness, mixed lymphocyte responses, and Ia antigens in natural populations of Norway rats. *J Immunol* (1979) 123:778–83.
29. Andrianaivoarimanana V, Telfer S, Rajerison M, Ranjalahy MA, Andriamiarimanana F, Rahaingosoamamitiana C, et al. Immune responses to plague infection in wild *Rattus rattus*, in Madagascar: a role in foci persistence? *PLoS One* (2012) 7:e38630. doi:10.1371/journal.pone.0038630
30. Beldomenico PM, Telfer S, Gebert S, Lukomski L, Bennett M, Begon M. Poor condition and infection: a vicious circle in natural populations. *Proc Biol Sci* (2008) 275:1753–9. doi:10.1098/rspb.2008.0147
31. Jackson JA, Begon M, Birtles R, Paterson S, Friberg IM, Hall A, et al. The analysis of immunological profiles in wild animals: a case study on immunodynamics in the field vole, *Microtus agrestis*. *Mol Ecol* (2011) 20:893–909. doi:10.1111/j.1365-294X.2010.04907.x
32. Arriero E, Wanelik KM, Birtles RJ, Bradley JE, Jackson JA, Paterson S, et al. From the animal house to the field: are there consistent individual differences in immunological profiles in wild populations of field voles (*Microtus agrestis*)? *PLoS One* (2017) 12:e0183450. doi:10.1371/journal.pone.0183450

33. Sinclair JA, Lochmiller RL. The winter immunoenhancement hypothesis: associations among immunity, density, and survival in prairie vole (*Microtus ochrogaster*) populations. *Can J Zool* (2000) 78:254–64. doi:10.1139/z99-203
34. Schwanz LE, Brisson D, Gomes-Solecki M, Ostfeld RS. Linking disease and community ecology through behavioural indicators: immunochallenge of white-footed mice and its ecological impacts. *J Anim Ecol* (2011) 80:204–14. doi:10.1111/j.1365-2656.2010.01745.x
35. Lehmer EM, Jones JD, Bego MG, Varner JM, Jeor SS, Clay CA, et al. Long-term patterns of immune investment by wild deer mice infected with Sin Nombre virus. *Phys Biochem Zool* (2010) 83:847–57. doi:10.1086/656215
36. Jackson JA, Friberg IM, Bolch L, Lowe A, Ralli C, Harris PD, et al. Immunoregulatory parasites and toll-like receptor-mediated tumour necrosis factor alpha responsiveness in wild mammals. *BMC Biol* (2009) 7:16. doi:10.1186/1741-7007-7-16
37. Finney OC, Riley EM, Walther M. Regulatory T cells in malaria – friend or foe? *Trend Parasitol* (2010) 31:63–70.
38. Darrigues J, van Meerwijk JPM, Romagnoli P. Age-dependent changes in regulatory T lymphocyte development and function: a mini-review. *Gerontology* (2017). doi:10.1159/000478044
39. Weldon L, Abolins S, Lenzi L, Bourne C, Riley EM, Viney ME. The gut microbiota of wild mice. *PLoS One* (2015) 10:e0134643. doi:10.1371/journal.pone.0134643
40. Nelson RJ, Demas GE, Klein SL, Kriegsfeld LJ. *Seasonal Patterns of Stress, Immune Function, and Disease*. Cambridge, UK: Cambridge University Press (2002).
41. Han BA, Kramer AM, Drake JM. Global patterns of zoonotic disease in mammals. *Trend Parasitol* (2006) 32:565–77.
42. Olival KJ, Hosseini PR, Zambrana-Torrelio C, Ross N, Bogich TL, Daszak P. Host and viral traits predict zoonotic spillover from mammals. *Nature* (2017) 546:646–50. doi:10.1038/nature22975
43. Breloer M, Abraham D. *Strongyloides* infection in rodents: immune responses and immune regulation. *Parasitology* (2017) 144:295–315. doi:10.1017/S0031182016000111
44. Abe T, Nawa Y. Worm expulsion and mucosal mast cell response induced by repetitive IL3 administration in *Strongyloides ratti*-infected nude mice. *Immunology* (1988) 63:181–5.
45. Sasaki Y, Yoshimoto T, Maruyama H, Tegoshi T, Ohta N, Arizono N, et al. IL-18 with IL-2 protects against *Strongyloides venezuelensis* infection by activating mucosal mast cell-dependent type 2 innate immunity. *J Exp Med* (2005) 202:607–16. doi:10.1084/jem.20042202

Conflict of Interest Statement: The authors declare that the research was conducted in the absence of any commercial or financial relationships that could be construed as a potential conflict of interest.

frontiers in Immunology

ORIGINAL RESEARCH
published: 03 May 2017
doi: 10.3389/fimmu.2017.00513

Comparative Analysis of Immune Checkpoint Molecules and Their Potential Role in the Transmissible Tasmanian Devil Facial Tumor Disease

Andrew S. Flies[1,2], Nicholas B. Blackburn[1,3], Alan Bruce Lyons[4], John D. Hayball[2,5] and Gregory M. Woods[1]*

[1] Menzies Institute for Medical Research, University of Tasmania, Hobart, TAS, Australia, [2] Department of Pharmacy and Medical Sciences, University of South Australia, Adelaide, SA, Australia, [3] School of Medicine, South Texas Diabetes and Obesity Institute, University of Texas Rio Grande Valley, Brownsville, TX, USA, [4] School of Medicine, University of Tasmania, Hobart, TAS, Australia, [5] Discipline of Obstetrics and Gynaecology, School of Medicine, Robinson Research Institute, The University of Adelaide, Adelaide, SA, Australia

OPEN ACCESS

Edited by:
*Evan W. Newell, Singapore Immunology Network (A*STAR), Singapore*

Reviewed by:
Daniel Olive, Institut national de la santé et de la recherche médicale (INSERM), France
Haidong Dong, Mayo Clinic Minnesota, USA

***Correspondence:**
Andrew S. Flies
andy.flies@utas.edu.au

Specialty section:
This article was submitted to Cancer Immunity and Immunotherapy, a section of the journal Frontiers in Immunology

Received: *04 March 2017*
Accepted: *18 April 2017*
Published: *03 May 2017*

Citation:
Flies AS, Blackburn NB, Lyons AB, Hayball JD and Woods GM (2017) Comparative Analysis of Immune Checkpoint Molecules and Their Potential Role in the Transmissible Tasmanian Devil Facial Tumor Disease. Front. Immunol. 8:513. doi: 10.3389/fimmu.2017.00513

Immune checkpoint molecules function as a system of checks and balances that enhance or inhibit immune responses to infectious agents, foreign tissues, and cancerous cells. Immunotherapies that target immune checkpoint molecules, particularly the inhibitory molecules programmed cell death 1 and cytotoxic T-lymphocyte-associated protein 4 (CTLA-4), have revolutionized human oncology in recent years, yet little is known about these key immune signaling molecules in species other than primates and rodents. The Tasmanian devil facial tumor disease is caused by transmissible cancers that have resulted in a massive decline in the wild Tasmanian devil population. We have recently demonstrated that the inhibitory checkpoint molecule PD-L1 is upregulated on Tasmanian devil (*Sarcophilus harrisii*) facial tumor cells in response to the interferon-gamma cytokine. As this could play a role in immune evasion by tumor cells, we performed a thorough comparative analysis of checkpoint molecule protein sequences among Tasmanian devils and eight other species. We report that many of the key signaling motifs and ligand-binding sites in the checkpoint molecules are highly conserved across the estimated 162 million years of evolution since the last common ancestor of placental and non-placental mammals. Specifically, we discovered that the CTLA-4 (MYPPPY) ligand-binding motif and the CTLA-4 (GVYVKM) inhibitory domain are completely conserved across all nine species used in our comparative analysis, suggesting that the function of CTLA-4 is likely conserved in these species. We also found that cysteine residues for intra- and intermolecular disulfide bonds were also highly conserved. For instance, all 20 cysteine residues involved in disulfide bonds in the human 4-1BB molecule were also present in devil 4-1BB. Although many key sequences were conserved, we have also identified immunoreceptor tyrosine-based inhibitory motifs (ITIMs) and immunoreceptor tyrosine-based switch motifs (ITSMs) in genes and protein domains that have not been previously reported in any species.

This checkpoint molecule analysis and review of salient features for each of the molecules presented here can serve as road map for the development of a Tasmanian devil facial tumor disease immunotherapy. Finally, the strategies can be used as a guide for veterinarians, ecologists, and other researchers willing to venture into the nascent field of wild immunology.

Keywords: devil, transmissible tumor, cosignaling immunotherapy, checkpoint blockade, wild immunity, allograft, transplant rejection, evolution

INTRODUCTION

The immune system plays a vital role in protecting an animal from pathogens and cancers through various immunosurveillance and effector mechanisms. The pathogenic cells and/or microbes that escape or neutralize host immunity produce more surviving descendants that are in turn more effective at evading immune responses. The architecture of the vertebrate immune system and the mechanisms by which immune responses are regulated are the result of this long and complex evolutionary arms race. This arms race drives continuous evolution of the immune system, but many defenses have persisted throughout this long-history and are conserved across speciation events.

Immune checkpoint molecules function as a complex system of checks and balances that promote or inhibit immune responses. Checkpoint molecules likely evolved to precisely balance the need to control pathogens and cancer with the need to maintain tolerance to healthy tissues and the microbiota (**Figure 1**). However, the delicate balance of tolerance and immunity can be upset by pathogens and tumor cells that subvert inhibitory pathways to evade host immune defenses.

Checkpoint molecule immunotherapy has recently surged onto the world stage, but this field emerged over three decades of basic immunobiological research, primarily focused on T cells. In general, activation of T cells requires signaling through the T cell receptor (TCR) (signal 1) and cosignaling through CD28 (signal 2), a constitutively expressed disulfide-linked homodimer on the surface of naïve T cells (1–3). Signal one is derived from interactions of the TCR with its cognate major histocompatibility complex (MHC) peptide-complex (4). Signal two is derived from CD28 binding with either CD80 (B7-1) or CD86 (B7-2), primarily expressed by dendritic cells (DCs) and other antigen-presenting cells (APCs), such as macrophages and B cells. TCR signaling in the absence of CD28 cosignaling can result in T cell anergy (5). Following activation of T cells, the inhibitory molecule cytotoxic T-lymphocyte-associated protein 4 (CTLA-4) is upregulated on the cell surface (6). CTLA-4 has a higher affinity for both CD80 and CD86 than does CD28 (7–9), and thus CD28 cosignaling is suppressed by CTLA-4 outcompeting CD28 for CD80 and CD86 binding. The result is a downregulation of the T cell response and loss of T cell function.

Immunotherapies targeting the CTLA-4 checkpoint molecule have opened new doors in the realm of human oncology. Two antagonistic anti-CTLA-4 mAbs, ipilimumab (IgG1 isotype) and tremelimumab (IgG2 isotype), that block interactions between CTLA-4 and its coreceptors CD80 and CD86 have been clinically approved for advanced stage cancers. The exact mechanisms by which anti-CTLA-4 works are not completely understood. Accumulating evidence suggests that anti-CTLA-4 works primarily in the secondary lymphoid organs by releasing pre-existing T cells from inhibitory signaling to target tumor neoantigens and by depleting Tregs in the tumor microenvironment (10, 11).

Despite the promising early results of anti-CTLA-4 mAb monotherapy in human clinical trials, objective response rates remained low in most cases. Improvements have been observed when anti-CTLA-4 was paired with other treatments, such as the chemotherapy drug dacarbazine (12). However, the most promising outcomes have been observed when anti-CTLA-4 mAb is paired with blockade of the programmed cell death 1 (PDCD1, PD-1) protein (13–15).

Anti-PD-1 has been the most successful checkpoint blocking monoclonal antibody in treating human cancer, in monotherapies or in combination therapies. Anti-CTLA-4 and anti-PD-1 combination therapies have achieved unprecedented objective response rates of nearly 60% in patients with stage III and IV melanoma (14, 15). PD-1 immunotherapies have focused largely on stimulating T cell antitumor responses by blocking binding of PD-1 to its ligands PD-L1 (B7-H1, CD274) and PD-L2 (B7-DC, CD273). PD-1 blockade abrogates the inhibitory effects of PD-1 ligation mediated by the immunoreceptor tyrosine-based inhibitory motif (ITIM) and immunoreceptor tyrosine-based switch motif (ITSM) in the PD-1 cytoplasmic tail (16–18). In addition to blocking the inhibitory effects of PD-1, blockade of PD-L1 ligation can render tumor cells less resistant to apoptosis (19). PD-L1 and PD-L2 proteins are largely absent in normal tissues, but PD-L1 expression is elevated in more than 20 types of human cancer [reviewed in Ref. (20)]. Furthermore, many cancers and healthy cells upregulate PD-L1 expression in response to inflammatory cytokines, such as interferon-gamma (IFN-γ).

In humans, PD-L1 expression in the tumor microenvironment is associated with an inhibited T cell antitumor response and reduced patient survival [reviewed in Ref. (20)]. PD-L1 expression in the tumor microenvironment plays an important role in shaping a dysfunctional immune response through reprogramming of APCs, regulatory T cells, and expression of inhibitory molecules. PD-L2 is not routinely detected on cancer cells, but is commonly expressed by DCs, which led to the alternative name of B7-DC (21). A second coreceptor for PD-L2, repulsive guidance molecule b, has recently been discovered and has been implicated in respiratory immune tolerance (22).

Orthologs of CTLA-4 and PD-1 and their coreceptors have been found in nearly all mammals and birds studied to date (23, 24), but comparatively little is known about the potential for checkpoint molecule immunotherapy in the field of veterinary

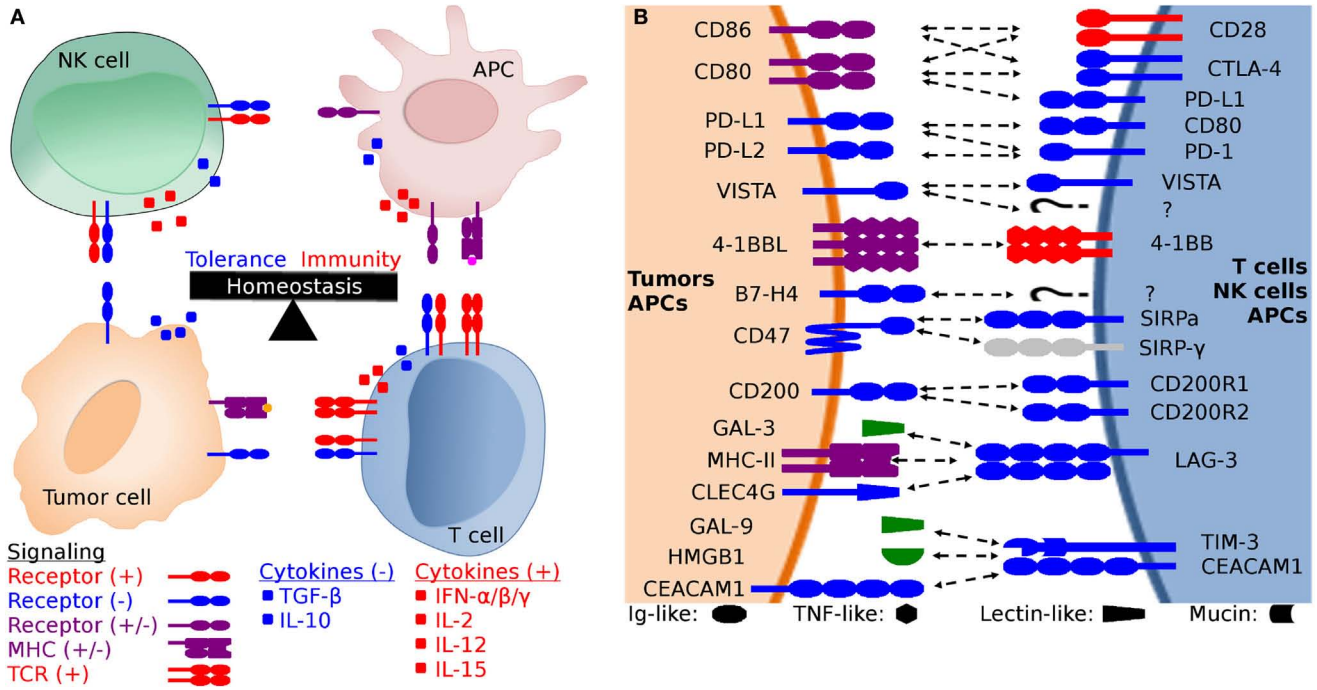

FIGURE 1 | Generalized schematic of checkpoint molecule structure and expression, and the balance between stimulatory and inhibitory signaling. **(A)** The net balance of inhibitory (–, blue) and stimulatory (+, red) signals regulates antitumor immune responses. The tumor microenvironment is dynamic and is molded by inhibitory and stimulatory signals both in the microenvironment and distant tissues (i.e., lymph nodes). Development of cytotoxic effector T cells and NK cells is regulated by the balance between inhibitory and stimulatory signaling, including both receptor:coreceptor interactions and cytokines. Both receptor and cytokine expression are also regulated by that balance of stimulatory and inhibitory signals, creating feedback loops that evolved to eliminate pathogens and cancer while simultaneously limiting collateral damage. **(B)** Expanded view of potential receptor:coreceptor interactions between T cells, NK cells, antigen-presenting cells (APCs), and tumor cells. The graphic here demonstrates some of the best characterized pathways, with a particular focus on T cell and NK cell interactions with tumor cells and APCs. Note that many of the ligands depicted here are expressed on several cell types and interactions with coreceptors and ligands can result in different functional outcomes depending on the cell types and microenvironment. For example, CD47 is expressed on all cells, but the pathway of primary interest for transmissible tumors is for the ability of tumor cell-expressed CD47 to inhibit phagocytosis *via* binding to SIRP-α on APCs. In addition to binding to SIRP-α, CD47 also binds to SIRP-β, SIRP-γ, THBS1, and THBS2, but we have only shown the CD47:SIRP-α interaction here to keep the figure relatively simple. Both V-domain Ig suppressor of T cell activation (VISTA) and B7-H4 have unknown coreceptors (labeled as "?" in the diagram) whose function has been studied using fusion proteins, but the genes for the coreceptors have yet to be identified.

medicine or in the realm of wildlife disease. Initial investigations into the function of CTLA-4, PD-1, and PD-L1 have been undertaken for canids (25–30), felids (31), and bovids (32–35), and results suggest that the CTLA-4 and PD-1/PD-L1 expression patterns and function are similar among these placental mammals.

An area where checkpoint molecule immunology could make a wildlife conservation impact is in the unusual cases of transmissible tumors. These transmissible tumors represent a unique immunological enigma because they can also simultaneously be considered infections and allografts. Disease progression, transmission, and the host immune response can only be properly understood when these tumors are considered in this complex tumor–infection–allograft context.

The Tasmanian devil facial tumor (DFT) was identified in 1996, and in 2006 the etiologic agent was found to be cancer cells that are transmitted between biting devils (36, 37). At the time of discovery, the only other known naturally transmissible tumors were the canine (*Canis lupus familiaris*) transmissible venereal tumor (38, 39) and a set of related Syrian hamster (*Mesocricetus auratus*) transmissible sarcomas (40, 41). In recent years, additional transmissible tumors have been discovered in soft-shell clams and other bivalves (42, 43). Remarkably, in 2015, we discovered a second transmissible devil facial tumor (DFT2) in wild Tasmanian devils (referred to as devils hereafter) that is genetically distinct from the original devil facial tumor (DFT1) (44).

Previous research has shown that reduced cell surface expression of MHC-I plays a major role in DFT1 immune evasion, but that IFN-γ can upregulate beta-2 microglobulin (β2m), ergo MHC-I expression (45). This immune evasion mechanism has been described in many types of cancer, and begs the question as to why the MHC-negative DFT cells are not targeted by NK cells in line with the "missing-self" hypothesis (46). Studies have demonstrated the NK cell genes are present in devils and that devil NK-like cells can mount an antitumor response (47–49). Despite the complimentary mechanisms of cytotoxic T cells and NK cells, immune responses against the DFTs are rare (50), suggesting that additional immune evasion mechanisms could be present.

Recent vaccination efforts have demonstrated that IFN-γ-stimulated DFT cells can induce antitumor responses and

tumor regressions in a subset of cases (51). However, initial forays into checkpoint molecule immunology of the DFT disease has shown that both DFT1 and DFT2 also upregulate PD-L1 upon exposure to IFN-γ (52), suggesting that anti-DFT immunotherapies could be enhanced by neutralizing the PD-1 inhibitory pathway. Given that the immune system has many redundant mechanisms for identifying and killing infectious agents and tumors, it is likely that the transmissible tumors employ additional methods beyond MHC-I downregulation and PD-L1 upregulation for evading host immune defenses and facilitating tumor transmission.

We have performed a comparative analysis of the protein sequences of key immune checkpoint molecules in the three mammalian species known to harbor naturally transmissible cancers (devils, dogs, and hamsters) and six other mammals (**Table 1**). We have not included the analysis of PD-1, PD-L1, and PD-L2 here, as we have previously published this information (52). Understanding the broad role of checkpoint molecules in these complex diseases has the potential to shed light on fundamental aspects of immune evasion, transplant tolerance and rejection, and infectious disease; this is logically relevant to both human and veterinary medicine. This checkpoint molecule analysis and review of salient features for each of the molecules presented here can serve as road map for the development of a DFT immunotherapy and as a guide for veterinarians, ecologists, and other researchers willing to venture into the nascent field of wild immunology.

MATERIALS AND METHODS

Species

We included nine species in our comparative analysis of checkpoint molecules. Humans and mice were included because checkpoint molecules have been best characterized in these species. We have included the little brown bat (*Myotis lucifugus*) in our comparative analyses because like devils, the species has recently undergone a dramatic population crash due to disease, and understanding bat immunology has become increasingly important due to the ability of bats to serve as reservoirs for viral pathogens (e.g., rabies, ebola, SARS). We have also included cats (*Felis catus*) and cattle (*Bos taurus*) due to their widespread distribution as important domestic animals. See **Table 1** for a full list of species names and abbreviations used.

TABLE 1 | Names and identifiers for species used in comparative sequence analysis.

#	Short name	Common name	Species name	Taxid
1	Devil	Tasmanian devil	*Sarcophilus harrisii*	9305
2	Opossum	Gray short-tailed opossum	*Monodelphis domestica*	13616
3	Bat	Little brown bat	*Myotis lucifugus*	59463
4	Cat	Domestic cat	*Felis catus*	9685
5	Cattle	Cattle	*Bos taurus*	9913
6	Dog	Domestic dog	*Canis familiaris*	9615
7	Hamster	Golden hamster	*Mesocricetus auratus*	10036
8	Human	Human	*Homo sapiens*	9606
9	Mouse	House mouse	*Mus musculus*	10090

Sequences

DNA sequences for all genes analyzed here were collected from GenBank and Ensembl and reference numbers for all sequences are available in Table S1 in Supplementary Material (53). All reference sequences current as of 30-Jan-2017, including the most current devil genome (Devil_ref v7.0). The complete coding sequence for the V-domain Ig suppressor of T cell activation (VISTA), CD47, and TIM-3 genes was not available from either GenBank or Ensembl, so sequences were obtained from a *de novo* transcriptome assembly (Table S2 in Supplementary Material) described below. The full coding sequences were submitted to GenBank with accession numbers: KY856749 (VISTA), KY856750 (CD47), and KY856751 (TIM-3). Where more than one sequence was present we generally chose GenBank transcript X1, unless preliminary alignments suggested that an alternative transcript was a better match to the other species used here. BLAST was used to find additional potential matching sequences for each gene (54). The available reference sequences for several genes that have not been characterized in their respective species contained elongated 5′ regions upstream of the likely start codon, so we manually truncated the amino acid sequences depicted in the alignment figures for the following genes: opossum CD80 and VISTA, bat CD86 and CD47, and hamster B7-H4.

RNA Sequencing (RNA-seq)

RNA sequencing data were generated as part of a previous study (55). Briefly, RNA was extracted from peripheral blood mononuclear cells (PBMCs) obtained from two disease-free devils. Illumina single-end 100 bp RNA-seq was conducted by the Australian Genome Research Facility. Sequencing generated 82,609,965 and 82,254,904 sequences, respectively. Fastq reads for each sample were assessed with FastQC version 0.11.5 (56), with both samples having acceptable per base sequence quality measurements. Genome-independent *de novo* assembly of the RNA-seq data was completed using the Trinity platform version 2.2.0 (57, 58) with default settings applied. This generated a reference transcriptome of assembled transcripts collectively from the two samples. The *de novo* transcriptome assembly was queried with BLASTN version 2.4.0+ (59) with coding sequences of the target genes obtained from Ensembl (53), database version 87.7, and UCSC Genome Browser (60). This identified transcript sequences from the assembled transcriptome of our target genes to use in comparative alignment analysis. Further information on this analysis is detailed in the Data Sheet S1 in Supplementary Material. Access to the raw fastq sequence data, Trinity assembled *de novo* transcriptome, and BLASTN results are detailed in the Data Sheet S1 in Supplementary Material.

Protein Sequence Alignments

Protein sequences were aligned with CLC sequence viewer using a progressive alignment algorithm with gap open cost = 5, gap extension cost = 1, end gap cost = free (61, 62). Pairwise protein sequence identities between devils and other species were determined using the default parameters on the Clustal Omega web server (63). We used the RasMol coloring scheme to highlight traditional amino acid properties in all sequence

alignments, which aids in interpretation of amino differences across species (64).

Analysis of Protein Sequences

All sequences were analyzed using the ExPASy server ProtParam tool to predict molecular weight and extinction coefficients (65). The eukaryotic linear motif (ELM) tool was used to predict key signaling motifs (66). The Simple Modular Architecture Research Tool (SMART) and the Phobius web server (67) were used to predict Ig-like domains and membrane topology (68). SignalP was used to confirm predicted signal peptides (69). Disulfide bonds and other unique features of each protein that were annotated on UniProt (70) were used to predict features in devil protein sequences.

RESULTS

The CTLA-4 and CD28 pathways are perhaps the most studied of the checkpoint molecules, but functional testing in species other than mice and humans is limited. A battery of tools (i.e.,

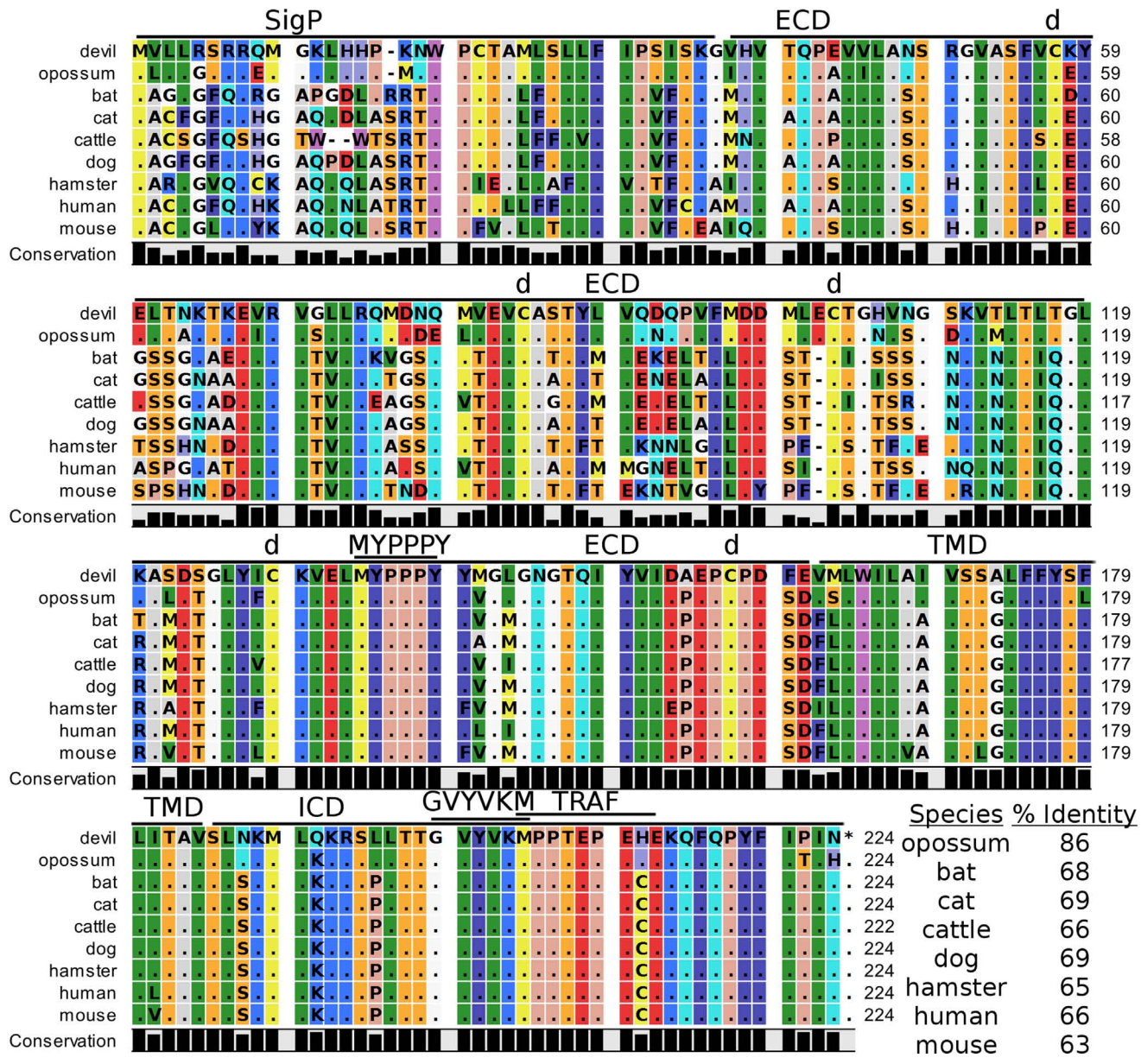

FIGURE 2 | Alignment of cytotoxic T-lymphocyte-associated protein 4 reference genes for nine species. The predicted signal peptides (SigP), extracellular domain (ECD), transmembrane domain (TMD), and intracellular domain (ICD) are demarcated with bars. "d" above the alignment represents predicted disulfide bonds. MYPPPY indicates the conserved CD80- and CD86-binding site. GVYVKM indicates a conserved cytoplasmic inhibitory domain and TRAF indicates a putative TRAF6-binding site. The black bars graphs below the alignment represent the conservation of amino acids across all nine species. The percent amino acid sequence identity between devils and other species is shown in the bottom right corner of the alignment.

TABLE 2 | Protein sequence percent identity between checkpoint molecules in devils and eight other species.

Species	Cytotoxic T-lymphocyte-associated protein 4	CD28	CD80	CD86	V-domain Ig suppressor of T cell activation	4-1BB	CD47	SIRP-α	CD200	TIM-3	Lymphocyte activation gene 3	B7-H4
Opossum	85.7	72.4	55.2	49.2	73.7	75.5	87.1	69.2	65.7	52.7	72.5	93.9
Bat	68.5	53.9	33.9	35.9	65.6	48.0	54.2	56.3	54.7	43.0	48.7	84.1
Cat	68.9	55.9	36.9	35.1	64.8	51.2	65.2	56.6	56.3	43.3	46.3	85.9
Cattle	66.1	56.0	36.3	35.9	65.8	50.8	67.4	55.3	53.2	42.1	50.6	85.9
Dog	68.9	56.4	35.0	37.8	63.2	53.8	67.1	56.7	52.8	43.1	43.0	87.7
Hamster	65.3	57.4	33.6	32.4	60.0	43.4	64.2	52.7	51.7	44.4	48.7	79.6
Human	65.8	56.2	35.5	36.6	64.9	52.2	66.8	55.8	56.2	43.2	51.9	87.0
Mouse	63.1	54.4	35.7	35.0	61.9	44.2	64.5	53.1	53.2	42.3	50.0	81.9

Percent identity was calculated by Clustal 2.1 algorithm.

recombinant proteins, monoclonal antibodies) and time are needed for proper testing of checkpoint molecule function, but much information and insight into function can be gained by analysis of protein sequences. For each molecule analyzed, we begin with a description of the general structure (i.e., Ig-like superfamily domains) and proceed to more nuanced details. This provides insight into potential functions of the molecules and can provide direction for designing critical experiments prior to the embarking on the time-consuming process of empirical testing of molecular function. See Table S3 in Supplementary Material for details of checkpoint molecule structure.

CTLA-4, CD28, CD80, and CD86

Devil CTLA-4 and CD28 are predicted to be 25 and 28 kDa, respectively, type-I transmembrane proteins with a single Ig-like V-type extracellular domain (ECD) (**Figure 1**). Protein sequence identity for CTLA-4 between devils and opossums was 86% and ranged from 63 to 69% between devils and placental mammals (**Figure 2**; **Table 2**). Percent identity for CD28 among species was lower than for CTLA-4, with 72% between devils and opossums and ranging from 54 to 57% between devils and placental mammals (**Figure 3**). Devil CTLA-4 had approximately 29% amino acid sequence identity with CD28. The CTLA-4 and CD28 coreceptors CD80 and CD86 are predicted to both be 35 kDa type-I transmembrane proteins that contain Ig-like V-type and an Ig-like C2-type domains. Devil CD80 and CD86 share only 21% sequence identity with each other, and the identity across the species analyzed here ranges from 34 to 55% and 32–49% for CD80 (**Figure 4**; **Table 2**) and CD86 (**Figure 5**; **Table 2**), respectively; the percent identity for CD80 and CD86 across species is the lowest of any of the checkpoint molecules compared here. All intra- and intermolecular disulfide bonds that have been identified in humans for CTLA-4, CD28, CD80, and CD86 are likely present in all the orthologs analyzed here, as we observed 100% conservation of cysteine residues at these sites in all species tested (**Figures 2**–**5**).

Key Ligand-Binding Regions Conserved in Devil CTLA-4 and CD28

Our analysis shows that devil CTLA-4 and CD28 both contain the MYPPPY motif that is necessary for binding of CTLA-4 and CD28 to CD80 and CD86 in humans and mice (**Figures 2** and **3**) (7). Of the 18 combined CTLA-4 and CD28 sequences aligned here, only cattle CD28 did not contain the $CD28_{MYPPPY}$ motif (71); cattle had a $CD28_{LYPPPY}$ sequence, which matches the $CD28_{LYPPPY}$ and $CTLA\text{-}4_{LYPPPY}$ that has been previously reported in pigs (*Sus scrofa*) and decreases affinity of porcine CTLA-4 for human CD80 and CD86 (35, 72). Additionally, all species also contain the $CTLA_{GVYVKM}$ inhibitory domain. Except for bats, all species also contain the key $CD28_{SDYMNM}$ and $CD28_{PYAP}$ motifs are critical for intracellular signaling that promotes T cell proliferation and survival *via* the CD28–PI3K–AKT [reviewed in Ref. (73)]. Bats have a $CD28_{M228L}$ substitution in the $CD28_{SDYMNM}$ motif.

Potential Unique Signaling Motifs Identified

The two marsupials examined contain a putative TRAF6-binding domain in CTLA-4 proteins that was not present in any of the placental mammals. We identified a putative ITIM in predicted the ECD of dog $CD80_{VKYGDL}$ and a TRAF1/2-binding site in the devil $CD80_{ATEEE}$ cytoplasmic domain (**Figure 4**). Our analysis predicted a TRAF6-binding site in the cytoplasmic tail of devil $CD86_{GHPKERDEV}$, a motif not predicted for CD86 in other species (**Figure 5**). Interestingly, the ELM tool predicted a putative ITIM domain in the second Ig-like segment of the human $CD86_{IEYDGI}$ ECD. To our knowledge, this putative ITIM has not been previously reported, and thus the potential inhibitory capacity of this motif is unknown.

V-Domain Ig Suppressor of T Cell Activation

Devil VISTA (PD-1H, C10orf54, Gi24, DD1α, Dies1) is a type-I transmembrane protein in the Ig superfamily predicted to be 33 kDa. The full coding sequence for this gene was previously not available in the devil genome (Devil_ref v7.0), but our *de novo* RNA transcriptome assembly uncovered a full coding devil VISTA transcript. Devil VISTA shares 60–74% sequence identity at the protein level with the other species analyzed here (**Figure 6**; **Table 2**). The ELM tool predicted a TRAF1/2-binding site in the ECD of devil $VISTA_{SIQE}$.

4-1BB

4-1BB (TNFRSF9, CD137) is a predicted 31 kDa member of the tumor necrosis factor (TNF) receptor family expressed predominantly as a type-I transmembrane homodimer (74, 75). 4-1BB ligand (4-1BBL, TNFSF9, CD137L) is a TNF family member

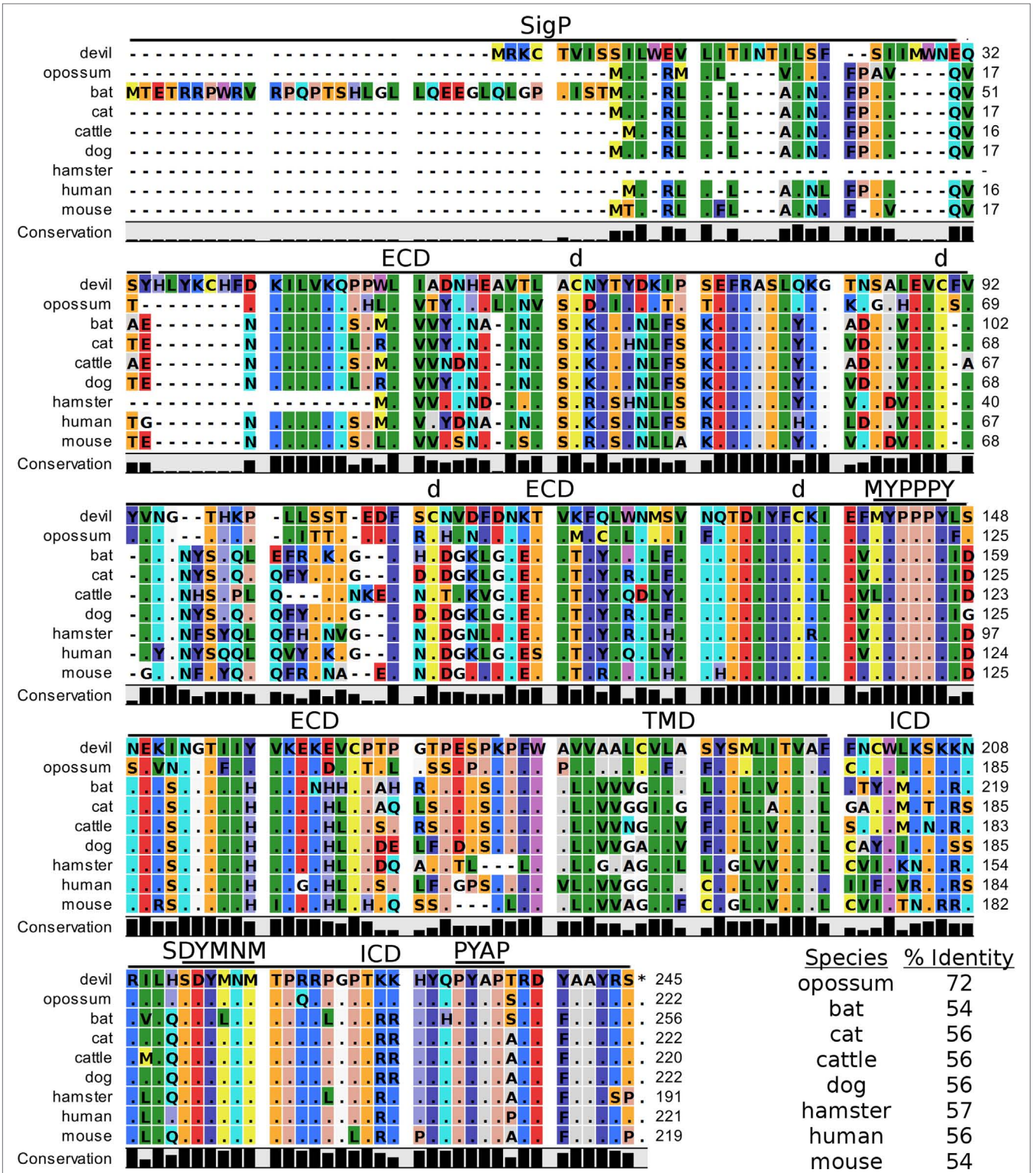

FIGURE 3 | Alignment of CD28 reference genes for nine species. The predicted signal peptides (SigP), extracellular domain (ECD), transmembrane domain (TMD), and intracellular domain (ICD) are demarcated with bars. "d" above the alignment represents predicted disulfide bonds. MYPPPY indicates the conserved CD80- and CD86-binding site, and SDYMNM and PYAP indicate key phosphorylation sites involved with cell proliferation and activation. The black bar graphs below the alignment represent the conservation of amino acids across all nine species. The percent amino acid sequence identity between devils and other species is shown in the bottom right corner of the alignment.

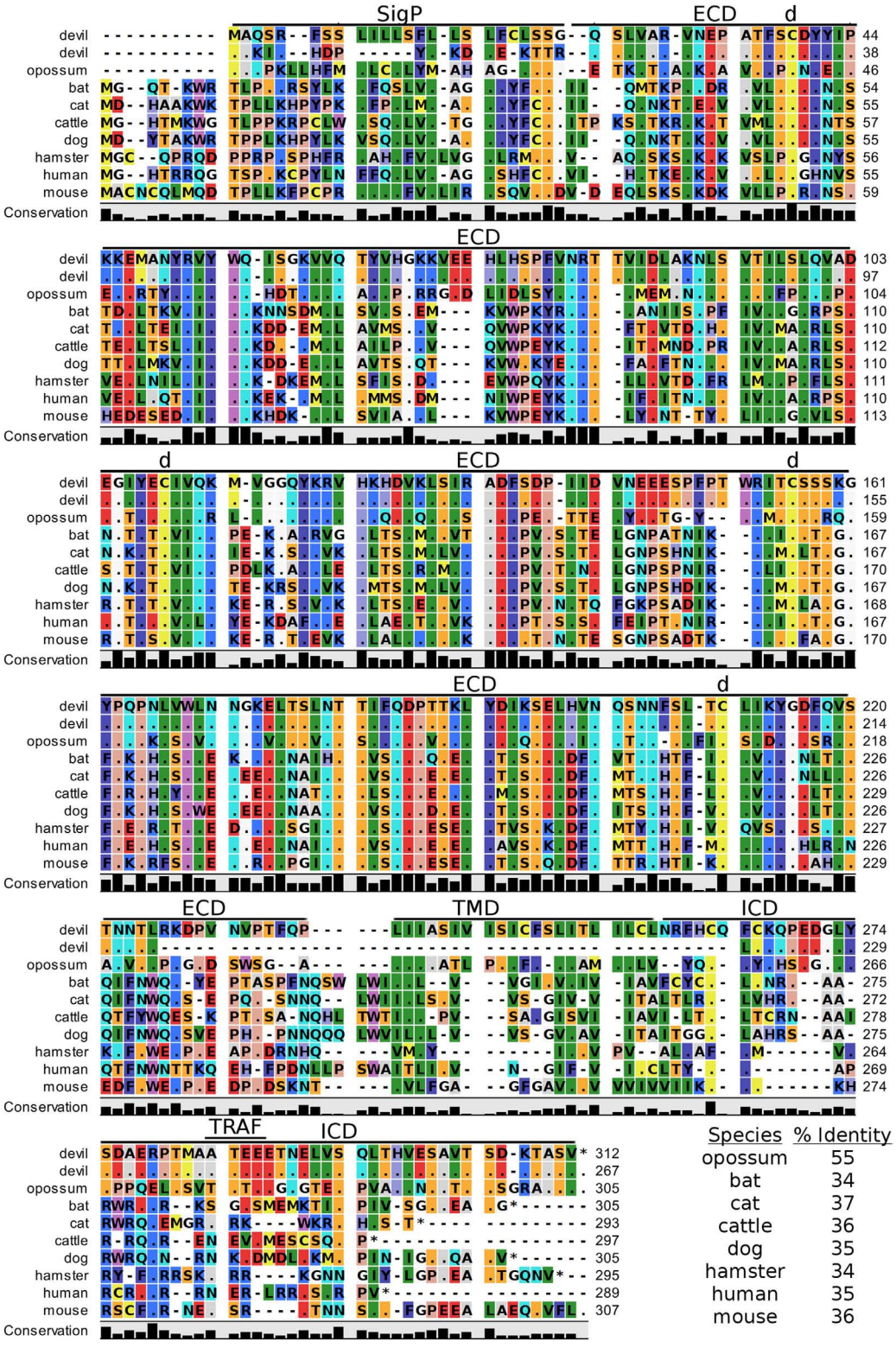

FIGURE 4 | **Alignment of CD80 reference genes for nine species**. The predicted signal peptides (SigP), extracellular domain (ECD), transmembrane domain (TMD), and intracellular domain (ICD) are demarcated with bars. The uppermost devil CD80 sequence is the full-length sequence and the lower devil CD80 is the potential secreted CD80 sequence. "d" above the alignment represents predicted disulfide bonds. TRAF indicates a putative TRAF1/2-binding site. The black bar graphs below the alignment represent the conservation of amino acids across all nine species. The percent amino acid sequence identity between devils and other species is shown in the bottom right corner of the alignment.

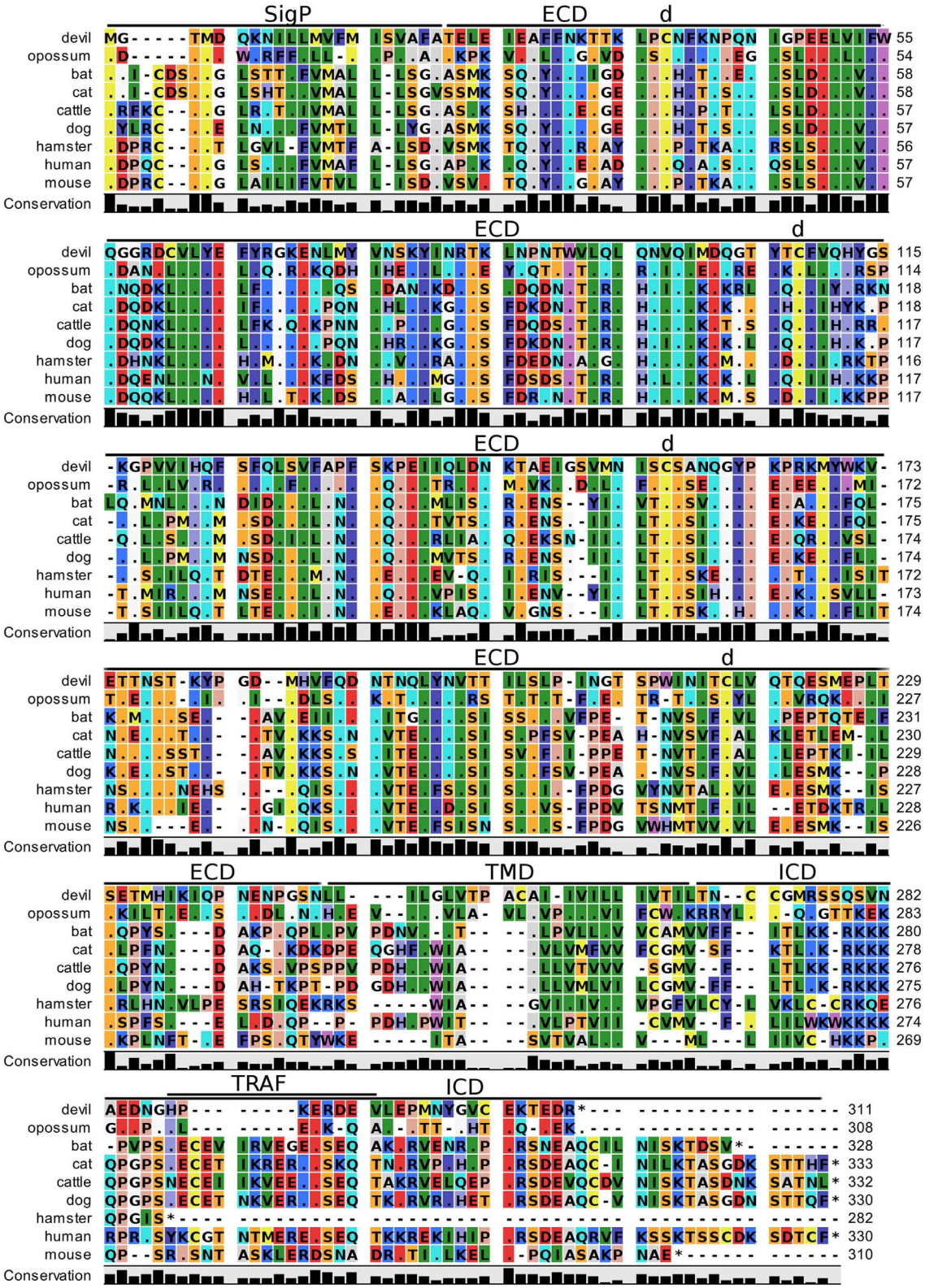

FIGURE 5 | **Alignment of CD86 reference genes for nine species**. The predicted signal peptides (SigP), extracellular domain (ECD), transmembrane domain (TMD), and intracellular domain (ICD) are demarcated with bars. "d" above the alignment represents predicted disulfide bonds. TRAF indicates a putative TRAF6-binding site. The black bar graphs below the alignment represent the conservation of amino acids across all nine species. The percent amino acid sequence identity between devils and other species is shown in the bottom right corner of the alignment. See **Table 2** for the sequence identity between devils and other species.

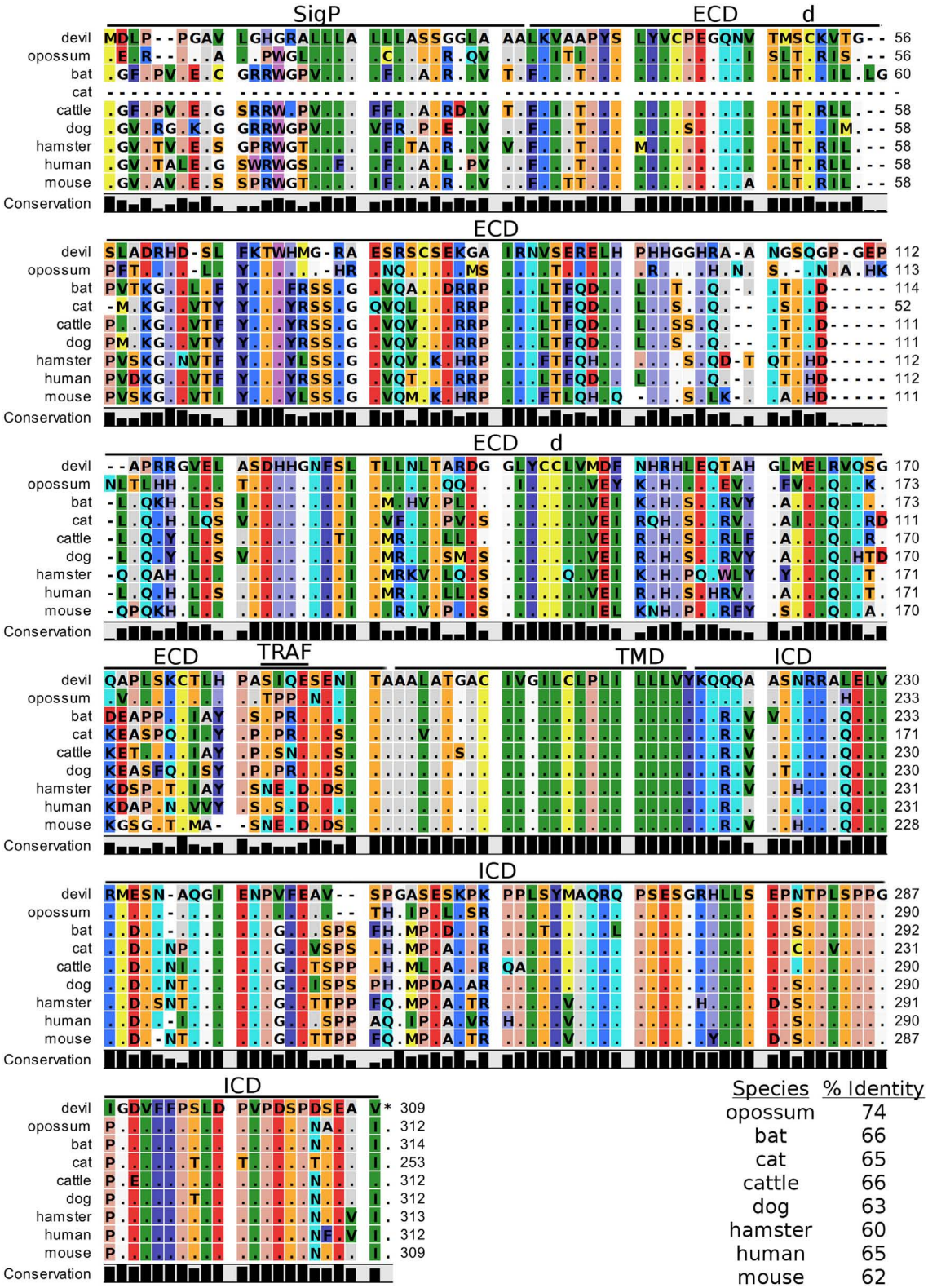

FIGURE 6 | **Alignment of V-domain Ig suppressor of T cell activation reference genes for nine species**. The predicted signal peptides (SigP), extracellular domain (ECD), transmembrane domain (TMD), and intracellular domain (ICD) are demarcated with bars. "d" above the alignment represents predicted disulfide bonds and "TRAF" indicates a potential TRAF1/2-binding site. The black bar graphs below the alignment represent the conservation of amino acids across all nine species. The percent amino acid sequence identity between devils and other species is shown in the bottom right corner of the alignment.

of 20 kDa, expressed as a type II transmembrane homotrimer (**Figure 1**). SMART analysis of devil 4-1BB identified two TNFR-Cys repeat domains, whereas human 4-1BB contains four TNFR-Cys repeats (**Figure 7**). All cysteine repeats in the four human TNFR-Cys domains were conserved in devils, suggesting that devil 4-1BB might also contain four TNFR-Cys domains despite not being predicted by the SMART program. Indeed, all 20 cysteine residues involved in disulfide bonds in human 4-1BB were also present in devil 4-1BB. Overall sequence identity among species compared here ranged from 43 to 75%, with mouse and hamster 4-1BB having the lowest percent identities with devil 4-1BB (**Table 2**).

We identified a putative inhibitory domain in devil 4-1BB$_{LPYFLK}$ based on alignment with a potential inhibitory domain in human 4-1BB$_{LLYIFK}$ (76, 77). The putative inhibitory domain resembles an ITIM domain but lacks the I, L, or V in the terminal amino acid position. To date, this potential inhibitory domain has only been reported in humans, but several species analyzed here have similar motifs. Additionally, mice have a 4-1BB$_{CXCP}$ motif in the cytoplasmic domain that facilitates binding of CD4 and CD8 molecules to p56^{lck}, a protein tyrosine kinase that is important for optimal T cell responses (78, 79); of the nine species compared here, mice are the only species that have the 4-1BB$_{CXCP}$ sequence. Our analysis using the ELM tool predicted two TRAF1/2 ligand-binding sites (devil 4-1BB$_{TAQEE,}$ 4-1BB$_{PEEE}$), which align with the known TRAF1/2-binding sites in human and mouse 4-1BB (80).

CD47

Human CD47, also known as integrin-associated protein for its role in cell adhesion, is a cell surface protein that contains five transmembrane segments and a single Ig-like V-type domain (81, 82). The most up-to-date gene sequences for devil CD47 in Ensembl (ENSSHAT00000014546.1) did not contain a full coding sequence (i.e., no start codon) and the GenBank (XM_012544496) gene had an extended 5′ region that did not align well with other species. Our *de novo* RNA transcriptome assembly uncovered a full coding transcript for CD47 from devil PBMCs that aligned well with other species analyzed here. Our analysis suggests that the 34 kDa devil CD47 also contains five transmembrane segments and a single Ig-like domain (**Figure 8**). The four cysteines needed for the disulfide bonds reported in human CD47 are conserved in all species examined here, and overall sequence identity across all species compared here ranges from 54 to 87% (**Table 2**). Curiously, the ELM tool predicted an ITIM in the devil CD47$_{LKYHVV}$ ECD. All other species except bats and hamsters also contain the putative ITIM domains, but the ELM tool classified the ITIM as an excluded motif due to the putative ITIM being located in ECD of the protein. We also identified a putative TRAF2-binding site in the third devil intracellular domain of CD47$_{KAVEE}$ that was conserved across all species examined here except bats.

SIRP-α

Devil SIRP-α is a predicted 56 kDa protein. Human SIRP-α binds to CD47 as either a monomer or a dimer (83, 84) and forms three intramolecular disulfide bonds. All six of the cysteines that form intramolecular disulfide bonds in humans are conserved in devils (Figure S1 in Supplementary Material). The percent sequence identity for SIRP-α ranged from 53 to 69%. Analysis of devil SIRP-α revealed two putative ITIM and one ITSM domain. The ITIM$_{ITYADL}$ shares 100% identity with all species except cattle, and the ITIM$_{LTYADL}$ is 100% conserved across all species. The devil ITSM$_{SQTEYASI}$ matches 5/7 amino acids with all other species; to our knowledge no ITSM has previously been reported in SIRP-α. We identified two potential SIRP-β1 orthologs in devils (ENSSHAT00000016950, XM_012553634.1) that contained ITIM motifs (SIRP-β1$_{VSYNLI}$) in the ECD. The putative SIRP-β1 (ENSSHAT00000016950) ITIM aligned with an SIRP-β1$_{VSYNIT}$ sequence in SIRP-α that contains the key tyrosine residue for ITIMs but did not contain the canonical 3′ I/V/L.

CD200

Devil CD200 is predicted to be a 31 kDa type-I transmembrane protein that shares 52–66% sequence identity across the species compared here (**Figure 9**; **Table 2**). The cysteine residues that form intramolecular and intermolecular disulfide bonds necessary for binding as either a monomer or homodimer to CD200 receptor (CD200R) are 100% conserved across all species examined here (**Figure 9**) (85). Additionally, the Ig-like V-type and Ig-like C2-type domains of human and mouse CD200 were identified by the SMART tool. Many key motifs, including endocytic sorting signals, and TRAF2, SH2, and SH3 binding motifs, are present in all species compared here. Our analysis using ELM predicts a potential ITSM only in devil CD200. However, the devil CD200$_{TLQE}$ TRAF1/2-binding site and CD200$_{NKTEYVVI}$ ITSM are both located in the predicted ECD of devil CD200, so empirical testing is needed to determine if these are functional sites. Although not analyzed in depth here, CD200R and CD200R-like proteins were identified in the nine species compared here. The primary reference sequence for each species contained the key CD200R$_{NPLY}$ motif (86), which has been shown to be a key motif for CD200R inhibitory function (87).

TIM-3

TIM-3, also known as T-cell immunoglobulin and mucin domain-containing protein 3, hepatitis A virus cellular receptor 2, and CD366, is a surface protein expressed on T cells, Tregs, monocytes, macrophages, and DCs in mice and humans [reviewed in Ref. (88)]. The most up-to-date gene sequences for devil TIM-3 in Ensembl (ENSSHAT00000018107.1) and GenBank (XM_012552117.1) had truncated 3′ region of the coding sequence, and the Ensembl gene had an extended 5′ region that did not align with other species. Our *de novo* RNA transcriptome assembly uncovered a full coding devil TIM-3 transcript from devil PBMCs that aligned well with other species analyzed here. Analysis of the devil TIM-3 predicted sequence suggests that it is a 24 kDa protein with a Ig-like V-type domain and mucin domain in the extracellular region of the protein (**Figure 10**). Percent amino acid sequence identity between devils and the other eight species analyzed here ranges from 42 to 53%, which is the lowest identity for any molecule analyzed here except for CD80 and CD86 (**Table 2**). Despite this relatively low conservation of protein sequence, many of the key TIM-3

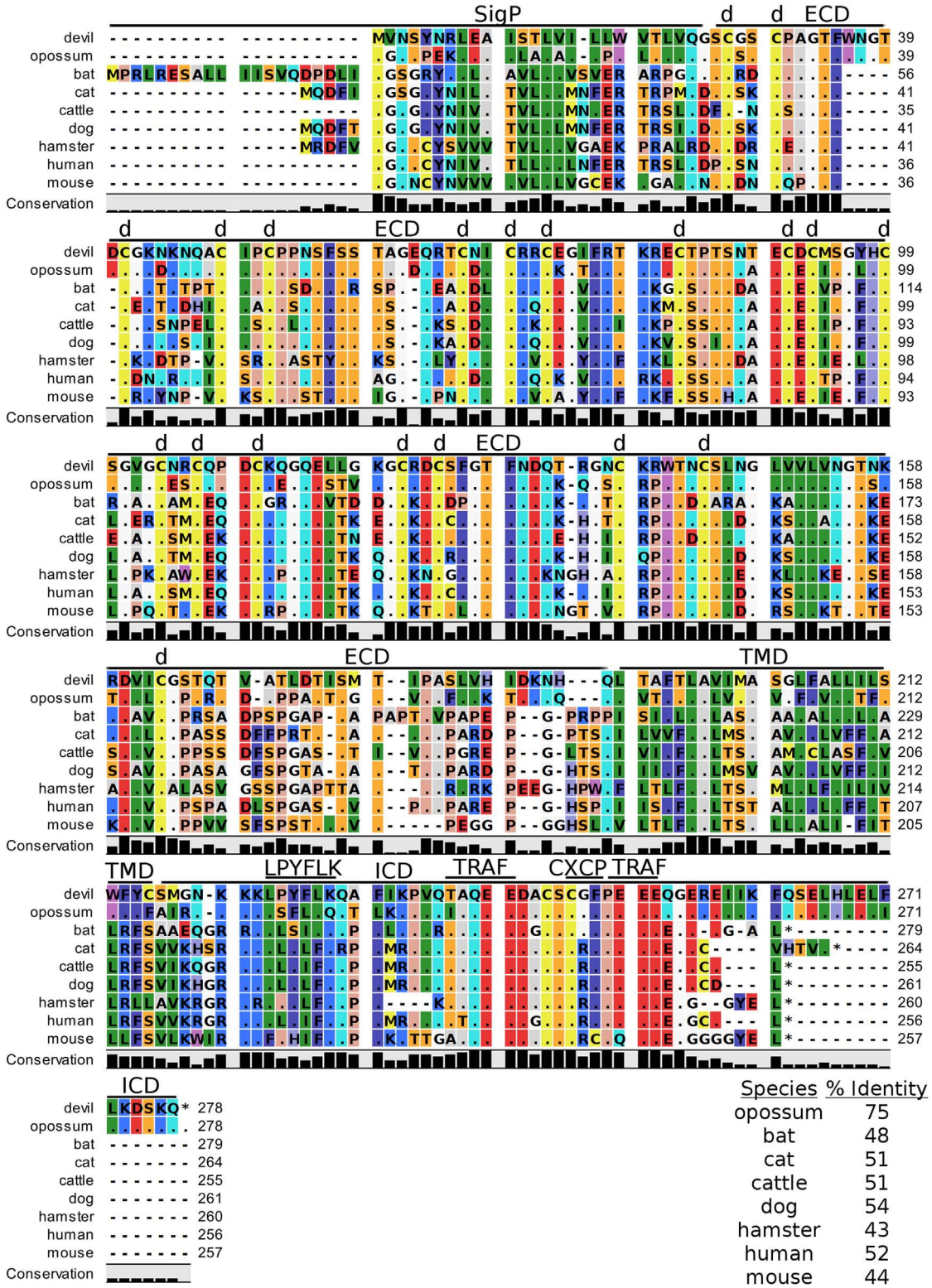

FIGURE 7 | Alignment of 4-1BB reference genes for nine species. The predicted signal peptides (SigP), extracellular domain (ECD), transmembrane domain (TMD), and intracellular domain (ICD) are demarcated with bars. "d" above the alignment represents predicted disulfide bonds. Two potential TRAF1/2-binding sites are demarcated by "TRAF." "CXCP" marks a motif associated with optimal T cell response in mice, and "LPYFLK" denotes a potential inhibitory domain in devils. The black bar graphs below the alignment represent the conservation of amino acids across all nine species. The percent amino acid sequence identity between devils and other species is shown in the bottom right corner of the alignment.

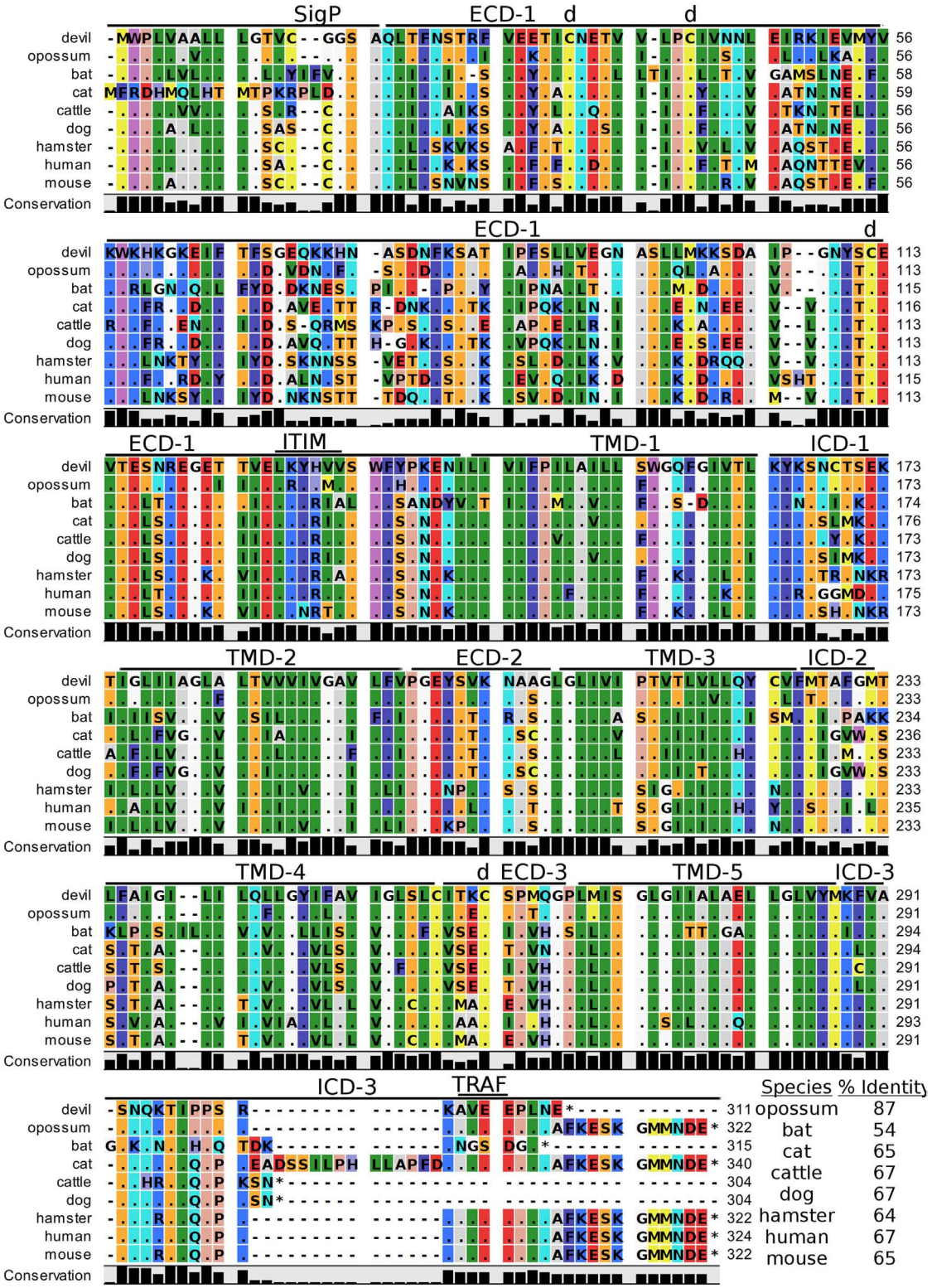

FIGURE 8 | Alignment of CD47 reference genes for nine species. The predicted signal peptides (SigP), extracellular domains (ECDs), transmembrane domains (TMDs), and intracellular domain (ICD) are demarcated with bars. "d" above the alignment represents predicted disulfide bonds. "TRAF" indicates a potential TRAF1/2-binding site and immunoreceptor tyrosine-based inhibitory motif (ITIM) marks a putative ITIM motif predicted in the ECD. The black bar graphs below the alignment represent the conservation of amino acids across all nine species. The percent amino acid sequence identity between devils and other species is shown in the bottom right corner of the alignment.

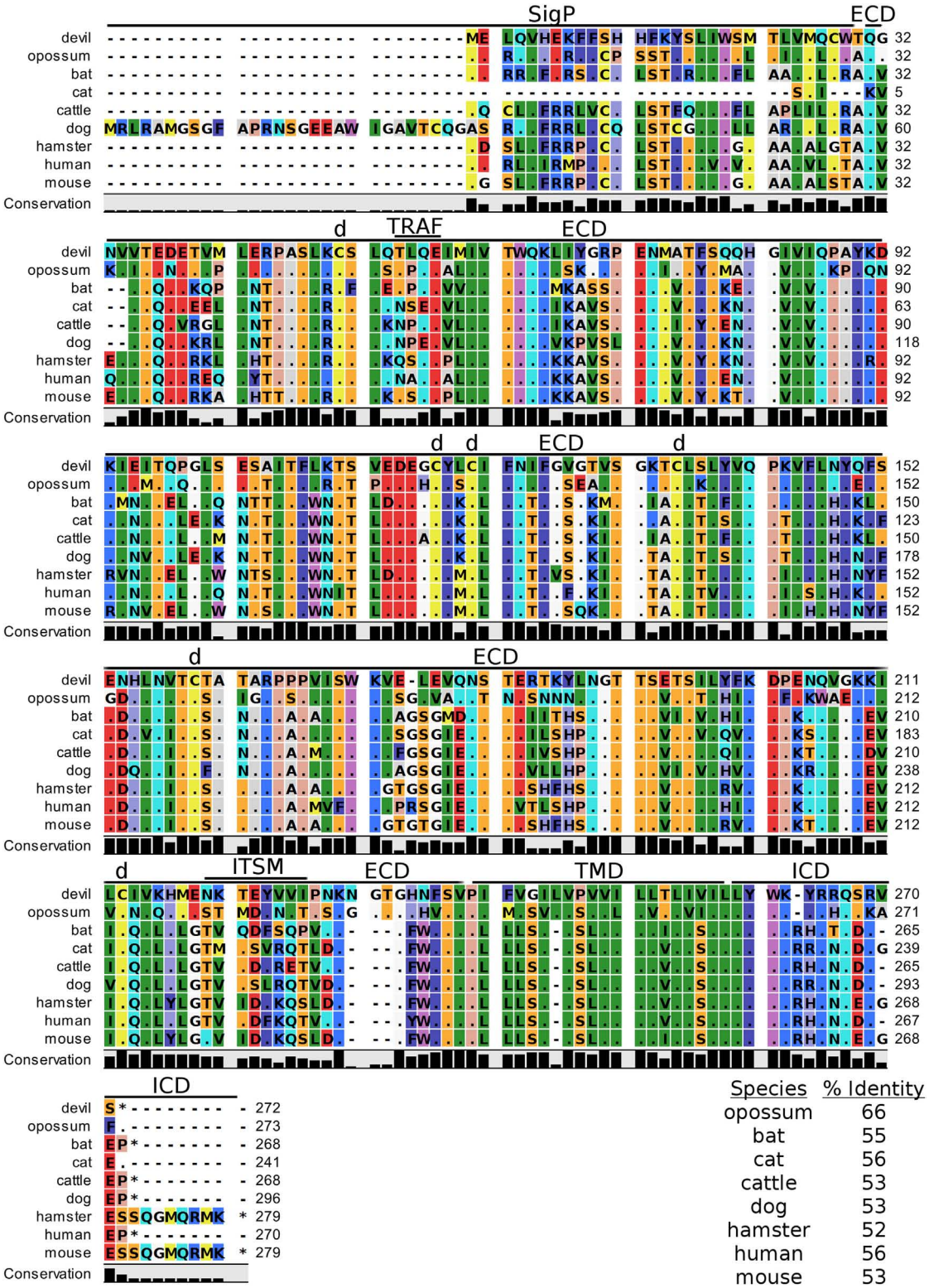

FIGURE 9 | Alignment of CD200 reference genes for nine species. The predicted signal peptides (SigP), extracellular domain (ECD), transmembrane domain (TMD), and intracellular domain (ICD) are demarcated with bars. "d" above the alignment represents predicted disulfide bonds. "TRAF" indicates a potential TRAF1/2-binding site and "ITSM" represents a putative immunoreceptor tyrosine-based switch motif (ITSM). The black bar graphs below the alignment represent the conservation of amino acids across all nine species. The percent amino acid sequence identity between devils and other species is shown in the bottom right corner of the alignment.

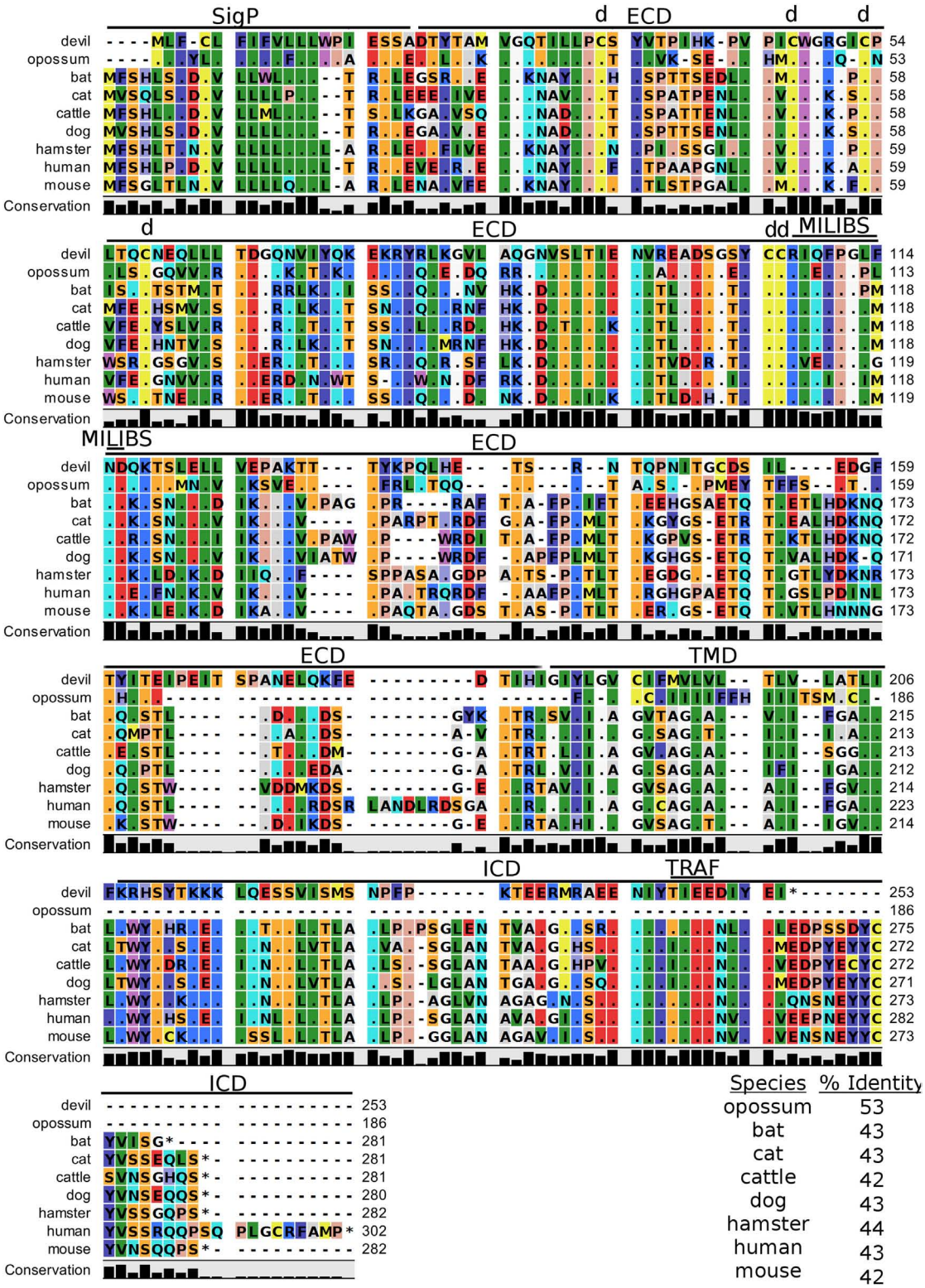

FIGURE 10 | Alignment of TIM-3 reference genes for nine species. The predicted signal peptides (SigP), extracellular domain (ECD), transmembrane domain (TMD), and intracellular domain (ICD) are demarcated with bars. "d" above the alignment represents predicted disulfide bonds. "TRAF" indicates a potential TRAF1/2-binding site and "MILIBS" demarcates a conserved metal ion-dependent ligand-binding site (MILIBS) found in phosphatidylserine on the surface of apoptotic cells. The black bar graphs below the alignment represent the conservation of amino acids across all nine species. The percent amino acid sequence identity between devils and other species is shown in the bottom right corner of the alignment.

features identified in mice and humans appear to be present in devil TIM-3.

A unique feature of human TIM-3 is the double cleft which facilitates binding to multiple ligands (89, 90). The six cysteines that form three intramolecular disulfide bonds in the Ig-like region of human TIM-3 (89) are all present in devil TIM-3 (**Figure 10**), suggesting that devil TIM-3 folding and structure might be similar to human TIM-3. Analysis of human TIM-3 sequences identified five key amino acids for the two ligand-binding clefts; four of the five key amino acids were conserved in devil TIM-3. All species analyzed here also have two critical tyrosine residues in the TIM-3 cytoplasmic domain that align with mouse TIM-3_{Y256} and TIM-3_{Y263} (**Figure 10**), which are phosphorylated following ligation by GAL-9 and are associated with increased NFAT/AP-1 and NF-κB activity (91). A TIM-3_{TIEE} TRAF1/2-binding site is located between these tyrosine residues in all species except for cats, dogs, and cattle (**Figure 10**). Also, mouse TIM-1, TIM-3, and TIM-4 all bind to phosphatidylserine on the surface of apoptotic cells *via* a conserved metal ion-dependent ligand-binding site (MILIBS). The mouse TIM-$3_{RIQFPGLMND}$ MILIBS motif is 100% conserved in cats, dogs, and cattle TIM-3, whereas devils have a phenylalanine instead of a methionine in this motif. Whether this TIM-3_{M114F} affects phosphatidylserine binding and clearance of apoptotic cells in devils is unknown.

Lymphocyte Activation Gene 3

In humans and mice, LAG-3 (CD223) is an inhibitory type-I transmembrane protein that is structurally homologous to CD4 (92). Human and mice LAG-3 each contain one Ig-like V-type and three Ig-like C-type domains, whereas devil LAG-3 is predicted to be a 54 kDa protein with three Ig-like domains. However, a 100 amino acid ($LAG3_{330–429}$) region downstream of the three predicted Ig-like domains could contain a fourth Ig-like domain that was not predicted by the SMART prediction tool (68, 93). Devil LAG-3 percent sequence identity with the other eight species analyzed here ranges from 43 to 73% (**Table 2**). In humans and mice, the LAG-3_{KIEELE} (Figure S2 in Supplementary Material) motif in the cytoplasmic domain is critical for downstream inhibitory signaling interactions, but this exact sequence is not present in the other species analyzed here. The critical lysine (LAG-3_{K468}) in this motif is present in devil (LAG-3_{KAEEME}) and all other mammals tested here, with the exception of opossums (LAG-3_{IAEQME}).

B7-H4

Devil V-set domain-containing T-cell activation inhibitor 1, or more commonly referred to as B7 homolog 4 (B7-H4), is a 30 kDa type-I membrane protein that contains two Ig-like V-type domains in the extracellular region (**Figure 11**). Devil B7-H4 protein shares 87% sequence identity with human B7-H4 and ranges from 80 to 94% for the other seven species analyzed here (**Table 2**). Based on homology to human and mouse B7-H4 and analysis of devil B7-H4 using cNLS Mapper (score of 3.4) (94, 95), it is likely that devil B7-$H4_{KKRGH}$ contains a bipartite nuclear localization signal (NLS). Interestingly, B7-H4 has only two amino acids in the cytoplasmic domain when expressed as a surface protein.

DISCUSSION

Evolutionary Conservation of Key Protein Regions

Despite an estimated 162 million years of evolution since the last common ancestor of placental and non-placental mammals, most of the checkpoint molecules we analyzed have orthologs in Tasmanian devils. Importantly, many of the key signaling motifs and ligand-binding sites are highly conserved in the genes analyzed, particularly cysteine residues for intra- and intermolecular disulfide bonds and transmembrane and intracellular tyrosine residues for receptor tyrosine kinases. The strong conservation of the key protein regions suggests that inhibitory and stimulatory function of these molecules, which is relatively well-documented in humans and mice, is conserved in devils. Importantly, by following established procedures and focusing on the checkpoint molecules that have proven most clinically effective in humans, we can rapidly characterize key checkpoint molecules in devils and incorporate potent immunomodulatory agents into our DFT disease vaccine-development efforts.

The Web of CD28–CTLA-4 Cosignaling Pathways

Our analysis shows for the first time that the key CTLA-4_{MYPPPY} and $CD28_{MYPPPY}$ are conserved in devils. Given that the MYPPPY motif present in chickens facilitates binding to mammalian CD80 and that a single leucine for methionine substitution in pig CTLA-4_{LYPPPY} is sufficient to disrupt binding of porcine CTLA-4 to human CD80 (35, 72, 96), the evolutionary conservation of CTLA-4_{MYPPPY} and $CD28_{MYPPPY}$ in devils suggests that the competitive binding of CTLA-4 and CD28 for CD80/86 should be present in devils.

In addition to the conserved binding motifs, the key $CD28_{SDYMNN}$ stimulatory domain (97) and $CTLA_{GVYVKM}$ inhibitory domains are also conserved in devils, suggesting that the complementary stimulatory and inhibitory functions of CD28 and CTLA-4 are present. The CTLA-4_{GVYVKM} motif, in association with T-cell receptor-interacting molecule (TRIM), regulates surface expression of CTLA-4 (98). The TRIM-mediated recycling of CTLA-4 from the surface provides the means for cell-extrinsic inhibitory function by trans-endocytosis of CD80/86 (99). By trans-endocytosing, or in other words stripping CD80/86 from the surface of an opposing cell (i.e., APCs) and degrading the CD80/86 molecules in the CTLA-4-expressing cell, the potential of costimulation *via* CD80/86 binding to CD28 is eliminated. Whether trans-endocytosis or trogocytosis (100) occurs in devils is unknown. It could be readily tested by developing CD80 transgenic cell lines that have a fluorescent protein, such as green fluorescent protein (GFP), fused to the 3′ tail of CD80. Flow cytometric or immunofluorescence observations of GFP transferred from the transgenic cell line to the CTLA-4 expressing cells would demonstrate that this inhibitory pathway is conserved in devils.

The complex interactions involving CTLA-4 are further complicated by some anti-CTLA-4 monoclonal antibody effects that are mediated through Fc receptor signaling (11, 101, 102). Tregs

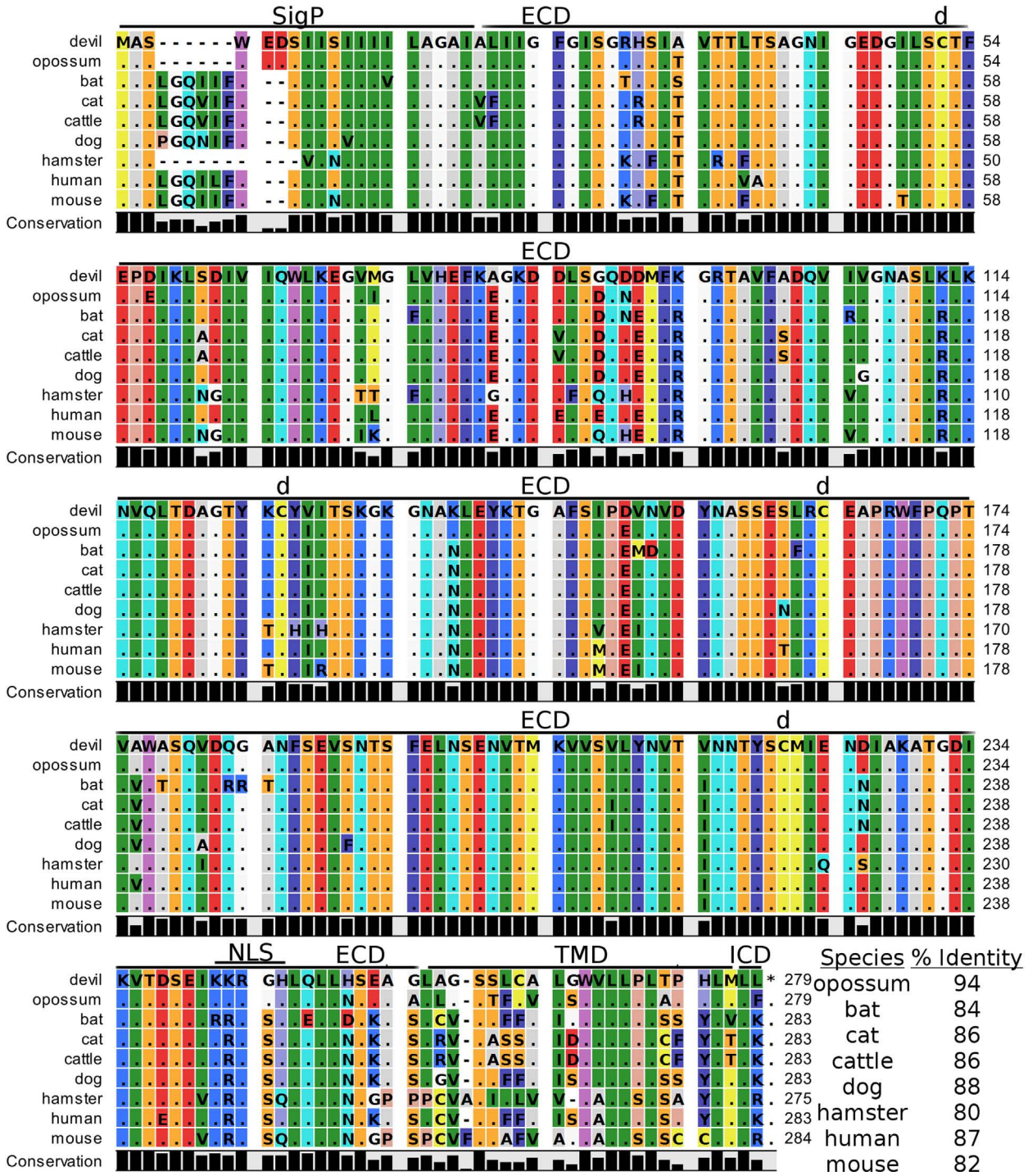

FIGURE 11 | Alignment of V-set domain-containing T-cell activation inhibitor 1 reference genes for nine species. The predicted signal peptides (SigP), extracellular domain (ECD), transmembrane domain (TMD), and intracellular domain (ICD) are demarcated with bars. "d" above the alignment represents predicted disulfide bonds. NLS indicates a predicted nuclear localization signal. The black bar graphs below the alignment represent the conservation of amino acids across all nine species. The percent amino acid sequence identity between devils and other species is show in the bottom right corner of the alignment.

expressing high levels of CTLA-4 can be killed *via* antibody-dependent cell-mediated cytotoxicity, thus reducing the inhibition of antitumor immunity. This could be a useful tactic for increasing T cell responses against neoantigens in DFT cells, but little is known about IgG isotypes and Fc receptors in devils (103). To our knowledge only a single IgG subclass has been identified in marsupials (103), and the number and type of Fc receptors are unknown. Investigations into devil isotypes and Fc receptors

are needed to aid development of potential monoclonal antibody immunotherapies for devils. Additionally, we identified a potential TRAF1/2-binding site in devil CD80 and a TRAF6-binding site in devil CD86. TRAF6 is associated with NF-κB activation and production of IL-6 and IL-8, whereas TRAF2 is associated with IκB-kinases. The binding site for TRAF2 but not TRAF6 is required CD40-mediated antibody class switching (104–106). Specific targeting of CD80 or CD86 by monoclonal antibodies or soluble ligands could help to determine if additional IgG subclasses exist in devils and to understand the potential role of IL-6 and IL-8 in immune evasion by DFT cells.

In addition to binding to both CTLA-4 and CD28 in humans and mice, CD80 binds to PD-L1 with a greater affinity than to CD28, but less than affinity of CD80 for CTLA and PD-L1 for PD-1 (107, 108). In humans, overexpression of CD80 blocks PD-L1 expression by sequestering PD-L1 in the cytoplasm while simultaneously providing costimulation (109). Additional pleiotropic effects of CD80 include its ability to stimulate NK cells through both CD28-dependent and -independent pathways (110–112). As DFT1 cells are poorly immunogenic and do not express MHC-I, the ability to stimulate NK cells using CD80 could provide immunotherapeutic potential.

Soluble CD80 can also effectively block PD-1:PD-L1 interactions and provide costimulation (113, 114). Interestingly, in addition to the full-length devil CD80, we identified a devil CD80 splice variant that lacks a transmembrane domain (TMD) and likely codes for soluble version of this key checkpoint molecule. Humans are also known to express soluble CD80 and soluble PD-L1, and high plasma levels of PD-L1 are associated with poor prognosis in B cell lymphomas (115–117). The anti-PD-L1 monoclonal antibodies we have previously developed could be used to screen devil plasma for soluble PD-L1 and possibly serve as a prognostic test for DFT disease.

Devil 4-1BB Function Is Predicted to Resemble Human 4-1BB Function

Despite the potential for enhanced immunotherapies targeting the 4-1BB/L pathway, actual progress has been slow, in part due to differences between mice and humans. 4-1BB costimulation in both mice and humans leads to enhanced T cell-mediated immunity, but the effects are contrasting in human and mouse NK cells. In mice, 4-1BB stimulation leads to enhanced NK cell effector mechanisms, but in humans 4-1BB signaling inhibits NK effector activity and reverse signaling through 4-1BBL on tumor cells can induce IL-10 and TNF-α (77, 118). This is potentially mediated by a putative inhibitory motif 4-1BB$_{LLYIFK}$ in the human cytoplasmic domain that resembles an ITIM domain (76, 77). Interestingly, devils have a similar putative 4-1BB$_{LPYFLK}$ inhibitory domain that includes the key tyrosine residue, but opossum 4-1BB does not contain the putative inhibitory motif (4-1BB$_{LSFLLQ}$). Comparative testing of opossum and devil 4-1BB should be able to determine the inhibitory capacity of these motifs. Devil 4-1BB also contains conserved TRAF1/2-binding sites that in humans are necessary for recruiting TRAF1 and TRAF2 and inducing expression of pro-survival genes, including Bcl-2, Bcl-XL, and Bfl-1 and decreasing expression of Bim, a pro-apoptotic molecule (119–121). Altogether, devil 4-1BB has key features that more closely resemble human 4-1BB, and thus devil 4-1BB might stimulate T cell function but inhibit NK cell function.

As expression of 4-1BB on T cells is largely dependent on activation state, combining agonistic anti-4-1BB immunotherapies with stimulatory cytokines presents an opportunity for promoting immune memory. For instance, CD28- or IL-15-mediated upregulation of 4-1BB combined with agonistic anti-4-1BB monoclonal antibodies or recombinant 4-1BBL could promote antigen-independent survival and expansion of memory CD8 T cells (122, 123); this could be critical for long-term memory against repeated exposure to DFT cells in the wild. Also of particular relevance to the DFT disease is that blockade of 4-1BB:4-1BBL pathways leads to prolonged allograft survival for heart (124), skin (124), eye (125), and intestinal (126) tissues in other species.

To Eat or Not to Eat: Phagocytic Checkpoints

CD47

CD47 functions as an identifier of "self" tissue and is expressed on nearly all human and mouse cells. It has become known as the "don't eat me" signal due to its ability to inhibit phagocytosis following ligation of SIRP-α (CD172a) on phagocytic cells (i.e., APCs, macrophages) (127). Of particular relevance to transmissible cancers, which are both allografts and cancer, CD47 appears to play a crucial role in transplant tolerance. The potent inhibitory signaling capacity of CD47 was clearly demonstrated in a xenotransplant model in which phagocytosis of pig cells by human macrophages was abrogated by transfecting the pig cells with human CD47 (128, 129). Several other studies have confirmed the importance of the CD47:SIRP-α interaction in graft and xenotransplant tolerance (129–132). Interestingly, the intraspecies CD47:SIRP-α interaction and function seems to be conserved in most species, but interspecies compatibility of CD47:SIRP-α is low (133). This suggests that CD47:SIRP-α binding could be a barrier to interspecies transmission of tumors. The closest extant relatives of devils, the Eastern quoll (*Dasyurus viverrinus*) and spotted-tail quoll (*Dasyurus maculatus*), are also a conservation priority, so understanding the role of CD47 in preventing interspecies transmission could prove useful for conservation of quolls.

DFT1 and DFT2 are not xenotransplants in devils, but the CD47:SIRP-α interaction could be a key mechanism of inhibiting phagocytosis and allo-responses against the DFT cells. Interestingly, in rats and mice, CD47 has been implicated in myelin phagocytosis through modulation of CD47:SIRP-α interactions (134) This is an immune evasion pathway that may have been exploited by DFT1, which originated from a Schwann cell and expresses high levels of myelin (37). Despite the nearly ubiquitous expression of CD47 by all cell types, expression levels are highly variable and can be modulated by inflammation (135, 136). High levels of CD47 found on many types of human cancer, including leukemia (137–139), lymphoma (140), and several types of solid tumor cancers (141, 142) and are often associated

with poor prognosis. Importantly, blockade of CD47:SIRP-α interactions stimulated enhanced antitumor responses in several mouse models of human cancer (141, 143, 144), and trials of anti-CD47 antagonistic monoclonal antibodies are underway in humans. The MYC oncogene transcription factor binds to the promotors of both CD47 and PD-L1 and expression of both CD47 and PD-L1 can be downregulated by targeting MYC (145), presenting an opportunity to simultaneously target both PD-L1 and CD47.

A drawback of the anti-CD47 monoclonal antibody treatment is that CD47 blockade can lead to anemia due to rapid depletion of red blood cells. However, this risk could potentially be minimized by injection of anti-CD47 mAbs or SIRP-α fusion proteins directly into accessible DFTs (i.e., tumors in the mouth and face) (146). In addition to facilitating cancer cell immune evasion, CD47 also affects T cell and NK cell homeostasis (147, 148). CD47 is suggested to facilitate longevity by reducing clearance by phagocytes (135). Blockade of CD47 could thus decrease memory cell longevity and increase turnover of T cells and NK cells and could be detrimental to long-term DFT immunity in wild devils that could be re-exposed to DFT.

V-Domain Ig Suppressor of T Cell Activation

In contrast to the "don't eat me" signal from CD47 ligation, VISTA can function as an "eat me" signal *via* intercellular homophilic binding that affects clearance of apoptotic cells and immune surveillance by macrophages and T cells (149, 150). VISTA expression is upregulated in response to genotoxic stress in a p53-dependent manner, and homophilic VISTA interactions both in *cis* and *trans* among tumor cells, APCs, and T cells may facilitate tumor cell escape from immune surveillance (149). No polymorphisms in devil p53 have been reported (151), but given the chromosomal rearrangements and greater than 17,000 somatic mutation reported in DFT1 cells (152, 153), it seems probable that p53 would be at least occasionally activated in DFT cells and could induce upregulation of tolerogenic VISTA signaling.

The tolerogenic role of VISTA in humans and mice and the strong conservation of VISTA across the nine species analyzed here (only B7-H4 and CTLA-4 were more conserved) suggest that VISTA may play an important evolutionary role in maintaining the balance between tolerance and immunity in mammals. Despite high sequence identity, the ELM tool unexpectedly predicted a putative TRAF1/2 ($VISTA_{SIQE}$) binding site in the ECD of devil VISTA. TRAF binding sites are most commonly found in TNF receptors, such as CD27, CD40, OX40, and 4-1BB.

Interestingly, two independent research groups first identified VISTA, but each reported contrasting functional effects of anti-VISTA monoclonal antibodies. One study reported that mouse VISTA inhibited T cell proliferation and cytokine production *in vitro*, that antagonistic anti-VISTA monoclonal antibody treatment exacerbated experimental autoimmune encephalomyelitis, and that VISTA overexpression on tumor cells led to reduced antitumor immunity in mice (154). By contrast, a single dose of agonistic anti-VISTA monoclonal antibody completely abrogated graft-versus-host disease in a partial and complete allogenic hematopoietic cell transplantation in mice with mismatched MHC between donor and host (155). This is of particular relevance to DFT, which in most cases likely has mismatched MHC, so blockade of VISTA could prove useful for breaking tolerance to DFT cells. In addition to the role of VISTA in transplant tolerance, early studies suggest that VISTA could play a more general role in immune escape by tumor cells. Several groups have independently demonstrated that VISTA-deficient mice have enhanced antitumor immunity compared to wild-type mice (156, 157). These effects are independent of PD-1 but are amplified in VISTA/PD-1 double knockout mice (158).

TIM-3

Like VISTA, TIM-3 plays a role in phagocytosis of apoptotic cells and T cell immunity [reviewed in Ref. (88)]. Ligation of TIM-3 by phosphatidylserine on apoptotic cells induces an "eat me" signal (159–161). The interaction of TIM-3 with its coreceptors has been associated with diverse functional outcomes, including both inhibitory and stimulatory functions. TIM-3 also binds to secreted and surface-expressed galectin-9 (GAL-9, LGALS9) and negatively regulates Th1 immunity and IFN-γ production (162, 163). As DFT1 cells do not naturally express MHC-I or PD-L1 but upregulate both MHC-I and PD-L1 in response to IFN-γ, the potential role of TIM-3 in IFN-γ production warrants further investigation. TIM-3 and PD-1 are often coexpressed on exhausted CD8+ T cells (164) in mice and exhausted TILs in mice and humans (165–168).

In contrast to the inhibitory function of TIM-3 on adaptive T cells, several types of innate immune cells can be activated by TIM-3 ligation (169). Ligation of TIM-3 on mouse and human DCs promotes secretion of inflammatory cytokines (169). TIM-3 is upregulated by TGF-β on tumor-associated macrophages (TAMs) of the M2 phenotype and ligation of TIM-3 leads to increased NF-κB and IL-6 production and is associated with reduced survival in human hepatocellular carcinoma (170). TIM-3 also binds to the pleiotropic alarmin HMGB1 and suppresses antitumor immunity *via* interfering with the ability of HMGB1 to transport tumor-derived DNA to the endosomes of DCs (171). As large DFTs often become ulcerated and/or necrotic, it will be interesting to see if HMGB1 or other alarmins are expressed.

In regard to receptor structure, TIM-3 is unique due to the formation of both *cis*- and *trans*-heterodimers with carcinoembryonic antigen cell adhesion molecule 1. The *cis* heterodimerization is critical for stable surface expression of TIM-3 and its inhibitory function (172, 173). Together, the conserved disulfide bonds and ligand-binding amino acids, suggest that devil TIM-3 function might be similar to humans and mice. Several of the most widely used cell lines in laboratory research, including Chinese hamster ovary cells, Jurkat RMA-S human lymphoma cells, and 3T3 mouse fibroblast cells, express natural ligands that bind to TIM-3 tetramers (89). This presents the opportunity for the use of cross-reactive reagents for devils and other non-traditional study species, but as a cautionary note, it also has the potential to cause confusing results in attempts to understand checkpoint molecule interactions.

Paired Inhibitory and Stimulatory Receptors

CD47 binds to several coreceptors, including SIRP-γ, THSB1, and THSB2, which induce either activation or inhibition signals (174, 175). An additional SIRP-family protein, SIRP-β1, does not bind to CD47 and no ligand for SIRP-β1 has been identified to date in humans (176). The SIRP-family proteins are hypothesized to be paired receptors that have evolved to reduce pathogen exploitation of conserved motifs found in inhibitory receptors, essentially a decoy target system that facilitates pathogen control. Pathogens that trigger inhibitory signals *via* conserved motifs in inhibitory receptors would thus also trigger activation signals when exploiting the similar motifs in the activating receptor (177, 178). Analysis of devil SIRP-α revealed two predicted cytoplasmic ITIM and one ITSM inhibitory domains, suggesting the inhibitory capacity of the CD47:SIRP-α interaction is conserved in devils and could be an immunotherapy target. The devil SIRP-α ITSM was not detected in any other species, so empirical testing will be needed to clarify the potential for targeting the CD47:SIRP-α pathway in devils.

Like the SIRP-family proteins, members of the CD200R family are hypothesized to have evolved as paired activating and inhibitory receptors. Specifically, herpesviruses, cytomegaloviruses, pox viruses, and adenoviruses inhibit macrophage activation *via* CD200 mimics that bind to CD200R-family members (179–181). In recent years, CD200 has received greater interest as an inhibitory checkpoint molecule associated with antitumor immunity. CD200 is expressed on a wide range of tumors, including lymphomas (182), myelomas (183), leukemias (184), and gliomas (185), and CD200 expression is correlated with expression of epithelial cancer stem cell markers on prostate, brain, breast, and colon cancers (186, 187).

Expression of CD200 on tumor cells has been associated with impaired NK cell function, increased frequencies of Tregs, suppression of memory T cells, decreased CTL activity, and induction of tolerance to allografts (184, 188, 189). Interestingly, CD200 expression has also been associated with Th2-skewed cytokine profiles and prolonged allograft survival (190–193). The transplantable EMT6 mouse breast cancer line expresses low levels of CD200 *in vitro*, but upregulates CD200 following inoculation into immunocompetent mice (194); this is similar to PD-L1, which is often expressed at low levels *in vitro*, but rapidly upregulated in immune active environments. Given the ongoing transmission of DFT for at least 20 years, immunohistochemical analysis of archived DFT tissue samples should determine expression levels of CD200 in the tumor microenvironment, and understanding this potential inhibitory pathway could help direct vaccine-development efforts.

Like devil PD-1, devil CD200 and SIRP-α are predicted to contain ITSM domains capable of regulating TCR signal transduction. ITSMs have been reported for both PD-1 and SIRP-α, but to our knowledge this is the first report of an ITSM in CD200. Interestingly, the CD200 ITSM was predicted only for devils and not any of the other eight species analyzed here, although it is possible that other isoforms of CD200 exist. There have only been a limited number molecules that have been predicted to contain ITSMs: BTLA; 2B4 (CD244); Siglec7; Siglec9; SLAMF1 (CD150); Ly9 (SLAMF3); CD84 (SLAMF5); SLAMF6 (CD352); and SLAMF7 (195, 196). Paired inhibitory and stimulatory receptors are hypothesized to have evolved in response to exploitation of inhibitory receptors by pathogens. Thus, pathogen motifs that utilize the inhibitory receptor will also trigger the stimulatory signal, so it is interesting that the three of the families that contain ITSMs are also predicted to be paired-receptor families (SIRP, CD200, Siglecs). The original ITSM was identified in CD150 and was named "switch-motif" due to its ability to switch from recruitment of SHP-2 to SHIP in the presence of SH2D1A (17, 197). This flexible switching aspect of the paired receptors could be an additional evolved response to exploitation of inhibitory receptors by common pathogens.

The Unexplored Function of ECD ITIMs and ITSMs

The short cytoplasmic tail of CD200 and known soluble forms in humans suggests that the primary inhibition through CD200 is mediated *via* ligation of CD200Rs. However, as mentioned above we identified a potential inhibitory ITSM in the extracellular region of $CD200_{NKTEYVVI}$. Interestingly, our analysis predicted putative inhibitory motifs in the extracellular region of several checkpoint molecules: devil $CD47_{LKYHVV}$ ITIM near the border of the first extracellular and TMDs; devil SIRP-$\beta1_{VSYNLI}$ extracellular ITIM; dog $CD80_{VKYGDL}$ extracellular ITIM; and human $CD86_{IEYDGI}$ extracellular ITIM.

To our knowledge, the function of ITIMs and ITSMs has only been explored in intracellular regions of checkpoint molecules. However, despite most checkpoint molecules being considered transmembrane proteins, the majority of checkpoint molecules covered in this analysis are only surface expressed in particular contexts. For instance, CTLA-4 protein can be detected in the cytoplasm prior to T cell activation, but then is transiently moved to the cell surface following activation. Trans-endocytosis of ITIM-containing CD80 (dog) or CD86 (human) could allow the ECD ITIMs to affect intracellular signaling. Also, CD80, CD86, CD200, CD47, all of which were identified to contain extracellular inhibitory domains, are part of multi-receptor or paired-receptor interactions and the potential role of ECD ITIMs and ITSMs may have been overlooked. This is potentially an understudied aspect of molecular and cellular immunology that warrants further investigation.

The Potential for LAG-3 As an Adjuvant

Although human LAG-3 has a higher affinity for MHC-II than CD4, the inhibitory effects of LAG-3 in humans and mice are thought to be mediated primarily *via* negative regulation of TCR:CD3 signal transduction rather than competition for MHC-II binding (198, 199). In addition to binding to MHC-II, LAG-3 also binds to C-type lectin domain family 4 member G (CLEC4G, LSECTin) and galectin 3 (Gal-3, LGALS3). In mice, Gal-3 expression can suppress CD8 antitumor responses and expansion of plasmacytoid DCs (200). Tumor cell expression of Gal-3 has also been associated with poor prognosis in non-small-cell lung cancer (201), Hodgkin

lymphoma (202), and acute myeloid leukemia (203), but the opposite effect has also been reported for breast (204) and gastric (205) cancer.

Of particular interest for devils is the potential for LAG-3 to facilitate anti-DFT immunity. Immunization of mice with LAG-3+ tumor cells, or irradiated tumor cells along with soluble LAG-3-Ig resulted in tumor regression or reduced tumor growth (206). In addition, soluble LAG-3-Ig binding to MHC-II reliably induced DC maturation, which is indicated by upregulation of MHC-II, costimulatory molecules CD40, CD80, CD83, CD86, and IL-12 and TNF-α cytokines (207, 208). In allogenic bone marrow transplant models, LAG-3 blockade abrogates CD8 T cell tolerance to tissue transplants (209), which suggests that LAG-3 blockade could be a target for inducing CD8 T cell responses to allogenic DFT cells. Additionally, because LAG-3 signaling is bidirectional, DFT expressed Gal-3 could inhibit T and NK cell responses *via* direct Gal-3:LAG-3 interactions. Finally, LAG-3 and PD-1 are coexpressed in exhausted T cells in viral infection and on TILs, and blockade of both LAG-3 and PD-1 has been demonstrated to have synergistic effects in mouse models (33, 210–212). Altogether, there is a strong potential for LAG-3 to stimulate anti-DFT immunity due to the potential for overexpression of LAG-3 on tumor cells and/or administration of soluble LAG-3-Ig to serve as an adjuvant, and to use monoclonal antibodies that block LAG-3 on T cells to reduce T cell inhibition.

Strong Conservation of B7-H4 Protein across All Species

Despite more than a decade of searching, the identity of the B7-H4 coreceptor remains unknown. Further complicating the functional role of B7-H4 protein is that it is commonly expressed in the cytoplasm and nucleus of cancer cells, and nuclear localization of B7-H4 is associated with cell cycle progression and proliferation of cancer cells (95). B7-H4 is upregulated to the cell surface on T and B cells by several mitogens (213, 214) and on monocytes, TAMs, and DCs in response to IL-6 and IL-10 (215, 216).

Despite the receptor for B7-H4 being unknown, the inhibitory function of B7-H4 in regard to T cell responses and apoptosis has been well-documented (213, 214, 217). Binding of B7-H4-Ig to the putative coreceptor inhibits T cell activation, which can be abrogated by monoclonal blockade of B7-H4 (213, 214). B7-H4 protein has been detected on breast, lung, ovarian, prostate, renal cell, and uterine endometrioid cancer cells and is associated with decreased survival [reviewed in Ref. (20, 218)]. The high sequence identity of B7-H4 between humans and devils (87%) suggests that B7-H4 function might be similar in devils, and thus could be used as a prognostic indicator for DFT in addition to the potential for anti-B7-H4 monoclonal antibody immunotherapy.

BTLA and TIGIT Inhibitory Genes Not Detected in Devils

The molecules described above demonstrated strong homology to other mammals, but another key inhibitory molecule in humans and mice, BTLA4, has not yet been identified in devils. Multiple BTLAs have been identified in bony fish (*Teleosts*), but have not been identified in amphibians or aves (24). Our search of GenBank and Ensembl and also our *de novo* assembly of a transcriptome from devil PBMCs failed to identify a BTLA gene and full coding sequence for the TIGIT gene in devils. Several TIGIT coreceptors are present in the devil genome and three TIGIT transcript variants reported in the opossum genome. Given that TIGIT expression appears to be tightly regulated in humans and mice (219), we believe it likely that a functional TIGIT gene will eventually be detected in devils through targeted laboratory methods (i.e., RACE PCR).

CONCLUSION

In addition to the highly conserved motifs in several molecules, we documented strong conservation of cysteine residues for intra- and intermolecular bonds. These remarkable similarities suggest that immunotherapies that have revolutionized human oncology might be translatable into immunotherapies for the DFT disease. The wealth of data on checkpoint molecule expression and function in humans should facilitate understanding of the key immune evasion pathways employed by the DFTs and allow development of vaccines that target these key pathways. However, given the general paucity of reagents for non-traditional study species, innovative new techniques may be needed to assess the potential roles of the putative signaling motifs, and more generally to assess checkpoint molecule function in species other than humans, mice, and rats.

Investigations into the function of checkpoint molecules in devils, dogs, and hamsters may provide insight into the transmissibility of these tumors and uncover potential immunotherapy targets relevant to both human and veterinary medicine. Additionally, our analysis has spawned new questions about the role of inhibitory ITIM and ITSM motifs and paired receptors that could be of highly relevant generally—not only to human medicine. Further insight into the evolution of the immune system might be gained by studying the role of checkpoint molecules in natural disease systems, such as white-nose syndrome in bats and chytridiomycosis in amphibians. Diversifying immunological studies into non-traditional species may facilitate a broader understanding of key immune defense pathways and elucidate general principles that are unlikely to be found when studying only a small number of model organisms.

AUTHOR CONTRIBUTIONS

AF collected, analyzed, and interpreted the data; prepared the figures; and wrote the manuscript. NB performed the *de novo* transcriptome assembly, provided intellectual input, and provided critical feedback on the manuscript. AL and GW provided intellectual input on immunological processes and assisted in the drafting of relevant sections of the manuscript. JH provided intellectual input into the overarching framework of the study, preclinical insight into feasibility of immunotherapeutically targeting immune checkpoint inhibition in species

other than humans and mice, and critical detailed review of the manuscript.

ACKNOWLEDGMENTS

The authors thank David Gearing and Sam Busfield (Nexvet Australia Pty. Ltd.) for critical review of the manuscript. The authors also would like to thank Alexander Kreiss, Amanda Patchett, Cesar Tovar, Georgina Kalodimos, Jocelyn Darby, Patrick Lennard, Chrissie Ong, and Ruth Pye for assistance in the lab and comments on research and/or manuscript, Elizabeth Murchison for advice in regard to the devil genome, Jac Charlesworth for help with data archiving, and Emily Flies for her ongoing research advice. The authors wish to thank Ginny Ralph and DPIPWE devil keepers who provided care for the devils used in these experiments.

FUNDING

Research support was provided by the Australian Research Council (ARC Linkage grant # LP0989727 and ARC Discovery grant # DP130100715) to GW, Morris Animal Foundation (# D14ZO-410), Sansom Institute Small Grants Scheme, University of Tasmania Foundation Dr Eric Guiler Tasmanian Devil Research Grant through funds raised by the Save the Tasmanian Devil Appeal (2013, 2015), and Entrepreneurs' Programme—Research Connections grant with Nexvet Australia Pty. Ltd. (RC50680) to AF.

SUPPLEMENTARY MATERIAL

The Supplementary Material for this article can be found online at http://journal.frontiersin.org/article/10.3389/fimmu.2017.00513/full#supplementary-material.

REFERENCES

1. Aruffo A, Seed B. Molecular cloning of a CD28 cDNA by a high-efficiency COS cell expression system. *Proc Natl Acad Sci U S A* (1987) 84:8573–7. doi:10.1073/pnas.84.23.8573
2. Linsley PS, Brady W, Grosmaire L, Aruffo A, Damle NK, Ledbetter JA. Binding of the B cell activation antigen B7 to CD28 costimulates T cell proliferation and interleukin 2 mRNA accumulation. *J Exp Med* (1991) 173:721–30. doi:10.1084/jem.173.3.721
3. Jenkins MK, Taylor PS, Norton SD, Urdahl KB. CD28 delivers a costimulatory signal involved in antigen-specific IL-2 production by human T cells. *J Immunol* (1991) 147:2461–6.
4. Janeway CA, Travers P, Walport M, Shlomchik M. *Immunobiology: The Immune System in Health and Disease*. 6th ed. New York, NY: Garland Science Publishing (2001).
5. Harding FA, McArthur JG, Gross JA, Raulet DH, Allison JP. CD28-mediated signalling co-stimulates murine T cells and prevents induction of anergy in T-cell clones. *Nature* (1992) 356:607–9. doi:10.1038/356607a0
6. Brunet JF, Denizot F, Luciani MF, Roux-Dosseto M, Suzan M, Mattei MG, et al. A new member of the immunoglobulin superfamily – CTLA-4. *Nature* (1987) 328:267–70. doi:10.1038/328267a0
7. Balzano C, Buonavista N, Rouvier E, Golstein P. CTLA-4 and CD28: similar proteins, neighbouring genes. *Int J Cancer Suppl* (1992) 7:28–32.
8. Stamper CC, Zhang Y, Tobin JF, Erbe DV, Ikemizu S, Davis SJ, et al. Crystal structure of the B7-1/CTLA-4 complex that inhibits human immune responses. *Nature* (2001) 410:608–11. doi:10.1038/35069118
9. Schwartz JC, Zhang X, Fedorov AA, Nathenson SG, Almo SC. Structural basis for co-stimulation by the human CTLA-4/B7-2 complex. *Nature* (2001) 410:604–8. doi:10.1038/35069112
10. Kvistborg P, Philips D, Kelderman S, Hageman L, Ottensmeier C, Joseph-Pietras D, et al. Anti-CTLA-4 therapy broadens the melanoma-reactive CD8+ T cell response. *Sci Transl Med* (2014) 6:254ra128. doi:10.1126/scitranslmed.3008918
11. Twyman-Saint Victor C, Rech AJ, Maity A, Rengan R, Pauken KE, Stelekati E, et al. Radiation and dual checkpoint blockade activate non-redundant immune mechanisms in cancer. *Nature* (2015) 520:373–7. doi:10.1038/nature14292
12. Ribas A, Kefford R, Marshall MA, Punt CJA, Haanen JB, Marmol M, et al. Phase III randomized clinical trial comparing tremelimumab with standard-of-care chemotherapy in patients with advanced melanoma. *J Clin Oncol* (2013) 31:616–22. doi:10.1200/JCO.2012.44.6112
13. Wolchok JD, Kluger H, Callahan MK, Postow MA, Rizvi NA, Lesokhin AM, et al. Nivolumab plus ipilimumab in advanced melanoma. *N Engl J Med* (2013) 369:122–33. doi:10.1056/NEJMoa1302369
14. Larkin J, Chiarion-Sileni V, Gonzalez R, Grob JJ, Cowey CL, Lao CD, et al. Combined nivolumab and ipilimumab or monotherapy in untreated melanoma. *N Engl J Med* (2015) 373:23–34. doi:10.1056/NEJMoa1504030
15. Postow MA, Chesney J, Pavlick AC, Robert C, Grossmann K, McDermott D, et al. Nivolumab and ipilimumab versus ipilimumab in untreated melanoma. *N Engl J Med* (2015) 372:2006–17. doi:10.1056/NEJMoa1414428
16. Chatterjee P, Patsoukis N, Freeman GJ, Boussiotis VA. Distinct roles of PD-1 ITSM and ITIM in regulating interactions with SHP-2, ZAP-70 and Lck, and PD-1-mediated inhibitory function. *Blood* (2013) 122:191.
17. Chemnitz JM, Parry RV, Nichols KE, June CH, Riley JL. SHP-1 and SHP-2 associate with immunoreceptor tyrosine-based switch motif of programmed death 1 upon primary human T cell stimulation, but only receptor ligation prevents T cell activation. *J Immunol* (2004) 173:945–54. doi:10.4049/jimmunol.173.2.945
18. Sheppard KA, Fitz LJ, Lee JM, Benander C, George JA, Wooters J, et al. PD-1 inhibits T-cell receptor induced phosphorylation of the ZAP70/CD3zeta signalosome and downstream signaling to PKCtheta. *FEBS Lett* (2004) 574:37–41. doi:10.1016/j.febslet.2004.07.083
19. Azuma T, Yao S, Zhu G, Flies AS, Flies SJ, Chen L. B7-H1 is a ubiquitous antiapoptotic receptor on cancer cells. *Blood* (2008) 111:3635–43. doi:10.1182/blood-2007-11-123141
20. Zou W, Chen L. Inhibitory B7-family molecules in the tumour microenvironment. *Nat Rev Immunol* (2008) 8:467–77. doi:10.1038/nri2326
21. Tseng SY, Otsuji M, Gorski K, Huang X, Slansky JE, Pai SI, et al. B7-DC, a new dendritic cell molecule with potent costimulatory properties for T cells. *J Exp Med* (2001) 193:839–46. doi:10.1084/jem.193.7.839
22. Xiao Y, Yu S, Zhu B, Bedoret D, Bu X, Francisco LM, et al. RGMb is a novel binding partner for PD-L2 and its engagement with PD-L2 promotes respiratory tolerance. *J Exp Med* (2014) 211:943–59. doi:10.1084/jem.20130790
23. Hansen JD, Du Pasquier L, Lefranc MP, Lopez V, Benmansour A, Boudinot P. The B7 family of immunoregulatory receptors: a comparative and evolutionary perspective. *Mol Immunol* (2009) 46:457–72. doi:10.1016/j.molimm.2008.10.007
24. Bernard D, Hansen JD, Du Pasquier L, Lefranc MP, Benmansour A, Boudinot P. Costimulatory receptors in jawed vertebrates: conserved CD28, odd CTLA4 and multiple BTLAs. *Dev Comp Immunol* (2007) 31:255–71. doi:10.1016/j.dci.2006.06.003
25. Esch KJ, Juelsgaard R, Martinez PA, Jones DE, Petersen CA. Programmed death 1-mediated T cell exhaustion during visceral leishmaniasis impairs phagocyte function. *J Immunol* (2013) 191(11):5542–50. doi:10.4049/jimmunol.1301810
26. Maekawa N, Konnai S, Ikebuchi R, Okagawa T, Adachi M, Takagi S, et al. Expression of PD-L1 on canine tumor cells and enhancement of IFN-g production from tumor-infiltrating cells by PD-L1 blockade. *PLoS One* (2014) 9:e98415. doi:10.1371/journal.pone.0098415
27. Hartley G, Faulhaber E, Caldwell A, Coy J, Kurihara J, Guth A, et al. Immune regulation of canine tumour and macrophage PD-L1 expression. *Vet Comp Oncol* (2016). doi:10.1111/vco.12197
28. Regan D, Guth A, Coy J, Dow S. Cancer immunotherapy in veterinary medicine: current options and new developments. *Vet J* (2015) 207:1–9. doi:10.1016/j.tvjl.2015.10.008

29. Khatlani TS, Ma Z, Okuda M, Onishi T. Molecular cloning and sequencing of canine T-cell costimulatory molecule (CD28). *Vet Immunol Immunopathol* (2001) 78:341–8. doi:10.1016/S0165-2427(01)00238-0
30. Shosu K, Sakurai M, Inoue K, Nakagawa T, Sakai H, Morimoto M, et al. Programmed cell death ligand 1 expression in canine cancer. *In Vivo* (2016) 30:195–204.
31. Folkl A, Wen X, Kuczynski E, Clark ME, Bienzle D. Feline programmed death and its ligand: characterization and changes with feline immunodeficiency virus infection. *Vet Immunol Immunopathol* (2010) 134:107–14. doi:10.1016/j.vetimm.2009.10.019
32. Ikebuchi R, Konnai S, Shirai T, Sunden Y, Murata S, Onuma M, et al. Increase of cells expressing PD-L1 in bovine leukemia virus infection and enhancement of anti-viral immune responses in vitro via PD-L1 blockade. *Vet Res* (2011) 42:103–17. doi:10.1186/1297-9716-42-103
33. Okagawa T, Konnai S, Deringer JR, Ueti MW, Scoles GA, Murata S, et al. Cooperation of PD-1 and LAG-3 contributes to T-cell exhaustion in *Anaplasma marginale*-infected cattle. *Infect Immun* (2016) 84:2779–90. doi:10.1128/IAI.00278-16
34. Ikebuchi R, Konnai S, Okagawa T, Yokoyama K, Nakajima C, Suzuki Y, et al. Blockade of bovine PD-1 increases T cell function and inhibits bovine leukemia virus expression in B cells in vitro. *Vet Res* (2013) 44:1–14. doi:10.1186/1297-9716-44-59
35. Parsons KR, Young JR, Collins BA, Howard CJ. Cattle CTLA-4, CD28 and chicken CD28 bind CD86: MYPPPY is not conserved in cattle CD28. *Immunogenetics* (1996) 43:388–91. doi:10.1007/s002510050080
36. Pearse A-M, Swift K. Allograft theory: transmission of devil facial-tumour disease. *Nature* (2006) 439:549. doi:10.1038/439549a
37. Murchison EP, Tovar C, Hsu A, Bender HS, Kheradpour P, Rebbeck CA, et al. The Tasmanian devil transcriptome reveals Schwann cell origins of a clonally transmissible cancer. *Science* (2010) 327:84–7. doi:10.1126/science.1180616
38. Murgia C, Pritchard JK, Kim SY, Fassati A, Weiss RA. Clonal origin and evolution of a transmissible cancer. *Cell* (2006) 126:477–87. doi:10.1016/j.cell.2006.05.051
39. vonHoldt BM, Ostrander EA. The singular history of a canine transmissible tumor. *Cell* (2006) 126:445–7. doi:10.1016/j.cell.2006.07.016
40. Ashbel R. Spontaneous transmissible tumours in the Syrian hamster. *Nature* (1945) 155:607–607. doi:10.1038/155607b0
41. Brindley DC, Banfield WG. A contagious tumor of the hamster. *J Natl Cancer Inst* (1961) 26:949–57. doi:10.1093/jnci/26.4.949
42. Metzger MJ, Villalba A, Carballal MJ, Iglesias D, Sherry J, Reinisch C, et al. Widespread transmission of independent cancer lineages within multiple bivalve species. *Nature* (2016) 534:705–9. doi:10.1038/nature18599
43. Metzger MJ, Reinisch C, Sherry J, Goff SP. Horizontal transmission of clonal cancer cells causes leukemia in soft-shell clams. *Cell* (2015) 161:255–63. doi:10.1016/j.cell.2015.02.042
44. Pye RJ, Pemberton D, Tovar C, Tubio JMC, Dun KA, Fox S, et al. A second transmissible cancer in Tasmanian devils. *Proc Natl Acad Sci U S A* (2016) 113:201519691. doi:10.1073/pnas.1519691113
45. Siddle HV, Kreiss A, Tovar C, Yuen CK, Cheng Y, Belov K, et al. Reversible epigenetic down-regulation of MHC molecules by devil facial tumour disease illustrates immune escape by a contagious cancer. *Proc Natl Acad Sci U S A* (2013) 110:5103–8. doi:10.1073/pnas.1219920110
46. Ljunggren HG, Karre K. In search of the missing self: MHC molecules and NK cell recognition. *Immunol Today* (1990) 11:237–44.
47. Brown GK, Kreiss A, Lyons AB, Woods GM. Natural killer cell mediated cytotoxic responses in the Tasmanian devil. *PLoS One* (2011) 6:e24475. doi:10.1371/journal.pone.0024475
48. Brown GK, Tovar C, Cooray AA, Kreiss A, Darby J, Murphy JM, et al. Mitogen-activated Tasmanian devil blood mononuclear cells kill devil facial tumour disease cells. *Immunol Cell Biol* (2016) 94:673–9. doi:10.1038/icb.2016.38
49. Van Der Kraan LE, Wong ESW, Lo N, Ujvari B, Belov K. Identification of natural killer cell receptor genes in the genome of the marsupial Tasmanian devil (*Sarcophilus harrisii*). *Immunogenetics* (2013) 65:25–35. doi:10.1007/s00251-012-0643-z
50. Pye R, Hamede R, Siddle HV, Caldwell A, Knowles GW, Swift K, et al. Demonstration of immune responses against devil facial tumour disease in wild Tasmanian devils. *Biol Lett* (2016) 12:20160553. doi:10.1098/rsbl.2016.0553
51. Tovar C, Pye RJ, Kreiss A, Cheng Y, Brown GK, Darby J, et al. Regression of devil facial tumour disease following immunotherapy in immunised Tasmanian devils. *Sci Rep* (2017) 7:43827. doi:10.1038/srep43827
52. Flies AS, Lyons AB, Corcoran LM, Papenfuss AT, Murphy JM, Knowles GW, et al. PD-L1 is not constitutively expressed on Tasmanian devil facial tumor cells but is strongly upregulated in response to IFN-γ and can be expressed in the tumor microenvironment. *Front Immunol* (2016) 7:581. doi:10.3389/fimmu.2016.00581
53. Aken BL, Achuthan P, Akanni W, Amode MR, Bernsdorff F, Bhai J, et al. Ensembl 2017. *Nucleic Acids Res* (2017) 45:D635–42. doi:10.1093/nar/gkw1104
54. Altschul SF, Gish W, Miller W, Myers EW, Lipman DJ. Basic local alignment search tool. *J Mol Biol* (1990) 215:403–10. doi:10.1016/S0022-2836(05)80360-2
55. Patchett AL, Latham R, Brettingham-Moore KH, Tovar C, Lyons AB, Woods GM. Toll-like receptor signaling is functional in immune cells of the endangered Tasmanian devil. *Dev Comp Immunol* (2015) 53:123–33. doi:10.1016/j.dci.2015.07.003
56. Andrews S, Babraham B. *FastQC A Quality Control Tool for High Throughput Sequence Data*. (2010). Available from: http://www.bioinformatics.babraham.ac.uk/projects/fastqc/
57. Grabherr MG, Haas BJ, Yassour M, Levin JZ, Thompson DA, Amit I, et al. Full-length transcriptome assembly from RNA-seq data without a reference genome. *Nat Biotechnol* (2011) 29:644–52. doi:10.1038/nbt.1883
58. Haas BJ, Papanicolaou A, Yassour M, Grabherr M, Blood PD, Bowden J, et al. De novo transcript sequence reconstruction from RNA-seq using the Trinity platform for reference generation and analysis. *Nat Protoc* (2013) 8:1494–512. doi:10.1038/nprot.2013.084
59. Zhang Z, Schwartz S, Wagner L, Miller W. A greedy algorithm for aligning DNA sequences. *J Comput Biol* (2000) 7:203–14. doi:10.1089/10665270050081478
60. James Kent W, Sugnet CW, Furey TS, Roskin KM, Pringle TH, Zahler AM, et al. The human genome browser at UCSC. *Genome Res* (2002) 12:996–1006. doi:10.1101/gr.229102
61. Knudsen B, Knudsen T, Flensborg M, Sandmann H, Heltzen M, Andersen A, et al. *CLC Sequence Viewer*. (2012). Available from: http://www.clcbio.com
62. Feng DF, Doolittle RF. Progressive sequence alignment as a prerequisite to correct phylogenetic trees. *J Mol Evol* (1987) 25:351–60. doi:10.1007/BF02603120
63. Sievers F, Wilm A, Dineen D, Gibson TJ, Karplus K, Li W, et al. Fast, scalable generation of high-quality protein multiple sequence alignments using clustal omega. *Mol Syst Biol* (2011) 7:539. doi:10.1038/msb.2011.75
64. Goodsell DS. Representing structural information with RasMol. In: Baxevanis AD, editor. *Current Protocols in Bioinformatics*. Hoboken, NJ: John Wiley and Sons, Inc. (2005). p. 5.4.1–5.4.23.
65. Gasteiger E, Gattiker A, Hoogland C, Ivanyi I, Appel RD, Bairoch A. ExPASy: the proteomics server for in-depth protein knowledge and analysis. *Nucleic Acids Res* (2003) 31:3784–8. doi:10.1093/nar/gkg563
66. Dinkel H, Van Roey K, Michael S, Davey NE, Weatheritt RJ, Born D, et al. The eukaryotic linear motif resource ELM: 10 years and counting. *Nucleic Acids Res* (2014) 42:D259–66. doi:10.1093/nar/gkt1047
67. Käll L, Krogh A, Sonnhammer ELL. Advantages of combined transmembrane topology and signal peptide prediction – the Phobius web server. *Nucleic Acids Res* (2007) 35:W429–32. doi:10.1093/nar/gkm256
68. Schultz J, Milpetz F, Bork P, Ponting CP. SMART, a simple modular architecture research tool: identification of signaling domains. *Proc Natl Acad Sci U S A* (1998) 95:5857–64. doi:10.1073/pnas.95.11.5857
69. Petersen TN, Brunak S, von Heijne G, Nielsen H. SignalP 4.0: discriminating signal peptides from transmembrane regions. *Nat Methods* (2011) 8:785–6. doi:10.1038/nmeth.1701
70. The UniProt Consortium. UniProt: a hub for protein information. *Nucleic Acids Res* (2014) 43:D204–12. doi:10.1093/nar/gku989
71. Metzler WJ, Bajorath J, Fenderson W, Shaw SY, Constantine KL, Naemura J, et al. Solution structure of human CTLA-4 and delineation of a CD80/CD86 binding site conserved in CD28. *Nat Struct Biol* (1997) 4:527–31. doi:10.1038/nsb0797-527
72. Vaughan AN, Malde P, Rogers NJ, Jackson IM, Lechler RI, Dorling A. Porcine CTLA4-Ig lacks a MYPPPY motif, binds inefficiently to human B7 and specifically suppresses human CD4+ T cell responses costimulated by pig but

not human B7. *J Immunol* (2000) 165:3175–81. doi:10.4049/jimmunol.165.6.3175
73. Chen L, Flies DB. Molecular mechanisms of T cell co-stimulation and co-inhibition. *Nat Rev Immunol* (2013) 13:227–42. doi:10.1038/nri3405
74. Schwarz H, Tuckwell J, Lotz M. A receptor induced by lymphocyte activation (ILA): a new member of the human nerve-growth-factor/tumor-necrosis-factor receptor family. *Gene* (1993) 134:295–8. doi:10.1016/0378-1119(93)90110-O
75. Pollok KE, Kim Y-J, Zhou Z, Hurtado J, Kim KK, Pickard RT, et al. Inducible T cell antigen 4-1BB. Analysis of expression and function. *J Immunol* (1993) 150:771–81.
76. Marvel J, Walzer T. CD137 in NK cells. *Blood* (2010) 115:2987–8. doi:10.1182/blood-2010-01-261404
77. Baessler T, Charton JE, Schmiedel BJ, Gru F, Krusch M, Wacker A, et al. CD137 ligand mediates opposite effects in human and mouse NK cells and impairs NK-cell reactivity against human acute myeloid leukemia cells. *Blood* (2010) 115:3058–69. doi:10.1182/blood-2009-06-227934.An
78. Barao I. The TNF receptor-ligands 4-1BB-4-1BBL and GITR-GITRL in NK cell responses. *Front Immunol* (2012) 3:402. doi:10.3389/fimmu.2012.00402
79. Kim YJ, Pollok KE, Zhou Z, Shaw A, Bohlen JB, Fraser M, et al. Novel T cell antigen 4-1BB associates with the protein tyrosine kinase p56lck1. *J Immunol* (1993) 151:1255–62.
80. Arch RH, Thompson CB. 4-1BB and Ox40 are members of a tumor necrosis factor (TNF)-nerve growth factor receptor subfamily that bind TNF receptor-associated factors and activate nuclear factor kappaB. *Mol Cell Biol* (1998) 18:558–65. doi:10.1016/j.bulcan.2015.03.022
81. Brown E, Hooper L, Ho T, Gresham H. Integrin-associated protein: a 50-kD plasma membrane antigen physically and functionally associated with integrins. *J Cell Biol* (1990) 111:2785–94. doi:10.1083/jcb.111.6.2785
82. Campbell IG, Freemont PS, Foulkes W, Trowsdale J. An ovarian tumor marker with homology to vaccinia virus contains an IgV-like region and multiple transmembrane domains advances in brief an ovarian tumor marker with homology to vaccinia virus contains an IgV-like region and multiple transmembrane domains. *Cancer Res* (1992) 52:5416–20.
83. Lee WY, Weber DA, Laur O, Stowell SR, McCall I, Andargachew R, et al. The role of cis dimerization of signal regulatory protein α (SIRPα) in binding to CD47. *J Biol Chem* (2010) 285:37953–63. doi:10.1074/jbc.M110.180018
84. Weiskopf K, Ring AM, Ho CCM, Volkmer J-P, Levin AM, Volkmer AK, et al. Engineered SIRPα variants as immunotherapeutic adjuvants to anticancer antibodies. *Science* (2013) 341:88–91. doi:10.1126/science.1238856
85. Hatherley D, Cherwinski HM, Moshref M, Barclay AN. Recombinant CD200 protein does not bind activating proteins closely related to CD200 receptor. *J Immunol* (2005) 175:2469–74. doi:10.4049/jimmunol.175.4.2469
86. Prigent SA, Gullick WJ. Identification of c-erbB-3 binding sites for phosphatidylinositol 3′-kinase and SHC using an EGF receptor/c-erbB-3 chimera. *EMBO J* (1994) 13:2831–41.
87. Zhang S, Phillips JH. Identification of tyrosine residues crucial for CD200R-mediated inhibition of mast cell activation. *J Leukoc Biol* (2005) 79:363–8. doi:10.1189/jlb.0705398
88. Le Mercier I, Lines JL, Noelle RJ. Beyond CTLA-4 and PD-1, the generation Z of negative checkpoint regulators. *Front Immunol* (2015) 6:418. doi:10.3389/fimmu.2015.00418
89. Cao E, Zang X, Ramagopal UA, Mukhopadhaya A, Fedorov A, Fedorov E, et al. T cell immunoglobulin mucin-3 crystal structure reveals a galectin-9-independent ligand-binding surface. *Immunity* (2007) 26:311–21. doi:10.1016/j.immuni.2007.01.016
90. Anderson AC, Xiao S, Kuchroo VK. Tim protein structures reveal a unique face for ligand binding. *Immunity* (2007) 26:273–5. doi:10.1016/j.immuni.2007.03.004
91. Lee J, Su EW, Zhu C, Hainline S, Phuah J, Moroco JA, et al. Phosphotyrosine-dependent coupling of tim-3 to T-cell receptor signaling pathways. *Mol Cell Biol* (2011) 31:3963–74. doi:10.1128/MCB.05297-11
92. Triebel F, Jitsukawa S, Baixeras E, Roman-Roman S, Genevee C, Viegas-Pequignot E, et al. LAG-3, a novel lymphocyte activation gene closely related to CD4. *J Exp Med* (1990) 171:1393–405. doi:10.1084/jem.171.5.1393
93. Letunic I, Doerks T, Bork P. SMART: recent updates, new developments and status in 2015. *Nucleic Acids Res* (2015) 43:D257–60. doi:10.1093/nar/gku949
94. Kosugi S, Hasebe M, Tomita M, Yanagawa H. Systematic identification of cell cycle-dependent yeast nucleocytoplasmic shuttling proteins by prediction of composite motifs. *Proc Natl Acad Sci U S A* (2009) 106:10171–6. doi:10.1073/pnas.0900604106
95. Zhang L, Wu H, Lu D, Li G, Sun C, Song H, et al. The costimulatory molecule B7-H4 promote tumor progression and cell proliferation through translocating into nucleus. *Oncogene* (2013) 32(46):5347–58. doi:10.1038/onc.2012.600
96. O'Regan MN, Parsons KR, Tregaskes CA, Young JR. A chicken homologue of the co-stimulating molecule CD80 which binds to mammalian CTLA-4. *Immunogenetics* (1999) 49:68–71. doi:10.1007/s002510050464
97. Yin L, Schneider H, Rudd CE. Short cytoplasmic SDYMNM segment of CD28 is sufficient to convert CTLA-4 to a positive signaling receptor. *J Leukoc Biol* (2003) 73:178–82. doi:10.1189/jlb.0702365
98. Rudd CE, Taylor A, Schneider H. CD28 and CTLA-4 coreceptor expression and signal transduction. *Immunol Rev* (2009) 229:12–26. doi:10.1111/j.1600-065X.2009.00770.x
99. Qureshi OS, Zheng Y, Nakamura K, Attridge K, Manzotti C, Schmidt EM, et al. Trans-endocytosis of CD80 and CD86: a molecular basis for the cell extrinsic function of CTLA-4. *Science* (2011) 332:600–3. doi:10.1126/science.1202947
100. Gu P, Fang Gao J, D'Souza CA, Kowalczyk A, Chou K-Y, Zhang L. Trogocytosis of CD80 and CD86 by induced regulatory T cells. *Cell Mol Immunol* (2012) 9:136–46. doi:10.1038/cmi.2011.62
101. Simpson TR, Li F, Montalvo-Ortiz W, Sepulveda MA, Bergerhoff K, Arce F, et al. Fc-dependent depletion of tumor-infiltrating regulatory T cells co-defines the efficacy of anti-CTLA-4 therapy against melanoma. *J Exp Med* (2013) 210:1695–710. doi:10.1084/jem.20130579
102. Bulliard Y, Jolicoeur R, Zhang J, Dranoff G, Wilson NS, Brogdon JL. OX40 engagement depletes intratumoral Tregs via activating FcγRs, leading to anti-tumor efficacy. *Immunol Cell Biol* (2014) 92:475–80. doi:10.1038/icb.2014.26
103. Sun Y, Wei Z, Li N, Zhao Y. A comparative overview of immunoglobulin genes and the generation of their diversity in tetrapods. *Dev Comp Immunol* (2012) 39:103–9. doi:10.1016/j.dci.2012.02.008
104. Zhang W, Zhang X, Wu X-L, He L-S, Zeng X-F, Crammer AC, et al. Competition between TRAF2 and TRAF6 regulates NF-kappaB activation in human B lymphocytes. *Chin Med Sci J* (2010) 25:1–12. doi:10.1016/S1001-9294(10)60013-2
105. Jabara HH, Laouini D, Tsitsikov E, Mizoguchi E, Bhan AK, Castigli E, et al. The binding site for TRAF2 and TRAF3 but not for TRAF6 is essential for CD40-mediated immunoglobulin class switching. *Immunity* (2002) 17:265–76. doi:10.1016/S1074-7613(02)00394-1
106. Purkerson JM, Smith RS, Pollock SJ, Phipps RP. The TRAF6, but not the TRAF2/3, binding domain of CD40 is required for cytokine production in human lung fibroblasts. *Eur J Immunol* (2005) 35:2920–8. doi:10.1002/eji.200526219
107. Butte MJ, Keir ME, Phamduy TB, Sharpe AH, Freeman GJ. Programmed death-1 ligand 1 interacts specifically with the B7-1 costimulatory molecule to inhibit T cell responses. *Immunity* (2007) 27:111–22. doi:10.1016/j.immuni.2007.05.016
108. Butte MJ, Peña-Cruz V, Kim M-J, Freeman GJ, Sharpe AH. Interaction of human PD-L1 and B7-1. *Mol Immunol* (2008) 45:3567–72. doi:10.1016/j.molimm.2008.05.014
109. Haile ST, Bosch JJ, Agu NI, Zeender AM, Somasundaram P, Srivastava MK, et al. Tumor cell programmed death ligand 1-mediated T cell suppression is overcome by coexpression of CD80. *J Immunol* (2011) 186:6822–9. doi:10.4049/jimmunol.1003682
110. Wilson JL, Charo J, Martín-Fontecha A, Dellabona P, Casorati G, Chambers BJ, et al. NK cell triggering by the human costimulatory molecules CD80 and CD86. *J Immunol* (1999) 163:4207–12.
111. Chambers BJ, Salcedo M, Ljunggren HG. Triggering of natural killer cells by the costimulatory molecule CD80 (B7-1). *Immunity* (1996) 5:311–7. doi:10.1016/S1074-7613(00)80257-5
112. Kocak E, Abdessalam SF, May K, Martin EW, Liu Y. CD28 is not required for B7-mediated costimulation of Nk cell proliferation in response to tumor challenge. *J Surg Res* (2003) 114:301. doi:10.1016/j.jss.2003.08.101
113. Haile ST, Dalal SP, Clements V, Tamada K, Ostrand-Rosenberg S. Soluble CD80 restores T cell activation and overcomes tumor cell programmed death ligand 1-mediated immune suppression. *J Immunol* (2013) 191:2829–36. doi:10.4049/jimmunol.1202777
114. Haile ST, Horn LA, Ostrand-Rosenberg S. A soluble form of CD80 enhances antitumor immunity by neutralizing programmed death ligand-1 and

simultaneously providing costimulation. *Cancer Immunol Res* (2014) 2:610–5. doi:10.1158/2326-6066.CIR-13-0204
115. Kakoulidou M, Giscombe R, Zhao X, Lefvert AK, Wang X. Human soluble CD80 is generated by alternative splicing, and recombinant soluble CD80 binds to CD28 and CD152 influencing T-cell activation. *Scand J Immunol* (2007) 66:529–37. doi:10.1111/j.1365-3083.2007.02009.x
116. Rossille D, Azzaoui I, Feldman AL, Maurer MJ, Labouré G, Parrens M, et al. Soluble programmed death-ligand 1 as a prognostic biomarker for overall survival in patients with diffuse large B-cell lymphoma: a replication study and combined analysis of 508 patients. *Leukemia* (2016) 31:988–91. doi:10.1038/leu.2016.385
117. Rossille D, Gressier M, Damotte D, Pangault C, Semana G, Le Gouill S, et al. High level of soluble programmed cell death ligand 1 in blood impacts overall survival in aggressive diffuse large B-Cell lymphoma: results from a French multicenter clinical trial. *Leukemia* (2014) 28:2367–75. doi:10.1038/leu.2014.137
118. Navabi S s, Doroudchi M, Tashnizi AH, Habibagahi M. Natural killer cell functional activity after 4-1BB costimulation. *Inflammation* (2015) 38:1181–90. doi:10.1007/s10753-014-0082-0
119. Ward-Kavanagh LK, Lin WW, Šedý JR, Ware CF. The TNF receptor superfamily in co-stimulating and co-inhibitory responses. *Immunity* (2016) 44:1005–19. doi:10.1016/j.immuni.2016.04.019
120. Mbanwi AN, Watts TH. Costimulatory TNFR family members in control of viral infection: outstanding questions. *Semin Immunol* (2014) 26:210–9. doi:10.1016/j.smim.2014.05.001
121. Wortzman ME, Clouthier DL, Mcpherson AJ, Lin GHY, Watts TH. The contextual role of TNFR family members in CD8+ T-cell control of viral infections. *Immunol Rev* (2013) 255:125–48. doi:10.1111/imr.12086
122. Zhu Y, Zhu G, Luo L, Flies AS, Chen L. CD137 stimulation delivers an antigen-independent growth signal for T lymphocytes with memory phenotype. *Blood* (2007) 109:4882–9. doi:10.1182/blood-2006-10-043463
123. Pulle G, Vidric M, Watts TH. IL-15-dependent induction of 4-1BB promotes antigen-independent CD8 memory T cell survival. *J Immunol* (2006) 176:2739–48. doi:10.4049/jimmunol.176.5.2739
124. Cho HR, Kwon B, Yagita H, La S, Lee EA, Kim JE, et al. Blockade of 4-1BB (CD137)/4-1BB ligand interactions increases allograft survival. *Transpl Int* (2004) 17:351–61. doi:10.1111/j.1432-2277.2004.tb00454.x
125. Asai T, Choi BK, Kwon PM, Kim WY, Kim JD, Vinay DS, et al. Blockade of the 4-1BB (CD137)/4-1BBL and/or CD28/CD80/CD86 costimulatory pathways promotes corneal allograft survival in mice. *Immunology* (2007) 121:349–58. doi:10.1111/j.1365-2567.2007.02581.x
126. Wang J, Guo Z, Dong Y, Kim O, Hart J, Adams A, et al. Role of 4-1BB in allograft rejection mediated by CD8+ T cells. *Am J Transpl* (2003) 3:543–51. doi:10.1034/j.1600-6143.2003.00088.x
127. Seiffert BM, Cant C, Chen Z, Rappold I, Brugger W, Kanz L, et al. Human signal-regulatory protein is expressed on normal, but not on subsets of leukemic myeloid cells and mediates cellular adhesion involving its counterreceptor CD47. *Blood* (1999) 94:3633–44.
128. Ide K, Wang H, Tahara H, Liu J, Wang X, Asahara T, et al. Role for CD47-SIRPalpha signaling in xenograft rejection by macrophages. *Proc Natl Acad Sci U S A* (2007) 104:5062–6. doi:10.1073/pnas.0609661104
129. Wang C, Wang H, Ide K, Wang Y, van Rooijen N, Ohdan H, et al. Human CD47 expression permits survival of porcine cells in immunodeficient mice that express SIRPa capable of binding to human CD47. *Cell Transplant* (2011) 20:1915–20. doi:10.3727/096368911X566253
130. Wang Y, Wang H, Wang S, Fu Y, Yang YG. Survival and function of CD47-deficient thymic grafts in mice. *Xenotransplantation* (2010) 17:160–5. doi:10.1111/j.1399-3089.2010.00578.x
131. Wang H, Verhalen J, Madariaga ML, Xiang S, Wang S, Lan P, et al. Attenuation of phagocytosis of xenogeneic cells by manipulating CD47. *Blood* (2007) 109:836–42. doi:10.1182/blood-2006-04-019794
132. Waern JM, Yuan Q, Rüdrich U, Becker PD, Schulze K, Strick-Marchand H, et al. Ectopic expression of murine CD47 minimizes macrophage rejection of human hepatocyte xenografts in immunodeficient mice. *Hepatology* (2012) 56:1479–88. doi:10.1002/hep.25816
133. Subramanian S, Boder ET, Discher DE. Phylogenetic divergence of CD47 interactions with human signal regulatory protein alpha reveals locus of species specificity: implications for the binding site. *J Biol Chem* (2007) 282:1805–18. doi:10.1074/jbc.M603923200
134. Gitik M, Liraz-Zaltsman S, Oldenborg P-A, Reichert F, Rotshenker S. Myelin down-regulates myelin phagocytosis by microglia and macrophages through interactions between CD47 on myelin and SIRPα (signal regulatory protein-α) on phagocytes. *J Neuroinflammation* (2011) 8:24. doi:10.1186/1742-2094-8-24
135. Van VQ, Raymond M, Baba N, Rubio M, Wakahara K, Susin SA, et al. CD47high expression on CD4 effectors identifies functional long-lived memory T cell progenitors. *J Immunol* (2012) 188:4249–55. doi:10.4049/jimmunol.1102702
136. Baba N, Van VQ, Wakahara K, Rubio M, Fortin G, Panzini B, et al. CD47 fusion protein targets CD172a+ cells in Crohn's disease and dampens the production of IL-1β and TNF. *J Exp Med* (2013) 210:1251–63. doi:10.1084/jem.20122037
137. Chao MP, Alizadeh AA, Tang C, Jan M, Weissman-Tsukamoto R, Zhao F, et al. Therapeutic antibody targeting of CD47 eliminates human acute lymphoblastic leukemia. *Cancer Res* (2011) 71:1374–84. doi:10.1158/0008-5472.CAN-10-2238
138. Jaiswal S, Jamieson CHM, Pang WW, Park CY, Chao MP, Majeti R, et al. CD47 is upregulated on circulating hematopoietic stem cells and leukemia cells to avoid phagocytosis. *Cell* (2009) 138:271–85. doi:10.1016/j.cell.2009.05.046
139. Majeti R, Chao MP, Alizadeh AA, Pang WW, Jaiswal S, Gibbs KD, et al. CD47 is an adverse prognostic factor and therapeutic antibody target on human acute myeloid leukemia stem cells. *Cell* (2009) 138:286–99. doi:10.1016/j.cell.2009.05.045
140. Chao MP, Alizadeh AA, Tang C, Myklebust JH, Varghese B, Gill S, et al. Anti-CD47 antibody synergizes with rituximab to promote phagocytosis and eradicate non-Hodgkin lymphoma. *Cell* (2010) 142:699–713. doi:10.1016/j.cell.2010.07.044
141. Willingham SB, Volkmer J-P, Gentles AJ, Sahoo D, Dalerba P, Mitra SS, et al. The CD47-signal regulatory protein alpha (SIRPa) interaction is a therapeutic target for human solid tumors. *Proc Natl Acad Sci U S A* (2012) 109:6662–7. doi:10.1073/pnas.1121623109
142. Chao MP, Jaiswal S, Weissman-Tsukamoto R, Alizadeh AA, Gentles AJ, Volkmer J, et al. Calreticulin is the dominant pro-phagocytic signal on multiple human cancers and is counterbalanced by CD47. *Sci Transl Med* (2010) 2:63ra94. doi:10.1126/scitranslmed.3001375
143. Tseng D, Volkmer J-P, Willingham SB, Contreras-Trujillo H, Fathman JW, Fernhoff NB, et al. Anti-CD47 antibody-mediated phagocytosis of cancer by macrophages primes an effective antitumor T-cell response. *Proc Natl Acad Sci U S A* (2013) 110:11103–8. doi:10.1073/pnas.1305569110
144. Chao MP, Tang C, Pachynski RK, Chin R, Majeti R, Weissman IL. Extranodal dissemination of non-Hodgkin lymphoma requires CD47 and is inhibited by anti-CD47 antibody therapy. *Blood* (2011) 118:4890–901. doi:10.1182/blood-2011-02-338020
145. Casey SC, Tong L, Li Y, Do R, Walz S, Fitzgerald KN, et al. MYC regulates the antitumor immune response through CD47 and PD-L1. *Science* (2016) 352:227–31. doi:10.1126/science.aac9935
146. Mittal D, Gubin MM, Schreiber RD, Smyth MJ. New insights into cancer immunoediting and its three component phases-elimination, equilibrium and escape. *Curr Opin Immunol* (2014) 27:16–25. doi:10.1016/j.coi.2014.01.004
147. Legrand N, Huntington ND, Nagasawa M, Bakker AQ, Schotte R, Strick-Marchand H, et al. Functional CD47/signal regulatory protein alpha (SIRP(alpha)) interaction is required for optimal human T- and natural killer- (NK) cell homeostasis in vivo. *Proc Natl Acad Sci U S A* (2011) 108:13224–9. doi:10.1073/pnas.1101398108
148. Sockolosky JT, Dougan M, Ingram JR, Ho CCM, Kauke MJ, Almo SC, et al. Durable antitumor responses to CD47 blockade require adaptive immune stimulation. *Proc Natl Acad Sci U S A* (2016) 113:E2646–54. doi:10.1073/pnas.1604268113
149. Yoon KW, Byun S, Kwon E, Hwang S-Y, Chu K, Hiraki M, et al. Control of signaling-mediated clearance of apoptotic cells by the tumor suppressor p53. *Science* (2015) 349:1261669. doi:10.1126/science.1261669
150. Muñoz-Fontela C, Mandinova A, Aaronson SA, Lee SW. Emerging roles of p53 and other tumour-suppressor genes in immune regulation. *Nat Rev Immunol* (2016) 16:741–50. doi:10.1038/nri.2016.99
151. Miller W, Hayes VM, Ratan A, Petersen DC, Wittekindt NE, Miller J, et al. Genetic diversity and population structure of the endangered marsupial *Sarcophilus harrisii* (Tasmanian devil). *Proc Natl Acad Sci U S A* (2011) 108:12348–53. doi:10.1073/pnas.1102838108

152. Deakin JE, Bender HS, Pearse AM, Rens W, O'Brien PCM, Ferguson-Smith MA, et al. Genomic restructuring in the Tasmanian devil facial tumour: chromosome painting and gene mapping provide clues to evolution of a transmissible tumour. *PLoS Genet* (2012) 8:e1002483. doi:10.1371/journal.pgen.1002483
153. Murchison EP, Schulz-Trieglaff OB, Ning Z, Alexandrov LB, Bauer MJ, Fu B, et al. Genome sequencing and analysis of the Tasmanian devil and its transmissible cancer. *Cell* (2012) 148:780–91. doi:10.1016/j.cell.2011.11.065
154. Wang L, Rubinstein R, Lines JL, Wasiuk A, Ahonen C, Guo Y, et al. VISTA, a novel mouse Ig superfamily ligand that negatively regulates T cell responses. *J Exp Med* (2011) 208:577–92. doi:10.1084/jem.20100619
155. Flies DB, Wang S, Xu H, Chen L. Cutting edge: a monoclonal antibody specific for the programmed death-1 homolog prevents graft-versus-host disease in mouse models. *J Immunol* (2011) 187:1537–41. doi:10.4049/jimmunol.1100660
156. Le Mercier I, Chen W, Lines JL, Day M, Li J, Sergent P, et al. VISTA regulates the development of protective antitumor immunity. *Cancer Res* (2014) 74:1933–44. doi:10.1158/0008-5472.CAN-13-1506
157. Flies DB, Han X, Higuchi T, Zheng L, Sun J, Ye JJ, et al. Coinhibitory receptor PD-1H preferentially suppresses CD4+ T cell-mediated immunity. *J Clin Invest* (2014) 124:1966–75. doi:10.1172/JCI74589
158. Liu J, Yuan Y, Chen W, Putra J, Suriawinata AA, Schenk AD, et al. Immune-checkpoint proteins VISTA and PD-1 nonredundantly regulate murine T-cell responses. *Proc Natl Acad Sci U S A* (2015) 112:6682–7. doi:10.1073/pnas.1420370112
159. Kobayashi N, Karisola P, Peña-Cruz V, Dorfman DM, Jinushi M, Umetsu SE, et al. TIM-1 and TIM-4 glycoproteins bind phosphatidylserine and mediate uptake of apoptotic cells. *Immunity* (2007) 27:927–40. doi:10.1016/j.immuni.2007.11.011
160. DeKruyff RH, Bu X, Ballesteros A, Santiago C, Chim Y-LE, Lee H-H, et al. T cell/transmembrane, Ig, and mucin-3 allelic variants differentially recognize phosphatidylserine and mediate phagocytosis of apoptotic cells. *J Immunol* (2010) 184:1918–30. doi:10.4049/jimmunol.0903059
161. Savill J, Gregory C. Apoptotic PS to phagocyte TIM-4: eat me. *Immunity* (2007) 27:830–2. doi:10.1016/j.immuni.2007.12.002
162. Oomizu S, Arikawa T, Niki T, Kadowaki T, Ueno M, Nishi N, et al. Cell surface galectin-9 expressing Th cells regulate Th17 and Foxp3+ Treg development by galectin-9 secretion. *PLoS One* (2012) 7:e48574. doi:10.1371/journal.pone.0048574
163. Zhu C, Anderson AC, Schubart A, Xiong H, Imitola J, Khoury SJ, et al. The Tim-3 ligand galectin-9 negatively regulates T helper type 1 immunity. *Nat Immunol* (2005) 6:1245–52. doi:10.1038/ni1271
164. Zhou Q, Munger ME, Veenstra RG, Weigel BJ, Hirashima M, Munn DH, et al. Coexpression of Tim-3 and PD-1 identifies a CD8+ T-cell exhaustion phenotype in mice with disseminated acute myelogenous leukemia. *Blood* (2011) 117:4501–10. doi:10.1182/blood-2010-10-310425
165. Gao X, Zhu Y, Li G, Huang H, Zhang G, Wang F, et al. TIM-3 expression characterizes regulatory T cells in tumor tissues and is associated with lung cancer progression. *PLoS One* (2012) 7:e30676. doi:10.1371/journal.pone.0030676
166. Sakuishi K, Apetoh L, Sullivan JM, Blazar BR, Kuchroo VK, Anderson AC. Targeting Tim-3 and PD-1 pathways to reverse T cell exhaustion and restore anti-tumor immunity. *J Exp Med* (2010) 207:2187–94. doi:10.1084/jem.20100643
167. Fourcade J, Sun Z, Benallaoua M, Guillaume P, Luescher IF, Sander C, et al. Upregulation of TIm-3 and PD-1 expression is associated with tumor antigen-specific CD8+ T cell dysfunction in melanoma patients. *J Exp Med* (2010) 207:2175–86. doi:10.1084/jem.20100637
168. Bauer CA, Kim EY, Marangoni F, Carrizosa E, Claudio NM, Mempel TR. Dynamic Treg interactions with intratumoral APCs promote local CTL dysfunction. *J Clin Invest* (2014) 124:2425–40. doi:10.1172/JCI66375
169. Anderson AC, Anderson DE, Bregoli L, Hastings WD, Kassam N, Lei C, et al. Promotion of tissue inflammation by the immune receptor tim-3 expressed on innate immune cells. *Science* (2007) 318:1141–3. doi:10.1126/science.1148536
170. Yan W, Liu X, Ma H, Zhang H, Song X, Gao L, et al. Tim-3 fosters HCC development by enhancing TGF-β-mediated alternative activation of macrophages. *Gut* (2015) 64:1593–604. doi:10.1136/gutjnl-2014-307671
171. Chiba S, Baghdadi M, Akiba H, Yoshiyama H, Kinoshita I, Dosaka-Akita H, et al. Tumor-infiltrating DCs suppress nucleic acid-mediated innate immune responses through interactions between the receptor TIM-3 and the alarmin HMGB1. *Nat Immunol* (2012) 13:832–42. doi:10.1038/ni.2376
172. Huang Y-H, Zhu C, Kondo Y, Anderson AC, Gandhi A, Russell A, et al. CEACAM1 regulates TIM-3-mediated tolerance and exhaustion. *Nature* (2015) 517:386–90. doi:10.1038/nature13848
173. Anderson AC, Joller N, Kuchroo VK. Lag-3, Tim-3, and TIGIT: co-inhibitory receptors with specialized functions in immune regulation. *Immunity* (2016) 44:989–1004. doi:10.1016/j.immuni.2016.05.001
174. Brown EJ, Frazier WA. Integrin-associated protein (CD47) and its ligands. *Trends Cell Biol* (2001) 11:130–5. doi:10.1016/S0962-8924(00)01906-1
175. Brooke G, Holbrook JD, Brown MH, Barclay AN. Human lymphocytes interact directly with CD47 through a novel member of the signal regulatory protein (SIRP) family. *J Immunol* (2004) 173:2562–70. doi:10.4049/jimmunol.173.4.2562
176. Barclay AN, van den Berg TK. The interaction between signal regulatory protein alpha (SIRPα) and CD47: structure, function, and therapeutic target. *Annu Rev Immunol* (2014) 32:25–50. doi:10.1146/annurev-immunol-032713-120142
177. Hatherley D, Graham SC, Turner J, Harlos K, Stuart DI, Barclay AN. Paired receptor specificity explained by structures of signal regulatory proteins alone and complexed with CD47. *Mol Cell* (2008) 31:266–77. doi:10.1016/j.molcel.2008.05.026
178. Hatherley D, Graham SC, Harlos K, Stuart DI, Barclay AN. Structure of signal regulatory protein alpha: a link to antigen receptor evolution. *J Biol Chem* (2009) 284:26613. doi:10.1074/jbc.M109.017566
179. Foster-Cuevas M, Wright GJ, Puklavec MJ, Brown MH, Barclay AN. Human herpesvirus 8 K14 protein mimics CD200 in down-regulating macrophage activation through CD200 receptor. *J Virol* (2004) 78:7667–76. doi:10.1128/JVI.78.14.7667-7676.2004
180. Foster-Cuevas M, Westerholt T, Ahmed M, Brown MH, Barclay AN, Voigt S. Cytomegalovirus e127 protein interacts with the inhibitory CD200 receptor. *J Virol* (2011) 85:6055–9. doi:10.1128/JVI.00064-11
181. Voigt S, Sandford GR, Hayward GS, Burns WH. The English strain of rat cytomegalovirus (CMV) contains a novel captured CD200 (vOX2) gene and a spliced CC chemokine upstream from the major immediate-early region: further evidence for a separate evolutionary lineage from that of rat CMV Maastricht. *J Gen Virol* (2005) 86:263–74. doi:10.1099/vir.0.80539-0
182. Dorfman DM, Shahsafaei A, Alonso MA. Utility of CD200 immunostaining in the diagnosis of primary mediastinal large B cell lymphoma: comparison with MAL, CD23, and other markers. *Mod Pathol* (2012) 25:1637–43. doi:10.1038/modpathol.2012.129
183. Tazawa S, Shiozawa E, Homma M, Arai N, Kabasawa N, Kawaguchi Y, et al. CD200 expression on plasma cell myeloma cells is associated with the efficacies of bortezomib, lenalidomide and thalidomide. *J Clin Exp Hematop* (2015) 55:1–5. doi:10.3960/jslrt.55.121
184. Coles S, Hills RK, Wang ECY, Burnett AK, Man ST, Darley RL, et al. Expression of CD200 on AML blasts directly suppresses memory T-cell function. *Leukemia* (2012) 26:2148–51. doi:10.1038/leu.2012.77
185. Moertel CL, Xia J, LaRue R, Waldron NN, Andersen BM, Prins RM, et al. CD200 in CNS tumor-induced immunosuppression: the role for CD200 pathway blockade in targeted immunotherapy. *J Immunother cancer* (2014) 2:46. doi:10.1186/s40425-014-0046-9
186. Kawasaki BT, Mistree T, Hurt EM, Kalathur M, Farrar WL. Co-expression of the toleragenic glycoprotein, CD200, with markers for cancer stem cells. *Biochem Biophys Res Commun* (2007) 364:778–82. doi:10.1016/j.bbrc.2007.10.067
187. Kawasaki BT, Farrar WL. Cancer stem cells, CD200 and immunoevasion. *Trends Immunol* (2008) 29:464–8. doi:10.1016/j.it.2008.07.005
188. Coles SJ, Wang ECY, Man S, Hills RK, Burnett AK, Tonks A, et al. CD200 expression suppresses natural killer cell function and directly inhibits patient anti-tumor response in acute myeloid leukemia. *Leukemia* (2011) 25:792–9. doi:10.1038/leu.2011.1
189. Coles S, Hills RK, Wang ECY, Burnett AK, Man ST, Darley RL, et al. Increased CD200 expression in acute myeloid leukemia is linked with an increased frequency of FoxP3+ regulatory T cells [Letter]. *Leukemia* (2012) 26:2146–8. doi:10.1038/leu.2012.75
190. Yu K, Gorczynski RM. Persistence of gene expression profile in CD200 transgenic skin allografts is associated with graft survival on

retransplantation to normal recipients. *Transplantation* (2012) 94:36–42. doi:10.1097/TP.0b013e318257ad5c
191. Gorczynski L, Chen Z, Hu J, Kai Y, Lei J, Ramakrishna V, et al. Evidence that an OX-2-positive cell can inhibit the stimulation of type 1 cytokine production by bone marrow-derived B7-1 (and B7-2)-positive dendritic cells. *J Immunol* (1999) 162:774–81.
192. Gorczynski RM, Chen Z, Khatri I, Yu K. Graft-infiltrating cells expressing a CD200 transgene prolong allogeneic skin graft survival in association with local increases in Foxp3 +Treg and mast cells. *Transpl Immunol* (2011) 25:187–93. doi:10.1016/j.trim.2011.07.006
193. Gorczynski RM, Chen Z, He W, Khatri I, Sun Y, Yu K, et al. Expression of a CD200 transgene is necessary for induction but not maintenance of tolerance to cardiac and skin allografts. *J Immunol* (2009) 183:1560–8. doi:10.4049/jimmunol.0900200
194. Gorczynski RM, Chen Z, Diao J, Khatri I, Wong K, Yu K, et al. Breast cancer cell CD200 expression regulates immune response to EMT6 tumor cells in mice. *Breast Cancer Res Treat* (2010) 123:405–15. doi:10.1007/s10549-009-0667-8
195. Odorizzi PM, Wherry EJ. Inhibitory receptors on lymphocytes: insights from infections. *J Immunol* (2012) 188:2957–65. doi:10.4049/jimmunol.1100038
196. Davis SJ, van der Merwe PA. The kinetic-segregation model: TCR triggering and beyond. *Nat Immunol* (2006) 7:803–9. doi:10.1038/ni1369
197. Shlapatska LM, Mikhalap SV, Berdova AG, Zelensky OM, Yun TJ, Nichols KE, et al. CD150 association with either the SH2-containing inositol phosphatase or the SH2-containing protein tyrosine phosphatase is regulated by the adaptor protein SH2D1A. *J Immunol* (2001) 166:5480–7. doi:10.4049/jimmunol.166.9.5480
198. Hannier S, Triebel F. The MHC class II ligand lymphocyte activation gene-3 is co-distributed with CD8 and CD3-TCR molecules after their engagement by mAb or peptide-MHC class I complexes. *Int Immunol* (1999) 11:1745–52. doi:10.1093/INTIMM/11.11.1745
199. Hannier S, Tournier M, Bismuth G, Triebel F. CD3/TCR complex-associated lymphocyte activation gene-3 molecules inhibit CD3/TCR signaling. *J Immunol* (1998) 161:4058–65.
200. Kouo T, Huang L, Pucsek AB, Cao M, Solt S, Armstrong T, et al. Galectin-3 shapes antitumor immune responses by suppressing CD8+ T cells via LAG-3 and inhibiting expansion of plasmacytoid dendritic cells. *Cancer Immunol Res* (2015) 3:412–23. doi:10.1158/2326-6066.CIR-14-0150
201. Yoshimura A, Gemma A, Hosoya Y, Komaki E, Hosomi Y, Okano T, et al. Increased expression of the LGALS3 (galectin 3) gene in human non-small-cell lung cancer. *Genes Chromosomes Cancer* (2003) 37:159–64. doi:10.1002/gcc.10205
202. Koh YW, Jung SJ, Park C-S, Yoon DH, Suh C, Huh J. LGALS3 as a prognostic factor for classical Hodgkin's lymphoma. *Mod Pathol* (2014) 27:1338–44. doi:10.1038/modpathol.2014.38
203. Cheng C, Hou H, Lee M, Liu C, Jhuang J, Lai Y, et al. Prognostic factor for overall survival in patients with acute myeloid higher bone marrow LGALS3 expression is an independent unfavorable prognostic factor for overall survival in patients with acute myeloid leukemia. *Blood* (2013) 121:3172–80. doi:10.1182/blood-2012-07-443762
204. Senkus E, Kyriakides S, Ohno S, Penault-Llorca F, Poortmans P, Rutgers E, et al. Primary breast cancer: ESMO Clinical Practice Guidelines for diagnosis, treatment and follow-up. *Ann Oncol* (2015) 26:v8–30. doi:10.1093/annonc/mdv298
205. Okada K, Shimura T, Suehiro T, Mochiki E, Kuwano H. Reduced galectin-3 expression is an indicator of unfavorable prognosis in gastric cancer. *Anticancer Res* (2006) 26:1369–76.
206. Prigent P, El Mir S, Dréano M, Triebel F. Lymphocyte activation gene-3 induces tumor regression and antitumor immune responses. *Eur J Immunol* (1999) 29:3867–76. doi:10.1002/(SICI)1521-4141(199912)29:12<3867::AID-IMMU3867>3.3.CO;2-5
207. Andreae S, Piras F, Burdin N, Triebel F. Maturation and activation of dendritic cells induced by lymphocyte activation gene-3 (CD223). *J Immunol* (2002) 168:3874–80. doi:10.4049/jimmunol.168.8.3874
208. Andreae S, Buisson S, Triebel F. MHC class II signal transduction in human dendritic cells induced by a natural ligand, the LAG-3 protein (CD223). *Blood* (2003) 102:2130–7. doi:10.1182/blood-2003-01-0273
209. Lucas CL, Workman CJ, Beyaz S, LoCascio S, Zhao G, Vignali DAA, et al. LAG-3, TGF-B, and cell-intrinsic PD-1 inhibitory pathways contribute to CD8 but not CD4 T-cell tolerance induced by allogeneic BMT with anti-CD40L. *Blood* (2011) 117:5532–40. doi:10.1182/blood-2010-11-318675
210. Grosso JF, Goldberg MV, Getnet D, Bruno TC, Yen H-R, Pyle KJ, et al. Functionally distinct LAG-3 and PD-1 subsets on activated and chronically stimulated CD8 T cells. *J Immunol* (2009) 182:6659–69. doi:10.4049/jimmunol.0804211
211. Grosso JF, Kelleher CC, Harris TJ, Maris CH, Hipkiss EL, De Marzo A, et al. LAG-3 regulates CD8+ T cell accumulation and effector function in murine self- and tumor-tolerance systems. *J Clin Invest* (2007) 117:3383–92. doi:10.1172/JCI31184
212. Woo SR, Turnis ME, Goldberg MV, Bankoti J, Selby M, Nirschl CJ, et al. Immune inhibitory molecules LAG-3 and PD-1 synergistically regulate T-cell function to promote tumoral immune escape. *Cancer Res* (2012) 72:917–27. doi:10.1158/0008-5472.CAN-11-1620
213. Sica GL, Choi IH, Zhu G, Tamada K, Wang SD, Tamura H, et al. B7-H4, a molecule of the B7 family, negatively regulates T cell immunity. *Immunity* (2003) 18:849–61. doi:10.1016/S1074-7613(03)00152-3
214. Prasad DVR, Richards S, Mai XM, Dong C. B7S1, a novel B7 family member that negatively regulates T cell activation. *Immunity* (2003) 18:863–73. doi:10.1016/S1074-7613(03)00147-X
215. Kryczek I, Wei S, Zou L, Zhu G, Mottram P, Xu H, et al. Cutting edge: induction of B7-H4 on APCs through IL-10: novel suppressive mode for regulatory T cells. *J Immunol* (2006) 177:40–4. doi:10.4049/jimmunol.177.1.40
216. Kryczek I, Wei S, Zhu G, Myers L, Mottram P, Cheng P, et al. Relationship between B7-H4, regulatory T cells, and patient outcome in human ovarian carcinoma. *Cancer Res* (2007) 67:8900–5. doi:10.1158/0008-5472.CAN-07-1866
217. Choi I-H, Zhu G, Sica GL, Strome SE, Cheville JC, Lau JS, et al. Genomic organization and expression analysis of B7-H4, an immune inhibitory molecule of the B7 family. *J Immunol* (2003) 171:4650–4. doi:10.4049/jimmunol.171.9.4650
218. Schildberg FA, Klein SR, Freeman GJ, Sharpe AH. Coinhibitory pathways in the B7-CD28 ligand-receptor family. *Immunity* (2016) 44:955–72. doi:10.1016/j.immuni.2016.05.002
219. Yu X, Harden K, Gonzalez LC, Francesco M, Chiang E, Irving B, et al. The surface protein TIGIT suppresses T cell activation by promoting the generation of mature immunoregulatory dendritic cells. *Nat Immunol* (2009) 10:48–57. doi:10.1038/ni.1674

Conflict of Interest Statement: AF and GW received funding from an Entrepreneurs' Programme Research Connections grant with Nexvet Australia Pty. Ltd. (RC50680). Nexvet is a global clinical-stage biopharmaceutical company focused on transforming the therapeutic market for companion animals by developing and commercializing novel biologic therapies. The other authors declare no conflict of interest.

frontiers in Immunology

HYPOTHESIS AND THEORY
published: 11 September 2017
doi: 10.3389/fimmu.2017.01098

Immunological Control of Viral Infections in Bats and the Emergence of Viruses Highly Pathogenic to Humans

Tony Schountz[1], Michelle L. Baker[2], John Butler[3] and Vincent Munster[4]*

[1] Arthropod-Borne and Infectious Diseases Laboratory, Department of Microbiology, Immunology and Pathology, Colorado State University, Fort Collins, CO, United States, [2] Australian Animal Health Laboratory, Health and Biosecurity Business Unit, Commonwealth Scientific and Industrial Research Organisation, Geelong, VIC, Australia, [3] Department of Microbiology, Carver College of Medicine, University of Iowa, Iowa City, IA, United States, [4] Virus Ecology Unit, Rocky Mountain Laboratories, National Institutes of Health, Hamilton, MT, United States

OPEN ACCESS

Edited by:
Greg Woods, University of Tasmania, Australia

Reviewed by:
Maria Forlenza, Wageningen University and Research, Netherlands
Alison Kell, University of Washington, United States
William Lee, Wadsworth Center, United States

***Correspondence:**
Tony Schountz
tony.schountz@colostate.edu

Specialty section:
This article was submitted to Comparative Immunology, a section of the journal Frontiers in Immunology

Received: *17 July 2017*
Accepted: *22 August 2017*
Published: *11 September 2017*

Citation:
Schountz T, Baker ML, Butler J and Munster V (2017) Immunological Control of Viral Infections in Bats and the Emergence of Viruses Highly Pathogenic to Humans. Front. Immunol. 8:1098. doi: 10.3389/fimmu.2017.01098

Bats are reservoir hosts of many important viruses that cause substantial disease in humans, including coronaviruses, filoviruses, lyssaviruses, and henipaviruses. Other than the lyssaviruses, they do not appear to cause disease in the reservoir bats, thus an explanation for the dichotomous outcomes of infections of humans and bat reservoirs remains to be determined. Bats appear to have a few unusual features that may account for these differences, including evidence of constitutive interferon (IFN) activation and greater combinatorial diversity in immunoglobulin genes that do not undergo substantial affinity maturation. We propose these features may, in part, account for why bats can host these viruses without disease and how they may contribute to the highly pathogenic nature of bat-borne viruses after spillover into humans. Because of the constitutive IFN activity, bat-borne viruses may be shed at low levels from bat cells. With large naive antibody repertoires, bats may control the limited virus replication without the need for rapid affinity maturation, and this may explain why bats typically have low antibody titers to viruses. However, because bat viruses have evolved in high IFN environments, they have enhanced countermeasures against the IFN response. Thus, upon infection of human cells, where the IFN response is not constitutive, the viruses overwhelm the IFN response, leading to abundant virus replication and pathology.

Keywords: bats, Chiroptera, zoonosis, antibody repertoire, emerging infectious disease, virus ecology

Bats have gained attention in recent years as reservoir or suspected reservoir hosts of many high-impact human pathogenic viruses that cause outbreaks and epidemics with high mortality (1, 2). In terms of viral species richness and zoonotic potential, bats may be the most important mammalian sources (3, 4). Each of these viruses, including the ebolaviruses, Marburg virus, severe acute respiratory syndrome and Middle East respiratory syndrome coronaviruses, rabies and other lyssaviruses, and Hendra and Nipah viruses, is thought to circulate in certain species of bats without significant disease. Chiroptera, to which bats belong, is the second largest mammalian order, with about 1,200 species. Bats originated about 80 million years ago (mya) and substantial radial divergence ensued soon after the K–T extinction event about 66 mya (5). Consequently, bats have been on independent evolutionary trajectories for most of the history of mammals. They belong to the mammalian superorder Laurasiatheria that includes ungulates and canines,

whereas rodents and primates belong to the superorder Euarchontoglires; these superorders diverged about 90 mya. Genome and transcriptome analyses suggest the immune systems of bats are substantially similar to those of other mammals; however, there are some significant differences, including the loss of the PYHIN locus that has the AIM2 cytosolic DNA sensor and inflammasome genes, loss of killer cell immunoglobulin-like (KIR), and killer cell lectin-like (KLR) receptor loci used by NK cells, expanded immunoglobulin heavy-chain VDJ segments and contraction of the interferon-α (IFNα) locus (6–11). Although bats share many immunological features with other mammals, little research into their immune systems or responses has been conducted and there are no well-developed bat research models to study infectious agents (12, 13).

Often, in zoonotic virus/reservoir host relationships, which have been best studied in rodents and primates (14–16), each virus is hosted by individuals of one or only a few species. There are exceptions, including slowly replicating viruses, such as rabies virus. However, viruses, like all other biological entities, are subject to the pressures of evolution and are likely genetically and biochemically adapted ("optimized") to circulate within their reservoir host populations to either cause persistent infection (often for the life of the host), or to replicate and be shed for a sufficient period to allow transmission to other susceptible hosts, without causing substantial disease within the population (17). They typically do not elicit robust immune responses in their reservoirs, which could lead to viral clearance or immunopathology. When spillover of pathogenic viruses to humans or other non-reservoir species occurs, they are not biochemically optimized for the new host cells, which can lead to disease and death, or immune clearance.

Because of the occurrence of severe human diseases caused by some of the bat-borne viruses, an important question is; how do bats host these viruses without becoming diseased? The answer to this question is likely complicated and will vary between species of bats and species of viruses. In rodent reservoirs of pathogenic hantaviruses, in which the viruses establish persistent infection without meaningful pathology (18–22), the immune response is slow to develop (21) and is mediated by Foxp3$^+$, TGFβ-expressing regulatory T (Treg) cells, which counter inflammatory disease (23, 24) but at the expense of sterilizing immunity. Do bats have Treg cells? If so, do bat viruses also elicit Treg responses in their reservoir hosts? T cell genes are found in bats, but there are no publications demonstrating antigen-specific T cell activities in bats. The lack of such studies underlies a significant deficit in the study of bat immune responses, considering the functional subsets of T cells that have been identified in other species (e.g., Th1, Th2, Th17, NKT, Tfh, CTL, etc.) and the effector functions mediated by T cells, including T cell help, inflammation, chemotaxis, and augmentation of macrophage activities such as phagocytosis and killing of microbes.

Even less is known about NK cells in bats. Does the loss of KIR/KLR genes in bats (8) mean that NK cells use alternative receptors to recognize MHC class I for activation and inhibition? Do bat NK cells have the same effector functions found in other species, such as granzyme-mediated cytolysis and antibody-dependent cell cytotoxicity? Genes for granzymes A and B and CD16 (FcRγIII) are found in bats (6, 7); thus, it is likely that bat NK cells are functionally similar to other species in this regard. Until methods are developed to assess T cell and NK cell functions in bats, our understanding of bat virus infections of reservoir hosts will be severely limited.

Pathogenic bat-borne viruses encode immune modulating accessory proteins that often target the innate antiviral responses of infected cells. It is thought that these proteins are contributory factors of human disease ("virulence factors") (25–32); however, because they evolved in their bat reservoirs (i.e., biochemically optimized), their impacts on the orthologous proteins of humans must somehow be different; otherwise, there would not be differential outcomes in bats (no disease) and humans (disease).

THE "FLIGHT AS FEVER" HYPOTHESIS

One proposed explanation for the lack of disease in virus-infected bats is the "flight as fever" hypothesis that suggests elevated body temperature during flight somehow mimics the effects of the fever response (33). However, the fever response after infection is much more sophisticated than simply elevated body temperature. In other mammals that have been studied, the production of interferons (IFN), interleukin-1, and prostaglandins have already occurred by the time fever is detectable (34, 35). There is no evidence that these effector molecules are expressed by bats during flight. Moreover, viral infections are complex processes; thus, it is unlikely that elevated body temperature alone is sufficient to explain how bats can host these viruses without signs of disease. The only experimental work assessing this effect showed that increasing incubation temperature of bat cells does not affect their ability to support ebolavirus replication (36). Although there is no experimental evidence supporting the flight as fever hypothesis, some have speculated this provides a metabolic mechanism for bats to host these viruses without disease (37).

THE "ALWAYS ON" IFN SYSTEM OF BATS

An interesting feature of pteropid bats is that parts of the type I IFN system appear to be constitutively active and it has been hypothesized that this "always on" activity may hamper early viral replication (10). We have also observed signatures of IFN receptor pathway activation in uninfected primary kidney cells cultured from Jamaican fruit bats (*Artibeus jamaicensis*), including constitutive STAT1 phosphorylation (unpublished data). In other mammals that have been examined, the type I IFN loci have undergone expansion by tandem duplication events, leading to multiple copies of *Ifna* genes. However, in bats there is compelling evidence that the type I IFN locus has undergone contraction leading to fewer *Ifna* genes (10). Despite this contraction, *Ifna* basal gene expression in bats is elevated relative to humans and rodents, as are the levels of many IFN-stimulated genes (ISG). The constitutive *Ifna* expression appears to induce a profile of ISGs that is not inflammatory, and this may be one of the reasons why *Ifna* expression can be elevated without leading to chronic inflammatory pathology. Furthermore, as the levels of IFNα protein expressed by bat cells remains to be determined, it is possible that much of the *Ifna* mRNA remains untranslated,

providing a source of transcripts for rapid translation when required. In addition, the type III IFN response appears to be restricted to immune cells and epithelial cells, and can be activated independently of type I IFN signaling (38, 39). Collectively, these aspects of the innate immune system suggest that bat cells are poised to respond to viral infections immediately, which may restrict, but not prevent, viral replication. It is unknown why bat IFN pathways are constitutively active but some species of bats can have extraordinarily high population densities with extensive mutual grooming behavior. Because transmission of infectious agents is related to population density, it may be evolutionarily favorable for bats to hamper virus replication and shedding to limit transmission within a population. However, viruses must also be able to sufficiently evade the response to transmit within the bat population; otherwise, they would be driven to extinction. Thus, it is likely that bat virus accessory proteins are finely tuned to modulate bat antiviral responses.

IMMUNOGLOBULIN REPERTOIRES OF BATS

The germline immunoglobulin loci of mammals contain tandem variable (V), diversity (D), and joining (J) gene segments that recombine during B cell development in the bone marrow to generate VDJ rearrangements at the immunoglobulin heavy-chain locus, and VJ rearrangements at the light chain locus (40). The number of segments varies between species (**Table 1**), and not all segments are functional. For example, humans have 87 immunoglobulin heavy-chain V segments, but only about 40 are functional. V(D)J recombination generates the naive B cell immunoglobulin repertoire of an individual with, in humans, about 2 million unique immunoglobulin specificities that typically have an IgM heavy chain (41). The result, termed *combinatorial diversity*, occurs prior to, and is independent of, the antigen stimulation of an immune response. Swine, on the other hand, have far fewer heavy-chain gene segments, with seven functional V segments, two D segments and one J segment for just 14 possible combinations (42). Increased junctional diversity of the developing naive immunoglobulin repertoire occurs during recombination of the V(D)J segments in which exonuclease activity removes nucleotides from the segment ends and the enzyme *terminal deoxynucleotidyl transferase* (TdT) adds nucleotides to the segment ends (41). The substantially limited swine VDJ is overcome by exonuclease and TdT activities (42).

Antigen exposure to naive B cells leads to secretion of IgM antibodies with typically low average affinities (~10^{-7} K_d). This low affinity is the result of the poor proximity of the amino acid residues of the antibody variable region to the residues of the antigenic epitope, thus, fewer non-covalent bonds can form at the antibody:antigen interface. However, as these B cells undergo clonal selection and expansion during an infection, *somatic hypermutation* (SHM) occurs in daughter cell V(D)J regions that leads to antibodies with higher average affinities by virtue of refined complimentary topology between the antibody and its epitope, and the inclusion of amino acids in the variable region that strengthen the non-covalent interactions with the epitope (43). This process, termed *affinity maturation*, requires T cell help and expression of the enzyme *activation-induced cytidine deaminase* (AID) in the dividing B cells. The result of this process is the generation of antibodies with affinities for antigen that are orders of magnitude greater (~10^{-10} to ~10^{-12} K_d) than those of the original naive parental B cell clones that recognized the antigen.

Affinity maturation can take weeks, but if the host survives the infection it typically produces antibodies that can bind antigen with nearly irreversible affinities under physiological conditions. Importantly, this process leads to memory B cells that have high affinity surface immunoglobulin receptors that have already class-switched to IgG or IgA, and can rapidly divide and secrete antibodies independent of T cell help should the same pathogen be encountered again. Indeed, affinity maturation principally accounts for the high antibody titers detected by the various serological end-point dilution assays.

In bats, combinatorial diversity may lead to the generation of a much larger naive immunoglobulin repertoire than it does in humans because bats may possess more heavy-chain VDJ germline gene segments. The heavy-chain locus of humans has 40 functional V segments, 24 D segments, and 6 J segments for a potential of 5,760 H chain specificities in its naive B cell repertoire through combinatorial diversity (44). The little brown

TABLE 1 | Immunoglobulin gene segments of select mammalian species (42).

Species	V_H (*F*[a])	D_H	J_H	V_λ (*F*)	J_λ	C_λ[b]	V_κ (*F*)	J_κ	C_κ	k:l[c]
Little brown bat	>250 (5)	?	13	?	?	?	? (?)	?	?	?:?
Human	87 (7)	30	9	70 (7)	7	7	66 (7)	5	1	60:40
Mouse	>100 (14)	11	4	3 (3)	4	4	140 (4)	4	1	95:5
Rabbit	>100 (1)	11	6	? (?)	2	2	>36 (?)	8	2[d]	95:5
Horse	>10 (2)	>7	>5	25 (3)	4	4	>20 (?)	5	5	5:95
Cattle	>15 (2)	3	5	83 (8)	>2	4	? (?)	?	1	5:95
Swine	>20 (1)	2[e]	1[e]	22 (>2)	>4	4	14–60 (5)	5	1	50:50

[a]*Number of families (F) of variable region genes.*

[b]*J_λ–C_λ duplicons are the common motif in most mammals.*

[c]*Ratio of expressed light chain in adults expressed as percent.*

[d]*Rabbits have a duplicate of the entire kappa locus.*

[e]*Functional D_H and J_H genes.*

?, number is unknown.

bat (*Myotis lucifugus*) has an estimated 236 V segments, at least 24 D segments, and at least 13 J segments, with a potential of more than 70,000 specificities in the naive B cell repertoire (9) (**Figure 1**). Pteropid bats also have a highly diverse genomic and expressed V_H repertoire, and evidence for multiple expressed D_H and J_H segments, consistent with their ability to recognize a range of antigenic epitopes (45). Bats appear to only express λ light chains but no research has been published about their light chain VJ segments nor their T cell receptor genes, thus it is not possible to compare them to other mammals.

In little brown bats, there appears to be less dependence on affinity maturation (9), suggesting the expanded repertoire from combinatorial diversity may have reduced, but not eliminated, the evolutionary need for SHM. Bats have and express the gene for AID (6–8), thus it is likely that some SHM occurs but AID appears to play a less prominent role in bats than it does in mice, humans, and swine. AID also facilitates class switching to other antibody classes (isotypes) in mice and humans, such as the IgG subclasses and IgA (46). If it is used less in bats, does this mean there is less class switching in bats? Or is it only the SHM function that is reduced? Do bats also generate junctional diversity through exonuclease and TdT activity? If bats do not use SHM does that lead to less robust memory B cell responses that can contribute to viral recrudescence?

Many of these questions are difficult to address because there are few immunoglobulin class-specific antibodies for bats of any species. Polyclonal rabbit antibodies to Australian black flying fox (*Pteropus alecto*) IgG, IgM, and IgA have been generated (47), but all others are polyclonal antibodies to whole bat IgG that likely recognize light chains as well as heavy chains. Because light chains are shared by all immunoglobulin classes, these polyclonal antibodies cannot discriminate IgD, IgM, IgG, IgA, or IgE. The number of immunoglobulin heavy-chain genes that encode IgG subclasses vary between species, with Seba's fruit bat (*Carollia perspicillata*) having only one, big brown bat (*Eptesicus fuscus*) having two, greater short-nosed bat (*Cynopterus sphinx*) having three and little brown bat having five (48). One monoclonal antibody to the immunoglobulin λ chain of the big brown bat has been generated and it has cross reactivity to little brown bat λ chains; thus, it likely will be useful for characterizing antibodies from these bats (49).

A recent report suggested that IgG, rather than IgA, is more abundant in mucosal secretions of the Australian black flying fox (47). Their approach used Jacalin, peptide M, and staphylococcal superantigen-like protein 7 to purify IgA; these reagents are routinely used to purify human IgA but it is unclear if they bind bat IgA efficiently, or at all. The suggestion that IgG is the most abundant secretory immunoglobulin in bats is inconsistent with established data on secretory immunoglobulins in other mammals and should be regarded with caution. The generation of isotype-specific monoclonal antibodies to bat immunoglobulins will be required to determine which isotype is most abundant in mucosal secretions of bats.

A HYPOTHESIS OF BAT IMMUNE RESPONSES TO VIRAL INFECTIONS

We propose that innate and adaptive immune responses in bats are different than in mice and humans, and these differences may account for why the viruses they host can be significant human pathogens. First, we suggest that because of higher constitutive expression of IFNα and persistent ISG activity, bat cells hamper virus replication relative to what occurs in cells from humans and rodent disease models. Second, because of the apparently larger bat naive immunoglobulin repertoires (from combinatorial diversity), bats may have more immunoglobulin specificities that favor clonal selection of B cells with immunoglobulin receptors that interact with substantially higher mean affinities for antigen. Because of this, and because of the reduced viral burden due to persistent IFN activity, there has been less evolutionary pressure for SHM to control viral infections in bats—the selected B cells can undergo clonal expansion without an urgent need for affinity maturation to generate high-titered antibodies.

This combination of events may lead to several expected outcomes that can be experimentally tested. First, because of their constitutively high expression of IFNα, less virus replication

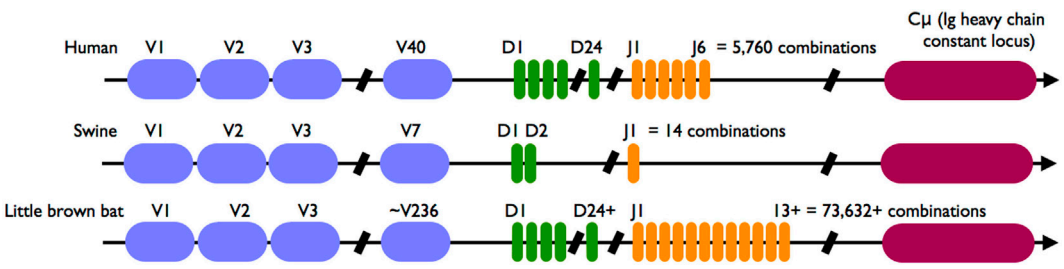

FIGURE 1 | Immunoglobulin VDJ combinatorial diversity potential of humans, swine and little brown bats. The human heavy (H) chain locus has about 40 variable (V), 24 diversity (D) and 6 joining (J) segments that are functional. Rearrangement of the locus occurs during B cell development in the bone marrow and provides the repertoire of immunoglobulin specificities that are clonotypic in naive B cells, usually with IgM constant (Cμ) heavy chains, which populate peripheral lymphoid tissues, such as lymph nodes and the spleen. The theoretical number of human H chain specificities is 40 × 24 × 6 = 5,760. In contrast, swine have 7 V, 2 D, and 1 J segments that are functional, totaling 14. In the little brown bat (*Myotis lucifugus*), the functional H chain locus is estimated to have 236 V segments, at least 24 D segments, and at least 13 J segments, for a theoretical number of at least 73,632 specificities in the naive B cell repertoire. Blue, V gene segments; green, D gene segments; orange, J chain segments; purple, C gene (IgM); other C genes not shown.

should occur in infected bat cells compared to human or rodent cells used in pathology models. Second, because of the hampered viral replication, antibody responses in bats likely are slower to develop and may not be as durable as those in mice or humans because fewer viruses will be available for T and B cell stimulation. Third, antibody titers, which are a function of affinity maturation, should be lower in bats (e.g., average affinities of 10^{-9} to 10^{-11} K_d) than those generated in mice. A poorer antibody response (i.e., lower titer) could prevent or delay clearance of virus from the reservoir bat, contribute to persistent infection, prolong shedding, and lead to periods of recrudescence as antibody wanes.

Although there are a few bat cell lines that are susceptible to these viruses, caution must be exercised when using them because of the potential for unusual genomic events that routinely occur during immortalization, such as deletions and duplications of genes, which can complicate interpretation of data. Therefore, assessment of viral infection kinetics will require isolation of identical susceptible primary cells from reservoir bats, and humans or rodents used in pathology studies. As one example, Nipah virus infects endothelial cells (50–52) and the Syrian hamster is a pathology model for its disease (53, 54). Isolation of primary endothelial cells (e.g., $PCAM1^+$ cells) from pteropid reservoir hosts and hamsters could be used to assess virus replication kinetics. If our hypothesis is correct, then we would expect less virus replication and shedding from primary pteropid endothelial cells than from hamster endothelial cells.

Consistent with our hypothesis, bat antibody responses appear to be slower to develop and less robust during infection (55, 56) and immunization (57, 58) compared to those of mice. Immunization of Brazilian free-tailed bats (*Tadarida brasiliensis*) and Egyptian fruit bats (*Rousettus aegyptiacus*) with rabies vaccines resulted in neutralizing antibody responses that are considered protective (59, 60). However, the vaccines used in these studies were inactivated, thus (1) were incapable of infecting cells and influencing the IFN response with the viral accessory proteins and (2) were formulated with adjuvant that simulates inflammation that contributes to more robust antibody responses. Experimental Marburg virus infection of Egyptian fruit bats, a natural reservoir host, leads to brief viremia, wide tissue distribution and low to modest viral loads and seroconversion (61–63) and transmission (64). Similarly, poor neutralizing antibody responses occur after experimental infection of artibeus bats with Tacaribe virus, even in surviving bats (65). To date, no direct comparisons of infections with bat-borne viruses in reservoir host bats and pathology models have been performed; thus, there are no direct comparisons of the antibody responses to determine differences or similarities between bats and other mammals. In addition to immune response studies of apathogenic infection of bat reservoir hosts and their viruses, it will be necessary to examine the immune response in pathogenic infections of bats for essential comparison, such as the aforementioned Tacaribe virus infection of artibeus bats (65) or rabies virus infection of bats of many species (60, 66). After all, if bat IFN responses are "always on," why does Tacaribe virus kill bats?

HAS PERSISTENT IFN ACTIVITY IN BATS DRIVEN THE EVOLUTION OF VIRUSES PATHOGENIC TO HUMANS?

With persistent activation of the IFN response in bat cells, it is reasonable to assume that viruses hosted by bats have evolved finely tuned countermeasures to dampen the response in the reservoir bat species. For example, STAT1, an essential component of the type I, II, and III IFN receptor signaling pathways, is a target of ebolavirus VP24, Marburg virus VP40, Nipah virus V and W, and SARS-CoV ORF6 (67–71). Because the viruses have evolved in bats, these proteins are likely optimized to disrupt STAT1 activity in the reservoir host bats in a qualitative and/or quantitative manner that permits virus replication and shedding without compromising the health of the host. Hendra virus antagonizes IFN production and signaling in an immortalized cell line from the Australian black flying fox, but only disrupts IFN production in an immortalized human cell line (72, 73). The impact of these proteins on STAT1 in the reservoir bats must be enough to allow some, perhaps periodic, viral replication to sustain the virus in bat populations, but not so much that it leads to high levels of viral replication and shedding from infected cells; otherwise, pathology and/or a robust adaptive immune response would ensue. But because the IFN receptor pathway is persistently activated in bat cells, it is likely that expression of these viral proteins occurs to counteract STAT1's cascading activation of the ISG pathways. Another important caveat of the experimental systems used to examine the effects of these viral proteins is that their genes are often cloned into high-expression plasmids or into other viruses that do not naturally infect bats. It is probable that expression levels of these genes by their viruses have been evolutionarily optimized for the reservoir bat species. But this presents logistical difficulties because most of these viruses require BSL-3 or BSL-4 containment, a significant hurdle for many investigators.

STAT1 is a highly conserved protein and the viral accessory proteins that target it have been shown to often interfere with human STAT1 activity (67–71). We hypothesize that because of persistent IFN activity in bat cells, these viruses may express these accessory proteins at substantially higher levels to counter the bat cell's elevated basal levels of the IFN response genes (**Figure 2**). STAT1 of the Australian black flying fox (Hendra virus reservoir) and the Egyptian fruit bat (*R. aegyptiacus*, Marburg virus reservoir) are 96% and 97% identical, respectively, to human STAT1. Because the human IFN system is "off" (i.e., low basal levels) until an infection, it may be that these viral proteins are expressed in such high abundance immediately upon infection of a human cell (because they have been evolutionarily programmed in bat cells) that they abrogate the cell's ability to mount an effective IFN response. This could lead to abundant viral replication and shedding from human cells, which would then disseminate and infect other cells, leading to direct viral pathology or immunopathology from the subsequent activation of immune cells that respond to viral infection, including macrophages, neutrophils, NK cells and cytotoxic T cells. Alternatively, or in conjunction with, the viral proteins may bind to STAT1 of humans and bats with different affinities that could contribute to the dichotomous outcomes (72).

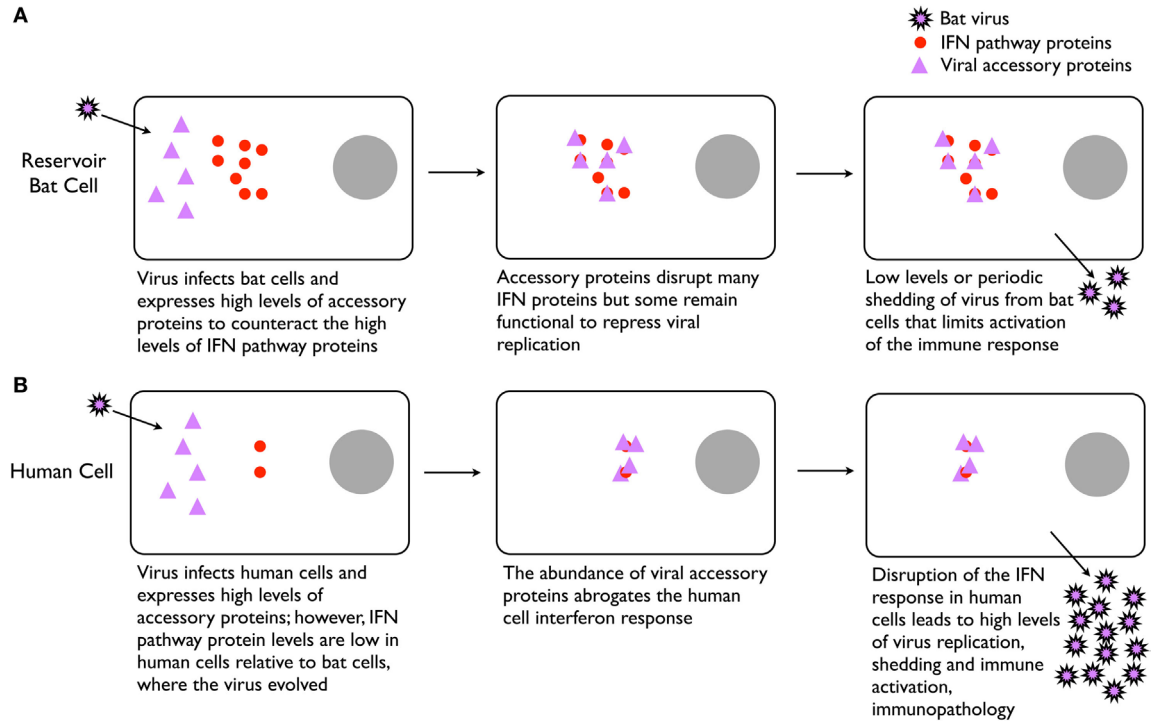

FIGURE 2 | Potential explanation for high virulence of certain bat-borne viruses in humans. **(A)** Infection of bat cells leads to high expression of viral accessory proteins that repress the constitutively active type I interferon (IFN) system, leading to low levels of virus replication and shedding. Low level or intermittent replication of virus delays and reduces stimulation of the immune system, thus resulting in weak adaptive immunity and poor antibody responses. **(B)** In human cells, the high expression of viral accessory proteins significantly disrupts the cell's ability to control the infection, leading to high levels of virus replication and immune stimulation that contributes to pathogenesis.

CAVEATS AND CHALLENGES OF THE HYPOTHESIS

We recognize that this hypothesis on its own may be insufficient to explain the biological relationships and interactions of hundreds of viruses, and probably many more (74), and bats of the ~1,200 different species. Is the IFN system "always on" for all 1,200 species of bats? Do they all have more V(D)J germline gene segments? Do they all rely more on combinatorial diversity and less on SHM for the generation of their immunoglobulin repertoires? Just as there are significant differences between bats and other mammals, there are likely significant differences between bat species. However, considering the current evidence, we believe that several aspects of these hypotheses can be experimentally addressed with appropriate animal studies. We also have not considered other aspects of immune systems that may be important in chiropteran immunology, including activities of cellular immunity, the roles of complement and antibody-dependent cell cytotoxicity, immune effector molecules such as cytokines, antigen processing and presentation, immunological memory, and the myriad other immunological factors. Virtually nothing is known about these aspects of bat immunology, thus it is difficult to imagine how they might be different or contribute to bats of a particular species being suitable reservoir hosts for viruses of a particular species. It also is likely that many other differences between bats and other mammals exist that are not directly related to the immune response (e.g., metabolism, physiology, hormonal changes, behavior, "flight as fever") that are contributory factors to reservoir host status of bats.

Of what is known, experimental approaches that examine the responses of infected bat cells (e.g., IFN response) and antibody responses seem to be the most tractable. A significant hurdle to accomplish these experiments is the lack of well-defined bat models for infectious disease research. Few closed colonies of bats are available for such purposes and of those, few reagents and methodologies have been developed to exploit them. These deficiencies can be rapidly overcome using the technological tools available today. For example, collection of low abundance antibodies (i.e., IgM, IgA) or immune cells from bats is challenging; most microbats are so small that collection of a few hundred microliters of blood can be lethal. But with deep sequencing, full genomes and transcriptomes can be rapidly generated and exploited to produce nearly any recombinant bat protein for use in experimental work. This approach could be deployed to generate monoclonal antibodies specific to not only IgM and IgA, but IgG subclasses, to help understand immune responses in bats. Moreover, with long-read RNA-Seq and bioinformatics, characterization of immunoglobulin and T cell receptor repertoires can identify

increased frequencies of V(D)J usage during B and T cell clonal expansion and SHM during infection (75, 76). This should clarify to what degree SHM is used by bats during immune responses, which has only been examined in naive little brown bats (9).

Regardless of the virus, it is essential that experimental infection studies of bat viruses should be done in bats. The use of other species, such as rodents and non-human primates, may provide information about pathogenesis, but they cannot address the biology, evolution and ecology of bat-borne viruses, and how they may emerge as human pathogens.

AUTHOR CONTRIBUTIONS

All authors listed have made substantial, direct, and intellectual contribution to the work and approved it for publication.

ACKNOWLEDGMENTS

The authors thank Charles H. Calisher for review of the manuscript and Jacalyn S. Strong for support. VM is supported by the Intramural Research Program of the National Institute of Allergy and Infectious Diseases, National Institutes of Health.

REFERENCES

1. Calisher CH, Childs JE, Field HE, Holmes KV, Schountz T. Bats: important reservoir hosts of emerging viruses. *Clin Microbiol Rev* (2006) 19(3):531–45. doi:10.1128/CMR.00017-06
2. Lau SK, Li KS, Tsang AK, Lam CS, Ahmed S, Chen H, et al. Genetic characterization of Betacoronavirus lineage C viruses in bats reveals marked sequence divergence in the spike protein of pipistrellus bat coronavirus HKU5 in Japanese pipistrelle: implications for the origin of the novel Middle East respiratory syndrome coronavirus. *J Virol* (2013) 87(15):8638–50. doi:10.1128/JVI.01055-13
3. Luis AD, Hayman DT, O'Shea TJ, Cryan PM, Gilbert AT, Pulliam JR, et al. A comparison of bats and rodents as reservoirs of zoonotic viruses: are bats special? *Proc Biol Sci* (2013) 280(1756):20122753. doi:10.1098/rspb.2012.2753
4. Olival KJ, Hosseini PR, Zambrana-Torrelio C, Ross N, Bogich TL, Daszak P. Host and viral traits predict zoonotic spillover from mammals. *Nature* (2017) 546(7660):646–50. doi:10.1038/nature22975
5. Benton MJ, Ayala FJ. Dating the tree of life. *Science* (2003) 300(5626):1698–700. doi:10.1126/science.1077795
6. Papenfuss AT, Baker ML, Feng ZP, Tachedjian M, Crameri G, Cowled C, et al. The immune gene repertoire of an important viral reservoir, the Australian black flying fox. *BMC Genomics* (2012) 13(1):261. doi:10.1186/1471-2164-13-261
7. Shaw TI, Srivastava A, Chou WC, Liu L, Hawkinson A, Glenn TC, et al. Transcriptome sequencing and annotation for the Jamaican fruit bat (*Artibeus jamaicensis*). *PLoS One* (2012) 7(11):e48472. doi:10.1371/journal.pone.0048472
8. Zhang G, Cowled C, Shi Z, Huang Z, Bishop-Lilly KA, Fang X, et al. Comparative analysis of bat genomes provides insight into the evolution of flight and immunity. *Science* (2013) 339(6118):456–60. doi:10.1126/science.1230835
9. Bratsch S, Wertz N, Chaloner K, Kunz TH, Butler JE. The little brown bat, *M. lucifugus*, displays a highly diverse V H, D H and J H repertoire but little evidence of somatic hypermutation. *Dev Comp Immunol* (2011) 35(4):421–30. doi:10.1016/j.dci.2010.06.004
10. Zhou P, Tachedjian M, Wynne JW, Boyd V, Cui J, Smith I, et al. Contraction of the type I IFN locus and unusual constitutive expression of IFN-alpha in bats. *Proc Natl Acad Sci U S A* (2016) 113(10):2696–701. doi:10.1073/pnas.1518240113
11. Ahn M, Cui J, Irving AT, Wang LF. Unique loss of the PYHIN gene family in bats amongst mammals: implications for inflammasome sensing. *Sci Rep* (2016) 6:21722. doi:10.1038/srep21722
12. Baker ML, Schountz T, Wang LF. Antiviral immune responses of bats: a review. *Zoonoses Public Health* (2013) 60(1):104–16. doi:10.1111/j.1863-2378.2012.01528.x
13. Schountz T. Immunology of bats and their viruses: challenges and opportunities. *Viruses* (2014) 6(12):4880–901. doi:10.3390/v6124880
14. Bean AG, Baker ML, Stewart CR, Cowled C, Deffrasnes C, Wang LF, et al. Studying immunity to zoonotic diseases in the natural host-keeping it real. *Nat Rev Immunol* (2013) 13(12):851–61. doi:10.1038/nri3551
15. Schountz T, Prescott J. Hantavirus immunology of rodent reservoirs: current status and future directions. *Viruses* (2014) 6(3):1317–35. doi:10.3390/v6031317
16. Mandl JN, Ahmed R, Barreiro LB, Daszak P, Epstein JH, Virgin HW, et al. Reservoir host immune responses to emerging zoonotic viruses. *Cell* (2015) 160(1–2):20–35. doi:10.1016/j.cell.2014.12.003
17. Drexler JF, Corman VM, Wegner T, Tateno AF, Zerbinati RM, Gloza-Rausch F, et al. Amplification of emerging viruses in a bat colony. *Emerg Infect Dis* (2011) 17(3):449–56. doi:10.3201/eid1703.100526
18. Yanagihara R, Amyx HL, Gajdusek DC. Experimental infection with Puumala virus, the etiologic agent of nephropathia epidemica, in bank voles (*Clethrionomys glareolus*). *J Virol* (1985) 55(1):34–8.
19. Botten J, Mirowsky K, Kusewitt D, Bharadwaj M, Yee J, Ricci R, et al. Experimental infection model for Sin Nombre hantavirus in the deer mouse (*Peromyscus maniculatus*). *Proc Natl Acad Sci U S A* (2000) 97(19):10578–83. doi:10.1073/pnas.180197197
20. Botten J, Mirowsky K, Kusewitt D, Ye C, Gottlieb K, Prescott J, et al. Persistent Sin Nombre virus infection in the deer mouse (*Peromyscus maniculatus*) model: sites of replication and strand-specific expression. *J Virol* (2003) 77(2):1540–50. doi:10.1128/JVI.77.2.1540-1550.2002
21. Schountz T, Acuna-Retamar M, Feinstein S, Prescott J, Torres-Perez F, Podell B, et al. Kinetics of immune responses in deer mice experimentally infected with Sin Nombre virus. *J Virol* (2012) 86(18):10015–27. doi:10.1128/JVI.06875-11
22. McGuire A, Miedema K, Fauver JR, Rico A, Aboellail T, Quackenbush SL, et al. Maporal hantavirus causes mild pathology in deer mice (*Peromyscus maniculatus*). *Viruses* (2016) 8(10):E286. doi:10.3390/v8100286
23. Easterbrook JD, Zink MC, Klein SL. Regulatory T cells enhance persistence of the zoonotic pathogen Seoul virus in its reservoir host. *Proc Natl Acad Sci U S A* (2007) 104(39):15502–7. doi:10.1073/pnas.0707453104
24. Schountz T, Prescott J, Cogswell AC, Oko L, Mirowsky-Garcia K, Galvez AP, et al. Regulatory T cell-like responses in deer mice persistently infected with Sin Nombre virus. *Proc Natl Acad Sci U S A* (2007) 104(39):15496–501. doi:10.1073/pnas.0707454104
25. Basler CF. Nipah and hendra virus interactions with the innate immune system. *Curr Top Microbiol Immunol* (2012) 359:123–52. doi:10.1007/82_2012_209
26. Mathieu C, Guillaume V, Volchkova VA, Pohl C, Jacquot F, Looi RY, et al. Nonstructural Nipah virus C protein regulates both the early host proinflammatory response and viral virulence. *J Virol* (2012) 86(19):10766–75. doi:10.1128/JVI.01203-12
27. Ramanan P, Edwards MR, Shabman RS, Leung DW, Endlich-Frazier AC, Borek DM, et al. Structural basis for Marburg virus VP35-mediated immune evasion mechanisms. *Proc Natl Acad Sci U S A* (2012) 109(50):20661–6. doi:10.1073/pnas.1213559109
28. Gralinski LE, Baric RS. Molecular pathology of emerging coronavirus infections. *J Pathol* (2015) 235(2):185–95. doi:10.1002/path.4454
29. Volchkova VA, Dolnik O, Martinez MJ, Reynard O, Volchkov VE. RNA editing of the GP gene of Ebola virus is an important pathogenicity factor. *J Infect Dis* (2015) 212(Suppl 2):S226–33. doi:10.1093/infdis/jiv309
30. Warren TK, Whitehouse CA, Wells J, Welch L, Heald AE, Charleston JS, et al. A single phosphorodiamidate morpholino oligomer targeting VP24

protects rhesus monkeys against lethal Ebola virus infection. *MBio* (2015) 6(1):e2344–2314. doi:10.1128/mBio.02344-14
31. Banadyga L, Dolan MA, Ebihara H. Rodent-adapted filoviruses and the molecular basis of pathogenesis. *J Mol Biol* (2016) 428(17):3449–66. doi:10.1016/j.jmb.2016.05.008
32. Thornbrough JM, Jha BK, Yount B, Goldstein SA, Li Y, Elliott R, et al. Middle east respiratory syndrome coronavirus NS4b protein inhibits host RNase L activation. *MBio* (2016) 7(2):e00258. doi:10.1128/mBio.00258-16
33. O'Shea TJ, Cryan PM, Cunningham AA, Fooks AR, Hayman DT, Luis AD, et al. Bat flight and zoonotic viruses. *Emerg Infect Dis* (2014) 20(5):741–5. doi:10.3201/eid2005.130539
34. Ching S, Zhang H, Belevych N, He L, Lai W, Pu XA, et al. Endothelial-specific knockdown of interleukin-1 (IL-1) type 1 receptor differentially alters CNS responses to IL-1 depending on its route of administration. *J Neurosci* (2007) 27(39):10476–86. doi:10.1523/JNEUROSCI.3357-07.2007
35. Wilhelms DB, Kirilov M, Mirrasekhian E, Eskilsson A, Kugelberg UO, Klar C, et al. Deletion of prostaglandin E2 synthesizing enzymes in brain endothelial cells attenuates inflammatory fever. *J Neurosci* (2014) 34(35):11684–90. doi:10.1523/JNEUROSCI.1838-14.2014
36. Miller MR, McMinn RJ, Misra V, Schountz T, Muller MA, Kurth A, et al. Broad and temperature independent replication potential of filoviruses on cells derived from old and new world bat species. *J Infect Dis* (2016) 214 (Suppl 3):S297–302. doi:10.1093/infdis/jiw199
37. Brook CE, Dobson AP. Bats as 'special' reservoirs for emerging zoonotic pathogens. *Trends Microbiol* (2015) 23(3):172–80. doi:10.1016/j.tim.2014.12.004
38. Zhou P, Cowled C, Marsh GA, Shi Z, Wang LF, Baker ML. Type III IFN receptor expression and functional characterisation in the pteropid bat, *Pteropus alecto*. *PLoS One* (2011) 6(9):e25385. doi:10.1371/journal.pone.0025385
39. Zhou P, Cowled C, Todd S, Crameri G, Virtue ER, Marsh GA, et al. Type III IFNs in pteropid bats: differential expression patterns provide evidence for distinct roles in antiviral immunity. *J Immunol* (2011) 186(5):3138–47. doi:10.4049/jimmunol.1003115
40. Jung D, Giallourakis C, Mostoslavsky R, Alt FW. Mechanism and control of V(D)J recombination at the immunoglobulin heavy chain locus. *Annu Rev Immunol* (2006) 24:541–70. doi:10.1146/annurev.immunol.23.021704.115830
41. Jackson KJ, Kidd MJ, Wang Y, Collins AM. The shape of the lymphocyte receptor repertoire: lessons from the B cell receptor. *Front Immunol* (2013) 4:263. doi:10.3389/fimmu.2013.00263
42. Butler JE, Wertz N. The porcine antibody repertoire: variations on the textbook theme. *Front Immunol* (2012) 3:153. doi:10.3389/fimmu.2012.00153
43. Peled JU, Kuang FL, Iglesias-Ussel MD, Roa S, Kalis SL, Goodman MF, et al. The biochemistry of somatic hypermutation. *Annu Rev Immunol* (2008) 26:481–511. doi:10.1146/annurev.immunol.26.021607.090236
44. Max EE, Fugmann S. *Fundamental Immunology*. Philadelphia: Lippincott (2013).
45. Baker ML, Tachedjian M, Wang LF. Immunoglobulin heavy chain diversity in Pteropid bats: evidence for a diverse and highly specific antigen binding repertoire. *Immunogenetics* (2010) 62(3):173–84. doi:10.1007/s00251-010-0425-4
46. Stavnezer J, Guikema JE, Schrader CE. Mechanism and regulation of class switch recombination. *Annu Rev Immunol* (2008) 26:261–92. doi:10.1146/annurev.immunol.26.021607.090248
47. Wynne JW, Di Rubbo A, Shiell BJ, Beddome G, Cowled C, Peck GR, et al. Purification and characterisation of immunoglobulins from the Australian black flying fox (*Pteropus alecto*) using anti-fab affinity chromatography reveals the low abundance of IgA. *PLoS One* (2013) 8(1):e52930. doi:10.1371/journal.pone.0052930
48. Butler JE, Wertz N, Zhao Y, Zhang S, Bao Y, Bratsch S, et al. The two suborders of chiropterans have the canonical heavy-chain immunoglobulin (Ig) gene repertoire of eutherian mammals. *Dev Comp Immunol* (2011) 35(3):273–84. doi:10.1016/j.dci.2010.08.011
49. Lee WT, Jones DD, Yates JL, Winslow GM, Davis AD, Rudd RJ, et al. Identification of secreted and membrane-bound bat immunoglobulin using a Microchiropteran-specific mouse monoclonal antibody. *Dev Comp Immunol* (2016) 65:114–23. doi:10.1016/j.dci.2016.06.024
50. Chua KB, Bellini WJ, Rota PA, Harcourt BH, Tamin A, Lam SK, et al. Nipah virus: a recently emergent deadly paramyxovirus. *Science* (2000) 288(5470):1432–5. doi:10.1126/science.288.5470.1432
51. Negrete OA, Levroney EL, Aguilar HC, Bertolotti-Ciarlet A, Nazarian R, Tajyar S, et al. EphrinB2 is the entry receptor for Nipah virus, an emergent deadly paramyxovirus. *Nature* (2005) 436(7049):401–5. doi:10.1038/nature03838
52. Lo MK, Miller D, Aljofan M, Mungall BA, Rollin PE, Bellini WJ, et al. Characterization of the antiviral and inflammatory responses against Nipah virus in endothelial cells and neurons. *Virology* (2010) 404(1):78–88. doi:10.1016/j.virol.2010.05.005
53. Wong KT, Grosjean I, Brisson C, Blanquier B, Fevre-Montange M, Bernard A, et al. A golden hamster model for human acute Nipah virus infection. *Am J Pathol* (2003) 163(5):2127–37. doi:10.1016/S0002-9440(10)63569-9
54. de Wit E, Bushmaker T, Scott D, Feldmann H, Munster VJ. Nipah virus transmission in a hamster model. *PLoS Negl Trop Dis* (2011) 5(12):e1432. doi:10.1371/journal.pntd.0001432
55. Williamson MM, Hooper PT, Selleck PW, Gleeson LJ, Daniels PW, Westbury HA, et al. Transmission studies of Hendra virus (equine morbillivirus) in fruit bats, horses and cats. *Aust Vet J* (1998) 76(12):813–8. doi:10.1111/j.1751-0813.1998.tb12335.x
56. Halpin K, Hyatt AD, Fogarty R, Middleton D, Bingham J, Epstein JH, et al. Pteropid bats are confirmed as the reservoir hosts of henipaviruses: a comprehensive experimental study of virus transmission. *Am J Trop Med Hyg* (2011) 85(5):946–51. doi:10.4269/ajtmh.2011.10-0567
57. Chakraborty AK, Chakravarty AK. Antibody-mediated immune response in the bat, *Pteropus giganteus*. *Dev Comp Immunol* (1984) 8(2):415–23. doi:10.1016/0145-305X(84)90048-X
58. Wellehan JF Jr, Green LG, Duke DG, Bootorabi S, Heard DJ, Klein PA, et al. Detection of specific antibody responses to vaccination in variable flying foxes (*Pteropus hypomelanus*). *Comp Immunol Microbiol Infect Dis* (2009) 32(5):379–94. doi:10.1016/j.cimid.2007.11.002
59. Peters C, Isaza R, Heard DJ, Davis RD, Moore SM, Briggs DJ. Vaccination of Egyptian fruit bats (*Rousettus aegyptiacus*) with monovalent inactivated rabies vaccine. *J Zoo Wildl Med* (2004) 35(1):55–9. doi:10.1638/03-027
60. Turmelle AS, Allen LC, Schmidt-French BA, Jackson FR, Kunz TH, McCracken GF, et al. Response to vaccination with a commercial inactivated rabies vaccine in a captive colony of Brazilian free-tailed bats (*Tadarida brasiliensis*). *J Zoo Wildl Med* (2010) 41(1):140–3. doi:10.1638/2008-0161.1
61. Paweska JT, Jansen van Vuren P, Masumu J, Leman PA, Grobbelaar AA, Birkhead M, et al. Virological and serological findings in *Rousettus aegyptiacus* experimentally inoculated with vero cells-adapted Hogan strain of Marburg virus. *PLoS One* (2012) 7(9):e45479. doi:10.1371/journal.pone.0045479
62. Amman BR, Jones ME, Sealy TK, Uebelhoer LS, Schuh AJ, Bird BH, et al. Oral shedding of Marburg virus in experimentally infected Egyptian fruit bats (*Rousettus aegyptiacus*). *J Wildl Dis* (2015) 51(1):113–24. doi:10.7589/2014-08-198
63. Paweska JT, Jansen van Vuren P, Fenton KA, Graves K, Grobbelaar AA, Moolla N, et al. Lack of Marburg virus transmission from experimentally infected to susceptible in-contact Egyptian fruit bats. *J Infect Dis* (2015) 212(Suppl 2):S109–18. doi:10.1093/infdis/jiv132
64. Schuh AJ, Amman BR, Jones ME, Sealy TK, Uebelhoer LS, Spengler JR, et al. Modelling filovirus maintenance in nature by experimental transmission of Marburg virus between Egyptian rousette bats. *Nat Commun* (2017) 8:14446. doi:10.1038/ncomms14446
65. Cogswell-Hawkinson A, Bowen R, James S, Gardiner D, Calisher CH, Adams R, et al. Tacaribe virus causes fatal infection of an ostensible reservoir host, the Jamaican fruit bat. *J Virol* (2012) 86(10):5791–9. doi:10.1128/JVI.00201-12
66. Turmelle AS, Jackson FR, Green D, McCracken GF, Rupprecht CE. Host immunity to repeated rabies virus infection in big brown bats. *J Gen Virol* (2010) 91(Pt 9):2360–6. doi:10.1099/vir.0.020073-0
67. Shaw ML, Garcia-Sastre A, Palese P, Basler CF. Nipah virus V and W proteins have a common STAT1-binding domain yet inhibit STAT1 activation from the cytoplasmic and nuclear compartments, respectively. *J Virol* (2004) 78(11):5633–41. doi:10.1128/JVI.78.11.5633-5641.2004

68. Frieman M, Yount B, Heise M, Kopecky-Bromberg SA, Palese P, Baric RS. Severe acute respiratory syndrome coronavirus ORF6 antagonizes STAT1 function by sequestering nuclear import factors on the rough endoplasmic reticulum/Golgi membrane. *J Virol* (2007) 81(18):9812–24. doi:10.1128/JVI.01012-07
69. Kopecky-Bromberg SA, Martinez-Sobrido L, Frieman M, Baric RA, Palese P. Severe acute respiratory syndrome coronavirus open reading frame (ORF) 3b, ORF 6, and nucleocapsid proteins function as interferon antagonists. *J Virol* (2007) 81(2):548–57. doi:10.1128/JVI.01782-06
70. Valmas C, Grosch MN, Schumann M, Olejnik J, Martinez O, Best SM, et al. Marburg virus evades interferon responses by a mechanism distinct from Ebola virus. *PLoS Pathog* (2010) 6(1):e1000721. doi:10.1371/journalppat.1000721
71. Zhang AP, Bornholdt ZA, Liu T, Abelson DM, Lee DE, Li S, et al. The ebola virus interferon antagonist VP24 directly binds STAT1 and has a novel, pyramidal fold. *PLoS Pathog* (2012) 8(2):e1002550. doi:10.1371/journal.ppat.1002550
72. Virtue ER, Marsh GA, Baker ML, Wang LF. Interferon production and signaling pathways are antagonized during henipavirus infection of fruit bat cell lines. *PLoS One* (2011) 6(7):e22488. doi:10.1371/journal.pone.0022488
73. Virtue ER, Marsh GA, Wang LF. Interferon signaling remains functional during henipavirus infection of human cell lines. *J Virol* (2011) 85(8):4031–4. doi:10.1128/JVI.02412-10
74. Anthony SJ, Epstein JH, Murray KA, Navarrete-Macias I, Zambrana-Torrelio CM, Solovyov A, et al. A strategy to estimate unknown viral diversity in mammals. *MBio* (2013) 4(5):e598–513. doi:10.1128/mBio.00598-13
75. Blachly JS, Ruppert AS, Zhao W, Long S, Flynn J, Flinn I, et al. Immunoglobulin transcript sequence and somatic hypermutation computation from unselected RNA-seq reads in chronic lymphocytic leukemia. *Proc Natl Acad Sci U S A* (2015) 112(14):4322–7. doi:10.1073/pnas.1503587112
76. Neave MJ, Sunarto A, McColl KA. Transcriptomic analysis of common carp anterior kidney during *Cyprinid herpesvirus* 3 infection: immunoglobulin repertoire and homologue functional divergence. *Sci Rep* (2017) 7:41531. doi:10.1038/srep41531

Conflict of Interest Statement: The authors declare that the research was conducted in the absence of any commercial or financial relationships that could be construed as a potential conflict of interest.

frontiers in Immunology

MINI REVIEW
published: 17 July 2017
doi: 10.3389/fimmu.2017.00827

Melanomacrophage Centers As a Histological Indicator of Immune Function in Fish and Other Poikilotherms

Natalie C. Steinel[1,2]* *and Daniel I. Bolnick*[1]

[1] Department of Integrative Biology, The University of Texas at Austin, Austin, TX, United States, [2] Department of Medical Education, Dell Medical School, The University of Texas at Austin, Austin, TX, United States

Melanomacrophage centers (MMCs) are aggregates of highly pigmented phagocytes found primarily in the head kidney and spleen, and occasionally the liver of many vertebrates. Preliminary histological analyses suggested that MMCs are structurally similar to the mammalian germinal center (GC), leading to the hypothesis that the MMC plays a role in the humoral adaptive immune response. For this reason, MMCs are frequently described in the literature as "primitive GCs" or the "evolutionary precursors" to the mammalian GC. However, we argue that this designation may be premature, having been pieced together from mainly descriptive studies in numerous distinct species. This review provides a comprehensive overview of the MMC literature, including a phylogenetic analysis of MMC distribution across vertebrate species. Here, we discuss the current understanding of the MMCs function in immunity and lingering questions. We suggest additional experiments needed to confirm that MMCs serve a GC-like role in fish immunity. Finally, we address the utility of the MMC as a broadly applicable histological indicator of the fish (as well as amphibian and reptilian) immune response in both laboratory and wild populations of both model and non-model vertebrates. We highlight the factors (sex, pollution exposure, stress, stocking density, etc.) that should be considered when using MMCs to study immunity in non-model vertebrates in wild populations.

Keywords: melanomacrophage center, germinal center, fish immunology, non-model organisms, comparative immunology

OPEN ACCESS

Edited by:
Andrew Steven Flies, University of Tasmania, Australia

Reviewed by:
Joachim Kurtz, Universität Münster, Germany
Hao-Ching Wang, Taipei Medical University, Taiwan

***Correspondence:**
Natalie C. Steinel
nsteinel@austin.utexas.edu

Specialty section:
This article was submitted to Comparative Immunology, a section of the journal Frontiers in Immunology

Received: *26 May 2017*
Accepted: *30 June 2017*
Published: *17 July 2017*

Citation:
Steinel NC and Bolnick DI (2017) Melanomacrophage Centers As a Histological Indicator of Immune Function in Fish and Other Poikilotherms. Front. Immunol. 8:827. doi: 10.3389/fimmu.2017.00827

INTRODUCTION

The study of immunology in wild vertebrates is hamstrung because many tools cannot readily be used in the field, and species-specific reagents do not exist for most non-model organisms. Melanomacrophage centers (MMCs) might offer a simple, cheap, and broadly applicable measure of adaptive immunity in poikilotherms. Here, we summarize and critically review this potentially valuable tool for wild immunology.

Abbreviations: MM, melanomacrophage; MMC, melanomacrophage center; GC, germinal center; RPMs, red pulp macrophages; TBMs, tingible body macrophages; FDC, follicular dendritic cell; T_{FH}, T follicular helper cell; Ig, immunoglobulin; SHM, somatic hypermutation; AID, activation-induced cytidine deaminase.

Melanomacrophages (or melanin-macrophages, MMs) are pigmented phagocytes found primarily in poikilotherm lymphoid tissues. MMs are darkly pigmented due to high lipofuscin, melanin, and haemosiderin content (1), making them histologically distinguishable *via* light microscopy (**Figure 1**). Nodular accumulations of closely packed MMs, known as MMCs, are primarily observed in the kidney, spleen, and liver. Generally, kidney and liver MMCs are diffuse and less structured, while splenic MMCs are more organized (2–4). As detailed below, the leading hypothesis is that MMCs represent a primitive site of adaptive immune system activation. As such, they may offer a valuable low-cost marker for measuring adaptive immunity across most of the vertebrate tree of life, in both model and non-model species. If so, MMCs could provide a widely applicable tool for wild immunology, as they are near-ubiquitous across vertebrates. MMCs are reported in over 130 fish species (Figure S1 and Table S1 in Supplementary Material) and are also present in amphibians and most reptiles (Figures S2 and S3 and Table S2 in Supplementary Material). This review centers on the well-studied piscine MMC but comments on the less-well known amphibian and reptile MMCs, where relevant.

NON-IMMUNOLOGICAL FUNCTIONS OF THE MMC

The MMC is thought to play dual roles, participating both in immune defenses and normal, non-immunological, physiological processes. This review focuses on MMC immune functions but touches briefly on non-immunological roles [detailed review by Wolke (5)]. Like other macrophages, MMs' primary function is phagocytosis. The presence and long-term storage of unmetabolized, effete materials, earned MMCs the title of "metabolic dumps" (6). This indigestible material, which gives MMs their characteristic pigmentation, can be of endogenous or exogenous origins. Endogenous materials are obtained through the phagocytosis of exhausted cells, particularly erythrocytes. Erythrophagocytosis by MMCs is widely reported and goes back to the earliest MMC description by Blumenthal in 1908 (7–13). More recent studies showed that turtle MMs can erythrophagocytose *in vitro* (14). The presence of degraded erythrocytes and hemosiderin suggests that MMs function in iron recycling (10, 11), much like the hemosiderin-laden splenic red pulp macrophages (RPMs) found in mammals (15). Exogenous materials, of natural or experimental origins, also collect within MMCs. Metal deposits (16, 17) and experimentally injected inert substances (13, 18–23) accumulate within MMs. These findings highlight the importance of MMCs in debris clearance and long-term storage of highly indigestible and/or toxic materials. The phagocytic nature of these cells is similar to that of the tingible body macrophage (TBM) found in the mammalian splenic germinal center (GC) (24). While the role of waste product repository is considered non-immunological, as we discuss in the following section, this physiological necessity may overlap with an important MMC immunological function: antigen retention.

IMMUNE FUNCTIONS OF THE MMC

Early descriptions proposed that MMCs function in both the innate and adaptive arms of the immune response (25). MM phagocytic activity is not limited to erythrocytes as they also phagocytose infectious materials (14, 21, 25–27). Turtle MMs are described as "aggressively phagocytic," attacking bacteria, fungi, and helminth parasite eggs *in vitro* (14). MMCs' close association with specialized capillaries in the spleen, known as ellipsoids (8, 28), suggests that they may scavenge blood borne pathogens. This notion is supported by the observation that, *in vivo*, MMCs quickly remove injected foreign materials from the circulation (13, 18–20, 27).

Morphological characteristics, organ location, and association with infection/immunization led to the hypothesis that MMCs are analogs, or "primitive" evolutionary precursors, of the mammalian GC (1, 5, 10, 21, 27–32). As such, they may participate in the adaptive immune response. In mammals, the GC response is crucial for the differentiation and clonal expansion of memory B cells and high-affinity plasma cells. Extensive experimentation has elucidated the complex spatial structure, cell–cell interactions, and molecular processes that occur within the mammalian GC (33). The GC has a well-defined architecture, with distinctive B-cell, follicular dendritic cell (FDC) and T follicular helper cell (T_{FH}) aggregates. Following antigen challenge, antigen-specific B cells accumulate and proliferate causing a transient increase in GC size (33). During the GC response, antigen-specific B cells, mediated by interactions with FDCs and T_{FH}, undergo clonal expansion and differentiate into memory and plasma cells (33).

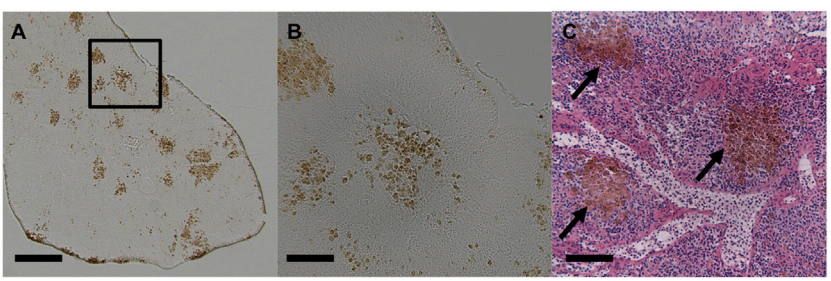

FIGURE 1 | Light micrographs of stickleback (*Gasterosteus aculeatus*) splenic melanomacrophage centers. **(A)** Unstained spleen at 50×. Scale bar equals 250 μm. Box outlines magnified section in panel **(B)**. **(B)** Unstained spleen at 200×. Scale bar equals 62.5 μm. **(C)** H&E-stained spleen at 200×, and black arrows indicate MMCs. Scale bar equals 62.5 μm.

FDCs serve as long-term antigen depots by maintaining intact antigen on their surface in the form of immune complexes (IC) (34). It is within GCs that antibody affinity maturation occurs. In this targeted microevolutionary process, immunoglobulin (Ig) genes undergo somatic hypermutation (SHM) and selection. In GC B cells, the enzyme activation-induced cytidine deaminase (AID) generates Ig gene mutations (35–37). GC B cells expressing mutated Ig genes are then selected based on their affinity for antigen (38, 39). This process hones antibody specificity and is necessary for an efficient humoral immune response.

Teleosts lack GCs; yet, nevertheless, they generate affinity-matured antibody in response to antigen challenge (40, 41). Descriptive studies, across many fish species, identified numerous similarities between GCs and MMCs (**Table 1**), raising the possibility that MMCs are the site of the teleost humoral adaptive immune response. MMs, like mammalian FDCs, stain positively with the CNA-42 monoclonal antibody (42) and express CSF1-R (43). Fish injected with both infectious and non-infectious substances demonstrated that MMCs are sites of antigen retention (18, 19, 21, 22, 30, 44–46). Notably, carp immunized with *Aeromonas hydrophila* retained antigen in and around splenic MMCs for at least a year (21). Antigen retained near or within MMCs is extracellular, trapped within IC, and the injection of preformed IC accelerates this retention (47, 48). While these findings highlight many similarities between MMs and FDCs, the erythrophagocytic and scavenging functions described in the previous section also suggest similarities between the MMC and RPMs and TBMs found in the mammalian spleen (**Table 1**).

Following immunization or infection, fish MMCs increase in size and/or number (10, 13, 26, 32, 49–52), much like mammalian GCs. Study of MMC kinetics in goldfish showed that MMs can both join existing aggregates or form new aggregates (22). Lymphoid cells are observed in close proximity to teleost MMCs (13, 21, 53) and increase in response to immunization (13). These studies, however, lacked species-specific reagents; so determination of cell identity was not possible. More recent immunohistochemical studies revealed MMC-adjacent Ig+ cells that increase in number in response to experimental infection (2–4). These Ig+ cells were presumed to be B cells, but the cells' identity has not been confirmed as these stains cannot differentiate between cells expressing Ig and those binding soluble Ig (or IC) on their cell surface (2–4). While some Ig+ cell aggregation was observed, they did not exhibit the highly compartmentalized structure characteristic of mammalian GCs (2–4). Unlike the GC, the MMC response in some teleost species does not correlate with an increased antibody production (13). More recently, AID-expressing cells were identified in or proximal to MMCs (54). Considering that AID expression is required for SHM in mammals, this finding strongly supports the notion of a GC-like MMC. However, SHM has not been directly documented in MMCs (54). These studies provide compelling evidence that MMCs and mammalian GCs likely perform similar functions, but differences do remain. A systematic investigation of MMC function has never been performed. Toward the end of this review, we suggest an experimental road map to fully characterize teleost MMC function.

TABLE 1 | Comparison of poikilotherm melanomacrophages with mammalian follicular dendritic cells (FDC), red pulp macrophages (RPM), and tingible body macrophages (TBM).

	Mammals			Poikilotherms
	FDC	**RPM**	**TBM**	**MMC**
Location	Spleen, LN	Spleen	Spleen, LN	Spleen, kidney, liver
Nodular aggregations	+	−	−	+
Erythrophagocytosis	−	+	−	+
Phagocytosis of exhausted/dead cells	−	−	+	+
Stain with CNA-42	+	−	−	+
Express CSF1-R	+	−	−	+
Retain antigen long-term within ICs	+	−	−	+
Found in close proximity to:				
Lymphoid cells	+	−	+	+
AID-expressing cells	+	−	+	+
B cells undergoing SHM	+	−	+	Unknown
Differentiating B cells	+	−	+	Unknown
Activated B cells	+	−	+	Unknown

LN, lymph node; IC, immune complexes; AID, activation-induced cytidine deaminase; SHM, somatic hypermutation.

EVOLUTIONARY HISTORY OF MMCs

Here, we consider both the likely timing and function of the early evolution of MMCs. MMCs are present in both jawless (Cyclostomata) and jawed vertebrates (Gnathostomata), implying that MMCs likely evolved at least 525 mya in a common ancestor of all Vertebrata (**Figure 2**). This evolutionary gain likely proceeds the evolution of adaptive immunity as jawed and jawless vertebrates evolved unique adaptive immune systems (55, 56). In "primitive" vertebrates like hagfish (Myxiniformes) and sharks and rays (Chondrichthyes), MMs are diffusely distributed, mostly in liver tissue. In contrast, bony vertebrates [Euteleostomi (a.k.a., Osteichthyes)] exhibit more aggregated MMs that form distinct MMCs primarily in the spleen and kidney (6). Because bony fish, amphibians, and reptiles share splenic aggregations, we infer that MMC concentration into the spleen must have evolved in a common ancestor to Euteleostomi. That is, splenic MMCs evolved between 430 and 460 mya, prior to the split between ray-finned fishes (Actinopterygii) from lobe-finned fishes and tetrapods (Sarcopterygii) but after their split from Chondrichthyes (**Figure 2**). Note that this inference is based on an assumption that MMCs are homologous structures (inherited from a common ancestor) rather than having independently evolved multiple times. This assumption has yet to be rigorously tested with transcriptomic and genetic data.

Melanomacrophage centers are retained in most poikilotherms, though they are reported absent in a handful of species. Admittedly, studies that did not locate MMCs (despite appreciable investigation) might be false negatives. Studies of MMCs in jawless vertebrates are underrepresented, with reports from only two Cyclostomata species (6). MMCs are reportedly absent in the lamprey, *Lampetra fluviatilis*, but present in hagfish (6) (**Figure 2**; Tables S1 and S3 in Supplementary Material). We are

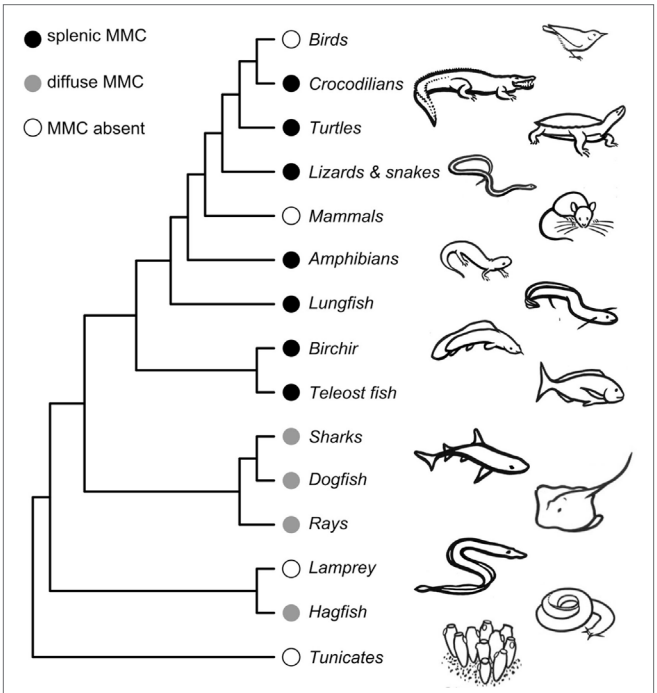

FIGURE 2 | Phylogeny showing melanomacrophage center (MMC) gains and losses across vertebrate species. Detailed phylogenies of fish, amphibian, and reptilian species can be found in Supplemental Material. The phylogeny is not time-calibrated and was plotted using the *ape* package in R (57), using a topology obtained from the OneZoom database (58). Drawings by Doreen J. Bolnick.

aware of only two bony fish species that reportedly lack MMCs: the fifteenspine stickleback, *Spinachia spinachia*, and the South American armored catfish, *Hypostomus francisci* (Figure S1 and Table S3 in Supplementary Material) (8, 59). In all three instances, MMC absence was determined by survey studies of a few individuals from a single location. From these limited studies, it is difficult to determine if the absence of MMCs represents species- or population-level variation. These absences should be investigated in greater detail but suggest that MMCs can be lost (or, replaced by another feature) without lethal effect. The sister genus to *Spinachia* (*Gasterosteus*, including threespine stickleback) has distinct MMCs (**Figure 1**), indicating that loss can occur over comparatively short macro-evolutionary time. MMCs have also been lost, probably two separate times, in Squamate reptiles (in vipers and a large snake clade including rat snakes and keelbacks) (Table S3 in Supplementary Material). But, MMCs were located in all amphibians we found reports for (Figure S2 in Supplementary Material), and in turtles, lizards, and crocodiles (Figure S3 in Supplementary Material). These aggregates are generally less organized than those observed in bony fish. MMCs are not observed in mammals or birds. If MMCs are indeed absent in birds and mammals, it is likely that they were independently lost. MMC loss in mammals is particularly note-worthy, because pigmented RPMs are still found in mammalian spleens. These macrophages perform physiological roles in erythrophagocytosis and metabolic recycling but have no known role in the GC response.

Collectively, evidence suggests several intriguing hypotheses for the evolutionary origins of MMs, MMCs, and mammalian GCs. We emphasize that these hypotheses are tentative but intriguing enough to warrant rigorous evaluation. The first hypothesis is that MMs initially evolved as molecular and cellular "garbage dumps" without a particular immunological role, in a common ancestor of all Vertebrata. Early MMs would have encountered pathogens or their antigens while acting in this clean-up capacity, which leads to a second hypothesis: MMs' incidental interaction with pathogens subsequently became entrenched and they gained immune function, perhaps in a common ancestor to Gnathostomata. The third (and oldest) hypothesis is that in early mammals, the MMCs evolved into GCs, with splenic RPMs remaining to carry out erythrocyte recycling function. We consider this third hypothesis in greater detail in the next section.

ARE MMCs AN EVOLUTIONARY PRECURSOR TO THE MAMMALIAN GC?

The notion of a "primitive GC"-like MMC has long been speculated (1, 5, 10, 21, 25, 27–32). However, this conclusion was drawn from descriptive studies, across many fish species, which did not directly investigate how MMC parameters correlate with immune function. As noted earlier, similarities between MMCs and GCs make this conclusion compelling (**Table 1**). Chiefly, both structures increase in size and/or number in response to immunization or infection (10, 13, 26, 31, 50–52). The structures also share cell types and expressed genes, but other observations call the "GC-precursor" hypothesis into question. Most notably, MMCs also respond to non-infectious settings, including poor body condition, pollution exposure, starvation, aging, and injury (discussed in detail below) (1, 10, 50, 60–63). When reconciling the MMC response to both infectious and non-infectious circumstances, these findings could be interpreted in several different ways.

First, it is possible that MMCs evolved from a purely physiological role, to gain immunological function, conducting both roles simultaneously. Subsequent GC evolution may be a case of sub-functionalization, in which a generalist tissue or cell type, performing multiple roles, evolves into specialist subpopulations. Second, the conditions that influence MMC status, including infection/immunization, are all associated with tissue destruction. So it is possible that the MMC response may not be immunological like the GC but may simply be a non-specific expansion of MMs in response to generalized tissue damage. In this case, the proposed immune function of MMCs may be a false lead.

Third, the association between MMCs and stress or tissue damage could be confounded with infection. Poor body condition, aging, injury, pollution exposure, and starvation can facilitate secondary infections. Thus, experiments that manipulate stressors might have incidental effects on infection, making it difficult to experimentally distinguish between non-infectious versus infectious MMC responses. Conversely, infection or pollution exposure may lead to poor body condition, injury, and/or suppressed appetite/starvation. As exposure to pathogens or contaminants

may not be readily detectible, an MMC response may mistakenly be attributed to other environmental or physiological factors.

FUTURE DIRECTIONS

To determine whether MMCs function in a GC-like capacity, further studies must directly test this hypothesis. Antigen-specific B-cell clonal expansion and high-affinity antibody production from mammalian GCs are the result of B-cell proliferation, differentiation, and SHM. To determine if MMCs are GC analogs, experiments must investigate if antigen-specific B cells proliferate and differentiate in association with MM aggregates. While the presence of AID-expressing cells within the MMC implies that affinity maturation is occurring (54), further experiments are necessary to assess whether antibody gene SHM occurs within and is dependent on the MMC. The mammalian GC response is T-cell dependent, as GC B-cell clonal expansion and differentiation requires help from T_{FH} cells (64). T-dependent (TD) antigens are proteins that induce GC reactions. T-independent (TI) antigens, in contrast, are polysaccharide based, cannot be presented to T_{FH} cells, and consequently do not stimulate a GC response (65). Therefore, a straightforward test of MMC function would compare the MMC response to TD and TI antigens. Using next generation sequencing tools, it would be useful to conduct a comparative transcriptomic analysis of MMCs and GCs to determine similarities and differences in gene expression. Lastly, MMC fine-scale structure should also be defined, for instance using single molecule fluorescent *in situ* hybridization to generate spatially explicit maps of gene expression and the distribution of cell types within MMCs. In the absence of functional studies that directly test the hypothesis of a GC-like MMC, an abundance of caution should be used when drawing conclusions regarding the nature of the MMC response in immune function.

NOTES FOR THE WILD IMMUNOLOGIST

Though fundamental experiments are needed to clarify the immunological significance of the MMC, we nevertheless assert that the MMC is potentially a practical biomarker of immune function in both laboratory and wild studies. As MMCs are evolutionarily conserved in many poikilothermic species, histological assays of the MMC state could provide a valuable tool for comparative studies of adaptive immunity across the diversity of vertebrates. Due to their inherent pigmentation, the MMC response can be easily visualized and quantified *via* light microscopy, without the need for costly species-specific reagents. This pigmentation also makes MMs highly autofluorescent, a feature that can be employed to isolate MMs *via* FACS sorting (43, 54). Though MMCs appear to be a useful bioindicator of poikilotherm immune function, several variables must be considered when designing and analyzing laboratory or wild studies.

Careful consideration should be given to sampling relevant tissues and quantifying the appropriate MMC parameters. Most immunological (and non-immunological) studies of the MMC focus on a single tissue. In light of the phylogenetic association of the MMC with different organs (6), researchers should be sure that the appropriate tissue(s) are sampled. The MMC response is quantified using various parameters including aggregate size, number, total pigmented area, pigmentation intensity, and aggregate circularity (shape factor). These variables can change through time in response to various stressors, and some are correlated (e.g., size and pigmented area). However, in the absence of a functional understanding of the nature of the MMC in the immune response it's not yet clear which metric(s) should be reported. Therefore, to avoid cherry-picking results, attention and justification should be given for choosing tissues to sample and MMC parameters to report.

The MMC can also respond to physiological and environmental changes. This presents a difficult situation for the wild immunologist. Histological MMC parameters vary in response to life history and environmental factors. Sex (60, 66), diet (52, 61, 63, 67), spawning phase (68), season (69), temperature (70), and UV exposure (71) influence MMC status. Several authors reported a linear correlation between age and elevated MMC metrics (17, 72–74). Studies also showed MMC responses to environmental stressors. In fish, farming increased MMC density compared to the same species raised in wild conditions (75). Other aquaculture variables, such as ranching time and stocking density, influence MMC metrics (67, 76).

Numerous investigations report correlations between "degraded environments" and MMC status. Decreased dissolved oxygen levels were associated with an increased fish MMC number (77). Several studies documented MMC responses to environmental contaminant exposure in wild fish and amphibians (66, 73, 77–81). However, many of these studies compared contaminant-exposed animals to those from uncontaminated "control" areas, without accounting for confounding effects of infection or other physiological or environmental factors. Nevertheless, controlled experimental exposure of lab-raised fish to environmental contaminants supports the notion of a pollutant-induced MMC response (52, 82–85). These observations, combined with MMC responses to life history and environmental factors (1, 10, 17, 31, 49, 50, 60–63, 72–74, 80), underscore the difficulty in interpreting MMC metrics in wild populations. If meaningful conclusions are to be drawn regarding the MMC response in wild (and lab-raised) animals, thoughtful consideration must be given to choosing appropriate controls and accounting for physiological and environmental variables in analyses. Therefore, we recommend wild studies employing the MMC assay without validation and appropriate controls be interpreted with caution.

CONCLUSION

The MMC shares many structural, cellular, and molecular similarities with the mammalian GC, suggesting an evolutionary tie to mammalian adaptive immunity. Parallels between these structures led researchers to recognize the potential for the MMC as a histological biomarker of poikilotherm immune response. We assert, however, that this tool should be used with caution. While descriptive studies have identified important features of the MMC, functional studies are needed to confirm its role in the adaptive immune system. If such studies validate this immunological tool,

they will pave the way for comparative studies of the evolutionary origins of vertebrate immunity and for experimental immunology in wild populations.

AUTHOR CONTRIBUTIONS

NS and DB wrote and edited the manuscript.

ACKNOWLEDGMENTS

We thank John Wiens for the reptile phylogeny, Mike Alfaro and Dan Rabosky for the ray-finned fish phylogeny, and Alex Pyron for the amphibian phylogeny. We thank Doreen J. Bolnick for providing line drawings for **Figure 2** and the Figure S1–S3 in Supplementary Material.

FUNDING

This work was supported by research funding from the Howard Hughes Medical Institute.

SUPPLEMENTARY MATERIAL

The Supplementary Material for this article can be found online at http://journal.frontiersin.org/article/10.3389/fimmu.2017.00827/full#supplementary-material.

REFERENCES

1. Agius C, Roberts RJ. Melano-macrophage centres and their role in fish pathology. *J Fish Dis* (2003) 26:499–509. doi:10.1046/j.1365-2761.2003.00485.x
2. Falk K, Press CM, Landsverk T, Dannevig BH. Spleen and kidney of Atlantic salmon (*Salmo salar* L.) show histochemical changes early in the course of experimentally induced infectious salmon anaemia (ISA). *Vet Immunol Immunopathol* (1995) 49:115–26. doi:10.1016/0165-2427(95)05427-8
3. Press CM, Dannevig BH, Landsverk T. Immune and enzyme histochemical phenotypes of lymphoid and nonlymphoid cells within the spleen and head kidney of Atlantic salmon (*Salmo salar* L.). *Fish Shellfish Immunol* (1994) 4:79–93. doi:10.1006/fsim.1994.1007
4. Bermúdez R, Vigliano F, Marcaccini A, Sitjà-Bobadilla A, Quiroga MI, Nieto JM. Response of Ig-positive cells to *Enteromyxum scophthalmi* (Myxozoa) experimental infection in turbot, *Scophthalmus maximus* (L.): a histopathological and immunohistochemical study. *Fish Shellfish Immunol* (2006) 21:501–12. doi:10.1016/j.fsi.2006.02.006
5. Wolke RE. Piscine macrophage aggregates: a review. *Annu Rev Fish Dis* (1992) 2:91–108. doi:10.1016/0959-8030(92)90058-6
6. Agius C. Phylogenetic development of melano-macrophage centres in fish. *J Zool* (1980) 191:11–31. doi:10.1111/j.1469-7998.1980.tb01446.x
7. Blumenthal R. Sur le rôle érythrolytique de la rate chez les poissons. *Comptes rendus hebdomadaires des seances de lAcademie des science* (1908) 146:190–1.
8. Yoffey JM. A contribution to the study of the comparative histology and physiology of the spleen, with reference chiefly to its cellular constituents: I. in fishes. *J Anat* (1929) 63:314–44.
9. Dawson AB. The hemopoietic response in the catfish, *Ameiurus nebulosus*, to chronic lead poisoning. *Biol Bull* (1935) 68:335–46. doi:10.2307/1537555
10. Agius C. The role of melano-macrophage centres in iron storage in normal and diseased fish. *J Fish Dis* (1979) 2:337–43. doi:10.1111/j.1365-2761.1979.tb00175.x
11. Fulop GMI, McMillan DB. Phagocytosis in the spleen of the sunfish *Lepomis* spp. *J Morphol* (1984) 179:175–95. doi:10.1002/jmor.1051790205
12. Agius C, Agbede SA. An electron microscopical study on the genesis of lipofuscin, melanin and haemosiderin in the haemopoietic tissues of fish. *J Fish Biol* (1984) 24:471–88. doi:10.1111/j.1095-8649.1984.tb04818.x
13. Herráez MP, Zapata AG. Structure and function of the melano-macrophage centres of the goldfish *Carassius auratus*. *Vet Immunol Immunopathol* (1986) 12:117–26. doi:10.1016/0165-2427(86)90116-9
14. Johnson JC, Schwiesow T, Ekwall AK, Christiansen JL. Reptilian melanomacrophages function under conditions of hypothermia: observations on phagocytic behavior. *Pigment Cell Res* (1999) 12:376–82. doi:10.1111/j.1600-0749.1999.tb00521.x
15. Klei TRL, Meinderts SM, van den Berg TK, van Bruggen R. From the cradle to the grave: the role of macrophages in erythropoiesis and erythrophagocytosis. *Front Immunol* (2017) 8:73. doi:10.3389/fimmu.2017.00073
16. Bunton TE, Baksi SM, George CJ, Frazier JM. Abnormal hepatic copper storage in a teleost fish (*Morone americana*). *Vet Pathol* (1987) 24:515–24. doi:10.1177/030098588702400608
17. Pulsford AL, Ryan KP, Nott JA. Metals and melanomacrophages in flounder, *Platichthys flesus*, spleen and kidney. *J Mar Biol Assoc U.K.* (1992) 72:483–98. doi:10.1017/S002531540003784X
18. Mackmull G, Michels NA. Absorption of colloidal carbon from the peritoneal cavity in the teleost, *Tautogolabrus adspersus*. *Am J Anat* (1932) 51:3–47. doi:10.1002/aja.1000510103
19. Ellis AE, Munroe A, Roberts RJ. Defence mechanisms in fish. 1. A study of the phagocytic system and the fate of intraperitoneally injected particulate material in the plaice (*Pleuronectes platessa* L.). *J Fish Biol* (1976) 8:67–79. doi:10.1111/j.1095-8649.1976.tb03908.x
20. Lamers CH, Parmentier HK. The fate of intraperitoneally injected carbon particles in cyprinid fish. *Cell Tissue Res* (1985) 242:499–503. doi:10.1007/BF00225414
21. Lamers CH, De Haas MJ. Antigen localization in the lymphoid organs of carp (*Cyprinus carpio*). *Cell Tissue Res* (1985) 242:491–8. doi:10.1007/BF00225413
22. Ziegenfuss MC, Wolke RE. The use of fluorescent microspheres in the study of piscine macrophage aggregate kinetics. *Dev Comp Immunol* (1991) 15:165–71. doi:10.1016/0145-305X(91)90007-L
23. Sayed AH, Younes HAM. Melanomacrophage centers in *Clarias gariepinus* as an immunological biomarker for toxicity of silver nanoparticles. *J Microsc Ultrastruct* (2016) 5:97–104. doi:10.1016/j.jmau.2016.07.003
24. Davies LC, Jenkins SJ, Allen JE, Taylor PR. Tissue-resident macrophages. *Nat Immunol* (2013) 14:986–95. doi:10.1038/sj.emboj.7600085
25. Roberts RJ. Melanin-containing cells of teleost fish and their relation to disease. In: Ribelin WE, Migaki G, editors. *The Pathology of Fishes*. University of Wisconsin (1975). p. 399–428.
26. Vogelbein WK, Fournie JW. Sequential development and morphology of experimentally induced hepatic melano-macrophage centres in *Rivulus marmoratus*. *J Fish Biol* (1987) 31:145–53. doi:10.1111/j.1095-8649.1987.tb05306.x
27. Brattgjerd S, Evensen O. A sequential light microscopic and ultrastructural study on the uptake and handling of *Vibrio salmonicida* in phagocytes of the head kidney in experimentally infected Atlantic salmon (*Salmo salar* L.). *Vet Pathol* (1996) 33:55–65. doi:10.1177/030098589603300106
28. Ferguson HW. The relationship between ellipsoids and melano-macrophage centres in the spleen of turbot (*Scophthalmus maximus*). *J Comp Pathol* (1976) 86:377–80. doi:10.1016/0021-9975(76)90005-0
29. Lamers CH. Histophysiology of a primary immune response against *Aeromonas hydrophila* in carp (*Cyprinus carpio* L.). *J Exp Zool* (1986) 238:71–80. doi:10.1002/jez.1402380109
30. Ellis AE. Antigen-trapping in the spleen and kidney of the plaice *Pleuronectes platessa* L. *J Fish Dis* (1980) 3:413–26. doi:10.1111/j.1365-2761.1980.tb00425.x
31. Kranz H, Peters N. Melano-macrophage centers in liver and spleen of ruffe (*Gymnocephalus cernua*) from the elbe estuary. *Helgol Meeresunters* (1984) 37:415–24. doi:10.1007/BF01989320

32. Secombes CJ. Histological changes in lymphoid organs of carp following injection of soluble or particulate antigens. *Dev Comp Immunol* (1982) 6(Suppl 2):53–8.
33. Victora GD, Nussenzweig MC. Germinal centers. *Annu Rev Immunol* (2012) 30:429–57. doi:10.1146/annurev-immunol-020711-075032
34. Heesters BA, Myers RC, Carroll MC. Follicular dendritic cells: dynamic antigen libraries. *Nat Rev Immunol* (2014) 14:495–504. doi:10.1038/nri3689
35. Muramatsu M, Kinoshita K, Fagarasan S, Yamada S. Class switch recombination and hypermutation require activation-induced cytidine deaminase (AID), a potential RNA editing enzyme. *Cell* (2000) 102:553–63. doi:10.1016/S0092-8674(00)00078-7
36. Nussenzweig A, Nussenzweig MC. Origin of chromosomal translocations in lymphoid cancer. *Cell* (2010) 141:27–38. doi:10.1016/j.cell.2010.03.016
37. Pavri R, Nussenzweig MC. AID targeting in antibody diversity. *Adv Immunol* (2011) 110:1–26. doi:10.1016/B978-0-12-387663-8.00005-3
38. Jacob J, Kelsoe G, Rajewsky K, Weiss U. Intraclonal generation of antibody mutants in germinal-centers. *Nature* (1991) 354:389–92. doi:10.1038/354389a0
39. Berek C, Berger A, Apel M. Maturation of the immune-response in germinal-centers. *Cell* (1991) 67:1121–9. doi:10.1016/0092-8674(91)90289-B
40. Solem ST, Stenvik J. Antibody repertoire development in teleosts – a review with emphasis on salmonids and *Gadus morhua* L. *Dev Comp Immunol* (2006) 30:57–76. doi:10.1016/j.dci.2005.06.007
41. Kaattari SL, Zhang HL, Khor IW, Kaattari IM, Shapiro DA. Affinity maturation in trout: clonal dominance of high affinity antibodies late in the immune response. *Dev Comp Immunol* (2002) 26:191–200. doi:10.1016/S0145-305X(01)00064-7
42. Vigliano FA, Bermúdez R, Quiroga MI, Nieto JM. Evidence for melano-macrophage centres of teleost as evolutionary precursors of germinal centres of higher vertebrates: an immunohistochemical study. *Fish Shellfish Immunol* (2006) 21:467–71. doi:10.1016/j.fsi.2005.12.012
43. Diaz-Satizabal L, Magor BG. Isolation and cytochemical characterization of melanomacrophages and melanomacrophage clusters from goldfish (*Carassius auratus,* L.). *Dev Comp Immunol* (2015) 48:221–8. doi:10.1016/j.dci.2014.10.003
44. Herráez MP, Zapata AG. Trapping of intraperitoneal-injected *Yersinia ruckeri* in the lymphoid organs of *Carassius auratus*: the role of melano-macrophages centres. *J Fish Biol* (1987) 31:235–7. doi:10.1111/j.1095-8649.1987.tb05321.x
45. Press CM, Evensen O, Reitan LJ, Landsverk T. Retention of furunculosis vaccine components in Atlantic salmon, *Salmo salar* L., following different routes of vaccine administration. *J Fish Dis* (1996) 19:215–24. doi:10.1111/j.1365-2761.1996.tb00128.x
46. Tsujii T, Seno S. Melano-macrophage centers in the aglomerular kidney of the sea horse (teleosts): morphologic studies on its formation and possible function. *Anat Rec* (1990) 226:460–70. doi:10.1002/ar.1092260408
47. Secombes CJ, Manning MJ. Comparative studies on the immune-system of fishes and amphibians – antigen localization in the carp *Cyprinus carpio* L. *J Fish Dis* (1980) 3:399–412. doi:10.1111/j.1365-2761.1980.tb00424.x
48. Secombes CJ, Manning MJ, Ellis AE. Localization of immune complexes and heat-aggregated immunoglobulin in the carp *Cyprinus carpio* L. *Immunology* (1982) 47:101.
49. Pierce KV, McCain B, Sherwood MJ. Histology of liver tissue from Dover sole. *Coastal Water Res Proj* (1977). p. 207–12.
50. Huizinga HW, Esch GW, Hazen TC. Histopathology of red-sore disease (*Aeromonas hydrophila*) in naturally and experimentally infected largemouth bass *Micropterus salmoides* (Lacepede). *J Fish Dis* (1979) 2:263–77. doi:10.1111/j.1365-2761.1979.tb00169.x
51. Kranz H. Changes in splenic melano-macrophage centers of dab *Limanda limanda* during and after infection with ulcer disease. *Dis Aquat Organ* (1989) 6:167–73. doi:10.3354/dao006167
52. Blazer VS, Fournie JW, Weeks-Perkins BA. Macrophage aggregates: biomarker for immune function in fishes? *Environ Toxicol Risk Assess* (1997) 6:360–75.
53. Ellis AE, De Sousa M. Phylogeny of the lymphoid system. I. A study of the fate of circulating lymphocytes in plaice. *Eur J Immunol* (1974) 4:338–43. doi:10.1002/eji.1830040505
54. Saunders HL, Oko AL, Scott AN, Fan CW, Magor BG. The cellular context of AID expressing cells in fish lymphoid tissues. *Dev Comp Immunol* (2010) 34:669–76. doi:10.1016/j.dci.2010.01.013
55. Flajnik MF, Kasahara M. Origin and evolution of the adaptive immune system: genetic events and selective pressures. *Nat Rev Genet* (2009) 11:47–59. doi:10.1038/nrg2703
56. Boehm T. Form follows function, function follows form: how lymphoid tissues enable and constrain immune reactions. *Immunol Rev* (2016) 271:4–9. doi:10.1111/imr.12420
57. Paradis E, Claude J, Strimmer K. APE: analyses of phylogenetics and evolution in R language. *Bioinformatics* (2004) 20:289–90. doi:10.1093/bioinformatics/btg412
58. Rosindell J, Harmon LJ. OneZoom: a fractal explorer for the tree of life. *PLoS Biol* (2012) 10:e1001406. doi:10.1371/journal.pbio.1001406
59. Sales CF, Silva RF, Amaral MGC, Domingos FFT, Ribeiro RIMA, Thomé RG, et al. Comparative histology in the liver and spleen of three species of freshwater teleost. *Neotrop Ichthyol* (2017) 15. doi:10.1590/1982-0224-20160041
60. Blazer VS, Wolke RE, Brown J, Powell CA. Piscine macrophage aggregate parameters as health monitors – effect of age, sex, relative weight, season and site quality in largemouth bass (*Micropterus salmoides*). *Aquat Toxicol* (1987) 10:199–215. doi:10.1016/0166-445X(87)90012-9
61. Agius C. The effects of splenectomy and subsequent starvation on the storage of haemosiderin by the melano-macrophages of rainbow trout *Salmo gairdneri* Richardson. *J Fish Biol* (1981) 18:41–4. doi:10.1111/j.1095-8649.1981.tb03757.x
62. Manrique WG, da Silva Claudiano G, Petrillo TR, de Castro MP, Pereira Figueiredo MA, de Andrade Belo MA, et al. Response of splenic melanomacrophage centers of *Oreochromis niloticus* (Linnaeus, 1758) to inflammatory stimuli by BCG and foreign bodies. *J Appl Ichthyol* (2014) 30:1001–6. doi:10.1111/jai.12445
63. Agius C, Roberts RJ. Effects of starvation on the melano-macrophage centres of fish. *J Fish Biol* (1981) 19:161–9. doi:10.1111/j.1095-8649.1981.tb05820.x
64. McHeyzer-Williams LJ, McHeyzer-Williams MG. Antigen-specific memory B cell development. *Annu Rev Immunol* (2005) 23:487–513. doi:10.1146/annurev.immunol.23.021704.115732
65. Fagarasan S, Honjo T. T-independent immune response: new aspects of B cell biology. *Science* (2000) 290:89–92. doi:10.1126/science.290.5489.89
66. Wolke RE, George CJ, Blazer VS. Parisitology and pathology of marine organisms of the world ocean. In: Hargis WJ, editor. *NOAA Tech Rep NMFS* (1985). p. 93–7.
67. Montero D, Blazer VS, Socorro J, Izquierdo MS, Tort L. Dietary and culture influences on macrophage aggregate parameters in gilthead seabream (*Sparus aurata*) juveniles. *Aquaculture* (1999) 179:523–34. doi:10.1016/S0044-8486(99)00185-4
68. Kumar R, Joy KP, Singh SM. Morpho-histology of head kidney of female catfish *Heteropneustes fossilis*: seasonal variations in melano-macrophage centers, melanin contents and effects of lipopolysaccharide and dexamethasone on melanins. *Fish Physiol Biochem* (2016) 42:1287–306. doi:10.1007/s10695-016-0218-2
69. Barni S, Bertone V, Croce AC, Bottiroli G, Bernini F, Gerzeli G. Increase in liver pigmentation during natural hibernation in some amphibians. *J Anat* (1999) 195:19–25. doi:10.1046/j.1469-7580.1999.19510019.x
70. De Souza Santos LR, Franco-Belussi L, Zieri R, Borges RE, de Oliveira C. Effects of thermal stress on hepatic melanomacrophages of *Eupemphix nattereri* (Anura). *Anat Rec* (2014) 297:864–75. doi:10.1002/ar.22884
71. Franco-Belussi L, Nilsson Sköld H, de Oliveira C. Internal pigment cells respond to external UV radiation in frogs. *J Exp Biol* (2016) 219:1378–83. doi:10.1242/jeb.134973
72. Brown CL, George CJ. Age-dependent accumulation of macrophage aggregates in the yellow perch, *Perca flavescens* (Mitchill). *J Fish Dis* (1985) 8:135–8. doi:10.1111/j.1365-2761.1985.tb01195.x
73. Couillard CM, Hodson PV. Pigmented macrophage aggregates: a toxic response in fish exposed to bleached-kraft mill effluent? *Environ Toxicol Chem* (1996) 15:1844–54. doi:10.1002/etc.5620151027
74. Christiansen JL, Grzybowski JM, Kodama RM. Melanomacrophage aggregations and their age relationships in the yellow mud turtle, *Kinosternon flavescens* (Kinosternidae). *Pigment Cell Res* (1996) 9:185–90. doi:10.1111/j.1600-0749.1996.tb00108.x

75. Kurtović B, Teskeredžić E, Teskeredžić Z. Histological comparison of spleen and kidney tissue from farmed and wild European sea bass (*Dicentrarchus labrax* L.). *Acta Adriat* (2008) 49:147–54.
76. Evans D, Nowak B. Effect of ranching time on melanomacrophage centres in anterior kidney and spleen of Southern bluefin tuna, *Thunnus maccoyii*. *Fish Shellfish Immunol* (2016) 59:358–64. doi:10.1016/j.fsi.2016.11.014
77. Fournie JW, Summers JK, Courtney LA, Engle VD, Blazer VS. Utility of splenic macrophage aggregates as an indicator of fish exposure to degraded environments. *J Aquat Anim Health* (2001) 13:105–16. doi:10.1016/0145-305X(91)90007-L
78. Pronina SV, Batueva MDD, Pronin NM. Characteristics of melanomacrophage centers in the liver and spleen of the roach *Rutilus rutilus* (Cypriniformes: Cyprinidae) in Lake Kotokel during the Haff disease outbreak. *J Ichthyol* (2014) 54:104–10. doi:10.1134/S003294521401010X
79. Haensly WE, Neff JM, Sharp JR. Histopathology of *Pleuronectes platessa* L. from Aber Wrac'h and Aber Benoit, Brittany, France: long-term effects of the Amoco Cadiz crude oil spill. *J Fish Dis* (1982) 5:365–91. doi:10.1111/j.1365-2761.1982.tb00494.x
80. Pierce KV, McCain BB, Wellings SR. Pathology of hepatomas and other liver abnormalities in English sole (*Parophrys vetulus*) from the Duwamish River estuary, Seattle, Washington. *J Natl Cancer Inst* (1978) 60:1445–53. doi:10.1093/jnci/60.6.1445
81. Jantawongsri K, Thammachoti P, Kitana J, Khonsue W, Varanusupakul P, Kitana N. Altered immune response of the rice frog *Fejervarya limnocharis* living in agricultura area with intensive herbicide utilization at Nan, Providence, Thailand. *Environ Asia* (2015) 8:68–74. doi:10.14456/ea.2015.9
82. Suresh N. Effect of cadmium chloride on liver, spleen and kidney melano macrophage centres in *Tilapia mossambica*. *J Environ Biol* (2009) 30:505–8.
83. Mela M, Randi MAF, Ventura DF, Carvalho CEV, Pelletier E, Oliveira Ribeiro CA. Effects of dietary methylmercury on liver and kidney histology in the neotropical fish *Hoplias malabaricus*. *Ecotoxicol Environ Saf* (2007) 68:426–35. doi:10.1016/j.ecoenv.2006.11.013
84. van der Weiden M, Bleumink R, Seinen W. Concurrence of P450 1A induction and toxic effects in the mirror carp (*Cyprinus carpio*), after administration of allow dose of 2, 3, 7, 8-tetrachlorodibenzo-p-dioxin. *Aquat Toxicol* (1994) 29:147–62. doi:10.1016/0166-445X(94)90065-5
85. Kranz H, Gercken J. Effects of sublethal concentrations of potassium dichromate on the occurrence of splenic melano-macrophage centres in juvenile plaice, *Pleuronectes platessa*, L. *J Fish Biol* (1987) 31:75–80. doi:10.1111/j.1095-8649.1987.tb05296.x

Conflict of Interest Statement: The authors declare that the research was conducted in the absence of any commercial or financial relationships that could be construed as a potential conflict of interest.

frontiers in Immunology

REVIEW
published: 19 December 2017
doi: 10.3389/fimmu.2017.01749

Tracing the Origins of IgE, Mast Cells, and Allergies by Studies of Wild Animals

Lars Torkel Hellman, Srinivas Akula, Michael Thorpe and Zhirong Fu*

Department of Cell and Molecular Biology, Uppsala University, Uppsala, Sweden

In most industrialized countries, allergies have increased in frequency quite dramatically during the past 50 years. Estimates show that 20–30% of the populations are affected. Allergies have thereby become one of the major medical challenges of the twenty-first century. Despite several theories including the hygiene hypothesis, there are still very few solid clues concerning the causes of this increase. To trace the origins of allergies, we have studied cells and molecules of importance for the development of IgE-mediated allergies, including the repertoire of immunoglobulin genes. These studies have shown that IgE and IgG most likely appeared by a gene duplication of IgY in an early mammal, possibly 220–300 million years ago. Receptors specific for IgE and IgG subsequently appeared in parallel with the increase in Ig isotypes from a subfamily of the recently identified Fc receptor-like molecules. Circulating IgE levels are generally very low in humans and laboratory rodents. However, when dogs and Scandinavian wolfs were analyzed, IgE levels were found to be 100–200 times higher compared to humans, indicating a generally much more active IgE synthesis in free-living animals, most likely connected to intestinal parasite infections. One of the major effector molecules released upon IgE-mediated activation by mast cells are serine proteases. These proteases, which belong to the large family of hematopoietic serine proteases, are extremely abundant and can account for up to 35% of the total cellular protein. Recent studies show that several of these enzymes, including the chymases and tryptases, are old. Ancestors for these enzymes were most likely present in an early mammal more than 200 million years ago before the separation of the three extant mammalian lineages; monotremes, marsupials, and placental mammals. The aim is now to continue these studies of mast cell biology and IgE to obtain additional clues to their evolutionary conserved functions. A focus concerns why the humoral immune response involving IgE and mast cells have become so dysregulated in humans as well as several of our domestic companion animals.

Keywords: IgE, Fc receptor, mast cell, IgE homeostasis, allergy, dermatitis, asthma

OPEN ACCESS

Edited by:
Greg Woods,
University of Tasmania, Australia

Reviewed by:
Axel Lorentz,
University of Hohenheim, Germany
Pierre Boudinot,
Institut National de la Recherche Agronomique, France

****Correspondence:***
Lars Torkel Hellman
lars.hellman@icm.uu.se

Specialty section:
This article was submitted to Comparative Immunology, a section of the journal Frontiers in Immunology

Received: *03 October 2017*
Accepted: *24 November 2017*
Published: *19 December 2017*

Citation:
Hellman LT, Akula S, Thorpe M and Fu Z (2017) Tracing the Origins of IgE, Mast Cells, and Allergies by Studies of Wild Animals. Front. Immunol. 8:1749. doi: 10.3389/fimmu.2017.01749

INTRODUCTION

During the past 50 years, allergies has increased in prevalence quite dramatically and in most industrialized countries 20–30% of the population are affected. In some school classes, the percentage of affected children can reach as high as 50. Allergies have thereby become one of the major medical challenges of the twenty-first century. Although relatively few die from an anaphylactic shock, the

severest form of allergic reaction, there are extensive burdens for sufferers, which in turn can also cause major economic loss. Asthma in children has in the USA been estimated to cost 56 billion $ per year and asthma in adults to cost 19 billion € per year in the EU so allergies involves large costs for the society (1, 2). Allergies not only affect humans but also our close domestic companions, including dogs, cats, and horses. In dogs, 3–15%, depending on the breed, suffer from atopic dermatitis, a type of allergic skin disease (3–5). By contrast, cats and horses suffer primarily from asthma. This indicates that domestication may be one contributing factor in this process. Rodents are the most frequently used animal models in allergy research and the numerous inbred strains of mice and rats may be seen as a form of domestication. However, neither rats nor mice can be considered naturally allergic. To obtain allergic mice or rats, these animals needs to be triggered by relatively high allergen doses and often complimented with additional immune stimulators to show allergy-like symptoms (6–8). These symptoms also disappear as soon as the sensitization protocol is terminated. Therefore, a life under controlled conditions with low pathogen load does not necessarily result in the induction of hypersensitivity. However, western lifestyle, with high hygiene levels, has been indicated as a potential contributing factor to the increase in allergy prevalence and been termed the "hygiene hypothesis" (9–11). The contact with high levels of bacteria, viruses, and parasites has likely been the normal condition for our immune system during the past millions of years of evolution (12). This has been an important component for the immune system to become educated and if we remove the normal triggers in our daily life, we may be more likely to develop allergies. There is evidence supporting this hypothesis but there is also data that do not fit into this model. One previously mentioned example is rodents living under controlled conditions in animal houses. There are certainly other contributing factors of major importance. Therefore in order to look deeper into these questions, we have turned our interest to the components of our immune system that are involved in an allergic immune response. This approach can be used to see if by studying of an array of different wild, domestic, and non-domestic animals, it is possible to trace the origins of these components and the factors that have resulted in the massive increase in allergies in humans and other domestic animals.

THE INDUCTION OF AN ALLERGIC IMMUNE RESPONSE

The absolute majority of allergies in humans belong to the immunoglobulin (Ig) E-mediated allergies, which also are named atopic allergies. The major focus of this review will be on this type of allergy, where dendritic cells, IgE, and IgE-binding cells, primarily mast cells, and basophils are central players (13).

The first time we are exposed to an allergen there will be no visible response. However, the immune system may start to recognize the target molecule *via* uptake of the protein antigen, the allergen, by local dendritic cells. Generally, allergens are proteins of a relatively low molecular weight and are often also relatively stable proteins, indicating they can more easily enter the mucosa in a native conformation. Dendritic cells are abundant at sites where allergens generally enter the body, for example, the skin, the lung, or the intestinal mucosa. These cells then process some of the protein into peptides of variable length in endosomal compartments using lysosomal proteases. The peptides, generally between 12 and 18 amino acids, are then presented onto major histocompatibility complex (MHC) class II molecules on the cell surface of the dendritic cell (**Figure 1**). A T helper cell may then recognize this peptide MHC complex with its specific T cell receptor (TCR) and when supported by several additional receptor ligand interactions, including CD28-B7:1 or B7:2, CD40L–CD40, CD48R–CD22, CD2–LFA3, the T cell becomes activated and starts to proliferate. Furthermore, the activated cell produces cytokines and also to upregulate receptors and receptor ligands that can support and trigger other immune cells (**Figure 1**). If there is no intracellular parasite or other potent danger signal in the area of allergen entry, the T cells are generally becoming T-helper cells of type 2, so called TH2 cells. TH2 cells promote humoral immunity, consisting primarily of soluble factors, involving B cells and Igs and not in cell-mediated immunity where cytotoxic T cells (CTLs) and NK cells are involved. The TH2 cells produce cytokines, including IL-4, IL-13, IL-5, IL-10, and sometimes also TNF-α (**Figure 1**) (14, 15). The B cells in the area of allergen contact bind with their surface IgM to the native protein antigen and thereby receive signal 1 to become activated. These B cells are then triggered by local IL-4 and/or IL-13 to switch to IgE and IgG1 producing cells in mice, and IgE and IgG4 in humans (**Figure 1**) (16–18). The locally produced IgE can then bind to high-affinity receptors on cells in the tissue. The cells that express the high-affinity receptor for IgE are primarily mast cells and basophilic granulocytes (**Figure 1**). Both of these cells store histamine and can also produce potent lipid mediators including prostaglandins and leukotrienes, which when released from the cells give the characteristic symptoms of allergies including tissue swelling, broncho constriction, and drop in blood pressure. The latter effects occur if mast cell activation involves larger regions of the body. This entire process, from the first antigen contact to the development of IgE and mast cell bound IgE, is termed sensitization and this can take weeks to months or even years to develop (13). In most cases, the immune system regulates itself so that more IgG than IgE is produced meaning no hypersensitivity appears and the individual does not become allergic (**Figure 1**). However, if this is dysregulated and more IgE is produced, the tissue becomes overly sensitive to contact with the allergen. When a sensitized person comes in contact with the same subsequent allergen, the mast cells release a number of vasoactive substances, which results in tissue swelling due to the influx of liquid into the tissue from the blood. The activation of mast cells also results in the recruitment of eosinophils to the tissue, a process at least partly dependent on locally produced IL-5 (**Figure 1**).

MAST CELLS AND BASOPHILS

Mast cells and basophils are the only two cells that express the complete high-affinity receptor for IgE (FcεRI) with all four polypeptide subunits (19) (**Figures 2A–C**). The FcεRI receptor belongs to a larger family of receptors binding to the constant domains of Igs, including IgG, IgA, and IgM receptors. The

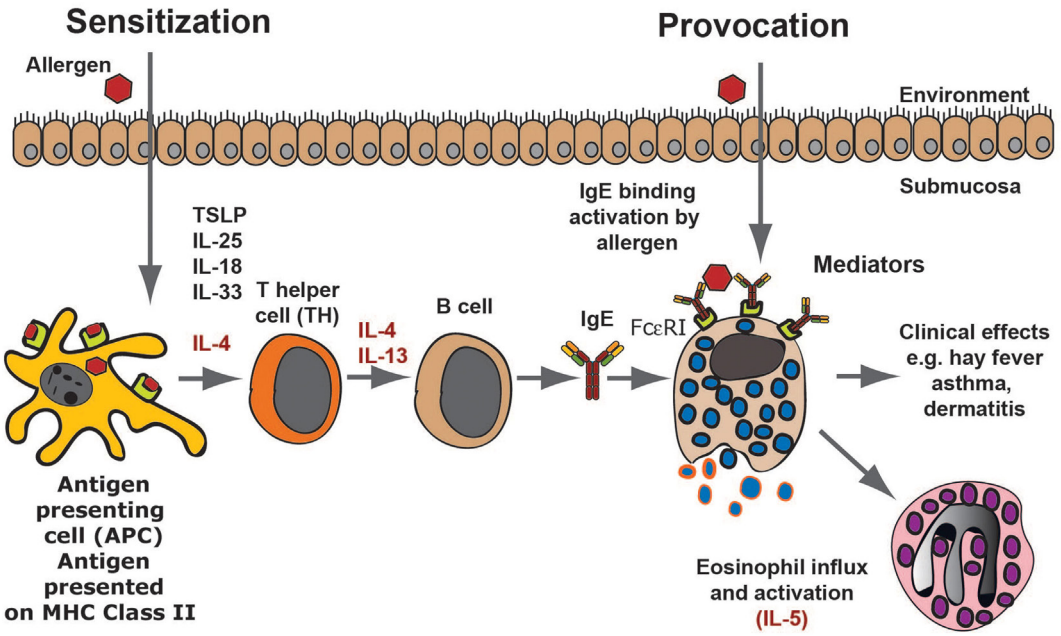

FIGURE 1 | An allergic immune response. The figure presents a schematic overview of an allergic immune response starting with the allergens first contact when it enters through the skin, lungs, or intestinal mucosa. Antigen-presenting cells, primarily dendritic cells, take up the antigen and process it into peptides, which are subsequently presented onto major histocompatibility complex class II molecules to naïve T cells. In an environment lacking major danger signals and in the presence of certain TH2-promoting cytokines, the T cell becomes a TH2 type of T cell. These T cells produce IL-4 and IL-13, which stimulates B cells to switch to IgE production. The IgE produced by these local B cells binds tissue mast cells, which have now become sensitized and can respond by degranulation as well as prostaglandin and leukotriene synthesis, which provides all the symptoms of an allergic reaction. As a next step, locally produced IL-5 results in eosinophil influx and the induction of a late phase response.

complete IgE receptor consists of an α chain, which is primarily located outside of the cell where it binds IgE; a β chain, which is a membrane protein with four transmembrane regions; and two identical γ chains. The γ chain has the majority of the protein on the cytoplasmic side of the membrane where it acts as the primary signal transducing subunit (**Figure 2C**). Other cells, such as dendritic cells and monocytes can in humans also express low levels of the IgE receptor; however in these cases, it is usually a three polypeptide variant, which lacks the β chain. This expression on dendritic cells and monocytes seems to be involved in IgE internalization and degradation, possibly also in antigen presentation (19). IgE binds to the FcεRI with high affinity, in the range of 10^{10} (20). Monomeric non-cross-linked IgE does not activate the mast cell or basophil. However, when two IgE-molecules bind the same allergen molecule they become cross-linked and if both molecules sit on the receptors, these receptors also become cross-linked. This receptor cross-linking changes the environment on the inside of the cell, favoring kinase activation at the expense of access of phosphatases to the cytoplasmic parts of the receptor subunits. This results in the phosphorylation of a number of cytoplasmic motifs on the β and the γ chains of the receptor (21). These activation motifs are called immune receptor tyrosine-based activation motifs, commonly referred to as ITAMs (**Figure 2C**). The phosphorylation of these short motifs result in the binding of signaling molecules including Lyn and Syk, which in turn result in a cascade of reactions including Ca^{2+} release from intracellular stores, activation of phospholipase A2 and thereby the release of arachidonic acid from membrane phospholipids and the generation of prostaglandins and leukotrienes by two different enzyme pathways. The receptor phosphorylation also results in the production of PIP3 and a few other intracellular signaling molecules as well as in the activation of the cells to release their pre-stored granule material, including histamine, heparin, and the very abundant granule proteases (**Figures 2A,B**).

Mast cells or mast cell-like cells have been described in most vertebrate lineages including mammals, birds, reptiles, amphibians, and bony fishes (29–32). Mast cell-like cells have also been described in an early ancestor of the vertebrates, the tunicate, or sea squirt (33, 34). Interestingly, these mast cell-like cells contain both histamine and heparin as well as some kind of trypsin-like enzyme indicating a relatively close resemblance to mammalian mast cells (33, 34).

IgE

Immunoglobulins and TCRs first appeared with jawed vertebrates. There has been a parallel increase in the different vertebrate lineages in the complexity of Ig classes and isotypes during vertebrate evolution through gene duplications, which have sometimes been followed by gene losses. In general, cartilaginous fish have three Ig classes IgM and IgW, which are of the classical type with both heavy and light chains and a third IgNAR, which lacks the light chain. The entire antigen-binding

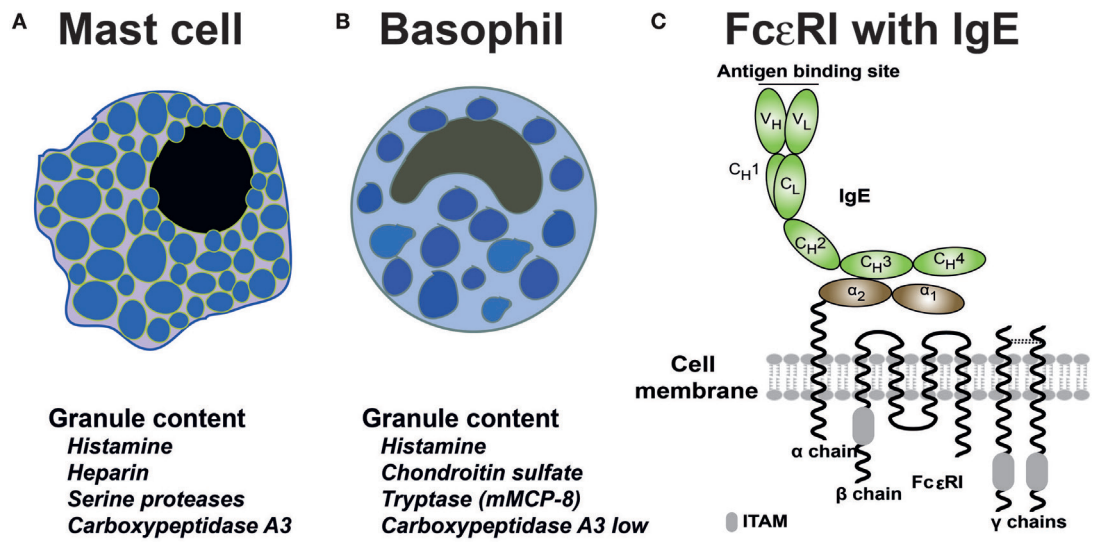

FIGURE 2 | Schematic representation of mast cells, basophils and the high-affinity IgE receptor. Below the schematic pictures of the cells is in **(A,B)** a listing of the most important granule components of the two cell types. The human basophil expresses the mast cell tryptase whereas the mouse basophil expresses mMCP-8, the first basophil-specific protein to be identified (22–24). **(C)** The high-affinity receptor for IgE consists of four subunits; the α chain, which binds the CH3 domain of IgE with its membrane proximal α2 domain, the β chain that spans the membrane four times and has one immunoreceptor tyrosine-based activation motif (ITAM) in its cytoplasmic region (marked by a gray box), and two identical γ chains, which are mostly intracellular, serving as the major signal transducing subunit (25). The γ chains contain two ITAMS, one in each subunit (26–28).

site of the IgNAR thereby resides in the variable region of the heavy chain (35). Interestingly, the cartilaginous fish have a different organization of the Ig locus compared to all other vertebrates in that there are multiple genes for each Ig class and there are large numbers of such small clusters compared to single genes, which are present in most other vertebrates. The genes are organized as small rearranging units consisting of a single V, one or two D segments, followed by a single J and subsequent constant region (V-D-D-J-C). This is in marked contrast to the translocon model used by almost all other vertebrates with multiple V regions followed by a number of D segments, often over 20, and then 3-7J segments followed by constant region gene segments (35). When looking at the bony fishes, which represent the largest single group of vertebrates, there are varying numbers of Ig classes and isotypes. As one example the gar, which represent an early branch of the bony fishes, seems to primarily depend on one Ig class IgM whereas the zebra fish and the rainbow trout expresses three Ig classes, each with only one isotype, IgM, IgD, and IgT/Z (T for teleost) (**Figure 3**) (36, 37). Amphibians as exemplified by the clawed frog *Xenopus laevis* or *tropicalis* have five Ig classes, also here with only one isotype each, i.e., IgM, IgD, IgY, IgX, and IgF (38). IgX appears to be the functional equivalent of IgA in birds and mammals, and IgY is the ancestor of mammalian IgG and IgE (**Figure 3**) (38). Reptiles have similar to the bony fishes very varying numbers of Ig classes and isotypes. For example, the anolis lizard (*Anolis carolinensis*) having only three Ig classes also here with one isotype for each class, IgM, IgD, and IgY whereas the American and Chinese alligators have 4 Ig classes and 10 isotypes (**Figure 3**) (39–41). The alligators have experienced a series of gene duplications resulting in several functional as well as a few pseudogenes for IgM, IgA, and IgY (**Figure 3**). Birds have relatively few Ig classes and isotypes, probably due to later gene losses. For example, chickens have only three Ig genes, one each for IgM, IgA, and IgY (42).

In general, mammals have five Ig classes IgM, IgD, IgG, IgE, and IgA, and a varying number of isotypes. Quite big differences have been observed between different mammalian species. For example, humans have nine isotypes, due to four different IgG isotypes and two IgA isotypes. Mice have 8 due to that they have only 1 IgA isotype, and rabbits have as many as 17 because of having 13 different copies of the IgA gene (**Figure 3**).

Interestingly, much of the functional diversification of the different Ig classes already came with the first tetrapods as the ancestors of IgA (IgX), IgG, and IgE (IgY) appeared with frogs and other amphibians. The most recent addition to the complexity came with early mammals from a gene duplication of IgY. One of the copies lost the second, CH2 encoding domain, and became a four domain Ig class with V, CH1, CH2, and CH3 domains. This gene was named IgG whereas the second duplicate, which became IgE, maintained all domains of IgY and thereby containing V, CH1, CH2, CH3, and CH4 domains (**Figure 4**) (43–46). Similarly to IgG, IgA also lost one domain in mammals, the CH2 domain, and instead gained a flexible hinge region (**Figure 4**).

IgG, IgE, and IgA are found in all three extant mammalian lineages in very similar forms (43–47). The gene duplication of IgY made it possible to separate the function of the mast cell activation *via* IgE, and the major plasma antibody, IgG, with functions in complement activation, immune complex clearance, and

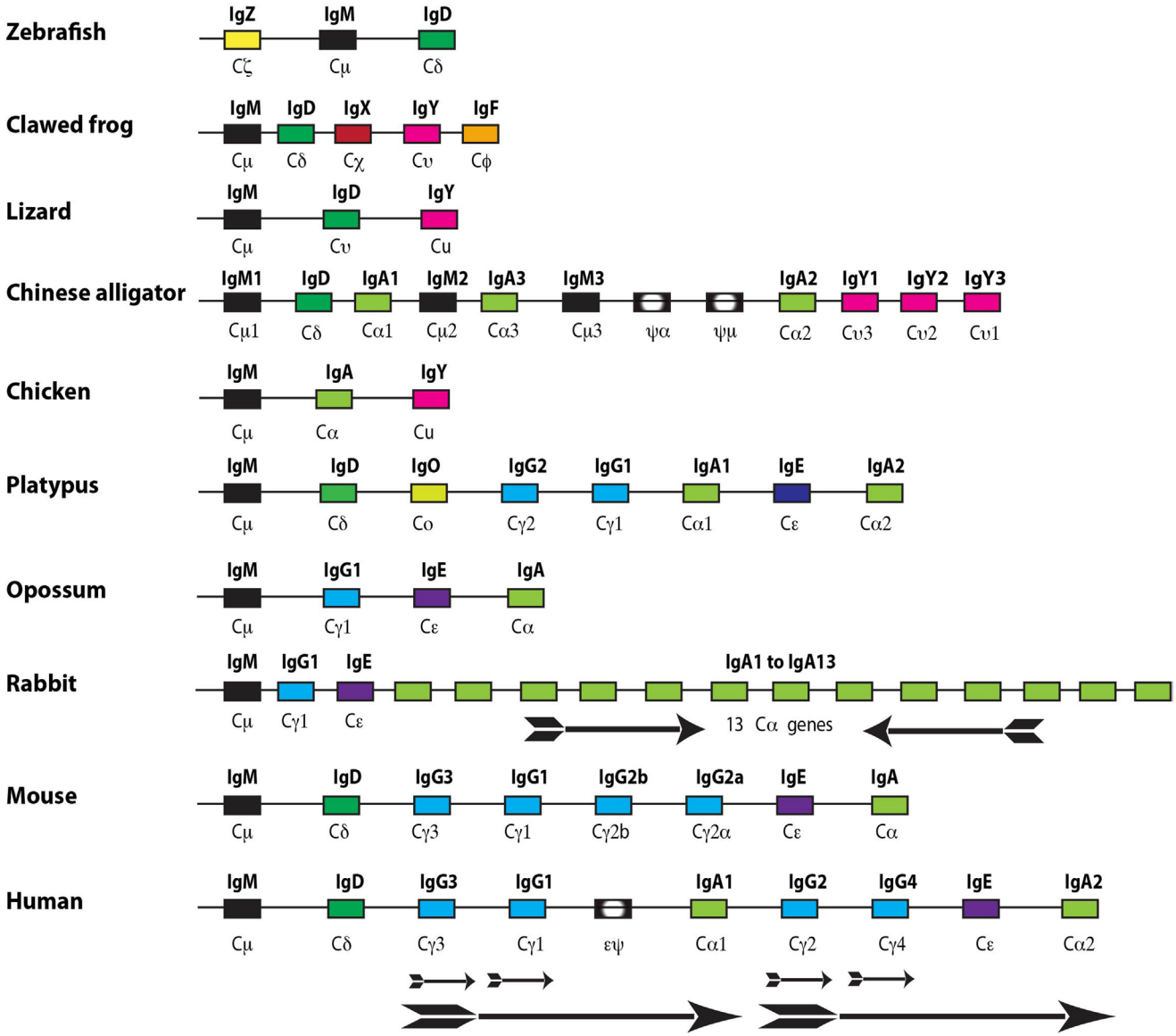

FIGURE 3 | The immunoglobulin heavy chain locus from a panel of different jawed vertebrates. The different genes are color coded with IgG in light blue, IgE in purple, IgM in black, IgA in light green, IgD in dark green, IgO in greenish yellow, IgZ in yellow, IgX in red, IgY in purple, and IgF in orange. The arrows show local duplications, and the direction of the arrow represents the transcription orientation of the genes within the duplicate. Pseudo genes are marked with black boxes with a white inner oval and a pseudo sign. The figure is not to scale.

antibody-dependent cellular cytotoxicity (ADCC). Interestingly the marsupials, exemplified by the American opossum only have four Ig classes, IgM, IgG, IgE, and IgA, and only one isotype for each Ig class (44, 48). This is likely due to a secondary loss of IgD. The monotremes, which are an early branch on the mammalian tree with only three extant surviving members of egg-laying mammals, the platypus and two variants of the ant-eating echidnas, the short and the long nosed, have unlike the marsupials all five mammalian Ig classes as well as one additional Ig class IgO (45, 47, 49–51). The gene for IgO is most likely a remaining extra duplicate of IgY, which seems to be expressed only in the spleen at very low levels, indicating that it is primarily a non-functional remnant of the duplication process (51). The platypus has eight isotypes, IgM, IgD, IgO, IgG1, IgG2, IgE, IgA1, and IgA2. One interesting observation in mammals is that despite the very varying number of isotypes across the species there always seems to be only one functional gene for IgE (46). Currently, the only exception to this rule is within the horse, which may have two genes. This indicates that IgE needs to be kept under very stringent control, most likely due to its potent mast cell-activating properties. Interestingly, there are three copies of the IgE gene in the human genome; two of them are a result of what appears to be a large duplication involving genes for IgG, IgE, and IgA (**Figure 3**) (52, 53). This duplication resulted in a

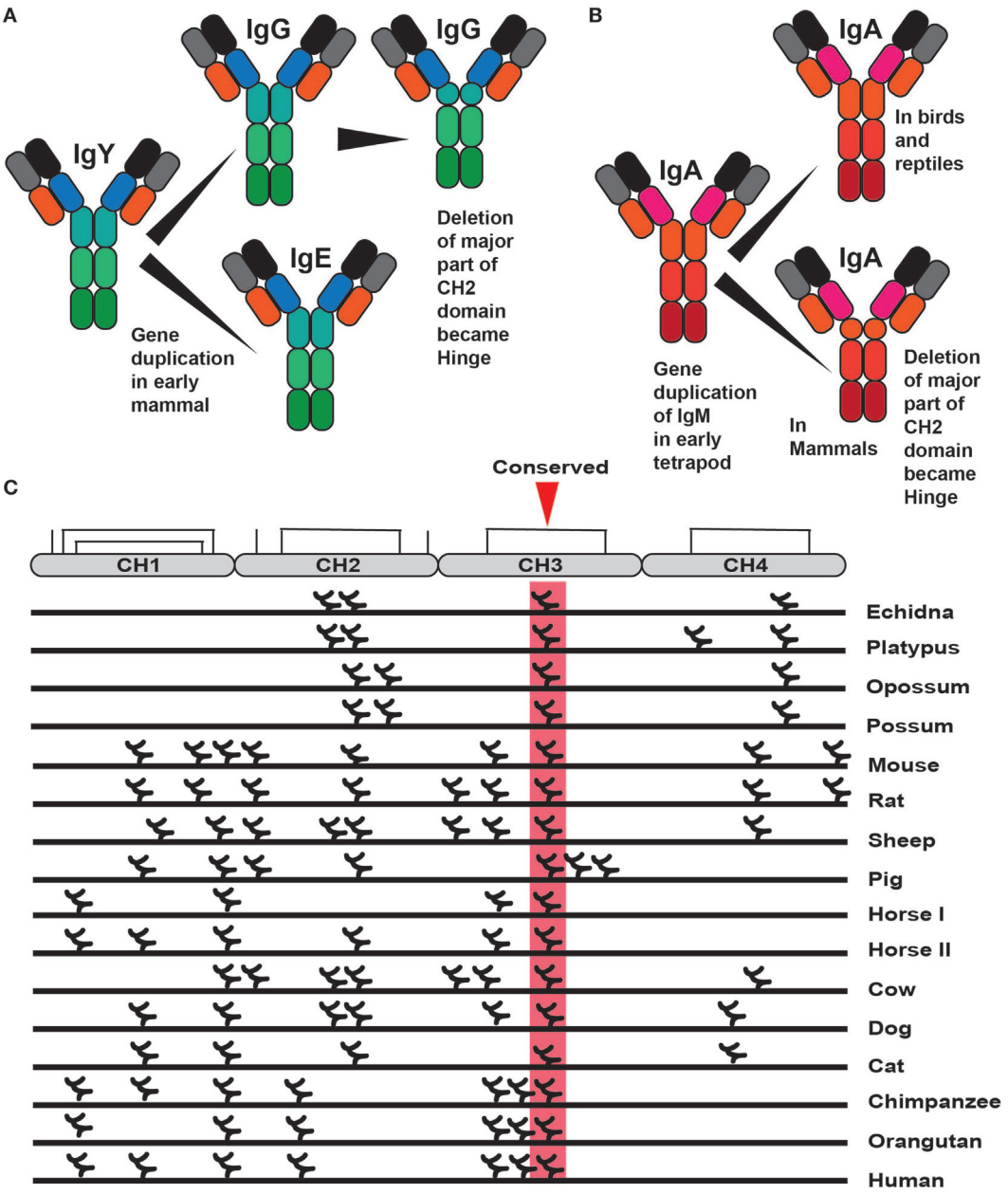

FIGURE 4 | The evolution of IgE, IgG, and IgA and the distribution of N-linked carbohydrates in IgE. Panel **(A)** shows the different steps in the evolution of IgE and IgG. It began with the duplication of IgY after which IgG lost one domain, the original CH2 domain, and became an Ig with three constant domains with one hinge region (46). Panel **(B)** shows the evolution of IgA. A four constant domain IgA is present in birds and reptiles. Sometime during early mammalian evolution IgA also lost one domain, the CH2 domain, and in its place gained a hinge region (47). This hinge region is very different in size between human IgA1 and IgA2 making the former more resistant to proteases and the later more flexible, facilitating binding of several antigens simultaneously. Panel **(C)** shows the positions of the different N-linked carbohydrates in a large panel of different IgE molecules from different species. Only one carbohydrate is conserved in a position shared by all of the different IgEs, marked in red, which is positioned in the middle of the CH3 domain where it has an important function in the folding of this domain.

doubling of the genes for IgG from two to four and a doubling of the genes for IgA into two. However, following the duplication of the genes for IgE one of them has suffered a large deletion involving part of the intron and the CH1 exon to render the gene non-functional (**Figure 3**) (52, 53). The third IgE gene is a non-functional intron-less copy on another chromosome, which appears as an mRNA copy inserted randomly without regulatory regions (54). The selective inactivation of the duplicate gene for IgE but not IgG or IgA strengthens the indication that there is an advantage of having only one functional gene for IgE (**Figure 3**). It should also be noted that within eutherians, IgE has been found in all of the major branches including the orders of Primates, Rodentia, Cetartiodactyla, Lagomorpha, Carnivora, Chiroptera, Afrotherians, and Xenarthra.

One noteworthy finding concerning IgE is in the pattern of glycosylation. Almost all of the Igs are glycosylated. Most often on asparagines, so called N-linked glycosylation. The glycosylation pattern does often differ between different species and the amount of carbohydrate also correlates with the amount of positive charge (46). Therefore, if the polypeptide backbone of an Ig is highly positively charged, then there is generally a higher number of attached, N-linked carbohydrates. These carbohydrates also tend to have several negatively charged sialic acid moieties. A neutral or acidic charge makes the antibodies "less sticky," a characteristic that may be essential for soluble effector molecules aimed to travel easily in the blood and through tissues. Of all the different carbohydrate chains of different IgGs and IgEs from different species, there is only one that is always conserved, which is in the middle of the CH3 domain of IgE (46). A carbohydrate chain is also found in the same position in the corresponding domain of IgG, the CH2 domain (46). This carbohydrate chain seems to be essential for proper domain folding and thereby for the interaction with the α chain of the IgE, and IgG receptors, which bind specifically to this domain (25, 26, 46). This indicates that with only one conserved carbohydrate position the function is to primarily to neutralize a high positive charge, where the position of the carbohydrate on the structure is of lower importance (46). Therefore, it is not the exact position rather the charge neutralization that is of importance. It also indicates that the interaction between IgE and its high-affinity receptor is a central characteristic feature of IgE, and this interaction has apparently been conserved for more than 200 years of mammalian evolution (46).

Fc Receptors (FcRs)

The IgE receptor α chain is one member of a complex set of proteins interacting with the constant domains of the Igs (55–59). These molecules, named FcRs, due to their interaction with the constant domain of the Igs, have a number of important functions in vertebrates including facilitating phagocytosis by opsonization, constituting key components in ADCC as well as activating cells to release their granular content. In placental mammals there are FcRs for all Ig classes, including four major types of classical FcRs for IgG as well as one high-affinity receptor for IgE, one for both IgM and IgA, one for IgM, and one for IgA (**Figures 5A,B**) (60, 61). Additionally, there is the transport receptor for IgA and IgM across epithelial layers the polymeric Ig receptor or PIGR (**Figures 5A,B**) (61). All of these receptors are related in structure, and they all contain Ig-like domains. Furthermore they all, with the exception of the IgA receptor, are found on chromosome 1 in humans, indicating that they originate from one or a few common ancestors via successive local gene duplications (**Figure 5A**) (60, 61). A new family of receptors, called FcR-like (FcRL), are related in structure to the classical IgG and IgE receptors, and were discovered upon the completion of full genome sequences from a number of mammalian species (62, 63). Eight different such FcRL genes have been identified in the human genome: FcRL1–FcRL6 as well as FcRLA and FcRLB (**Figures 5A,B**).

All of the FcRs, including the PIGRs and the FcRL molecules, contain one or several Ig type domains. These domains have a similar fold to the Ig constant or variable domains and belong to the large family of Ig-like domains. The Ig domains have been classified into four basic types depending on the number of antiparallel beta-sheets and the positions of cysteine and other conserved amino acids. These are described as the V, C1, C2, and I type of domains (64, 65). V domains are generally found in variable regions of Igs and TCRs as well as in cluster of differentiation markers including CD2, CD4, CD80, and CD86. C1 domains are found in the constant regions of Igs, TCRs, and in MHC class I and II. C2 domains are found in CD2, CD4, CD80, VCAM, and ICAM, and I domains are found in VCAM, ICAM, NCAM, MADCAM, and numerous other diverse protein families (EMBL-EBI InterPro). All Ig domains of the FcRL and classical FcRs are classed as C2 domains, whereas the Ig domains of the PIGRs, IgM receptors (FcμRs), and IgA/IgM receptors (FcαμRs) are V type domains (64, 65). In a phylogenetic analysis of the individual domains of these receptors, the C2 and V type domains separate into clear individual branches. This is also true for the individual domains within the different receptors (**Figure 5C**) (60, 61).

The important signaling molecule for the classical FcRs, the common γ chain, is a member of a small family of non Ig-domain-containing molecules including the TCR zeta chain, DAP10, and DAP12 (60, 66–70). The latter two proteins serve as signaling components of NK cell receptors and as well as the related Ig-domain containing receptors (70).

Based on a phylogenetic tree (shown in **Figure 6**), we have found strong indications that the classical receptors for IgG and IgE likely appeared as a separate subfamily of the FcRL molecules during early mammalian evolution (60). Related genes are also found in the Western clawed frog (*Xenopus tropicalis*) and the Chinese alligator, indicating that the processes forming the subfamily of receptors that later became the classical IgG and IgE receptors may have started already during early tetrapod evolution. However, this subfamily probably did not appear as a distinct subfamily until the appearance of the mammals (60). In the Western clawed frog, these receptors have a similar structure to the human high affinity IgG receptor, FcγRI, with three extracellular Ig domains of the C2 type. In the platypus there are both two- and three-domain receptors, which are similar to the human three-domain FcγRI as well as the low-affinity IgG receptors FcγRII and III, both of which have two domains. This indicates that the development of high and low affinity receptors also took place during early mammalian evolution (60). Despite this knowledge, currently none of these amphibian, reptile, or non-placental mammalian receptors have been studied for their isotype specificities and affinities.

Interestingly, no gene related to any of the FcRs, including the PIGRs is found in cartilaginous fish. They first seem to appear with the bony fish. In bony fish, there are the PIGRs and genes closely related to the mammalian FcRL genes. There is also a gene for the signaling molecule for the classical FcRs the common γ chain, which is lacking in cartilaginous fish. This indicates a major step in evolution of the FcRs at the base of bony fish with the appearance of the PIGR, the FcR γ chain, and the FcRL molecules (60, 61). Subsequently, the second major step was the appearance of the classical receptors for IgG and IgE as a subfamily of the

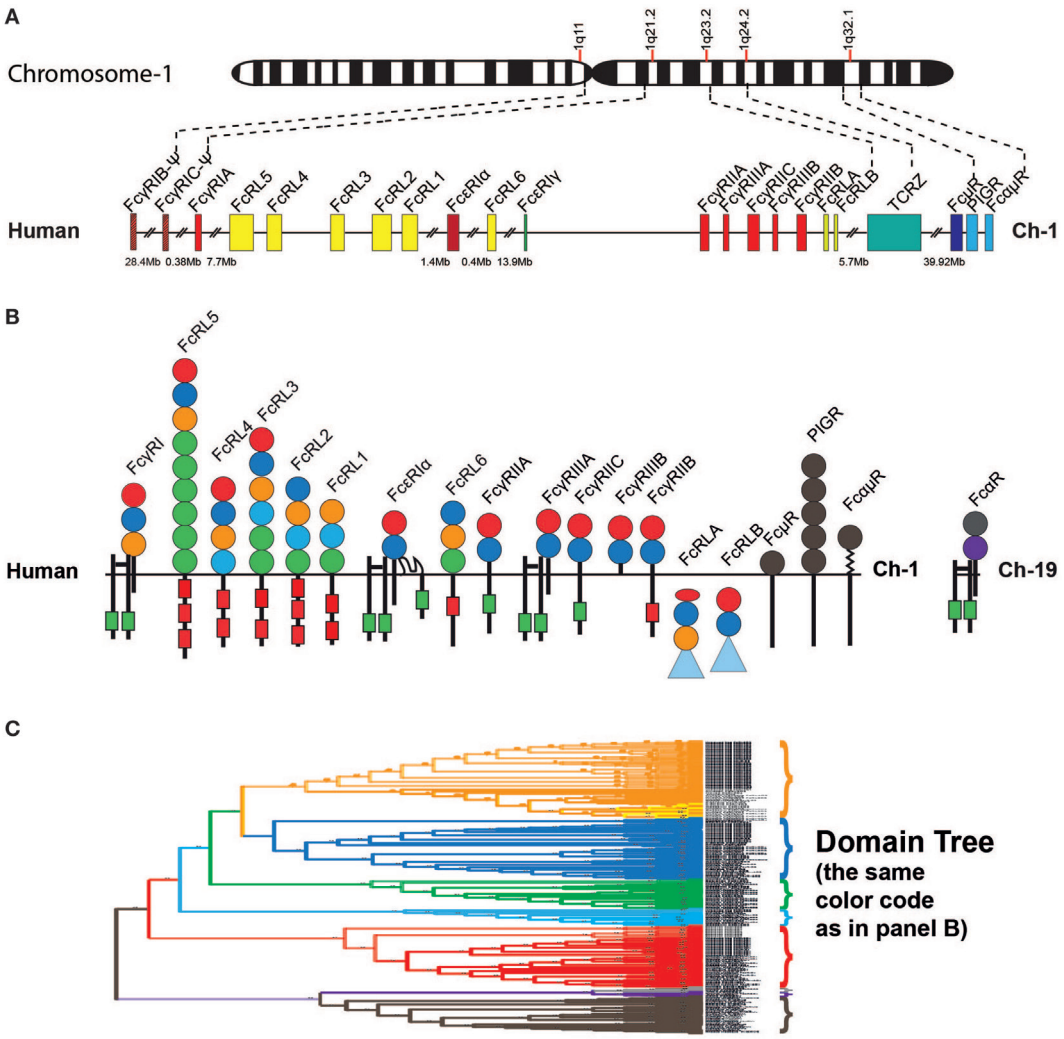

FIGURE 5 | Fc receptor (FcR) genes and proteins. Panel **(A)** shows the regions within chromosome 1 in the human genome that encodes all the different FcR genes except for the specific receptor for IgA, the FcαRI, which is located together with the NK cell receptors on chromosome 19 in the humans (60, 61). Panel **(B)** shows the domain structure of the different FcRs with their different subunits. All of these receptors except FcRLA and FcRLB are transmembrane proteins. FcRLA and FcRLB are both cytoplasmic proteins. Panel **(C)** shows a phylogenetic tree of the individual domains of a panel of the FcRs, which are color coded to reflect the same subunits shown in panel **(B)**. The tree is strongly reduced in size. However, even in its reduced format, it shows the striking separation of the different domains into clearly separate branches. Only the filled circles represent the individual Ig-like domains that are included in the phylogenetic tree. The extracellular regions, the transmembrane regions, and cytoplasmic tails are not to scale in order to show the positions of potential signaling motifs such as immunoreceptor tyrosine-based activation motifs (ITAMs) (green boxes) and immunoreceptor tyrosine-based inhibitory motifs (ITIMs) (red boxes), which regulate the biological function the FcRs. Some of the intracellular proteins contain C-terminal mucin-like regions, which are depicted as blue triangles. The PIGR domains are depicted in gray.

FcRL molecules, most likely in parallel with the duplication of IgY and the slowly emerging separation of the functions of IgG and IgE. It therefore appears to be a close evolution of the new Ig classes and their receptors.

IgE and the Connection between Innate and Adaptive Immunity

IgE and IgG are only found in mammals and we know that in all eutherian mammals studied mast cells interact with IgE and often also IgG with isotype-specific receptors (43–45). However, Igs are found in all jawed vertebrates and mast cells are also present in most, if not all, jawed vertebrates. Therefore, one central question is when mast cells and the adaptive immunity as represented by antibodies did connect through isotype-specific FcRs. This step in the evolution is a very important step where innate immunity, which is the core of the immune system in all multicellular organisms connected with adaptive immunity. Adaptive immunity has most likely appeared a number of times and in very different shapes, which has later become an essential part of immunity in complex multicellular organisms such as the vertebrates. Although studies of the mammalian Ig repertoire and the FcR repertoires have not conclusively shown it, the results suggest that it is likely that all three extant mammalian lineages,

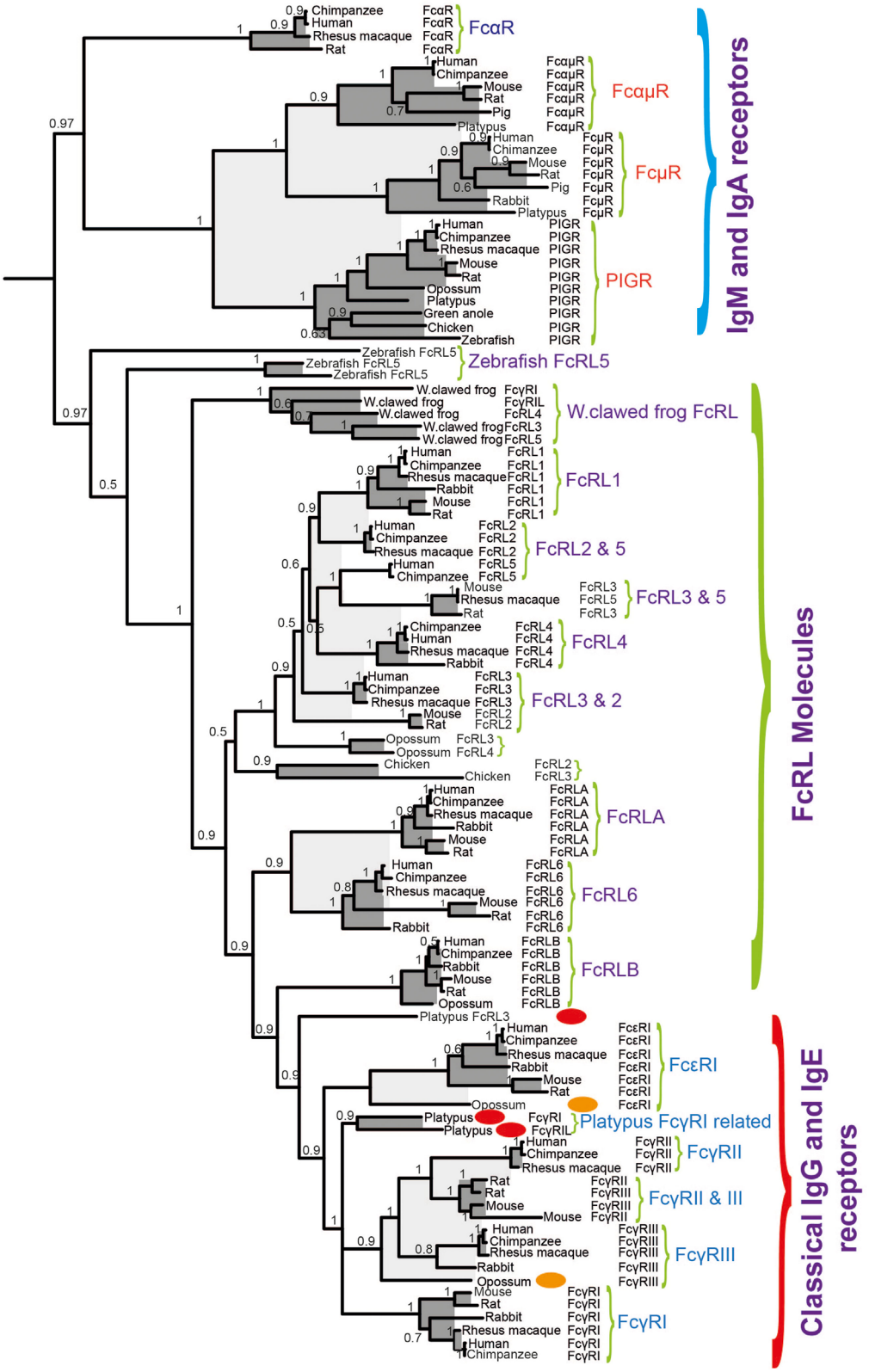

FIGURE 6 | A phylogenetic tree of different Fc receptor (FcR) and FcR-like (FcRL) protein sequences. A few sequences of particular interest for the early evolution of specific IgG and IgE receptors, the discussed opossum, and platypus are marked with red and orange ovals. The Fc γ and ε sequences form a separate subfamily within the FcRL sequences, indicating that they originate as a subfamily from the FcRL genes.

that is, monotremes, marsupials, and placental mammals have mast cells, which are armed with high-affinity receptors for IgE (43–45, 60). However, the situation in reptiles, birds, and amphibians is much less clear. Do their mast cells have receptors for IgY? Are other isotypes involved or are there no Ig receptors on mast cells in these tetrapods?

In marsupials, represented by the American opossum, there is, based on phylogenetics, a direct ortholog of the human and mouse IgE receptor α chain (**Figure 6**) (60). Although it is most likely that this receptor binds IgE, it has not yet been proven. The situation in the monotremes, represented by the platypus, is even less clear, although there are receptors in the platypus genome, which are closely related to the IgG and IgE receptors in placental mammals (**Figure 6**). The two receptors that are most closely related to the IgG and IgE receptors in placental mammals appear as a separate branch in-between the IgG and IgE receptors in the phylogenetic three (**Figure 6**) (60). The isotype specificities of these two receptors and the single receptor, which is located just outside of the IgG and IgE receptors in the tree have not yet been studied but it is reasonable to think that one of them is IgE specific and the other is IgG specific. There are no direct homologs to the IgG and IgE receptors in birds and reptiles. However in the clawed frog, *Xenopus laevis*, there are three genes, which may be a very early ancestor to the IgG and IgE receptors (**Figure 6**) (60). However in a similar manner to the platypus, there is not yet any information on their isotype specificity, therefore we do not know if they bind IgY, IgX, IgM, or IgF or perhaps none of them.

Mast Cell and Basophil Granule Components

Both mast cells and basophils contain a large number of cytoplasmic granules (**Figures 2A,B**). These granules that are functionally related to lysosomes, store a number of substances of low and high molecular weight substances. Histamine, one of these low molecular weight compounds, is stored by both mast cells and basophils (71). It is based on the amino acid histidine where the carboxyl acid, i.e., COOH group, has been removed by the enzyme histidine decarboxylase (72). The removal of the acid group results in a positively charged molecule of a size smaller than that of an amino acid. Histamine is a highly potent inflammatory mediator due to its interaction with four different receptors termed H1, H2, H3, and H4 (73, 74). Binding of histamine to these receptors induces a number of processes including vascular leakage and itching (73, 74). The mast cell granules also contain large and heavily sulfated, negatively charged polysaccharides; heparin in the case of mast cells, and chondroitin sulfate in basophils (75–78). One function of these charged proteoglycans is most likely to counteract the positive charge of histamine. The cell would otherwise not be able to store such large amounts of a positively charged molecule (77). Heparin is also a potent anticoagulant *via* its binding and activation of anti-thrombin (78).

Mast cells also store massive amounts of proteases primarily chymotrypsin/trypsin-related serine proteases but also the mast cell-specific carboxypeptidase A3 (79–85). These proteases can make up to 35% of the total protein, thereby constituting the absolute majority of the protein content of the mast cell granules (86). Most of these proteases are positively charged and therefore bind to the long, negatively charged proteoglycan polysaccharide chains. Tryptases are one subfamily of serine proteases, which are also dependent on heparin for maximal activity (87). The mast cell tryptases form tetramers where the dependency on heparin keeps these formations together, as well as increasing their proteolytic activity (88, 89). Basophils also express proteases but to a much lesser extent. Human basophils primarily express the tryptase whereas mouse basophils express the basophil-specific protease mMCP-8 (22–24).

One of the major questions in the field is the function of these very abundant proteases. To trace the origin of these proteases and thereby get additional clues to their conserved primary functions, we have performed several evolutionary studies of the different loci encoding the different mast cell and basophil proteases (85, 90). These proteases belong to a larger subfamily of related proteases that are expressed by a number of hematopoietic cells and have therefore been named hematopoietic serine proteases. They are expressed by mammalian mast cells, basophils, neutrophils, CTLs, and NK cells. In mammals, these serine proteases are encoded from four loci (85, 90–92). One additional locus with related proteases is found in reptiles, indicating a loss of one locus in mammals (90). In mammals, the four loci include the chymase locus, which in humans encodes the mast cell chymotryptic enzyme, the chymase; the neutrophil cathepsin G; and a few T cell- and NK cell-expressed granzymes (**Figure 7**). In humans, only two granzymes are present in this locus, granzyme B and H (**Figure 7**). A massive expansion of the chymase locus both in size and number of functional genes has occurred in rodents. The mouse chymase locus has, for example, 15 functional genes, including two new classes of genes, the β-chymases and the mMCP-8 gene and also several additional granzyme genes (**Figure 7**) (85, 90). The rat locus is fifteen times larger than the dog chymase locus and contains 28 functional genes (85). In ruminants, i.e., cows and sheep, an additional subfamily called the duodenases has appeared *via* gene duplications, most likely from the granzymes or from cathepsin G (85, 90). The duodenases in cow have changed tissue specificity and are now not expressed in hematopoietic cells but in secretory cells in the duodenum, where they most likely take part in food digestion (93, 94). The second locus is the metase locus, which encodes most of the neutrophil proteases; *N*-elastase, proteinase-3, neutrophil serine protease-4, and an inactive variant, azurocidine that acts as an antibacterial substance without protease activity. This locus also encodes a complement component, complement component D (**Figure 7**) (85, 90). The third locus encodes two T-cell expressed proteases, granzyme A and K, which are both tryptic enzymes (**Figure 7**). The fourth locus is the mast cell tryptase locus, which is divided into two regions, one expressing primarily the mast cell-expressed soluble tryptases and the second, which primarily encodes membrane bound tryptases that show a relatively broad pattern of expression (**Figure 7**) (95–97). The fifth locus has completely different bordering genes and is only found in reptiles, birds, and amphibians, where it encodes a few proteases that are distantly related to the mammalian chymase locus genes (**Figure 7**) (85, 90). By looking into the genomes of a panel of

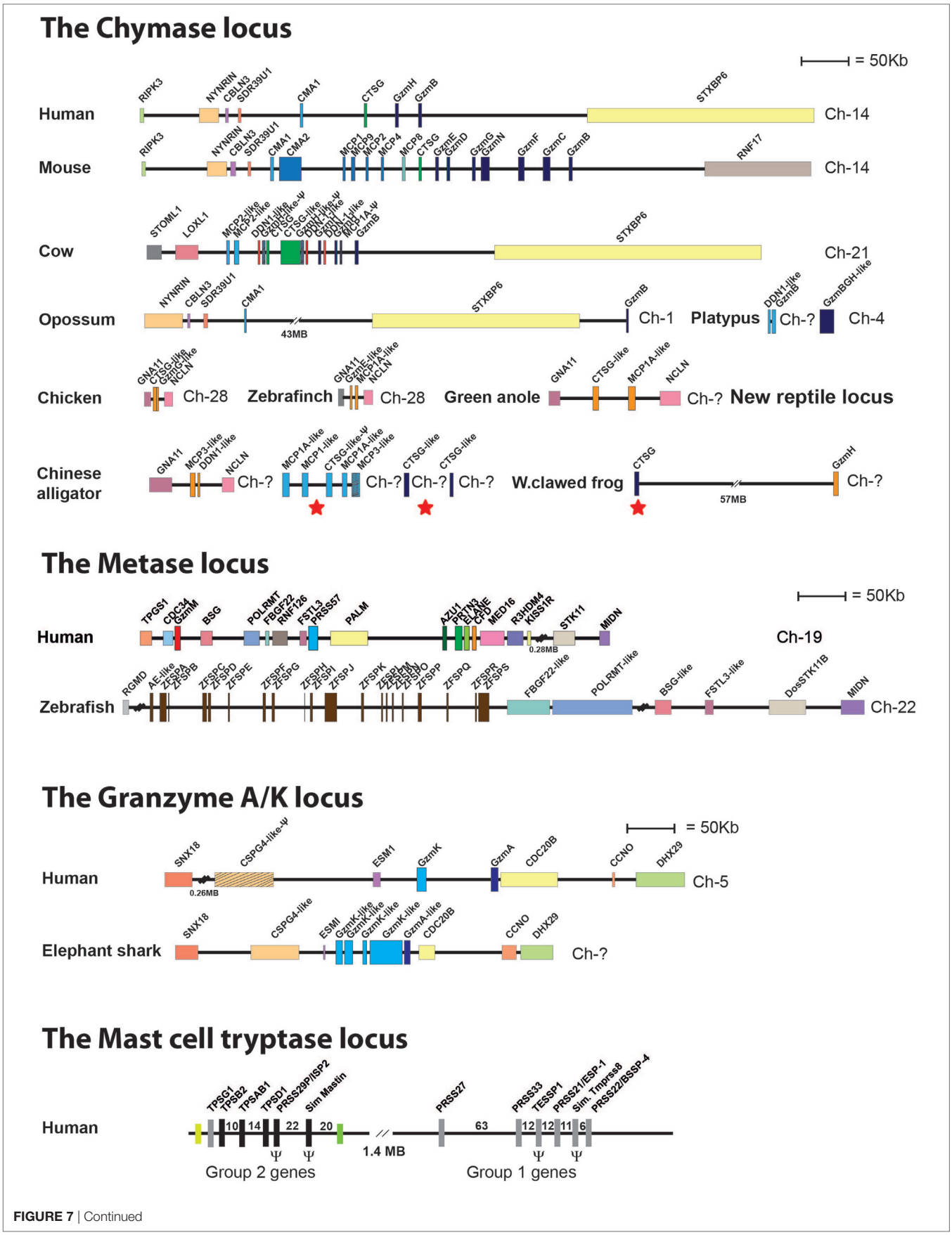

FIGURE 7 | Continued

FIGURE 7 | Chromosomal loci encoding hematopoietic serine proteases. A selection of such loci representing the five different loci encoding hematopoietic serine proteases is shown; the chymase locus, the metase locus, the granzyme A/K locus, the mast cell tryptase locus, and the new chymase locus related locus found in amphibians, reptiles, and birds. The section of the figure showing the chymase loci includes this new amphibian, bird, and reptile locus. These chymase locus related genes are marked in orange. A number of bordering genes are also included to show the similarity in the surrounding regions between the different species. The loci or genes marked with red stars in the alligator and frog genes (under chymase locus genes) are the genes closely related to the mammalian chymase locus genes and thereby may represent an early variant of the mammalian chymase locus. A more detailed analysis of these protease genes and their evolution containing a much larger number of species is found in Akula et al. (90).

vertebrates, it has been possible to trace the origin of these genes during vertebrate evolution. There is evidence for the existence of the T cell tryptase locus, encoding granzymes A and K, from cartilaginous fish to humans but not in jawless fish, including the lamprey and hagfish. Similarly, this locus is not found in tunicates or echinoderms, indicating an appearance with early jawed vertebrates. This locus is the only one of the five loci that is found in cartilaginous fish, indicating that it is the oldest of them all (**Figure 7**) (85, 90). In bony fish, there is evidence for the presence of the metase locus, and in frogs, the first gene that can be directly seen as an ancestor of the mammalian chymase locus is found. In frogs, a gene for the fifth locus exists, which is present in reptiles and birds but not in mammals. In this manner, we can start to see a gradual and probably parallel appearance of these proteases in the different vertebrate lineages during vertebrate evolution (85, 90).

In order to obtain additional functional information concerning these proteases, we have used an unbiased technique with a very large number of potential target sequences. This consists of a phage library with 50 million different 9 amino acid long random sequences to study the extended cleavage specificity of a number of these hematopoietic serine proteases (85, 98).

Using a combination of genomic analyses and functional analyses of the extended cleavage specificities of a selected panel of the proteases, we have started to get a more detailed view of their emergence, evolution, cleavage specificities, and the basic functions performed by these proteases (22, 23, 80, 82, 85, 90, 98–106). The proteases we have focused on are the most interesting ones from an evolutionary perspective, i.e., ones that represent major branches on the phylogenetic tree and that can be most easily studied for their *in vivo* function based on available model systems (**Figure 8**) (85, 90).

Both chymotryptic and tryptic enzymes appear to have been a central component of mast cell granules from early mammals. This is based solely on the presence of the protease genes in marsupials and monotremes and not on a direct analysis of their mast cells. However, based on the presence of proteases with close structural similarities and with very similar cleavage specificities to the well-characterized ones in several placental animals, we can with reasonable certainty claim that they are also likely to be part of the mast cell phenotype (90, 103). The picture is less clear when we look at reptiles, birds, and amphibians. In birds, none of the classical chymase locus genes are present and in frogs, there is one such gene, which has structural similarity of its active site pocket that closely matches one of the T cell enzymes, granzyme B (**Figure 7**) (90). We have now also started to study the related fish proteases (**Figure 8**, brown colored branch) (90, 107), and have so far produced recombinant protein for three catfish proteases. Two of them are expressed in CTLs or NK-like cells and one from a macrophage-like cell line. One of these proteases, catfish granzyme-like I is a highly specific protease, probably the serine proteases with the highest specificity characterized so far. The cleavage specificity of this protease, which is expressed by fish NK-like cells, has an ability *in vitro* to cleave a sequence within catfish caspase 6, indicating it may have similar function as mammalian granzyme B, thereby inducing apoptosis in target cells (108). The second catfish protease is a highly specific tryptase, as of yet an unknown function, which is expressed by fish macrophage-like cells (unpublished results). The third of these three catfish proteases is not yet characterized at all and we do not know its specificity (90, 107). Several other fish proteases have also been produced as recombinant proteins, including ones from gar, zebrafish, and platyfish (**Figure 8**). However, no information concerning their tissue specificities, cleavage specificities, or potential targets are known yet; therefore currently, we cannot say if these fish proteases show similarities to any of the mast cell proteases in mammals. These studies are in their infancy and hopefully a more detailed picture will emerge within a few years' time.

Despite numerous studies concerning the major functions and major targets of mammalian hematopoietic serine proteases, the picture concerning these proteases is still relatively incomplete. An array of potential targets has been described, some more and some less likely to represent evolutionary conserved functions of these proteases.

The five most interesting and in our minds most logical roles for the mast cell proteases include the following: they most likely have a central role in the defense against various snake, scorpion, and bee venoms (109–111). There is sufficient evidence that they probably also take an active part in connective tissue remodeling by cleaving connective tissue components, as for example, fibronectin, and/or by activating other proteases, for example, matrix metalloproteases (MMPs), which can degrade several components including collagen (112–117). In addition, they are likely involved in both activation and degradation of cytokines, primarily inflammatory cytokines to dampen inflammation (106, 118). The mast cell chymase is also a potent activator of angiotensin from Ang I to Ang II thereby with the potential to increase blood pressure, which may be needed after a systemic mast cell activation where blood pressure drops due to the outflow of liquid from the blood into the surrounding tissue (117, 119–121). During the opening of blood vessels to enhance the flow of blood components including antibodies and complement, there is a major risk that the inflow is blocked by coagulation. Here, mast cell proteases and heparin may act cooperatively as an anticoagulant by cleaving thrombin and other coagulation components (114, 122, 123). Although not to be ignored, there are many other suggested functions. However, given the evidence,

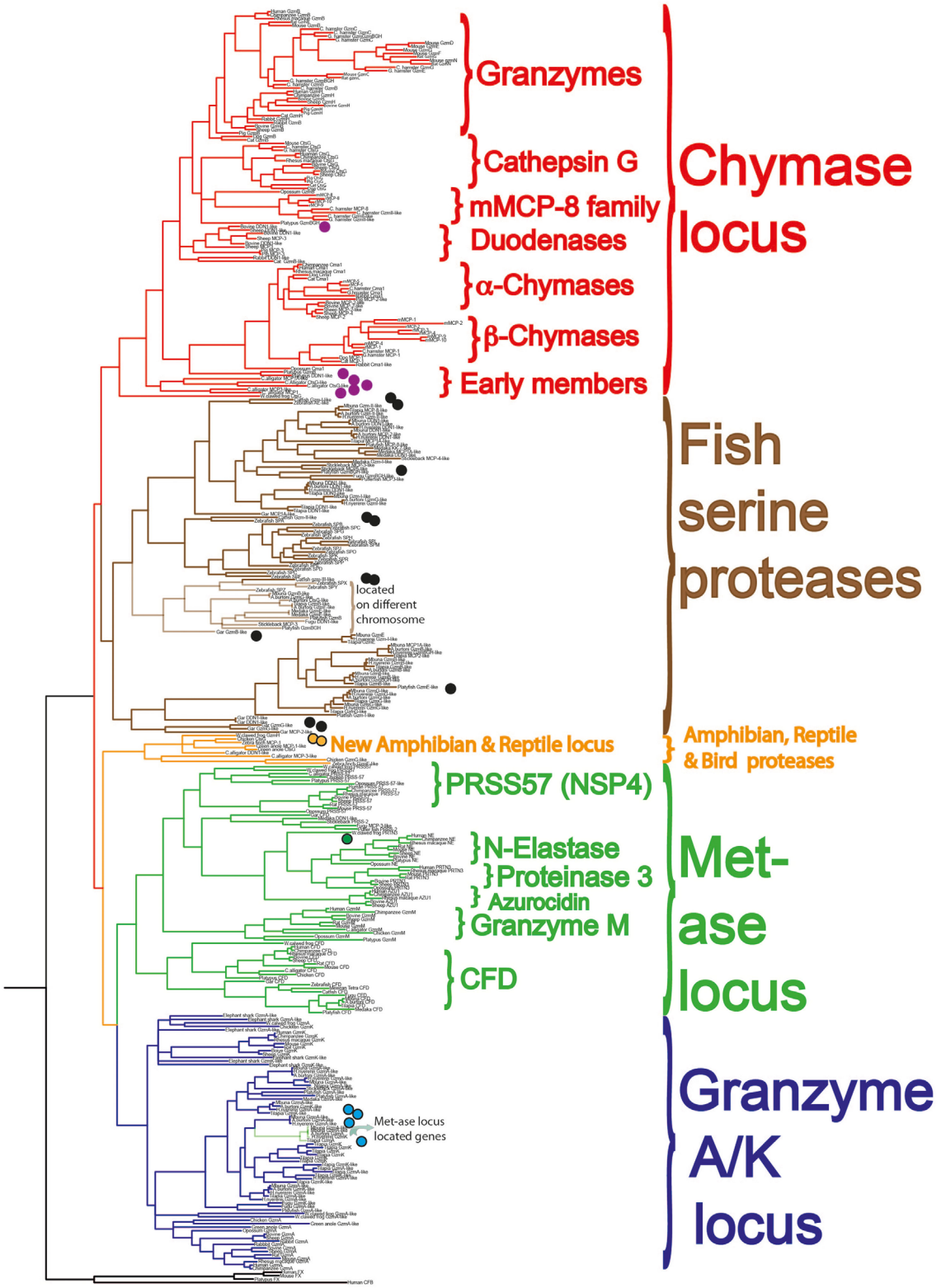

FIGURE 8 | A phylogenetic analysis of a large panel of hematopoietic serine proteases. Three coagulation and complement components are used as outgroup. The proteases of the different genetic loci cluster together in separate branches of the tree and are color coded in similar fashion to **Figure 7**: the metase locus genes marked in green, the granzyme A/K locus in dark blue, the new reptile and amphibian locus in orange, the chymase locus marked in red in one branch, and the majority of the fish proteases in brown. The proteases we are currently analyzing for their extended cleavage specificities and tissue or cell type expression patterns are marked with small filled circles. A more detailed analysis of these protease genes and their evolution is found in Akula et al. (90).

we feel that these five are among the most likely. These proteases may have adapted a relatively broad array of functions, which may also explain their relatively broad specificities.

What Is the Physiological Role of IgE?

One of the major questions in the field of IgE biology is why this gene that on face value causes us so much trouble has been maintained for several hundred million years of mammalian evolution. The indications for a coevolution of IgE and its receptors on mast cells and basophils strongly support an evolutionary selective advantage of the system. During the writing of my PhD thesis in 1985 I (LH) proposed a theory that IgE together with mast cells may actually function as a door or gate keeper, stopping the antigen at the site of entry (124). Much of the evidence that has accumulated on the subject now strengthens this hypothesis. By triggering a rapid release of histamine, prostaglandins, leukotrienes, proteoglycans, proteases, and cytokines mast cells can activate and recruit immune cells to the site of entry. Histamine and the arachidonic acid metabolites (leukotrienes and prostaglandins) open blood vessels, which facilitates the entry of antibodies, complement and immune cells. The proteases and heparin that are also being released by the mast cells can limit coagulation, which would otherwise inhibit the movement of inflammatory cells. The proteases can also function by loosening up the connective tissue allowing the entry of the immune cells and other molecules. The location of mast cells in regions where most pathogens enter, for example, the intestinal and lung mucosa, the skin as well as around organs and blood vessels, also provides strong support for the role of IgE and mast cells as part of a door keeper or sentry function. At these sites mast cells can also exert an important role in the process of venom inactivation. Likewise at these locations, the processing of Ang I into Ang II by the mast cell chymase can potentially counteract the resulting effect of the blood pressure drop after mast cell degranulation. Release of Ang II can result in a rapid increase in blood pressure. The tissue remodeling function of mast cells by activation of MMPs and cleavage of fibronectin, collagen, and other connective tissue components is probably relatively IgE independent, whereas cytokine activation or inactivation may be important for limiting the inflammation initiated by the IgE-dependent mast cell activation. We have also observed a peculiar early IgE response already at days 3 and 4 after antigen/allergen contact that seems to precede the rise in IgG (unpublished observations). IgE responses have also been seen to occur primarily against low levels of antigen. This would indicate that the IgE system is focused on early responses to low levels of antigen, possibly to sample the environment. The antigen-specific IgE, often locally produced, can then bind mast cells and prime the immune system for a second encounter with this antigen possibly in the form of a parasite, a virus, or a bacteria. The individual is subsequently already primed for a relatively strong response involving the majority of immune components. The IgE covered mast cell is an extremely potent amplifier of an inflammatory response, where cross-linking of less than 100 IgE molecules on the cell surface is sufficient for full activation/degranulation of the cell. Such a sensitive and massive response may be necessary to manage a massive infection of an intestinal worm parasite. Therefore, in our minds many aspects related to IgE and mast cells, including their location and homeostasis, favor a role of these components in an early, door keeper function.

IgE Levels under Parasite-Free and Parasite-Rich Conditions

Non-allergic persons have generally very low levels of IgE in their circulation, ranging from 20 to 400 ng/ml in blood (125). In comparison to the IgG levels, which range from 8 to 16 mg/ml, IgE levels are between 100,000 times to a million times lower. Persons with the relatively mild allergies, rhinitis, and conjunctivitis, often have slightly elevated IgE levels, where asthmatics have even higher ranging from 400 ng to 1 or 2 μg per ml. The patients with the highest IgE levels are generally persons with severe atopic dermatitis where IgE levels may reach as high as 10 μg/ml.

An interesting question here is if these very low levels of IgE are reflected in the general situation in both domestic and wild animal populations, and how this affects our view of the function of IgE. Most inbred mouse and rat strains have similar low IgE levels to non-allergic humans, below 200 ng/ml, with many strains having less than 50 ng/ml (7, 126). However, there are some notable exceptions with strains such as the Balb/c mice, which may reach 100 μg of IgE/ml as well as the Brown Norway rats, which can have IgE in the range of several micrograms per milliliter (7). Both of these rodent strains are considered so called TH2 type of strains, with a dominance of humoral immunity compared to many strains with low IgE levels that are more TH1 prone, thereby having a stronger tendency to use cell-mediated immunity. Therefore, genetic factors are clearly important for the levels of circulating IgE.

However, other factors are also very significant. Both humans and rodents living under laboratory conditions are generally free from worm infections, which are known to be potent inducers of IgE production (127). By contrast, most wild animal populations have massive amounts of intestinal worm parasites.

A few years ago we developed a reliable assay testing for dog IgE based on monoclonals raised against recombinant dog IgE. This made it possible to study IgE levels in both dogs and wolves, with high accuracy, which had not been possible with previously existing reagents. Analysis of a panel of 76 adult dogs showed that adult dogs have IgE levels that are between 10 and 40 μg/ml, which is almost 100 times higher than non-allergic humans, but that young dogs started with low with levels often below 1 μg/ml of IgE (**Figure 9**) (128). A collaboration with Professors Jon Arnemo and Olof Liberg, which involved a large interdisciplinary study on the Scandinavian wolves, Scandulv, made it possible to obtain serum samples from approximately 30% of the total Scandinavian wolf population, around 65 individuals. By analyzing their IgE levels, we could see that wolves in general have twice as high IgE levels compared to domestic dogs, having a median value of 67 μg/ml (**Figure 9**) (129). The relatively high levels seen in domestic dogs (compared to non-allergic humans) were somewhat surprising as they are a domestic population. However, dogs are frequently parasite infected, then undergo treatment for this, but often get re-infected. This indicates that after infection levels of IgE tends to stay high for relatively long periods of time.

Dogs IgE levels ug/ml

Dog breed	Number of dogs	Health status	Value range	IgE, µg/ml Median value
Beagle	9	Healthy	19-31	20
Germ. shepherd	18	Healthy	1-22	13
Irish Setter	2	Healthy	8-16	12
American Cocker	2	Healthy	2-17	9
Engelsk Cocker	1	Healthy	15	15
Tolling Retriever	3	Healthy	11-19	17
Pudel	1	Healthy	35	35
Pug	1	Healthy	20	20
Sw. farm dog	1	Healthy	25	25
Tervueren	2	Healthy	17-20	18
Beauceron	1	Healthy	20	20
Rottweiler	1	Healthy	22	22
Border Collie	1	Healthy	22	22

Dog Pups

Dog breed	Number of dogs	Age Weeks	IgE, µg/ml Median value
Rh. Ridgeback	1	Adult	20
Rh. Ridgeback	14	0-4	1
Rh. Ridgeback	9	0-19	0.2
Rh. Ridgeback	10	0.6-3.6	0.8

Wolf Pups

Wolf pups	Number	IgE, µg/ml Range
Pups from ZOO	5	84-138

Wolves IgE levels ug/ml

Wolf	Age &weight	IgE/ml	Wolf	Age &weight	IgE/ml	Wolf	Age &weight	IgE/ml
1	0 (35kg)	51	21	0 (38kg)	69	41	1 (46kg)	53
2	7-8 (53kg)	35	22	0 (33kg)	61	42	1-2 (47kg)	58
3	5-6 (38kg)	47	23	4-5 (38kg)	57	43	3-4 (51kg)	61
4	0 (38kg)	89	24	3-4 (49kg)	72	44	0 (35kg)	49
5	4-5 (35kg)	44	25	0 (24kg)	50	45	3-4 (36kg)	15
6	0 (37kg)	61	26	0 (33kg)	34	46	puppy	26
7	0 (37kg)	22	27	0 (36kg)	51	47	4 (46kg)	95
8	0 (35kg)	33	28	4-5 (52kg)	26	48	0 (31kg)	22
9	5-6 (53kg)	63	29	3-4 (43kg)	66	49	0 (30kg)	48
10	5-6 (40kg)	48	30	1 (39kg)	73	51	1 (38kg)	40
11	0 (36kg)	68	31	4 (39kg)	11	52	0 (32kg)	55
12	4-5 (42kg)	21	32	0 (39kg)	27	53	2 (44kg)	92
13	2-3 (53kg)	42	33	0 (30kg)	64	54	1 (35kg)	74
14	2 (49kg)	71	34	0 (38kg)	68	55	0 (36kg)	37
15	3 (51kg)	66	35	1-2 (45kg)	92	56	1 (42kg)	37
16	4 (42kg)	62	36	0 (34kg)	49	57	2 (51kg)	74
17	5-7 (49kg)	48	37	0 (30kg)	48	58	2 (47kg)	33
18	0 (40kg)	42	38	0 (31kg)	68	59	1 (47kg)	103
19	Wolf/dog hybrid	84	39	4-5 (46kg)	60			
20	0 (31kg)	81	40	2 (52kg)	52			

FIGURE 9 | IgE levels in a panel of domestic dogs and wild wolves. The IgE levels, in micrograms per milliliter, are marked in red after each animal or group of animals. Values from 33 young dogs and 5 young wolves are also included in the figure. The young wolves were from a zoo due to the difficulty obtaining samples from wild wolf pups.

A similar situation is seen with horses. Domestic horses have been found to have very high levels of IgE, twice the levels seen in wolves somewhere between 30 and 180 µg/ml (130). Horses also often get re-infected with worm parasites when grazing, which means they tend to need repeated treatment for intestinal worm infections (131, 132). Analysis of the young dogs previously described showed relatively low IgE levels, below 1 µg, indicating that parasite infections may be the major cause of the high IgE levels seen in adult dogs (**Figure 9**) (128). This also suggests that the puppies stay uninfected until they start to go outside their homes. Interestingly by contrast, the few young wolves coming from a zoo that were analyzed showed even higher IgE levels than the adult wolves, possibly indicating an early parasite infection or a genetic difference in IgE regulation between dogs and wolves (**Figure 9**). During the cloning and analysis of Ig isotypes in the platypus, we also found that transcript levels for IgE in the spleen were only six times lower than the IgG levels of these free-living animals, which further support the finding that IgE levels are much higher in wild compared to domestic animals (45).

A very interesting study of Ethiopian Jews has also been performed, which provides indications further in line with these animal findings. When IgE levels were analyzed on people that had moved from Ethiopia to Israel at an adult age their IgE levels were high and stayed high during the entire study, whereas their children who were born and raised in Israel had similar low levels of IgE as other children born in Israel (125). The situation seen

in dogs, horses, platypus and the migrating Ethiopian Jews show that IgE levels tend to stay high for long periods of time even after being free from parasite infection. The reasons for this are not known but indicates that the cytokine environment may change more permanently after a long or repeated exposure to intestinal worm parasites (133).

Domestication and the Appearance of Allergies

A number of factors have been indicated to be of importance for the high incidence of allergies in industrialized countries. One factor that seems to have a major impact is general domestication, as it is primarily among ourselves and among domestic animals that we find allergic individuals. To our knowledge, allergies have not been described in wild animals. One potential factor could be a genetic drift due to strong selection for phenotypic characteristics like coat color, long or short noses, running fast, or wanted social behaviors. Such strong selections are seen in the breeding programs for dogs, horses, and cats, but a questionable cause for human allergies. However, it is possible that we constantly need to be selecting against hypersensitivities, which may occur due to minor shift in immune functions caused by spontaneous point mutations. A strong such selection process most likely exists in wild animals under tough environmental conditions but not in domestic animals and in humans. Another factor could be parasite infections. However, the presence or absence of parasites cannot be the only explanation as we see allergies both in ourselves, who are generally free from intestinal parasites, at least in the industrialized world, whereas dogs and horses are often parasite infected.

There could also be numerous other contributing factors, which are only partly dependent on domestication such as hygiene including a reduced complexity of intestinal microbiome. For humans, one factor could be the reduced use of fermented food. The list has become relatively long for potential causes of this increase and there are studies, which favor and disfavor almost all of them, making the situation very complex. It is clear that not only one single factor is involved but a combination of many and often also diverse factors, which together provides the imbalance of the immune system to overreact against often harmless substances such as pollen, nuts, animal fur, cow milk proteins, eggs, fish, and shellfish.

What We Can Learn from Wild Animals

By studying only a few species, which live under very similar conditions we most likely get a fairly limited view of the regulation of the immune system. For example, many of the knockout strains of mice have been shown to display a very mild phenotype, indicating that many cell types and molecules are dispensable and not essential. However, this may be the situation under low pathogen loads and under conditions of good access to nutrients and clean water. A more pronounced phenotype may be seen under stress, under conditions of limited water and food supply, when individuals have to fight for territory and mating partners and under heavy parasite loads. Similarly, we may not see the factors regulating a normal immune response by only looking at a few species, which are essentially living under very similar and limited environmental conditions, including absence of parasites, a lack of fighting for territory, and an almost unlimited supply of food and water. One interesting finding relating to this idea is that persons lacking IgE seem to live a relatively normal life in spite of the fact that the connection between IgE and mast cells has been evolutionary conserved for what it seems at least 200 million years (134). By studying wild animals under natural conditions, we may get a better picture of the factors that have shaped our immune system. Recent data from the currently rapidly evolving field concerning the role of the microbiome show that as we are eating the same foods with low amount of fiber and high fat or high sugar, this can reduce the complexity of the intestinal flora (135, 136). A similar effect may also come from a massive overuse of antibiotics (137). A diverse microbiome obtained from eating different foods and not using antibiotics may be one factor in this picture (126, 138, 139). We know that the microbiome is important for stimulating the immune system, and that microbes are important for the production of vitamins and for the degradation of hormones and other substances. This may be suggestive as to why a reduced food complexity may be one factor that limits the development and functional diversity of our immune system. We are bombarded by the idea that lactobacilli, for example, are beneficial for our health. However, numerous trials with probiotics, including eating live lactobacilli in the form of yogurt or fermented foods have not shown any significant effects [reviewed in Ref. (140)]. Here the problems may be partly related to that these added lactobacilli only appearing to live for a short period of time in the intestine, thereby only marginally affecting the intestinal mucosa and the immune cells residing in the area just under the epithelial cells. In the industrialized world, we are almost completely free of both ecto and intestinal parasites. This is a factor that we as species are not so well adapted for. For example, studying the intestines of wild mice reveals that they are typically full of intestinal parasites, yet interestingly they are otherwise in reasonable health. Similarly, they are usually also infested with ecto-parasites including lice, fleas, and ticks factors that may markedly affect the immune system by triggering inflammatory cells, thereby affecting the cytokine environment. Although these factors may be of importance for the development of our immune system we do not perceive that anyone of us would like to return to such conditions. However, the lesson here is that factors such as parasite loads and complexity of the intestinal flora may be of importance for many diseases including allergy, autoimmunity, diabetes, and possibly even certain cancers (127, 141, 142). Here studies of wild animals can shed light upon how the immune system reacts to, and handles, all of these parasites and also how a diverse intestinal flora may affect these processes. Respiratory virus infections are most likely also an important factor where respiratory syncytial virus and rhino virus are of prime interest for asthma development (143). There are other, more discrete factors, for example, there is an ever increasing amount of hormone-like substances in our environment, such as estrogens from contraceptives that enter the sewage system. These may also be other factors to take into account, as it is well known that such substances can markedly affect reproduction of local fish and amphibian species. Wild animals are often more exposed to such pollutants than us, for example, fish and amphibians can live directly within the polluted water and thereby take up the substances more effectively.

Studies of such animals in the wild can provide information on how such pollutants affect their immune functions and thereby give us clues to as to how these substances will also affect us. Such substances may affect us more subtly by shifting the balance of the immune system. The question is very complex, and here by looking at wild populations may present us with a more multifaceted

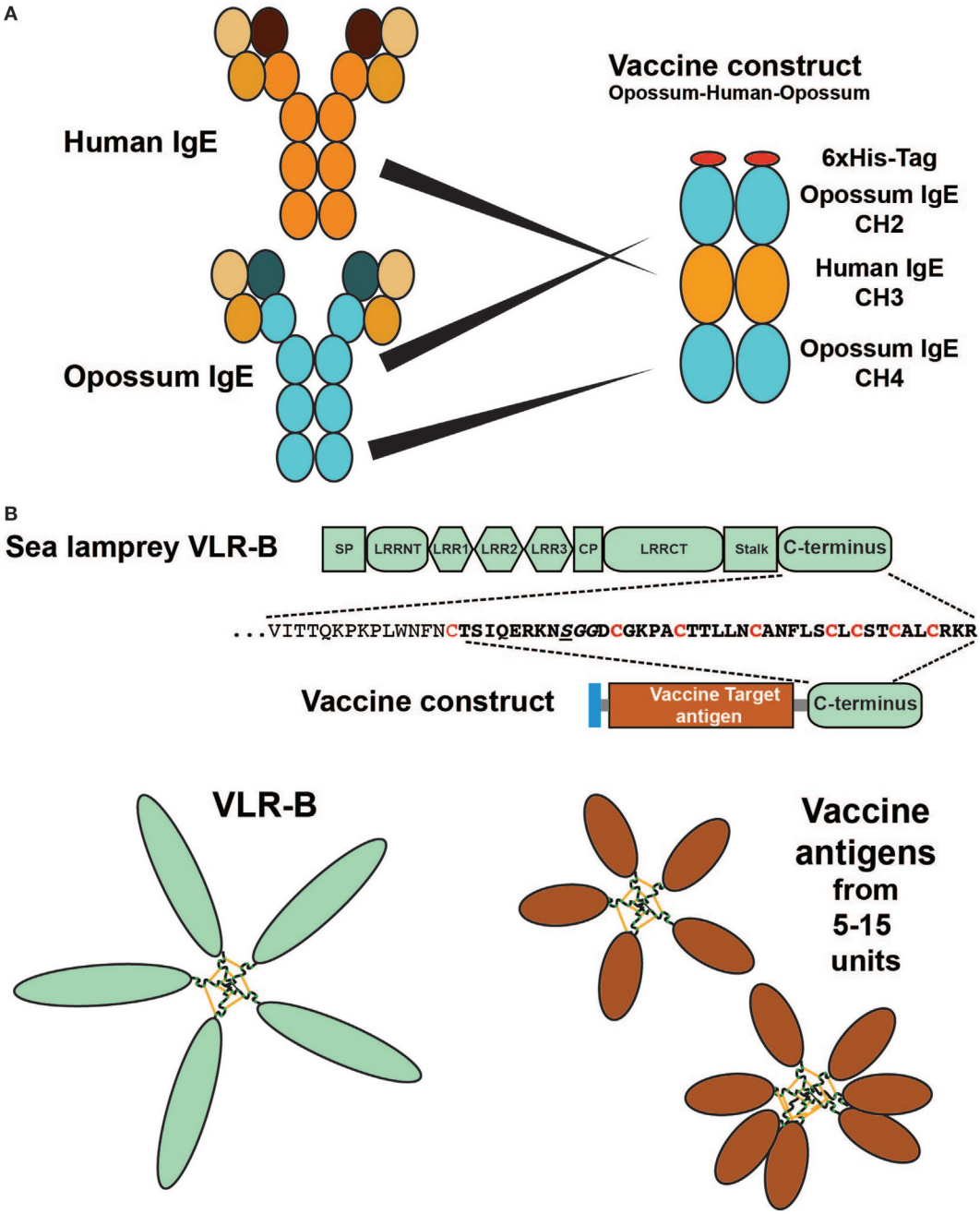

FIGURE 10 | Therapeutic vaccine proteins where parts of the vaccine antigen originate from a wild animal. Panel **(A)** shows a vaccine antigen consisting of a fusion protein between the CH2 and CH4 domains of opossum IgE together with the target region for the vaccine: the CH3 domain from the target animal, a human, dog, or rat. The figure shows the human variant of the vaccine. The rat variant of the vaccine antigen has been shown to induce a strong anti-self-IgE response in rats of several strains and to reduce circulating IgE levels in these animals (7). Panel **(B)** shows a multimeric vaccine component generated by the use of the C terminal tail of the lamprey antigen-specific receptor variable leukocyte receptor B (VLR-B). VLR-B is the functional but not the structural equivalent of human IgM, a pentameric antigen-binding molecule. Using the C terminal 30–40 amino acids from VLR-B fused to the C terminal of any soluble vaccine antigen, it is possible to obtain a multimeric vaccine antigen that serves as a very potent antigen due to their similarity to virus particles or bacterial surfaces with multiple identical epitopes. Using three cancer vaccine antigens as test antigens, we have shown that they are soluble when produced in bacteria (*E. coli*) and form stable cysteine-bridged multimers with from 5 to at least 15 monomers, in the multimeric structures (150).

view of the factors involved in shaping immunity and where these factors can go wrong. Our life style has changed dramatically, and the strong genetic selection acting upon us during early evolution is presently most likely not as efficient, which may be contributing factors to the increase in allergies. However, what factors that dominate this increase are still not known, which may also vary from person to person as both genetic and environmental factors seem to be of importance (127, 140).

Wild Animals As a Source of Therapeutic Proteins

In addition to giving us a more detailed view of the regulation and the evolution of our immune system, wild animals may also be a rich source of therapeutic proteins and other potential therapeutic molecules. As a separate line of research we have also been trying to develop new treatment strategies against atopic allergies. One such line of research has been the development of therapeutic vaccines targeting IgE and several of the early TH2 inducing cytokines including IL-33, IL-18, and TSLP (**Figure 1**) (6–8, 13, 144). Induction of an immune response against self-molecules, as is the case for all of these targets, is considerably more difficult than inducing an immune response against a foreign molecule. We are generally tolerant to self-molecules, and therefore, we need to use a number of tricks to overcome these tolerance mechanisms in order to induce an immune response strong enough to give a therapeutic effect. Here, adjuvants are very important and in order to obtain a strong anti-self-immune response potent adjuvants are a necessity (145, 146). On top of this issue are other factors including having to modify the self-protein by coupling it to a non-self carrier (6, 144, 147). This results in the recruitment of non-tolerized T cells to provide help to self-reactive B cells to expand and differentiate (144). In the design of a vaccine targeting IgE, we produced a fusion protein between opossum IgE and human, rat or dog IgE (**Figure 10A**). The rat variant of this vaccine antigen induced a strong anti-rat IgE response in sensitized rats and resulted in a marked reduction in circulating IgE titers in these animals (7). Another important factor is the form the self-antigen is being presented (148). Multimeric antigens such as a virus particle or a bacterial surface are very potent antigens, probably due to their potent B cell-activating properties (148, 149). A multimeric antigen can crosslink IgM on the surface of the naïve B cell very efficiently and thereby giving a very strong activating signal 1 to the B cell. During the process of optimizing parameters to obtain potent therapeutic vaccines against allergies and different solid cancers, we identified a region of a molecule coming from a wild animal a jawless fish. The protein and region is the tail-piece of the variable leukocyte receptor B (VLR-B) that facilitates the pentamerization of the VLRB, which is the functional but not structural Ig equivalent in lamprey and hagfish, similar to pentameric human IgM. Using the 30 amino acid C-terminal region of lamprey VLR-B, this resulted in very efficient multimerization of the target antigen and in a marked enhancement of the anti-target immune response (**Figure 10B**) (150). In this context, wild animals can not only give us a more detailed view of the function and evolution of our immune system but can also be a rich source of potential therapeutic proteins.

CONCLUSION

Wild animals can teach us a lot about our own immune system, including how it is regulated, how it has evolved, and which functions are essential for a potent immune defense. These reasons are but a few to consider, where non-domestic animals may facilitate new solutions to difficult therapeutic challenges.

AUTHOR CONTRIBUTIONS

The review was co-written by LH, SA, MT, and ZF.

FUNDING

Work related to the review was funded by The Swedish Research Council (VR-NT) (621-2011-5007).

REFERENCES

1. Pearson WS, Goates SA, Harrykissoon SD, Miller SA. State-based medicaid costs for pediatric asthma emergency department visits. *Prev Chronic Dis* (2014) 11:E108. doi:10.5888/pcd11.140139
2. Accordini S, Corsico AG, Braggion M, Gerbase MW, Gislason D, Gulsvik A, et al. The cost of persistent asthma in Europe: an international population-based study in adults. *Int Arch Allergy Immunol* (2013) 160:93–101. doi:10.1159/000338998
3. Griffin C. Canine atopic disease. In: Griffin C, Kwochka K, McDonald J, editors. *Current Veterinary Dermatology: The Science and Art of Practice*. St Louis: Mosby Yearbook (1993). 1993 p.
4. Reedy LM, Miller WH, Willemse T. *Allergic Skin Diseases of Cats and Dogs*. Philadelphia: W.B. Saunders (1997).
5. Lund EM, Armstrong PJ, Kirk CA, Kolar LM, Klausner JS. Health status and population characteristics of dogs and cats examined at private veterinary practices in the United States. *J Am Vet Med Assoc* (1999) 214:1336–41.
6. Hellman L. Profound reduction in allergen sensitivity following treatment with a novel allergy vaccine. *Eur J Immunol* (1994) 24:415–20. doi:10.1002/eji.1830240222
7. Vernersson M, Ledin A, Johansson J, Hellman L. Generation of therapeutic antibody responses against IgE through vaccination. *FASEB J* (2002) 16:875–7. doi:10.1096/fj.01-0879fje
8. Lei Y, Boinapally V, Zoltowska A, Adner M, Hellman L, Nilsson G. Vaccination against IL-33 inhibits airway hyperresponsiveness and inflammation in a house dust mite model of asthma. *PLoS One* (2015) 10:e0133774. doi:10.1371/journal.pone.0133774
9. Strachan DP. Hay fever, hygiene, and household size. *BMJ* (1989) 299:1259–60. doi:10.1136/bmj.299.6710.1259
10. von Mutius E. Allergies, infections and the hygiene hypothesis – the epidemiological evidence. *Immunobiology* (2007) 212:433–9. doi:10.1016/j.imbio.2007.03.002
11. Okada H, Kuhn C, Feillet H, Bach JF. The 'hygiene hypothesis' for autoimmune and allergic diseases: an update. *Clin Exp Immunol* (2010) 160:1–9. doi:10.1111/j.1365-2249.2010.04139.x
12. Stear MJ, Singleton D, Matthews L. An evolutionary perspective on gastrointestinal nematodes of sheep. *J Helminthol* (2011) 85:113–20. doi:10.1017/S0022149X11000058
13. Hellman L. Regulation of IgE homeostasis, and the identification of potential targets for therapeutic intervention. *Biomed Pharmacother* (2007) 61:34–49. doi:10.1016/j.biopha.2006.10.001
14. Mosmann TR, Cherwinski H, Bond MW, Giedlin MA, Coffman RL. Two types of murine helper T cell clone. I. Definition according to profiles of lymphokine activities and secreted proteins. *J Immunol* (1986) 136:2348–57.
15. Zhu J, Paul WE. CD4 T cells: fates, functions, and faults. *Blood* (2008) 112:1557–69. doi:10.1182/blood-2008-05-078154

16. de Vries JE, Punnonen J, Cocks BG, de Waal Malefyt R, Aversa G. Regulation of the human IgE response by IL4 and IL13. *Res Immunol* (1993) 144:597–601. doi:10.1016/S0923-2494(05)80009-4
17. McKenzie GJ, Fallon PG, Emson CL, Grencis RK, McKenzie AN. Simultaneous disruption of interleukin (IL)-4 and IL-13 defines individual roles in T helper cell type 2-mediated responses. *J Exp Med* (1999) 189:1565–72. doi:10.1084/jem.189.10.1565
18. Stavnezer J, Amemiya CT. Evolution of isotype switching. *Semin Immunol* (2004) 16:257–75. doi:10.1016/j.smim.2004.08.005
19. Greer AM, Wu N, Putnam AL, Woodruff PG, Wolters P, Kinet JP, et al. Serum IgE clearance is facilitated by human FcepsilonRI internalization. *J Clin Invest* (2014) 124:1187–98. doi:10.1172/JCI68964
20. Ye H, Housden JE, Hunter MJ, Sabban S, Helm BA. The role of Cepsilon2, Cepsilon3, and Cepsilon4 domains in human and canine IgE and their contribution to FcepsilonRIalpha interaction. *Mol Immunol* (2014) 57:151–9. doi:10.1016/j.molimm.2013.08.004
21. Barua D, Goldstein B. A mechanistic model of early FcepsilonRI signaling: lipid rafts and the question of protection from dephosphorylation. *PLoS One* (2012) 7:e51669. doi:10.1371/journal.pone.0051669
22. Lutzelschwab C, Huang MR, Kullberg MC, Aveskogh M, Hellman L. Characterization of mouse mast cell protease-8, the first member of a novel subfamily of mouse mast cell serine proteases, distinct from both the classical chymases and tryptases. *Eur J Immunol* (1998) 28:1022–33. doi:10.1002/(SICI)1521-4141(199803)28:03<1022::AID-IMMU1022>3.0.CO;2-1
23. Lutzelschwab C, Lunderius C, Enerback L, Hellman L. A kinetic analysis of the expression of mast cell protease mRNA in the intestines of *Nippostrongylus brasiliensis*-infected rats. *Eur J Immunol* (1998) 28:3730–7. doi:10.1002/(SICI)1521-4141(199811)28:11<3730::AID-IMMU3730>3.0.CO;2-0
24. Lunderius C, Hellman L. Characterization of the gene encoding mouse mast cell protease 8 (mMCP-8), and a comparative analysis of hematopoietic serine protease genes. *Immunogenetics* (2001) 53:225–32. doi:10.1007/s002510100316
25. Garman SC, Kinet JP, Jardetzky TS. Crystal structure of the human high-affinity IgE receptor. *Cell* (1998) 95:951–61. doi:10.1016/S0092-8674(00)81719-5
26. Helm B, Marsh P, Vercelli D, Padlan E, Gould H, Geha R. The mast cell binding site on human immunoglobulin E. *Nature* (1988) 331:180–3. doi:10.1038/331180a0
27. Henry AJ, Cook JP, McDonnell JM, Mackay GA, Shi J, Sutton BJ, et al. Participation of the N-terminal region of Cepsilon3 in the binding of human IgE to its high-affinity receptor FcepsilonRI. *Biochemistry* (1997) 36:15568–78. doi:10.1021/bi971299+
28. Henry AJ, McDonnell JM, Ghirlando R, Sutton BJ, Gould HJ. Conformation of the isolated cepsilon3 domain of IgE and its complex with the high-affinity receptor, FcepsilonRI. *Biochemistry* (2000) 39:7406–13. doi:10.1021/bi9928391
29. Dobson JT, Seibert J, Teh EM, Da'as S, Fraser RB, Paw BH, et al. Carboxypeptidase A5 identifies a novel mast cell lineage in the zebrafish providing new insight into mast cell fate determination. *Blood* (2008) 112:2969–72. doi:10.1182/blood-2008-03-145011
30. Baccari GC, Pinelli C, Santillo A, Minucci S, Rastogi RK. Mast cells in non-mammalian vertebrates: an overview. *Int Rev Cell Mol Biol* (2011) 290:1–53. doi:10.1016/B978-0-12-386037-8.00006-5
31. Crivellato E, Travan L, Ribatti D. The phylogenetic profile of mast cells. *Methods Mol Biol* (2015) 1220:11–27. doi:10.1007/978-1-4939-1568-2_2
32. Reite OB, Evensen O. Inflammatory cells of teleostean fish: a review focusing on mast cells/eosinophilic granule cells and rodlet cells. *Fish Shellfish Immunol* (2006) 20:192–208. doi:10.1016/j.fsi.2005.01.012
33. Cavalcante MC, de Andrade LR, Du Bocage Santos-Pinto C, Straus AH, Takahashi HK, Allodi S, et al. Colocalization of heparin and histamine in the intracellular granules of test cells from the invertebrate *Styela plicata* (Chordata-Tunicata). *J Struct Biol* (2002) 137:313–21. doi:10.1016/S1047-8477(02)00007-2
34. Wong GW, Zhuo L, Kimata K, Lam BK, Satoh N, Stevens RL. Ancient origin of mast cells. *Biochem Biophys Res Commun* (2014) 451:314–8. doi:10.1016/j.bbrc.2014.07.124
35. Dooley H, Flajnik MF. Antibody repertoire development in cartilaginous fish. *Dev Comp Immunol* (2006) 30:43–56. doi:10.1016/j.dci.2005.06.022
36. Danilova N, Bussmann J, Jekosch K, Steiner LA. The immunoglobulin heavy-chain locus in zebrafish: identification and expression of a previously unknown isotype, immunoglobulin Z. *Nat Immunol* (2005) 6:295–302. doi:10.1038/ni1166
37. Castro R, Jouneau L, Pham HP, Bouchez O, Giudicelli V, Lefranc MP, et al. Teleost fish mount complex clonal IgM and IgT responses in spleen upon systemic viral infection. *PLoS Pathog* (2013) 9:e1003098. doi:10.1371/journal.ppat.1003098
38. Zhao Y, Pan-Hammarstrom Q, Yu S, Wertz N, Zhang X, Li N, et al. Identification of IgF, a hinge-region-containing Ig class, and IgD in *Xenopus tropicalis*. *Proc Natl Acad Sci U S A* (2006) 103:12087–92. doi:10.1073/pnas.0600291103
39. Gambon Deza F, Sanchez Espinel C, Magadan Mompo S. The immunoglobulin heavy chain locus in the reptile *Anolis carolinensis*. *Mol Immunol* (2009) 46:1679–87. doi:10.1016/j.molimm.2009.02.019
40. Cheng G, Gao Y, Wang T, Sun Y, Wei Z, Li L, et al. Extensive diversification of IgH subclass-encoding genes and IgM subclass switching in crocodilians. *Nat Commun* (2013) 4:1337. doi:10.1038/ncomms2317
41. Magadan-Mompo S, Sanchez-Espinel C, Gambon-Deza F. IgH loci of American alligator and saltwater crocodile shed light on IgA evolution. *Immunogenetics* (2013) 65:531–41. doi:10.1007/s00251-013-0692-y
42. Zhao Y, Rabbani H, Shimizu A, Hammarstrom L. Mapping of the chicken immunoglobulin heavy-chain constant region gene locus reveals an inverted alpha gene upstream of a condensed upsilon gene. *Immunology* (2000) 101:348–53. doi:10.1046/j.1365-2567.2000.00106.x
43. Warr GW, Magor KE, Higgins DA. IgY: clues to the origins of modern antibodies. *Immunol Today* (1995) 16:392–8. doi:10.1016/0167-5699(95)80008-5
44. Aveskogh M, Hellman L. Evidence for an early appearance of modern post-switch isotypes in mammalian evolution; cloning of IgE, IgG and IgA from the marsupial *Monodelphis domestica*. *Eur J Immunol* (1998) 28:2738–50. doi:10.1002/(SICI)1521-4141(199809)28:09<2738::AID-IMMU2738>3.0.CO;2-I
45. Vernersson M, Aveskogh M, Munday B, Hellman L. Evidence for an early appearance of modern post-switch immunoglobulin isotypes in mammalian evolution (II); cloning of IgE, IgG1 and IgG2 from a monotreme, the duck-billed platypus, *Ornithorhynchus anatinus*. *Eur J Immunol* (2002) 32:2145–55. doi:10.1002/1521-4141(200208)32:8<2145::AID-IMMU2145>3.0.CO;2-I
46. Vernersson M, Aveskogh M, Hellman L. Cloning of IgE from the echidna (*Tachyglossus aculeatus*) and a comparative analysis of epsilon chains from all three extant mammalian lineages. *Dev Comp Immunol* (2004) 28:61–75. doi:10.1016/S0145-305X(03)00084-3
47. Vernersson M, Belov K, Aveskogh M, Hellman L. Cloning and structural analysis of two highly divergent IgA isotypes, IgA1 and IgA2 from the duck billed platypus, *Ornithorhynchus anatinus*. *Mol Immunol* (2010) 47:785–91. doi:10.1016/j.molimm.2009.10.007
48. Aveskogh M, Pilstrom L, Hellman L. Cloning and structural analysis of IgM (mu chain) and the heavy chain V region repertoire in the marsupial *Monodelphis domestica*. *Dev Comp Immunol* (1999) 23:597–606. doi:10.1016/S0145-305X(99)00050-6
49. Belov K, Hellman L. Immunoglobulin genetics of *Ornithorhynchus anatinus* (platypus) and *Tachyglossus aculeatus* (short-beaked echidna). *Comp Biochem Physiol A Mol Integr Physiol* (2003) 136:811–9. doi:10.1016/S1095-6433(03)00165-X
50. Belov K, Hellman L, Cooper DW. Characterisation of echidna IgM provides insights into the time of divergence of extant mammals. *Dev Comp Immunol* (2002) 26:831–9. doi:10.1016/S0145-305X(02)00030-7
51. Zhao Y, Cui H, Whittington CM, Wei Z, Zhang X, Zhang Z, et al. *Ornithorhynchus anatinus* (platypus) links the evolution of immunoglobulin genes in eutherian mammals and nonmammalian tetrapods. *J Immunol* (2009) 183:3285–93. doi:10.4049/jimmunol.0900469
52. Flanagan JG, Rabbitts TH. Arrangement of human immunoglobulin heavy chain constant region genes implies evolutionary duplication of a segment containing gamma, epsilon and alpha genes. *Nature* (1982) 300:709–13. doi:10.1038/300709a0
53. Max EE, Battey J, Ney R, Kirsch IR, Leder P. Duplication and deletion in the human immunoglobulin epsilon genes. *Cell* (1982) 29:691–9. doi:10.1016/0092-8674(82)90185-4

54. Battey J, Max EE, McBride WO, Swan D, Leder P. A processed human immunoglobulin epsilon gene has moved to chromosome 9. *Proc Natl Acad Sci U S A* (1982) 79:5956–60. doi:10.1073/pnas.79.19.5956
55. Nimmerjahn F, Ravetch JV. Fcgamma receptors as regulators of immune responses. *Nat Rev Immunol* (2008) 8:34–47. doi:10.1038/nri2206
56. van der Poel CE, Spaapen RM, van de Winkel JG, Leusen JH. Functional characteristics of the high affinity IgG receptor, FcgammaRI. *J Immunol* (2011) 186:2699–704. doi:10.4049/jimmunol.1003526
57. Rivera J, Fierro NA, Olivera A, Suzuki R. New insights on mast cell activation via the high affinity receptor for IgE. *Adv Immunol* (2008) 98:85–120. doi:10.1016/S0065-2776(08)00403-3
58. Klimovich VB. IgM and its receptors: structural and functional aspects. *Biochemistry (Mosc)* (2011) 76:534–49. doi:10.1134/S0006297911050038
59. Bakema JE, van Egmond M. The human immunoglobulin A Fc receptor FcalphaRI: a multifaceted regulator of mucosal immunity. *Mucosal Immunol* (2011) 4:612–24. doi:10.1038/mi.2011.36
60. Akula S, Mohammadamin S, Hellman L. Fc receptors for immunoglobulins and their appearance during vertebrate evolution. *PLoS One* (2014) 9:e96903. doi:10.1371/journal.pone.0096903
61. Akula S, Hellman L. The appearance and diversification of receptors for IgM during vertebrate evolution. *Curr Top Microbiol Immunol* (2017) 408:1–23. doi:10.1007/82_2017_22
62. Davis RS. Fc receptor-like molecules. *Annu Rev Immunol* (2007) 25:525–60. doi:10.1146/annurev.immunol.25.022106.141541
63. Ehrhardt GR, Cooper MD. Immunoregulatory roles for fc receptor-like molecules. *Curr Top Microbiol Immunol* (2011) 350:89–104. doi:10.1007/82_2010_88
64. Nikolaidis N, Klein J, Nei M. Origin and evolution of the Ig-like domains present in mammalian leukocyte receptors: insights from chicken, frog, and fish homologues. *Immunogenetics* (2005) 57:151–7. doi:10.1007/s00251-004-0764-0
65. Viertlboeck BC, Gobel TW. The chicken leukocyte receptor cluster. *Vet Immunol Immunopathol* (2011) 144:1–10. doi:10.1016/j.vetimm.2011.07.001
66. Kaetzel CS. Coevolution of mucosal immunoglobulins and the polymeric immunoglobulin receptor: evidence that the commensal microbiota provided the driving force. *ISRN Immunol* (2014):1–20. doi:10.1155/2014/541537
67. Blank U, Ra C, Miller L, White K, Metzger H, Kinet JP. Complete structure and expression in transfected cells of high affinity IgE receptor. *Nature* (1989) 337:187–9. doi:10.1038/337187a0
68. Rodewald HR, Arulanandam AR, Koyasu S, Reinherz EL. The high affinity Fc epsilon receptor gamma subunit (Fc epsilon RI gamma) facilitates T cell receptor expression and antigen/major histocompatibility complex-driven signaling in the absence of CD3 zeta and CD3 eta. *J Biol Chem* (1991) 266:15974–8.
69. Weissman AM, Hou D, Orloff DG, Modi WS, Seuanez H, O'Brien SJ, et al. Molecular cloning and chromosomal localization of the human T-cell receptor zeta chain: distinction from the molecular CD3 complex. *Proc Natl Acad Sci U S A* (1988) 85:9709–13. doi:10.1073/pnas.85.24.9709
70. Lanier LL. DAP10- and DAP12-associated receptors in innate immunity. *Immunol Rev* (2009) 227:150–60. doi:10.1111/j.1600-065X.2008.00720.x
71. Riley JF, West GB. Histamine in tissue mast cells. *J Physiol* (1952) 117:72–3.
72. Ohtsu H, Tanaka S, Terui T, Hori Y, Makabe-Kobayashi Y, Pejler G, et al. Mice lacking histidine decarboxylase exhibit abnormal mast cells. *FEBS Lett* (2001) 502:53–6. doi:10.1016/S0014-5793(01)02663-1
73. Parsons ME, Ganellin CR. Histamine and its receptors. *Br J Pharmacol* (2006) 147(Suppl 1):S127–35. doi:10.1038/sj.bjp.0706440
74. Khanfar MA, Affini A, Lutsenko K, Nikolic K, Butini S, Stark H. Multiple targeting approaches on histamine H3 receptor antagonists. *Front Neurosci* (2016) 10:201. doi:10.3389/fnins.2016.00201
75. Kjellen L, Pettersson I, Lillhager P, Steen ML, Pettersson U, Lehtonen P, et al. Primary structure of a mouse mastocytoma proteoglycan core protein. *Biochem J* (1989) 263:105–13. doi:10.1042/bj2630105
76. Angerth T, Huang RY, Aveskogh M, Pettersson I, Kjellen L, Hellman L. Cloning and structural analysis of a gene encoding a mouse mastocytoma proteoglycan core protein; analysis of its evolutionary relation to three cross hybridizing regions in the mouse genome. *Gene* (1990) 93:235–40. doi:10.1016/0378-1119(90)90230-O
77. Forsberg E, Pejler G, Ringvall M, Lunderius C, Tomasini-Johansson B, Kusche-Gullberg M, et al. Abnormal mast cells in mice deficient in a heparin-synthesizing enzyme. *Nature* (1999) 400:773–6. doi:10.1038/23488
78. Ronnberg E, Melo FR, Pejler G. Mast cell proteoglycans. *J Histochem Cytochem* (2012) 60:950–62. doi:10.1369/0022155412458927
79. Reynolds DS, Stevens RL, Lane WS, Carr MH, Austen KF, Serafin WE. Different mouse mast cell populations express various combinations of at least six distinct mast cell serine proteases. *Proc Natl Acad Sci U S A* (1990) 87:3230–4. doi:10.1073/pnas.87.8.3230
80. Huang RY, Blom T, Hellman L. Cloning and structural analysis of MMCP-1, MMCP-4 and MMCP-5, three mouse mast cell-specific serine proteases. *Eur J Immunol* (1991) 21:1611–21. doi:10.1002/eji.1830210706
81. Irani AM, Goldstein SM, Wintroub BU, Bradford T, Schwartz LB. Human mast cell carboxypeptidase. Selective localization to MCTC cells. *J Immunol* (1991) 147:247–53.
82. Lutzelschwab C, Pejler G, Aveskogh M, Hellman L. Secretory granule proteases in rat mast cells. Cloning of 10 different serine proteases and a carboxypeptidase A from various rat mast cell populations. *J Exp Med* (1997) 185:13–29. doi:10.1084/jem.185.1.13
83. Pejler G, Ronnberg E, Waern I, Wernersson S. Mast cell proteases: multifaceted regulators of inflammatory disease. *Blood* (2010) 115:4981–90. doi:10.1182/blood-2010-01-257287
84. Caughey GH. Mast cell proteases as protective and inflammatory mediators. *Adv Exp Med Biol* (2011) 716:212–34. doi:10.1007/978-1-4419-9533-9_12
85. Hellman L, Thorpe M. Granule proteases of hematopoietic cells, a family of versatile inflammatory mediators – an update on their cleavage specificity, in vivo substrates, and evolution. *Biol Chem* (2014) 395:15–49. doi:10.1515/hsz-2013-0211
86. Schwartz LB, Irani AM, Roller K, Castells MC, Schechter NM. Quantitation of histamine, tryptase, and chymase in dispersed human T and TC mast cells. *J Immunol* (1987) 138:2611–5.
87. Lindstedt KA, Kokkonen JO, Kovanen PT. Regulation of the activity of secreted human lung mast cell tryptase by mast cell proteoglycans. *Biochim Biophys Acta* (1998) 1425:617–27. doi:10.1016/S0304-4165(98)00115-9
88. Matsumoto R, Sali A, Ghildyal N, Karplus M, Stevens RL. Packaging of proteases and proteoglycans in the granules of mast cells and other hematopoietic cells. A cluster of histidines on mouse mast cell protease 7 regulates its binding to heparin serglycin proteoglycans. *J Biol Chem* (1995) 270:19524–31. doi:10.1074/jbc.270.33.19524
89. Hallgren J, Karlson U, Poorafshar M, Hellman L, Pejler G. Mechanism for activation of mouse mast cell tryptase: dependence on heparin and acidic pH for formation of active tetramers of mouse mast cell protease 6. *Biochemistry* (2000) 39:13068–77. doi:10.1021/bi000973b
90. Akula S, Thorpe M, Boinapally V, Hellman L. Granule associated serine proteases of hematopoietic cells – an analysis of their appearance and diversification during vertebrate evolution. *PLoS One* (2015) 10:e0143091. doi:10.1371/journal.pone.0143091
91. Gallwitz M, Hellman L. Rapid lineage-specific diversification of the mast cell chymase locus during mammalian evolution. *Immunogenetics* (2006) 58:641–54. doi:10.1007/s00251-006-0123-4
92. Gallwitz M, Reimer JM, Hellman L. Expansion of the mast cell chymase locus over the past 200 million years of mammalian evolution. *Immunogenetics* (2006) 58:655–69. doi:10.1007/s00251-006-0126-1
93. Zamolodchikova TS, Scherbakov IT, Khrennikov BN, Svirshchevskaya EV. Expression of duodenase-like protein in epitheliocytes of Brunner's glands in human duodenal mucosa. *Biochemistry (Mosc)* (2013) 78:954–7. doi:10.1134/S0006297913080130
94. Zamolodchikova TS, Vorotyntseva TI, Antonov VK. Duodenase, a new serine protease of unusual specificity from bovine duodenal mucosa. Purification and properties. *Eur J Biochem* (1995) 227:866–72. doi:10.1111/j.1432-1033.1995.tb20212.x
95. Caughey GH, Raymond WW, Blount JL, Hau LW, Pallaoro M, Wolters PJ, et al. Characterization of human gamma-tryptases, novel members of the chromosome 16p mast cell tryptase and prostasin gene families. *J Immunol* (2000) 164:6566–75. doi:10.4049/jimmunol.164.12.6566
96. Trivedi NN, Tong Q, Raman K, Bhagwandin VJ, Caughey GH. Mast cell alpha and beta tryptases changed rapidly during primate speciation and evolved from gamma-like transmembrane peptidases in ancestral vertebrates. *J Immunol* (2007) 179:6072–9. doi:10.4049/jimmunol.179.9.6072

97. Reimer JM, Samollow PB, Hellman L. High degree of conservation of the multigene tryptase locus over the past 150-200 million years of mammalian evolution. *Immunogenetics* (2010) 62:369–82. doi:10.1007/s00251-010-0443-2
98. Karlson U, Pejler G, Froman G, Hellman L. Rat mast cell protease 4 is a beta-chymase with unusually stringent substrate recognition profile. *J Biol Chem* (2002) 277:18579–85. doi:10.1074/jbc.M110356200
99. Huang R, Hellman L. Genes for mast-cell serine protease and their molecular evolution. *Immunogenetics* (1994) 40:397–414. doi:10.1007/BF00177823
100. Lunderius C, Xiang Z, Nilsson G, Hellman L. Murine mast cell lines as indicators of early events in mast cell and basophil development. *Eur J Immunol* (2000) 30:3396–402. doi:10.1002/1521-4141(2000012)30:12<3396::AID-IMMU3396>3.0.CO;2-O
101. Poorafshar M, Helmby H, Troye-Blomberg M, Hellman L. MMCP-8, the first lineage-specific differentiation marker for mouse basophils. Elevated numbers of potent IL-4-producing and MMCP-8-positive cells in spleens of malaria-infected mice. *Eur J Immunol* (2000) 30:2660–8. doi:10.1002/1521-4141(200009)30:9<2660::AID-IMMU2660>3.0.CO;2-I
102. Karlson U, Pejler G, Tomasini-Johansson B, Hellman L. Extended substrate specificity of rat mast cell protease 5, a rodent alpha-chymase with elastase-like primary specificity. *J Biol Chem* (2003) 278:39625–31. doi:10.1074/jbc.M301512200
103. Reimer JM, Enoksson M, Samollow PB, Hellman L. Extended substrate specificity of opossum chymase – implications for the origin of mast cell chymases. *Mol Immunol* (2008) 45:2116–25. doi:10.1016/j.molimm.2007.10.015
104. Fu Z, Thorpe M, Hellman L. rMCP-2, the major rat mucosal mast cell protease, an analysis of its extended cleavage specificity and its potential role in regulating intestinal permeability by the cleavage of cell adhesion and junction proteins. *PLoS One* (2015) 10:e0131720. doi:10.1371/journal.pone.0131720
105. Fu Z, Thorpe M, Akula S, Hellman L. Asp-ase activity of the opossum granzyme B supports the role of granzyme B as part of anti-viral immunity already during early mammalian evolution. *PLoS One* (2016) 11:e0154886. doi:10.1371/journal.pone.0154886
106. Fu Z, Thorpe M, Alemayehu R, Roy A, Kervinen J, de Garavilla L, et al. Highly selective cleavage of cytokines and chemokines by the human mast cell chymase and neutrophil cathepsin G. *J Immunol* (2017) 198:1474–83. doi:10.4049/jimmunol.1601223
107. Wernersson S, Reimer JM, Poorafshar M, Karlson U, Wermenstam N, Bengten E, et al. Granzyme-like sequences in bony fish shed light on the emergence of hematopoietic serine proteases during vertebrate evolution. *Dev Comp Immunol* (2006) 30:901–18. doi:10.1016/j.dci.2005.10.014
108. Thorpe M, Akula S, Hellman L. Channel catfish granzyme-like I is a highly specific serine protease with metase activity that is expressed by fish NK-like cells. *Dev Comp Immunol* (2016) 63:84–95. doi:10.1016/j.dci.2016.05.013
109. Metz M, Piliponsky AM, Chen CC, Lammel V, Abrink M, Pejler G, et al. Mast cells can enhance resistance to snake and honeybee venoms. *Science* (2006) 313:526–30. doi:10.1126/science.1128877
110. Akahoshi M, Song CH, Piliponsky AM, Metz M, Guzzetta A, Abrink M, et al. Mast cell chymase reduces the toxicity of Gila monster venom, scorpion venom, and vasoactive intestinal polypeptide in mice. *J Clin Invest* (2011) 121:4180–91. doi:10.1172/JCI46139
111. Mukai K, Tsai M, Starkl P, Marichal T, Galli SJ. IgE and mast cells in host defense against parasites and venoms. *Semin Immunopathol* (2016) 38(5):581–603. doi:10.1007/s00281-016-0565-1
112. Vartio T, Seppa H, Vaheri A. Susceptibility of soluble and matrix fibronectins to degradation by tissue proteinases, mast cell chymase and cathepsin G. *J Biol Chem* (1981) 256:471–7.
113. Tchougounova E, Forsberg E, Angelborg G, Kjellen L, Pejler G. Altered processing of fibronectin in mice lacking heparin. a role for heparin-dependent mast cell chymase in fibronectin degradation. *J Biol Chem* (2001) 276:3772–7. doi:10.1074/jbc.M008434200
114. Tchougounova E, Pejler G, Abrink M. The chymase, mouse mast cell protease 4, constitutes the major chymotrypsin-like activity in peritoneum and ear tissue. A role for mouse mast cell protease 4 in thrombin regulation and fibronectin turnover. *J Exp Med* (2003) 198:423–31. doi:10.1084/jem.20030671
115. Okumura K, Takai S, Muramatsu M, Katayama S, Sakaguchi M, Kishi K, et al. Human chymase degrades human fibronectin. *Clin Chim Acta* (2004) 347:223–5. doi:10.1016/j.cccn.2004.04.019
116. Tchougounova E, Lundequist A, Fajardo I, Winberg JO, Abrink M, Pejler G. A key role for mast cell chymase in the activation of pro-matrix metalloprotease-9 and pro-matrix metalloprotease-2. *J Biol Chem* (2005) 280:9291–6. doi:10.1074/jbc.M410396200
117. Thorpe M, Yu J, Boinapally V, Ahooghalandari P, Kervinen J, Garavilla LD, et al. Extended cleavage specificity of the mast cell chymase from the crab-eating macaque (*Macaca fascicularis*): an interesting animal model for the analysis of the function of the human mast cell chymase. *Int Immunol* (2012) 12:771–82. doi:10.1093/intimm/dxs081
118. Piliponsky AM, Chen CC, Rios EJ, Treuting PM, Lahiri A, Abrink M, et al. The chymase mouse mast cell protease 4 degrades TNF, limits inflammation, and promotes survival in a model of sepsis. *Am J Pathol* (2012) 181:875–86. doi:10.1016/j.ajpath.2012.05.013
119. Caughey GH, Raymond WW, Wolters PJ. Angiotensin II generation by mast cell alpha- and beta-chymases. *Biochim Biophys Acta* (2000) 1480:245–57. doi:10.1016/S0167-4838(00)00076-5
120. Wintroub BU, Schechter NB, Lazarus GS, Kaempfer CE, Schwartz LB. Angiotensin I conversion by human and rat chymotryptic proteinases. *J Invest Dermatol* (1984) 83:336–9. doi:10.1111/1523-1747.ep12264144
121. Chandrasekharan UM, Sanker S, Glynias MJ, Karnik SS, Husain A. Angiotensin II-forming activity in a reconstructed ancestral chymase. *Science* (1996) 271:502–5. doi:10.1126/science.271.5248.502
122. Pejler G, Karlstrom A. Thrombin is inactivated by mast cell secretory granule chymase. *J Biol Chem* (1993) 268:11817–22.
123. Pejler G, Soderstrom K, Karlstrom A. Inactivation of thrombin by a complex between rat mast-cell protease 1 and heparin proteoglycan. *Biochem J* (1994) 299(Pt 2):507–13. doi:10.1042/bj2990507
124. Hellman, L. *Genes for Immunoglobulin E: Structure, Rearrangement and Expression [Thesis]*. Uppsala: Acta Universitatis Upsaliensis (1985). 1–54 p.
125. Iancovici Kidon M, Stein M, Geller-Bernstein C, Weisman Z, Steinberg S, Greenberg Z, et al. Serum immunoglobulin E levels in Israeli-Ethiopian children: environment and genetics. *Isr Med Assoc J* (2005) 7:799–802.
126. Cahenzli J, Koller Y, Wyss M, Geuking MB, McCoy KD. Intestinal microbial diversity during early-life colonization shapes long-term IgE levels. *Cell Host Microbe* (2013) 14:559–70. doi:10.1016/j.chom.2013.10.004
127. Yazdanbakhsh M, van den Biggelaar A, Maizels RM. Th2 responses without atopy: immunoregulation in chronic helminth infections and reduced allergic disease. *Trends Immunol* (2001) 22:372–7. doi:10.1016/S1471-4906(01)01958-5
128. Ledin A, Bergvall K, Hillbertz NS, Hansson H, Andersson G, Hedhammar A, et al. Generation of therapeutic antibody responses against IgE in dogs, an animal species with exceptionally high plasma IgE levels. *Vaccine* (2006) 24:66–74. doi:10.1016/j.vaccine.2005.07.052
129. Ledin A, Arnemo JM, Liberg O, Hellman L. High plasma IgE levels within the Scandinavian wolf population, and its implications for mammalian IgE homeostasis. *Mol Immunol* (2008) 45:1976–80. doi:10.1016/j.molimm.2007.10.029
130. Wagner B, Radbruch A, Rohwer J, Leibold W. Monoclonal anti-equine IgE antibodies with specificity for different epitopes on the immunoglobulin heavy chain of native IgE. *Vet Immunol Immunopathol* (2003) 92:45–60. doi:10.1016/S0165-2427(03)00007-2
131. Lyons ET, Tolliver SC, Kuzmina TA, Collins SS. Critical tests evaluating efficacy of moxidectin against small strongyles in horses from a herd for which reduced activity had been found in field tests in Central Kentucky. *Parasitol Res* (2010) 107:1495–8. doi:10.1007/s00436-010-2025-5
132. Matthews JB. Facing the threat of equine parasitic disease. *Equine Vet J* (2011) 43:126–32. doi:10.1111/j.2042-3306.2010.00356.x
133. Mitre E, Nutman TB. IgE memory: persistence of antigen-specific IgE responses years after treatment of human filarial infections. *J Allergy Clin Immunol* (2006) 117:939–45. doi:10.1016/j.jaci.2005.12.1341
134. Levy DA, Chen J. Healthy IgE-deficient person. *N Engl J Med* (1970) 283:541. doi:10.1056/NEJM197009032831018
135. Thorburn AN, Macia L, Mackay CR. Diet, metabolites, and "western-lifestyle" inflammatory diseases. *Immunity* (2014) 40:833–42. doi:10.1016/j.immuni.2014.05.014

136. Daien CI, Pinget GV, Tan JK, Macia L. Detrimental impact of microbiota-accessible carbohydrate-deprived diet on gut and immune homeostasis: an overview. *Front Immunol* (2017) 8:548. doi:10.3389/fimmu.2017.00548
137. Hill DA, Siracusa MC, Abt MC, Kim BS, Kobuley D, Kubo M, et al. Commensal bacteria-derived signals regulate basophil hematopoiesis and allergic inflammation. *Nat Med* (2012) 18:538–46. doi:10.1038/nm.2657
138. McCoy KD, Koller Y. New developments providing mechanistic insight into the impact of the microbiota on allergic disease. *Clin Immunol* (2015) 159:170–6. doi:10.1016/j.clim.2015.05.007
139. Hong SW, Kim KS, Surh CD. Beyond hygiene: commensal microbiota and allergic diseases. *Immune Netw* (2017) 17:48–59. doi:10.4110/in.2017.17.1.48
140. Jatzlauk G, Bartel S, Heine H, Schloter M, Krauss-Etschmann S. Influences of environmental bacteria and their metabolites on allergies, asthma, and host microbiota. *Allergy* (2017) 72(12):1859–67. doi:10.1111/all.13220
141. Abrahamsson TR, Jakobsson HE, Andersson AF, Bjorksten B, Engstrand L, Jenmalm MC. Low diversity of the gut microbiota in infants with atopic eczema. *J Allergy Clin Immunol* (2012) 129:434–40, 440.e1–2. doi:10.1016/j.jaci.2011.10.025
142. Abrahamsson TR, Jakobsson HE, Andersson AF, Bjorksten B, Engstrand L, Jenmalm MC. Low gut microbiota diversity in early infancy precedes asthma at school age. *Clin Exp Allergy* (2014) 44:842–50. doi:10.1111/cea.12253
143. Dulek DE, Peebles RS Jr. Viruses and asthma. *Biochim Biophys Acta* (2011) 1810:1080–90. doi:10.1016/j.bbagen.2011.01.012
144. Hellman L. Therapeutic vaccines against IgE-mediated allergies. *Expert Rev Vaccines* (2008) 7:193–208. doi:10.1586/14760584.7.2.193
145. Johansson J, Ledin A, Vernersson M, Lovgren-Bengtsson K, Hellman L. Identification of adjuvants that enhance the therapeutic antibody response to host IgE. *Vaccine* (2004) 22:2873–80. doi:10.1016/j.vaccine.2003.12.029
146. Ringvall M, Huijbers EJ, Ahooghalandari P, Alekseeva L, Andronova T, Olsson AK, et al. Identification of potent biodegradable adjuvants that efficiently break self-tolerance – a key issue in the development of therapeutic vaccines. *Vaccine* (2009) 28:48–52. doi:10.1016/j.vaccine.2009.09.122
147. Saupe F, Huijbers EJ, Hein T, Femel J, Cedervall J, Olsson AK, et al. Vaccines targeting self-antigens: mechanisms and efficacy-determining parameters. *FASEB J* (2015) 29:3253–62. doi:10.1096/fj.15-271502
148. Johansson J, Hellman L. Modifications increasing the efficacy of recombinant vaccines; marked increase in antibody titers with moderately repetitive variants of a therapeutic allergy vaccine. *Vaccine* (2007) 25:1676–82. doi:10.1016/j.vaccine.2006.10.055
149. Lechner F, Jegerlehner A, Tissot AC, Maurer P, Sebbel P, Renner WA, et al. Virus-like particles as a modular system for novel vaccines. *Intervirology* (2002) 45:212–7. doi:10.1159/000067912
150. Saupe F, Reichel M, Huijbers EJ, Femel J, Markgren PO, Andersson CE, et al. Development of a novel therapeutic vaccine carrier that sustains high antibody titers against several targets simultaneously. *FASEB J* (2017) 31:1204–14. doi:10.1096/fj.201600820R

Conflict of Interest Statement: The patents for the VLR-B sequence used to enhance immunogenicity to therapeutic vaccines targeting self-molecules is owned by a company owned by LH. All other authors declare that the research was conducted in the absence of any commercial or financial relationships that could be construed as a potential conflict of interest.

frontiers in Immunology

ORIGINAL RESEARCH
published: 19 February 2018
doi: 10.3389/fimmu.2018.00259

Immunization Strategies Producing a Humoral IgG Immune Response against Devil Facial Tumor Disease in the Majority of Tasmanian Devils Destined for Wild Release

Ruth Pye[1], Amanda Patchett[1], Elspeth McLennan[2], Russell Thomson[3], Scott Carver[4], Samantha Fox[5], David Pemberton[5], Alexandre Kreiss[1], Adriana Baz Morelli[6], Anabel Silva[6], Martin J. Pearse[6], Lynn M. Corcoran[7,8], Katherine Belov[2], Carolyn J. Hogg[2], Gregory M Woods[1] and A. Bruce Lyons[9]**

[1] Menzies Institute for Medical Research, University of Tasmania, Hobart, TAS, Australia, [2] Faculty of Science, School of Life and Environmental Sciences, The University of Sydney, Sydney, NSW, Australia, [3] Centre for Research in Mathematics, School of Computing, Engineering and Mathematics, Western Sydney University, Penrith, NSW, Australia, [4] School of Biological Sciences, University of Tasmania, Hobart, TAS, Australia, [5] Save the Tasmanian Devil Program, Tasmanian Department of Primary Industries, Parks, Water and the Environment, Hobart, TAS, Australia, [6] CSL Ltd., Bio21 Institute, Melbourne, VIC, Australia, [7] The Walter and Eliza Hall Institute of Medical Research, Melbourne, VIC, Australia, [8] Department of Medical Biology, The University of Melbourne, Melbourne, VIC, Australia, [9] School of Medicine, University of Tasmania, Hobart, TAS, Australia

OPEN ACCESS

Edited by:
Rayne Rouce, Baylor College of Medicine, United States

Reviewed by:
Alexandre Corthay, Oslo University Hospital, Norway
Thorbald Van Hall, Leiden University, Netherlands

***Correspondence:**
Ruth Pye
ruth.pye@utas.edu.au;
A. Bruce Lyons
bruce.lyons@utas.edu.au

Specialty section:
This article was submitted to Cancer Immunity and Immunotherapy, a section of the journal Frontiers in Immunology

Received: *01 November 2017*
Accepted: *29 January 2018*
Published: *19 February 2018*

Citation:
Pye R, Patchett A, McLennan E, Thomson R, Carver S, Fox S, Pemberton D, Kreiss A, Baz Morelli A, Silva A, Pearse MJ, Corcoran LM, Belov K, Hogg CJ, Woods GM and Lyons AB (2018) Immunization Strategies Producing a Humoral IgG Immune Response against Devil Facial Tumor Disease in the Majority of Tasmanian Devils Destined for Wild Release. Front. Immunol. 9:259. doi: 10.3389/fimmu.2018.00259

Devil facial tumor disease (DFTD) is renowned for its successful evasion of the host immune system. Down regulation of the major histocompatabilty complex class I molecule (MHC-I) on the DFTD cells is a primary mechanism of immune escape. Immunization trials on captive Tasmanian devils have previously demonstrated that an immune response against DFTD can be induced, and that immune-mediated tumor regression can occur. However, these trials were limited by their small sample sizes. Here, we describe the results of two DFTD immunization trials on cohorts of devils prior to their wild release as part of the Tasmanian Government's Wild Devil Recovery project. 95% of the devils developed anti-DFTD antibody responses. Given the relatively large sample sizes of the trials (N = 19 and N = 33), these responses are likely to reflect those of the general devil population. DFTD cells manipulated to express MHC-I were used as the antigenic basis of the immunizations in both trials. Although the adjuvant composition and number of immunizations differed between trials, similar anti-DFTD antibody levels were obtained. The first trial comprised DFTD cells and the adjuvant combination of ISCOMATRIX™, polyIC, and CpG with up to four immunizations given at monthly intervals. This compared to the second trial whereby two immunizations comprising DFTD cells and the adjuvant combination ISCOMATRIX™, polyICLC (Hiltonol®) and imiquimod were given a month apart, providing a shorter and, therefore, more practical protocol. Both trials incorporated a booster immunization given up to 5 months after the primary course. A key finding was that devils in the second trial responded more quickly and maintained their antibody levels for longer compared to devils in the first trial. The different adjuvant combination incorporating the RNAase

resistant polyICLC and imiquimod used in the second trial is likely to be responsible. The seroconversion in the majority of devils in these anti-DFTD immunization trials was remarkable, especially as DFTD is hallmarked by its immune evasion mechanisms. Microsatellite analyzes of MHC revealed that some MHC-I microsatellites correlated to stronger immune responses. These trials signify the first step in the long-term objective of releasing devils with immunity to DFTD into the wild.

Keywords: Tasmanian devil facial tumour disease, vaccination, adjuvant, humoral immunity/antibody response, wild immunology

INTRODUCTION

The Tasmanian devil is the largest living carnivorous marsupial species and is unique to Australia's island state of Tasmania. The species was listed as Endangered in 2008 due to mortality from devil facial tumor disease (DFTD) (1). DFTD is a fatal transmissible cancer whereby the cancer cells are the infectious agent and pass between individual devils by biting behavior. The cancer's ability to evade the host's immune response as it acts as an allograft has been the subject of ongoing research. The devil's immune system has demonstrated competence from both humoral and cell-mediated perspectives (2–5). The DFTD cancer cells' ability to avoid an allogeneic immune response is, therefore, not considered due to a defective devil immune system, but rather due to DFTD's immune escape mechanisms (6, 7). While DFTD immunology and the marsupial devil immune system are in themselves fascinating research topics, the insights gained from such research have a practical application for DFTD vaccine development. A protective vaccine against DFTD would provide an extremely useful tool for managing the endangered species and may help prevent DFTD-driven extinction of the wild devil.

As previously mentioned, successful transmission of DFTD between individuals is considered to be primarily due to the tumor's immune escape mechanisms. A primary mechanism is the down regulation of the major histocompatibility class I molecule (MHC-I) on the DFTD cell surface (8). Despite this, naturally occurring immune responses against DFTD have been identified in a small number of wild devils (9). Furthermore, immunization trials have demonstrated that humoral and cell-mediated immune recognition of DFTD can be induced (10). Subsequent trials found these immune responses could lead to immune-mediated rejection of the tumors (11). These trials used DFTD cells manipulated to express surface MHC-I as the antigenic basis of the vaccine. This approach was intended to make the tumor cells immunogenic and, therefore, increase the likelihood of raising both antibody and allospecific T-cell responses. However, limitations of these trials included small sample sizes and senescent individuals. The opportunity to address these shortcomings arose with the implementation of the Wild Devil Recovery project by the Tasmanian state government's Save the Tasmanian Devil Program (STDP; http://www.tassiedevil.com.au/tasdevil.nsf/Wild-Devil-Recovery/8A632773F33E4920CA257EC9001912CE). The ongoing project involves the release of devils from the STDP's captive insurance and DFTD-free island populations to augment local wild devil populations that have been decimated by DFTD.

The first wild release took place in September 2015 in Narawntapu National Park (NNP) in Tasmania's north. The devils selected for release were held in free range enclosures (FREs) for several months prior to the release date and 19 were included in this first DFTD immunization trial. The selection of the immunization protocol for this trial was based on results from the previously mentioned trial whereby DFTD cells manipulated *in vitro* to express MHC-I on the cell surface were used as the antigenic basis for the immunizations.

A second release of 33 devils in Stony Head (SH) in the state's north east took place in August 2016. The SH immunization protocol was shortened in light of the NNP trial results. It also incorporated an improved adjuvant combination that was identified between the NNP and SH releases (12).

Post release monitoring at NNP and SH was carried out by the STDP. Not all devils were trapped following release, but those that had serum samples collected to assess the duration of their anti-DFTD immune responses. Booster immunizations were given to the SH devils that were trapped during the final month of monitoring, which was 5 months after the primary immunization course.

These immunization trials provided the first opportunity to use comparatively large sample sizes. This meant a more robust assessment of anti-DFTD immune responses in Tasmanian devils, as determined by seroconversion, could be made. The responses generated by the different protocols used in the NNP and SH trials with respect to the number of immunizations given and adjuvant combination could also be compared.

Since the initiation of these trials, a second DFTD was discovered (13) and named DFT2 to distinguish it from the first DFTD, which is now referred to as DFT1. The work described here refers to DFT1.

MATERIALS AND METHODS

Tasmanian Devils

There were 19 devils in the NNP trial and 33 devils in the SH trial. All of the NNP devils came from the captive insurance population. Eleven of these NNP devils were originally born in the wild and brought into captivity at the age of 1 year ($N = 10$) or 2 years ($N = 1$). They were quarantined for a period of 30 months to ensure that they were disease free. The other eight NNP devils were born in captivity. Of the SH devils, 16 were born in captivity as part of the captive insurance population. The remaining 17 of the SH devils were from Maria Island, the DFTD-free island population. See **Table 1** for age and sex details of the trial devils.

TABLE 1 | Summary of devil age, sex, and immunization protocols for Narawntapu National Park (NNP) and Stony Head (SH) trials.

Age	1 year	2 years	3 years	4 years	5 years	Total
NNP devils						
No. of males	4	0	0	7	0	11
No. of females	1	1	2	3	1	8
SH devils						
No. of males	1	13	8	0	0	22
No. of females	0	1	6	4	0	11

Complete NNP immunization protocol

Primary course (four immunizations given at monthly intervals)	
Date of each immunization	Composition of immunizations[a]
1st: February 2015	2×10^7 MHC-I^{+ve} sonicated cells
2nd: March 2015	2×10^7 MHC-I^{+ve} sonicated cells
3rd: April 2015	2×10^6 MHC-I^{+ve} irradiated cells
4th: May 2015	2×10^6 MHC-I^{+ve} irradiated cells
Booster immunization	
Date of booster	Composition of booster immunization[a]
September 2015 (pre-release)	2×10^6 MHC-I^{+ve} irradiated cells

Complete SH immunization protocol

Primary course (2 immunizations given at monthly intervals)	
Date of each immunization	Composition of immunizations[b]
1st: June 2016	2×10^7 MHC-I^{+ve} sonicated cells
2nd: July 2016	2×10^6 MHC-I^{+ve} irradiated cells
Booster immunization	
Date of booster	Composition of booster immunization[b]
December 2016 (post release)	2×10^6 MHC-I^{+ve} irradiated cells

[a]*The combination of adjuvants used in each immunization and booster was as follows: 50 µl ISCOMATRIX™ (provided by CSL Ltd., VIC, Australia), 100 µg polyIC (Sigma-Aldrich, P1530), 50 µg CpG-ODN-1585 (GeneWorks, 1141231), and 50 µg CpG-ODN-2395 (GeneWorks, 1141232).*

[b]*The combination of adjuvants used in each immunization and booster was as follows: 50 µl ISCOMATRIX™, 100 µg polyICLC (Hiltonol®, Oncovir Inc., lot PJ215-1-10-01), and 100 µg Imiquimod (Sigma-Aldrich, 15159).*

Devil Enclosures, Trapping, and Blood Sample Collection

The NNP devils were kept in two 11 ha FREs for at least 8 months prior to their release. Males and females were kept separately. The devils were trapped fortnightly during the primary 3-month immunization course. Blood samples were collected each time. For the 4 months prior to the booster immunization, the devils were monitored weekly with camera traps by STDP staff. Blood samples were collected 2 weeks after the booster and a week later the devils were released. The SH devils were kept in two FRE's, one 11 ha and one 22 ha, for 14 weeks prior to release, and sexes were not separated. They were trapped on three occasions while in the FRE's for blood collection and immunization.

For each trial, not all devils were trapped each time, and consequently there were some differences in the immunization protocols given, and the blood samples available. Traps were set in each FRE the afternoon before procedures were performed (body weight, physical examination, blood collection, and immunization if required). The traps were baited with possum or lamb flaps and checked the following morning. Each trapped devil was transferred into a hessian sack and the handling and procedures were carried out by two veterinarians/devil keepers. General anesthesia was given in the rare event of not being able to handle the devil in the sack. Devils were released into the FRE immediately following the procedures. Blood sample collection and general anesthesia were performed as described in Ref. (11).

Vaccine Protocol and Preparation

Devil facial tumor disease immunizations were pre-prepared by treating C5065 DFTD cells with recombinant devil interferon gamma (IFN-γ) [produced by the Walter and Eliza Hall Institute for Medical Research as described in Ref. (11)] diluted 5,000× in culture medium for 24 h. This was to upregulate cell surface expression of the MHC-I molecule (8), and these cells are referred to as MHC-I^{+ve} DFTD cells. The non-manipulated DFTD cells, i.e., cells not expressing surface MHC-I, are referred to as MHC-I^{-ve} DFTD cells. After treatment, MHC-I^{+ve} DFTD cells were inactivated by either four ultrasonic cycles at 50% power on an ultrasonic cell disruptor (sonication) (Misonix Inc., Farmingdale, NY, USA), or by two doses of 40 Gy gamma radiation 24 h apart using a Varian Clinac 23-EX linear accelerator (irradiation) (Varian Medical Systems Inc., Palo Alto, CA, USA).

One day of travel was required prior to the administration of the immunizations. On the morning of the travel day, sonicated preparations in 1 ml phosphate buffered saline (PBS) were taken from −80°C, thawed and adjuvants added. Irradiated cell preparations were thawed, washed twice (with PBS at 500 *g* for 5 min), counted and resuspended in 1 ml, and adjuvants added. The composition of the immunizations, including adjuvants, is detailed in **Table 1**. The immunizations were kept on ice or at 4°C for 24 h prior to administration. Immunizations were given as a subcutaneous injection between the devils' scapulae.

Serum Antibody Detection

Indirect immunofluorescence and flow cytometry to measure serum anti-DFTD IgG antibody levels were performed on the serum samples against MHC-I^{-ve} DFTD cells and MHC-I^{+ve} DFTD cells. Preparation of MHC-I^{+ve} cells was described in the Section "Vaccine Protocol and Preparation," and this and the serum antibody detection method are also described in Ref. (11). In brief, DFTD cells were washed twice with PBS (500 *g*, 5 min). Pre-immune and immune serum samples were diluted 1:50 with washing buffer and mixed with DFTD cells for 1 h. Cells were washed twice with washing buffer, and incubated with 50 µl of 10 µg/ml of a monoclonal mouse anti-devil IgG (provided by the Walter and Eliza Hall Institute for Medical Research) for 30 min, then washed and incubated with 50 µl of 2 µg/ml Alexa Fluor 647 conjugated goat anti-mouse IgG antibody (Life Technologies, A21235) for 30 min. After washing, cells were resuspended in 200 µl of washing buffer containing 200 ng/ml of the cell viability dye 4′,6-Diamidino-2-Phenylindole, Dilactate (Sigma-Aldrich, D9542). Data acquisition was performed on a BD FACSCanto™ II flow cytometer (BD Biosciences, Franklin Lakes, NJ, USA). The median fluorescence intensity ratio (MFIR) was used to classify the antibody responses. The MFIR is defined as the median fluorescence intensity (MFI) of DFTD cells labeled with immune serum divided by the MFI of DFTD cells labeled

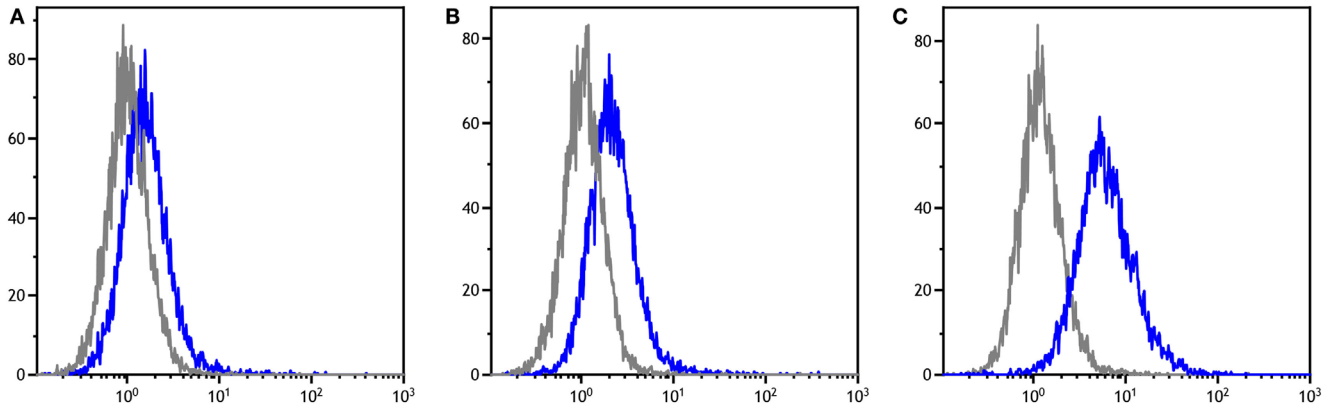

FIGURE 1 | Flow cytometry histograms for three individual devils showing antibodies for MHC-I^{-ve} devil facial tumor disease cells in their pre-immune (gray) and post-immune (blue) serum samples. The fluorescence intensity is in log scale and shown on the *x*-axis, the cell count is on the *y*-axis. **(A–C)** demonstrate the range of responses found across the cohorts.

with pre-immune serum. This ratio accounts for any background serum IgG present prior to the immunizations and standardizes the responses between individual devils. Examples of antibody staining patterns are shown in **Figure 1**.

Devil Release and Post-Release Monitoring

Prior to the releases, the incumbent devil populations in NNP and SH were each estimated at 18 individuals, with a DFTD prevalence of 15% (Samantha Fox, personal communication 2016). The NNP trial devils were released on 25 September 2015. The monitoring trips included in this analysis were carried out at 2, 6, and 12 weeks post release. Serum was collected from the immunized devils trapped during the monitoring trips. The SH trial devils were released on 30 August 2016. Monitoring was carried out almost continuously during the 4 months post release, and blood was collected when possible. A booster immunization was given to the SH devils that were trapped in December 2016, 5 months after completion of the primary course.

Serum Antibody Data Analysis of NNP and SH Trials

The NNP trial took place 1 year before the SH trial. The SH immunization protocol was, therefore, a modified version of the NNP protocol, based on the NNP results and the findings of an adjuvant trial that took place prior to the SH trial. The NNP protocol was longer than SH's and so had more time points from which serum antibody levels were analyzed. The pre-release responses of the NNP and SH trials are presented here separately, and then compared. The post-release antibody responses of both trials follow.

Statistical Analysis of Serum Antibody Data

All MFIR values were log transformed prior to analysis.

A four-way repeated-measures ANOVA comparing protocol, age and sex over time was performed to compare antibody responses at three time points for the NNP trial (**Figure 2**). Repeated-measures one-way ANOVAs, paired or unpaired *t*-tests (**Figures 3–6**) were performed to compare overall anti-DFTD IgG antibody responses at different time periods. Tukey's *post hoc* analyzes were performed, and for the one-way ANOVAs, multiplicity adjusted *P* values reported.

One-way ANOVAs and t-tests were performed using GraphPad Prism version 6 for Mac OS X, GraphPad Software, La Jolla, CA, USA, www.graphpad.com. The four-way ANOVA was performed using R statistical software (R Core Team 2014).

MHC Analysis

To determine an association between diversity at MHC-linked microsatellites and individual antibody score, each devil was screened at 12 polymorphic loci (MHC-I 01, 02, 05, 06, 07, 08, 09, 10, 11, 12; MHC-II 02, 03) with devil specific primers (14) (Day, personal communication). Ear biopsies ($N = 52$) were stored in 70% ethanol at −20°C and DNA was extracted using both standard phenol/chloroform protocols and a PureLink Genomic DNA Mini Kit (Thermofisher Scientific, MA, USA). The DNA concentration of each sample was quantified using a Nanodrop 2000 Spectrophotometer (Thermofisher Scientific, MA, USA) and samples normalized to a concentration of 10 ng/μl. Loci were grouped into previously formulated multiplexes (14) determined by the fluorescent tag on either the forward or reverse primer using Multiplex Manager (15).

Polymerase chain reactions (PCR) were performed using the Qiagen Type-it Microsatellite PCR Kit (Qiagen, CA, USA) in a total volume of 10 μl containing 1 × Type-it Multiplex PCR Master Mix (HotStarTaq *Plus* DNA polymerase, Type-it Microsatellite PCR buffer, dNTPs, 2 nM $MgCl_2$), 0.2 μM of primer multiplex, and 1 μl of DNA. A negative control using water in place of DNA was included in each 96-well plate run. Products were amplified on a T100 Thermocycler (Biorad, CA, USA) following the manufacturer's instructions. Amplicon products were sent to AGRF (Westmead, NSW, Australia) for capillary separation using an ABi 3130XL Genetic Analyzer (Applied Biosystems, CA, USA) and scored against the size ladder McLab Orange DMSO 100

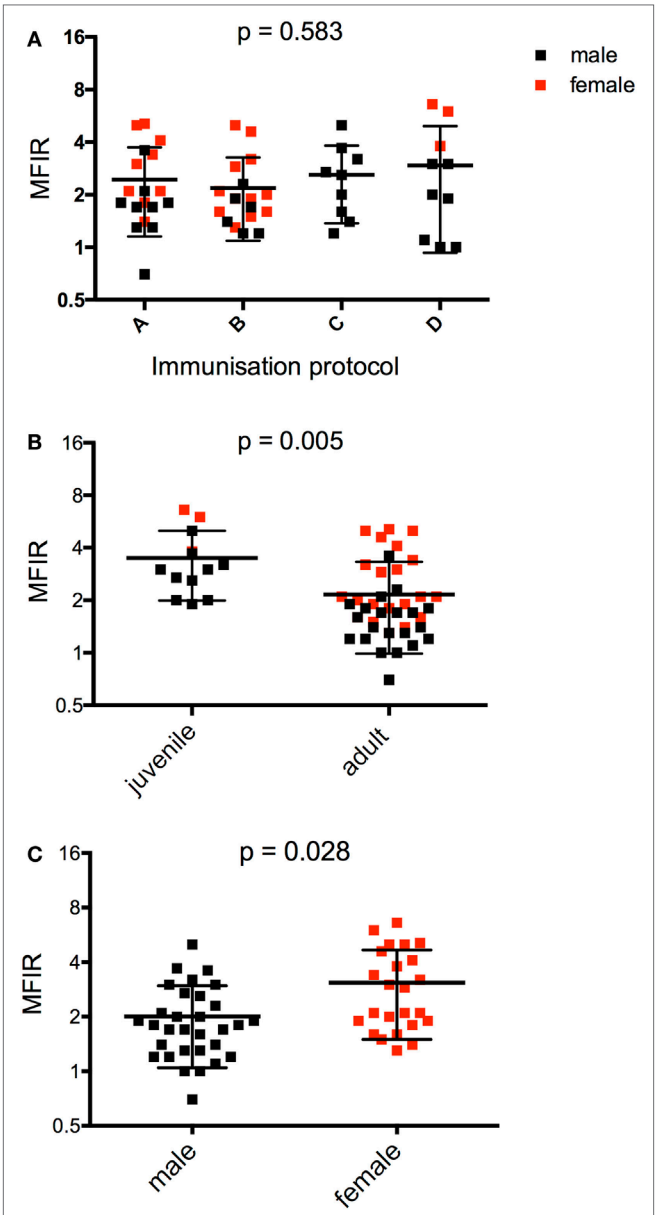

FIGURE 2 | Serum anti-devil facial tumor disease IgG antibody levels (MFIR) for Narawntapu National Park devils showing effect of **(A)** protocol, **(B)** age, and **(C)** sex. The MFIR for each devil at each time point (2 weeks after primary course, on the day of the booster and 2 weeks after the booster) has been plotted on each graph. Protocol A = 4 immunizations at 4-week intervals, B = 4 immunizations at 4- or 6-week intervals, C = 3 immunizations at 4-week intervals, D = 2 immunizations at 2- or 4-week intervals. The *p* values for **(A–C)** were obtained with a four-way ANOVA analysis. See **Table 3** for detailed ANOVA results. MFIR, median fluorescence intensity ratio.

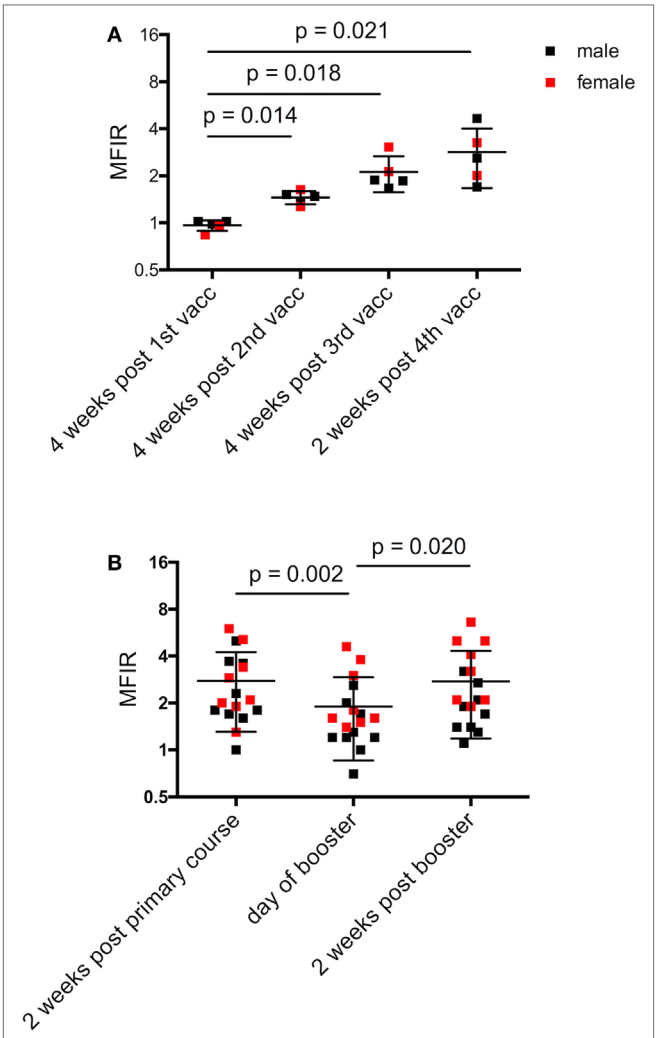

FIGURE 3 | Narawntapu National Park (NNP) devils' serum anti-devil facial tumor disease IgG antibody levels (MFIR). **(A)** Responses of devils that had all four immunizations in their primary course, i.e., protocol A or B, **Table 2**. Only those devils for which sera samples were available at all time points are included. **(B)** Responses of all devils for each of three time points: end of primary immunization course, day of booster (4 months later) and 2 weeks post booster. Statistical analysis was performed with repeated-measures one-way ANOVA and only significant *p* values are shown on the graphs. See **Table 5** for statistical details. Pre-immune MFIR for each devil is equal to 1 and is, therefore, not shown. MFIR, median fluorescence intensity ratio.

(Molecular Cloning Laboratories, SF). Genotypes were assigned to individuals *via* automated allele binning and confirmed visually using GeneMarker 1.95 (Soft Genetics LLC, PA, USA).

MHC Statistical Analysis

The association between antibody score and MHC marker was examined using multiple linear regression. Each individual was given a value of 0, 1, or 2 for each allele, depending on the number of copies of the allele that individual carried. In order to adjust for age, sex, and population (NNP or SH), all analyses included these covariates in the models. A model was fitted separately for each marker in MHC-I and MHC-II. The overall significance of a marker was obtained from a likelihood ratio test, where models with/without the marker in question were compared. The effect size of an allele on antibody score are presented as the coefficient from the regression model and its significance was determined using a Wald Test. All analyses were performed using R statistical software (R Core Team 2014).

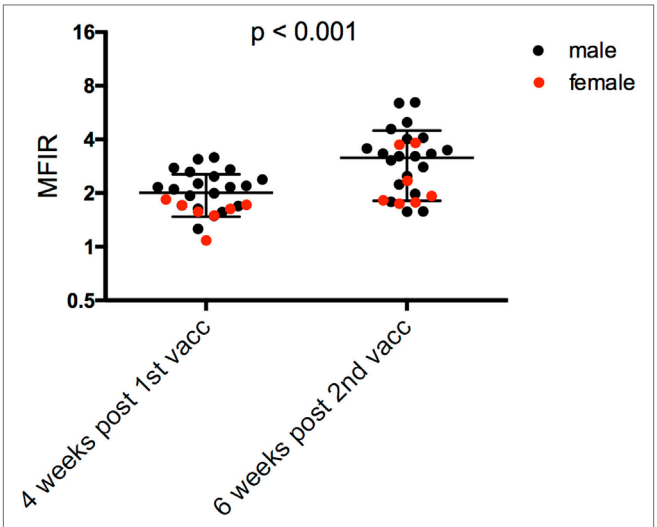

FIGURE 4 | Serum anti-devil facial tumor disease IgG antibody levels (MFIR) of Stony Head devils after their 1st and 2nd immunizations. Pre-immune MFIR for each devil is equal to 1 and is, therefore, not shown. MFIR, median fluorescence intensity ratio.

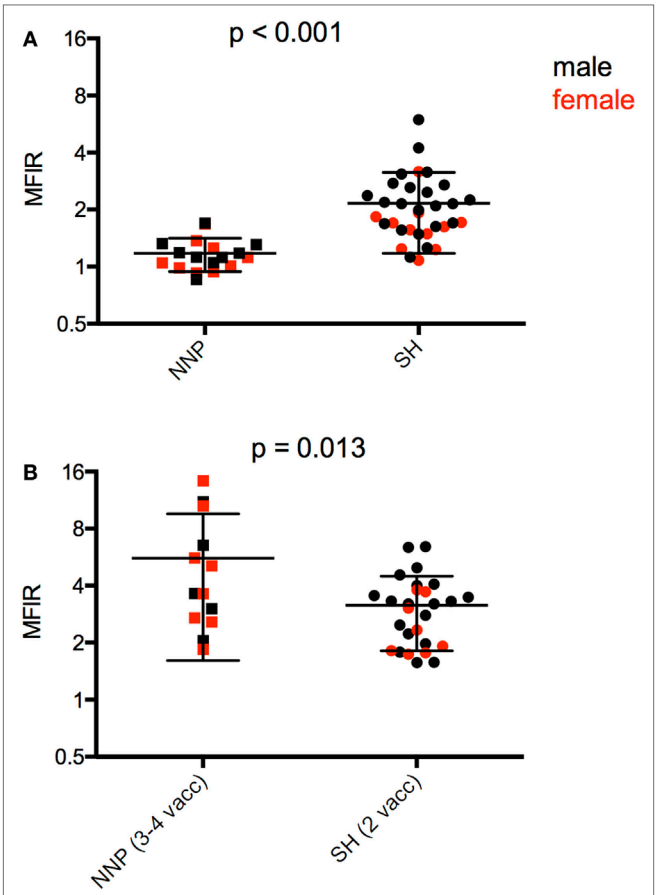

FIGURE 5 | Serum anti-devil facial tumor disease (DFTD) IgG antibody levels [median fluorescence intensity ratio (MFIR)] of **(A)** Stony Head (SH) and Narawntapu National Park (NNP) devils 4 weeks post 1st immunization; **(B)** SH and NNP devils just at the end of their primary immunization courses.

RESULTS

Immunization Protocols

For the NNP trial in particular, the primary immunization protocol each devil received was dependent on trapping success, as well as the time the devils came into the trial. For example, the five juveniles (1-year-old devils) were late entries and, therefore, received only two or three initial immunizations. **Table 2** summarizes the different NNP immunization protocols and the number of devils that received each one. All the NNP devils had a booster immunization 4 months after the primary course, just prior to their release.

Of the 33 SH devils, 27 had the primary immunization protocol as outlined in **Table 1**. There were six devils that had their second immunization on the final pre-release visit since they were not trapped on both the first and second visits. Consequently, there was no blood sample collected after their second immunization and so they were left out of some of the analyses.

Antibody Responses Prior to Wild Release

The anti-DFTD IgG antibody responses were assessed separately against MHC-I^{-ve} and MHC-I^{+ve} DFTD cells. There were no significant differences between results for the cell types (data not shown), so the results presented below are responses against MHC-I^{-ve} DFTD cells only. This applied to the post release analysis as well. **Figure 1** shows representative histograms of the flow cytometry data for serum samples on MHC-I^{-ve} DFTD cells. The negative control for each devil is its pre-immune serum sample and this is compared to the post-immunization serum samples for each individual.

Narawntapu Trial

The effects of protocol, age, and sex on the antibody responses measured at three time points were assessed with a four-way ANOVA (**Table 3**). The primary immunization protocol, whether two, three, or four immunizations, did not make a significant difference to the antibody responses (**Figure 2A**). However, both age and sex were found to have significant effects on these (**Figures 2B,C**; **Table 3**). Juveniles had higher responses on average than adults, and females had higher responses than males.

Figure 3A shows the responses for devils that received four immunizations in the primary course, either protocol A or B, for which serum samples were available at each time point. Antibody levels were significantly higher after the second, third, and fourth immunizations compared to the first (**Table 4**).

Antibody levels of all devils were then compared at three time points: 2 weeks after the primary course; on the day of the booster; and 2 weeks after the booster. At the end of the primary immunization course, only two NNP devils failed to respond (MFIR < 1.5) (**Figure 3B**). There was a significant difference in MFIR over time (**Table 4**). The levels on average were lowest on the day of the booster which was 4 months after the primary course. The booster resulted in an increase in antibody levels similar to the level at the end of the primary course (**Figure 3B**).

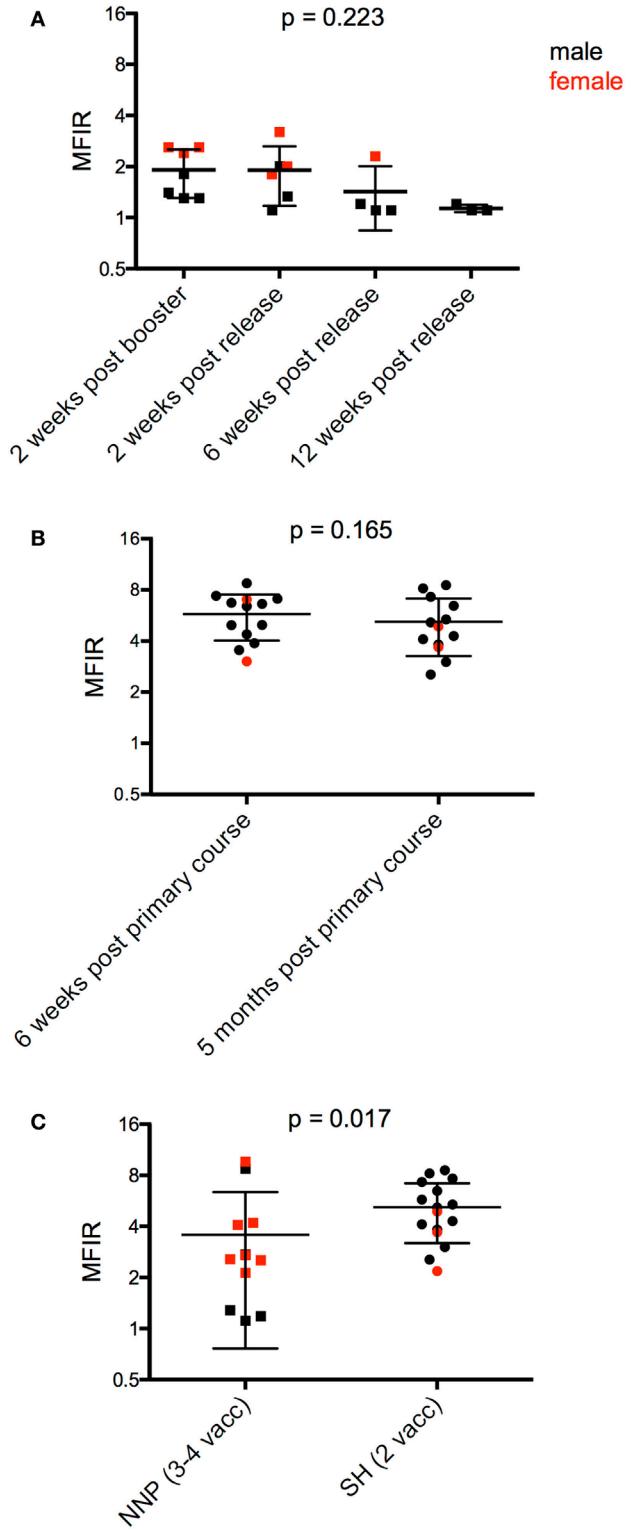

FIGURE 6 | Serum anti-devil facial tumor disease (DFTD) IgG antibody levels [median fluorescence intensity ratio (MFIR)] of **(A)** Narawntapu National Park (NNP) devils post release compared to their post booster response in September 2015; **(B)** Stony Head (SH) devils after their primary course compared to 5 months later; and **(C)** NNP and SH devils, 5 months after their primary immunization course, just prior to the booster administration.

TABLE 2 | Description of Narawntapu National Park (NNP) immunization protocols.

Protocol	Protocol description[a]	Number of devils receiving the protocol
A	4 immunizations at 4-week intervals: 1st and 2nd: sonicated cells 3rd and 4th: irradiated cells	6
B	4 immunizations at 4- or 6-week intervals[b]: 1st and 2nd: sonicated cells 3rd and 4th: irradiated cells	6
C	3 immunizations at 4-week intervals: 1st and 2nd: sonicated cells 3rd: irradiated cells	3 (including 2 juveniles)
D	2 immunizations at 2- or 4-week intervals: 1st: sonicated cells 2nd: irradiated cells	4 (including 3 juveniles)

[a]*See* **Table 1** *for complete description of immunization composition.*
[b]*Two male devils had their 2nd immunizations 6 weeks after the 1st. There were 4-week intervals between their 2nd and 3rd, and their 3rd and 4th immunizations. Four female devils had 4-week intervals between their 1st and 2nd, and 2nd and 3rd immunizations. The 4th immunization was given 6 weeks after the 3rd immunization. Juvenile = 1-year-old devil.*

TABLE 3 | Results of statistical tests comparing serum antibody responses for (A) **Figure 2**.

Four-way ANOVA (Figure 1. Narawntapu National Park: effect of protocol, age, and sex on serum antibody)

	df	*F*	*P*
Sex	1	6.609	0.028
Age	1	12.417	0.005
Protocol	3	0.682	0.583
Sex:age	1	0.348	0.569
Sex:protocol	1	0.234	0.639
Sex:time	1	3.811	0.061
Age:time	1	0	0.984
Protocol:time	3	0.820	0.494
Sex:age:time	1	1.364	0.253
Sex:protocol:time	1	0.163	0.690
Age:protocol:time	1	1.279	0.268
Error	27		

A sex difference was apparent whereby post booster antibody levels in the adult males did not reach the levels found after the primary immunization course. By contrast, there was a trend for the booster to result in female devils having antibody levels that were equal to or higher than levels achieved after the primary course (**Figure 3B**; **Table 5**).

SH Trial

Antibody levels were significantly higher for the SH devils 6 weeks after the second immunization compared to 4 weeks after the first immunization (**Figure 4**; **Table 4**). Sex did not have a significant effect on the SH devils' responses at the end of their primary immunization course. There was only one juvenile devil in the SH trial so a comparison between juvenile and adult responses was not possible.

TABLE 4 | Results of statistical tests comparing serum antibody responses for (B) **Figures 3–6**.

Repeated-measures ANOVA					
Figure	**df**	***F***	***P***	**Adjusted *P* values for multiple comparisons (not shown on graphs)**	
				Columns[a]	***P***
3 (A) NNP devils that received protocol A or B	3	18.10	0.001	B–C B–D C–D	0.067 0.072 0.543
3 (B) NNP, both sexes	2	7.061	0.005	A–C	0.986
3 (B) NNP, males	2	19.190	<0.001	A–B A–C B–C	0.004 0.035 0.003
3 (B) NNP, females	2	9.552	0.008	A–B A–C B–C	0.257 0.071 0.003
6 (A) NNP, post release compared to post booster[b]	2	2.200	0.223	A–B A–C B–C	0.976 0.200 0.199
Figure	**df**	***t***	***P***		
Paired *t*-test					
4. SH after 1st and 2nd immunizations, both sexes	26	5.438	<0.001		
4. SH males	19	4.798	<0.001		
4. SH females	6	2.405	0.053		
6 (B) SH, post primary course compared to time of booster	12	1.480	0.165		
Unpaired *t*-test					
5 (A) SH and NNP, 4 weeks post 1st immunization	49	5.713	<0.001		
5 (B) SH and NNP after primary immunization course	38	2.600	0.013		
6 (C) NNP and SH just prior to booster administration	26	2.540	0.017		

[a]*A, B, C, and D refer to columns in the graphs, i.e., A, 1st column, B, 2nd column; C, 3rd column; D, 4th column.*

[b]*Only 3 time points compared statistically due to missingness.*

NNP, Narawntapu National Park trial; SH, Stony Head trial.

Comparison of SH and NNP Trials

The only directly comparable time point for the NNP and SH trials was 4 weeks after the first immunization. The SH devils had significantly higher serum antibody levels than NNP devils (**Figure 5A**; **Table 4**). At the end of the primary course, the NNP devils that had three or four immunizations had higher serum antibody levels than the SH devils (**Figure 5B**; **Table 4**).

A the end of their primary course, 17 of the 19 NNP devils, and all 33 of the SH devils had seroconverted providing an overall percentage of 96% for seroconversion in response to the DFTD immunizations.

Antibody Responses after Wild Release

Following the release into NNP, monitoring trips included in this analysis were carried out at 2, 6, and 12 weeks. There were six devils trapped on the first post monitoring trip, and only three devils at 12 weeks. There was a trend for antibody levels to decrease over this time to almost baseline levels at 12 weeks (**Figure 6A**; **Table 4**).

Monitoring at SH was carried out almost continuously for 4 months post release, i.e., up until 5 months after the primary course. There were 17 devils that were trapped, had blood collected, and given a booster immunization in the final month of monitoring. Of these devils, 13 had blood samples collected 6 weeks after their second immunization. Antibody levels were maintained by these 13 devils over the 5-month period between their second immunization and booster (**Figure 6B**; **Table 4**). This contrasts with the NNP devils whose antibody levels dropped over a similar time frame (**Figure 2B**, 2 weeks post primary course compared to at time of booster). Five months after the primary course, the SH devils, which all received a total of two immunizations, had a higher overall antibody level than the NNP devils which had received three or four immunizations (**Figure 6C**; **Table 4**).

MHC Microsatellites Markers

Microsatellites across the MHC-I and MHC-II were compared to the antibody responses (MFIR). Highly significant ($p < 0.005$) associations occurred between antibody responses and MHC-I_10, and a significant association ($p < 0.05$) was identified for MHC-I_02 and MHC-I_08 (**Table 5**). No significant associations were found with MHC-I loci 01, 05, 06, 07, and 11. There was limited diversity across MHC-II loci (02 and 03) and no associations were identified. The significance of the effect of each MHC-I and MHC-II microsatellite markers on serum antibody are shown in Table S1 in Supplementary Material.

The statistical analysis of the MHC data and its association with antibody response was adjusted for age, sex, and population (NNP or SH). A significant effect of age on antibody score was demonstrated, with an average decrease in antibody score of 0.76 for every year of a devil's life ($p < 0.001$). There were non-significant effects observed for population (NNP devils having an antibody score of 0.12 greater than SH devils, $p = 0.77$) and sex (females having an antibody score of 0.1 greater than males, $p = 0.81$).

The DFTD tumor cell line used in the immunizations was assessed for the presence of microsatellites. None of the three alleles associated with a higher antibody response were present in the C5065 cell line that was used for the immunizations (**Table 5**).

DISCUSSION

These trials brought about the first cohorts of devils immunized against DFTD and released to the wild in the STDP's Wild Devil Recovery project. The collaboration combined two innovative management strategies to prevent the extinction of devils in the wild: DFTD immunization and population augmentation. The immunization trials were performed on a much larger number of devils than had previously been possible, allowing for a robust assessment of the induced immune responses. The two trials differed with respect to the number and timing of the immunizations given in the primary course, and the adjuvant combination.

There are other examples of vaccinating captive bred and/or wild populations of endangered species against fatal diseases, e.g., black-footed ferrets against plague and canine distemper virus

TABLE 5 | Devil MHC microsatellite markers that have alleles significantly associated with a high antibody response.

MHC marker	*P*-value of marker (adjusted for age, sex, and population)	Allele	Effect size	*P*-value of allele (adjusted for age, sex, and population)	Mean antibody score (median fluorescence intensity ratio), and number of devils with 1 or 2 copies of the allele	Vaccine cell line alleles
MHC-I 02	0.041[a]	201	0.56	0.048[a]	3.5, *N* = 20	/
		203	NA	NA	2.9, *N* = 40	203, 203
MHC-I 08	0.029[a]	216	0.95	0.195	2.5, *N* = 23	/
		218	1.91	0.054	3.3, *N* = 3	/
		220	1.4	0.069	3.2, *N* = 20	220
		222	1.73	0.030[a]	3.5, *N* = 17	/
		224	NA	NA	1.8, *N* = 3	224
MHC-I 10	0.003[a]	243	3.37	0.039[a]	6.4, *N* = 1	/
		245	0.71	0.535	3.3, *N* = 33	/
		247	0.09	0.938	2.5, *N* = 27	/
		249	NA	NA	1.8, *N* = 1	249
		251	NA	NA	*N* = 0	251

Models were adjusted for age, sex, and population. Age was found to have a significant association with antibody response. The alleles of the MHC markers significantly associated with high serum antibody are also shown, along with their P values. The effect size indicates the average increase in serum antibody observed for each copy of the allele. P values for alleles were obtained from a likelihood ratio test/Wald test, respectively. The last column shows the alleles of the C5065 cell line used in the vaccine.

[a]*Indicates significance.*

NA = not available; / = none shared with respect to MHC allele.

(16, 17), kakapo against erysipelas (18), and Ethiopian wolves against rabies (19, 20). An experimental chlamydia vaccine trial has also been carried out on a wild population of koalas in south east Queensland (21). The DFTD immunization trials shared aspects of these examples, notably a focus on an endangered species facing a primary threat of disease which might be addressed by vaccination. However, most of the previous examples are against microorganisms for which vaccines have been established.

A vaccine protecting against DFTD would be a valuable conservation tool to secure the future of the wild devil population. There are suggestions that responses to DFTD are occurring in the wild. Natural immune responses against DFTD have been found in a small percentage of wild devils (9). There is also evidence that genetic selection associated with DFTD has occurred in certain populations (22). However, there has not been a measurable reduction of the DFTD effect on these populations. DFTD has resulted in dramatic devil population decline to the point where the species is functionally extinct in certain locations (23). Even with the assumption that adequate anti-DFTD responses are evolving, the ecological impacts of a decimated devil population are profound and relying on natural selection of resistant animals for population recovery at this stage seems risky. A protective DFTD vaccine would aid in timelier restoration of a functional devil population while helping to ensure maintenance of the genetic diversity of the species.

With respect to DFTD vaccine development, the biggest advantage of the trials described in this study was the sample size. Previous immunization studies have been carried out on a maximum of four devils at a time. The comparatively large sample sizes here allowed for greater confidence in the assessment of anti-DFTD immune responses. It also allowed for the effects of age, sex, differing immunization protocols, and MHC variation to be evaluated. Prior immunization trials on captive devils have demonstrated that an immune response against DFTD is achievable. However, it was unknown if results could be generalized to the wider devil population due to the small sample sizes. The high number of responders in these trials suggests most devils are capable of producing an immune response against DFTD which is encouraging for vaccine development.

MHC-linked microsatellite analysis of the immunized devils showed that particular MHC alleles were associated with a higher antibody response to the immunizations. These alleles were not present in the tumor cell line that was used as the basis of the immunization. This suggests that the MHC type of the individual devil may influence its response to DFTD immunizations. It also implies that an immune response against DFTD is more likely if the MHC of the devil and the tumor are mismatched. However, there is no evidence in the literature that MHC type affects devil responses to naturally occurring DFTD infection (24, 25). Sequencing analysis of the MHC genes themselves and their expression may provide further insight into the relationship between MHC and a devil's ability to respond to immunization. IgG responses in both NNP and SH trials were specific for both non-manipulated and MHC-I upregulated DFTD cells, suggesting that immune responses against DFTD surface antigens other than MHC were generated. These responses will be critical for recognition of MHC-I^{-ve} DFTD cells upon exposure to the disease in the wild.

The statistical analysis of the MHC data and its association with antibody response found a significant effect of age. This result is in accordance with previous research showing the decline of the devil's immune capacity with age (26). The NNP trial included five juvenile devils which allowed for the effect of age (juvenile compared to adult) on the immune response to be assessed. The juveniles showed, on average, higher antibody responses than the adult devils. This was despite the juveniles receiving fewer immunizations in the primary course than the majority of adults. Only one juvenile was in the SH trial, which precluded a comparison between juvenile and adult responses. The NNP trial showed female devils to have significantly higher antibody responses than males. There was no overall significant sex difference found in the

SH trial. SH males did, however, show a significant increase in antibody levels after their second immunization, whereas there was only a trend for antibody levels to increase in the females. There is evidence that sex affects immune responses *via* a combination of genetic, hormonal, and environmental factors with human studies generally showing females to have heightened immunity to pathogens, and a tendency toward higher responses to bacterial and viral vaccines than males (27).

Compared to conventional immunization protocols against microbial pathogens, the NNP immunization protocol was long, taking 7 months including the booster prior to the release date. Not all devils received the entire primary immunization course, and results suggested that a reduced number of primary immunizations did not affect the post booster antibody response. This evidence that similar antibody responses could be achieved with fewer immunizations was used to refine the protocol for the SH trial. Similarly, results from an adjuvant study on captive devils that took place prior to the SH trial influenced the choice of adjuvant used in the SH protocol (12). A shorter and, therefore, more practical protocol with a promising adjuvant combination was implemented for SH. Both the NNP and SH trials resulted in similar levels of serum antibody. The improvements identified in the SH trial were that antibody levels were achieved more rapidly and were of longer duration. Following their first immunization, the SH devils had higher overall antibody levels than the NNP devils. These levels in the SH devils were maintained over the 5 months prior to the booster compared to the NNP devils which had a significant decline in antibody levels pre-booster. In addition, the NNP devils trapped 3 months after release had antibody levels approaching baseline. This suggests that superior immune memory was stimulated in the SH devils. It is likely that the adjuvant combination used in the SH trial was responsible for the improved speed and duration of response.

The adjuvant component in both trials included ISCOMATRIX ™, a proprietary saponin-based adjuvant which has previously been shown to generate antigen-specific CD8+ T cells and result in regression of established solid tumors when combined with toll-like receptor (TLR) agonists (28). The adjuvant component of the NNP and SH trials differed in their use of TLR agonists. The NNP trial included the TLR9 agonist, CpG- oligodeoxynucleotide (CpG), and the TLR3 agonist, polyinosinic:polycytidylic acid (polyIC). This combination was in keeping with the DFTD immunization trials that documented tumor regression (11).

As mentioned above, a study was undertaken prior to the SH trial to assess adjuvant effects on the immune responses of devils to the model antigen, keyhole limpet hemocyanin (KLH) (12). The study used the TLR-7 agonist imiquimod, and polyICLC (Hiltonol®) which is more stable than polyIC due to its ribonuclease resistance. Imiquimod alone resulted in a minimal immune response to KLH. PolyICLC, however, gave a robust antibody response when used alone and also in combination with imiquimod. In light of these results, the SH trial protocol omitted CpG and replaced it with imiquimod, and the polyIC was replaced with polyICLC.

As discussed in Patchett et al. (12), polyICLC and imiquimod activate potent antigen-specific immunity through the stimulation of multiple immune pathways in human and animal studies. PolyIC results in production of large amounts of type-1 IFN. In mice immunized with polyICLC, substantial increases in $CD8^+$ T-cell cytotoxicity occurred (29, 30). Imiquimod is also a potent stimulator of type-1 IFN *via* TLR-7-dependent activation of plasmacytoid dendritic cells (pDCs) (31). Previous studies of adjuvant efficacy have demonstrated improved generation of T-cell memory in response to polyICLC or imiquimod compared to other adjuvants (32, 33). Similar responses in Tasmanian devils to DFTD immunizations containing polyICLC may offer a greater likelihood of protection against DFTD.

There were two notable limitations to these trials. The first was the inability to measure the cell-mediated immune response to the immunizations due to the absence of a reliable cytotoxicity assay. The challenges of designing and implementing accurate T-cell assays in human clinical trials are substantial and well reviewed (34). Furthermore, *in vitro* evidence for specific T-cell responses does not always predict vaccine-mediated protection and Saade et al. highlight the need for better correlates of vaccine-induced T-cell immunity.

Here, serum IgG antibodies specific for DFTD were used to measure the responses induced by the immunizations (11). Since IgG production is T cell dependent, this provides indirect evidence for T-cell involvement. Previous research has suggested that a humoral immune response can inhibit development of a protective cellular immune response (35), the latter being requisite for a cancer vaccine. However, the correlation between anti-DFTD serum antibodies and DFTD regression has been documented in both wild and captive devils (9, 11) indicating the relevance of serum antibodies in an anti-DFTD response. As was postulated in these references, antibody-dependent cell-mediated cytotoxicity is a mechanism by which antibodies could facilitate tumor cell killing.

Another limitation associated with the trials was the low post-release trapping success of immunized devils. This applied particularly to the NNP trial. The low NNP recapture rate was partly due to the devils' likely dispersal beyond the trap lines, but also due to deaths from road traffic accidents (36). Trapping at SH was more successful due to the SH devils being fitted with GPS collars just prior to their release. The devils were, therefore, trackable until the collars were removed within 4 months of release, and it was possible to collect serum from 17 SH devils 4 months after the release date. Future trapping success will dictate whether the duration of antibody responses and the effect of the immunization protocol on DFTD susceptibility can be confidently ascertained. At the time of publication, three of the devils released at SH have been confirmed positive for DFTD due to natural exposure. Longitudinal sample collection and analysis are required before drawing conclusions on whether the immunization responses influence tumor growth rate in the devils that acquire disease.

Despite the limitations, these trials signify a notable advance in DFTD vaccine research. Although it remains unclear what protection the immunization protocols provided against a natural DFTD challenge, the serum antibodies detected in the majority of devils in response to the immunizations suggest that development of an effective DFTD vaccine is a realistic expectation. The improved antibody response obtained with the shorter protocol used in the SH trial was most likely a function of the adjuvant used and was a particularly encouraging finding for the eventual feasibility of an immune solution to DFTD.

ETHICS STATEMENT

All procedures were approved by the University of Tasmania Animal Ethics Committee (permit number A0014599). Permission to obtain samples was approved by the Tasmanian Department of Primary Industries, Parks, Water and Environment (DPIPWE) for the period 20 September 2016 to 19 September 2021 inclusive.

AUTHOR CONTRIBUTIONS

The field work and experiments were conceived and designed by RP, AM, AS, MP, AK, SF, CH, GW, AL, DP, and LC. The laboratory experiments were performed by RP, AP, and EM. The data was analyzed by EM, RT, SC, AP, RP, KB, CH, GW, and AL. The manuscript was written by RP, GW, and AL. All authors approved the manuscript.

ACKNOWLEDGMENTS

Judy Clarke and Save the Tasmanian Devil Program staff; Jocelyn Darby and the Tasmanian devil immunology research group, Menzies Institute for Medical Research; Tasmania Zoo; East Coast Nature World; the Holman Clinic, Royal Hobart Hospital; Tasmania Parks and Wildlife Service; Saffire; Dr. Andres Salazar, Oncovir (Washington DC). We acknowledge suggestions from, Jim Kaufman (University of Cambridge), Hannah Siddle (University of Southampton), Wilf Jefferies (University of British Columbia), James Murphy (Walter and Eliza Institute for Medical Research).

FUNDING

This work was supported by the Australian Research Council [LP130100218; LP140100508]; and the University of Tasmania Foundation through funds raised by the Save the Tasmanian Devil Program Appeal and Wildcare Inc. The Wild Devil Recovery Project received funding from the Australian Commonwealth and Tasmanian State Governments.

SUPPLEMENTARY MATERIAL

The Supplementary Material for this article can be found online at http://www.frontiersin.org/articles/10.3389/fimmu.2018.00259/full#supplementary-material.

REFERENCES

1. Hawkins CE, McCallum H, Mooney N, Jones M, Holdsworth M. *Sarcophilus harrisii. In IUCN Red List of Threatened Species Version 2016-2. e.T40540A10331066 ed*. International Union for the Conservation of Nature (2008).
2. Kreiss A, Fox N, Bergfeld J, Quinn SJ, Pyecroft S, Woods GM. Assessment of cellular immune responses of healthy and diseased Tasmanian devils (*Sarcophilus harrisii*). *Dev Comp Immunol* (2008) 32:544–53. doi:10.1016/j.dci.2007.09.002
3. Kreiss A, Wells B, Woods GM. The humoral immune response of the Tasmanian devil (*Sarcophilus harrisii*) against horse red blood cells. *Vet Immunol Immunopathol* (2009) 130:135–7. doi:10.1016/j.vetimm.2009.02.003
4. Brown GK, Kreiss A, Lyons AB, Woods GM. Natural killer cell mediated cytotoxic responses in the Tasmanian devil. *PLoS One* (2011) 6:e24475. doi:10.1371/journal.pone.0024475
5. Kreiss A, Cheng Y, Kimble F, Wells B, Donovan S, Belov K, et al. Allorecognition in the Tasmanian devil (*Sarcophilus harrisii*), an endangered marsupial species with limited genetic diversity. *PLoS One* (2011) 6:e22402. doi:10.1371/journal.pone.0022402
6. Woods GM, Howson LJ, Brown GK, Tovar C, Kreiss A, Corcoran LM, et al. Immunology of a transmissible cancer spreading among Tasmanian devils. *J Immunol* (2015) 195:23–9. doi:10.4049/jimmunol.1500131
7. Pye RJ, Woods GM, Kreiss A. Devil facial tumor disease. *Vet Pathol* (2015) 53(4):726–36. doi:10.1177/0300985815616444
8. Siddle HV, Kreiss A, Tovar C, Yuen CK, Cheng Y, Belov K, et al. Reversible epigenetic down-regulation of MHC molecules by devil facial tumour disease illustrates immune escape by a contagious cancer. *Proc Natl Acad Sci U S A* (2013) 110:5103–8. doi:10.1073/pnas.1219920110
9. Pye R, Hamede R, Siddle HV, Caldwell A, Knowles GW, Swift K, et al. Demonstration of immune responses against devil facial tumour disease in wild Tasmanian devils. *Biol Lett* (2016) 12(10):5. doi:10.1098/rsbl.2016.0553
10. Kreiss A, Brown GK, Tovar C, Lyons AB, Woods GM. Evidence for induction of humoral and cytotoxic immune responses against devil facial tumor disease cells in Tasmanian devils (*Sarcophilus harrisii*) immunized with killed cell preparations. *Vaccine* (2015) 33(26):3016–25. doi:10.1016/j.vaccine.2015.01.039
11. Tovar C, Pye RJ, Kreiss A, Cheng Y, Brown GK, Darby J, et al. Regression of devil facial tumour disease following immunotherapy in immunised Tasmanian devils. *Sci Rep* (2017) 7:43827. doi:10.1038/srep43827
12. Patchett AL, Tovar C, Corcoran LM, Lyons AB, Woods GM. The toll-like receptor ligands Hiltonol(R) (polyICLC) and imiquimod effectively activate antigen-specific immune responses in Tasmanian devils (*Sarcophilus harrisii*). *Dev Comp Immunol* (2017) 76:352–60. doi:10.1016/j.dci.2017.07.004
13. Pye RJ, Pemberton D, Tovar C, Tubio JM, Dun KA, Fox S, et al. A second transmissible cancer in Tasmanian devils. *Proc Natl Acad Sci U S A* (2016) 113:374–9. doi:10.1073/pnas.1519691113
14. Cheng Y, Belov K. Isolation and characterisation of 11 MHC-linked microsatellite loci in the Tasmanian devil (*Sarcophilus harrisii*). *Conserv Genet Resour* (2011) 4:463–5. doi:10.1007/s12686-011-9575-4
15. Holleley CE, Geerts PG. Multiplex manager 1.0: a cross-platform computer program that plans and optimizes multiplex PCR. *Biotechniques* (2009) 46:511–7. doi:10.2144/000113156
16. Marinari PE, Kreeger JS. An adaptive management approach for black-footed ferrets in captivity. In: Roelle JE, Miller BJ, Godbey JL, Biggins DE, editors. *Recovery of the Black-Footed Ferret: Progress and Continuing Challenges*. U.S. Geological Survey Scientific Investigations Report 2005–5293 (2006). 288 p.
17. US Fish and Wildlife Service. *Recovery Plan for the Black-Footed Ferret (Mustela nigripes)*. Wellington, CO: U.S. Fish and Wildlife Service (2013).
18. Gartrell BD, Alley MR, Mack H, Donald J, Mcinnes K, Jansen P. Erysipelas in the critically endangered kakapo (*Strigops habroptilus*). *Avian Pathol* (2005) 34:383–7. doi:10.1080/03079450500268583
19. Randall DA, Williams SD, Kuzmin IV, Rupprecht CE, Tallents LA, Tefera Z, et al. Rabies in endangered Ethiopian wolves. *Emerg Infect Dis* (2004) 10:2214–7. doi:10.3201/eid1012.040080
20. Sillero-Zubiri C, Marino J, Gordon CH, Bedin E, Hussein A, Regassa F, et al. Feasibility and efficacy of oral rabies vaccine SAG2 in endangered Ethiopian wolves. *Vaccine* (2016) 34:4792–8. doi:10.1016/j.vaccine.2016.08.021
21. Waugh C, Khan SA, Carver S, Hanger J, Loader J, Polkinghorne A, et al. A prototype recombinant-protein based *Chlamydia pecorum* vaccine results in reduced chlamydial burden and less clinical disease in free-ranging koalas (*Phascolarctos cinereus*). *PLoS One* (2016) 11:e0146934. doi:10.1371/journal.pone.0146934
22. Epstein B, Jones M, Hamede R, Hendricks S, Mccallum H, Murchison EP, et al. Rapid evolutionary response to a transmissible cancer in Tasmanian devils. *Nat Commun* (2016) 7:12684. doi:10.1038/ncomms12684
23. Hollings T, Mccallum H, Kreger K, Mooney N, Jones M. Relaxation of risk-sensitive behaviour of prey following disease-induced decline of an apex

predator, the Tasmanian devil. *Proc Biol Sci* (2015) 282:20150124. doi:10.1098/rspb.2015.0124
24. Wright B, Willet CE, Hamede R, Jones M, Belov K, Wade CM. Variants in the host genome may inhibit tumour growth in devil facial tumours: evidence from genome-wide association. *Sci Rep* (2017) 7:423. doi:10.1038/s41598-017-00439-7
25. Lane A, Cheng Y, Wright B, Hamede R, Levan L, Jones M, et al. New insights into the role of MHC diversity in devil facial tumour disease. *PLoS One* (2012) 7:e36955. doi:10.1371/journal.pone.0036955
26. Cheng Y, Heasman K, Peck S, Peel E, Gooley RM, Papenfuss AT, et al. Significant decline in anticancer immune capacity during puberty in the Tasmanian devil. *Sci Rep* (2017) 7:44716. doi:10.1038/srep44716
27. Klein SL, Flanagan KL. Sex differences in immune responses. *Nat Rev Immunol* (2016) 16:626–38. doi:10.1038/nri.2016.90
28. Silva A, Mount A, Krstevska K, Pejoski D, Hardy MP, Owczarek C, et al. The combination of ISCOMATRIX adjuvant and TLR agonists induces regression of established solid tumors in vivo. *J Immunol* (2015) 194:2199–207. doi:10.4049/jimmunol.1402228
29. Cho HI, Barrios K, Lee YR, Linowski AK, Celis E. BiVax: a peptide/poly-IC subunit vaccine that mimics an acute infection elicits vast and effective anti-tumor CD8 T-cell responses. *Cancer Immunol Immunother* (2013) 62:787–99. doi:10.1007/s00262-012-1382-6
30. Kato H, Takeuchi O, Sato S, Yoneyama M, Yamamoto M, Matsui K, et al. Differential roles of MDA5 and RIG-I helicases in the recognition of RNA viruses. *Nature* (2006) 441:101–5. doi:10.1038/nature04734
31. Gibson SJ, Lindh JM, Riter TR, Gleason RM, Rogers LM, Fuller AE, et al. Plasmacytoid dendritic cells produce cytokines and mature in response to the TLR7 agonists, imiquimod and resiquimod. *Cell Immunol* (2002) 218:74–86. doi:10.1016/S0008-8749(02)00517-8
32. Goldinger SM, Dummer R, Baumgaertner P, Mihic-Probst D, Schwarz K, Hammann-Haenni A, et al. Nano-particle vaccination combined with TLR-7 and -9 ligands triggers memory and effector CD8(+) T-cell responses in melanoma patients. *Eur J Immunol* (2012) 42:3049–61. doi:10.1002/eji.201142361
33. Martins KA, Cooper CL, Stronsky SM, Norris SL, Kwilas SA, Steffens JT, et al. Adjuvant-enhanced CD4 T cell responses are critical to durable vaccine immunity. *EBioMedicine* (2016) 3:67–78. doi:10.1016/j.ebiom.2015.11.041
34. Saade F, Gorski SA, Petrovsky N. Pushing the frontiers of T-cell vaccines: accurate measurement of human T-cell responses. *Expert Rev Vaccines* (2012) 11:1459–70. doi:10.1586/erv.12.125
35. Hamilton DH, Bretscher PA. Different immune correlates associated with tumor progression and regression: implications for prevention and treatment of cancer. *Cancer Immunol Immunother* (2008) 57:1125–36. doi:10.1007/s00262-007-0442-9
36. Grueber CE, Reid-Wainscoat EE, Fox S, Belov K, Shier DM, Hogg CJ, et al. Increasing generations in captivity is associated with increased vulnerability of Tasmanian devils to vehicle strike following release to the wild. *Sci Rep* (2017) 7:2161. doi:10.1038/s41598-017-02273-3

Conflict of Interest Statement: The authors declare that the research was conducted in the absence of any commercial or financial relationships that could be construed as a potential conflict of interest.

frontiers in Immunology

ORIGINAL RESEARCH
published: 11 January 2018
doi: 10.3389/fimmu.2017.01944

Detection of Pathogen Exposure in African Buffalo Using Non-Specific Markers of Inflammation

Caroline K. Glidden[1], Brianna Beechler[2], Peter Erik Buss[3], Bryan Charleston[4], Lin-Mari de Klerk-Lorist[5], Francois Frederick Maree[6,7], Timothy Muller[2], Eva Pérez-Martin[4], Katherine Anne Scott[6], Ockert Louis van Schalkwyk[5] and Anna Jolles[1,2]*

[1] Department of Integrative Biology, Oregon State University, Corvallis, OR, United States, [2] College of Veterinary Medicine, Oregon State University, Corvallis, OR, United States, [3] SANPARKS, Veterinary Wildlife Services, Skukuza, South Africa, [4] The Pirbright Institute, Woking, United Kingdom, [5] Office of the State Veterinarian, Department of Agriculture, Forestry and Fisheries, Skukuza, South Africa, [6] Vaccine and Diagnostic Development Programme, Transboundary Animal Diseases, Onderstepoort Veterinary Institute, Agricultural Research Council, Onderstepoort, South Africa, [7] Department of Microbiology and Plant Pathology, Faculty of Agricultural and Natural Sciences, University of Pretoria, Pretoria, South Africa

Detecting exposure to new or emerging pathogens is a critical challenge to protecting human, domestic animal, and wildlife health. Yet, current techniques to detect infections typically target known pathogens of humans or economically important animals. In the face of the current surge in infectious disease emergence, non-specific disease surveillance tools are urgently needed. Tracking common host immune responses indicative of recent infection may have potential as a non-specific diagnostic approach for disease surveillance. The challenge to immunologists is to identify the most promising markers, which ideally should be highly conserved across pathogens and host species, become upregulated rapidly and consistently in response to pathogen invasion, and remain elevated beyond clearance of infection. This study combined an infection experiment and a longitudinal observational study to evaluate the utility of non-specific markers of inflammation [NSMI; two acute phase proteins (haptoglobin and serum amyloid A), two pro-inflammatory cytokines (IFNγ and TNF-α)] as indicators of pathogen exposure in a wild mammalian species, African buffalo (*Syncerus caffer*). Specifically, in the experimental study, we asked (1) How quickly do buffalo mount NSMI responses upon challenge with an endemic pathogen, foot-and-mouth disease virus; (2) for how long do NSMI remain elevated after viral clearance and; (3) how pronounced is the difference between peak NSMI concentration and baseline NSMI concentration? In the longitudinal study, we asked (4) Are elevated NSMI associated with recent exposure to a suite of bacterial and viral respiratory pathogens in a wild population? Among the four NSMI that we tested, haptoglobin showed the strongest potential as a surveillance marker in African buffalo: concentrations quickly and consistently reached high levels in response to experimental infection, remaining elevated for almost a month. Moreover, elevated haptoglobin was indicative of recent exposure to two respiratory pathogens assessed in the longitudinal study. We hope this work motivates studies investigating suites of NSMI as indicators for pathogen exposure in a broader range of both pathogen and host species, potentially transforming how we track disease burden in natural populations.

Keywords: emerging infectious disease, disease surveillance, wildlife, inflammation, haptoglobin, serum amyloid A, IFNγ, TNF-α

OPEN ACCESS

Edited by:
Jayne Hope, University of Edinburgh, United Kingdom

Reviewed by:
Viskam Wijewardana, International Atomic Energy Agency, Austria
Noemi Sevilla, Instituto Nacional de Investigación y Tecnología Agraria y Alimentaria (INIA), Spain

****Correspondence:***
Caroline K. Glidden
gliddeca@science.oregonstate.edu

Specialty section:
This article was submitted to Comparative Immunology, a section of the journal Frontiers in Immunology

Received: *20 October 2017*
Accepted: *18 December 2017*
Published: *11 January 2018*

Citation:
Glidden CK, Beechler B, Buss PE, Charleston B, de Klerk-Lorist L-M, Maree FF, Muller T, Pérez-Martin E, Scott KA, van Schalkwyk OL and Jolles A (2018) Detection of Pathogen Exposure in African Buffalo Using Non-Specific Markers of Inflammation. Front. Immunol. 8:1944. doi: 10.3389/fimmu.2017.01944

INTRODUCTION

Emerging infectious diseases cause human suffering (1, 2), threaten food security (3), and contribute to the decline of vulnerable populations and species (4). As such, in the face of elevated rates of infectious disease emergence in humans (5, 6), domestic animals (7) and wildlife (8–10), effective surveillance for pathogen exposure is increasingly important.

Surveillance for emerging infections is challenging because it requires detection of previously unreported infectious agents, and/or diagnosis of exposure or infection in understudied animal species. Indeed, animals are hosts to hundreds of pathogens and parasites (11) with previously unidentified species regularly documented (12–14). Yet, available disease diagnostics typically target known infections that cause detectable pathology in humans or economically important domestic animals resulting in a relatively narrow range of tests that are highly pathogen specific. Common molecular techniques to detect pathogens include tests that detect genetic material of the pathogen itself and antibody-based diagnostics that detect the host's antibodies to a given pathogen. Advancing sequencing methods show promise for simultaneously detecting a wider range of pathogens (15, 16) but, while genetically based techniques often have high sensitivity and specificity, they are limited to detection of active infections. Many infections last only a few days and thus may escape detection unless sampling can occur on a tight time frame. Most importantly, diagnostic techniques based on amplifying pathogen genetic material still require pathogen specific primers and/or previous publication of genetic sequences and are, thus, unsuitable in situations where the identity of pathogens is uncertain. Antibody-based techniques, such as enzyme-linked immunosorbent assays or immnuofluorescence assays, offer a way to detect infection after pathogen exposure has occurred because antibody titers to many infections can remain elevated for months to years after primary infection (17). However, antibody-based techniques typically used in disease diagnostics are highly pathogen specific, which limits their utility in detecting novel infections.

An ideal diagnostic approach for monitoring (often unknown) infections in natural populations would complement existing genetic and antibody techniques by detecting the presence of pathogens non-specifically, using immunological markers that indicate recent presence of infection. Ideal markers should increase rapidly and reliably in response to a broad range of pathogens and remain elevated for a consistent period after active infection has subsided. A test that detects exposure both early in infection as well as past pathogen clearance could aid in monitoring population health and improve surveillance for emerging infections.

Here, we suggest that non-specific markers of inflammation (NSMI hereafter) have potential for use in detecting pathogen exposure in natural populations. NSMI include APP [this study: haptoglobin, serum amyloid A (SAA)] and cytokines (here: TNF-α, IFNγ). APP are an integral part of the acute inflammatory response to pathogen exposure and engage in opsonization of pathogens and scavenging of toxic substances (18). SAA is produced by the liver after acute phase induction by pro-inflammatory cytokines; its main functions include binding cholesterol from inflammation sites, modulating the function of innate immune cells, and opsonizing pathogens for destruction by immune cells (18). Haptoglobin binds hemoglobin, which prevents oxidative damage and deprives bacteria of iron needed to grow (18). Cytokines are small "messenger" proteins secreted by immune cells to mediate the immune response. TNF-α is a primary signaling molecule in systemic inflammatory reactions and is a vital component of the acute phase response; IFNγ is a key signaling molecule in clearance of intracellular pathogen infections (19).

We combined an infection experiment and a longitudinal observational study to evaluate the utility of these four NSMI as indicators of pathogen exposure in a wild mammalian species, African buffalo (*Syncerus caffer*) (**Figure 1**). Specifically, in the experimental study we asked (1) How quickly do buffalo mount NSMI responses upon challenge with an endemic pathogen, foot-and-mouth disease virus (FMDV); (2) for how long do NSMI remain elevated after viral clearance; and (3) how pronounced is the difference between peak NSMI concentration and baseline NSMI concentration? In the longitudinal study, we asked (4) Are elevated NSMI associated with recent exposure to seven bacterial and viral respiratory pathogens, in a natural host population?

MATERIALS AND METHODS

African buffalo (*Syncerus caffer*) included for this study were located within Kruger National Park (KNP), a 19,000 km^2 reserve located in northeastern South Africa. Two populations were used for the study: (1) 12 1- to 2-year-old bovine tuberculosis (BTB) and FMDV free wild-caught buffalo obtained from Hluwluwe iMfolozi Park and transferred to the Skukuza State Veterinary enclosure (FMDV experiment buffalo, hereafter); (2) a herd of 60–75 wild buffalos, of mixed age and sex, contained within a 900-ha enclosure near Satara camp in the central area of KNP (cohort buffalo, hereafter). The first population was used in a FMDV challenge experiment identifying triggers of FMDV transmission and tracing viral evolution; the second population is part of an ongoing observational study identifying drivers of FDMV dynamics. The study was conducted under South Africa Department of Agriculture, Forestry and Fisheries Section 20 permits Ref 12/11/1 and Ref 12/11/1/8/3, ACUP project number 4478 and 4861, Onderstepoort Veterinary Research Animal Ethics Committee project number 100261-Y5, and the Kruger National Park Animal Care and Use Committee project number JOLAE1157-12 and JOLAE1157-13.

Field Sampling

FMDV Experiment Buffalo

Foot-and-mouth disease virus is an endemic viral infection of cloven-hoofed ungulates, with African buffalo acting as the maintenance host (20). Briefly, 12 buffalo were exposed to FMDV (day 2) by allowing them to mix with recently infected [*via* injection, using protocols optimized previously for buffalo: Maree et al. (21)] animals. All 12 recipient animals were sedated on days 2, 4, 6, 8, 11, 14, and 30 days post FMDV exposure to

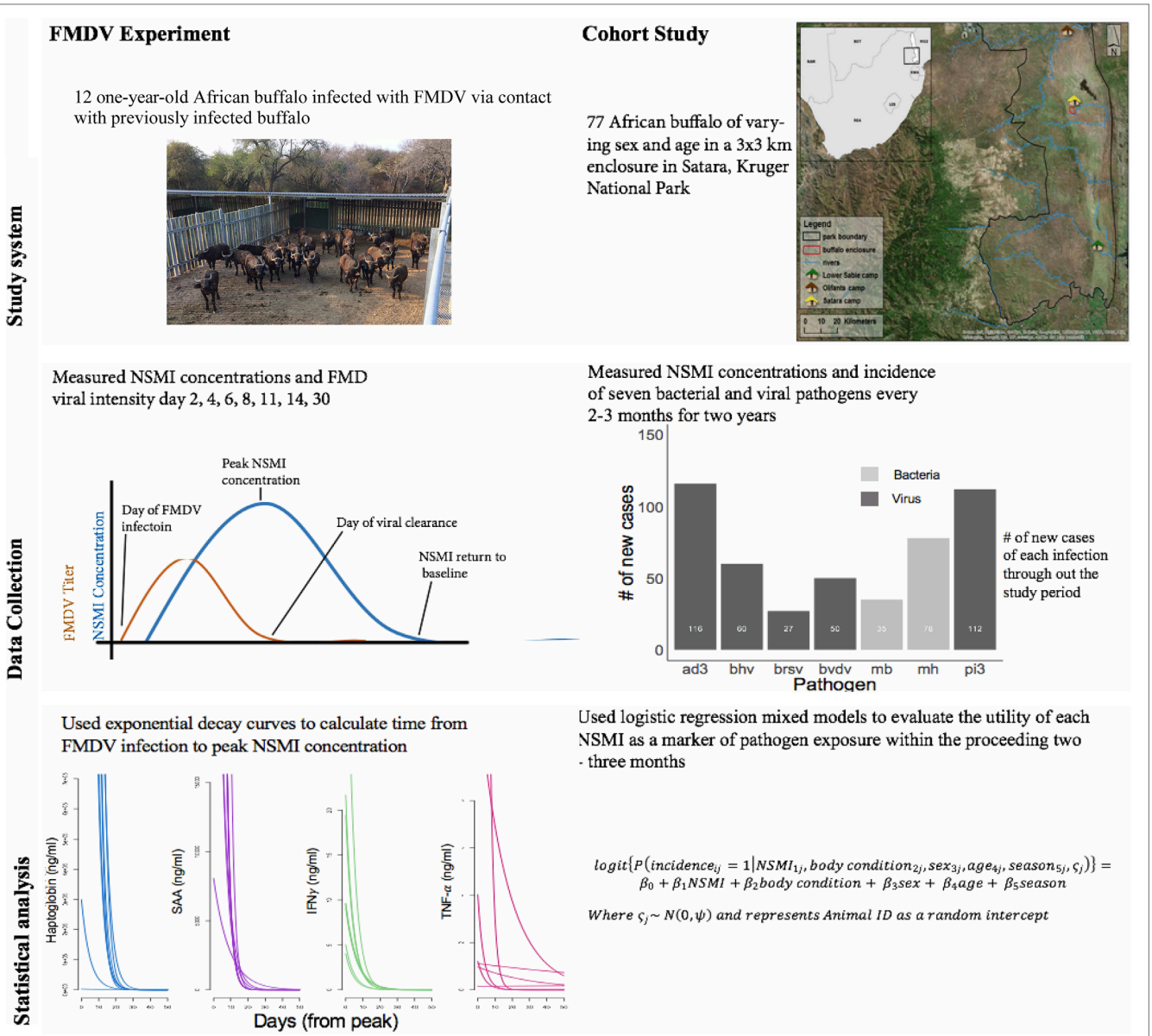

FIGURE 1 | A schematic illustrating the study design and analysis for the foot-and-mouth disease virus (FMDV) experiment and cohort buffalo longitudinal study. The bar graph (cohort study, middle panel) depicts the number of new cases throughout the study period of seven respiratory parasites. The number of new cases of viral parasites are displayed in dark gray (ad3 = Adenovirus; bhv = bovine herpes virus II; brsv = bovine respiratory syncytial virus; bvdv = bovine viral diarrheal virus; pi3 = Parainfluenza virus), the number of new cases of bacterial parasites are displayed in light gray (mb = *Mycoplasma bovis,* mh = *Mannheimia haemolytica*). The line graphs (FMDV experiment, bottom panel) illustrate the exponential decay curve fit from day of peak NSMI concentration to day NSMI returned to baseline for each animal. All animals mounted haptoglobin, SAA, and IFNγ responses, however, only three animals mounted a TNF-α response.

allow for collection of blood samples for quantification of NSMI and FMD viremia. Immobilizations were conducted by South African State Veterinarians using standard protocols for buffalo (22). Blood was collected *via* jugular venipuncture directly into vacutainer tubes with (plasma, whole blood) or without (serum) heparin, and stored on ice for transport back to the laboratory. Immediately upon arrival at the laboratory, blood was centrifuged at 5000 × *g* for 10 min; plasma and serum pipetted off the cellular layer into sterile microcentrifuge tubes and stored at −80°C until analysis. In addition, 1.5 ml of whole blood, collected in tubes with heparin, was aliquoted into separate, sterile microcentrifuge tubes and incubated at 37 C for 72 h. After 72 h, plasma was pipetted off the cellular layer and stored at 4 C until cytokine analysis 24–72 h later (23). Samples collected within 3 days of each other were all processed on the same cytokine assay; therefore, samples collected 3 days prior to running the assays were stored at 4 C for 72 h, samples collected 2 days prior to running the assays were stored at 4 C for 48 h and samples

collected 1 day prior to running the assays were stored at 4 C for 24 h.

Cohort Buffalo

Cohort buffalo were originally captured in 2001 from the North of KNP and have been maintained since then in the enclosure as a BTB free breeding herd. During our study period (2014–2016), the herd included 65–70 animals. Natural births and deaths occurred during the study, leading to a total of 77 individuals included in analyses.

The enclosure is entirely within KNP and has numerous other wild animals typical of the ecosystem (e.g., giraffe, zebra, warthogs, small mammals, and small predators). However, the enclosure excludes megaherbivores (rhino, hippo, elephant) and large predators (lion, leopard). Cohort buffalo graze and breed naturally and find water in seasonal pans and manmade (permanent) water points. In extreme dry seasons, supplemental grass and alfalfa hay are supplied.

Cohort buffalo were caught every 2–3 months from February 2014 to February 2016, totaling 10 capture periods. To sample, buffalo were herded into a capture corral, separated into groups of 4–10 animals, and sedated. Buffalo that evaded corral capture were darted individually from a helicopter. Sedation procedures are outlined in Couch et al. (24). Animals were released from the capture corral within 1–5 days after captures.

The animals' sex was determined visually. Age was determined by a combination of incisor wear and tooth emergence for animals older than 2.5 years, and *via* body size and horn growth in younger calves, as described in Jolles et al. (25). Body condition was determined by assigning a score from 1 to 5 based on manually palpating four sites (ribs, hips, spine, and tail base); average score was used in all analyses (26). At each capture period, blood was collected and processed identically to FMDV experiment procedures, with the addition of serum being stored for analysis of exposure by respiratory pathogens.

Laboratory Methods

Foot-and-mouth disease virus qRT-PCR and respiratory pathogen ELISAs were run using serum samples. NSMI markers were quantified using plasma samples; cytokine assays were run using incubated plasma samples (outlined in field methods section) whereas haptoglobin and SAA assay were run using non-incubated plasma samples.

FMDV Experimental Buffalo

The number of FDMV RNA genome copies per ml of serum, expressed as $\log_{10}$, was measured using quantitative qRT-PCR methods outlined in Ref. (21). Buffalo were considered to have an active viral infection if genome copies per ml of serum were >3.2 $\log_{10}$. Thus, one individual was removed from the study as serum qRT-PCR results never exceeded >3.2 $\log_{10}$ genome copies/ml of serum.

Non-specific markers of inflammation were measured *via* sandwich ELISA per manufacturers' instructions (Haptoglobin: Life Diagnostics 2410; Serum amyloid A: Life Diagnostics SAA-11; TNF-α: Ray-Bio ELB-TNFa; IFNγ: Bio-Rad MCA5638KZZ). All NSMI ELISAs were run within 1 month of collection.

Importantly, FMDV experimental buffalo were monitored for exposure to seven common respiratory pathogens, however, no animals seroconverted during the experiment. Pathogens tested for, and methods used to estimate, sero-conversion are identical to methods outlined below (Methods, laboratory methods, cohort buffalo).

Cohort Buffalo

Identical to the FMDV experiment, APP were measured *via* sandwich ELISA per manufacturers' instructions (Haptoglobin: Life Diagnostics 2410; Serum amyloid A: Life Diagnostics SAA-11; TNF-α: Ray-Bio ELB-TNFa; IFNγ: Bio-Rad MCA5638KZZ).

Sero-conversion, a proxy for incidence, of seven common viral and bacterial respiratory pathogens (**Figure 1**) was measured for each capture period *via* sandwich ELISAs per manufacturers' instructions [Adenovirus (AD-3), parainfluenza virus (Pi-3), bovine herpes virus, *Mannheimia hemolytica*, *Mycoplasma bovis* (MB): Bio-X IPAMM; bovine diarrhea virus (BVDV): Bio-X BVDV; bovine respiratory syncytial virus: Bio-X BRSV]. Samples were considered positive for pathogen antibodies if antibody titers exceeded threshold absorbance values calculated using the quality control procedures outlined in each Bio-X kit. Incidence was calculated as a binomial variable. Incidence was assigned a 1 if an animal seroconverted from t_0 to t_1 (i.e., absorbance values were below threshold concentrations at t_0 but above threshold absorbance at t_1) and 0 if the animal had not seroconverted.

With the exception of SAA, all NSMI and respiratory pathogen ELISAs were run within 2 weeks of capture periods. All SAA ELISAs were run in September 2016.

Statistical Analyses

FMDV Experimental Buffalo

Mathematical modeling was carried out using R [R Core Team (27)]. To evaluate the response of each NSMI to FMDV infection, we calculated (i) the time to NSMI peak from initial FMDV exposure (i.e., from the first day FMDV serum genome copies/1 ml of serum >3.2 $\log_{10}$), and (ii) the period for which NSMI remained elevated after the host cleared the virus. In addition, mean peak concentration and baseline concentration were calculated for each NSMI.

The period for which NSMI remained elevated past viral clearance was calculated as follows: first, an exponential decay curve Eq. 1 was fit starting from peak NSMI concentration (**Figure 1**):

$$y = ae^{kt}. \tag{1}$$

Next, decay rate (k) and intercept (a) were extracted from individual exponential decay equations, and baseline NSMI (y_{BL}) levels were estimated from averaging day-2 and day-14 NSMI concentrations. The time when NSMI returned to baseline levels after their peak, (t_{BL}), was calculated using Eq. 2:

$$t_{BL} = \frac{\log(y_{BL}) - \log(a)}{k}. \tag{2}$$

Time at viral clearance (t_{VC}) was assigned based on the first-day FMDV genome copies dropped below 3.2 $\log_{10}$/ml of serum after

initial incidence. Days' NSMI was elevated past viral clearance which was calculated by Eq. 3:

$$t_{\text{NSMI elevated from vc}} = t_{\text{BL}} - t_{\text{VC}}. \quad (3)$$

Animals in which the NSMI concentration did not exceed twofold baseline levels were determined not to have mounted that particular NSMI response and removed from future analysis (for that NSMI). If NSMI concentrations did not peak until 30 days post FMDV challenge these animals were removed from the analysis as their exponential decay curve would have been fit to only one data point. Final sample sizes included in each NSMI analysis are included in **Table 1**.

Raw data of NSMI concentration by day is presented in SF1.

Cohort Buffalo

Statistical analyses for cohort buffalo were performed in R using lme4 (28) and lmerTest (29).

Mixed effects logistic regressions were used to evaluate the effect of NSMI on respiratory disease incidence. Multiple samples per individual were used for all analyses, thus Animal ID was included as a random intercept to avoid pseudo-replication. Host traits (body condition, age, sex) and season may influence respiratory disease incidence (30); therefore, they were included as fixed effects within each model. A model was run for each combination of respiratory pathogen × NSMI (mixed effects logistic regression model example Eq. 4):

$$\begin{aligned}\text{logit}\left\{P\left(\begin{array}{l}\text{incidence}_{ij}=1|\text{NSMI}_{1j},\\ \text{Body Condition}_{2j},\text{sex}_{3j},\text{age}_{4j},\varsigma_j\end{array}\right)\right\}\\ =\beta_0+\beta_1*\text{NSMI}_{1j}+\beta_2*\text{Body Condtion}\\ +\beta_3*\text{sex}+\beta_4*\text{age}+\beta_5*\text{season}+\varsigma_j\end{aligned} \quad (4)$$

where $\varsigma_j \sim N(0,\psi)$ represents Animal ID as a random intercept.

The association of NSMI with respiratory disease incidence was evaluated post sero-conversion. Our models asked whether prior disease incidence between [t_0 and t_1] was associated with elevated NSMI at t_1. Thus, each model was run with explanatory variables corresponding to the t_1 time step, and disease incidence measured for the preceding capture interval.

Haptoglobin and SAA spanned several orders of magnitude and were severely right skewed, thus were $\log_2$ transformed to increase model stability and avoid issues with influential data points.

To prevent errors that can arise from multiple testing, statistical significance of each dependent variable was defined using significance levels corrected via the Benjamini and Hochberg's false discovery rate controlling procedure (31). Benjamini and Hochberg's false discovery rate controlling procedure assigns a significance level based upon rank of *p*-value within the family of tests; therefore, the particular significance level for each model is specified within **Table 2**. The test statistic and resulting *p*-value were calculated using Satterthwaite's approximation of degrees of freedom (29).

For significant associations between pathogen incidence and NSMI, average marginal predicted probabilities for given levels of NSMI concentration and area under the curve (AUC) were calculated using R packages lme4 (28) and pROC (32). Marginal predicted probabilities were calculated using models described in Eq. 4. 1,000 marginal predicted probabilities of pathogen incidence were calculated for 100 fixed values of NSMI and randomly selected (from the data) values of age, sex, body condition, season, and animal id. Average marginal predicted probability and 95% CI intervals for pathogen incidence were then constructed from the 1,000 values calculated for each fixed NSMI concentration. AUC, or the area under the receiving operating characteristic curve, is a standard diagnostic analysis used to measure how well a parameter can distinguish between two diagnostic groups based upon the specificity (true negative rate) and sensitivity (true positive rate) of the test.

TABLE 1 | Foot-and-mouth disease virus (FMDV) experiment: mean (±SE) baseline non-specific marker of inflammation (NSMI) concentration, peak NSMI concentration, days from FDMV incidence to peak concentration and days elevated from viral clearance for the FMDV virus.

NSMI	#Buffalo that responded	Baseline concentration (ng/ml)		Peak concentration (ng/C)	
		Mean	SE	Mean	SE
Haptoglobin	11	401.26	22.38	491,891	22,722.45
Serum amyloid A (SAA)	11	273.46	20.02	13,806.5	135.45
TNF-α	3	0.88	0.45	3.18	1.61
IFNγ	11	0.52	0.08	7.3	0.49
NSMI		**Days to peak**		**Days elevated post viral clearance**	
		Mean	**SE**	**Mean**	**SE**
Haptoglobin		5.4	0.29	21.23	0.39
SAA		3.33	1.17	11.18	2.66
TNF-α		6.67	0.19	7.75	2.56
IFNγ		4.4	0.3	16.51	1.74

Animals were considered to have mounted a NSMI response if NSMI concentration exceeded 2× baseline concentration after FMDV infection; with a total of 11 animals participating in the study. Days to peak was calculated by counting the number of days between the first day FMDV RNA copies exceeded 3.2 copies/5 μl of serum and the day NSMI reached peak concentration. Days elevated from viral clearance was calculated by estimating the time it took for NSMI to return to baseline concentrations after viral clearance (when FMDV RNA copies were less than 3.2 copies/5 μl serum post FDMV incidence). If peak concentrations were only reached on day 30, animals were excluded from mean calculations of days to peak and days elevated from viral clearance. Notably, mean peak concentration for haptoglobin was approximately 1,226 times higher than mean baseline levels, 50 times higher for SAA, 14 times higher for IFNγ, and four times higher for TNF-α.

RESULTS

FMDV Experiment Buffalo

Buffalo mounted robust NSMI responses to FMDV infection, as evidenced by differences between mean peak and baseline NSMI concentrations (**Table 1**; **Figure 2**).

The mean time from FMDV incidence to peak NSMI concentration was 3–7 days for all NSMI (**Table 1**; **Figure 3**). On average, viral clearance occurred at 4.72 (±0.20) days after initial FMDV

TABLE 2 | Cohort study: results of logistic regression models examining the non-specific markers of inflammation (NSMI) as indicators of recent (2–3 months) parasite exposure after accounting for body condition, sex, age, season, and animal id.

NSMI	Pathogen	β	SE	Test statistic	FDR sig level	*p*-Value
log_2 (Haptoglobin)						
	Bovine herpes virus (BHV)	−0.06307	0.038	−1.66	0.021	0.09695
	PI-3	0.12049	0.03749	3.214	0.007	**0.00131**
	Bovine respiratory syncytial virus (BRSV)	−0.05834	0.05671	−1.029	0.043	0.655834
	Bovine diarrhea virus (BVDV)	−0.03116	0.03953	−0.788	0.029	0.4309
	AD-3	0.01374	0.03651	0.376	0.05	0.707
	Mycoplasma bovis (MB)	0.19008	0.0598	3.178	0.014	**0.00148**
	Mannheimia hemolytica (MH)	−0.02125	0.03593	−0.592	0.036	0.55414
log_2 (Serum amyloid A)						
	BHV	−0.04368	0.02235	−1.954	0.007	0.0507
	PI-3	0.003432	0.019632	0.175	0.05	0.86123
	BRSV	−0.03458	0.03394	−1.019	0.036	0.308322
	BVDV	−1.32E−01	8.95E−02	−1.471	0.029	0.14131
	AD-3	0.01316	0.02144	0.614	0.043	0.53946
	MB	0.3577	0.19031	1.88	0.014	0.060174
	MH	−0.04644	0.02661	−1.745	0.021	0.0809
TNF-α						
	BHV	−0.19076	0.3101	−0.615	0.036	0.5384
	PI-3	−0.32148	0.26095	−1.232	0.007	0.21798
	BRSV	−0.62706	71187	−0.881	0.021	0.378
	BVDV	−0.24408	0.35926	−0.679	0.029	0.496886
	AD-3	−0.099964	0.212616	−0.47	0.043	0.638
	MB	0.277238	0.22845	1.192	0.014	0.233131
	MH	−0.064314	0.235515	−0.273	0.05	0.784793
IFNγ						
	BHV	−0.77378	0.58834	−1.315	0.029	0.18844
	PI-3	0.20225	0.18011	1.123	0.043	0.26148
	BRSV	−3.63397	2.19124	−1.658	0.021	0.0972
	BVDV	0.17317	0.1457	1.189	0.036	0.234609
	AD-3	0.34937	0.18254	1.914	0.014	0.0556
	MB	−2.23E+00	1.03E + 00	−2.157	0.007	0.031
	MH	0.26631	0.29246	0.125	0.05	0.900229

FDR significance levels are false discovery rate significance levels, which avoid issues for false positives that can occur when using multiple testing procedures.
Bold values indicate statistically significant relationships.

infection (i.e., the first-day FMDV RNA copies >3.2 log_{10}/ml of serum). Haptoglobin remained elevated for the greatest number of days past viral clearance (21 days on average), with the lowest interindividual variation in time elevated, followed by IFNγ, SAA, and TNF-α (**Figures 1** and **3**; **Table 1**).

All individuals showed increases in haptoglobin, SAA, and IFNγ, however, only 3/11 contact buffalo mounted detectable TNF-α responses. Haptoglobin displayed the greatest difference in mean peak and baseline concentration, followed by SAA, IFNγ, and TNF-α.

Cohort Buffalo

For each NSMI, we tested whether elevated levels of the marker were indicative of infection by a range of respiratory pathogens during the preceding 2–3 months. Haptoglobin was a significant indicator of two respiratory pathogens: MB and Pi-3 (**Table 2**; **Figure 4**). After controlling for animal traits and season, for every twofold increase in haptoglobin there was a 21% increase in the odds of prior MB incidence and a 13% increase in the odds of prior Pi-3 incidence. As expected for NSMI, the sensitivity and specificity of haptoglobin as a marker of each particular pathogen was significant (Lower CI of AUC > 0.5) but moderate. The AUC for haptoglobin as a classifier of MB was 0.67 (95% CI 0.52–0.77) and Pi-3 was 0.586 (95% CI 0.53–0.64) (**Figure 5**).

Although not significant by standards of the Benjamini and Hochberg's false discovery rate controlling procedure, there was suggestive evidence (p-value <0.05) that IFNγ was an indicator of MB incidence (**Table 2**). For every unit increase in IFNγ, there was an 11% decrease in the odds of prior MB incidence.

DISCUSSION

Mitigating disease outbreaks and identifying pathogen presence is crucial in evaluating ecosystem health (33, 34), creating effective wildlife conservation plans (35–37) and improving global health (38–40). Current techniques to detect pathogen exposure are primarily limited to (1) tests that are highly specific to both pathogen and host and (2) pathogens that cause detectable pathology in humans and economically important animals; yet, the diversity of pathogen communities in natural populations is only beginning to be uncovered (41, 42) with specific diagnostic tools for novel infections generally unavailable.

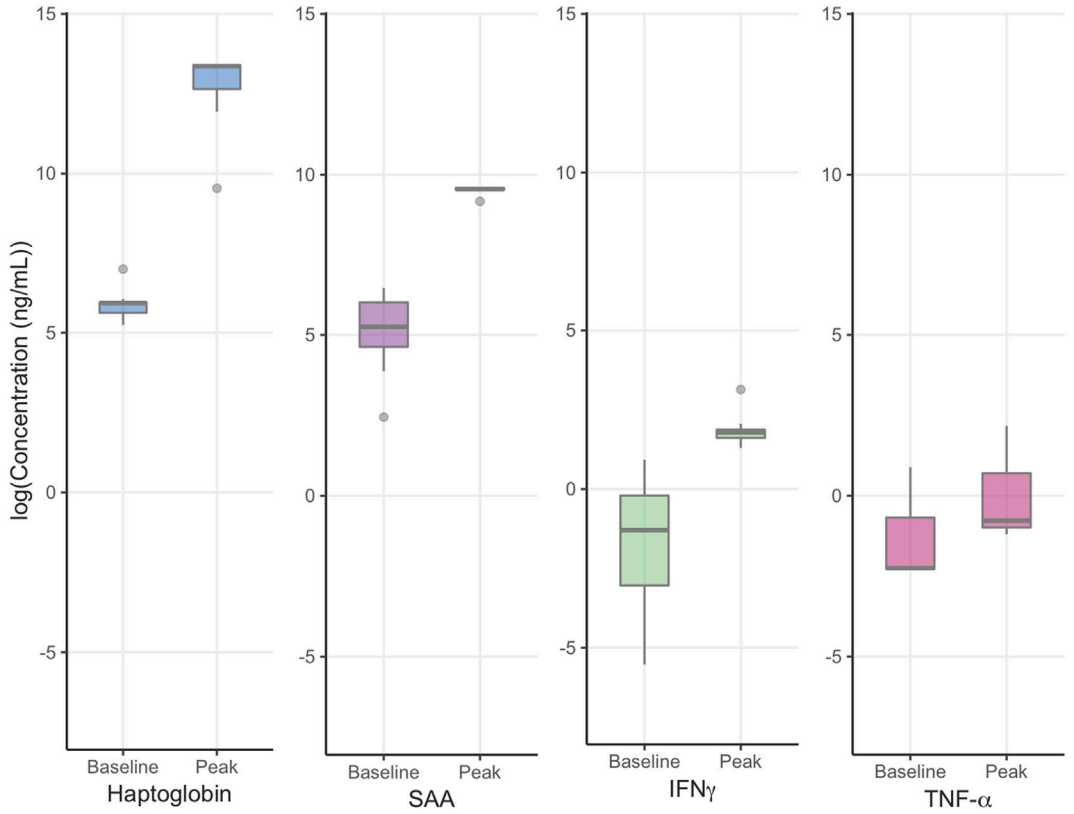

FIGURE 2 | Foot-and-mouth disease virus experiment: mean baseline and peak NSML. *Y* axes are log transformed for ease of visual comparison between non-specific markers of inflammation peak and baseline concentrations. Haptoglobin peak and baseline concentrations displayed the greatest difference and least variability followed by serum amyloid A (SAA), IFNγ, and TNF-α. The horizontal bands represent the 25, 50, and 75% quartiles whereas the vertical lines represent 1.5 times the interquartile range above the upper quartile and below the lower quartile, and dots represent outliers.

Given the current surge in infectious disease emergence (43), new diagnostic approaches, which can detect diverse pathogens, over an extended time frame within a broad range of hosts, are urgently needed. Our study demonstrates a possible approach to detecting infections non-specifically, using inflammatory molecular.

Despite the overwhelming diversity of pathogen species that can infect a given host, early stages of immunological response are considered evolutionarily conserved, and primary defenses are similar for a diversity of pathogens (44) within many hosts (45). Consequently, tracking first-line immune response has potential as a non-specific diagnostic approach for monitoring the burden of disease in a population of interest. Invertebrate and vertebrate hosts initially respond to pathogen challenge by mounting an inflammatory response (45). Due to the ubiquity of the inflammatory response, proteins upregulated during this initial stage of infection may hold promise as non-specific markers of pathogen exposure.

In this study, we used experimental and observational approaches to explore the utility of four NSMI in detecting pathogen exposure. We included two APP (haptoglobin and SAA) and two cytokines involved in inflammatory responses (IFNγ and TNF-α).

Buffalo mounted quick and robust acute phase responses to experimental challenge with FMDV, with the magnitude of NSMI responses similar to those reported in cattle (46). We found that, in response to FMDV infection, haptoglobin remained elevated the greatest number of days past viral clearance with the smallest degree of interindividual variation. Haptoglobin reached peak concentrations within a week of FMDV incidence and remained elevated for more than 3 weeks past FMDV clearance. Elevated haptoglobin levels were, thus, detectable both during and for several weeks after FMDV infection. Complementary to this, we found in our cohort study that haptoglobin was a significant indicator of recent natural incidence by two out of seven viral and bacterial respiratory pathogens.

Within the last 20 years, haptoglobin has been used to study inflammation in domestic animals (46) but has been more strongly associated with bacterial infections (47). We found haptoglobin to be significantly associated with both a viral (Pi-3) and a bacterial (MB) pathogen. Abnormal haptoglobin concentrations have been found in cattle infected with FMDV (48, 49) and Pi-3 (50).

All buffalo included in the experimental study mounted SAA and IFNγ responses to experimental FMDV infection within a week, however, on average, SAA remained elevated for just under 2 weeks and IFNγ remained elevated for just over 1 week. IFNγ was also a suggestive indicator of MB in our cohort study. TNF-α responses were detectable in one-fourth of our experimentally FMDV-infected buffalo, were short-lived for animals that

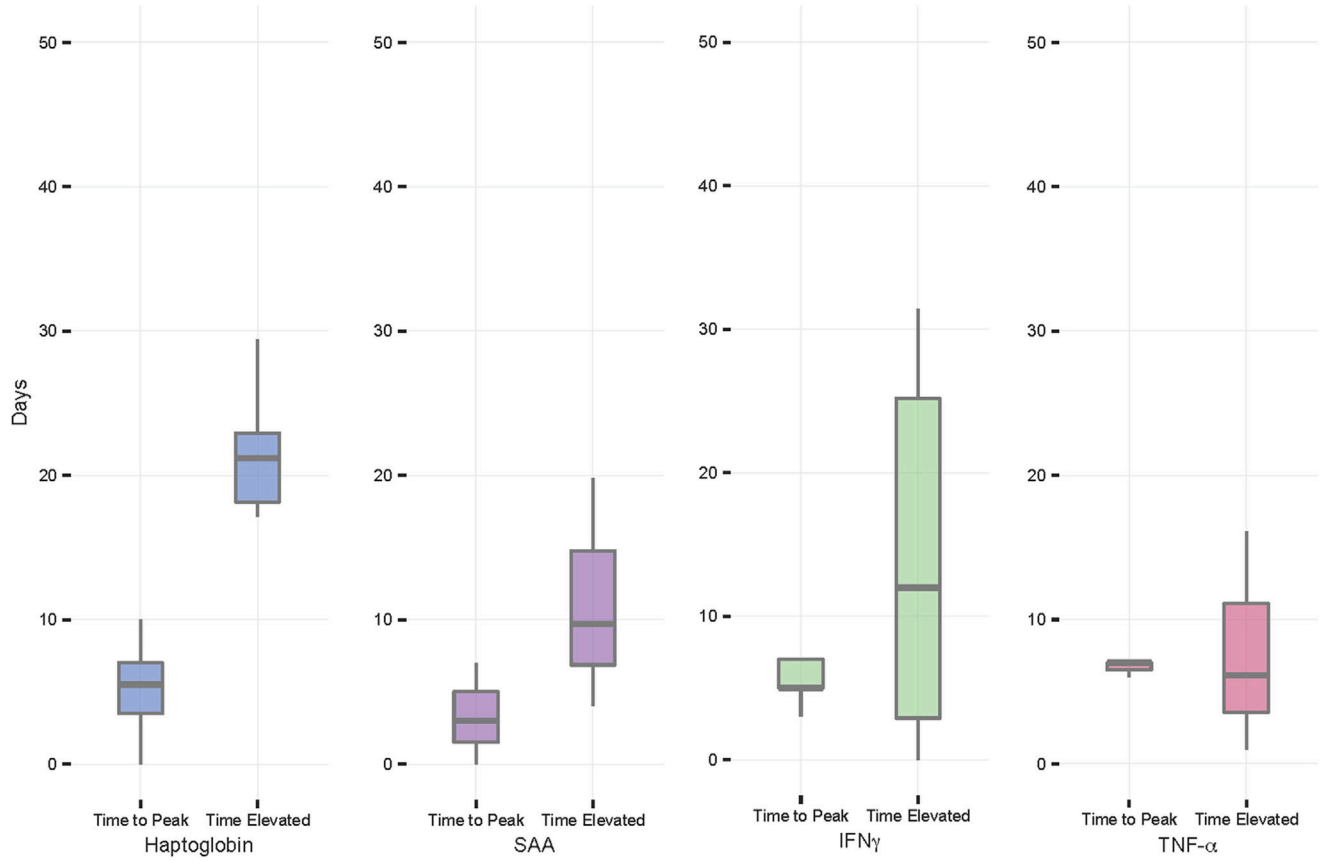

FIGURE 3 | Foot-and-mouth disease virus experiment: time from initial FMDV incidence to peak non-specific markers of inflammation concentration and time NSMI elevated from viral clearance. On average, all NSMI concentrations reached peak in 3–7 days. Haptoglobin concentrations remained elevated the longest past viral clearance, with the least variability, followed by serum amyloid A (SAA), IFNγ, and TNF-α. Individuals where NSMI concentrations peaked on day 30 were excluded from calculations as this was thought to be due to a secondary infection. The horizontal bands represent the 25, 50, and 75% quartiles, whereas the vertical lines represent 1.5 times the interquartile range above the upper quartile and below the lower quartile, and dots represent outliers.

mounted a response, and showed no associations with respiratory pathogens we monitored in our cohort study. Our results for SAA and IFNγ, especially IFNγ, suggest potential of NSMI for disease monitoring. Perhaps, inflammatory cytokines, particularly TNF-α, responses are mounted quickly, either very localized or low in magnitude, and short lived because of the collateral damage they elicit (51, 52). Haptoglobin contributes to "cleaning up" products of inflammation (19) and, thus, should cause significantly less immunopathology. The function of haptoglobin may, thus, explain the comparatively long lived, high magnitude responses we observed.

We found haptoglobin to be a significant classifier of MB and Pi-3, however, specificity would be considered low by veterinary and human medical diagnostic standards. Low specificity is expected, given that haptoglobin responds to multiple inflammatory processes including exposure to unknown pathogens, stress, trauma, and autoimmune disorders (46); and indeed, the goal here was to find non-specific markers indicative of pathogen exposure. Although sensitivity and specificity was low, and haptoglobin only detected two out of seven respiratory pathogens, our results are particularly encouraging because we are likely to be underestimating the true sensitivity of haptoglobin and other NSMI in the cohort study, due to the "mismatch" between capture interval (2–3 months) and NSMI response (e.g., haptoglobin: 3 weeks). This is likely cause an increased number of false negatives—animals that were exposed to a given pathogen, but have no detectable elevation in NSMI at time of capture. More frequent captures should thus improve the performance of NSMI in detecting pathogen exposures. In addition, using a combination of NSMI may help to tease apart sources of inflammation, allowing researchers to filter out non-infectious processes and improve test specificity.

Our work points to the possibility of defining markers for non-specific disease surveillance, but raises many new questions about discovering which combinations of markers can potentially work in different host species, and for detection of different suites of pathogens.

For example, future research could investigate a broader range of cytokines, such as inflammatory cytokines, Il-6 and Il-1beta, and additional APP, such as fibrinogen or C-reactive protein, and negative APP such as albumin or transferrin. Dugovich et al. (53) recently described the utility of natural antibodies (nAbs),

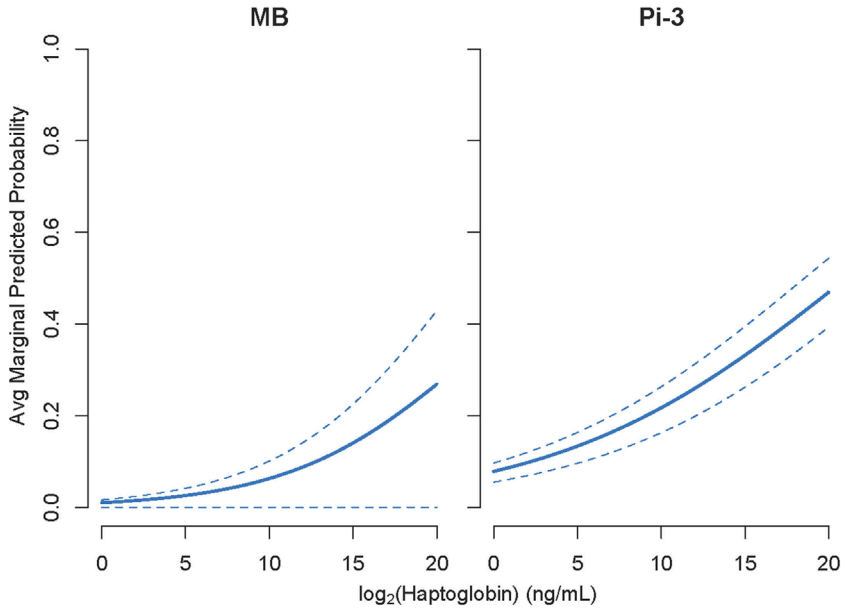

FIGURE 4 | Cohort study: elevated haptoglobin was associated with *Mycoplasma bovis* (MB) and *Parainfluenza virus III* (PI3) exposure during the preceding 2–3 months. *Y* axes show average marginal predicted probabilities of pathogen incidence. Marginal predicted probabilities were calculated using models described in Eq. 4. 1,000 marginal predicted probabilities of pathogen incidence were calculated for 100 fixed values of NSMI and randomly selected (from the data) values of age, sex, body condition, season, and animal id. Average marginal predicted probability and 95% CI intervals for parasite incidence were then constructed from the 1,000 values calculated for each fixed NSMI concentration. Due to large seasonal variation, the lower confidence interval of MB is small.

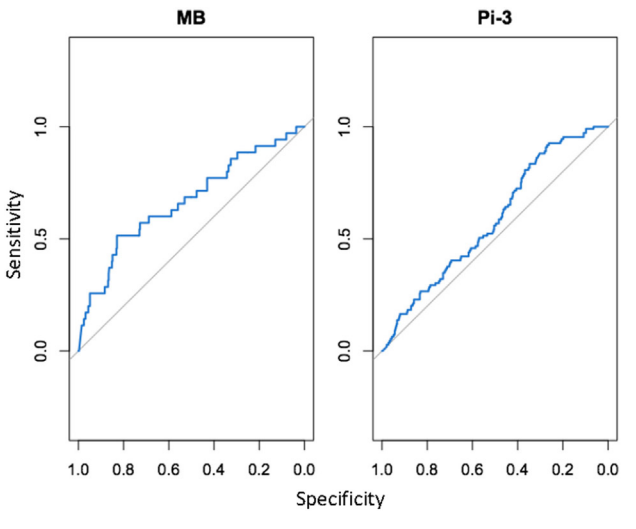

FIGURE 5 | Cohort study: area under the curve (AUC) for detection *of Mycoplasma bovis* (Mb) and *Parainfluenza Virus* (PI3) based on elevated haptoglobin. AUC, or the area under the receiving operating characteristic (ROC) curve, is a standard diagnostic analysis used to measure how well a parameter can distinguish between two diagnostic groups based on the specificity (true negative rate) and sensitivity (true positive rate) of the test. The gray line represents the trend the diagnostic parameter would follow if the AUC was equal to 0.5. The blue line represents the observed trend; the closer the curve follows the left and top border of the graph, the more accurate the test. If the blue line falls below the gray line (AUC < 0.5), it indicates that the test is not significantly better than random.

antibodies that associate with the innate immune response and bind to multiple microbial agents, in assessing immunological status of desert bighorn sheep. In addition, in mammals, toll-like receptors (TLRs), proteins integral in recognition of infection, are highly conserved to recognize broad groups of pathogens (54). As such, the utility of nABs and TLR expression as disease surveillance tools warrants future research.

A systematic approach could follow host responses to pathogenic challenge, from pathogen recognition to inflammation, and define effectors that typify responses to different groups of pathogens. Immunologists could potentially tailor NSMI panels for detecting different groups of parasites, such as hemoparasites or gastro-intestinal infections—and explore whether taxonomic relatedness of parasites, or similarity of infection sites are most important in selecting appropriate NSMI.

Assays for APP and pro-inflammatory cytokines have been developed for domestic animals and laboratory model species, including cows, sheep, goats, horses, dogs, cats, mice, and rats. A handful of studies have used serum and urine based assays to monitor health and disease incidence in wildlife species including Grant's zebra (55), European mouflon (56), Przewalkski's horses (57), rhesus macaques (58). As such, the tools for beginning to define panels of NSMI for disease monitoring, already exist for a broad range of mammalian host species. Due to the devastation that emerging infectious diseases have elicited in amphibian (59) and marine invertebrate (60, 61) systems, identifying inflammatory markers that detect pathogen exposure in non-mammalian vertebrates and invertebrates could prove invaluable to conservation biologists.

For NSMI that are stable in stored samples, such as frozen sera, the utility of NSMI could extend beyond current surveillance to include retrospective studies—biobanks are a commonly available but underused resource for human, animal, and wildlife studies. Beechler et al. (62) demonstrated that haptoglobin concentrations in stored serum remain stable for at least 4 years, and (63) documented stability of haptoglobin, nAbs, and total immunoglobulins during extended storage, suggesting that undertaking retrospective evaluations of populations is a feasible and viable option for future studies.

Developing non-specific diagnostic tools is essential to detect emerging infections in animal and human populations and effectively tracking the burden of infection in natural populations. In the face of the vast diversity of pathogens and host species, an approach that tracks conserved inflammatory responses to a range of infections may provide a tractable pathway toward recognizing changes in disease burden that can then be followed up with specific diagnostic testing. Our study on infections in African buffalo provides a proof of concept, showing that APP and/or pro-inflammatory cytokines can provide useful information about pathogen exposures. It is our hope that this work will open opportunities for investigating suites of NSMI as indicators for pathogen exposure, potentially transforming how we measure disease in natural populations.

ETHICS STATEMENT

The study was conducted under South Africa Department of Agriculture, Forestry and Fisheries Section 20 permits Ref 12/11/1 and Ref 12/11/1/8/3, Oregon State University ACUP project number 4478 and 4861, Onderstepoort Veterinary Research Animal Ethics Committee project number 100261-Y5, and the Kruger National Park Animal Care and Use Committee project number JOLAE1157-12 and JOLAE1157-13.

AUTHOR CONTRIBUTIONS

AJ: project PI, PhD advisor of lead author CG, involved in idea, field work, lab work, analyses, and manuscript writing. CG: lead author involved in field work, lab work, leads analyses, and manuscript writing. BB: involved in idea, field work, lab work, analyses, and manuscript writing. PB: scientific liaison for South African National Parks Veterinary Wildlife Services. Involved in project design and field work. BC: Project PI for the Pirbright Institute. Involved in project design, lab work, and field work. LK-L: state veterinarian involved in project design, lead experimental study, and manuscript preparation. FM: involved in diagnostic lab work, experimental study design and implementation, and manuscript preparation. TM: involved in data analysis. EP-M: involved in field work, lab work, and manuscript preparation. KS: involved in field work, lab work, and manuscript preparation. OS: state veterinarian involved in project design, lead experimental study, and manuscript preparation.

ACKNOWLEDGMENTS

We thank Kruger National Park Veterinary Wildlife Services and State Veterinarians for their help with animal capture. Lab work and field work was completed by members of the Jolles Lab group: Hannah Tavalire, Brian Dugovich, Courtney Coon, Claire Couch, Henri Combrink, Juliana Masseloux, Danielle Sisson, Daniel Trovillion, Abby Sage, Emma Devereux, and Kath Forssman. We would also like to thank two anonymous reviewers for helpful feedback that improved the manuscript. Both experimental and longitudinal studies were supported by the USDA-NIFA AFRI grant # 2013-67015-21291and by the UK Biotechnology and Biological Sciences Research Council grant # BB/L011085/1 as part of the joint USDA-NSF-NIH-BBSRC Ecology and Evolution of Infectious Diseases program. C. Glidden was supported by ARCS and NSF GRFP fellowships.

SUPPLEMENTARY MATERIAL

The Supplementary Material for this article can be found online at http://www.frontiersin.org/articles/10.3389/fimmu.2017.01944/full#supplementary-material.

REFERENCES

1. Kelser EA. Meet dengue's cousin, Zika. *Microbes Infect* (2016) 18(3):163–6. doi:10.1016/jmicinf.2015.12.003
2. Shears P, O'Dempsey TJD. Ebola virus disease in Africa: epidemiology and nosocomial transmission. *J Hosp Infect* (2015) 90(1):1–9. doi:10.1016/j.jhin.2015.01.002
3. Vurro M, Bonciani B, Vannacci G. Emerging infectious diseases of crop plants in developing countries: impact on agriculture and socio-economic consequences. *Food Sec* (2010) 2:113. doi:10.1007/s12571-01-00627
4. Genton C, Cristescu R, Gatti S, Levréro F, Bigot E, Caillaud D, et al. Recovery potential of a western lowland gorilla population following a major Ebola outbreak: results from a ten year study. *PLoS One* (2012) 7(5):e37106. doi:10.1371/journal.pone.0037106
5. Brierley L, Vonhof MJ, Olival KJ, Daszak P, Jones KE. Quantifying global drivers of zoonotic bat viruses: a process-based perspective. *Am Nat* (2016) 187(2):E53–64. doi:10.1086/684391
6. Meyer Steiger DB, Ritchie SA, Laurance SGW. Mosquito communities and disease risk influenced by land use change and seasonality in the Australian tropics. *Parasit Vectors* (2016) 9:387. doi:10.1186/s13071-016-1675-2
7. Openshaw JJ, Hegde S, Sazzad HM, Khan SU, Hossain MJ, Epstein JH, et al. Increased morbidity and mortality in domestic animals eating dropped and bitten fruit in Bangladeshi villages: implications for zoonotic disease transmission. *Ecohealth* (2016) 13(1):39–48. doi:10.1007/s10393-015-1080-x
8. Adlard RD, Miller TL, Smit NJ. The butterfly effect: parasite diversity, environment, and emerging disease in aquatic wildlife. *Trends Parasitol* (2015) 31(4):160–6. doi:10.1016/j.pt.2014.11.001
9. Ingersoll TE, Sewall BJ, Amelon SK. Effects of white-nose syndrome on regional population patterns of 3 hibernating bat species. *Conserv Biol* (2016) 30(5):1048–59. doi:10.1111/cobi.12690
10. Price SJ, Garner TWJ, Cunningham AA, Langton TES, Nichol RA. Reconstructing the emergence of a lethal infectious disease of wildlife supports a key role for spread through translocations by humans. *Proc Biol Sci* (2016) 283:20160952. doi:10.1098/rspb.2016.0952

11. Pérez JM, Meneguz PG, Dematteis A, Rossi L, Serrano E. Parasites and conservation biology: the 'ibex-ecosystem'. *Biodivers Conserv* (2006) 15:2033–47. doi:10.1007/s10531-005-0773-9
12. Blackwell M. The fungi: 1,2,3…5.1 million species? *Am J Bot* (2011) 98(3):426–38. doi:10.3732/ajb.1000298
13. Woolhouse M, Scott F, Hudson Z, Howey R, Chase-Topping M. Disease invasion impacts on biodiversity and human health. *Philos T R Soc B* (2012) 367(1604):2804–6. doi:10.1098/rstb.2012.0331
14. Rodicio MR, Mendoza MC. Identification of bacteria through 16S rRNA sequencing: principles, methods, and applications in clinical microbiology. *Enferm Infecc Microbiol Clin* (2004) 22(4):238–45. doi:10.1157/13059055
15. Metzker M. Sequencing technologies – the next generation. *Nat Rev Genet* (2010) 11(1):31–46. doi:10.1038/nrg2626
16. Petti CA. Detection and identification of microorganisms by gene amplification and sequencing. *Clin Infect Dis* (2007) 44(8):1108–14. doi:10.1086/512818
17. Guerrant RL, Walker DH, Weller PF. *Tropical Infectious Diseases*. Edinburgh: Elsevier (2011).
18. Ceciliani F, Ceron JJ, Eckersall PD, Sauerwein H. Acute phase proteins in ruminants. *J Proteomics* (2012) 75(14):4207–31. doi:10.1016/j.jprot.2012.04.004
19. Murphy K. *Janeway's Immunobiology*. New York, USA: Taylor & Francis Inc. (2011).
20. Vosloo W, Thomson GR. Natural habitats in which foot-and-mouth disease viruses are maintained. In: Sobrino F, Domingo E, editors. *Foot-and-Mouth Disease Virus: Current Research and Emerging Trends*. Madrid, Spain: CSIC-UAM (2017). p. 179–210.
21. Marree F, de Klerk-Lorist LM, Gubbins S, Zhang F, Seago J, Pérez-Martin E, et al. Differential persistence of foot-and-mouth disease virus in African buffalo is related to virus virulence. *J Virol* (2016) 90(10):5132–40. doi:10.1128/JVI.00166-16
22. McKenzie A. *The Capture and Care Manual: Capture, Care, and Accommodation, and Transportation of Wild African Animals*. Lynwood Ridge, South Africa: South African Veterinary Foundation (1993).
23. Ezenwa VO, Jolles AE. Opposite effects of anthelmintic treatment on microbial infection at individual versus population scale. *Science* (2015) 347: 175–7. doi:10.1126/science.1261714
24. Couch CE, Movius MA, Jolles AE, Gorman ME, Rigas JD, Beechler BR. Serum biochemistry panels in African buffalo: defining reference intervals and assessing variability across season, age, sex. *PLoS One* (2017) 12(5):e0176830. doi:10.1371/journal.pone.0176830
25. Jolles AE, Cooper DV, Levin SA. Hidden effects of chronic tuberculosis in African buffalo. *Ecology* (2005) 86(9):2358–64. doi:10.1890/05-0038
26. Ezenwa VO, Jolles AE, O'Brien MP. A reliable body condition scoring technique for estimating condition in African buffalo. *Afr J Ecol* (2009) 47(4):476–81. doi:10.1111/j.1365-2028.2008.00960.x
27. R Core Team. *R: A Language and Environment for Statistical Computing*. Vienna, Australia: R Foundation for Statistical Computing (2015).
28. Bates D, Maechler M, Bolker B, Walker S. Fitting linear mixed-effects models using lme4. *J Stat Softw* (2015) 67(1):1–48. doi:10.18637/jss.v067.i01
29. Kuznetsova A, Brockhoff P, Christensen RHB. *lmerTest: Tests in Linear Mixed Effects Models. R Package Version 2.0-33* (2016). Available from: https://CRAN.R-project.org/package=lmerTest.
30. McNulty C. *African Buffalo as Reservoir Hosts for Infectious Respiratory Pathogens in Kruger National Park*. MS Thesis, University of Wisconsin-Madison College of Veterinary Medicine, South Africa (2015).
31. Benjamini Y, Yekutieli D. The control of the false discovery rate in multiple testing under dependency. *Ann Statist* (2001) 29(4):665–1188.
32. Xavier R, Turck N, Hainard A, Tiberti N, Lisacek F, Sanchez J, et al. pROC: an open-source package for R and S+ to analyze and compare ROC curves. *BMC Bioinformatics* (2011) 12:77. doi:10.1186/1471-2105-12-77
33. Preston DL, Mishler JA, Townsend AR, Johnson PTJ. Disease ecology meets ecosystem science. *Ecosystems* (2016) 19:737–48. doi:10.1007/s10021-016-9965-2
34. Polley L. Navigating parasite webs and parasite flow: emerging and re-emerging parasitic zoonoses of wildlife origin. *Int J Parasitol* (2005) 35 (11–12):1279–94. doi:10.1016/j.ijpara.2005.07.003
35. Heard MJ, Smith KF, Ripp KJ, Berger M, Chen J, Dittmeier J, et al. The threat of disease increases as species move toward extinction. *Conserv Biol* (2013) 27(6):1378–88. doi:10.1111/cobi.12143
36. Thompson RCA, Lymbery AJ, Smith A. Parasites, emerging disease and wildlife conservation. *Int J Parasitol* (2010) 40(10):1163–70. doi:10.1016/j.ijpara.2010.04.009
37. Smith KF, Sax DF, Lafferty KD. Evidence for the role of infectious disease in species extinction and endangerment. *Conserv Biol* (2006) 20(5):1349–57. doi:10.1111/j.1523-1739.2006.00524.x
38. Macpherson CN. The epidemiology and public health importance of toxocariasis: a zoonosis of global importance. *Int J Parasitol* (2013) 43(12–13): 999–1008. doi:10.1016/j.ijpara.2013.07.004
39. Colwell DD, Dantas-Torres F, Otranto D. Vector-borne parasitic zoonoses: emerging scenarios and new perspectives. *Vet Parasitol* (2013) 182(1):14–21. doi:10.1016/j.vetpar.2011.07.012
40. Vandegrift KJ, Wale N, Epstein JH. An ecological and conservation perspective on advances in the applied virology of zoonoses. *Viruses* (2011) 3(4):379–97. doi:10.3390/v3040379
41. Anthony SJ, Epstein JH, Murray KA, Navarrete-Macias I, Zambrana-Torrelio CM, Solovyov A, et al. A strategy to estimate unknown viral diversity in mammals. *mBio* (2013) 4(5):e000598. doi:10.1128/mBio.00598-13
42. Bailey AL, Lauck M, Ghai RR, Nelson CW, Heimbruch K, Hughes AL, et al. Arteriviruses, pegiviruses, and lentiviruses are common among wild African monkeys. *J Virol* (2016) 90(15):6724–37. doi:10.1128/JVI.00573-16
43. Jones KE, Patel NG, Levy MA, Storeygard A, Balk D, Gittleman JL, et al. Global trends in emerging infectious disease. *Nature* (2008) 451:990–3. doi:10.1038/nature06536
44. Mogensen TH. Pathogen recognition and inflammatory signaling in innate immune defenses. *Clin Microbiol Rev* (2009) 22(2):240–73. doi:10.1128/CMR.00046-08
45. Rowley AF. The evolution of inflammatory mediators. *Mediators Inflamm* (1996) 5(1):3–13. doi:10.1155/S0962935196000014
46. Cray C, Zaias J, Altman NH. Acute phase response in animals: a review. *Comp Med* (2009) 59(6):517–26.
47. Godson DL, Campos M, Attah-Poku SK, Redmond MJ, Corediro DM, Manjeet SS, et al. Serum haptoglobin as an indicator of the acute phase response in bovine respiratory disease. *Vet Immunol Immunopathol* (1996) 51(3–4):277–92. doi:10.1016/0165-2427(95)05520-7
48. Stenfeldt C, Heegaard PMH, Stockman A, Tjomehoj K, Belsham GJ. Analysis of the acute phase responses of serum amyloid A, haptoglobin and type 1 interferon in cattle experimentally infected with foot-and-mouth disease virus serotype O. *Vet Res* (2011) 42:66. doi:10.1186/1297-9716-42-66
49. Höfner MC, Fosbery MW, Eckersall PD. Haptoglobin response of cattle infected with foot-and-mouth disease virus. *Res Vet Sci* (1994) 57(1):125–8. doi:10.1016/0034-5288(94)90093-0
50. Rodrigues MC, Cooke RF, Marques RS, Cappellozza BI, Arispe SA, Keisler DH, et al. Effects of vaccination against respiratory pathogens on feed intake, metabolic, and inflammatory responses in beef heifers. *J Anim Sci* (2015) 93(9):4443–52. doi:10.2527/jas.2015-9277
51. Graham AL, Allen JE, Read AF. Evolutionary causes and consequences of immunopathology. *Annu Rev Ecol Evol Syst* (2005) 36(1):373–97. doi:10.1146/annurev.ecolsys.36.102003.152622
52. Sears BF, Rohr JR, Allen JE, Martin LB. The economy of inflammation: when is less more? *Trends Parasitol* (2011) 27(9):382–7. doi:10.1016/j.pt.2011.05.004
53. Dugovich BS, Peel MJ, Palmer AL, Zielke RA, Sikora AE, Beechler BR, et al. Detection of bacterial-reactive natural IgM antibodies in desert bighorn sheep populations. *PLoS One* (2017) 12(6):e0180415. doi:10.1371/journal.pone.0180415
54. Takeda K, Kaisho T, Akira S. Toll-like receptors. *Annu Rev Immunol* (2003) 21:335–76. doi:10.1146/annurev.immunol.21.120601.141126
55. Cray C, Hammond E, Haefele H. Acute phase protein and protein electrophoresis values for captive Grant's zebra (*Equus burchelli*). *J Zoo Wildl Med* (2013) 44(4):1107–10. doi:10.1638/2013-0033R.1
56. Smitka P, Tóthová C, Curlík J, Lazar P, Bíres J, Posiváková T. Serum concentration of haptoglobin in European mouflon (*Ovis musimon* L.) from a game reserve. *Acta Vet Brno* (2015) 84:25–8. doi:10.2754/avb201584010025
57. Sander SJ, Joyner PH, Cray C, Rostein DS, Aitken-Palmer C. Acute phase proteins as a marker of respiratory inflammation in Prezewalski's horse (*Equus ferus prezwalski*). *J Zoo Wildl Med* (2016) 47(2):654–8. doi:10.1638/2015-0059.1

58. Krogh AK, Lundsgaard JF, Bakker J, Langermans JA, Verreck FA, Kjelgaard-Hansen M, et al. Acute-phase responses in healthy and diseased rhesus macaques (*Macaca mulatta*). *J Zoo Wildl Med* (2014) 45(2):306–14. doi:10.1638/2013-0153R.1
59. Daszak P, Berger L, Cunningham AA, Hyatt AD, Green DE, Speare R. Emerging infectious diseases and amphibian population declines. *Emerg Infect Dis* (1999) 5(6):735–48. doi:10.3201/eid0506.990601
60. Menge BA, Cerny-Chipman EB, Johnson A, Sullivan J, Gravem A, Chen F. Insights into differential population impacts, recovery, predation rate and temperature effects from long-term research. *PLoS One* (2016) 11(5): e0153994. doi:10.1371/journal.pone.0153994
61. Maynard J, van Hooidonk R, Harvell CD, Eakin CM, Liu G, Willis BL, et al. Improving marine disease surveillance through sea temperature monitoring, outlooks and projections. *Phil Trans R Soc* (2016) 371:20150208. doi:10.1098/rstb.2015.0208
62. Beechler BR, Jolles AE, Budischak SA, Corstjens PLAM, Ezenwa VO, Smith M, et al. Host immunity, nutrition and coinfection alter longitudinal infection patterns of schistosomes in a free ranging African buffalo population. *PLoS Negl Trop Dis* (2017) 11(12):e0006122. doi:10.1371/journal.pntd.0006122
63. Hegemann A, Pardal S, Matson KD. Indices of immune function used by ecologists are mostly unaffected by repeated freeze-thaw cycles and methodological deviations. *Front Zool* (2017) 14:43. doi:10.1186/s12983-017-0226-9

Conflict of Interest Statement: The authors declare that the research was conducted in the absence of any commercial or financial relationships that could be construed as a potential conflict of interest.

frontiers in Immunology

ORIGINAL RESEARCH
published: 12 September 2017
doi: 10.3389/fimmu.2017.01071

Gene Expression Contributes to the Recent Evolution of Host Resistance in a Model Host Parasite System

Brian K. Lohman[1], Natalie C. Steinel[1,2], Jesse N. Weber[1,3] and Daniel I. Bolnick[1]*

[1] Department of Integrative Biology, The University of Texas at Austin, Austin, TX, United States, [2] Department of Medical Education, Dell Medical School, The University of Texas at Austin, Austin, TX, United States, [3] Division of Biological Sciences, The University of Montana, Missoula, MT, United States

Heritable population differences in immune gene expression following infection can reveal mechanisms of host immune evolution. We compared gene expression in infected and uninfected threespine stickleback (*Gasterosteus aculeatus*) from two natural populations that differ in resistance to a native cestode parasite, *Schistocephalus solidus*. Genes in both the innate and adaptive immune system were differentially expressed as a function of host population, infection status, and their interaction. These genes were enriched for loci controlling immune functions known to differ between host populations or in response to infection. Coexpression network analysis identified two distinct processes contributing to resistance: parasite survival and suppression of growth. Comparing networks between populations showed resistant fish have a dynamic expression profile while susceptible fish are static. In summary, recent evolutionary divergence between two vertebrate populations has generated population-specific gene expression responses to parasite infection, affecting parasite establishment and growth.

Keywords: gene expression, host–parasite, ecoimmunology, stickleback, reactive oxygen species

OPEN ACCESS

Edited by:
Andrew Steven Flies, University of Tasmania, Australia

Reviewed by:
Katherine Buckley, George Washington University, United States
Magdalena Chadzińska, Jagiellonian University, Poland

****Correspondence:***
Brian K. Lohman
brian.keith.lohman@gmail.com

Specialty section:
This article was submitted to Comparative Immunology, a section of the journal Frontiers in Immunology

Received: *14 June 2017*
Accepted: *16 August 2017*
Published: *12 September 2017*

Citation:
Lohman BK, Steinel NC, Weber JN and Bolnick DI (2017) Gene Expression Contributes to the Recent Evolution of Host Resistance in a Model Host Parasite System. Front. Immunol. 8:1071. doi: 10.3389/fimmu.2017.01071

INTRODUCTION

Helminths are a diverse group of parasitic worms, which often establish long lasting infections in their vertebrate hosts (1), despite host immune activity. Curiously, in many host-parasite systems, helminths can persist in some host genotypes, whereas other hosts successfully eliminate infections. Therefore, a key question in biology is, why does parasite resistance differ among host individuals or populations? Host resistance depends on a complex signaling cascade, starting with the detection of pathogen molecules or pathogen induced damage to host tissues, followed by activation of a diverse suite of innate and adaptive immune cell populations. These cells may proliferate, migrate, or produce molecules that signal to other immune cells or directly attack the parasite. If the infection is cleared, the host must downregulate this costly response (1–4). Natural genetic variation in host resistance could arise from any stage(s) in an immune cascade.

Classically, the search for genes important to host immunity has been conducted in the lab using a combination of forward genetic experiments and screens for abnormal phenotypes (5, 6). Such approaches typically identify genes in which natural or induced mutations lead to loss of immunological function. In contrast, natural selection provides a powerful genetic screen for alleles that confer adaptive benefits within the complex ecological milieu in which wild vertebrates have evolved and currently live, including diverse stresses and coinfections (7, 8). Isolated host populations are often exposed to distinct local parasite species or genotypes, and consequently

evolve divergent immune traits. Spatially varying coevolution thus leads to adaptive geographic variation in host genotypes and corresponding immune traits (9, 10). In contrast to lab knockout screens, this natural genetic variation is more likely to entail genes whose alleles confer a change or gain of immune function. Loss of function is of course also a possibility, if parasites exploit a given host trait, or if a trait confers insufficient benefits to warrant its costs. By identifying these evolutionarily labile genes, biologists seek to understand the genetic and immunological mechanisms of vertebrate resistance to, and coevolution with, helminth parasites. The genes identified in this manner will be of interest not only for what they tell us about the basic biology of host parasite interactions but also as a possible source of new therapeutic strategies for controlling parasitic infections or manipulating vertebrate immunity (11, 12).

One way to identify genes favored by natural selection is to look for evolution of gene expression in response to infection. Recent advances in sequencing technology and genetic mapping have made this an accomplishable goal (13, 14). Previous studies have uncovered variation in gene expression associated with disease in rat, mouse, and human populations (15–18), but few studies have used wild populations (19–22). These studies are often underpowered, as the historically high cost of RNAseq library prep and sequencing limited biological replication (23). Few studies of variation in disease in wild populations have included more than a single population (20) or considered the effect of exposure on those individuals who did not ultimately become infected. Finally, linking changes in gene expression to host immune function requires concurrent measurement of multiple immune phenotypes, which are also missing from the majority of existing studies of wild populations of hosts. Here, we seek to close these gaps by testing the effect of exposure or infection on gene expression, using a large number of individuals from two populations with independent evidence of immune trait divergence.

We tested whether host genotype and infection status alter host gene expression, using the threespine stickleback fish (*Gasterosteus aculeatus*) and its native cestode parasite *Schistocephalus solidus* as a model host-parasite system. The cestode's eggs are deposited into freshwater *via* bird feces, then hatch and are consumed by copepods, which are in turn consumed by stickleback (their obligate host). Cestodes mature only in sticklebacks' peritoneum, then mate inside the gut of piscivorous birds. This life cycle can be recapitulated in the lab, permitting controlled genetic crossing (24) and controlled infections among host or parasite genotypes. There is naturally occurring variation in cestode infection rates among stickleback populations throughout their native range (25, 26). This is mirrored by differences in expression of a selected few immune genes, between wild caught stickleback from six populations, and between wild caught fish with vs. without cestodes (27, 28).

Recently, Weber et al. (26) identified natural populations of stickleback with dramatically different resistance to *S. solidus*. Marine stickleback, which resemble the likely ancestral state for modern freshwater populations, rarely encounter the cestode because its eggs do not hatch in brackish water. These fish genotypes are therefore highly susceptible to infection in laboratory exposure trials. When marine stickleback colonized post-glacial freshwater lakes, they encountered cestodes and evolved increased resistance to infection by cestodes (26).

However, not all derived freshwater populations are equally resistant. On Vancouver Island in British Columbia, Gosling Lake (Gos) stickleback are heavily infected by cestodes (50–80% of fish, per year, from 10 years of observations). In contrast, the cestode is absent in stickleback from nearby Roberts Lake (Rob) over the same period of time (18 km away) (29). The first host (copepods) and terminal hosts (piscivorous birds, mostly loons, and mergansers) are common in both lakes. Diet data from both lakes shows that Rob and Gos fish consume copepods at an equal rate (29, 30). The difference in infection rates is therefore not likely to be merely ecological. Accordingly, Weber et al. (29) used experimental infections to confirm that Rob fish are more resistant to infection than Gos fish. In the lab, cestodes infect Rob and Gos stickleback at statistically indistinguishable rates, but Rob fish greatly reduce cestode growth (by two orders of magnitude). Rob fish are able to subsequently kill established cestodes by initiating peritoneal fibrosis which sometimes leads to the formation of a cyst and cestode death. While the mechanism underlying this cestode growth suppression and killing is uncertain, potential correlates are suggestive. Lab-reared Rob fish (or, F_1 hybrids with a Rob dam, i.e., mother) have a higher granulocyte:lymphocyte ratio following infection. In Rob fish, a higher fraction of the granulocytes generate reactive oxygen species (ROS), and these constitutively produce more ROS than cells from Gos fish. ROS is thought to damage the cestode tegument, and ROS production was negatively correlated with cestode growth. This higher ROS production by Rob fish is constitutive rather than induced by infection (29).

Given the immune phenotypes that differ between Rob and Gos stickleback, we hypothesized that these populations would exhibit constitutive and infection-induced differences in gene expression. Furthermore, we expected these differences to involve differential expression of immune genes, particularly those involved in ROS production and fibrosis. To test these hypotheses, we quantified gene expression of head kidneys from lab-reared Rob and Gos stickleback from three treatments: control, exposed but uninfected, and infected by *S. solidus*. We tested for: (i) genes whose expression differs constitutively between populations, (ii) genes which are involved in general responses to cestodes shared by both host populations, and (iii) genes whose expression depends on the interaction between host population and infection status. Genes whose expression depends on an interaction between population and infection status are prime candidates for explaining how these populations respond differently to cestodes, ultimately resulting in significantly different parasite burdens. Additionally, we tested for correlations between modules of coexpressed genes and immune phenotypes (e.g., ROS production or granulocyte:lymphocyte ratio). The number of correlated suites of genes and their correlations with various immune phenotypes can give insight into pathway level phenotypes for further study. In particular, we wish to know whether cestode establishment and cestode growth are correlated with similar or different gene expression modules, implying a shared or separate immunological cause.

RESULTS AND DISCUSSION

We measured gene expression of the head kidney, the major site of immune cell differentiation, using TagSeq, an RNAseq method that focuses on the 3′ end of transcripts (31). We connected these results to prior work on ROS production and cell population characterization (29). We further described these cell culture results with new flow cytometry analysis, and correlated ratios of cell sub-populations with TagSeq measurements of gene expression.

Populations Differ in Expression of Genes Underlying Divergent Immune Phenotypes

Our negative binomial linear models (see Materials and Methods) identified 643 genes that were differentially expressed as a function of stickleback population (Wald, $p < 0.1$ after 10% FDR correction; 361 genes after 5% FDR. See **Table 1** for summary statistics.). These main effects of population represent genes whose expression differs constitutively between populations (regardless of infection status). Because these differences occur in lab-raised fish, they represent heritable between-population differences in RNA abundance. Because we measured gene expression from the entire head kidney, expression differences could reflect evolved changes in gene regulation per cell, changes in cell population composition, or both. A caveat is that because we used first-generation lab-reared fish, we are as yet unable to rule out maternal or other epigenetic effects. However, comparison of Rob, Gos, and reciprocal F_1 hybrids revealed little evidence for maternal effects on infection outcomes or immune traits (with the exception of granulocyte:lymphocyte ratio) (29). So, we consider maternal effects unlikely for most of the differentially expressed genes documented here.

Previous studies have considered the effect of genotype on changes in stickleback immune gene expression in controlled lab infection experiments. However, these results are conflated with other factors such as environment (i.e., comparing wild-caught lake, stream, and estuary stickleback) and multiple exposures to parasites (27). Host genotype was also considered in an experimental infection of honeybees, revealing significant host genotype effects on both gene expression and infection phenotypes (32). Furthermore, host genotype effects could be potentially very important in mosquito-malaria interactions, including a unique example of dual-species trancriptomics (33). Clearly host genotype effects in macroparasite infection are worthy of future study.

Gene ontogeny (GO) showed that these differentially expressed genes are significantly enriched for several categories related to mitochondrial respiration, which can affect ROS production (**Figure 1**, cellular components, Mann–Whitney *U*-test). Rob lake fish also have higher expression of B-cell lymphoma 2 (*bcl2*, ENSGACG00000004283, log2foldchange = 0.99, Wald $p < 0.01$ after 10% FDR correction), a mitochondrial membrane protein which mediates the release of ROS-producing cytochrome C into the cell and promotes cell survival in the presence of oxidative stress (34). We observed significant differences in expression of two copies of another mitochondrial adaptor, tripartite motif 14 (TRIM14). Surprisingly, expression of each gene copy changes in opposite direction between the two host populations (ENSGACG00000018044: log2fold change = −1.78, Wald $p < 0.01$ after 10% FDR correction, ENSGACG00000011287: log2fold change = 1.26, Wald $p < 0.01$ after 10% FDR correction). TRIM14 is part of the innate immune system (35) and shows signatures of balancing selection among other populations of stickleback (36). While the majority of differences in TRIM14 expression are constitutive population effects, there is a single copy that depends on an interaction between population and infection status (see below). Together, the population differences in ROS-associated gene expression support our observation of significantly greater ROS production in Rob stickleback. It is important to note that these genes are differentially expressed between populations regardless of infection status, consistent with prior observations that ROS production is constitutive, insensitive to infection status (29).

Major histocompatibility complex II (MHC II) is a key element of the adaptive immune system, involved in pathogen

TABLE 1 | Candidate genes; Ensembl IDs, gene names, log2 fold changes, 10% FDR corrected *p*-values, term in the model for which they are significant, putative function, and interpretation.

Ensemble ID	Gene name	Log2 fold change	10% FDR corrected *p*-value	Model term	Putative function
ENSGACG00000004283	*bcl2*	0.99	<0.01	Population	Reactive oxygen species (ROS) production
ENSGACG00000018044	Tripartite motif 14 (TRIM14)	−1.78	<0.01	Population	Mitochondria
ENSGACG00000011287	TRIM14	1.26	<0.01	Population	Mitochondria
ENSGACG00000000336	Major histocompatibility complex II (MHC II)	3.67	<0.01	Population	Antigen presentation
ENSGACG00000017967	MHC II	3.39	<0.01	Population	Antigen presentation
ENSGACG00000017764	*Ndufs8*	0.88	<0.08	Infection	ROS production
ENSGACG00000012552	*blvrb*	1.14	<0.07	Infection	ROS removal
ENSGACG00000005065	*nfkbiaa*	−0.49	<0.07	Infection	Inflammation
ENSGACG00000011155	CD40	−0.38	<0.1	Infection	Macrophage/ROS
ENSGACG00000015164	*fibronectin*	0.89	<0.07	Infection	Build cysts
ENSGACG00000019698	*Tspan33*	1.04	<0.07	Infection	Helminth immunity
ENSGACG00000010455	*gpx1a*	−1.86	<0.07	Interaction	ROS removal
ENSGACG00000015963	*cox4i1*	0.43	<0.06	Interaction	ROS production
ENSGACG00000002844	*csf1b*	−1.11	<0.08	Interaction	Macrophage activation
ENSGACG00000019078	*cxcl19*	−1.17	<0.06	Interaction	B-cell targeting

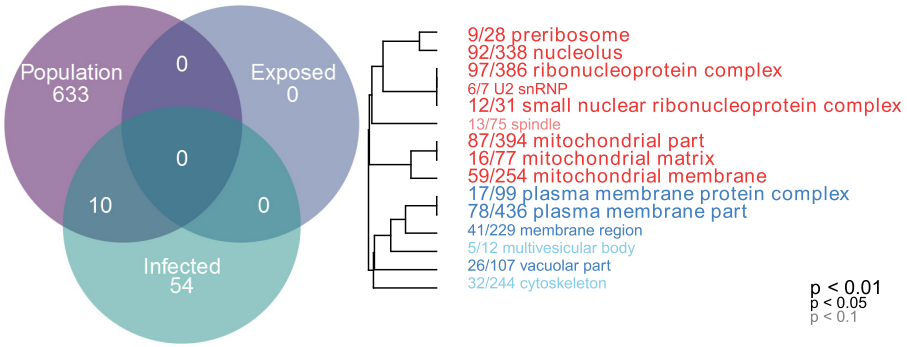

FIGURE 1 | Linear modeling reveals differences between populations and by infection status (all genes $p < 0.1$ after 10% FDR correction). Genes which are differentially expressed between Rob and Gos are enriched for mitochondrial respiration (cellular components, Mann–Whitney *U*-test, $p < 0.01$ after 10% FDR correction). GO categories in red are upregulated in Rob fish, while blue indicates downregulated, relative to Gos. Numbers indicate genes present in category/total genes in category. Text size indicates statistical significance of GO term enrichment among differentially-expressed genes. See Figure S1 in Supplementary Material for molecular function and biological processes.

recognition. Regardless of infection status, Rob fish have higher MHC II expression than do Gos fish, for two different copies of MHC II (ENSGACG00000000336: log2fold change = 3.67, Wald $p < 0.01$ after 10% FDR correction, ENSGACG00000017967: log2fold change = 3.39, Wald $p < 0.01$ after 10% FDR correction). This difference in transcript abundance could be due to changes in the relative abundance of antigen-presenting cells (APCs) such as macrophages, which express MHC II (37). To explore this possibility, we used another statistical model to determine whether variance-stabilized expression of each MHC copy covaried with the proportion of granulocytes (as opposed to lymphocytes, described in **Figure 2**) in a head kidney primary cell culture, controlling for population and infection status. Rob fish have relatively more granulocytes when infected (29), so we expected a positive correlation between MHC II expression and granulocyte production. Instead, the correlation was negative (ENSGACG00000000336: $\beta = -0.0262$, $t = -1.76$ ENSGACG00000017967: $\beta = -0.022$, $t = -1.98$). Our working model to explain this result is that Rob fish have constitutively higher abundance of MHC II in their head kidneys because they have higher numbers of APCs regardless of infection status. When challenged by cestodes, Rob fish initiate a strong innate immune response, expanding the granulocyte population, but not APCs. This infection-dependent proliferation of non-APC granulocytes may dilute the relative abundance of MHC transcript, resulting in the observed negative correlation between MHC and granulocyte abundance.

Previous work has focused on the role of MHC allelic variation in stickleback–parasite interaction, resistance, and local adaptation (38–40). However, most of this work centers on MHC allelic composition and its correlation to infection and growth phenotypes (as a proxy for fitness). Many fewer studies quantify expression of MHC alleles. One study noted increased expression of MHC II in wild fish which were more heavily parasitized, especially when MHC allele diversity was low (39). However, only a single population of fish was considered, so our discovery of significant effect of population (Rob vs. Gos) on MHC II expression is therefore novel. It is important to note that copy number variation may complicate this result. Previous sequencing efforts have suggested that stickleback have between four and six copies of MHC II throughout their genome (41–43). Because TagSeq does not sequence the entirety of the mRNA, we cannot distinguish all MHC haplotypes present in individual fish. It is therefore possible that differences in expression of the two variants described here is due to altered regulation of only particular alleles or paralogs. Poor annotation is also a problem, but because the identity of a read is based on mapping in a relatively conserved region of the mRNA, we believe we have captured the broad patterns at play.

Infection Changes Gene Expression but Exposure Does Not

Surprisingly, no genes differed between control vs. exposed-but-uninfected fish (Wald, $p < 0.1$ after 10% FDR correction). This could be because resistant fish quickly mounted a response to the cestode, eliminated the parasite, and then downregulated immune function by our 42-day sample date. Or, early-acting resistance to the cestode may involve physical or chemical barriers to entry that entail constitutive gene expression or non-genetic effects (e.g., gut epithelial mucous, protective symbiotic bacteria, etc). Finally, early-stage infections may induce localized immune responses in the intestinal epithelium or peritoneum that are not reflected in systemic responses that are measured by head-kidney gene expression.

Once the cestode establishes in the peritoneum, however, it induces some shared changes in gene expression of all host genotypes. We identified 64 genes that were differentially expressed between control and infected fish (Wald, $p < 0.1$ after 10% FDR correction), across both host genotypes. Several of these genes are promising candidates because of their known role in host immunity. For example, infected fish increase expression of *ndufs8*, a component of complex I which is the main ROS producer in cells (ENSGACG00000017764: log2fold change = 0.88, Wald $p < 0.08$ after 10% FDR correction) (44). Other subunits of complex I are more highly expressed in Rob

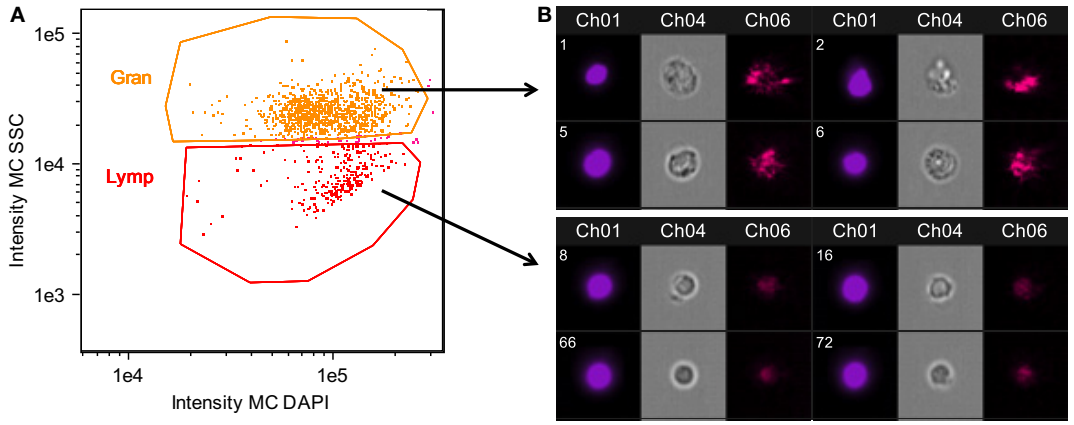

FIGURE 2 | Confirmation of granulocyte and lymphocyte identity confirmed using Amnis imaging flow cytometry. Side scatter (SSC) high cells were morphologically consistent with granulocytes, while SSC low cells were consistent with lymphocytes. Head kidney leukocytes were permeabilized and stained with DAPI. **(A)** Singlet, DAPI+ cells were divided into granulocyte and lymphocyte populations based on SSC. **(B)** Representative images of cells within the granulocyte and lymphocyte gates. Chanel 1: DAPI nuclear stain, Chanel 4: bright field, Chanel 6: SSC.

fish regardless of infection status, consistent with their higher constitutive production of ROS. Therefore, *ndufs8* may be particularly important in regulating the production of ROS in response to infection, because it is the only complex I subunit upregulated upon infection. ROS are reduced when they act on their targets, and the raw materials can be recycled through the biliverdin/billiruben redox cycle (45). Infected fish from both populations have higher levels of *blvrb* (biliverden reductase B), one of the two enzymes in this ROS-recycling system (ENSGACG00000012552: log2fold change = 1.14, Wald $p < 0.07$ after 10% FDR correction). This upregulation should facilitate removal of ROS that may limit damage to host tissues, or facilitate subsequent ROS production.

Another important aspect of ROS-based immunity is the associated inflammation. Infected fish have decreased expression of *nfkbiaa* (nuclear factor kappa light polypeptide gene enhancer in B-cell inhibitor alpha a), which interacts with NF-kB to suppress inflammation (ENSGACG00000005065: log2fold change = −0.49, Wald $p < 0.07$ after 10% FDR correction). *Nfkbiaa* inhibits the pro-inflammatory NF-kB by either preventing NF-kB proteins from entering the nucleus, where they are active, or by blocking NF-kB transcription factor binding sites. NF-kB activation by TNFa or LPS reverses this binding and allows NF-kB to activate expression of pro-inflammatory genes (46). Thus, decreased *nfkbiaa* expression suggests an increased inflammatory response following successful infection.

Infected fish also have a slight decrease in expression of CD40 (ENSGACG00000011155: log2foldchange = −0.38, Wald $p < 0.1$), a co-stimulatory molecule expressed on dendritic cells, macrophages, and B-cells, which activates T- and B-cells (37). Previous studies have suggested that helminths could potentially suppress stickleback adaptive immunity (47), and the downregulation of CD40 is one plausible mechanism. Alternatively, fish with inherently lower CD40 expression may be more susceptible to infection. This raises a broader question that we are not yet able to answer, but which warrants further study: to what extent are the expression differences between infected and control fish a result of host immune response or parasite immune suppression? One plausible approach might be to measure gene expression in both host and parasite simultaneously and model host expression as a function of parasite expression and *vice versa*.

CD40 expression is not limited to immune cells, but can also be expressed in fibroblasts (48), so its precise function in stickleback infection by cestodes is unclear. This dual role is intriguing because fibroblast activation is associated with the formation of fibrotic cysts that encapsulate cestodes (49). These cysts likely restrict cestode movement and concentrate ROS while limiting damage to host tissues. Recall that this is a population specific defense, exhibited by Rob but not Gos fish (29), and in this statistical contrast the effect of population is averaged. In addition to changes in CD40, our linear model identified an increase of expression of *fibronectin* in infected Rob fish, which contributes to fibrinogen production to build cysts (3, 50) (ENSGACG00000015164: log2fold change = 0.89, Wald $p < 0.07$ after 10% FDR correction).

Adaptive immune system genes also respond to cestode infection. *Tspan33* has recently been shown to be a marker for activated B-cells in vertebrates (51, 52). The presence of activated B-cells indicates the host immune system has recognized the parasite and is actively mounting a defense. In our study, infected fish show higher levels of *tspan33* compared to controls (ENSGACG00000019698: log2fold change = 1.04, Wald $p < 0.07$ after 10% FDR correction). Increased expression of *tspan33* in infected fish is consistent with increased activation of B-cells, an integral part of the adaptive immune response.

Population Dependent Expression Supports Prior Observations of Divergent Immune Phenotypes

The higher resistance to *S. solidus* infection in Rob compared to Gos stickleback could be due to constitutive differences in gene expression (as documented above), or differences in the induced

immune response to infection. The latter can be detectable *via* interactions between host genotype and infection status. Linear modeling results identified 16 genes significant for this interaction (Wald $p < 0.1$ after 10% FDR correction). Most of these genes are known to affect the immune traits that Weber et al. (29) already showed are divergent between Rob and Gos fish. For example, glutathione peroxidase 1a (*gpx1a*) is an enzyme that degrades hydrogen peroxide, a type of ROS, into glutathione and water (53). Expression of *gpx1a* in Gos fish increases upon infection and therefore should tend to decrease the amount of ROS (hydrogen peroxide) available to defend against cestodes (ENSGACG00000010455: log2foldchange = −1.86, Wald $p < 0.07$ after 10% FDR correction). We speculate that this proactive downregulation upon infection might be a tolerance response to mitigate autoimmune damage by Gos fish, which are commonly infected and therefore might not be able to tolerate a strong ROS response. The cytochrome c complex produces ROS (53), and we see increased expression of Cytochrome c oxidase subunit IV (*cox4i1*) in Rob fish that are infected, while Gos fish decrease expression (ENSGACG00000015963: log2foldchange = 0.43, Wald $p < 0.06$ after 10% FDR correction). These gene expression data are consistent with our phenotypic data showing that Rob fish have more ROS-producing macrophages than Gos fish, and more ROS per cell. This *cox4il* upregulation in Rob fish may be amplified by population differences in *bcl2* (see above). Oddly, we do not observe a significant infection-induced increase in ROS production in fish of either genotype. This discrepancy may reflect our head-kidney cell-culture based ROS assay, which does not rule out changes in ROS *in vivo* or in other tissues.

The one contrary result involves colony stimulating factor 1b (*csf1b)*, a paralog of *csf1/mcsf*, a well-studied regulator of monocytes in mammals (54). *csf1* increases the production of head kidney leukocytes (which includes granulocytes) in trout (*Oncorhynchus mykiss*)(55). In our study, *csf1b* is downregulated in infected Rob fish even though they have more granulocytes relative to either Gos fish or to uninfected Rob fish (ENSGACG00000002844: log2foldchange = −1.11, Wald $p < 0.08$ after 10% FDR correction). This discrepancy may be resolved by recognizing that we examined a single time point post-exposure. It is likely that Rob fish initially increase *csf1b* or another gene to drive expansion of the granulocyte population that we observe after infection. The downregulation of *csf1b* 42 days after infection could be a homeostatic mechanism to suppress further macrophage proliferation, after they already reached sufficient abundance. Further time series analyses would be necessary to resolve this hypothesis.

Finally, adaptive immune system genes also exhibit population specific responses to infection. Activated B-cells are critical to mounting an adaptive immune response, and they are targeted by various cytokines (37). When challenged by cestodes, Rob fish increase expression of C-X-C motif chemokine ligand 19 (*cxcl19*). In contrast, cestode infection reduces *cxcl19* expression in Gos fish, which otherwise exhibit constitutively higher expression than Rob fish (ENSGACG00000019078: log2foldchange = −1.17, Wald $p < 0.06$ after 10% FDR correction; **Figure 2**). Ligands with this motif induce migration of leukocytes (56). Literature on *cxcl19* is rare, but it has been suggested that the zebrafish *cxcl19* gene is orthologous to *Il-8*, a major mediator of leukocyte migration to sites of inflammation (55). Regardless of whether *cxcl19* is involved specifically leukocyte trafficking to sites inflammation or increasing migration of leukocytes in the absence of inflammation, both of these immune mechanisms could play an important role in defense against cestodes.

Network Analysis Suggests Two Traits: Establishment and Growth

We tested for correlations between patterns of gene expression and immune/cestode phenotypes using weighted gene co-expression network analysis (WGCNA). WGCNA provides an unbiased data-driven hierarchical clustering of genes with similar expression patterns, thereby reducing the number of genes under consideration (reduced multiple test correction) and identifying functionally similar gene modules which can be used for further statistical analysis (57). WGCNA is a more appropriate analysis for incorporating additional immune phenotype data that was collected during the infection experiment not only because of its continuous nature (vs. the categorical predictors of population and infection status) but also because the correlation between suites of co-expressed genes and traits is estimated independently for each trait, rather than simultaneously (as under the linear modeling framework), resulting in lower unexplained variance to be assigned to other traits. We used a two-step process, first looking for general pathways and subsequent correlations to phenotypes by using all samples to construct a signed network. Second, we tested for genotype-dependent network structure and module-trait correlation by building signed networks for each population of stickleback. The latter case may be especially pertinent if the regulation of gene expression plays a strong role in the genotype dependent response to infection. To explore this, we calculated module similarity between the Rob and Gos signed networks as the fraction of genes shared between any two given modules.

When all samples were combined to build a single signed coexpression network, WGCNA analysis revealed modules that were correlated with host population, ROS production, infection status, number of cestodes, total cestode mass, density of cells in host head kidney, frequency of granulocytes/lymphocytes, fraction of cells gated into various subpopulations including precursors, myeloid, and eosinophils, and finally, host families (data not shown, but this highlights the need to include family as a nested factor in the linear modeling of DESeq2).

Population differences are mainly captured by the turquoise, green, magenta, and greenyellow modules, with lesser contributions by the blue and red modules (**Figure 3**). These population-dependent modules have connections to population-dependent phenotypes such as ROS production. For example, top kME genes (those genes which most strongly represent a module) in the turquoise modules (positive correlation with Rob) include ROS producing cytochrome c oxidase genes and ROS recycling *gpx1a* (**Figure 4**). Together, we would expect the action of these genes to increase ROS levels. As expected, the turquoise module has a positive correlation with ROS production ($r = 0.36$, $p = 2e{-}4$, **Figure 3**).

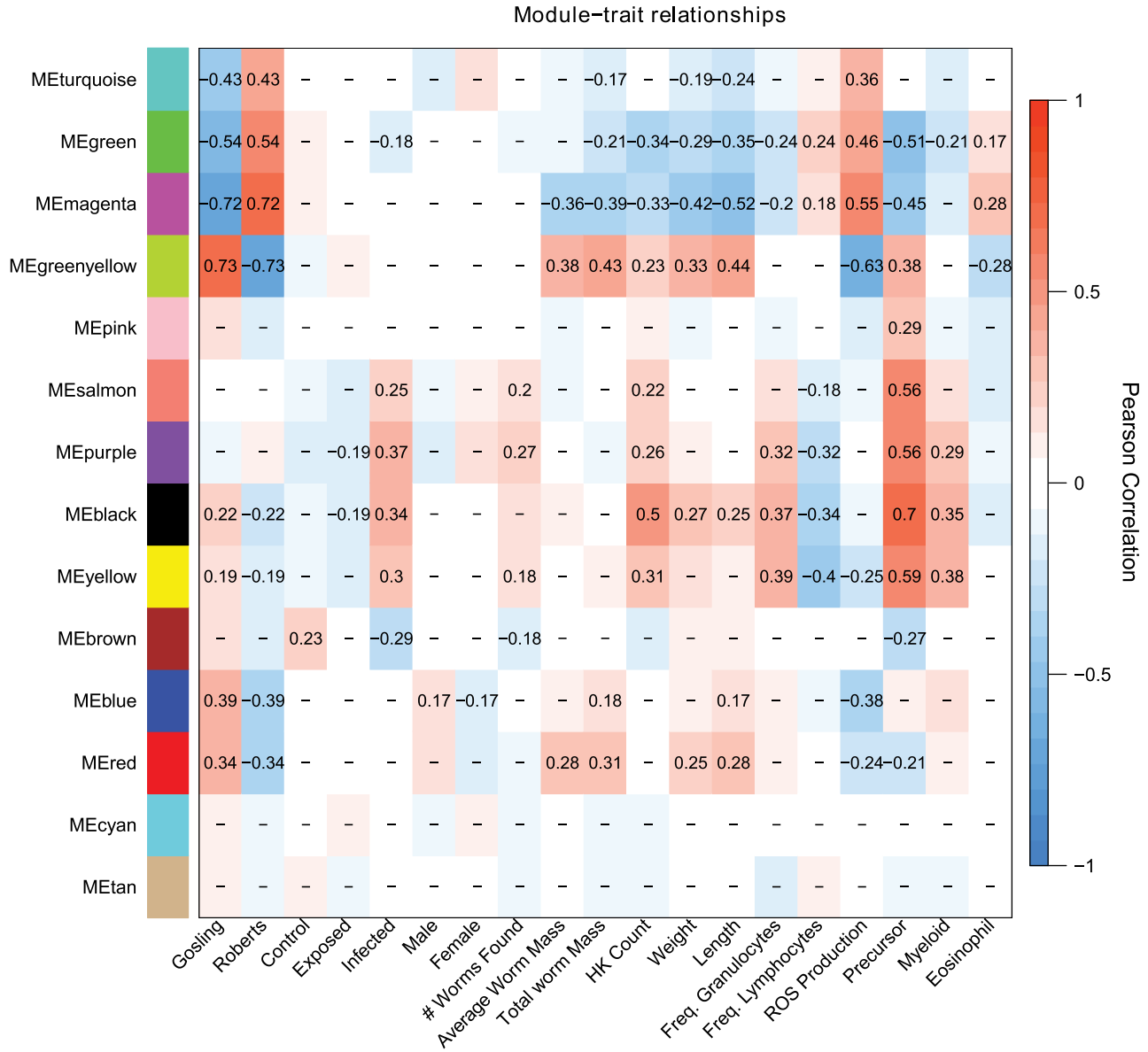

FIGURE 3 | Weighed coexpression gene network analysis suggest that host response to cestodes involves two traits, the initial immune response (salmon, purple, black, yellow, brown) and the control over parasite growth (magenta and greenyellow). Each cell indicates the correlation between the module and a given trait. Correlations with *p*-values greater than 0.1 are omitted.

Some module-trait correlations reinforce prior inferences about the immunological basis of stickleback resistance to the cestode. For example, the black module has modest to strong correlations with infection status, cell population phenotypes including density of all cells, precursors, and myeloids but is not correlated to ROS production ($r = 0.13$, $p = 0.2$, **Figure 3**). In contrast, the magenta and greenyellow modules are correlated with ROS production and also with cestode size, but much less so with cell population phenotypes and not at all with infection status (**Figure 3**). These observations imply that stickleback prevention of cestode establishment, and suppression of cestode growth, entail two distinct immune pathways (innate response and ROS production, respectively).

The magenta module has a modest, but strongly significant correlation to the fraction of cells that are eosinophils ($r = 0.28$, $p = 0.005$). A recent review highlighted the importance of eosinophils in host-helminth interactions. Specifically, at the site of host tissue damage, eosinophils are primed by fibronectin, and produce a variety of proteins which are toxic to helminths. Furthermore, the diversity of eosinophil cell surface receptors makes them central to mediate the inflammation response. Finally, helminths appear to have a number of anti-eosinophil proteins which both evade and dampen host response to the presence of helminths (58).

Constructing separate signed coexpression networks for each population reveals dramatic differences in network structure.

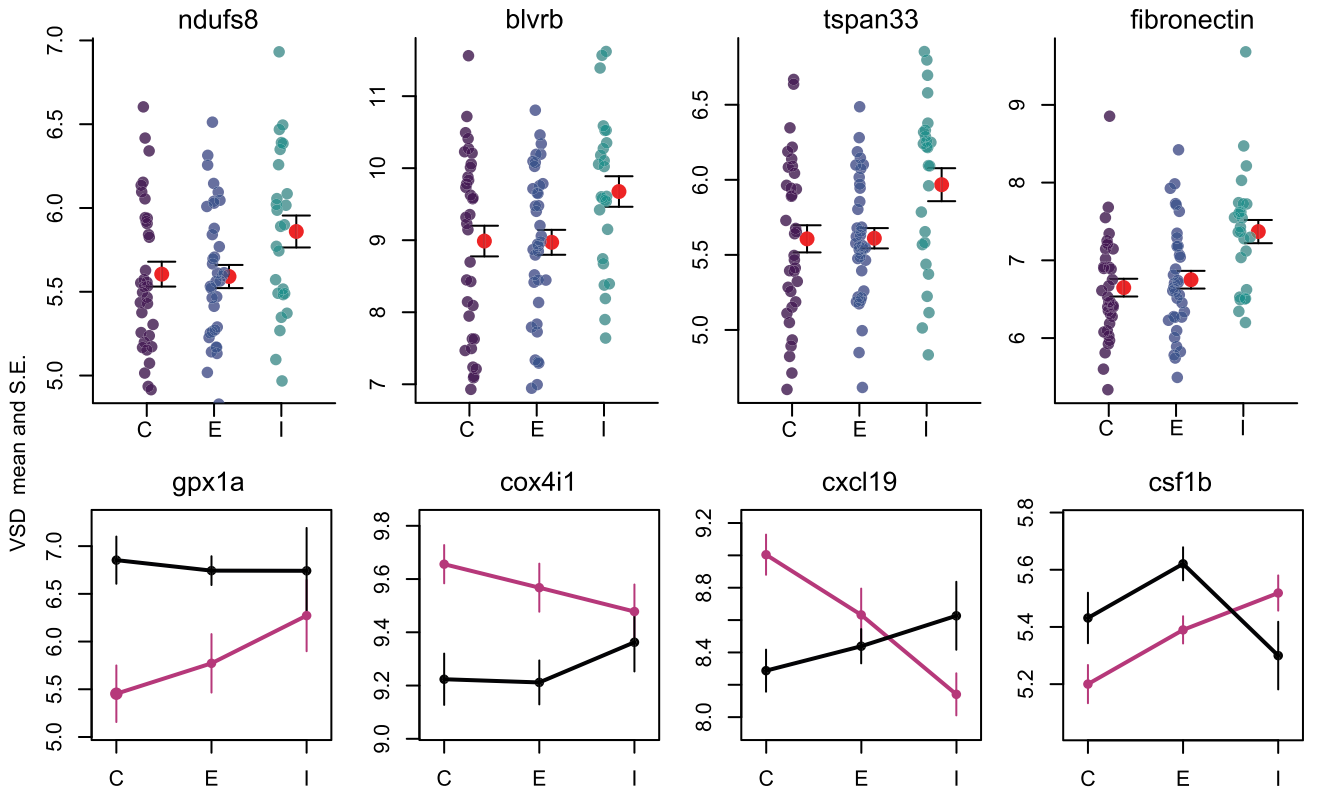

FIGURE 4 | Reactive oxygen species production and B cells respond to infection by cestodes, both in a population independent, and dependent manner. *Y* axis is variance stabilized count data, the product of log transforming and library size correcting raw gene counts. For upper row, purple, blue, and teal points indicate individuals, while red points and fences indicate mean and SE. C, control; E, exposed; I, infected. Black lines are Rob and magenta lines are Gos.

Using the same construction parameters for each population, the Rob network resembles the combined population network, showing strong module-trait correlations for worm size, cell population phenotypes, ROS production, and sex across many different modules. In stark contrast, the Gos network is much more static, with only a subset of traits which were previously significant correlated to a single module. Overall, Gos fish have many fewer total modules and correlations between modules and traits are much weaker. To estimate relationships between networks, we calculated module similarity between every pair of Rob and Gos modules by shared gene membership. Broadly, large modules in Gos are split into many smaller modules in Rob. Thus, we conclude that there are two possible outcomes: (1) the Rob fish have evolved a more modular and dynamic repertoire of expression with which to fend off cestodes, or (2) the Gos fish evolved to maintain constitutive gene expression in response to cestodes, instead adopting a tolerance strategy (See Figures S2–10 in Supplementary Material for additional details on shared and population specific signed networks, and module similarity heat map).

Our WGCNA results confirm observed population differences in immune function and patterns of gene expression in the linear modeling. Furthermore, they support our hypothesis that there are two traits involved in stickleback resistance to cestodes: (1) innate immune response to prevent cestode establishment and (2) limiting worm growth once cestodes become established. These two traits separate into distinct modules of gene expression, each enriched for genes with immunological function matching *a priori* expectations. This two-trait perspective refines the question of variation in cestode prevalence among stickleback populations by focusing attention to both early and late stage infection. Future studies will be needed to describe the full time-series of gene expression as exposure and infection proceeds in these study populations, and to establish directionality of the interaction between cestodes and stickleback. While others have argued that cestodes are the primary drivers of coevolution (47), only by sequencing both host and parasite mRNAs can we hope to detail this interaction at the molecular level. Host genotype by parasite genotype interactions offers a promising opportunity for further study. Such GxG interaction was recently described in the stickleback-cestode system, but only documented growth phenotypes, and no attempt to describe the genetic basis for such traits has been made (59). We maintain that this type of study provides a means to identify evolutionarily labile genes, which underlie beneficial shifts in immune function across the geographic mosaic of host-parasite coevolution.

Summary

Using a large scale controlled laboratory infection experiment, we find changes in gene expression between two host populations,

and as a function of infection status. For a smaller portion of genes, the expression response to infection differed between the two host populations. These findings are consistent with observations of host immune function in the same infection experiment (29). ROS production and recycling, B cell activation and targeting, and fibrosis appear to play important roles in stickleback defense against cestodes. Our analysis also suggests that host resistance involved two components; response to challenge by cestodes, and control over cestode growth. Furthermore, differences in coexpression networks between populations suggest that either Rob fish have evolved a more elaborate expression profile or that Gos fish are shutting down expression to tolerate cestodes. Our results not only suggest a mechanistic link between host immune phenotypes and candidate genes, but also provide the foundation for studying the direct effects of host alleles on parasite fitness.

MATERIALS AND METHODS

We obtained mRNA from the head kidneys of stickleback from three experimental groups: unexposed controls ($N = 16$ and 19, Rob and Gos fish, respectively), exposed but ultimately uninfected stickleback ($N = 21$ and 16), or exposed and infected ($N = 17$ and 9) fish. Tissues from the latter two groups were harvested 42 days post exposure. A brief summary is presented below, but see Weber et al. (29) for full experimental methods. We focus on expression in head kidneys as it is the major site of immune cell development in fish (47, 60–62), and head kidney cell cultures were used to measure immune function independently of gene expression (stickleback have two head kidneys).

Summary of Breeding and Infection As Described in Weber et al. (29)

Weber et al. (29) generated 17 pure Rob and 16 pure Gos families by *in vitro* fertilization of wild caught parents. F_1 fish were raised to adulthood. Members of each family were either sham exposed or exposed to cestodes *via* uninfected/infected copepods, respectively. Infection and screening of copepods was done by hand in a laboratory setting. After exposure, fish were grown for 42 days before being euthanized. For the present study, we subsampled from these fish, attempting to balance both population and infection status. We incorporated at least one individual from each treatment per family. Our final sample sizes (TagSeq libraries post outlier removal) are: Gos: Control: 19, Exposed: 21, Infected: 17, across 11 families. Rob: Control: 16, Exposed: 16, Infected: 9 across, 8 families (detailed in Table S1 in Supplementary Material).

Sample Collection, Sequence Library Construction, and Analysis of Flow Cytometry Data

Briefly, head kidneys were dissected from stickleback; one head kidney was used for flow cytometry (measuring ROS and describing cell populations) and the other was preserved in RNAlater at −20°C. Detailed protocols can be found in Weber et al. (29). From the stored head kidney, RNAseq libraries were constructed according to Lohman et al. (31). This method focuses sequencing effort on short "tags" adjacent to the poly-A tail of mRNAs rather than distributing sampling effort across the entire mRNA as in traditional RNAseq. Samples were sequenced on the Illumina HiSeq 2500 at the Genome Sequence and Analysis Facility at the University of Texas at Austin, producing ~6.7M raw reads per sample. See Weber et al. (29) for full ROS and flow cytometry methods. Flow cytometry data were analyzed using FlowJo software (Treestar). Granulocyte and lymphocyte populations were defined based linear forward scatter (FSC) and side scatter (SSC) gating described in Weber et al. (29). Precursor, myeloid, lymphoid, and eosinophil populations were defined using linear FSC and logarithmic SSC gating as described in Wittamer et al. (63).

Bioinformatics

TagSeq reads were processed (removal of PCR duplicates, adapter contamination, and average base quality score *–n* 20) according to the iRNAseq pipeline (64) using version 79 of the stickleback transcriptome from Ensemble. Resulting genes were filtered for mean counts greater than 1 among all samples, producing 9077 genes among all samples. Transcriptome annotations were based on the UniProtKB database (http://www.uniprot.org/help/uniprotkb) and followed previously described procedures (64). Code for the iRNAseq pipeline can be found here: https://github.com/z0on/tag-based_RNAseq. Code for the annotation pipeline can be found here: https://github.com/z0on/annotating Transcriptomes.

Statistical Analysis with DESeq2

We scanned for outliers using arrayQualityMetrics (65) and removed one sample because of insufficient read depth (final $N = 98$). To test for differential gene expression, we used the following model in DESeq2:

$$Y_{ij} \sim \beta_{\text{Batch}} + \beta_{\text{Population}} + \beta_{\text{InfectionStatus}} + \beta_{\text{Population*InfectionStatus}} + \varepsilon_{ij} \quad (1)$$

where Y_{ij} is the count of gene i in individual j, $\beta_{\text{Population}}$ is a fixed effect with two levels: Rob and Gos, $\beta_{\text{InfectionStatus}}$ is a fixed effect with three levels: control, exposed (but not infected), and infected, and full-sibling families are nested within populations. β_{Batch} is the lane on which samples were sequenced. An additional predictor β_{Sex} was included for genes when appropriate (lower AIC score) and improved the model fit of 839 genes total. We fit the full model (including sex) to all genes and then extracted only the 839 that were improved by the addition of sex and looked for significant p values for main effects and interactions. With the full model, 67 of these "sex improved" genes were significantly different between populations. No genes were significant for either exposure or infection, and one gene was significant for the interaction of population and infection status (myosin 5ab, ENSGACG00000006025: log2foldchange = 2.98, Wald $p = 0.07$). All p-values were multiple test corrected using 10% FDR (Benjamini–Hochberg). Although fish from the controlled infection experiment were exposed to three different parasite genotypes (each family exposed to only one parasite genotype), we are only interested in the host response to any parasite, and

therefore average across parasite genotypes by simply not including this as a term in our linear model.

GO with GO_MWU

We used the Mann–Whitney *U* test for GO analysis. This approach has been described (66) and the code for analysis can be found here: https://github.com/z0on/GO_MWU.

Weighted Coexpression Gene Network Analysis

Raw read counts were normalized using limma (67) for input into WGCNA (57). All genes included in the post filter data were included in the WGCNA analysis. Following the walkthrough in Langfelder and Horvath (57), we built a signed network with a soft thresholding power of 7, and a minimum module size of 30 genes. Following dynamic tree cut, we merged modules with greater than 80% similarity, producing 14 modules. We separated Rob and Gos samples and repeated this process with the same parameters.

Caveats and Limitations

Our study flips the traditional search for immune candidate genes from inbred lab strains to wild populations, using historical natural selection as a tool to screen for changes in gene expression associated with parasite infection. While our host-parasite model system is powerful, it does have some limitations. The reference genome is of generally good quality but annotation is lacking (approximately 22.5% of the entries in the stickleback genome are either unnamed or labeled as novel genes). Thus, GO analysis is performed after assigning GO accession terms by BLAST homology, rather than functional verification, a common solution for non-model systems. The features of the stickleback genome may be missing potentially interesting immunological genes which are sufficiently diverged from human or mouse genes and therefore may be unannotated. In particular, the number and location of MHC II paralogs remains uncertain, illustrating need for genome sequence improvement. With respect to MHC II in particular, the unknown number of gene copies in the populations of interest may potentially complicate our estimates of gene expression.

Our linear modeling with DESeq2 employs appropriate FDR correction, but we choose to accept higher than "standard" *p*-values associated with LFC because of the direct connection between candidate genes and independently observed immune phenotypes. If, for example, we had not measured immune phenotypes, we would not accept $\log_2$ fold changes in expression with associated *p*-values greater than 0.05 but less than 0.1. Furthermore, we chose a very low base min mean filter because we have high confidence in detecting lowly expressed genes (31).

We also wished to include more genes in our enrichment analysis and this also detracts from our power due to multiple test correction. We accordingly accept slightly larger than normally allowed *p*-values. Our TagSeq based approach has been shown to be at least as good as total RNAseq methods (having an equal or higher correlation between observed and known values of a spike in control) but does not account for splice variants or copy number variation, which may be potentially important in the evolution of immune responses.

Our study used tissue from a single organ (head kidneys) for both gene expression and immune phenotype measures. Head kidneys are a crucial hematopoetic organ in fish, but analysis of other tissues may produce different results. Moreover, head kidneys contain multiple immune cell populations that we are unable to sort effectively for cell-type-specific expression studies. We do use cell population counts (proportion granulocytes vs. lymphocytes) as a covariate, which as noted for MHC weakly contributes to expression variation of a few genes. But, lacking monoclonal antibodies to many immune cell receptors in stickleback, we cannot readily distinguish among finer subdivisions of cell types. This resource limitation, typical of most non-model organisms, limits our ability to statically detect effects of cell population composition on expression.

DATA ARCHIVAL LOCATION

Instructions for accessing the code for analysis and plotting, and raw sequence data from UT Austin's permanent data archive are located in supplementary materials.

AUTHOR CONTRIBUTIONS

BL built, sequenced, and analyzed TagSeq libraries. NS and JW provided samples, flow cytometry data, and comments on analysis and interpretation of results. BL and DB wrote the manuscript with comments from NS and JW. All authors approved the final version.

ACKNOWLEDGMENTS

This work was supported by the Howard Hughes Medical Institute (DB). We thank John Lovell and Marie Strader for helpful comments during data analysis and writing.

SUPPLEMENTARY MATERIAL

The Supplementary Material for this article can be found online at http://journal.frontiersin.org/article/10.3389/fimmu.2017.01071/full#supplementary-material.

REFERENCES

1. Maizels RM, Balic A, Gomez-Escobar N, Nair M, Taylor MD, Allen JE. Helminth parasites – masters of regulation. *Immunol Rev* (2004) 201(1): 89–116. doi:10.1111/j.0105-2896.2004.00191.x
2. Maizels RM, Yazdanbakhsh M. Immune regulation by helminth parasites: cellular and molecular mechanisms. *Nat Rev Immunol* (2003) 3(9):733–44. doi:10.1038/nri1183
3. Anthony RM, Rutitzky LI, Urban JF, Stadecker MJ, Gause WC. Protective immune mechanisms in helminth infection. *Nat Rev Immunol* (2007) 7(12):975–87. doi:10.1038/nri2199
4. Gause WC, Wynn TA, Allen JE. Type 2 immunity and wound healing: evolutionary refinement of adaptive immunity by helminths. *Nat Rev Immunol* (2013) 13(8):607–14. doi:10.1038/nri3476
5. Beutler B, Jiang Z, Georgel P, Crozat K, Croker B, Rutschmann S, et al. Genetic analysis of host resistance: toll-like receptor signaling and

immunity at large. *Annu Rev Immunol* (2006) 24:353–89. doi:10.1146/annurev.immunol.24.021605.090552
6. Beutler B, Du X, Xia Y. Precis on forward genetics in mice. *Nat Immunol* (2007) 8(7):659–64. doi:10.1038/ni0707-659
7. Beraldi D, McRae AF, Gratten J, Pilkington JG, Slate J, Visscher PM, et al. Quantitative trait loci (QTL) mapping of resistance to strongyles and coccidia in the free-living Soay sheep (*Ovis aries*). *Int J Parasitol* (2007) 37(1):121–9. doi:10.1016/j.ijpara.2006.09.007
8. Schielzeth H, Husby A. Challenges and prospects in genome-wide quantitative trait loci mapping of standing genetic variation in natural populations. *Ann N Y Acad Sci* (2014) 1320(1):35–57. doi:10.1111/nyas.12397
9. Eizaguirre C, Lenz TL, Kalbe M, Milinski M. Rapid and adaptive evolution of MHC genes under parasite selection in experimental vertebrate populations. *Nat Commun* (2012) 3:621. doi:10.1038/ncomms1632
10. Stutz WE, Bolnick DI. Natural selection on MHC IIβ in parapatric lake and stream stickleback: balancing, divergent, both or neither? *Mol Ecol* (2017). doi:10.1111/mec.14158
11. Geary TG, Thompson DP, Klein RD. Mechanism-based screening: discovery of the next generation of anthelmintics depends upon more basic research. *Int J Parasitol* (1999) 29(1):105–12. doi:10.1016/S0020-7519(98)00170-2
12. Geary TG, Sakanari JA, Caffrey CR. Anthelmintic drug discovery: into the future. *J Parasitol* (2015) 101(2):125–33. doi:10.1645/14-703.1
13. Cookson W, Liang L, Abecasis G, Moffatt M, Lathrop M. Mapping complex disease traits with global gene expression. *Nat Rev Genet* (2009) 10(3):184–94. doi:10.1038/nrg2537
14. Pasaniuc B, Price AL. Dissecting the genetics of complex traits using summary association statistics. *Nat Rev Genet* (2016) 18(2):117–27. doi:10.1038/nrg.2016.142
15. Hubner N, Wallace CA, Zimdahl H, Petretto E, Schulz H, Maciver F, et al. Integrated transcriptional profiling and linkage analysis for identification of genes underlying disease. *Nat Genet* (2005) 37(3):243–53. doi:10.1038/ng1522
16. Barrett JC, Hansoul S, Nicolae DL, Cho JH, Duerr RH, Rioux JD, et al. Genome-wide association defines more than 30 distinct susceptibility loci for Crohn's disease. *Nat Genet* (2008) 40(8):955–62. doi:10.1038/ng.175
17. Emilsson V, Thorleifsson G, Zhang B, Leonardson AS, Zink F, Zhu J, et al. Genetics of gene expression and its effect on disease. *Nature* (2008) 452(7186):423–8. doi:10.1038/nature06758
18. Wijayawardena BK, Minchella DJ, DeWoody JA. The influence of trematode parasite burden on gene expression in a mammalian host. *BMC Genomics* (2016) 17(1):600. doi:10.1186/s12864-016-2950-5
19. Hawley DM, Altizer SM. Disease ecology meets ecological immunology: understanding the links between organismal immunity and infection dynamics in natural populations. *Funct Ecol* (2011) 25(1):48–60. doi:10.1111/j.1365-2435.2010.01753.x
20. Pedersen AB, Babayan SA. Wild immunology. *Mol Ecol* (2011) 20(5):872–80. doi:10.1111/j.1365-294X.2010.04938.x
21. Viney M, Lazarou L, Abolins S. The laboratory mouse and wild immunology. *Parasite Immunol* (2015) 37(5):267–73. doi:10.1111/pim.12150
22. Huang Y, Chain FJ, Panchal M, Eizaguirre C, Kalbe M, Lenz TL, et al. Transcriptome profiling of immune tissues reveals habitat-specific gene expression between lake and river sticklebacks. *Mol Ecol* (2016) 25(4):943–58. doi:10.1111/mec.13520
23. Todd EV, Black MA, Gemmell NJ. The power and promise of RNA-seq in ecology and evolution. *Mol Ecol* (2016) 25(6):1224–41. doi:10.1111/mec.13526
24. Schärer L, Wedekind C. Lifetime reproductive output in a hermaphrodite cestode when reproducing alone or in pairs: a time cost of pairing. *Evol Ecol* (1999) 13(4):381–94. doi:10.1023/A:1006789110502
25. MacColl ADC. Parasite burdens differ between sympatric three-spined stickleback species. *Ecography* (2009) 32(1):153–60. doi:10.1111/j.1600-0587.2008.05486.x
26. Weber JN, Kalbe M, Shim KC, Erin NI, Steinel NC, Ma L, et al. Resist globally, infect locally: a transcontinental test of adaptation by stickleback and their tapeworm parasite. *Am Nat* (2017) 189(1):43–57. doi:10.1086/689597
27. Lenz TL, Eizaguirre C, Rotter B, Kalbe M, Milinski M. Exploring local immunological adaptation of two stickleback ecotypes by experimental infection and transcriptome-wide digital gene expression analysis. *Mol Ecol* (2013) 22(3):774–86. doi:10.1111/j.1365-294X.2012.05756.x
28. Stutz WE, Schmerer M, Coates JL, Bolnick DI. Among-lake reciprocal transplants induce convergent expression of immune genes in threespine stickleback. *Mol Ecol* (2015) 24(18):4629–46. doi:10.1111/mec.13295
29. Weber JN, Steinel NC, Shim KC, Bolnick DI. Recent evolution of cestode growth suppression by threespine stickleback. *Proc Natl Acad Sci U S A* (2017). doi:10.1073/pnas.1620095114
30. Snowberg LK, Hendrix KM, Bolnick DI. Covarying variances: more morphologically variable populations also exhibit more diet variation. *Oecologia* (2015) 178(1):89–101. doi:10.1007/s00442-014-3200-7
31. Lohman BK, Weber JN, Bolnick DI. Evaluation of TagSeq, a reliable low-cost alternative for RNAseq. *Mol Ecol Resour* (2016) 16(6):1315–21. doi:10.1111/1755-0998.12529
32. Barribeau SM, Sadd BM, du Plessis L, Schmid-Hempel P. Gene expression differences underlying genotype-by-genotype specificty in a host-parasite system. *Proc Natl Acad Sci U S A* (2014) 111:3496–501. doi:10.1073/pnas.1318628111
33. Choi Y-J, Aliota MT, Mayhew GF, Erickson SM, Christensen BM. Dual RNA-seq of parasite and host reveals gene expression dynamics during filarial worm–mosquito interactions. *PLoS Negl Trop Dis* (2014) 8(5):e2905. doi:10.1371/journal.pntd.0002905
34. Martindale JL, Holbrook NJ. Cellular response to oxidative stress: signaling for suicide and survival. *J Cell Physiol* (2002) 192(1):1–15. doi:10.1002/jcp.10119
35. Zhou Z, Jia X, Xue Q, Dou Z, Ma Y, Zhao Z, et al. TRIM14 is a mitochondrial adaptor that facilitates retinoic acid-inducible gene-I-like receptor-mediated innate immune response. *Proc Natl Acad Sci U S A* (2014) 111(2):E245–54. doi:10.1073/pnas.1316941111
36. Hohenlohe PA, Bassham S, Etter PD, Stiffler N, Johnson EA, Cresko WA. Population genomics of parallel adaptation in threespine stickleback using sequenced RAD tags. *PLoS Genet* (2010) 6(2):e1000862. doi:10.1371/journal.pgen.1000862
37. Murphy KM. *Janeway's Immunobiology*. New York: Garland Science (2011).
38. Kurtz J, Kalbe M, Aeschilmann PB, Haberli MA, Wegner KM, Reusch TBH, et al. Major histocompatibility complex diversity influences parasite resistance and innate immunity in sticklebacks. *Proc Biol Sci* (2004) 271:197–204. doi:10.1098/rspb.2003.2567
39. Wegner KM, Kalbe M, Rauch G, Kurtz J, Schaschl H, Reusch TBH. Genetic variation in MHC class II expression and interactions with MHC sequence polymorphism in three-spined sticklebacks. *Mol Ecol* (2006) 15(4):1153–64. doi:10.1111/j.1365-294X.2006.02855.x
40. Lenz TL, Eizaguirre C, Kalbe M, Milinski M. Evaluating patters of convergent evolution and trans-species polymorphism at MHC immunogenes in two sympatric stickleback species. *Evolution* (2013) 67:2400–12. doi:10.1111/evo.12124
41. Sato A, Figueroa F, O'hUigin C, Steck N, Klein J. Cloning of major histocompatibility complex (MHC) genes from threespine stickleback, *Gasterosteus aculeatus*. *Mol Mar Biol Biotechnol* (1998) 7:221–31.
42. Reusch TB, Schaschl H, Wegner KM. Recent duplication and inter-locus gene conversion in major histocompatibility class II genes in a teleost, the three-spined stickleback. *Immunogenetics* (2004) 56(6):427–37. doi:10.1007/s00251-004-0704-z
43. Reusch TBH, Langefors Å. Inter- and intralocus recombination drive MHC class IIB gene diversification in a teleost, the three-spined stickleback *Gasterosteus aculeatus*. *J Mol Evol* (2005) 61(4):531–41. doi:10.1007/s00239-004-0340-0
44. Procaccio V, Depetris D, Soularue P, Mattei M-G, Lunardi J, Issartel J-P. cDNA sequence and chromosomal localization of the NDUFS8 human gene coding for the 23 kDa subunit of the mitochondrial complex I. *Biochim Biophys Acta* (1997) 1351(1):37–41. doi:10.1016/S0167-4781(97)00020-1
45. Barañano DE, Rao M, Ferris CD, Snyder SH. Biliverdin reductase: a major physiologic cytoprotectant. *Proc Natl Acad Sci U S A* (2002) 99(25):16093–8. doi:10.1073/pnas.252626999
46. Verma IM, Stevenson JK, Schwarz EM, Van Antwerp D, Miyamoto S. Rel/NF-kappa B/I kappa B family: intimate tales of association and dissociation. *Genes Dev* (1995) 9(22):2723–35. doi:10.1101/gad.9.22.2723
47. Scharsack JP, Koch K, Hammerschmidt K. Who is in control of the stickleback immune system: interactions between *Schistocephalus solidus* and its specific vertebrate host. *Proc Biol Sci* (2007) 274(1629):3151–8. doi:10.1098/rspb.2007.1148

48. Grewal IS, Flavell RA. CD40 and CD154 in cell-mediated immunity. *Annu Rev Immunol* (1998) 16(1):111–35. doi:10.1146/annurev.immunol.16.1.111
49. Zeisberg M, Strutz F, Müller GA. Role of fibroblast activation in inducing interstitial fibrosis. *J Nephrol* (1999) 13:S111–20.
50. Gratchev A, Guillot P, Hakiy N, Politz O, Orfanos C, Schledzewski K, et al. Alternatively activated macrophages differentially express fibronectin and its splice variants and the extracellular matrix protein βIG-H3. *Scand J Immunol* (2001) 53(4):386–92. doi:10.1046/j.1365-3083.2001.00885.x
51. Hevezi P, Vences-Catalan F, Maravillas-Montero JL, White CA, Casali P, Llorente L, et al. TSPAN33 is a novel marker of activated and malignant B cells. *Clin Immunol* (2013) 149(3):388–99. doi:10.1016/j.clim.2013.08.005
52. Perez-Martinez C, Zlotnik A, Santos-Argumedo L. Tspan33 is differentially expressed during B cell differentiation (LYM7P. 620). *J Immunol* (2015) 194(1 Suppl):200–12.
53. Turrens JF. Mitochondrial formation of reactive oxygen species. *J Physiol* (2003) 552(2):335–44. doi:10.1113/jphysiol.2003.049478
54. Akagawa KS, Komuro I, Kanazawa H, Yamazaki T, Mochida K, Kishi F. Functional heterogeneity of colony-stimulating factor-induced human monocyte-derived macrophages. *Respirology* (2006) 11(Suppl 1): S32–6. doi:10.1111/j.1440-1843.2006.00805.x
55. Wang T, Hanington PC, Belosevic M, Secombes CJ. Two macrophage colony-stimulating factor genes exist in fish that differ in gene organization and are differentially expressed. *J Immunol* (2008) 181(5):3310–22. doi:10.4049/jimmunol.181.5.3310
56. Belperio JA, Keane MP, Arenberg DA, Addison CL, Ehlert JE, Burdick MD, et al. CXC chemokines in angiogenesis. *J Leukoc Biol* (2000) 68(1):1–8.
57. Langfelder P, Horvath S. WGCNA: an R package for weighted correlation network analysis. *BMC Bioinformatics* (2008) 9(1):559. doi:10.1186/1471-2105-9-559
58. Shin MH, Lee YA, Min D-Y. Eosinophil-mediated tissue inflammatory responses in helminth infection. *Korean J Parasitol* (2009) 47(Suppl):S125–31. doi:10.3347/kjp.2009.47.S.S125
59. Kalbe M, Eizaguirre C, Scharsack JP, Jakobsen PJ. Reciprocal cross infection of sticklebacks with the diphyllobothriidean cestode *Schistocephalus solidus* reveals consistent population differences in parasite growth and host resistance. *Parasit Vectors* (2016) 9(1):1. doi:10.1186/s13071-016-1419-3
60. Scharsack JP, Kalbe M, Derner R, Millinski M. Modulation of granulocyte responses in three-spined sticklebacks *Gasterosteus aculeatus* infected with the tapeworm *Schistocephalus solidus*. *Dis Aquat Organ* (2004) 59:141–50. doi:10.3354/dao059141
61. Fischer U, Utke K, Somamoto T, Kollner B, Ototake M, Nakanishi T. Cytotoxic activities of fish leucocytes. *Fish Shellfish Immunol* (2006) 20(2):209–26. doi:10.1016/j.fsi.2005.03.013
62. Fischer U, Koppang EO, Nakanishi T. Teleost T and NK cell immunity. *Fish Shellfish Immunol* (2013) 35(2):197–206. doi:10.1016/j.fsi.2013.04.018
63. Wittamer V, Bertrand JY, Gutschow PW, Traver D. Characterization of the mononuclear phagocyte system in zebrafish. *Blood* (2011) 117(26):7126–35. doi:10.1182/blood-2010-11-321448
64. Dixon GB, Davies SW, Aglyamova GA, Meyer E, Bay LK, Matz MV. Genomic determinants of coral heat tolerance across latitudes. *Science* (2015) 348(6242):1460–2. doi:10.1126/science.1261224
65. Kauffmann A, Gentleman R, Huber W. arrayQualityMetrics—a bioconductor package for quality assessment of microarray data. *Bioinformatics* (2009) 25(3):415–6. doi:10.1093/bioinformatics/btn647
66. Wright RM, Aglyamova GV, Meyer E, Matz MV. Gene expression associated with white syndromes in a reef building coral, *Acropora hyacinthus*. *BMC Genomics* (2015) 16(1):371. doi:10.1186/s12864-015-1540-2
67. Ritchie ME, Phipson B, Wu D, Hu Y, Law CW, Shi W, et al. Limma powers differential expression analyses for RNA-sequencing and microarray studies. *Nucleic Acids Res* (2015) 43(7):e47. doi:10.1093/nar/gkv007

Conflict of Interest Statement: The authors declare that the research was conducted in the absence of any commercial or financial relationships that could be construed as a potential conflict of interest.

frontiers in Immunology

ORIGINAL RESEARCH
published: 22 December 2017
doi: 10.3389/fimmu.2017.01831

The Kinetics of the Humoral and Interferon-Gamma Immune Responses to Experimental *Mycobacterium bovis* Infection in the White Rhinoceros (*Ceratotherium simum*)

Sven D. C. Parsons[1,2,3], Darshana Morar-Leather[4], Peter Buss[5], Jennifer Hofmeyr[5], Ross McFadyen[1,2,3,6†], Victor P. M. G. Rutten[4,7], Paul D. van Helden[1,2,3], Michele A. Miller[1,2,3] and Anita Luise Michel[4,8]*

[1] DST/NRF Centre of Excellence for Biomedical Tuberculosis Research, Cape Town, South Africa, [2] SAMRC Centre for TB Research, Cape Town, South Africa, [3] Division of Molecular Biology and Human Genetics, Faculty of Medicine and Health Sciences, Stellenbosch University, Cape Town, South Africa, [4] Bovine Tuberculosis and Brucellosis Research Programme, Faculty of Veterinary Science, Department of Veterinary Tropical Diseases, University of Pretoria, Onderstepoort, South Africa, [5] Veterinary Wildlife Services, South African National Parks, Kruger National Park, Skukuza, South Africa, [6] Centre for Proteomic and Genomic Research (CPGR), Cape Town, South Africa, [7] Faculty of Veterinary Medicine, Department of Infectious Diseases and Immunology, Utrecht University, Utrecht, Netherlands, [8] National Zoological Gardens of South Africa, Pretoria, South Africa

Mycobacterium bovis is the cause of tuberculosis (TB) in a wide range of species, including white rhinoceroses (*Ceratotherium simum*). Control of the disease relies on the indirect detection of infection by measuring pathogen-specific responses of the host. These are poorly described in the white rhinoceros and this study aimed to characterize the kinetics of immune responses to *M. bovis* infection in this species. Three white rhinoceroses were infected with *M. bovis* and their immune sensitization to this pathogen was measured monthly for 20 months. Cell-mediated immunity was characterized in whole blood samples as the differential release of interferon-gamma in response to bovine purified protein derivative (PPDb) and avian PPD (PPDa) as well as the release of this cytokine in response to the *M. bovis* proteins 6 kDa early secretory antigenic target (ESAT-6)/10 kDa culture filtrate protein (CFP-10). Humoral immunity was quantified as the occurrence or the magnitude of antibody responses to the proteins ESAT-6/CFP-10, MPB83, MPB83/MPB70, and PPDb. The magnitude and duration of immune reactivity varied between individuals; however, peak responses to these antigens were detected in all animals circa 5–9 months postinfection. Hereafter, they gradually declined to low or undetectable levels. This pattern was associated with limited TB-like pathology at postmortem examination and appeared to reflect the control of *M. bovis* infection following the development of the adaptive immune response. Measurement of these markers could prove useful for assessing the disease status or treatment of naturally infected animals. Moreover, immune responses identified in this study might be used to detect infection; however, further studies are required to confirm their diagnostic utility.

Keywords: immune response, interferon-gamma, serology, *Mycobacterium bovis*, tuberculosis, white rhinoceros

OPEN ACCESS

Edited by:
Andrew Steven Flies, University of Tasmania, Australia

Reviewed by:
Francisco Javier Salguero, University of Surry, United Kingdom
David E. MacHugh, University College Dublin, Ireland
Maria A. Risalde, Instituto Maimonides de Investigación Biomédica de Cordoba (IMIBIC), Spain

****Correspondence:***
Sven D. C. Parsons
sparsons@sun.ac.za

†Present address:
Ross McFadyen, Centre for Proteomic and Genomic Research (CPGR), Cape Town, South Africa

Specialty section:
This article was submitted to Comparative Immunology, a section of the journal Frontiers in Immunology

Received: *18 June 2017*
Accepted: *04 December 2017*
Published: *22 December 2017*

Citation:
Parsons SDC, Morar-Leather D, Buss P, Hofmeyr J, McFadyen R, Rutten VPMG, van Helden PD, Miller MA and Michel AL (2017) The Kinetics of the Humoral and Interferon-Gamma Immune Responses to Experimental Mycobacterium bovis Infection in the White Rhinoceros (Ceratotherium simum). Front. Immunol. 8:1831. doi: 10.3389/fimmu.2017.01831

INTRODUCTION

White rhinoceroses (*Ceratotherium simum*) are classified as "Near Threatened" by the International Union for Conservation of Nature, with the majority of animals occurring in South Africa (1). Of these, a substantial number occur in the greater Kruger National Park (KNP) and the Hluhluwe-iMfolozi Park (HiP). However, because of their economic value and threatened conservation status, animals from these populations are regularly translocated to other reserves and privately owned collections. Importantly, movement of animals from these areas could present a risk of translocating *Mycobacterium bovis*, a major cause of tuberculosis (TB). This pathogen can infect a wide variety of domestic and wildlife hosts, including rhinoceros species (2) and has become established in both the KNP and HiP (3). The recent detection, in the KNP, of a case of severe pulmonary TB in a black rhinoceros (4) and confirmed *M. bovis* granulomas in lymph nodes of four white rhinoceroses (unpublished data) highlights the potential risk of movement of these species.

Tuberculosis is slowly progressive and the causative organisms may initially be contained within well circumscribed granulomas (5). For this reason, detection of the pathogen can be challenging and, as in other species, TB in rhinoceroses might only be diagnosed postmortem or once animals have developed advanced disease (2). Infection is therefore often diagnosed indirectly by measuring the host's adaptive immune response toward *M. bovis* antigens. This is commonly done by quantifying either the *in vivo* or the *in vitro* immune response to purified protein derivative (PPD), a preparation containing a broad range of *M. bovis* antigens (6, 7). Alternatively, recombinant proteins that are more specific to *M. bovis* can be utilized as test antigens and these include 6 kDa early secretory antigenic target (ESAT-6), 10 kDa culture filtrate protein (CFP-10), MPB70, and MPB83 (8). Assessment of immune responses to these and other antigens might also be used to distinguish between latent infection and progressive disease or to monitor treatment in both humans and animals (8, 9).

The present study forms part of a broader project that characterized the clinical features and associated gross and histopathology of the experimental infection of three white rhinoceroses with *M. bovis* (10). In all cases, 20 months after infection, animals had shown no clinical signs of TB disease and had limited TB-like pathology (10). We hypothesized that quantifying the adaptive immune responses to *M. bovis* in these animals would provide an indirect measure of their infection and disease status. As such, we aimed to characterize (i) their immune sensitization to selected antigens following infection and (ii) the kinetics of their humoral and cell-mediated immune responses.

Abbreviations: CFP-10, 10 kDa culture filtrate protein; ELISA, enzyme-linked immunoassay; ESAT-6, 6 kDa early secretory antigenic target; HiP, Hluhluwe-iMfolozi Park; IFN-γ, interferon-gamma; KNP, Kruger National Park; OD, optical density; PBS, phosphate-buffered saline; PI, postinfection; PPDa, avian purified protein derivative; PPDb, bovine purified protein derivative; QFT, modified QuantiFERON TB Gold (In-Tube) assay; TMB, 3, 3′, 5, 5′- tetramethylbenzidine.

MATERIALS AND METHODS

Animals

The capture, maintenance, chemical immobilization, infection, and sampling of animals in the KNP, as well as biohazard containment, have previously been described in detail (10). Briefly, three subadult male white rhinoceroses, identified as PB1, PB2, and PB4, were infected by endoscopic endobronchial instillation of the *M. bovis* strain SB0121, a genotype commonly isolated from wildlife in the KNP. The inocula for the three animals contained approximately 2.1×10^3 colony forming units (cfu), 1.8×10^2 and 1.4×10^3 cfu, respectively. Each month, from 3 months prior to infection until 20 months postinfection (PI), animals were chemically immobilized and blood was collected from the radial vein into lithium heparin and serum vacutainer tubes (Fisher Scientific, Suwanee, GA, USA) and used in the immunological assays described below (**Table 1**). On these occasions, endoscopic bronchoalveolar lavages were performed for mycobacterial culture. Twenty months after infection, animals were euthanized, postmortem examinations performed, and systematic tissue sampling conducted to determine the presence or absence of *M. bovis* by histopathology, mycobacterial culture, and polymerase chain reaction (PCR) and findings have been previously reported in detail (10). Approval for the study was obtained from the Animal Ethics Committees of the South African National Parks and Stellenbosch University (proposal SU-ACUM12-00012) as well the South African National Department of Agriculture, Forestry and Fisheries in terms of Section 20 of the Animal Diseases Act (Permit 12/11/1/1/6/1).

Rhinoceros-Specific Interferon-Gamma (IFN-γ) Release Assay

Blood collected in heparin tubes was processed within 12 h after collection as previously described (11). Briefly, whole blood samples were incubated at 37°C in 5% CO_2 for 24 h with *M. bovis* PPD (PPDb, 20 μg/ml) and *M. avium* PPD (PPDa, 20 μg/ml), PMA/CaI (0.1/2 μg/ml—positive control), culture medium (Nil—negative control), respectively. Plasma was harvested following centrifugation at $1{,}088 \times g$ for 5 min and stored at −80°C until tested, in duplicate, in the rhinoceros-specific IFN-γ capture enzyme-linked immunoassay (ELISA) (11). The results of the ELISA were determined at 490 nm using an ELISA plate reader (BioTek, Powerwave XS2, Gen5 software). An initial reference/blank reading was performed on the plate prior to the blocking step, at the same wavelength, and final optical density (OD) values were determined by subtracting the mean reference value from the mean test value for each sample well. Antigen- and mitogen-specific release of IFN-γ was calculated as the OD value derived from the PPD- and PMA/CaI-stimulated samples minus that derived from the Nil sample. *M. bovis*-specific release of IFN-γ was calculated as the PPDb value minus the PPDa value (ΔPPDb-a).

Modified QuantiFERON TB Gold (In-Tube) (QFT) Assay

One milliliter of heparinized whole blood was transferred to a "Nil" tube (containing saline) and a "TB Antigen" tube (coated

TABLE 1 | Immunoassays utilized to measure immune sensitization to selected antigens in *Mycobacterium bovis*-infected white rhinoceroses.

Assay	Supplier	Test antigens	Assay format	Reference
Rhinoceros-specific assay	In-house assay	*M. bovis* PPD; *M. avium* PPD	IGRA	(11)
Modified QFT assay	Components supplied by Qiagen and Mabtech	ESAT-6, CFP-10, TB 7.7	IGRA	N/A
PPD ELISA	In-house assay	*M. bovis* PPD	ELISA	N/A
ElephantTB STAT-PAK® assay	Chembio Diagnostic Systems	ESAT-6/CFP-10/MPB83	LFD	(8, 12)
Dual Path Platform (DPP)® VetTB assay	Chembio Diagnostic Systems	MPB83; ESAT-6/CFP-10	LFD	(12)
Bovid DPP assay	Chembio Diagnostic Systems	MPB83/MPB70	LFD	N/A

PPD, purified protein derivative; IGRA, interferon-gamma release assay; QFT, QuantiFERON TB Gold (In Tube); N/A, not applicable; ELISA, enzyme-linked immunosorbent assay; LFD, lateral flow device.

with peptides simulating ESAT-6, CFP-10, and TB 7.7) of the QFT system (Qiagen, Hilden, Germany). In addition, as a measure of cell viability, 1 ml blood was incubated with phytohemagglutinin (PHA) (Sigma-Aldrich, St. Louis, MO, USA) in phosphate-buffered saline (PBS) at a final concentration of 10 µg/ml. The tubes were shaken according to the manufacturer's instructions and incubated for 20–24 h at 37°C. Hereafter, the tubes were centrifuged at 1,600 × *g* for 10 min and plasma was harvested and stored at −80°C. Plasma samples were assayed in duplicate using a commercial bovine IFN-γ ELISA cross-reactive with IFN-γ of sheep and horses (Kit 3115-1H-20; Mabtech AB, Nacka Strand, Sweden) that has previously been shown to detect recombinant rhinoceros IFN-γ (data not shown). Reactions were visualized using 3,3′,5,5′-tetramethylbenzidine (TMB) (BD Biosciences, NJ, USA) as a color substrate. The IFN-γ concentration in each sample was measured as the OD of each well, at a wavelength of 450 nm, using a Labtech LT-4000 microplate reader (Lasec, Cape Town, South Africa). The *M. bovis*-specific release of IFN-γ was calculated as the mean OD derived for plasma harvested from the TB Ag tube minus the mean OD derived for plasma harvested from the Nil tube.

PPD ELISA

Flat-bottomed 96-well microtiter plates (Nunc, New York, NY, USA) were coated with 100 µl of a 10 µg/ml PPDb solution (Prionics, Schlieren-Zurich, Switzerland) in 0.05 M carbonate-bicarbonate buffer (pH 9.6) and incubated overnight at 4°C. For each well coated with antigen, a corresponding control well was coated with 100 µl blocking buffer (BB) consisting of 5% milk powder (Clover, Roodepoort, South Africa) in PBS + 0.05% Tween-20 (Sigma-Aldrich, St. Louis, MO, USA). After incubation, plates were decanted and washed five times with PBS containing 0.05% Tween-20, then blocked with 200 µl/well of BB for 1 h at room temperature (RT). The plates were washed as above and serum samples diluted 1:200 in BB were added to duplicate wells (100 µl/well). Plates were incubated at RT for 1 h and then washed five times as above. Plates were then incubated with 100 µl/well of peroxidase-conjugated recombinant protein A/G (Thermo Scientific, MA, USA) diluted 1:100,000 in PBS, for 1 h at RT. Plates were washed as above before addition of 100 µl/well of TMB and subsequently incubated in the dark for 15 min. The reaction was stopped using 50 µl/well of 2 M H_2SO_4 and the OD of each well was measured at 450 nm using a LT-4000 Microplate Reader (Lasec). For each animal, an assay result was calculated as the mean OD value derived from duplicate PPD-coated wells minus that of duplicate BB-coated wells.

ElephantTB STAT-PAK® Assay

Rhinoceros sera were tested using the ElephantTB STAT-PAK® assay (Chembio Diagnostic Systems, Inc., Medford, NY, USA). The assay has been optimized for the detection of *M. tuberculosis* infection in elephants but is not specific for a particular host species and has previously been found useful in measuring antibody responses in a black rhinoceros infected with *M. tuberculosis* (12). Briefly, 30 µl of serum was added to the sample well followed by three drops of diluent/antibody detection conjugate. If the sample contained antibodies to *M. bovis* antigens (ESAT-6/CFP-10/MPB83), a positive line appeared as a blue band. Any visible band observed in the test line area by two independent observers and read at 20 min was considered as an antibody positive result.

Dual Path Platform (DPP)® VetTB and Bovid DPP Assays

The DPP® VetTB and Bovid DPP assays (Chembio Diagnostic Systems, Inc.) were performed according to the manufacturer's instructions as previously described (12). After 15 min, the test results were read. A DPP optical reader device (Chembio Diagnostic Systems, Inc.) was used to measure the reflectance of test strips and a result was quantified as a numerical score, represented as reflectance units (RU). The DPP® VetTB assay includes two test lines containing the antigens MPB83 and ESAT-6/CFP-10, along with a positive control. In the Bovid DPP assay, a single test line contained MPB83/MPB70, along with a positive control.

RESULTS

Rhinoceros-Specific IFN-γ Assay

The release of IFN-γ in unstimulated blood was negligible, resulting in median ELISA OD values of 0.08, 0.05, and 0.07 for PB1, PB2, and PB4, respectively. All animals displayed strong IFN-γ responses to PMA/CaI stimulation, with mean mitogen-specific OD values of 0.86, 0.83, and 0.86, respectively. The kinetics of PPDa and PPDb-specific IFN-γ release in whole blood from these animals are illustrated in **Figure 1A**. Immune sensitization to these antigens was negligible prior to infection and first observed at 2–3 months PI. The release of IFN-γ in response to both antigens was greatest between 4 and 10 months PI and the *M. bovis*-specific

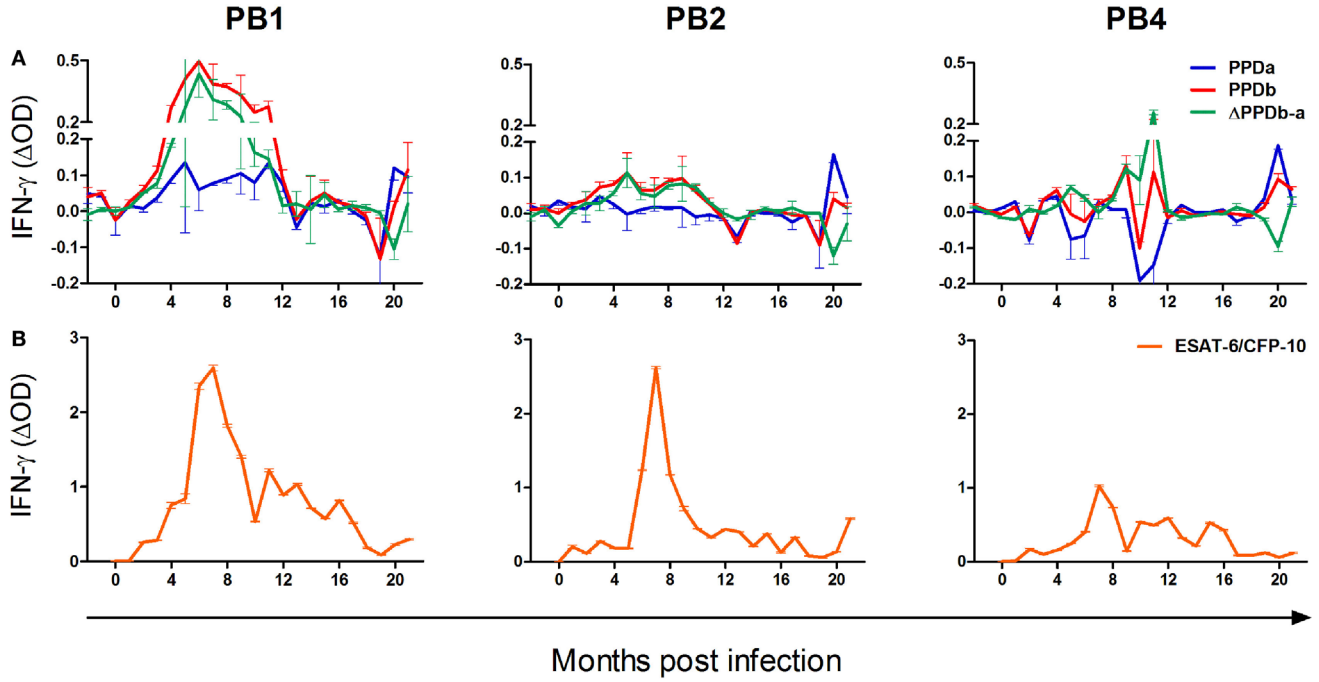

FIGURE 1 | The kinetics of the cell-mediated immune response to *Mycobacterium bovis* infection in the white rhinoceros. Following *M. bovis* infection, whole blood from three animals (PB1, PB2, and PB4) was incubated overnight at 37°C without stimulation, or stimulation with bovine PPD purified protein derivative (PPDb), avian PPD (PPDa), and 6 kDa early secretory antigenic target (ESAT-6)/10 kDa culture filtrate protein (CFP-10)/TB7.7 peptides, respectively. Plasma interferon-gamma (IFN-γ) was measured by enzyme-linked immunoassay, in duplicate, as the optical density (OD), and antigen-specific release calculated as the OD derived for the unstimulated sample subtracted from that derived for each antigen (mean ΔOD ± SD). **(A)** Antigen-specific IFN-γ release in response to PPDb and PPDa, and the differential response to these antigens (ΔPPDb-a); **(B)** Antigen-specific IFN-γ release in response to ESAT-6/CFP-10/TB7.7 peptides.

PPD responses (ΔPPDb-a) peaked at circa 5–6 months PI in PB1 and PB2 and at 11 months PI in PB4. Subsequently, IFN-γ release in responses to both PPDa and PPDb were low until 20 months PI when all animals again showed substantial responses to these antigens. At this time, IFN-γ release was notably greater in response to PPDa than PPDb in PB2 and PB4, while in PB1, the PPDb response was higher than that to PPDa.

Modified QFT Assay

The release of IFN-γ in unstimulated blood was negligible, resulting in median ELISA OD values of 0.09, 0.08, and 0.09 for PB1, PB2, and PB3, respectively. As a result of experimental error, measurements of PHA-induced IFN-γ responses were available for only 14/21 sampling occasions for each animal. On these occasions, median mitogen-specific OD values were 0.81, 0.35, and 0.89, respectively. The kinetics of ESAT-6/CFP-10/TB7.7-specific IFN-γ release in whole blood from PB1, PB2, and PB4 are illustrated in **Figure 1B**. These antigen-specific responses were first observed at 1 month PI in PB2 and at 2 months PI in PB1 and PB4. Following infection, peak responses occurred at circa 6–9 months PI, after which IFN-γ release decreased gradually over time. At 20 months PI, PB2 displayed a moderate but distinct increase in IFN-γ release in response to ESAT-6/CFP-10/TB7.7.

PPD ELISA, ElephantTB STAT-PAK®, and DPP Assays

The kinetics of the humoral responses to *M. bovis* antigens in PB1, PB2, and PB4 are illustrated in **Figure 2**. Using the ElephantTB STAT-PAK® assay, PB1 displayed humoral sensitization to the combined antigens ESAT-6/CFP-10/MPB83 at all time points from 1 to 10 months PI (**Figure 2A**). In contrast, antibodies to this antigen pool were not detected in PB2 for the duration of the study and only on a single occasion in PB4, i.e., 2 months PI (**Figure 2A**). Using the DPP assays, only PB1 displayed a strong and sustained humoral response to the *M. bovis* antigens ESAT-6/CFP-10, MPB83, and MPB83/MPB70, with sensitization to all three antigens detected at 5 and 6 months PI. Hereafter, the humoral response to MBP83 alone was not again detected in this animal; however, responses to MBP83/MPB70 were sustained until 10 months PI and responses to ESAT-6/CFP-10 peaked again at 14 months PI. Both PB2 and PB4 displayed very low antibody quantities specific for these antigens, with PB4 showing only a moderate response to MPB83/MPB70 at 17 months PI.

Prior to infection, levels of circulating antibodies to PPDb (**Figure 2B**) were similar in all animals, with levels rising from 2 to 4 months PI. A peak in the PPDb-specific humoral response occurred circa 6 months PI, after which this gradually decreased in all animals.

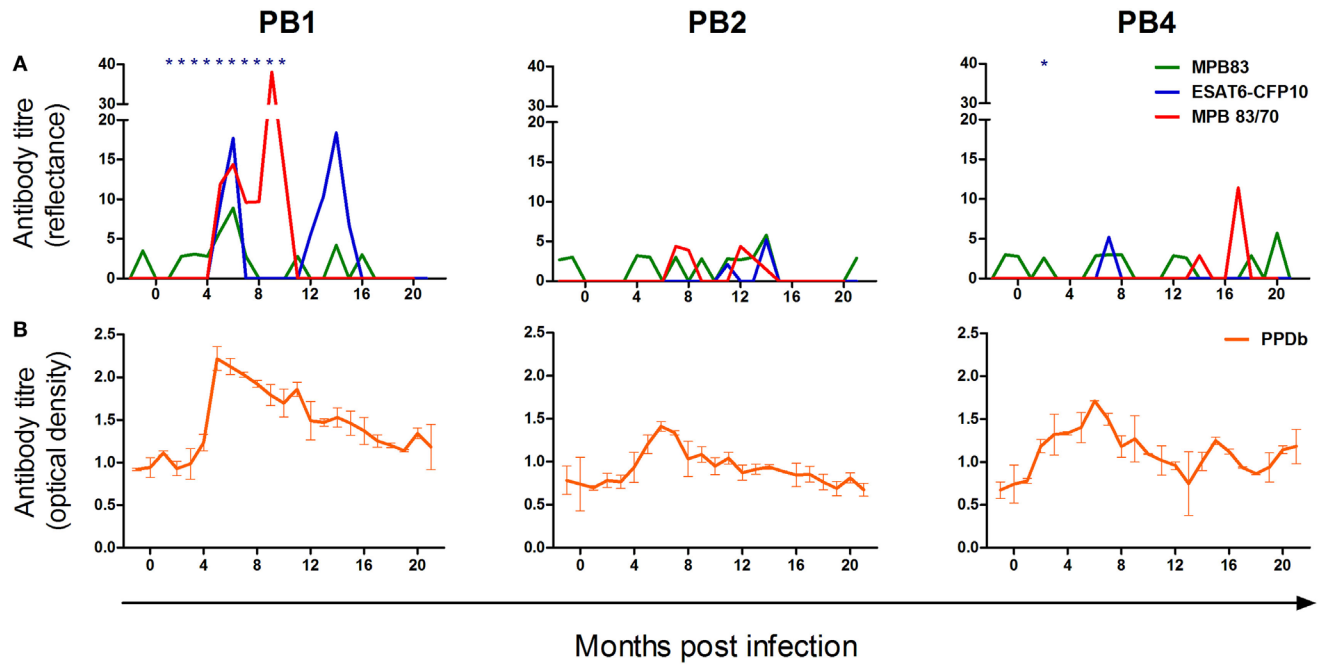

FIGURE 2 | The kinetics of the humoral response to *Mycobacterium bovis* infection in the white rhinoceros. Following *M. bovis* infection, serum antibodies of three animals (PB1, PB2, and PB4) were measured using selected commercial assays and an in-house bovine purified protein derivative (PPDb) enzyme-linked immunoassay (ELISA). **(A)** Serological responses to MPB83 and 6 kDa early secretory antigenic target (ESAT-6)/10 kDa culture filtrate protein (CFP-10) (Dual Path Platform (DPP)® VetTB assay) and MPB83/70 (Bovid DPP assay); seroreactivity to ESAT-6/CFP-10/MPB83 (ElephantTB STAT-PAK® assay) is indicated (*). **(B)** Serological responses to PPDb, measured in duplicate by indirect ELISA, and calculated as the difference in optical density (OD) between control wells and PPDb-coated wells (mean ΔOD ± SD).

DISCUSSION

Following experimental endobronchial instillation of *M. bovis* in 3 white rhinoceroses, these developed time-dependent humoral and cell-mediated immune responses toward the antigens PPDa, PPDb, ESAT-6/CFP-10, MPB83, MPB83/MPB70, and ESAT-6/CFP-10/MPB83. Notably, cell-mediated responses toward ESAT-6/CFP-10 and PPD showed greater consistency between individuals than did humoral responses toward MPB83, MPB83/MPB70, and ESAT-6/CFP-10/MPB83. While the specific patterns of immune reactivity varied between individuals, peak responses were detected in all three animals circa 5–9 months PI, after which they gradually declined to low or undetectable levels.

In mice, the onset of adaptive immunity toward *M. tuberculosis* requires the active replication of the pathogen in lymph nodes draining the site of infection (13). Moreover, the progression and magnitude of this response is associated with the amount of antigen produced in these lymph nodes (13, 14). Similarly, *M. bovis* infection in cattle and deer invariably results in the development of granulomatous disease in lymph nodes draining the site of infection, suggesting that these tissues are the primary site of antigen presentation and immune activation (15). In the present study, during the first 5–9 months PI, the rhinoceroses displayed a consistent rise in immune reactivity toward *M. bovis* antigens, strongly suggesting the establishment of this infection in all three animals.

The magnitude and duration of *M. bovis*-specific immune reactivity appeared to reflect the disease status of each animal. PB1, which displayed the most robust and sustained responses to all test antigens was the only animal from which viable *M. bovis* was isolated, i.e., from a bronchoalveolar lavage sample collected 5 months following infection (10). Moreover, at postmortem examination of PB1, acid fast bacterial rods and *M. bovis* DNA were detected in tracheobronchial and lung lesions, respectively (10). In contrast, PB4 displayed substantially lower responses of both humoral and cell-mediated immunity (CMI) and no definitive confirmation of *M. bovis* infection was made in this animal by culture, histopathology, or PCR (10).

Following an initial peak circa 5–9 months PI, all rhinoceroses displayed a gradual decline in the magnitude of their immune responses, and antigen-induced IFN-γ release reached low levels within 12–16 months after infection. In cattle, the severity of TB disease correlates with both the magnitude of ESAT-6-specific CMI (5) and the humoral response to *M. bovis* (6). Similarly, in rabbits experimentally infected with *M. tuberculosis*, progressive disease is associated with strongly rising titers of anti-PPD antibodies (16), while control of the infection is characterized by low seroreactivity to PPD that declines over time (17). A similar pattern of waning sensitization to ESAT-6/CFP-10 has been documented in naturally infected black rhinoceroses during treatment for *M. tuberculosis* infection (8). Such patterns are associated with a decrease in pathogen burden and antigenic

load (17). Notably, for PB1, the peak in CMI responses at 5 months PI occurred at the only time point that viable *M. bovis* was isolated from the respiratory tract. Hereafter, the gradual decline in *M. bovis*-specific immune responses, as for the other two experimentally infected animals, was associated with limited TB-like pathology at postmortem examination and a failure to isolate viable organisms from multiple tissues. Together, these immune response patterns appear to reflect the control of *M. bovis* infection in these animals following the development of the adaptive immune response.

Humoral responses broadly mirrored those of CMI, with PB1 showing strong seroreactivity to all test antigens. However, PB2 and PB4 showed limited detectable sensitization to the *M. bovis*-specific antigens MPB83, MPB83/MPB70, and ESAT-6/CFP-10. Similar differences in seroreactivity of individual animals are seen following experimental infection in other species, including cattle and badgers (18, 19). As for these hosts, this phenomenon in rhinoceroses could be related to the infection dose administered to each animal or reflect a natural animal-to-animal diversity in antigen recognition (18, 19). Nonetheless, following infection, PB2 and PB4 did display a transient elevation in seroreactivity to PPDb. In part, this may reflect the far greater range of antigenic epitopes present in PPDb compared to the more specific antigens such as MPB83 and ESAT-6. Alternatively, because PPD includes antigens that are shared between various mycobacterial species (20), the detection of immunological sensitization to PPDb might in part reflect the boosting of immune responses to cross-reactive antigens. Evidence of such cross-reactivity is indicated by the distinct CMI response of PB1 to PPDa following *M. bovis* infection.

At 20 months PI, all rhinoceroses displayed a rapid increase in IFN-γ release in response to the antigens PPDb, PPDa, and ESAT-6/CFP-10/TB7.7. This boosting of the immune response might have reflected acute progression of TB disease in these animals (5); however, this is unlikely given the paucity of *M. bovis*-associated pathology at postmortem examination shortly after this sampling time point (10). Alternatively, this observation may be related to viral pneumonia observed in PB2 and PB4 (10). The immune response associated with acute viral infections can induce non-specific "bystander" activation and proliferation of lymphocytes (21), giving rise to IFN-γ production (22). Notably, at this time, PB2 and PB4 displayed a greater response to PPDa than to PPDb. This may be further evidence that this phenomenon resulted from a non-specific mycobacterial or viral infection rather than an *M. bovis*-specific event.

Results from the present study provide insight into the temporal patterns of immunological responses to *M. bovis* infection in white rhinoceroses. However, limitations in the study design must be considered when extrapolating findings to animals under natural conditions. First, the nature of the study precluded statistical analysis of data, partly because of the limited sample size and partly because of the substantial variation in immune responses between individuals. Unlike studies using inbred species such as experimental mice (13), this limitation is commonly experienced in studies investigating outbred animals, especially wildlife (19). Second, differences in the infective doses administered to each animal may have accounted for the differences in pathological outcomes and immune response profiles and these may not reflect natural infection. Nonetheless, it is notable that while the magnitude of these responses differed between individuals, their kinetics were comparable. Lastly, the three experimentally infected individuals were all relatively young, had been treated for ectoparasites, were generally free from severe stressors and were well fed (10). As such, the immunological profiles described in this study may reflect an optimal outcome of infection and not necessarily a scenario in which these and other factors might affect either disease progression or resolution.

In summary, this study has characterized antigen-specific immune response patterns of white rhinoceroses that appear to reflect the effective control of *M. bovis* infection by this host. Importantly, the measurement of these responses might prove useful for assessing the disease status or response to treatment of naturally infected animals. Moreover, the immunological markers identified in this study might be used for the detection of infection; however, further studies investigating these markers in *M. bovis*-uninfected animals are required to confirm their diagnostic utility.

ETHICS STATEMENT

This study was carried out with the approval of the Animal Ethics Committees of the South African National Parks (SANParks) and Stellenbosch University. Animal care was in accordance with the SANParks Standard Operating Procedures for the Capture, Transportation and Maintenance in Holding Facilities of Wildlife.

AUTHOR CONTRIBUTIONS

AM, MM, VR, and PH designed the study; MM, PB, and JH provided animal care and performed chemical immobilization and blood collection; SP, DM-L, JH, RM, and MM performed laboratory assays; data analysis was done by SP, DM-L, VR, PH, MM, and AM; the first draft of the manuscript was written by SP and all authors contributed to editorial revision.

ACKNOWLEDGMENTS

The authors are grateful for the expert support of Guy Hausler of Stellenbosch University and Nomkosi Mathebula of SANParks Veterinary Wildlife Services (VWS), for their contribution to the processing of blood. We are also thank Dr. Markus Hofmeyr, Marius and Melandie Kruger and the VWS boma team for the husbandry and care of the rhinoceroses.

FUNDING

Research reported in this publication was supported by the South African Medical Research Council (SAMRC) and the South African National Research Foundation (grants 41744, 86949 as well as the Incentive Funding for Rated Researchers). The content is solely the responsibility of the authors and does not necessarily represent the official views of the SAMRC or the NRF.

REFERENCES

1. Emslie, R. *Ceratotherium simum*. The IUCN Red List of Threatened Species 2012: e.T4185A16980466. (2012). Available from: http://dx.doi.org/10.2305/IUCN.UK.2012.RLTS.T4185A16980466.en
2. Miller M, Michel A, van Helden P, Buss P. Tuberculosis in rhinoceros: an underrecognized threat? *Transbound Emerg Dis* (2017) 64(4):1071–8. doi:10.1111/tbed.12489
3. Michel AL, Bengis RG, Keet DF, Hofmeyr M, de Klerk LM, Cross PC, et al. Wildlife tuberculosis in South African conservation areas: implications and challenges. *Vet Microbiol* (2006) 112:91–100. doi:10.1016/j.vetmic.2005.11.035
4. Miller MA, Buss P, Van Helden P, Parsons SDC. *Mycobacterium bovis* in a free-ranging black rhinoceros, Kruger National Park, South Africa, 2016. *Emerg Infect Dis* (2017) 23:557–8. doi:10.3201/eid2303.161622
5. Vordermeier HM, Chambers MA, Cockle PJ, Whelan AO, Simmons J, Hewinson RG. Correlation of ESAT-6-specific gamma interferon production with pathology in cattle following *Mycobacterium bovis* BCG vaccination against experimental bovine tuberculosis. *Infect Immun* (2002) 70:3026–32. doi:10.1128/IAI.70.6.3026-3032.2002
6. Welsh MD, Cunningham RT, Corbett DM, Girvin RM, McNair J, Skuce RA, et al. Influence of pathological progression on the balance between cellular and humoral immune responses in bovine tuberculosis. *Immunology* (2005) 114:101–11. doi:10.1111/j.1365-2567.2004.02003.x
7. Griffin JFT, Nagai S, Buchan GS. Tuberculosis in domesticated red deer: comparison of purified protein derivative and the specific protein MPB70 for in vitro diagnosis. *Res Vet Sci* (1991) 50:279–85. doi:10.1016/0034-5288(91)90124-7
8. Duncan AE, Lyashchenko K, Greenwald R, Miller M, Ball R. Application of elephant TB Stat-Pak assay and Mapia (multi-antigen print immunoassay) for detection of tuberculosis and monitoring of treatment in black rhinoceros (*Diceros bicornis*). *J Zoo Wildl Med* (2009) 40:781–5. doi:10.1638/2009-0044.1
9. Chegou NN, Black GF, Kidd M, van Helden PD, Walzl G. Host markers in Quantiferon supernatants differentiate active TB from latent TB infection: preliminary report. *BMC Pulm Med* (2009) 9:21. doi:10.1186/1471-2466-9-21
10. Michel AL, Lane EP, De Klerk-Lorist L-M, Hofmeyr M, Van der Heijden EMDL, Botha L, et al. Experimental *Mycobacterium bovis* infection in three white rhinoceroses (*Ceratotherium simum*): susceptibility, clinical and anatomical pathology. *PLoS One* (2017) 12:e0179943. doi:10.1371/journal.pone.0179943
11. Morar D, Schreuder J, Mény M, van Kooten PJS, Tijhaar E, Michel AL, et al. Towards establishing a rhinoceros-specific interferon-gamma (IFN-γ) assay for diagnosis of tuberculosis. *Transbound Emerg Dis* (2013) 60:60–6. doi:10.1111/tbed.12132
12. Miller MA, Greenwald R, Lyashchenko KP. Potential for serodiagnosis of tuberculosis in black rhinoceros (*diceros bicornis*). *J Zoo Wildl Med* (2015) 46:100–4. doi:10.1638/2014-0172R1.1
13. Wolf AJ, Desvignes L, Linas B, Banaiee N, Tamura T, Takatsu K, et al. Initiation of the adaptive immune response to *Mycobacterium tuberculosis* depends on antigen production in the local lymph node, not the lungs. *J Exp Med* (2008) 205:105–15. doi:10.1084/jem.20071367
14. Reiley WW, Calayag MD, Wittmer ST, Huntington JL, Pearl JE, Fountain JJ, et al. ESAT-6-specific CD4 T cell responses to aerosol *Mycobacterium tuberculosis* infection are initiated in the mediastinal lymph nodes. *Proc Natl Acad Sci U S A* (2008) 105:10961–6. doi:10.1073/pnas.0801496105
15. Behr MA, Waters WR. Is tuberculosis a lymphatic disease with a pulmonary portal? *Lancet Infect Dis* (2014) 14:250–5. doi:10.1016/S1473-3099(13)70253-6
16. Subbian S, Tsenova L, Yang G, O'Brien P, Parsons S, Peixoto B, et al. Chronic pulmonary cavitary tuberculosis in rabbits: a failed host immune response. *Open Biol* (2011) 1:110016. doi:10.1098/rsob.110016
17. Subbian S, Tsenova L, O'Brien P, Yang G, Kushner NL, Parsons S, et al. Spontaneous latency in a rabbit model of pulmonary tuberculosis. *Am J Pathol* (2012) 181:1711–24. doi:10.1016/j.ajpath.2012.07.019
18. Lyashchenko KP, Pollock JM, Colangeli R, Gennaro ML. Diversity of antigen recognition by serum antibodies in experimental bovine tuberculosis. *Infect Immun* (1998) 66:5344–9.
19. Lesellier S, Corner L, Costello E, Sleeman P, Lyashchenko KP, Greenwald R, et al. Immunological responses following experimental endobronchial infection of badgers (*Meles meles*) with different doses of *Mycobacterium bovis*. *Vet Immunol Immunopathol* (2009) 127:174–80. doi:10.1016/j.vetimm.2008.09.012
20. Michel AL. *Mycobacterium fortuitum* infection interference with *Mycobacterium bovis* diagnostics: natural infection cases and a pilot experimental infection. *J Vet Diagn Invest* (2008) 20:501–3. doi:10.1177/104063870802000415
21. Murali-Krishna K, Altman JD, Suresh M, Sourdive DJD, Zajac AJ, Miller JD, et al. Counting Antigen-Specific CD8 T Cells: a re-evaluation of bystander activation during viral infection. *Immunity* (1998) 8:177–87. doi:10.1016/S1074-7613(00)80470-7
22. Gilbertson B, Germano S, Steele P, Turner S, Fazekas de St Groth B, Cheers C. Bystander activation of CD8+ T Lymphocytes during experimental mycobacterial infection. *Infect Immun* (2004) 72:6884–91. doi:10.1128/IAI.72.12.6884-6891.2004

Conflict of Interest Statement: The research was conducted in the absence of any commercial or financial relationships that could be construed as a potential conflict of interest.

frontiers in Immunology

ORIGINAL RESEARCH
published: 08 January 2018
doi: 10.3389/fimmu.2017.01914

Feeding Immunity: Physiological and Behavioral Responses to Infection and Resource Limitation

Sarah A. Budischak[1], Christina B. Hansen[1], Quentin Caudron[1], Romain Garnier[1,2], Tyler R. Kartzinel[3], István Pelczer[4], Clayton E. Cressler[5], Anieke van Leeuwen[1,6] and Andrea L. Graham[1]*

[1] Department of Ecology and Evolutionary Biology, Princeton University, Princeton, NJ, United States, [2] Department of Veterinary Medicine, University of Cambridge, Cambridge, United Kingdom, [3] Department of Ecology and Evolutionary Biology, Brown University, Providence, RI, United States, [4] Department of Chemistry, Princeton University, Princeton, NJ, United States, [5] School of Biological Sciences, University of Nebraska, Lincoln, NE, United States, [6] NIOZ Royal Netherlands Institute for Sea Research, Department of Coastal Systems, and Utrecht University, Texel, Netherlands

Resources are a core currency of species interactions and ecology in general (e.g., think of food webs or competition). Within parasite-infected hosts, resources are divided among the competing demands of host immunity and growth as well as parasite reproduction and growth. Effects of resources on immune responses are increasingly understood at the cellular level (e.g., metabolic predictors of effector function), but there has been limited consideration of how these effects scale up to affect individual energetic regimes (e.g., allocation trade-offs), susceptibility to infection, and feeding behavior (e.g., responses to local resource quality and quantity). We experimentally rewilded laboratory mice (strain C57BL/6) in semi-natural enclosures to investigate the effects of dietary protein and gastrointestinal nematode (*Trichuris muris*) infection on individual-level immunity, activity, and behavior. The scale and realism of this field experiment, as well as the multiple physiological assays developed for laboratory mice, enabled us to detect costs, trade-offs, and potential compensatory mechanisms that mice employ to battle infection under different resource conditions. We found that mice on a low-protein diet spent more time feeding, which led to higher body fat stores (i.e., concentration of a satiety hormone, leptin) and altered metabolite profiles, but which did not fully compensate for the effects of poor nutrition on albumin or immune defenses. Specifically, immune defenses measured as interleukin 13 (IL13) (a primary cytokine coordinating defense against *T. muris*) and as *T. muris*-specific IgG1 titers were lower in mice on the low-protein diet. However, these reduced defenses did not result in higher worm counts in mice with poorer diets. The lab mice, living outside for the first time in thousands of generations, also consumed at least 26 wild plant species occurring in the enclosures, and DNA metabarcoding revealed that the consumption of different wild foods may be associated with differences in leptin concentrations. When individual foraging behavior was accounted for, worm infection significantly reduced rates of host weight gain. Housing laboratory mice in outdoor enclosures provided new insights into the resource costs of immune defense to helminth infection and how hosts modify their behavior to compensate for those costs.

Keywords: *Trichuris muris*, resource–immune trade-offs, compensatory feeding, DNA metabarcoding, nuclear magnetic resonance spectroscopy metabolite profiling, rewilding mice

OPEN ACCESS

Edited by:
Andrew Steven Flies, University of Tasmania, Australia

Reviewed by:
Claudio Silva, Federal University of Uberlandia, Brazil
Jamie Kopper, Michigan State University, United States
William Parker, Duke University, United States

****Correspondence:***
Sarah Budischak
sabudischak@gmail.com

Specialty section:
This article was submitted to Comparative Immunology, a section of the journal Frontiers in Immunology

Received: *29 September 2017*
Accepted: *14 December 2017*
Published: *08 January 2018*

Citation:
Budischak SA, Hansen CB, Caudron Q, Garnier R, Kartzinel TR, Pelczer I, Cressler CE, van Leeuwen A and Graham AL (2018) Feeding Immunity: Physiological and Behavioral Responses to Infection and Resource Limitation. Front. Immunol. 8:1914. doi: 10.3389/fimmu.2017.01914

INTRODUCTION

Ecologists have long-studied energy and nutrient flows in ecosystems to understand their function and how they may respond to environmental changes (1–4). In ecological communities, these flows are often a core currency of species interactions in food webs. Parasite–host interactions represent a trophic interaction in their own right, and elucidating resource flows within infected hosts can reveal crucial processes that determine immunity and infection outcomes. Resources ingested by hosts must first be metabolized and used for maintenance (i.e., baseline metabolism), and can subsequently be used for host growth (including growth of immune cells), or be diverted to parasite growth and reproduction (**Figure 1**).

Resource flow models also capture the total cost of infection, including nutrients going to immunity, parasites, and host tissue repair. By modeling the priority of resource allocation to the host's immune system vs. resources captured by parasites, Cressler et al. (5) illustrated how increasing resource acquisition can have qualitatively different effects on host immunity and parasite loads: the immune priority scenario (i.e., when additional resources go first into immune system components) quickly clears infections, while the parasite priority scenario (i.e., additional resources are first nabbed by the parasite), results in chronic infections. At molecular and cellular levels, immunologists are increasingly describing how nutrients and metabolites affect particular immune pathways (6–8). For example, receptors for glucose and leptin, a signal of body fat (9), are found on T- and B-lymphocytes, macrophages, neutrophils, and natural killer cells and can stimulate inflammatory responses [reviewed in Ref. (6, 10)]. While great progress has been achieved in understanding how nutrition affects immunity (7), scaling-up our understanding of resource–immune interactions from molecules and cells to entire organisms and populations remains challenging (11). Here, we use semi-natural enclosures to investigate resource flow through parasitized hosts by examining trade-offs among immunity, host condition (protein and fat stores), and parasite growth and survival under two levels of resource availability.

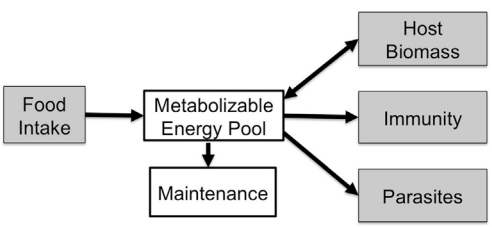

FIGURE 1 | Within an infected host, resources are metabolized and allocated to baseline maintenance costs. Remaining resources are put toward immunity and host biomass, or are captured by parasites to use for their own growth and reproduction. Resources, therefore, must trade-off between these competing demands unless hosts are able to increase the quality or quantity of food intake to compensate for those costs.

Because of their tractability and the plethora of tools available for studying immune pathways, laboratory (lab) mice have been integral in building our basic understanding of immunology, as well as how parasite-infected hosts respond to energy, macronutrient, and micronutrient limitation (12–17). However, when scaling to organism-level questions of nutrition and resource flows during infection, it is becoming apparent that lab mouse experiments do not recapitulate some critical biological features (**Table 1**). The *ad lib*, energy-rich, readily accessible resource conditions of lab mice differ from those of most human and wildlife populations. Additionally, ties between immunity, metabolism, and the gut microbiome are increasingly recognized (18, 19), and the low diversity microbiomes and low activation state of T cells of lab mice most closely resemble neonates (20) and diverge widely from wild mice (21). Furthermore, gastrointestinal (GI) helminths also play a role in training and modulating immunity (22, 23), with increasing risks of allergic and autoimmune conditions in human populations devoid of their coevolved worms (24). Thus, this and other studies of helminth infection in

TABLE 1 | Studying laboratory mice in semi-natural enclosures provides a tractable experimental system that recapitulates more aspects of wild systems than traditional laboratory experiments while avoiding confounding complexities such as unknown exposure histories and coinfections.

	Lab	Enclosures	Wild
Host genotype, age, sex	+ selectable, − not diverse	+ selectable, − not diverse	Natural but added source of variation
Previous exposure	Controlled	Controlled	Unknown and can affect immune investment
Coinfections	Controlled	Controlled	Unknown and can affect immune investment
Thermoregulation	Artificial constant temperature	Natural	Natural
Foraging	Only chow, accessed with minimal foraging effort	Chow accessible with moderate effort, natural forage	Natural forage requiring greater energetic investment to acquire
Diet manipulation and feeding behavior	Manipulatable but cannot track individual feeding	Manipulatable and can track individual feeding	Limited to providing supplementary food, cannot track individual feeding
Predators and competitors	None	Excluded	Natural
Reproduction	None[a]	None[b]	Natural
Seasonality	None	Present	Present
Microbiome	Limited (20)	More diverse (See text footnote 1)	Natural
Immunological tools	Widely commercially available	Widely commercially available	Limited, more tools available for species closely related to lab and veterinary animals

[a]*Unless breeding pairs are purposely put together.*

[b]*None if housed in single-sex enclosures, but possibly reproduce if both sexes are cohoused.*

rewilded mice[1] provide the opportunity to study how these key components of immunological regulation interact to affect the health of humans and other animals.

Fortunately, recent studies offer a promising compromise between realism and tractability for studying immune–resource interactions in lab mice. For example, immune traits of lab mice can be made more representative by generating more diverse microbiomes or exposure histories in the laboratory (20, 25). An even greater degree of realism can be achieved by putting lab mice in outdoor enclosures (**Table 1**) that arguably mimic aspects of their evolutionary history as commensals of humans engaged in agriculture (26). Outdoors, lab mice develop more diverse microbiomes, elevated T cell responses and higher parasite loads compared with indoor lab mouse controls (See text footnote 1). Additionally, in outdoor enclosures, mice experience more natural variation in activity and thermo-regimes that may make trade-offs between immunity and other physiological processes more apparent than under lab conditions (**Table 1**).

Host behavior is central to scaling-up immune–resource interactions from the cellular to organismal level. Mice on low-quality (i.e., protein) diets may consume a greater quantity of chow, which can alter their body fat composition and immune profiles (27). From livestock studies, we know that GI nematodes, or host immune responses to them, can reduce host appetite, decreasing the energy budget the host has to allocate to defense, repair, and other physiological functions (28). Reciprocally, hosts can alter foraging during infection by consuming medicinal plants (29) or by increasing foraging to mitigate costs of infection and immunity (30). In free-ranging populations, increased foraging may come with increased energetic costs, parasite exposure, social stress, and predation risks (11, 28, 31, 32). Thus, assessing feeding behavior is critical for understanding how organisms respond to resource limitation and the resultant fitness consequences (7).

Using a semi-natural field system (See text footnote 1), we manipulate resource availability to examine the resource costs of infection and immunity. Our goal was to investigate the costs of infection (including resources diverted to parasites and immunity) and to learn how hosts may use foraging behavior to mitigate those costs in lab mice (C57BL/6) infected with the GI nematode *Trichuris muris*. *T. muris* is a whipworm that lives in the cecum, and is a congener of the parasite *Trichuris trichiura* that infects over 450 million people worldwide (33). To assess how hosts respond to infection under resource limitation, we manipulate levels of dietary protein, which is known to have strong effects on host immune defenses (7, 17, 34–37). We might expect mice fed the high-protein diet to have stronger immune responses and lower parasite loads than those on the low-protein diet. Alternatively, mice on the high-protein diet could tolerate infection while mice on the low-protein diet resist (17), which would turn the expected observation around and show stronger immune responses and lower parasite loads in the low-protein treatment. At the individual level-scale, we track whether mice compensate for potential joint costs of infection or a low-protein diet by altering foraging behavior. We predict that there will be trade-offs between food intake, investment in immunity, and parasite load (**Figure 1**). Infected mice may either feed less due to infection-induced inappetence (28, 38, 39), or feed more to compensate for costs of infection and immunity. Our findings do indeed suggest complex repercussions of behavioral changes for the flow of resources into infection and immunity.

[1]Leung JM, Budischak SA, Chung HT, Hansen C, Bowcutt R, Neill R, et al. The shock of the new: rapid environmental effects on gut nematode susceptibility in re-wilded mice. Under review.

MATERIALS AND METHODS

Experimental Design

Our experiment to examine trade-offs between infection, immunity, and within-host resources (i.e., diet quality) included four treatment groups: high-protein infected, high-protein uninfected, low-protein infected, and low-protein uninfected. Eighty-eight female C57Bl/6 mice aged 5–6 weeks were obtained from Jackson Laboratories and individually identified with both ear tags and RFID tags (see below). All animal care was conducted in accordance with protocols approved by the Princeton University Animal Care and Use Committee (Protocol no. 1982-14). Mice were housed in groups of five in the laboratory and randomly assigned to the two diet treatments as well as two cohorts that were staggered by 2 days for logistical purposes (**Figure 2**). The high-protein (HP; 20%; Envigo Teklad Custom Diet TD.91352) and low-protein (LP; 6%; Envigo Teklad Custom Diet TD.90016) diets had the same energy density (3.8 kcal/g) and micronutrient composition. The typical chow fed to lab mice (e.g., PicoLab® Rodent Diet 20) has very similar composition to the HP diet. For 10 days mice were fed the assigned diets in the lab while temperature and light cycles were gradually altered to mimic outdoor conditions (June/July in New Jersey, USA: 26 ± 1°C with a 15-h light–9-h dark cycle; **Figure 2**).

Next, the 22 mice in each diet–cohort combination were transported to four outdoor enclosures (**Figure 2**), two of which contained the HP chow and the other two the LP chow (**Figure 2** inset). The enclosures are replicate pens of approximately 180 m^2, fenced in by zinced iron walls extending 1.5-m high and 80-cm deep, and topped with electric fencing and reflective aluminum pans to deter ground and aerial predators, respectively (See text footnote 1). Diets were provided *ad libitum* at feeding stations monitored by two RFID readers to track each individual's time spent feeding. The natural environment could serve as an additional source of food (e.g., berries, seeds, insects). Each enclosure provided two watering stations inside a small (180 cm × 140 cm × 70 cm) straw-filled shed (See text footnote 1). Mice were weighed at the start of the experiment, the day of release, and approximately weekly thereafter as they were trapped overnight in the outdoor enclosures using chow-baited Longworth traps. At each weekly trapping, fecal samples were collected and blood samples were taken *via* shallow cutaneous tail snips into heparinized capillary tubes.

Mice were acclimated to the enclosures for 2 weeks (14–17 days) prior to *T. muris* infection (**Figure 2**). A dose of 200 embryonated *T. muris* eggs (strain E) was then given *via* oral gavage to the first 16 mice trapped per enclosure. If more than 16 mice

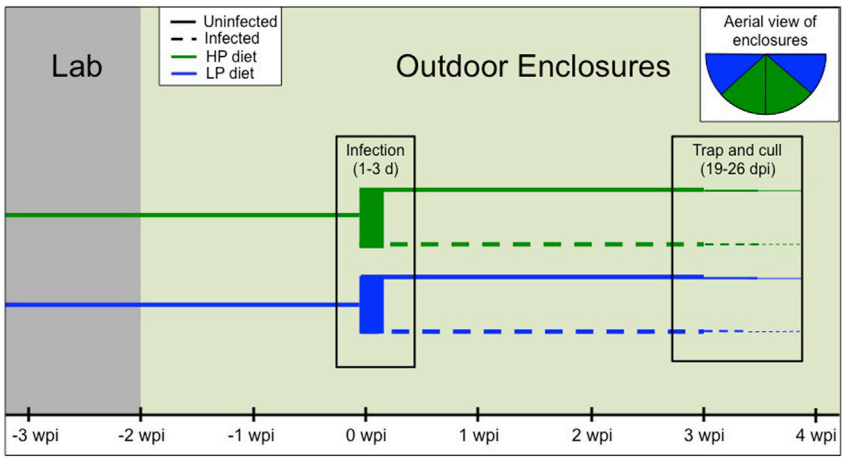

FIGURE 2 | Timeline of the experimental design. First, mice were randomly assigned to diet treatment and cohort [–3 weeks postinfection (wpi)]. Diets were provided to the second cohort 2 days later, but since both groups subsequently followed the same timeline, only one cohort is depicted for clarity. After 10 days in the lab (–2 wpi), all mice were moved to four outdoor enclosures (n = 22/enclosure). After 2 weeks, 16 mice per enclosure were trapped and infected with 200 *T. muris* eggs over the course of 1–3 days. Final trapping and culling occurred around 3–4 wpi (19–26 days postinfection). Inset shows an aerial view of the enclosures by diet treatment, and infected and uninfected mice were cohoused.

were trapped on a given day, individuals were randomly assigned to infection treatment. In total, 29 mice on the HP diet and 31 mice on the LP diet were infected. Thus, infected and uninfected animals were cohoused in the same enclosures. The remaining mice (15 HP, 13 LP) served as uninfected controls. Nematode infection could not be transmitted between mice assigned to different treatments in the shared enclosures due to the long life cycle of *T. muris* [>28 days to maturity (40)], and the relatively short duration of the experiment [<26 days postinfection (dpi)].

Approximately 3 weeks postinfection (mean ± SE: 21.5 ± 1.7 dpi), range: 19–26 (dpi), all mice were trapped, weighed, and transported back to the laboratory (**Figure 2**). Mice were anesthetized via isoflurane inhalation followed by terminal cardiac puncture. Cardiac blood was drawn from each mouse, spun in a heparinized tube, and plasma was separated and stored at −80°C. During necropsy, mesenteric lymph nodes (MLNs) were excised for cell culture (see below). Finally, to determine carcass weight, all major organs (except the brain) were removed and weighed. The spleen, large intestine (emptied of contents), and cecum were separated and weighed. Ceca were frozen for later dissection and parasite enumeration.

Quantifying Feeding Behavior

Individual-level feeding behavior was assessed using a custom-built monitoring system (Datasheet S1 in Supplementary Material). To track feeding behavior, Radio Frequency IDentification tags (RFID; 8 mm × 1.4 mm FDX-B "Skinny" PIT Tag, Oregon RFID, Portland, OR, USA) were injected subcutaneously. When in the vicinity of an antenna, the RFID tag emits a unique string of numbers that serves as an individual's identifier (i.e., RFID number). In each enclosure, Feeding Event Tracking Apparatuses (FETA) with RFID antennas were deployed. The FETA transmit a signal to an Event Acquisition and Reporting System (EARS), which automatically compiles the data produced by the FETA (FETA number, RFID number, and timestamp). Two FETA were placed in sequence and connected on one end to the sole entrance to the chow hopper.

The directionality of mouse movement through the sequential FETA boxes was used to determine when mice were in the feeder. Specifically, mice were inferred to be in the feeder for the duration of time between two EARS readings on the FETA nearest the chow hopper. Intervals <5 s in duration (7.5% of visits) were removed because they allowed insufficient time to feed. Intervals greater than 2 h were also removed because mice were likely not eating for such a long duration and this small fraction (<0.1%) of visits skewed feeding time distributions. Intervals when chow was not available in the feeder (i.e., during trapping sessions) were also dropped. Next, total time feeding was summed per mouse, then divided by the number of days each mouse was in the enclosure because some mice were in the enclosures for longer than others (35–40 days depending on when they were trapped). This produced a comparable measurement of time spent feeding (min) per experiment day. Mice that lost their RFID tags (n = 6) and two individuals that did not eat at the feeder (working RFIDs but stopped visiting feeder) were excluded from feeding behavior analyses. Chow consumption was monitored by weighing each chow hopper every time it was removed for trapping as well as before and after refilling (i.e., every 1–3 days).

Immune Response Measurements

Following established protocols (See text footnote 1, 41), MLN tissue was excised during necropsy, prepared into single-cell suspensions at a density of 5 × 10^6 cells/mL, stimulated with *T. muris* antigen at 5 μg/mL, and cultured for 48 h. Supernatants were collected and analyzed in duplicate for interleukin 13 (IL13), interleukin 10 (IL10), interleukin 17 (IL17), and interferon gamma (IFNg) using half-reactions of Beckton Dickinson Cyometric Bead Array Mouse/Rat Soluble Protein Flex Set system

(BD Biosciences, Oxford, UK) and an LSRII flow cytometer (BD Biosciences) (See text footnote 1). Concentrations were analyzed with the FCAP Array software (version 3.0.1, BD Biosciences).

Worm-specific IgG1 titers were measured using sandwich enzyme-linked immunoassays (ELISA). Ninety-six-well plates were coated with *T. muris* excretory-secretory (ES) antigen at a concentration of 5 μg/mL in carbonate buffer (0.06 M, pH = 9.6) with 2% bovine serum albumin (BSA). Plates were then blocked overnight with 2% powdered milk in carbonate buffer. After a 2-h incubation at 37°C, plates were washed three times with *tris*-buffered saline-Tween (TBST). Plasma samples were added and serially diluted from 1:50 to 1:6,400 with TBST and incubated for 2 h at 37°C. After washing five times with TBST, horseradish peroxidase (HRP) conjugated IgG1 antibody (1:4,000 in TBST) was added. Following a 1-h incubation at 37°C, plates were washed five times and Substrate ABTS (Sigma-Aldrich) was added. Plates were developed for 20 min at 37°C, then stopped with a 1% sodium dodecyl sulfate solution. Absorbance was measured at 405 nm using a Multiscan™ GO spectrophotometer (Thermo Scientific). Titers were determined by the dilution at which absorbance exceeded 4 SDs above background, defined as the plate-wide average absorbance of the two most dilute concentrations of each sample.

To quantify total IgG, a mouse antibody IgG pair was purchased from StemCell Tech (Catalog no. 01998C). Plates were coated at 1 μg/mL 50 μL per well with carbonate buffer (pH 9.6) overnight at 4°C. Plates were blocked for an hour with TBST 20 with 0.1% BSA at 37°C, then washed. Preliminary assays revealed that IgG levels were quite high, so to fall in the range of the standards, samples were diluted 1:81,920 in TBST containing 0.1% BSA. After incubation for 2 hat 37°C and washing, a secondary antibody was applied at a concentration of 1:1,000 in TBST with 0.1% BSA. Plates were incubated at 37°C for 1 h then washed. Next, we added 100 μL/well of p-nitrophenyl phosphate (pNPP) substrate to all wells. Finally, plates were incubated for 30 min and read at 405 nm. Concentrations were calculated in comparison to a plate-specific standard curve (all $R^2 > 0.999$).

Parasite Quantification

Caeca were cut open longitudinally and examined under a dissecting microscope by an observer blind to infection status. Worms were isolated by scraping the gut mucosa into a series of clean petri dishes of water. After enumeration, worms were stored in 70% ethanol for subsequent length measurements. Each worm was photographed under a dissecting scope (2–4× power) and ImageJ (version 1.49, NIH, USA) was used to measure total length.

Condition and Nutritional Measurements

Plasma albumin concentrations were measured colorimetrically. QuantiChrom BCG albumin assay kits (BioAssays) were used following the manufacturer's instructions. Briefly, 5-μL duplicates of each standard and sample (diluted 1:2 with ultrapure water) were mixed with 200 μL of BCG reagent. Plates were incubated at 23°C for 5 min before being read at 620 nm. Concentrations were determined in comparison to a standard curve run in duplicate ($R^2 = 0.997$).

Plasma leptin concentrations were analyzed using a RayBio® Mouse Leptin ELISA kit following manufacturer's instructions (RayBiotech, Norcross, GA, USA). Briefly, 10 μL of plasma samples were diluted 1:10, incubated on a 96-well plate coated with mouse leptin antibody. After washing, a biotinylated anti-mouse leptin antibody was added. Next, the plate was washed, horseradish peroxidase-conjugated streptavidin was added. Following another washing step, a buffered 3,3,5,5′-tetramethylbenzidine solution was used to produce a color change reaction stopped after 30 min with 0.2-M sulfuric acid. Color intensity was read at 450 nm. Concentrations were calculated using a standard curve (standards run in duplicate, $R^2 = 0.995$).

Characterizing Herbivory on Wild Plants Using DNA Metabarcoding

To compare the wild plant species diversity and composition with which lab mice supplemented their diets, we employed a DNA metabarcoding method that involves sequencing and identifying undigested plant DNA obtained from fecal pellets (42, 43). The plant DNA in fecal pellets is likely to reflect very recent foraging activity because the half-life of ingesta in lab mice is approximately 74 min (44), meaning that <1% of contents are retained after 8 h. Thus, the resulting dietary profiles represent plants eaten over the ~2.5- to 5-h period prior to sample collection (44, 45).

Fecal samples from 26 mice ($n = 7$ HP inf, 9 LP inf, 6 HP uninf, 4 LP uninf) from the end of the study were obtained for dietary analysis. Samples were frozen on dry ice and stored at −80°C to preserve DNA prior to extraction. Total DNA from 1 to 2 pellets (~15–30 mg) per mouse was extracted using a Zymo Xpedition Soil/Fecal DNA mini kit with an extraction blank to monitor for potential cross-contamination. Using PCR, the P6 loop of the chloroplast *trnL*(UAA) marker was amplified with primers *g* and *h* (42). The PCRs were run with unique combinations of the *g* and *h* primers that had been modified with 8-nt multiplex identification (MID) tags in order to enable pooling of amplicons for sequencing using established protocols (46). These PCR products were cleaned and normalized using SequelPrep normalization plates, then pooled for sequencing in a 170-nt single-end run of the Illumina HiSeq2500 at Princeton University's Lewis Sigler Institute following Kartzinel et al. (46).

The resulting DNA sequence data were assigned to samples of origin (i.e., demultiplexed), screened to reduce potential sequencing errors, and identified by comparison to a plant DNA reference library. The sequences were demultiplexed and primers were removed using the *ngsfilter* command in the Obitools software (47). We discarded sequences that contained ambiguous base calls (i.e., non-A, T, C, or G characters) that were <9-nt long or that had mean Illumina quality scores of <32. Unique sequences were merged and tabulated within samples to permit quantification of DNA sequence relative read abundance (RRA), a measure of the proportion of each dietary plant species in each dietary sample. Putative errors were screened by using the *obiclean* command to identify sequences that differed by 1 nt from another sequence in the same sample, but that occurred at <5% of the abundance. These sequences were removed from further analyses. Plant DNA

was identified by comparison to a reference library developed using the European Molecular Biology Laboratories (EMBL) (Database release no. 130). From this archive, we extracted 35,776 unique sequences (229,430 entries) with ≤3 mismatches to the *trnL*-P6 primers *g* and *h*. Unique dietary sequences were identified by comparison to this reference database using the *ecoTag* command. Operational taxonomic units (OTUs) were identified by clustering at the >97% level using the uclust algorithm (48). To focus on abundant and well-identified plant taxa, we considered only OTUs with >80% identity to the EMBL database and those representing >5% of reads within each sample. Samples were rarefied to even sequencing depth using phyloseq (49) in R (50).

We inspected taxonomic identifications to identify imprecision that could arise from gaps or misidentified DNA sequences in the reference library. Any OTUs that exactly matched a taxon not known to occur in the region were revised to higher taxonomic levels, and the set of references matching any OTUs that were poorly identified (family or higher taxonomic levels) were scrutinized for taxonomic outliers (Table S2 in Supplementary Material). Only two plant taxa were included in the manufacturing process of the chow provisioned to lab mice in this experiment were corn (*Zea mays*) and beets (*Beta vulgaris*), and DNA from these plant products was expected to be destroyed by irradiation during the chow production process; indeed, no DNA sequences that match either of these plant species were identified in the final set of OTUs from our analysis. We calculated RRA by converting the rarefied number of reads into a proportion of reads per sample (i.e., ranging 0–1). Although RRA is not always a reliable measure of proportional dietary utilization in DNA metabarcoding studies (51), the analysis of RRA based on the *trnL*-P6 protocol employed in this study has been supported at least to the level of plant family and functional group in independent studies from different systems (46, 52, 53).

NMR of Dietary Metabolites

Nuclear magnetic resonance spectroscopy (NMR) was used to examine dietary metabolites from a random subsample of uninfected mice (12 HP and 8 LP) with sufficient frozen fecal samples from the end of the experiment. Fecal pellets from the mice were weighed, crushed, and diluted 1:3 with phosphate buffered saline (PBS). Samples were vortexed, allowed to dissolve overnight, and re-vortexed. After centrifugation, the supernatant was decanted and brought to ca. 30 µL with PBS in a 1.7-mm OD capillary tube (New Era Enterprises, Vineland, NJ, USA). This capillary was inserted into a 5/2.5-mm OD NMR tube containing small amount of D_2O, which served as an external lock material. Samples were analyzed on an 800-MHz Bruker Avance III HD NMR spectrometer equipped with a custom-made $^{1}H/^{19}F/^{13}C/^{15}N//^{2}H$ cryoprobe using Topspin v.3.2. Water suppression was done using the first increment of the NOESY pulse sequence (delay–G1–90°–t_1–90°–t_m–G2–90°–acquisition) applying weak presaturation during the relaxation delay and the 100-ms mixing time period. Data processing was done offline using MNova v.11.0 (Mestrelab Research, Santiago de Compostela, Spain). After zero filling, apodization with 1-Hz Gaussian broadening, careful phase and baseline correction were applied manually. In order to compensate for variance of concentrations the spectral intensities were normalized to total integral, excluding the small region of the residual water signal. Local peak alignment was applied where necessary and possible using the inherent function in MNova. A few key metabolites were identified based on literature data (54). Out of the 20 samples, two were discarded because of technical problems (poor shimming and water suppression) to maintain statistical integrity of the residual data. The collection of 18 spectra was then exported to a spreadsheet.

Statistical Analysis

The final sample size of this study was 80 (LP infected = 31, LP uninfected = 10, HP infected = 24, HP uninfected = 15). Several mice eluded capture for over 20 days beyond when the rest were trapped and sampled; these were excluded from statistical analyses. An additional mouse that had a severe congenital uterine defect was also excluded.

We assessed effects of diet and infection on immunity and condition. No uninfected mice had detectable IL13 concentrations, so a Kruskal–Wallis rank sum test was first used to compare infected and uninfected mice. The other cytokines (IFNγ, IL10, IL17) also had highly skewed distributions that could not be normalized. Thus, effects of diet and infection were analyzed using Kruskal–Wallis tests. Next, a general linear model (GLM) was used to test the effect of diet on log-transformed IL13 concentration among infected mice. GLMs were also used to test effects of diet and infection on log-transformed worm-specific IgG1, total IgG, and spleen weight relative to carcass weight. Using GLMs, we next tested for effects of diet and infection on mouse condition, including weight gain per day, plasma albumin concentration, plasma leptin concentration, and carcass weight. Plasma albumin and leptin concentrations were log transformed for the analysis. Diet–infection interaction terms were dropped when non-significant. To account for potential correlation structure among plasma components, we conducted a principal component analysis (PCA) of worm-specific IgG1, total IgG, albumin, and leptin. All components were log transformed and scaled prior to analysis. Next, the relationship between diet and infection status and each principal component (PC) was tested using GLMs. This PCA yielded no new insights beyond the univariate analyses described above, and results can be found in Table S1 in Supplementary Material.

To assess differences in fecal metabolites between the diet treatments, the SIMCA-P v.12.1 software package was used (Umetrics, Umea, Sweden). To determine if there was spectrum-wide variation between the diets, partial least squares-discriminant analysis (PLS-DA) was performed and orthogonal atrial least squares-discriminant analysis (OPLS-DA) were performed. Widely used in metabolic phenotyping studies, the PLS-DA analyses are better able to detect clusters than traditional PCA, and OPLS-DA provides even stronger discrimination based on known groupings (e.g., diet) (55). The DA methods were validated by calculating R^2 and Q^2. Prior to PLS-DA and OPLS-DA analysis, both UV and Pareto scaling were applied. UV scaling is a better choice for maintaining uniform contribution from all peaks regardless of their absolute intensity, while Pareto scaling provides access to "spectrum-like" loadings plot.

To examine morphological and behavioral changes, we first tested for effects of diet and infection on large intestine size (tissue weight/carcass weight) using a GLM. Similarly, we used a GLM to determine if time spent feeding per day in the enclosures varied with diet or infection status. Third, we examined supplemental foraging on natural plants in the enclosures using fecal DNA metabarcoding data. We tested for significant differences in the composition of plant species eaten according to diet, infection status, and leptin levels (log-transformed) using permutational MANOVA (perMANOVA) in *vegan* (56) in R. For the perMANOVA, we calculated pairwise Bray–Curtis dissimilarity metrics for each pair of samples, which ranges from 0 to 1 (from completely identical to mutually exclusive dietary compositions, respectively). For the six wild-plant families with the greatest overall RRA, we compared mean RRA between treatment groups (infected vs. uninfected and LP vs. HP diets) and across levels of leptin. Exploratory trend lines were fit to the data using generalized linear modeling. We investigated differences in RRA between genera of the legume family (Fabaceae) in more detail because this family comprised greatest overall RRA.

Lastly, we tested for differences in parasite load and weight gain, corrected for the amount of time each individual spent feeding. Among infected individuals, a non-parametric Kruskal–Wallis test was used to determine if diet affected worm count. In infected individuals, we also tested for an effect of diet on worm length (log transformed for normality) with a GLM. The amount of weight each mouse gained while in the enclosures was divided by the amount of time each spent feeding. Weight gain per minute feeding was compared between diets and infection status using a GLM. All analyses were run in R version 3.1.2.

RESULTS

Dietary Quality and Infection Affected Immunity

Measures of immune function were affected by both diet and infection. MLN cells of the uninfected mice produced no detectable IL13 [a cytokine strongly induced by nematodes (57)] in response to stimulation with nematode antigen, making them significantly lower than the infected mice (Kruskal–Wallis $\chi^2 = 7.52$, df = 1, $p = 0.0061$; **Figure 3A**). Among infected mice, those on the high-protein diet had higher IL13 concentrations in culture supernatants than those on the low-protein diet [Est (±SE): 0.56 ± 0.25, $t = 2.20$, $p = 0.033$; **Figure 3A**]. The cytokines IFNγ and IL17 mediate pro-inflammatory responses, primarily to intracellular pathogens and extracellular bacteria and fungi, respectively (58, 59). IL10 mediates anti-inflammatory, regulatory responses (58, 60). Surprisingly, IFNγ, IL17, and IL10 were also higher in infected mice but did not differ between diets (Figure S1 in Supplementary Material). In mice and many other mammals, IgG1 is an important antibody class for fighting GI nematode infection (57). In addition to being higher in infected mice ($p = 0.00006$), *T. muris* specific IgG1 titers were elevated in mice eating the high-protein diet ($p = 0.032$; **Table 2**; **Figure 3B**). Total IgG concentrations did not vary with diet or infection status (all $p > 0.33$; **Table 2**; **Figure 3C**), so we cannot account for the elevated IgG1 titers observed in uninfected mice eating the high-protein diet as a correlate of high total IgG concentrations. Spleen size also did not differ significantly with infection status or diet (all $p > 0.10$; **Table 2**; **Figure 3D**).

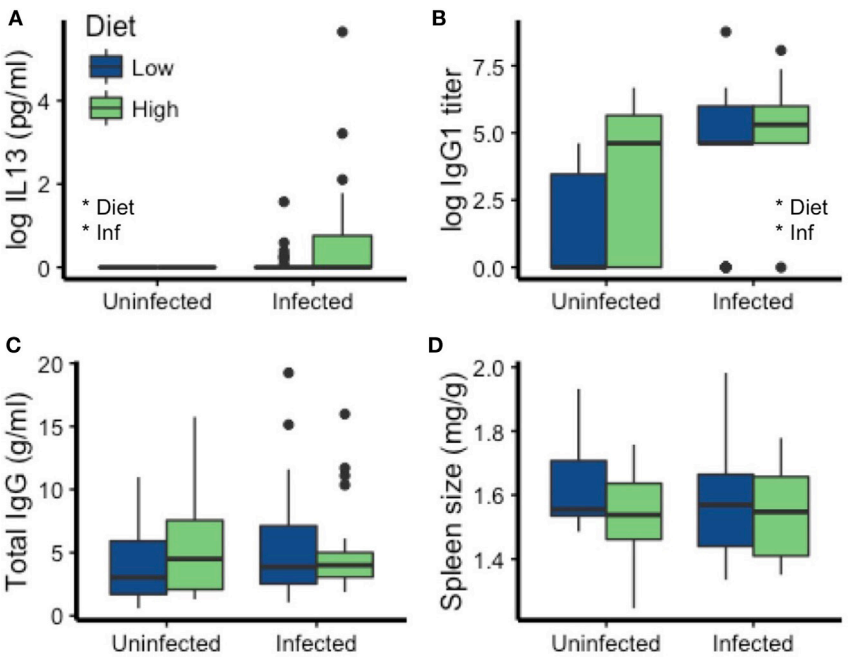

FIGURE 3 | Diet and infection status affected some mediators of immunity to *T. muris* but not others. Specifically, **(A)** interleukin 13 (IL13) and **(B)** immunoglobulin G1 (IgG1) were affected by diet and infection, but not **(C)** total IgG concentration or **(D)** spleen size (weight/carcass weight). Asterisks denote significant effects of diet or infection (Inf).

TABLE 2 | Results of general linear models testing the effects of diet (HP) and infection on immunity, condition, morphology, behavior, and costs of infection.

	Estimate	SE	*t*-Value	*p*-Value
Log (*T. muris* IgG1 titer)				
Diet	0.367	0.168	2.18	**0.032**
Infection	0.769	0.182	4.23	**0.00006**
Log (total IgG g/mL)				
Diet	0.171	0.175	0.98	0.332
Infection	0.129	0.188	0.68	0.496
Spleen size (g/mm)				
Diet	−0.056	0.034	−1.64	0.106
Infection	−0.022	0.037	−0.59	0.560
Weight gain/day (g/day)				
Diet	−0.013	0.009	1.33	0.187
Infection	−0.020	0.010	1.97	0.052
Log (albumin mg/mL)				
Diet	0.161	0.057	−2.83	**0.006**
Infection	0.082	0.061	−1.34	0.184
Carcass weight (g)				
Diet	−0.626	0.219	2.86	**0.006**
Infection	−0.341	0.236	1.44	0.154
Log (leptin pg/mL)				
Diet	−0.289	0.141	2.05	**0.044**
Infection	−0.018	0.151	0.12	0.904
Large intestine size (mg/g)				
Diet	0.56	0.41	1.37	0.176
Infection	1.03	0.44	2.34	**0.022**
Cecum size (mg/g)				
Diet	0.148	0.061	2.45	**0.017**
Infection	0.130	0.065	1.99	**0.050**
Time spent feeding (min/day)				
Diet	−13.7	3.7	−3.69	**0.0004**
Infection	−0.49	4.04	−0.12	0.904
Weight gain/time feeding (g/day)				
Diet	−0.088	0.265	−0.33	0.742
Infection	−0.596	0.287	−2.07	**0.042**

Significant effects are highlighted in bold.

Dietary Quality Affected Nutrition and Condition

Dietary protein affected multiple aspects of mouse nutrition and condition, whereas parasite infection did not. Although neither diet ($p = 0.19$) nor infection ($p = 0.052$) significantly affected rates of weight change (**Figure 4A**; **Table 2**), other condition measures were more sensitive. Mice on the LP diet had significantly lower albumin concentrations ($p = 0.006$; **Figure 4B**; **Table 2**) than those on the high-protein chow. The low-protein diet also led to elevated leptin concentrations, a metabolic and immune-regulatory hormone released in proportion to body fat, as well as to higher carcass weights ($p = 0.044$; **Figures 4C,D**; **Table 2**). Infection did not affect any of these other condition measures (all $p > 0.15$; **Table 2**).

Dietary Quality Affected Fecal Metabolites

Nuclear magnetic resonance spectroscopy provides data and information on metabolites at the molecular level. The average spectrum of the 18 fecal samples, after normalization, peak alignment, and identification of some components (54), is shown in **Figure 5A**. PLS-DA (UV scaled) revealed distinct clustering by diet (**Figure 5B**), with a high proportion of variance explained by PC1 and PC2 ($R^2Y = 0.993$) and decent predictability ($Q^2 = 0.533$). The OPLS-DA (Pareto scaled) coefficient plot (**Figure 5C**) shows many positive and negative intensities, corresponding to metabolites in higher or lower relative concentrations in LP and HP diets, respectively. A great variety of sugars are present in the fecal extract, and aliphatic amino acids are clearly in higher abundance in the LP diet group (**Figure 5C**). The differences in metabolite relative abundances between the diet treatment indicates the LP diet produces clear alterations in the metabolism of the mice and/or their gut microbiota.

Dietary Quality and Infection Altered Aspects of Morphology and Behavior

The morphology and behavior of the mice was affected by diet and infection. First, infected mice had significantly heavier large intestines (emptied large intestinal tissue, weight relative to carcass weight) than uninfected mice ($p = 0.022$; **Figure 6A**; **Table 2**). Diet and infection status affected cecum size, with larger ceca in infected mice on the HP diet (diet: $p = 0.017$, infection: $p = 0.050$; **Figure 6B**; **Table 2**). Additionally, mice on the LP diet spent more time feeding than those on the HP diet ($p = 0.0004$; **Figure 6C**; **Table 2**).

Herbivory on Wild Plant Species Varied among Individuals

Our DNA metabarcoding strategy yielded a total of 1,433,421 demultiplexed sequence reads of high quality, 14,521 of which were unique. After removing putative sequencing errors and picking OTUs, our cleaned-up database comprised 3,017 OTUs representing 1,296,521 sequence reads (>90% of the original). Sequence counts per sample were uneven (range = 1,648–162,180, mean = 49,702), and all were much higher than the extraction blank ($N = 229$). After removing sequences that poorly matched the reference database and that were never >5% of reads in any sample, we were left with 82% of the raw DNA sequence reads (1,167,514; of raw DNA sequence reads). These raw DNA sequence reads represented 26 plant OTUs in subsequent analyses (Table S3 in Supplementary Material). We rarefied samples to an even depth of 1,301 sequences/sample. The six most heavily utilized wild plant families (RRA > 0.05; Table S3 in Supplementary Material) included legumes (Fabaceae, cumulative RRA across all samples = 0.32), grasses (Poaceae = 0.18), wood sorrel (Oxalidaceae = 0.12), roses (Rosaceae = 0.08), violets (Violaceae = 0.07), and asters (Asteraceae = 0.07).

Individuals varied considerably in the composition of wild plants eaten, but the overall composition of wild foods eaten did not differ between treatment groups. The composition of consumed wild plants did not differ by diet quality (perMANOVA: pseudo-$F_{1,22} = 0.83$, $R^2 = 0.03$, $p > 0.05$) or infection status (pseudo-$F_{1,22} = 0.96$, $R^2 = 0.04$, $p > 0.05$; **Figure 7A**) of the mice, at least in part reflecting the high inter-individual variation in diet composition (mean pairwise Bray–Curtis dissimilarity = 0.89). Diet compositions were more closely associated with leptin levels (pseudo-$F_{1,22} = 1.61$, $R^2 = 0.06$, $p = 0.06$; **Figure 7B**), although this trend was marginally non-significant.

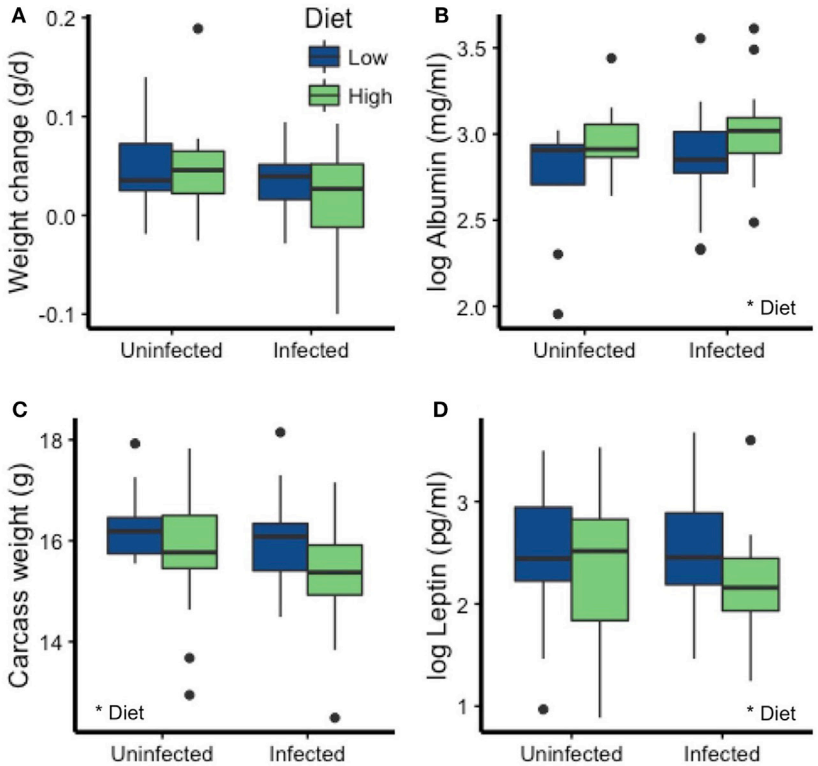

FIGURE 4 | Diet, but not infection status, affected most measures of condition. **(A)** Weight change over the course of the experiment (corrected for no. of days in the enclosure) was not affected by diet or *T. muris* infection. However, the LP diet led to reduced **(B)** albumin concentration and increased **(C)** carcass weight and **(D)** leptin levels. Asterisks denote significant effects of diet.

Nevertheless, some variation among groups in their proportional utilization of different plant types was apparent. Most strikingly, legumes (family Fabaceae) were virtually unutilized by LP-uninfected lab mice even though the mean RRA of legumes eaten by mice in other treatments ranged from ~0.3 to 0.4 (**Figure 7A**). Within Fabaceae, clover (*Trifolium* sp.) was proportionally more utilized by individuals assigned to all groups except the LP-uninfected group, while beggar's lice (*Desmodium* sp.) was proportionally more utilized by infected individuals (**Figure 7C**). Legumes tended to have higher RRA in the diets of individuals with high leptin levels, and there was a trend of decreasing Oxalidaceae and Violaceae RRA with leptin (**Figure 6B**). Lab mice from the LP-uninfected treatment utilized proportionally more Oxalidaceae (mean RRA ~0.3 vs. <0.1) and Violaceae (mean RRA ~0.2 vs. <0.1; **Figure 7A**). These trends did not, however, reflect a significant relationship ($p > 0.05$).

Effects of Infection Visible Despite Low-Intensity Infections

Perhaps due to the greater chow consumption of mice on the LP diet and increased large intestine size of infected mice, the net effects of diet and infection reveal the dynamic complexity of scaling-up this host–parasite interaction to the individual level. For example, worm counts did not differ by diet treatment (Kruskal–Wallis $\chi^2 = 0.27$, df = 1, $p = 0.60$; **Figure 8A**). Worm length also did not vary with dietary quality ($t = 0.57$, $p = 0.57$).

Costs of infection were nonetheless detectable if individual-level feeding behavior was accounted for. Although overall weight change did not vary among treatments (**Figure 4A**), mice on the LP diet spent more time feeding ($p = 0.0004$; **Figure 6C**). Examining weight gain per time feeding revealed that infected mice gained weight at a slower rate than the uninfected mice ($p = 0.042$; **Figure 8B**; **Table 2**), suggesting that they had to invest that food energy into something other than growth (e.g., the immune response) or that parasites usurped it.

DISCUSSION

Above all, this study shows that a broad perspective on the resource demands of parasites and immunity is needed to understand mammalian defense. In order to gain this understanding as well as insight into the ecology and evolution of host defenses in general, we must incorporate behavioral as well as physiological responses to resource limitation and infection. Using diverse data types, we discovered that within-host dynamics of infection and defense were strongly impacted by the interactions of the host with its wider environment. Most importantly, effects of infection, in terms of reduced weight gain, were only visible after accounting for variation in individual feeding behavior,

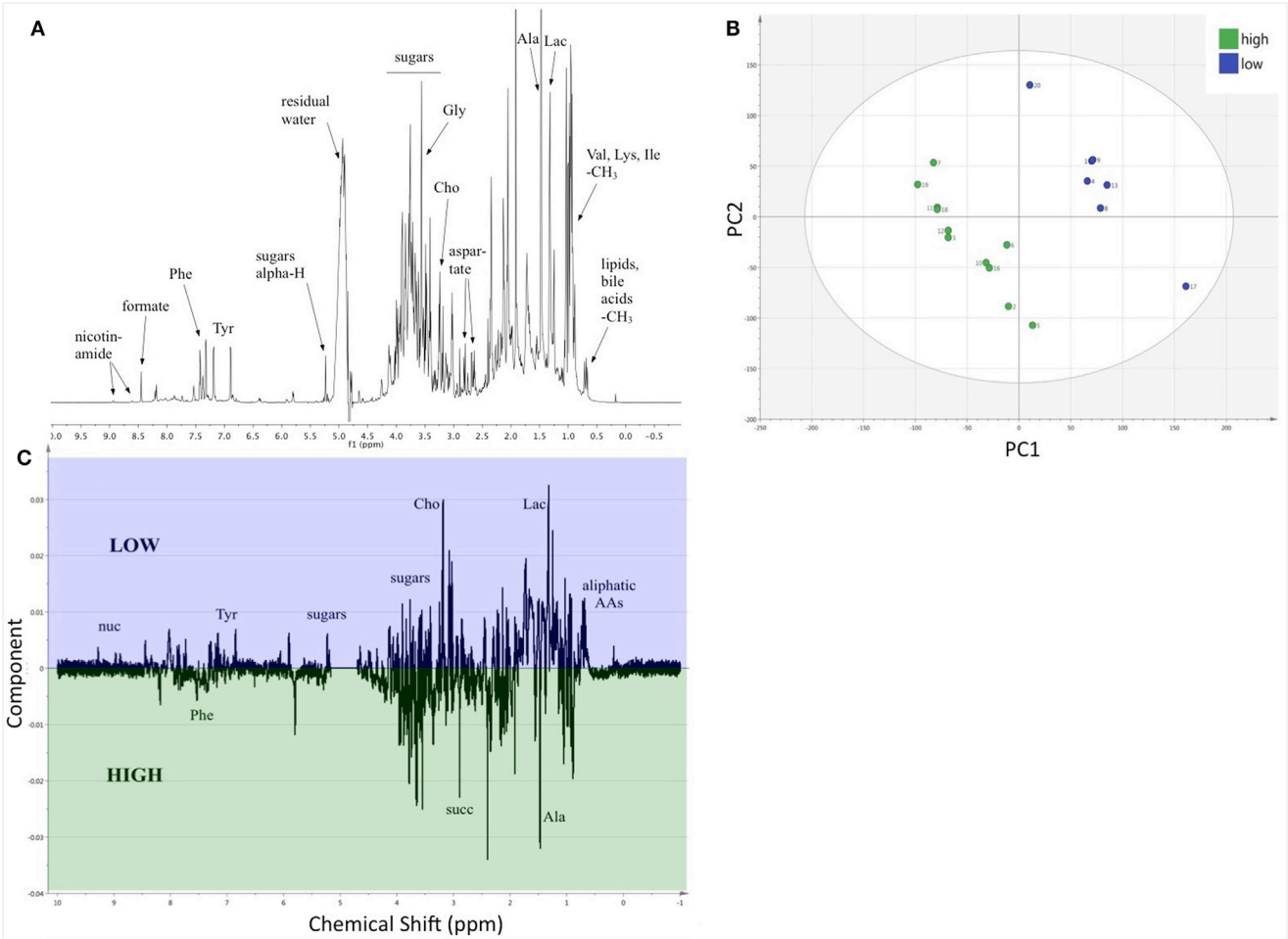

FIGURE 5 | The relative composition of fecal metabolites differed between the two diets. **(A)** A representative ^{1}H-NMR spectrum, the average of the 18 samples, with identification of selected metabolites. **(B)** PLS-DA scores plot (UV scaling); the subgroups of mice on HP and LP diets are clearly separated into distinct clusters. For three components R^2Y(cum) = 0.993 and Q^2(cum) = 0.533, showing decent validity of the statistics. The ellipse denotes Hotelling's T2. **(C)** Loading data along the NMR spectrum (Pareto scaling) reveals that there are a great number of metabolites, which are present in distinct quantity in the separated clusters of samples. All the negative intensities belong to peaks of metabolites, which are present in greater quantity in the cohort on HP diet (green), while the positive intensities depict metabolites in larger concentration in the LP diet group (blue), respectively. Some tentative assignments are shown on the plot. Abbreviations: AAs, amino acids; Ala, alanine; Cho, aldehydes; Gly, glycine; Ile, isoleucine; Lac, lactones; Lys, lysine; nuc, nucleic acids; Phe, phenylalanine; Tyr, tyrosine; succ, succinate; Val, valine.

highlighting the complexity of resource–immune–infection relationships at the individual scale. In the sections below, we discuss each aspect of our results in detail before returning to the broader implications in a concluding section.

Dietary Quality and Infection Affected Immunity but Not Parasite Loads

The 6% protein (low protein) chow reduced investment in both IgG1 and IL13. The direction of the effect of dietary protein on IgG1 responses to *T. muris* E/S antigen, the predominant antibody response to primary infection (61), was difficult to predict since both higher and lower responses are reasonable given previous studies. In the lab, higher IgG1 antibody concentrations during protein restriction were documented in mice infected with *T. muris* (14). However, mice infected with the nematode *Heligmosomoides polygyrus* experience lower levels of total IgG1 (15) when fed a 3% protein diet. Interestingly, a 7% protein diet permitted total IgG1 levels indistinguishable from those in mice fed a 24% protein diet (15). Similarly, the reduction in IL13 on the LP diet was not a certainty; in a previous laboratory experiment, IL13 concentrations did not vary with dietary protein level in mice infected with *H. polygyrus* (27). Spleen size was not sensitive to dietary protein, a somewhat unexpected result given that low-protein diets reduce spleen size during *H. polygyrus* infection (15, 34). However, differences between these nematodes in their infection sites (small intestine vs. cecum) and the immune responses they typically induce in C57BL/6 mice (Treg vs. Th2) (62), could account for their different effects in protein-limited hosts.

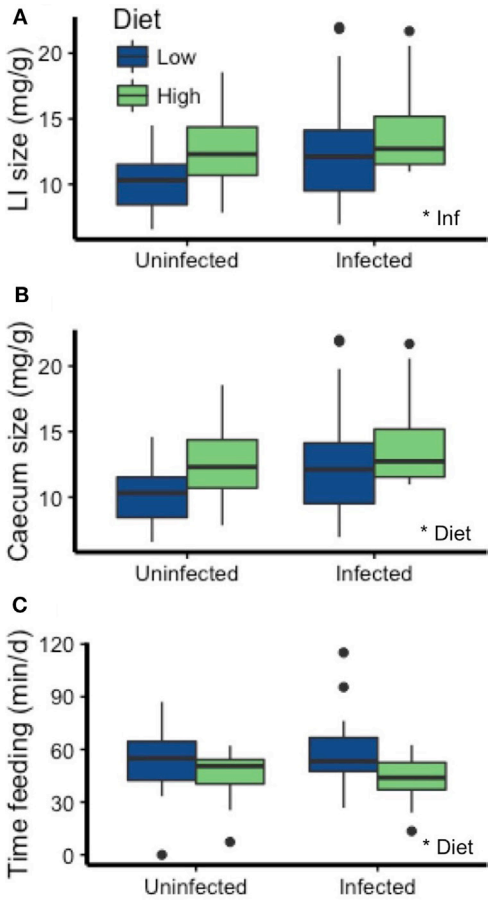

FIGURE 6 | Mouse physiology and feeding behavior were affected by infection and diet. **(A)** Infection was associated with a heavier large intestine size (emptied of contents, relative to carcass weight), whereas **(B)** the HP diet was associated with a heavier cecum relative to carcass weight. **(C)** Mice on the LP diet spent more time feeding than mice on the HP diet. Asterisks denote significant effects of diet or infection (Inf).

The reductions in IgG1 and IL13 could be due to direct effects of protein limitation on T- and B-cell function, which are known to be regulated by host metabolic activity (63, 64). Indeed, trade-offs between markers of protein nutrition and worm-specific antibodies to the nematode *Teladorsagia circumcinta* were visible in a wild Soay sheep population. Moreover, these trade-offs predicted overwinter survival with nutrition increasing survival for older individuals while investment in immunity led to greater survival odds for young sheep (37). Alternatively, the elevated carcass weights and leptin concentrations of the LP mice, due to increased chow consumption, suggest they had a higher body fat content than HP mice. Food intake in uninfected mice may be regulated by dietary protein content (65). Increased chow consumption, weight, and leptin levels have also been detected in mice fed a low-protein diet in previous nematode infection-diet manipulation experiments (27, 66). Carcass weight has been posited as an indicator of tolerance during helminth infection (67), but our data suggest that compensatory feeding may disrupt that association. Obesity is associated with pro-inflammatory responses (68), which may be mediated in part by leptin (6, 69, 70). Thus, the reduced IgG1 and IL13 levels could be a consequence of the fatter LP mice shifting from Th2 responses to pro-inflammatory Th1 responses. Although it is a common finding across multiple nematodes (27, 66), it remains unknown whether protein limitation itself or increased body fat due to limitation-induced overeating drive the pro-inflammatory shift during protein limitation.

Given how integral IgG1 and IL13 are to the development of an effective Th2 response to *T. muris* infection (61, 71), it is surprising—and contrary to our initial hypotheses regarding potential relationships between diet and immunoparasitological outcome—that parasite load did not differ between the dietary treatments. IgG1 levels in uninfected HP mice were much higher than those in uninfected LP mice, which contributed to the overall effect of diet on IgG1 levels. Among infected mice, IgG1 levels were more similar across diets, offering a potential explanation for their indistinguishable worm counts. Yet, among infected mice, IL13 concentrations were over 70 times higher in mice eating the HP diet, so it is unclear why that did not translate to differences in parasite load. Across both diets, infected mice had cleared most of their parasites by the time they were sampled at the end of the study. Due to this clearance rate and the high numbers of individuals with below-detection immune responses, there was insufficient statistical power to examine individual-level variation in immunity and its relation to parasite load. The treatment-level patterns suggest that perhaps the lower concentrations of IL13 in the mice given the LP diet were also sufficient to reduce *T. muris* survival by that time point, while those on the HP protein treatment had excess expression. Alternatively, the higher IL13 concentration (generated by stimulating MLN cells with *T. muris* antigen), might indicate the strength of the memory response. Thus, mice on the HP diet might be better protected during reinfection, a pattern also seen during protein limitation and infection with *H. polygyrus* (27, 34).

The low worm counts are surprising, given the 5.5-fold higher loads observed at a similar time point in a prior experiment (mean ± SE; Leung et al.: 34.2 ± 7.7 worms, this experiment: 6.1 ± 1.9 worms) in these same enclosures with similar mouse age and weight at infection, enclosure acclimation time, experiment duration, and parasite dosing performed by the same technician (See text footnote 1). The number of dpi was a strong predictor of worm counts, which declined quickly over time. If sampled sooner, differences in burden between diet treatments may have been more detectable. However, this rate of decline was indistinguishable from the prior experiment (See text footnote 1), and thus cannot explain the overall lower worm counts.

Instead, differences in hatching ability between batches of *T. muris* eggs, differential availability or composition of supplementary forage, slightly different sampling time points and/or effects of the different brand and composition of chow could contribute to the disparity in worm counts between experiments. For example, although the chow used by Leung et al. (See text footnote 1) had a similar macronutrient composition to the HP diet in this study, the highly refined ingredients in the specialty diet might have altered the gut microbial flora, reduced *T. muris* hatching,

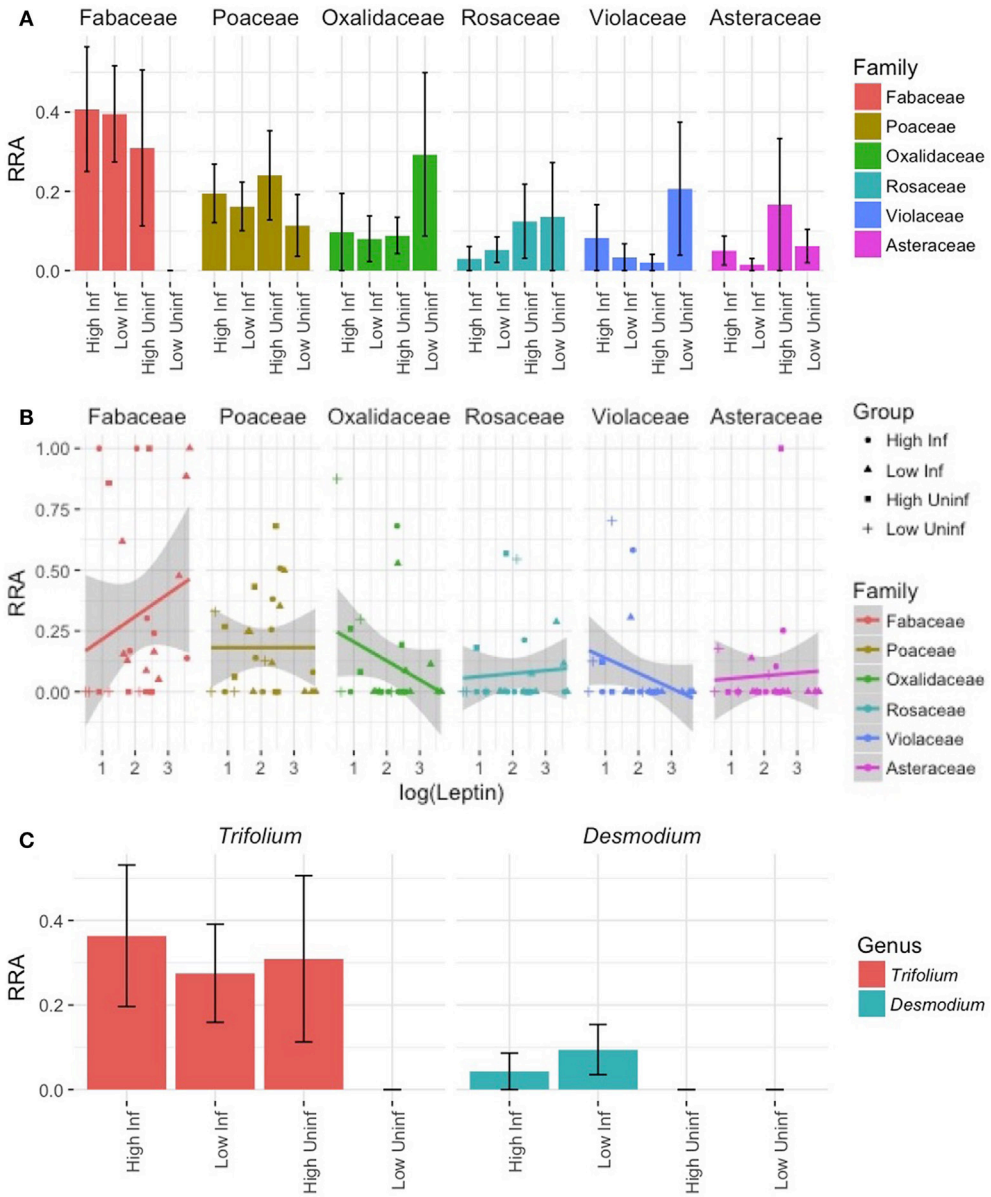

FIGURE 7 | Dietary DNA metabarcoding revealing the diversity of wild plants eaten by lab mice. **(A)** The mean (±SE) relative read abundances (RRA) of plants representing the top-6 most heavily utilized families of wild plants reveal considerable dietary variation within and among treatment groups. Families are ordered according to decreasing total RRA across all samples. **(B)** The correlations between leptin, a measure of body fat, and the RRA of plant families in each sample suggest differing relationships, but none reached significance (all $p > 0.05$). **(C)** Within the family exhibiting the highest overall RRA (Fabaceae), an OTU-representing *Trifolium* (clover) was common in all but the LP-uninfected treatment and an OTU-representing *Desmodium* (beggar's lice) was eaten only by infected mice.

made the intestines a less hospitable environment for *T. muris*, and/or increased the efficacy of mouse immune defenses. This is an important area of future inquiry. In any case, IgG1 and IL13 data confirm that the mice in the current study were infected for long enough to stimulate an immune defense to *T. muris*.

Dietary Quality Affected Fecal Metabolites

In the uninfected mice, the dietary quality significantly altered the nutrient environment within the mouse; in infected hosts, *T. muris* would likely experience similar nutrient alterations. Estimating cecum nutrient content from those in feces using NMR revealed that sugar metabolites varied greatly between diets, and amino acids like phenylalanine and alanine were higher in the HP group. This is not surprising given that the difference in protein between the treatments was compensated with a higher percentage of carbohydrates to achieve equal calorie density. Relative abundances of tyrosine, which is involved in the regulation of immune signaling pathways (72), and the aliphatic amino acids tended to be higher among mice on the LP diet. This preliminary exploration demonstrates that NMR metabolite

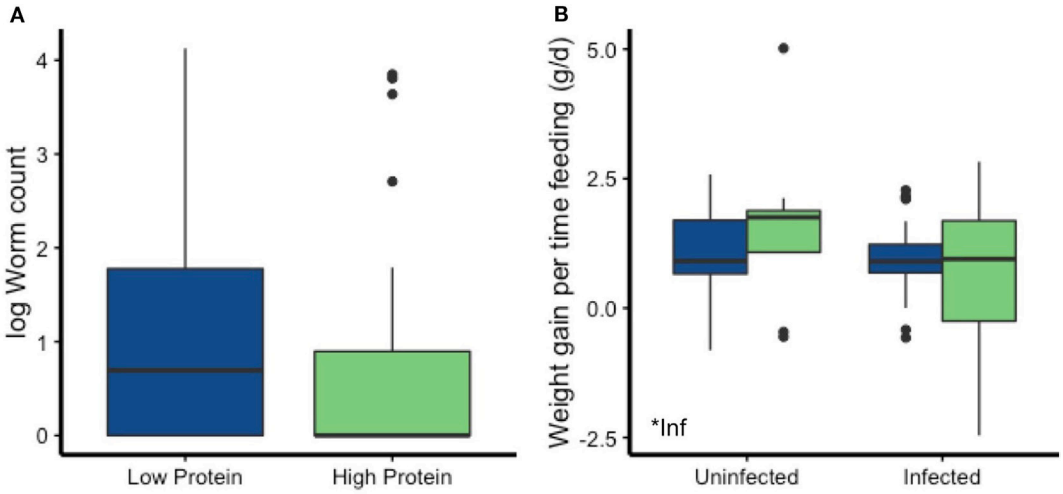

FIGURE 8 | Despite there being no differences in worm counts by diet, infected mice gained less body weight than uninfected mice when corrected for time spent feeding. **(A)** Among infected mice, worm counts did not differ by diet. **(B)** Infection status affected weight gain for the amount of time individual mice spent feeding.

analysis is a powerful, non-species-specific tool for examining host nutrition. Further analysis can include 2D NMR and spiking to identify additional metabolites, quantification of absolute concentrations using reference samples [PULCON method (73)], and metabolic pathway analysis [STOCSY (74)]. Despite differences in the nutrient environment revealed by NMR, *T. muris* counts and length did not differ between the dietary treatments. *T. muris* may feed on intestinal tissues and secretions (75, 76), rather than host blood or ingesta. *T. muris* also strongly affects, and is affected by, the host intestinal microbiome (76–78), so any changes in metabolic profile that alter microbiome composition could potentially have stronger effects on *T. muris* hatching, development, and survival. Future work could explore how host gut microbiome and metabolites effect *T. muris* infection success, and in turn, how they are affected by helminth infection.

Dietary Quality and Infection Altered Aspects of Morphology and Behavior

Our data support the hypothesis that mice attempted to compensate for differences in the protein composition of the chow by altering their physiology and behavior. Mice spent 30% more time eating the LP diet per day, a significant time investment that could also come with increased predation risk in fully natural settings (79). While this investment could partially close the gap in protein acquisition between treatments, consumption would need to be 400% higher in the LP treatment to achieve similar protein levels to individuals on the HP diet. However, dietary protein does not affect host metabolic rate (16), so maintenance costs (**Figure 1**) are likely similar between treatments. Insects were also present in the enclosures and diet metabarcoding tools could be used in future studies to examine if, and to what degree, lab mice are able to utilize them as a food source. Albumin was reduced on the LP diet, revealing protein limitation within those hosts. Albumin's primary role is maintaining osmotic pressure in the blood (80), and, in wildlife, lower levels can reflect costs of reproduction (81) and indicate reduced survival probability in wildlife (37).

Interestingly, the choice of supplemental wild forage was marginally associated with differences in leptin concentrations. Leptin concentrations tended to be higher in animals that ate proportionally more plants in the legume family, Fabaceae, which includes clover (*Trifolium* sp.) and beggar's lice (*Desmodium* sp.). These plants have a higher protein content and are widely known to be good forage for livestock and wildlife (82), even increasing sheep weight gain by an average of 40% compared with feeding on ryegrass alone (83). Thus, behavioral compensation for immunological or infection costs may explain the trend toward higher consumption of these plants in infected mice. Conversely, lab mice that ate proportionally more plants in the families Oxalidaceae (*Oxalis* sp.; wood sorrel) and Violaceae (Viola sp.) tended to have low leptin levels. Mice consumed similar amounts of chow in the enclosures (g chow/g mouse) as they did in the laboratory setting, so wild plants probably do not represent a replacement food source for most individuals. We cannot quantify the *amount* of wild plant matter eaten by mice in the different treatments using DNA metabarcoding, but these emerging trends are suggestive of compensatory foraging behaviors worth further investigation.

Infected mice found physiological ways to compensate for the costs of *T. muris* infection, rather than following our alternate hypotheses of increased foraging or infection-induced inappetence. The increased cecum size of infected individuals could be a consequence of parasite manipulation to create more habitat space, but the increase in large intestine size with infection is more difficult to explain. Large intestines, emptied of contents and relative to body size, were over 10% heavier in infected mice. This additional weight was not due to the worms themselves, which were located in the cecum. In the average size mouse, this difference translates to a 15-mg increase in colon weight. Hosts

could increase colonic tissues to enhance water balance, nutrient reabsorption, or house more commensal microbes to aid in digestion. Similarly, *H. polygyrus*, which resides in the small intestine, is associated with increased investment in small intestine tissues (67). An influx of immune cells or an increase in gut microbe communities could also contribute to these differences; this hypothesis could be examined histologically in future studies. However, given estimates of approximately 1 pg per *E. coli* cell (84) and 2.2 pg per lymphocyte (85), they cannot fully account for the increase in colon size in *T. muris*-infected mice.

To some degree, infected mice may also supplement their food intake with clovers. This trend was driven by a lack of beggar's lice in feces of uninfected mice and an absence of clover in LP-uninfected mice. Plants in the Fabaceae family, including clovers and beggar's lice, tend to be high in protein (82), and that could help hosts either resist infection by providing more resources for immune defense or tolerate infection by compensating for costs of infection and immune defense. A larger sample size, particularly of LP-uninfected mice, would help elucidate the efficacy and generality of this potential behavioral compensation mechanism. At this stage, however, we can conclude that infected mice gained less weight per minute of chow feeding than uninfected mice, despite increased large intestine size and use of potentially high-protein wild forage. This in turn suggests that their compensation for the costs of infection (e.g., parasite resource theft, elevation of immune defenses, tissue repair, etc.) was incomplete.

CONCLUSION

Ultimately, biomedical and evolutionary immunology both aim to explain how resource costs of immunity and infection at the cellular level scale up to the whole organism embedded in its natural environment. Seeking such an explanation—and indeed bridging from biomedical to evolutionary immunology—requires altered experimental designs that allow organisms to modify both their behavior and physiology in response to infection. An experimental approach is critical given the plausibility of alternate hypotheses (e.g., increased or reduced investment in immunity with a high-protein diet; increased or reduced foraging in response to parasite infection). Laboratory mice in semi-natural enclosures such as those studied here provide such an opportunity. The enclosures provided an environment with natural thermal regimes and space for activity (e.g., foraging, digging burrows) that could generate stronger energetic demands, and therefore stronger trade-offs than under typical laboratory conditions. Given the importance of gut microbiomes in *T. muris* infection (76–78) and in nutrition–immune interactions in general (19, 86, 87), the more diverse gut microbiomes generated by the enclosures (See text footnote 1) likely provide more realistic results than laboratory settings would. Additionally, this system shows potential for future studies of microbiome-helminth-diet interactions pertinent to the increasing rates of diseases linked to nutrition and immune dysregulation in developed nations (e.g., diabetes, obesity, autoimmune disorders). Our custom-built feeding monitoring system and dietary DNA metabarcoding allowed detection of compensatory feeding on chow and wild plants, respectively, that otherwise masked effects of infection.

By investigating lab mice, we were able to utilize a large suite of physiological and immunological tools, which proved useful given their variable responses to protein and infection. Much work remains to deploy such tools and new experimental designs to definitively dissect the mechanisms of the host–parasite interaction. In semi-natural enclosures, we observed high inter-individual variation that reduces statistical power and, therefore, requires much larger sample sizes than traditional laboratory studies. For example, the relationship between infection and weight gain was just above the significance threshold ($p = 0.052$), but our power to detect an effect with total sample size of 80 individuals was only 0.45, far below the ideal power of 0.8. Thus, although we failed to detect an effect of infection on weight gain, we cannot conclude that *T. muris* does not affect mouse weight gain. Indeed, once we corrected for variation in weight gain due to time spent feeding, an effect of infection on weight gain was detectable ($p = 0.042$). Additionally, to prevent uncontrolled disease transmission and "contamination" of the enclosures with parasite eggs, we ended the experiment before *T. muris* could develop into adults, which may be a more energetically costly parasite life-stage. Longer term studies and those with trickle infections (i.e., small doses over time) will provide additional insight into this host–parasite interaction. Finally, variation in individual movement and thermoregulatory behavior is difficult to monitor in the enclosures, but may contribute to overall energy budgets and weight gain. With some weatherproofing alterations, remote activity monitoring systems such as those developed to study the activity of barn mice (88), plus temperature-sensing chips, could be a useful addition to such field enclosure studies.

Nonetheless, examining the interactions among diet, nutrients, immunity, and parasites in a realistic context revealed the central role of feeding behavior in infection outcomes and the complexity of interactions among environmental resources and within-host dynamics. Future experiments must therefore account for behavioral heterogeneity among individuals if we are to elucidate costs of parasitism and defense. Moreover, in the wild, altering feeding behavior in response to infection is a strategy available to individuals, but it may come with costs in terms of energy spent foraging, predation risk, and less time available for other behaviors (e.g., reproduction). Housing laboratory mice in outdoor enclosures provided new insights into the resource costs of immune defense to helminth infection and how hosts modify their feeding behavior to compensate for those costs.

ETHICS STATEMENT

This research was conducted in accordance with animal care protocols approved by the Princeton University Animal Care and Use Committee (Protocol no. 1982-14).

AUTHOR CONTRIBUTIONS

SB and AG designed the study, with intellectual contributions from CC and AL. SB, CH, and AG carried out the experiment and performed immune and condition measurements. QC and

RG designed and built the feeding monitoring system. Diet metabarcoding was performed by CH and TK, and analyzed by SB and TK. NMR was performed and analyzed by IP. SB analyzed the data (unless otherwise noted) and wrote the manuscript. All coauthors provided editorial feedback.

ACKNOWLEDGMENTS

We thank Sriveena Chittamuri, William Craigens, Justine Hamilton, Jackie Leung, Daniel Navarrete, Rebecca Neill, Hannah Priddy, Rob Pringle, Ross Pringle, and Alison Salamandran for assistance in the lab and field. P'ng Loke and Rowann Bowcutt kindly provided *T. muris* parasites. We also thank J. Leung for comments on the draft manuscript. Funding was provided by the Princeton University's Department of Ecology and Evolutionary and Center for Health and Wellbeing, and National Science Foundation Research Experience for Undergraduates program (DBI—1358737). License for the SIMCA software was generously provided for student use by Umetrics (Umea, Sweden).

SUPPLEMENTARY MATERIAL

The Supplementary Material for this article can be found online at http://www.frontiersin.org/articles/10.3389/fimmu.2017.01914/full#supplementary-material.

FIGURE S1 | Interferon gamma (IFNg), interleukin 10 (IL10), and interleukin 17 (IL17) concentrations were higher in infected mice than uninfected mice (Wilcoxon tests; IFNg: $W = 506$, $p = 0.046$, IL10: $W = 483$, $p = 0.010$, IL17: $W = 441$, $p = 0.0036$), but did not vary with diet (IFNg: $W = 843$, $p = 0.67$, IL10: $W = 929$, $p = 0.13$, IL17: $W = 899$, $p = 0.28$).

REFERENCES

1. Fittkau EJ, Klinge H. On biomass and trophic structure of the Central Amazonian rain forest ecosystem. *Biotropica* (1973) 5:2–14. doi:10.2307/2989676
2. McNaughton SJ. Ecology of a grazing ecosystem: the Serengeti. *Ecol Monogr* (1985) 55:260–94. doi:10.2307/1942578
3. Lindeman RL. The trophic-dynamic aspect of ecology. *Ecology* (1942) 23:399–417. doi:10.2307/1930126
4. Thompson RM, Brose U, Dunne JA, Hall RO, Hladyz S, Kitching RL, et al. Food webs: reconciling the structure and function of biodiversity. *Trends Ecol Evol* (2012) 27:689–97. doi:10.1016/j.tree.2012.08.005
5. Cressler CE, Nelson WA, Day T, McCauley E. Disentangling the interaction among host resources, the immune system and pathogens. *Ecol Lett* (2014) 17:284–93. doi:10.1111/ele.12229
6. Fernandez-Riejos P, Najib S, Santos-Alvarez J, Martin-Romero C, Perez-Perez A, Gonzalez-Yanes C, et al. Role of leptin in the activation of immune cells. *Mediators Inflamm* (2010) 2010:e568343. doi:10.1155/2010/568343
7. Ponton F, Wilson K, Holmes AJ, Cotter SC, Raubenheimer D, Simpson SJ. Integrating nutrition and immunology: a new frontier. *J Insect Physiol* (2013) 59:130–7. doi:10.1016/j.jinsphys.2012.10.011
8. Buck MD, O'Sullivan D, Pearce EL. T cell metabolism drives immunity. *J Exp Med* (2015) 212:1345–60. doi:10.1084/jem.20151159
9. Frederich RC, Hamann A, Anderson S, Löllmann B, Lowell BB, Flier JS. Leptin levels reflect body lipid content in mice: evidence for diet-induced resistance to leptin action. *Nat Med* (1995) 1:1311–4. doi:10.1038/nm1295-1311
10. Cohen S, Danzaki K, MacIver NJ. Nutritional effects on T-cell immunometabolism. *Eur J Immunol* (2017) 47:225–35. doi:10.1002/eji.201646423
11. Becker DJ, Hall RJ. Too much of a good thing: resource provisioning alters infectious disease dynamics in wildlife. *Biol Lett* (2014) 10:20140309. doi:10.1098/rsbl.2014.0309
12. Ehrenford FA. Effects of dietary protein on the relationship between laboratory mice and the nematode *Nematospiroides dubius*. *J Parasitol* (1954) 40:486–486. doi:10.2307/3273912
13. Bundy DA, Golden MH. The impact of host nutrition on gastrointestinal helminth populations. *Parasitology* (1987) 95(Pt 3):623–35. doi:10.1017/S0031182000058042
14. Michael E, Bundy DAP. Protein content of CBA/Ca mouse diet: relationship with host antibody responses and the population dynamics of *Trichuris muris* (Nematoda) in repeated infection. *Parasitology* (1992) 105:139–50. doi:10.1017/S0031182000073790
15. Boulay M, Scott ME, Conly SL, Stevenson MM, Koski KG. Dietary protein and zinc restrictions independently modify a *Heligmosomoides polygyrus* (Nematoda) infection in mice. *Parasitology* (1998) 116:449–62. doi:10.1017/S0031182098002431
16. Martel SI, Riquelme SA, Kalergis AM, Bozinovic F. Dietary effect on immunological energetics in mice. *J Comp Physiol B* (2014) 184:937–44. doi:10.1007/s00360-014-0852-x
17. Budischak SA, Sakamoto K, Megow LC, Cummings KR, Urban JF Jr, Ezenwa VO. Resource limitation alters the consequences of co-infection for both hosts and parasites. *Int J Parasitol* (2015) 45:455–63. doi:10.1016/j.ijpara.2015.02.005
18. Simpson SJ, Clissold FJ, Lihoreau M, Ponton F, Wilder SM, Raubenheimer D. Recent advances in the integrative nutrition of arthropods. *Annu Rev Entomol* (2015) 60:293–311. doi:10.1146/annurev-ento-010814-020917
19. Leulier F, MacNeil LT, Lee W, Rawls JF, Cani PD, Schwarzer M, et al. Integrative physiology: at the crossroads of nutrition, microbiota, animal physiology, and human health. *Cell Metab* (2017) 25:522–34. doi:10.1016/j.cmet.2017.02.001
20. Beura LK, Hamilton SE, Bi K, Schenkel JM, Odumade OA, Casey KA, et al. Normalizing the environment recapitulates adult human immune traits in laboratory mice. *Nature* (2016) 532:512–6. doi:10.1038/nature17655
21. Abolins S, King EC, Lazarou L, Weldon L, Hughes L, Drescher P, et al. The comparative immunology of wild and laboratory mice, *Mus musculus domesticus*. *Nat Commun* (2017) 8:14811. doi:10.1038/ncomms14811
22. McSorley HJ, Hewitson JP, Maizels RM. Immunomodulation by helminth parasites: defining mechanisms and mediators. *Int J Parasitol* (2013) 43:301–10. doi:10.1016/j.ijpara.2012.11.011
23. Ramanan D, Bowcutt R, Lee SC, Tang MS, Kurtz ZD, Ding Y, et al. Helminth infection promotes colonization resistance via type 2 immunity. *Science* (2016) 352:608–12. doi:10.1126/science.aaf3229
24. Loke P, Lim YaL. Helminths and the microbiota: parts of the hygiene hypothesis. *Parasite Immunol* (2015) 37:314–23. doi:10.1111/pim.12193
25. Reese TA, Bi K, Kambal A, Filali-Mouhim A, Beura LK, Bürger MC, et al. Sequential infection with common pathogens promotes human-like immune gene expression and altered vaccine response. *Cell Host Microbe* (2016) 19:713–9. doi:10.1016/j.chom.2016.04.003
26. Cucchi T, Auffray J-C, Vigne J-D. On the origin of the house mouse synanthropy and dispersal in the Near East and Europe: zooarchaeological review and perspectives. In: Macholan M, Baird S, Munclinger P, Pialek J, editors. *Evolution of the House Mouse*. New York, NY: Cambridge University Press (2012). p. 65–93.
27. Tu T, Koski KG, Scott ME. Mechanisms underlying reduced expulsion of a murine nematode infection during protein deficiency. *Parasitology* (2008) 135:81–93. doi:10.1017/s0031182007003617
28. Gunn A, Irvine RJ. Subclinical parasitism and ruminant foraging strategies—a review. *Wildl Soc Bull* (2003) 31:117–26.
29. Huffman MA. Animal self-medication and ethno-medicine: exploration and exploitation of the medicinal properties of plants. *Proc Nutr Soc* (2003) 62:371–81. doi:10.1079/PNS2003257
30. Hutchings MR, Athanasiadou S, Kyriazakis I, Gordon IJ. Can animals use foraging behaviour to combat parasites? *Proc Nutr Soc* (2003) 62:361–70. doi:10.1079/PNS2003243
31. Hutchings MR, Kyriazakis I, Papachristou TG, Gordon IJ, Jackson F. The herbivores' dilemma: trade-offs between nutrition and parasitism in foraging decisions. *Oecologia* (2000) 124:242–51. doi:10.1007/s004420000367

32. Hall SR, Sivars-Becker L, Becker C, Duffy MA, Tessier AJ, Caceres CE. Eating yourself sick: transmission of disease as a function of foraging ecology. *Ecol Lett* (2007) 10:207–18. doi:10.1111/j.1461-0248.2006.01011.x
33. Pullan RL, Smith JL, Jasrasaria R, Brooker SJ. Global numbers of infection and disease burden of soil transmitted helminth infections in 2010. *Parasit Vectors* (2014) 7:37. doi:10.1186/1756-3305-7-37
34. Ing R, Su Z, Scott ME, Koski KG. Suppressed T helper 2 immunity and prolonged survival of a nematode parasite in protein-malnurished mice. *Proc Natl Acad Sci U S A* (2000) 97:7078–83. doi:10.1073/pnas.97.13.7078
35. Koski KG, Scott ME. Gastrointestinal nematodes, nutrition and immunity: breaking the negative spiral. *Annu Rev Nutr* (2001) 21:297–321. doi:10.1146/annurev.nutr.21.1.297
36. Povey S, Cotter SC, Simpson SJ, Lee KP, Wilson K. Can the protein costs of bacterial resistance be offset by altered feeding behaviour? *J Anim Ecol* (2009) 78:437–46. doi:10.1111/j.1365-2656.2008.01499.x
37. Garnier R, Cheung CK, Watt KA, Pilkington JG, Pemberton JM, Graham AL. Joint associations of blood plasma proteins with overwinter survival of a large mammal. *Ecol Lett* (2017) 20:175–83. doi:10.1111/ele.12719
38. Mercer JG, Mitchell PI, Moar KM, Bissett A, Geissler S, Bruce K, et al. Anorexia in rats infected with the nematode, *Nippostrongylus brasiliensis*: experimental manipulations. *Parasitology* (2000) 120:641–7. doi:10.1017/s0031182099005922
39. Stephenson LS, Latham MC, Ottesen EA. Malnutrition and parasitic helminth infections. *Parasitology* (2000) 121:S23–38. doi:10.1017/S0031182000006491
40. Panesar TS. The moulting pattern in *Trichuris muris* (Nematoda: Trichuroidea). *Can J Zool* (1989) 67:2340–3. doi:10.1139/z89-330
41. Bowcutt R, Bell LV, Little M, Wilson J, Booth C, Murray PJ, et al. Arginase-1-expressing macrophages are dispensable for resistance to infection with the gastrointestinal helminth *Trichuris muris*. *Parasite Immunol* (2011) 33:411–20. doi:10.1111/j.1365-3024.2011.01300.x
42. Taberlet P, Coissac E, Pompanon F, Gielly L, Miquel C, Valentini A, et al. Power and limitations of the chloroplast trnL (UAA) intron for plant DNA barcoding. *Nucleic Acids Res* (2007) 35:e14. doi:10.1093/nar/gkl938
43. Pompanon F, Deagle BE, Symondson WOC, Brown DS, Jarman SN, Taberlet P. Who is eating what: diet assessment using next generation sequencing. *Mol Ecol* (2012) 21:1931–50. doi:10.1111/j.1365-294X.2011.05403.x
44. Schwarz R, Kaspar A, Seelig J, Künnecke B. Gastrointestinal transit times in mice and humans measured with 27Al and 19F nuclear magnetic resonance. *Magn Reson Med* (2002) 48:255–61. doi:10.1002/mrm.10207
45. Anitha M, Reichardt F, Tabatabavakili S, Nezami BG, Chassaing B, Mwangi S, et al. Intestinal dysbiosis contributes to the delayed gastrointestinal transit in high-fat diet fed mice. *Cell Mol Gastroenterol Hepatol* (2016) 2:328–39. doi:10.1016/j.jcmgh.2015.12.008
46. Kartzinel TR, Chen PA, Coverdale TC, Erickson DL, Kress WJ, Kuzmina ML, et al. DNA metabarcoding illuminates dietary niche partitioning by African large herbivores. *Proc Natl Acad Sci U S A* (2015) 112:8019–24. doi:10.1073/pnas.1503283112
47. Boyer F, Mercier C, Bonin A, Le Bras Y, Taberlet P, Coissac E. obitools: a unix-inspired software package for DNA metabarcoding. *Mol Ecol Resour* (2016) 16:176–82. doi:10.1111/1755-0998.12428
48. Edgar RC. Search and clustering orders of magnitude faster than BLAST. *Bioinformatics* (2010) 26:2460–1. doi:10.1093/bioinformatics/btq461
49. McMurdie PJ, Holmes S. phyloseq: an R package for reproducible interactive analysis and graphics of microbiome census data. *PLoS One* (2013) 8:e61217. doi:10.1371/journal.pone.0061217
50. Core Team R. *R: A Language and Environment for Statistical Computing*. Vienna, Austria: R Foundation for Statistical Computing (2014). Available from: http://www.R-project.org/
51. De Barba M, Miquel C, Boyer F, Mercier C, Rioux D, Coissac E, et al. DNA metabarcoding multiplexing and validation of data accuracy for diet assessment: application to omnivorous diet. *Mol Ecol Resour* (2014) 14:306–23. doi:10.1111/1755-0998.12188
52. Willerslev E, Davison J, Moora M, Zobel M, Coissac E, Edwards ME, et al. Fifty thousand years of Arctic vegetation and megafaunal diet. *Nature* (2014) 506:47–51. doi:10.1038/nature12921
53. Craine JM, Towne EG, Miller M, Fierer N. Climatic warming and the future of bison as grazers. *Sci Rep* (2015) 5:16738. doi:10.1038/srep16738
54. Lin H, An Y, Hao F, Wang Y, Tang H. Correlations of fecal metabonomic and microbiomic changes induced by high-fat diet in the pre-obesity state. *Sci Rep* (2016) 6:sre21618. doi:10.1038/srep21618
55. Fonville JM, Richards SE, Barton RH, Boulange CL, Ebbels TMD, Nicholson JK, et al. The evolution of partial least squares models and related chemometric approaches in metabonomics and metabolic phenotyping. *J Chemom* (2010) 24:636–49. doi:10.1002/cem.1359
56. Oksanen J, Blanchet FG, Kindt R, Legendre P, Minchin PR, O'Hara RB, et al. *vegan: Community Ecology Package*. (2013). Available from: http://CRAN.R-project.org/package=vegan
57. Grencis RK. Immunity to helminths: resistance, regulation, and susceptibility to gastrointestinal nematodes. *Annu Rev Immunol* (2015) 33:201–25. doi:10.1146/annurev-immunol-032713-120218
58. Abbas AK, Murphy KM, Sher A. Functional diversity of helper T lymphocytes. *Nature* (1996) 383:787–93. doi:10.1038/383787a0
59. Jin W, Dong C. IL-17 cytokines in immunity and inflammation. *Emerg Microbes Infect* (2013) 2:e60. doi:10.1038/emi.2013.58
60. Chaudhry A, Samstein RM, Treuting P, Liang Y, Pils MC, Heinrich J-M, et al. Interleukin-10 signaling in regulatory T cells is required for suppression of Th17 cell-mediated inflammation. *Immunity* (2011) 34:566–78. doi:10.1016/j.immuni.2011.03.018
61. Else K, Wakelin D. Genetic variation in the humoral immune responses of mice to the nematode *Trichuris muris*. *Parasite Immunol* (1989) 11:77–90. doi:10.1111/j.1365-3024.1989.tb00650.x
62. Maizels RM, Balic A, Gomez-Escobar N, Nair M, Taylor MD, Allen JE. Helminth parasites—masters of regulation. *Immunol Rev* (2004) 201:89–116. doi:10.1111/j.0105-2896.2004.00191.x
63. MacIver NJ, Michalek RD, Rathmell JC. Metabolic regulation of T lymphocytes. In: Littman DR, Yokoyama WM, editors. *Annual Review of Immunology*. (Vol. 31), Palo Alto: Annual Reviews (2013). p. 259–83.
64. Boothby M, Rickert RC. Metabolic regulation of the immune humoral response. *Immunity* (2017) 46:743–55. doi:10.1016/j.immuni.2017.04.009
65. Solon-Biet SM, McMahon AC, Ballard JWO, Ruohonen K, Wu LE, Cogger VC, et al. The ratio of macronutrients, not caloric intake, dictates cardiometabolic health, aging, and longevity in ad libitum-fed mice. *Cell Metab* (2014) 19:418–30. doi:10.1016/j.cmet.2014.02.009
66. Athanasiadou S, Jones LA, Burgess STG, Kyriazakis I, Pemberton AD, Houdijk JGM, et al. Genome-wide transcriptomic analysis of intestinal tissue to assess the impact of nutrition and a secondary nematode challenge in lactating rats. *PLoS One* (2011) 6(6):e20771. doi:10.1371/journal.pone.0020771
67. Athanasiadou S, Tolossa K, Debela E, Tolera A, Houdijk JG. Tolerance and resistance to a nematode challenge are not always mutually exclusive. *Int J Parasitol* (2015) 45:277–82. doi:10.1016/j.ijpara.2014.12.005
68. DeFuria J, Belkina AC, Jagannathan-Bogdan M, Snyder-Cappione J, Carr JD, Nersesova YR, et al. B cells promote inflammation in obesity and type 2 diabetes through regulation of T-cell function and an inflammatory cytokine profile. *Proc Natl Acad Sci U S A* (2013) 110:5133–8. doi:10.1073/pnas.1215840110
69. Cava AL, Matarese G. The weight of leptin in immunity. *Nat Rev Immunol* (2004) 4:371–9. doi:10.1038/nri1350
70. Park H-K, Ahima RS. Physiology of leptin: energy homeostasis, neuroendocrine function and metabolism. *Metabolism* (2015) 64:24–34. doi:10.1016/j.metabol.2014.08.004
71. Bancroft AJ, Artis D, Donaldson DD, Sypek JP, Grencis RK. Gastrointestinal nematode expulsion in IL-4 knockout mice is IL-13 dependent. *Eur J Immunol* (2000) 30:2083–91. doi:10.1002/1521-4141(200007)30:7<2083:AID-IMMU2083>3.0.CO;2-3
72. Johnson P, Cross JL. Tyrosine phosphorylation in immune cells: direct and indirect effects on toll-like receptor-induced proinflammatory cytokine production. *Crit Rev Immunol* (2009) 29:347–67. doi:10.1615/CritRevImmunol.v29.i4.50
73. Wider G, Dreier L. Measuring protein concentrations by NMR spectroscopy. *J Am Chem Soc* (2006) 128:2571–6. doi:10.1021/ja055336t
74. Cloarec O, Dumas M-E, Craig A, Barton RH, Trygg J, Hudson J, et al. Statistical total correlation spectroscopy: an exploratory approach for latent biomarker identification from metabolic 1H NMR data sets. *Anal Chem* (2005) 77:1282–9. doi:10.1021/ac048630x

75. Wright KA. The feeding site and probable feeding mechanism of the parasitic nematode *Capillaria hepatica* (Bancroft, 1893). *Can J Zool* (1974) 52:1215–20. doi:10.1139/z74-161
76. Hayes KS, Bancroft AJ, Goldrick M, Portsmouth C, Roberts IS, Grencis RK. Exploitation of the intestinal microflora by the parasitic nematode *Trichuris muris*. *Science* (2010) 328:1391–4. doi:10.1126/science.1187703
77. Houlden A, Hayes KS, Bancroft AJ, Worthington JJ, Wang P, Grencis RK, et al. Chronic *Trichuris muris* infection in C57BL/6 mice causes significant changes in host microbiota and metabolome: effects reversed by pathogen clearance. *PLoS One* (2015) 10:e0125945. doi:10.1371/journal.pone.0125945
78. Holm JB, Sorobetea D, Kiilerich P, Ramayo-Caldas Y, Estellé J, Ma T, et al. Chronic *Trichuris muris* infection decreases diversity of the intestinal microbiota and concomitantly increases the abundance of *Lactobacilli*. *PLoS One* (2015) 10:e0125495. doi:10.1371/journal.pone.0125495
79. Verdolin JL. Meta-analysis of foraging and predation risk trade-offs in terrestrial systems. *Behav Ecol Sociobiol* (2006) 60:457–64. doi:10.1007/s00265-006-0172-6
80. Peters T Jr. *All About Albumin: Biochemistry, Genetics, and Medical Applications*. San Diego, CA: Academic Press (1995).
81. Schoepf I, Pillay N, Schradin C. Trade-offs between reproduction and health in free-ranging African striped mice. *J Comp Physiol B* (2017) 187:625–37. doi:10.1007/s00360-016-1054-5
82. Hoffman P, Sievert S, Shaver R, Welch D, Combs D. In-situ dry-matter, protein, and fiber degradation of perennial forages. *J Dairy Sci* (1993) 76:2632–43. doi:10.3168/jds.S0022-0302(93)77599-2
83. Nicol AM, Edwards GR. Why is clover better than ryegrass? *Proc N Z Soc Anim Prod* (2011) 71:71–8.
84. Cayley S, Lewis BA, Guttman HJ, Record MT. Characterization of the cytoplasm of *Escherichia coli* K-12 as a function of external osmolarity. Implications for protein-DNA interactions in vivo. *J Mol Biol* (1991) 222:281–300. doi:10.1016/0022-2836(91)90212-O
85. Segel GB, Cokelet GR, Lichtman MA. The measurement of lymphocyte volume: importance of reference particle deformability and counting solution tonicity. *Blood* (1981) 57:894–9.
86. Cho I, Blaser MJ. The human microbiome: at the interface of health and disease. *Nat Rev Genet* (2012) 13:260–70. doi:10.1038/nrg3182
87. Read MN, Holmes AJ. Towards an integrative understanding of diet–host–gut microbiome interactions. *Front Immunol* (2017) 8:538. doi:10.3389/fimmu.2017.00538
88. König B, Lindholm AK, Lopes PC, Dobay A, Steinert S, Buschmann FJ-U. A system for automatic recording of social behavior in a free-living wild house mouse population. *Anim Biotelemetry* (2015) 3:39. doi:10.1186/s40317-015-0069-0

Conflict of Interest Statement: The authors declare that the research was conducted in the absence of any commercial or financial relationships that could be construed as a potential conflict of interest.

frontiers in Immunology

ORIGINAL RESEARCH
published: 05 February 2018
doi: 10.3389/fimmu.2018.00056

The Immune and Non-Immune Pathways That Drive Chronic Gastrointestinal Helminth Burdens in the Wild

Simon A. Babayan[1], Wei Liu[1], Graham Hamilton[2], Elizabeth Kilbride[1], Evelyn C. Rynkiewicz[3], Melanie Clerc[3] and Amy B. Pedersen[3]*

[1] Institute of Biodiversity, Animal Health & Comparative Medicine, University of Glasgow, Glasgow, United Kingdom, [2] Glasgow Polyomics, Glasgow, United Kingdom, [3] Institute of Evolutionary Biology and Centre for Immunity, Infection and Evolution, School of Biological Sciences, University of Edinburgh, Edinburgh, United Kingdom

Parasitic helminths are extremely resilient in their ability to maintain chronic infection burdens despite (or maybe because of) their hosts' immune response. Explaining how parasites maintain these lifelong infections, identifying the protective immune mechanisms that regulate helminth infection burdens, and designing prophylactics and therapeutics that combat helminth infection, while preserving host health requires a far better understanding of how the immune system functions in natural habitats than we have at present. It is, therefore, necessary to complement mechanistic laboratory-based studies with studies on wild populations and their natural parasite communities. Unfortunately, the relative paucity of immunological tools for non-model species has held these types of studies back. Thankfully, recent progress in high-throughput 'omics platforms provide powerful and increasingly practical means for immunologists to move beyond traditional lab-based model organisms. Yet, assigning both metabolic and immune function to genes, transcripts, and proteins in novel species and assessing how they interact with other physiological and environmental factors requires identifying quantitative relationships between their expression and infection. Here, we used supervised machine learning to identify gene networks robustly associated with burdens of the gastrointestinal nematode *Heligmosomoides polygyrus* in its natural host, the wild wood mice *Apodemus sylvaticus*. Across 34 mice spanning two wild populations and across two different seasons, we found 17,639 transcripts that clustered in 131 weighted gene networks. These clusters robustly predicted *H. polygyrus* burden and included well-known effector and regulatory immune genes, but also revealed a number of genes associated with the maintenance of tissue homeostasis and hematopoiesis that have so far received little attention. We then tested the effect of experimentally reducing helminth burdens through drug treatment on those putatively protective immune factors. Despite the near elimination of *H. polygyrus* worms, the treatment had surprisingly little effect on gene expression. Taken together, these results suggest that hosts balance tissue homeostasis and protective immunity, resulting in relatively stable immune and, consequently, parasitological profiles. In the future, applying our approach to larger numbers of samples from additional populations will help further increase our ability to detect the immune pathways that determine chronic gastrointestinal helminth burdens in the wild.

Keywords: wild immunology, *Apodemus sylvaticus*, transcriptome, machine learning applied to immunology, *Heligmosomoides polygyrus*, anthelminthics

OPEN ACCESS

Edited by:
Lluis Tort, Universitat Autònoma de Barcelona, Spain

Reviewed by:
Katherine Buckley, George Washington University, United States
Jorge Galindo-Villegas, Universidad de Murcia, Spain

****Correspondence:***
Simon A. Babayan
simon.babayan@glasgow.ac.uk

Specialty section:
This article was submitted to Comparative Immunology, a section of the journal Frontiers in Immunology

Received: *07 October 2017*
Accepted: *09 January 2018*
Published: *05 February 2018*

Citation:
Babayan SA, Liu W, Hamilton G, Kilbride E, Rynkiewicz EC, Clerc M and Pedersen AB (2018) The Immune and Non-Immune Pathways That Drive Chronic Gastrointestinal Helminth Burdens in the Wild. Front. Immunol. 9:56. doi: 10.3389/fimmu.2018.00056

INTRODUCTION

Chronic helminth infections challenge our understanding of how the immune system functions. In natural populations, while individuals are continually exposed to helminth parasites, there is substantial variability in infection burdens, with some consistently showing no active infection (1, 2). This suggests that individuals can potentially control infection. In addition, while anthelminthics are commonly employed to reduce helminth burdens, after drug clearance, infections typically return to their initial burdens (3–5), suggesting that the immune system does not or cannot easily acquire complete protection against helminths. Such observations have lead to the hypothesis that hosts must balance the costs of helminth infection with the immunopathology and/or protein-energy-related costs associated with eliminating these parasites (6–8). If this trade-off exists, it suggests that the host can regulate the intensity of its immune attack on the parasites, and, alternatively, that these parasites can avoid and suppress host immune responses (9, 10). While these ideas have received substantial theoretical and experimental support, the mechanisms that underlie chronic helminth infection dynamics "in the real world," and whether or how the balance of resistance and susceptibility might change over the lifetime of an individual, either naturally or in response to vaccination, remain very poorly understood. We suggest that addressing these questions is necessary for the development of more effective and sustainable treatment and immunization against parasitic helminths, which are the leading cause of productivity loss in livestock (11–13) and remain a substantial agent of poverty in the developing world (14, 15). It is, therefore, paramount to study hosts in their natural environment, outside of the controlled laboratory, where the data may be messy, but where relationships between hosts and their natural parasite communities are the result of millions of years of coevolution and more likely to be biomedically relevant.

Identifying protective immune mechanisms in inherently variable natural populations warrants relatively large sample sizes, the possibility to manipulate parasitological, physiological, and environmental parameters, and the ability to monitor individuals repeatedly over time. The wood mouse *Apodemus sylvaticus* has been extensively studied by disease biologists since the 1960s (16, 17) and is now increasingly used for immunological studies (18, 19). It offers many of the features that originally made small rodents attractive experimental models (i.e., affordable, easy to maintain and handle, prolific breeding, and short time to maturity) and adds features that make it an ecologically and epidemiologically sound model for mammalian, including human, immunology, and parasitology (i.e., high diversity and prevalence of parasites, good trapability, large population sizes, genetic relatedness to *Mus musculus*). Indeed, *A. sylvaticus* harbors a diverse and prevalent community of parasite and pathogens that closely resembles those found in larger mammals, including humans (20–24), and domestic animals (25). Importantly, unlike *Mus musculus* which is naturally infected by very few gastrointestinal helminth parasites (26, 27), *A. sylvaticus* is the natural host of the nematode *Heligmosomoides polygyrus*, which is routinely found in >50% of wild wood mice (28) and is closely related to *H. bakeri* (29), a species extensively studied as a model of human gastrointestinal helminths that is known for its ability to suppress the immune system of its host (30). In this study, we therefore used *H. polygyrus* as a model for chronic endemic helminthiasis, and aimed to identify immune networks that regulate infection burden in a natural host–helminth system. Due to the preponderance of the laboratory mouse model in immunology, there are few, if any, reagents developed and optimized for non-model organisms (31). We, therefore, utilized a transcriptomics approach. While the genome itself provides invaluable information about immune resistance to infection (32–34), messenger RNA expression profiles provide a time- and context-sensitive picture of the immune system as it responds to antigenic stimuli. Moreover, unlike PCR and other candidate gene-driven approaches, transcriptomics allow discovery of unexpected correlates of immune protection and inclusion of physiological processes in the discovery of determinants of resistance to disease that would otherwise be overlooked in a purely immunology-focused approach.

In this study, we aimed (i) to identify gene networks that were either positively or negatively associated with *H. polygyrus* infection burden, (ii) to use those genes to identify immune pathways that promoted immunity to *H. polygyrus*, and (iii) to test whether those protective pathways were affected by sex and anthelminthic drug treatment. We used a newly published *A. sylvaticus* genome for the assembly and analysis of RNAseq samples generated from the spleens of 34 wild-caught wood mice from two distinct populations showing natural variation in helminth burdens, and then randomly treated a subset with anthelminthics to experimentally reduce their nematode infection burdens. Identifying transcripts predictive of infection burdens in a natural system, and maximizing the chances of these associations to generalize across populations requires detecting potentially weak signals among many variables, while simultaneously avoiding spurious variation (false positives). We addressed this challenge by reducing transcripts into co-expression gene networks, and identifying therein robust predictors of immunity to *H. polygyrus* using supervised machine learning—a class of statistical models that can integrate multiple variables that each carry weak signal into a stronger predictor by mapping them to a response variable, here *H. polygyrus* burdens. These types of supervised machine learning approaches hold promise for ecological and immunological studies (35, 36). We then applied a similar supervised approach to a narrower set of transcripts explicitly associated with immunity to assess how the immune system regulates its response to chronic helminth burdens in both male and female mice. To ensure that our models were not specific to a single population, time point, and sequencing platform, and thereby to increase the generalizability of our conclusions, we split samples spanning two wood mouse populations repeatedly at random into training sets on which predictive models were generated, and corresponding test sets on which the predictions of trained models were validated against observed values. Finally, given the widely reported propensity of anthelminthic-treated individuals (humans included) to return to their initial helminth burdens within weeks, we assessed whether the correlates of protection identified by our supervised learning approach were impacted by anthelminthic treatment.

MATERIALS AND METHODS

Ethics Statement

All procedures on animals were approved by the University of Glasgow ethics committee and the UK Home Office (PPL60/4572) and conducted in accordance with the Animals (Scientific Procedures) Act 1986.

Wood Mouse Field Treatment and Sampling

To minimize false discovery and ensure that our findings could generalize to other wood mouse populations, we included samples from two geographically and temporally distinct *A. sylvaticus* populations at two woodland sites: Haddon Wood (N 53.16°, W 3.1°, hereafter referred to as HW) in north-west England in 2011, and Callendar Wood (N 55.99°, W 3.78° hereafter referred to as CW) in the Central Lowlands of Scotland in 2015.

Mice were trapped using Sherman live traps (H. B. Sherman 2 × 2.5 × 6.5 inch folding trap, Tallahassee, FL, USA) baited with grain, carrot, and bedding material. Two traps were placed every 10 m in a 70 m × 70 m (total 128 traps per grid). At first capture, each individual was microchipped (AVID microchips, Lewes, UK). In CW only, mice were allocated to one of two sex-balanced groups: anthelminthic drug-treated or control. Age and reproductive status, assessed by the body mass, color of the coat, position of testes, occlusion of the vagina, and visible signs of lactation and pregnancy were also recorded. The drug treatment removed gastrointestinal nematodes, which are typically the most abundant parasites in wood mice (4). Drugs were given as a single oral dose of 2 µl g^{-1} of body weight of a mixture of 9.4 mg kg^{-1} Ivermectin and 100 mg kg^{-1} Pyrantel (IVM + PYR), and controls consisted of oral delivery of 2 µl g^{-1} of body weight of water (H_2O). Mice that were recaptured 14 ± 3 days post first capture were sacrificed on site. After cervical dislocation and exsanguination by cardiac puncture, the spleen of each individual was extracted and immediately transferred to a tube containing 4 ml RNA later, followed by whole removal of the intestine and storage in phosphate-buffered saline for subsequent dissection and parasite identification.

Parasitology

Heligmosomoides polygyrus are ingested at their third larval (L3) stage, penetrate the submucosa of the small intestine within 24 h, and migrate to the muscularis externa, where they develop into L4-stage larvae. 8–10 days after infection, adult worms begin to emerge into the lumen of the intestine and attach to the intestinal villi within ~14 days, where they mate and release eggs. We measured adult *H. polygyrus* intestinal burdens of all sacrificed mice to assess immune resistance to infection. Worm burdens are preferred over fecal egg counts because they have much lower variability and likely reflect interactions with the host's immune system during larval development. While it was not possible to measure individual level differences in exposure to parasite infective L3s in the wild, we selected mice of similar ages within both sexes, and assumed lifetime exposure levels were similar across all selected mice. Worm burdens were compared between sites (CW or HW), sexes and treatment groups using negative binomial generalized linear models because of the significant left-skew coupled with high worm prevalence, over a zero-inflated distribution.

RNA Sequencing, Assembly, Annotation, and Quantification

A transversal segment of each spleen was cut under sterile conditions, weighed, and processed following the RNeasy kit (Qiagen). RNA quantity and quality were assessed using a Tapestation (Agilent Technologies), and stored at −80 until RNA sequencing. All RNA samples were evaluated on a Bioanlayzer (Agilent Technologies) immediately prior to Poly-A selection of messenger RNA. Ten wood mice from Haddon Wood were sequenced on an Illumina Solexa 454 with 100 bp paired end reads by Edinburgh Genomics (2011). Twenty-four wood mice from Callendar wood were sequenced on an Illumina NextSeq 500 with 75 pb paired end reads by Glasgow Polyomics (2015). Raw reads generated by the sequencers were quality-checked using FastQC v. 0.11.5 (37) and sequences of low-quality and sequencer adapters trimmed using cutadapt v. 1.14 (38). The resulting trimmed reads were then quality-checked using FastQC and MultiQC (39) as above (see MultiQC report in Supplementary Data Sheet 1), and aligned to a reference transcriptome and quantified using Kallisto v. 0.43.1 (40). An *A. sylvaticus* transcriptome generated from a recently published genome (assembly ASM130590v1, https://www.ncbi.nlm.nih.gov/nuccore/LIPJ00000000.1) was used as the reference for assembly and read counts.

Transcriptome Analysis

Dimensionality Reduction

To select within the full transcriptome only the genes that had a potential role in resistance or tolerance to *H. polygyrus* across the full wood mouse transcriptome, we first grouped highly interconnected transcripts that may form distinct biological pathways by applying a weighted correlation network analysis (41) with the R package WGCNA (42). This entailed constructing gene networks (or modules) using a co-expression similarity measure defined as:

$$A_{ij} = \left(0.5 + 0.5\mathrm{cor}(x_i, x_j)\right)^{\beta}$$

where A_{ij} is the pairwise correlation between gene expressions (x_i, x_j), and β is the soft-threshold weight which is set at 6 in our analysis based on scale-free topology criterion (41). The WGCNA cluster eigengenes, which summarize the expression levels of all transcripts within each cluster, were used for further analysis as combining such clusters into biologically linked "meta-networks" as been shown to help identify biologically meaningful pathways (43–45). In addition to identifying the strongest correlates of protection across the full transcriptome, we sought to describe how genes explicitly associated with immunity might be functionally associated with *H. polygyrus* infection burdens. We, therefore, selected all genes for which the BLAST annotation contained the following immunological terms: "chemokine," "cytokine," "gata3," "immunoglobulin," "interferon," "interleukin," "platelet," "relm," "resistin," "ror-gamma," "t-bet," "TBX21," "TGF," "TNF,"

or "toll-like" for their reported roles in immunity or regulation of responses to parasitic nematodes (9, 46–49).

Supervised Learning

To identify WGCNA clusters or immune genes ("features") that may have a role in regulating *H. polygyrus* burdens, we trained supervised learning models to map them to parasite counts of untreated individuals from both CW and HW populations. All features were scaled to unit variance to ensure homoscedasticity, and worm counts were log10+1-transformed to improve machine learning algorithm performance. To predict *H. polygyrus* burdens, we used a regression analysis with the task of minimizing mean squared errors (MSE) between parasitic worm burdens observed in a test set and burdens predicted by a model trained on an independent training subset of the full dataset.

To select which algorithm was most likely to generate the best models from our data, we began by comparing the baseline performance of widely used algorithms using their default settings on the full dataset using 10-fold cross-validation: Elastic Net; k-Nearest Neighbors for Regression; Random Forest regressor; and eXtreme Gradient Boosting regressor using either a linear (GLM) booster, or a tree booster.

The full dataset was then split 75/25 into a training set and the corresponding test set 10 times repeatedly at random without replacement to avoid sampling bias affecting our choice of trained model. For each of the random train-test paired subsets, the selected algorithm was tuned on the training set using a wide range of possible parameter settings on the training subset using fivefold cross-validation, and the trained models that achieved the lowest MSE between predicted and observed burdens in the test set were retained. Summary statistics (mean and SEM) of all 50 resulting MSE, and of all 50 weights applied to each cluster within the trained models were used for ranking the importance of each gene transcript or cluster in predicting *H. polygyrus* burdens.

Statistical Analysis

Immune features (WGCNA clusters and transcripts) that contributed most to the predictive performance of each model were used as response variables in generalized linear models to assess the effects of host sex (two level factor) and anthelminthic treatment (two level factor) on their expression. To reduce type 1 errors due to multiple testing, statistical significant was considered at $p \leq 0.01$.

All data processing, machine learning, statistical analyses, and graphs were performed using Python 3.6 packages pandas (50), scikit-learn (51), statsmodels (52), and seaborn (53), respectively.

RESULTS

Infection by *H. polygyrus* Was Prevalent but Infection Intensity Varied Substantially between Individuals and Populations

As is typical of parasite burdens where a minority of the animals carry most of the infection (54), *H. polygyrus* infection burdens followed a negative binomial distribution in the 61 individuals sampled in the two field populations (CW and HW), with burdens ranging from 0 to 135 worms (**Figure 1A**). Of those, 34 adult mice selected at random with *H. polygyrus* burdens at post mortem ranging 0–86 were retained for further analysis. While worm burdens within each population did not to differ significantly between sexes (**Figure 1B**), they were markedly higher in CW than in HW (**Figure 1C**, $p < 0.0001$, $n = 22$ untreated wood mice). All males and all females from CW included in subsequent analyses were infected with *H. polygyrus*, while prevalence was 60% for the females from HW (**Figure 1B**), amounting to a 91% prevalence of *H. polygyrus* in our untreated individuals. Half of the males and females caught in CW were treated with anthelminthic drugs to test associations between transcript expression (Illumina RNA-seq counts) and gastrointestinal helminth burdens. Treatment was equally effective at reducing *H. polygyrus* numbers and prevalence in both sexes but failed to remove the parasites completely (**Figure 1C**, 60× reduction in burden $p < 0.0001$; prevalence $X^2 = 0.0007$, $n = 24$ in CW only). Taken together, these results confirm that this parasite is common in *A. sylvaticus*, suggest that *H. polygyrus* varies substantially in intensity between and within populations, and that anthelminthic treatment, while effective, did not completely eliminate gastrointestinal helminths from the treated individuals.

Transcriptome-Wide Correlates of Resistance and Susceptibility to *H. polygyrus* Were Highly Predictive of Worm Burden

To identify transcriptome-wide gene expression profiles that might explain the observed variation in worm burdens and help identify immune mechanisms that regulate *H. polygyrus* burdens in wild wood mice, we began by clustering transcripts into co-expression networks to reduce the number of variables for further analysis. WGCNA reduced the 17,639 transcripts contained in the full transcriptome to 131 clusters. We used the eigengene (or first principle component) of each cluster to capture the majority of variation of all the genes contained within that cluster. Despite differences in infection burdens reported above, we found no clustering of transcription profiles by sampling origin, sex, or treatment (Figure S2 in Supplementary Material), indicating that our sampling procedure, use of different sequencing platforms, host sex, and drug treatment did not cause transcriptome-wide biases between individuals. All 34 transcriptomes were, thus, treated as belonging to the same statistical population. To identify the clusters associated with chronic *H. polygyrus* burdens, we used a supervised learning approach with clusters entered as explanatory variables and log10+1-transformed *H. polygyrus* counts as the response variable. Only mice that were not treated with anthelminthics were considered. A comparison of machine learning algorithms using fivefold cross-validation suggested two classes of algorithms were best suited for generating models mapping gene expression clusters to *H. polygyrus* burdens, gradient boosting with a linear booster (55) and Elastic Nets (Figure S3 in Supplementary Material). Elastic Nets identified several positively and negatively

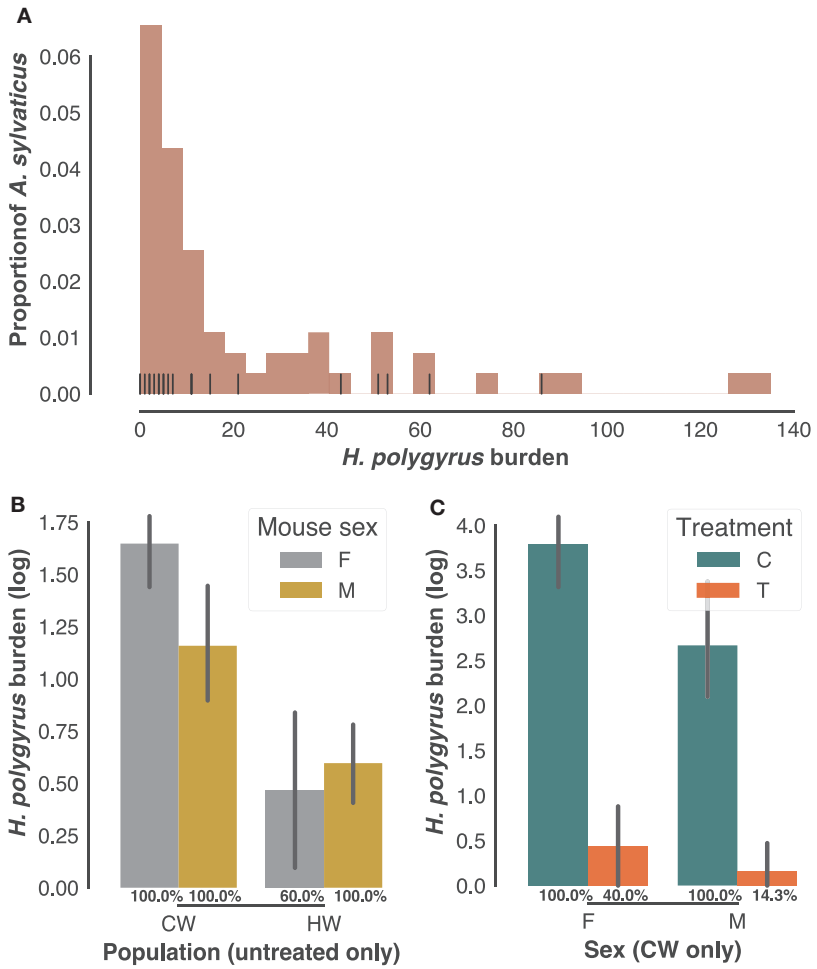

FIGURE 1 | *Heligmosomoides polygyrus* prevalence and burdens in sampled *Apodemus sylvaticus*. **(A)** Distribution of *H. polygyrus* intestinal burdens in 61 *A. sylvaticus* sampled in HW and CW (histogram) and among those the 34 individuals randomly selected for the transcriptome analysis (vertical black lines). **(B)** *H. polygyrus* burdens of untreated male (M) and female (F) mice from CW and HW. **(C)** *H. polygyrus* burdens of treated (T) and untreated controls (C) from CW only. In **(B,C)** *H. polygyrus* prevalences in each category are given as percentages, bars represent mean log-transformed worm counts and error bars show the SEM.

correlated clusters with robust statistical support. Elastic nets are particularly useful when the number of predictors is larger than the number of observations, as they tend to group together highly correlated features, a desirable behavior when selecting gene expression variables (56). Conversely, the XGBoost algorithm selected few clusters with clear positive of negative associations with worm burdens and appeared too sensitive to outliers, suggesting that it was likely to overfit (Figure S4 in Supplementary Material)—we, therefore, retained only Elastic Nets for further analysis. We then trained Elastic Nets as described in the section "Materials and Methods" on 10 randomly selected training subsets of untreated only mice from both CW and HW. The resulting models predicted log10+1-transformed *H. polygyrus* burdens in the corresponding test sets with a MSE of 0.24 ± 0.01. To identify clusters that were most informative to the prediction models, we ranked them using the Elastic Net coefficients, of which both positively- and negatively associated transcript expression networks were identified (**Figure 2A**). Within the 10 top-ranking clusters, we only retained for further analysis the five clusters that correlated significantly with worm burden at $p \leq 0.01$ (**Figure 2B**). The KEGG pathways associated with the gene transcripts that correlated positively with parasite burdens included farnesylated proteins-converting enzyme 1, ubiquitin protein ligase synthesis and terpenoid backbone synthesis, ATP-dependant RNA helicase activity, and the NOD-like receptor signaling pathway (see Table S1 in Supplementary Material for details of all clusters positively associated with worm burdens). Pathways negatively correlated with parasite burdens included apoptosis, phosphatidylinositol 3-kinase regulatory subunit binding, glucosidase activity, C2H2 zinc finger domain binding, disordered domain specific binding, protein tyrosine kinase activity, and ATP-binding cassette transporters (see Table S2 in Supplementary Material for details of all clusters negatively associated with worm burdens). Host sex did not significantly

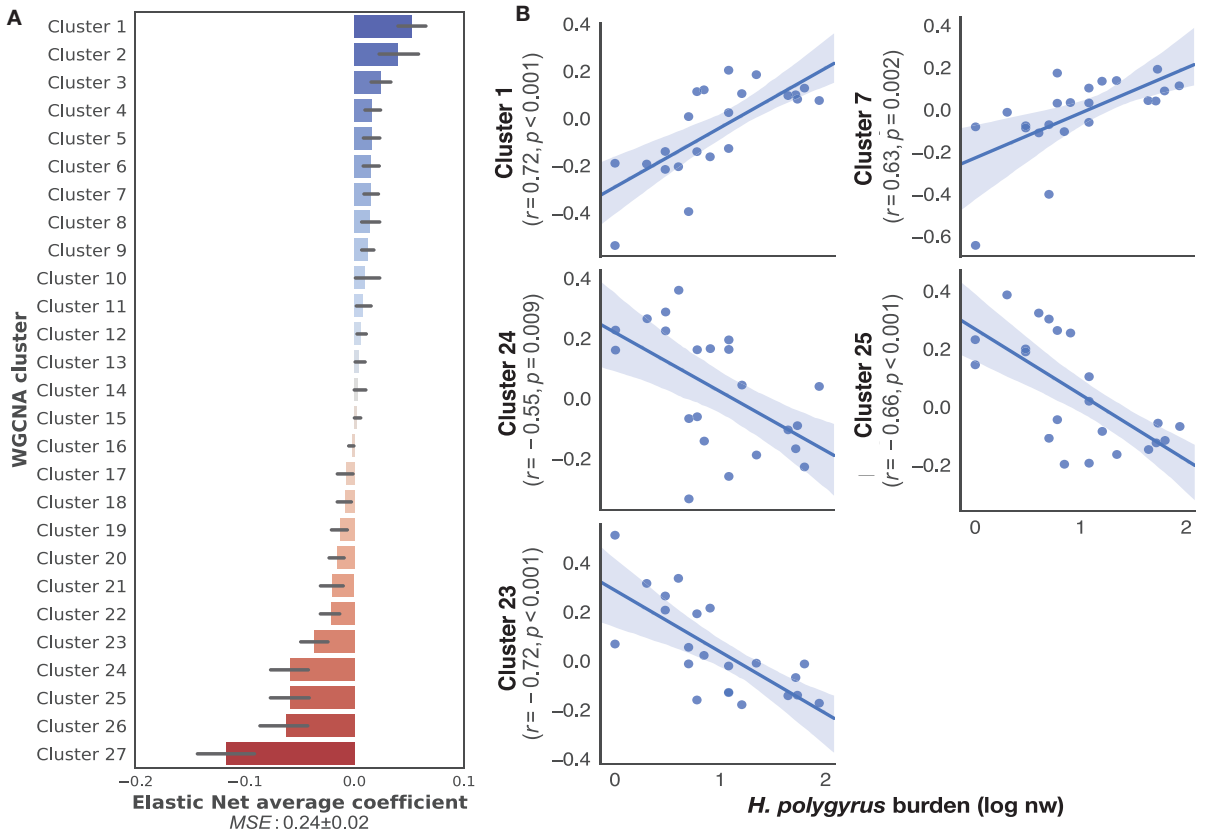

FIGURE 2 | Top gene networks predictive of chronic *Heligmosomoides polygyrus* worm burdens in wild wood mice. **(A)** Average ranking of WGCNA clusters based on Elastic Net coefficients of 50 models trained on 22 untreated wood mice from HW and CW (see Materials and Methods for description details). **(B)** Regression plots of the top five positive and negative clusters based on their coefficients against log-transformed *H. polygyrus* burdens, for which $p \leq 0.01$. Each point represents a wood mouse, the solid line is the regression line and the shaded areas represent the corresponding 95% bootstrapped confidence intervals. KEGG pathways (human and mouse) associated with: Cluster 1: ubiquitin protein ligase synthesis and terpenoid backbone synthesis; Cluster 7: ATP-dependant RNA helicase activity, NOD-like receptor signaling pathway; Cluster 24: phosphatidylinositol 3-kinase regulatory subunit binding, glucosidase activity, apoptosis; Cluster 25: C2H2 zinc finger domain binding, disordered domain specific binding; Cluster 23: protein tyrosine kinase activity, ATP-binding cassette transporters.

affect the expression of either sets of genes (Figure S5 in Supplementary Material).

Immune Gene Transcription Correlates of Resistance and Susceptibility to *H. polygyrus*

To specifically identify, within the transcriptome, only immune genes associated with the regulation of *H. polygyrus* burdens, we applied our supervised learning approach to transcripts selected on the basis of their BLAST annotations containing explicit reference to immune function (see Materials and Methods for details). This retained a list of 222 unique genes out of the 12,437 present in the full transcriptome. Elastic nets mapping those immune transcripts to log10+1-transformed *H. polygyrus* burdens predicted *H. polygyrus* burdens of mice in the test datasets with a MSE of 0.33 ± 0.02 (**Figure 3A**). Among the transcripts that contributed most to the prediction, eight were significantly ($p \leq 0.01$) correlated with parasite burden (**Figure 3B**), 2 positively—which included TGF-β-activated kinase 1 and MAP3K7-binding protein 2 (TAB 2), and dedicator of cytokinesis protein 7 (DOCK7), and 4 negatively—which included interleukin-5 receptor alpha, interleukin-17 receptor alpha, atypical chemokine receptor 3 (ACKR3), and platelet endothelial aggregation receptor 1.

Effect of Sex and Treatment on Immune Pathways Correlated with Parasite Burdens

Sex effects are widely reported to affect gastrointestinal parasite burdens (57–60). Although there was little sex bias in *H. polygyrus* burdens in our study population (**Figure 1B**; Figure S1B in Supplementary Material), we did investigate whether the expression of protective pathways identified above differed between sexes. In addition, we predicted that experimental reduction of parasite burdens through anthelminthic treatment, which had resulted in a dramatic reduction in *H. polygyrus* worm burdens (**Figure 1C**), would profoundly affect the expression of immune genes associated with responses

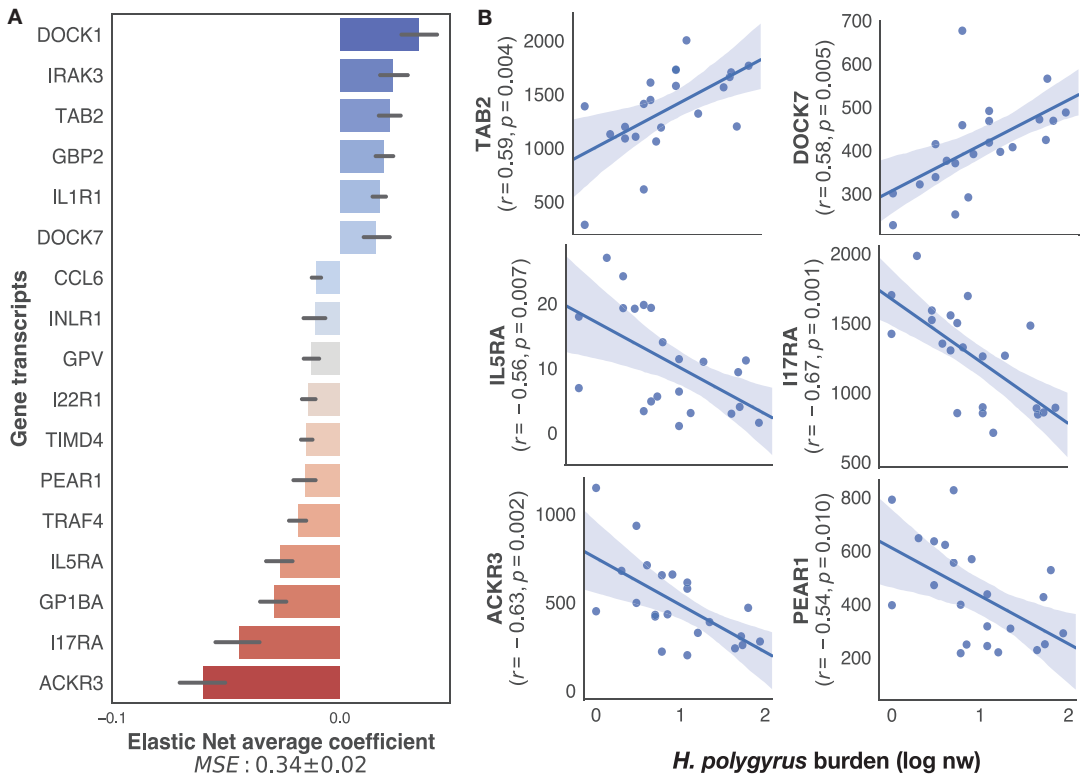

FIGURE 3 | Top immune predictors of chronic *Heligmosomoides polygyrus* worm burdens in wild wood mice. **(A)** Average ranking of immune gene transcripts based on Elastic Net coefficients of 50 models trained on 22 untreated wood mice from HW and CW (see Materials and Methods for details on immune gene selection procedure and model training). **(B)** Regression plots of the top five positive and negative clusters based on their coefficients against log-transformed *H. polygyrus* burdens, for which $p \leq 0.01$. In regression plots, each point represents a wood mouse, the solid line is the regression line and the shaded areas represent the corresponding 95% bootstrapped confidence intervals.

to these parasites. Contrary to our expectations, neither sex nor drug treatment resulted in major differences in expression of gene networks (Figure S2 in Supplementary Material), nor specifically in the expression of genes that correlated with *H. polygyrus* burdens in untreated individuals (**Figure 4**). Because our choice of Elastic Nets favored linear relationships and may, thus, have failed to identify non-linear relationships between gene expression and worm counts, we repeated the analyses above using gradient boosted trees. Consistent with expectations (Figure S3 in Supplementary Material), XGBoost achieved very similar predictive performances to the Elastic Nets (mean MSE [range] = 0.34 [0.11–3.3], Figure S6 in Supplementary Material), and of the top features, two out of the four that were significantly correlated with parasite burden were in agreement with those identified by the Elastic Nets (DOCK7 and IL17RA, Figure S6B in Supplementary Material). The two other genes identified by XGBoost were suppressor of cytokine signaling 2 (SOCS2) and interferon-stimulated 20 kDa exonuclease-like 2 (I20L2), which both showed greater variance in gene expression at intermediate parasite burdens. SOCS2 and I20L2 were expressed at only marginally different levels between treated and untreated animals ($p = 0.04$ and $p = 0.05$, respectively), and between sexes ($p = 0.15$ and $p = 0.03$, respectively) (Figure S7 in Supplementary Material).

DISCUSSION

The distribution of parasite infection burdens within a population is typically highly dispersed, with a small proportion of the hosts harboring the heaviest infections (61). Here, the prevalence of *H. polygyrus* was high in both populations studied, and remained detectable even after drug treatment. This suggests, assuming similar exposure to infection at a given age, that most individuals limited their parasite burdens but did not eliminate infection completely, consistent with reports on chronic helminth infections across diverse host species (61–63). Furthermore, drug treatment usually needs to be administered regularly to control helminth infections, as otherwise worms recrudesce within weeks (3, 5, 64). We sought to better understand how the immune system, under natural exposure and chronic helminth infection, regulates its response to infection, what immune traits allow some hosts to maintain low infection burdens, and how anthelminthic treatment and the subsequent reduction in parasite burdens impact those protective immune traits.

Addressing these questions required choosing a species that naturally harbors a diverse community of parasites at high prevalence and densities to maximize our chance of detecting the effects of their removal on the host. This ruled out *M. musculus*, which despite being a powerful model for immunology, is a

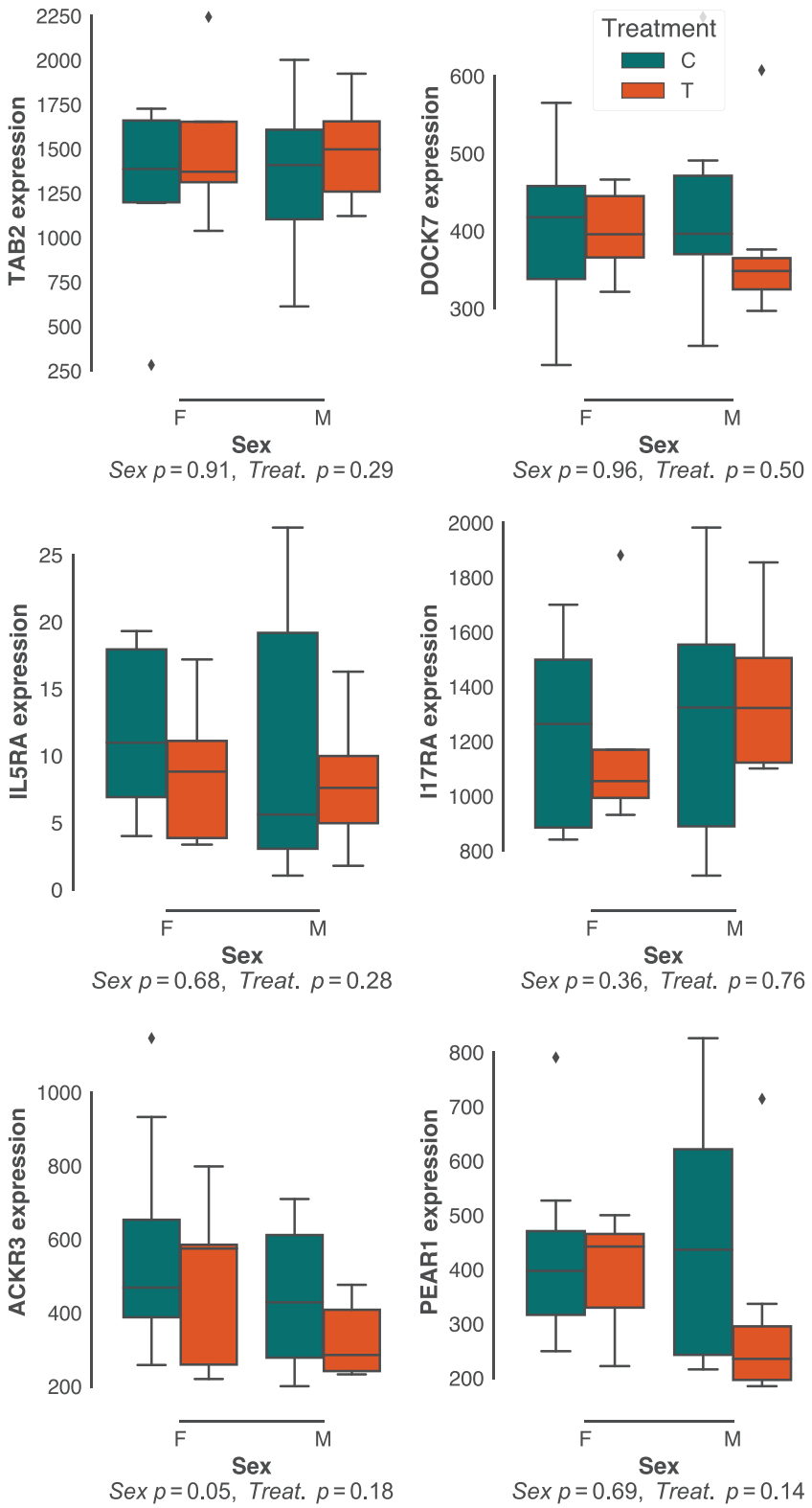

FIGURE 4 | Effects of host sex and drug treatment on protective immune gene expression. No statistically significant effects of host sex and drug treatment were detected among the best predictors of *Heligmosomoides polygyrus* burdens identified in untreated mice only. Each plot represents transcript counts scaled to unit variance but not centered. Horizontal bars represent the median, boxes represent the interquartile range, whiskers the range, and diamonds transcript counts that lay beyond 1.5× of the interquartile range.

relatively poor model for parasitology owing to the uncharacteristically low helminth infections naturally present in that species (26, 27). Wood mice, however, resemble species of greater societal importance in the diversity and prevalence of the parasite communities (21, 65). Here, we chose to focus on the gastrointestinal nematode *H. polygyrus* due to its prevalence in wood mice, and to its extensive use as a laboratory model (24, 66, 67), thus providing a powerful way to compare lab-based and field-based immune responses to this parasite. In our study populations, *H. polygyrus* was present in 91% of the wood mice we caught.

The immune system of *A. sylvaticus* is poorly known, thus we chose to take a transcriptomic approach to discover specific host–parasite interactions. In addition, having the full transcriptome also allowed us to use a candidate gene approach based on BLAST annotations. Moreover, it is likely that a significant amount of variation in chronic helminth burdens could be driven by processes not typically classified as immunological. We, therefore, decided to combine the discovery approach afforded by our sequencing of the full transcriptome with an approach focused on the genes explicitly associated with the immune system. However, RNAseq risks overestimating transcript abundance due to splicing variants, or being dominated by the more abundantly transcribed genes. While a technical solution would be to combine platforms with different read depths and lengths, here we used analytical solutions (e.g., FastQC reports of overrepresented sequences), and supervised learning to focus on transcripts that had statistically significant correlation with a biological read-out, here, parasite burdens. In short, we used parasite burdens to select the genes and co-expression networks for further analysis. By using Elastic Nets to identify correlates of parasite burdens, we ensured that redundant transcripts would feature together in the ranking of coefficients once models were trained. Yet, after removing all exact duplicates from the raw transcript counts, our models generated lists of uniquely represented genes, suggesting that for any that may have had differently expressed isoforms, only one of each correlated significantly with parasite burden.

We found that within the transcriptome, the best predictors of parasite burdens included both immune and non-immune genes. Among non-immune genes that were associated with *H. polygyrus*, were farnesylated proteins-converting enzyme 1 (FACE1), which is involved in protein hydrolysis (68), dedicator of cytokinesis protein 7 (DOCK7), which is reported to influence lipid regulation (69, 70), and proteases, helicases, and ABC transporters—genes generally involved in protein and energy metabolism, and potentially tissue growth and/or repair. Although nutrition plays an important role in resistance to helminth infections (71), how these specific pathways relate to immunity or exposure to *H. polygyrus* is currently unclear.

Examining immune genes more specifically confirmed known associations between gastrointestinal helminths and immune factors, and revealed others that merit further study. Among previously reported associations was the negative correlation between parasite burdens and the receptor for IL-5, which is the main cytokine involved in the activation of eosinophils, part of the group-2 innate lymphoid cell-driven responses to helminths in the gut (48). Also consistent with previous reports in laboratory models was the negative relationship between *H. polygyrus* and IL-17A. Indeed, this parasite has previously been reported to inhibit IL-17 production in the gut mucosa (72), and more recently, that this interaction may be mediated by a subset of gut-resident eosinophils that suppress IL-17 (47, 73–75). Furthermore, interactions between *H. polygyrus*, Th17, and regulatory T cell responses have been reported to interact with the gut microbiota and be genotype dependent. Indeed, a susceptible mouse strain has elevated IL-17 and increased proportions of *Lactobacilli* whereas in a resistant mouse strain, *H. polygyrus* has no effect on *Lactobacillus* abundance (76). In wild wood mice, these interactions are likely to be driven, in part, by seasonal changes in diet (77), which is consistent with three-way interactions observed between hosts, helminths, and their microbiota in wild seabirds (78). We also detected strong positive associations between *H. polygyrus* burdens and TAB 2 expression, which is reported to activate IL-1 *via* JNK and NF-κB (79). This is consistent with their positive correlation with the reactive oxygen species-expressing NOD-like receptor signaling pathway (80) we identified among WGCNA clusters. This suggests either an inflammatory response to *H. polygyrus* or to the damage it may cause in the gut (81), or that immune systems already skewed toward inflammation are less able to control parasitic helminths. While we did not detect clear signatures of regulatory T cell activation in the spleen, two genes potentially involved in immune regulation correlated strongly with parasite burdens: IL17RA, as mentioned above, and ACKR3, a chemokine scavenger (82) that is widely expressed in the hematopoietic system, heart, vascular endothelial cells, bone, kidney, and brain, and that is reported to be upregulated in many cancers (83) and also mimicked by a herpesvirus agonist (84, 85).

Interestingly, we did not detect significant associations between worm burdens and cytokines or chemokines, but rather with that of their receptors. Likewise, we might expect GATA-3 to correlate with *H. polygyrus* burdens, since this transcription factor is central to ILC2 initiating Th2 responses to helminths in the gut (48). This suggests that in the spleen associations between infection burdens and RNA expression of cytokine receptor genes are more statistically robust, and thus more functionally interpretable, than those between infection burdens and cytokine messenger RNA.

Having observed no significant difference between male and female mice in their parasite burdens, we also did not detect significant differences in the expression of any of the top predictors of parasite burdens, and host sex only marginally explaining the variation in the expression of ACKR3. More surprising was that a 60-fold reduction in *H. polygyrus* burdens within an individual mouse would have so little effect on the immune pathways that predict their chronic burdens. This may be due to the target of the anthelminthic drugs we used, ivermectin and pyrantel (86). The combination of immune-regulatory predictors of chronic infection burdens, the mode of action of commonly used anthelminthics, and the ensuing lack of immune response to

drug-induced worm death may explain the high reinfection rates post drug-removal (3–5).

Finally, while wood mice infected with high worm burdens may be more tolerant to infection [i.e., the ability of hosts to minimize adverse fitness consequences of increasing parasite burdens (87)], our study could not address this question satisfactorily because we did not collect data to assess fitness-relevant effects of infection nor of drug treatment in the wood mice. While recent studies suggest a complex relationship between protective immunity, resource limitation, and immunopathology (88, 89), how organisms balance the benefits of eliminating helminth infection and the costs of mounting the anthelminthic immune responses to do so is poorly understood. A further limitation of this study is its reliance on the transcriptome to assess immune responses: in the future, it will be important not only to validate our findings in additional wood mouse populations, e.g., using quantitative RT-PCR, but also to integrate protein, cellular, and metabolomic data alongside transcriptomic data (90) to reduce the risk of overlooking important processes that vary in their post-transcriptional regulation.

In conclusion, we have generated the first transcriptome for *A. sylvaticus* and identified a number of transcriptional predictors of chronic infection chronic infection burdens by *H. polygyrus* that include previously known immune pathways as well as novel candidates which merit further investigation. Notably, resolving the causal relationships between hosts, parasitic helminths and microbiota in the maintenance of immune homeostasis even in the face of drug-induced parasite removal, merits further attention. By combining two distinct wood mouse populations, integrating two different sequencing platforms, and applying machine-learning-based cross-validation procedures to map transcript expression levels to parasite burdens, we have sought to maximize the generalizability and functional relevance of our analysis of the wood mouse immune system. In the future, longer term studies and the integration of multiple biological levels, from genomes to cells, should help further our understanding of how the immune system maintains the health of the organism in its natural habitat.

ETHICS STATEMENT

All procedures on animals were approved by the University of Glasgow ethics committee and the UK Home Office (PPL60/4572) and conducted in accordance with the Animals (Scientific Procedures) Act 1986.

AUTHOR CONTRIBUTIONS

SB and AP conceived, designed, and secured funding for the study, ran the field sites, participated in the field and lab work, and wrote the manuscript. SB performed all statistics and machine learning analyses. WL performed the digital transcriptomics and helped write the manuscript. GH performed all assembly and annotation of the transcriptomes. EK extracted and quality-checked all RNA samples. MC and ER participated in the field work and analyzed the parasite samples.

FUNDING

This work and the next-generation sequencing performed by Glasgow Polyomics were supported by the Wellcome Trust ISSF grant [097821/Z/11/Z] to SB, NBAF grant (#NBAF528) to AP and SB, a targeted Institute of Biodiversity, Animal Health & Comparative Medicine Research Fellowship to SB, a Wellcome Trust Strategic Grant for the Centre for Immunity Infection and Evolution (095831 Advanced Fellowship) to AP, a University of Edinburgh Chancellors Fellowship to AP, and a National Science Foundation Postdoctoral Research Fellowship in Biology (DBI-1306608) to ER.

SUPPLEMENTARY MATERIAL

The Supplementary Material for this article can be found online at http://www.frontiersin.org/articles/10.3389/fimmu.2018.00056/full#supplementary-material.

REFERENCES

1. Hoerauf A, Brattig N. Resistance and susceptibility in human onchocerciasis – beyond Th1 vs. Th2. *Trends Parasitol* (2002) 18:25–31. doi:10.1016/S1471-4922(01)02173-0
2. Nagaraj SH, Harsha HC, Reverter A, Colgrave ML, Sharma R, Andronicos N, et al. Proteomic analysis of the abomasal mucosal response following infection by the nematode, *Haemonchus contortus*, in genetically resistant and susceptible sheep. *J Proteomics* (2012) 75:2141–52. doi:10.1016/j.jprot.2012.01.016
3. Nfon CK, Makepeace BL, Njongmeta LM, Tanya VN, Trees AJ. Lack of resistance after re-exposure of cattle cured of *Onchocerca ochengi* infection with oxytetracycline. *Am J Trop Med Hyg* (2007) 76:67–72.
4. Knowles SC, Fenton A, Petchey OL, Jones TR, Barber R, Pedersen AB. Stability of within-host-parasite communities in a wild mammal system. *Proc Biol Sci* (2013) 280:20130598. doi:10.1098/rspb.2013.0598
5. Speich B, Moser W, Ali SM, Ame SM, Albonico M, Hattendorf J, et al. Efficacy and reinfection with soil-transmitted helminths 18-weeks post-treatment with albendazole-ivermectin, albendazole-mebendazole, albendazole-oxantel pamoate and mebendazole. *Parasit Vectors* (2016) 9:123. doi:10.1186/s13071-016-1406-8
6. Mideo N, Nelson WA, Reece SE, Bell AS, Read AF, Day T. Bridging scales in the evolution of infectious disease life histories: application. *Evolution* (2011) 65:3298–310. doi:10.1111/j.1558-5646.2011.01382.x
7. Long GH, Graham AL. Consequences of immunopathology for pathogen virulence evolution and public health: malaria as a case study. *Evol Appl* (2011) 4:278–91. doi:10.1111/j.1752-4571.2010.00178.x
8. Choisy M, de Roode JC. Mixed infections and the evolution of virulence: effects of resource competition, parasite plasticity, and impaired host immunity. *Am Nat* (2010) 175:E105–18. doi:10.1086/651587
9. Ludwig-Portugall I, Layland LE. TLRs, Treg, and B cells, an interplay of regulation during helminth infection. *Front Immunol* (2012) 3:8. doi:10.3389/fimmu.2012.00008
10. Guivier E, Bellenger J, Sorci G, Faivre B, Metcalf CJE, Winn AA. Helminth interaction with the host immune system: short-term benefits and costs in relation to the infectious environment. *Am Nat* (2016) 188:253–63. doi:10.5061/dryad.7017n
11. Charlier J, De Waele V, Ducheyne E, van der Voort M, Vande Velde F, Claerebout E. Decision making on helminths in cattle: diagnostics, economics and human behaviour. *Ir Vet J* (2015) 69:14. doi:10.1186/s13620-016-0073-6

12. Coop RL, Sykes AR, Angus KW. The effect of three levels of intake of *Ostertagia circumcincta* larvae on growth rate, food intake and body composition of growing lambs. *J Agric Sci* (1982) 98:247–55. doi:10.1017/S0021859600041782
13. Coop RL, Kyriazakis I. Influence of host nutrition on the development and consequences of nematode parasitism in ruminants. *Trends Parasitol* (2001) 17:325–30. doi:10.1016/S1471-4922(01)01900-6
14. Muller O, Krawinkel M. Malnutrition and health in developing countries. *CMAJ* (2005) 173:279–86. doi:10.1503/cmaj.050342
15. Pullan R, Brooker S. The health impact of polyparasitism in humans: are we under-estimating the burden of parasitic diseases. *Parasitology* (2008) 135:783–94. doi:10.1017/S0031182008000346
16. Rioux JA, Golvan YJ. [Mange caused by *Psorergates musculinus* (Michael 1889) (Acari; Myobiidae) in the field mice *Apodemus sylvaticus* (Linne 1758) of the mass of Caroux (Herault)]. *Ann Parasitol Hum Comp* (1961) 36:785–7. doi:10.1051/parasite/1961365785
17. Pokorny J, Havlik O. [Experimental infection of *Apodemus sylvaticus L.* with leptospiras (*L. grippotyphosa*)]. *Cesk Epidemiol Mikrobiol Imunol* (1960) 9:88–92.
18. Friberg IM, Little S, Ralli C, Lowe A, Hall A, Jackson JA, et al. Macroparasites at peripheral sites of infection are major and dynamic modifiers of systemic antimicrobial pattern recognition responses. *Mol Ecol* (2013) 22:2810–26. doi:10.1111/mec.12212
19. Jackson JA, Hall AJ, Friberg IM, Ralli C, Lowe A, Zawadzka M, et al. An immunological marker of tolerance to infection in wild rodents. *PLoS Biol* (2014) 12(7):e1001901. doi:10.1371/journal.pbio.1001901
20. Goüy de Bellocq J, Charbonnel N, Morand S. Coevolutionary relationship between helminth diversity and MHC class II polymorphism in rodents. *J Evol Biol* (2008) 21:1144–50. doi:10.1111/j.1420-9101.2008.01538.x
21. Behnke JM, Eira C, Rogan M, Gilbert FS, Torres J, Miquel J, et al. Helminth species richness in wild wood mice, *Apodemus sylvaticus*, is enhanced by the presence of the intestinal nematode *Heligmosomoides polygyrus*. *Parasitology* (2009) 136:793–804. doi:10.1017/S0031182009006039
22. Poulin R. Interactions between species and the structure of helminth communities. *Parasitology* (2001) 122:S3–11. doi:10.1017/S0031182000016991
23. Montgomery SSJ, Montgomery WI. Structure, stability and species interactions in helminth communities of wood mice, *Apodemus sylvaticus*. *Int J Parasitol* (1990) 20:225–42. doi:10.1016/0020-7519(90)90105-V
24. Behnke JM, Menge DM, Noyes H. *Heligmosomoides bakeri*: a model for exploring the biology and genetics of resistance to chronic gastrointestinal nematode infections. *Parasitology* (2009) 136:1565–80. doi:10.1017/S0031182009006003
25. Taylor MA, Coop RL, Wall RL. *Veterinary Parasitology*. Oxford, UK: John Wiley & Sons (2015).
26. Abolins S, King EC, Lazarou L, Weldon L, Hughes L, Drescher P, et al. The comparative immunology of wild and laboratory mice, *Mus musculus domesticus*. *Nat Commun* (2017) 8:14811. doi:10.1038/ncomms14811
27. Beura LK, Hamilton SE, Bi K, Schenkel JM, Odumade OA, Casey KA, et al. Normalizing the environment recapitulates adult human immune traits in laboratory mice. *Nature* (2016) 532(7600):512–6. doi:10.1038/nature17655
28. Behnke JM, Lewis JW, Zain SN, Gilbert FS. Helminth infections in *Apodemus sylvaticus* in southern England: interactive effects of host age, sex and year on the prevalence and abundance of infections. *J Helminthol* (1999) 73:31–44.
29. Cable J, Harris PD, Lewis JW, Behnke JM. Molecular evidence that *Heligmosomoides polygyrus* from laboratory mice and wood mice are separate species. *Parasitology* (2006) 133:111–22. doi:10.1017/S0031182006000047
30. Maizels RM, Hewitson JP, Murray J, Harcus YM, Dayer B, Filbey KJ, et al. Immune modulation and modulators in *Heligmosomoides polygyrus* infection. *Exp Parasitol* (2012) 132:76–89. doi:10.1016/j.exppara.2011.08.011
31. Pedersen AB, Babayan SA. Wild immunology. *Mol Ecol* (2011) 20:872–80. doi:10.1111/j.1365-294X.2010.04938.x
32. Behnke JM, Menge DM, Nagda S, Noyes H, Iraqi FA, Kemp SJ, et al. Quantitative trait loci for resistance to *Heligmosomoides bakeri* and associated immunological and pathological traits in mice: comparison of loci on chromosomes 5, 8 and 11 in F2 and F6/7 inter-cross lines of mice. *Parasitology* (2010) 137:311–20. doi:10.1017/S0031182009991028
33. Beraldi D, McRae AF, Gratten J, Pilkington JG, Slate J, Visscher PM, et al. Quantitative trait loci (QTL) mapping of resistance to strongyles and coccidia in the free-living Soay sheep (*Ovis aries*). *Int J Parasitol* (2007) 37:121–9. doi:10.1016/j.ijpara.2006.09.007
34. Venturina VM, Gossner AG, Hopkins J. The immunology and genetics of resistance of sheep to *Teladorsagia circumcincta*. *Vet Res Commun* (2013) 37:171–81. doi:10.1007/s11259-013-9559-9
35. Stephens PR, Altizer S, Smith KF, Alonso Aguirre A, Brown JH, Budischak SA, et al. The macroecology of infectious diseases: a new perspective on global-scale drivers of pathogen distributions and impacts. *Ecol Lett* (2016) 19:1159–71. doi:10.1111/ele.12644
36. Urrutia A, Duffy D, Rouilly V, Posseme C, Djebali R, Illanes G, et al. Standardized whole-blood transcriptional profiling enables the deconvolution of complex induced immune responses. *Cell Rep* (2016) 16:2777–91. doi:10.1016/j.celrep.2016.08.011
37. Andrews S. *FastQC: A Quality Control Tool for High Throughput Sequence Data*. (2010). Available from: http://www.bioinformatics.babraham.ac.uk/projects/fastqc/
38. Martin M. Cutadapt removes adapter sequences from high-throughput sequencing reads. *EMBnet J* (2011) 17:10–2. doi:10.14806/ej.17.1.200
39. Ewels P, Magnusson M, Lundin S, Käller M. MultiQC: summarize analysis results for multiple tools and samples in a single report. *Bioinformatics* (2016) 32:3047–8. doi:10.1093/bioinformatics/btw354
40. Bray NL, Pimentel H, Melsted P, Pachter L. Near-optimal probabilistic RNA-seq quantification. *Nat Biotechnol* (2016) 34:525–7. doi:10.1038/nbt.3519
41. Zhang B, Horvath S. A general framework for weighted gene co-expression network analysis. *Stat Appl Genet Mol Biol* (2005) 4:Article17. doi:10.2202/1544-6115.1128
42. Langfelder P, Horvath S. WGCNA: an R package for weighted correlation network analysis. *BMC Bioinformatics* (2008) 9:559. doi:10.1186/1471-2105-9-559
43. Langfelder P, Horvath S. Eigengene networks for studying the relationships between co-expression modules. *BMC Syst Biol* (2007) 1:54. doi:10.1186/1752-0509-1-54
44. Albert R. Scale-free networks in cell biology. *J Cell Sci* (2005) 118:4947–57. doi:10.1242/jcs.02714
45. Horvath S, Zhang B, Carlson M, Lu KV, Zhu S, Felciano RM, et al. Analysis of oncogenic signaling networks in glioblastoma identifies ASPM as a molecular target. *Proc Natl Acad Sci U S A* (2006) 103:17402–7. doi:10.1073/pnas.0608396103
46. Wynn TA. Type 2 cytokines: mechanisms and therapeutic strategies. *Nat Rev Immunol* (2015) 15:271–82. doi:10.1038/nri3831
47. Pathak M, Sharma P, Sharma A, Verma M, Srivastava M, Misra-Bhattacharya S. Regulatory T-cell neutralization in mice during filariasis helps in parasite clearance by enhancing T helper type 17-mediated pro-inflammatory response. *Immunology* (2016) 147:190–203. doi:10.1111/imm.12550
48. Pelly VS, Kannan Y, Coomes SM, Entwistle LJ, Rückerl D, Seddon B, et al. IL-4-producing ILC2s are required for the differentiation of TH2 cells following *Heligmosomoides polygyrus* infection. *Mucosal Immunol* (2016) 9(6):1407–17. doi:10.1038/mi.2016.4
49. Anthony RM, Rutitzky LI, Urban JFJ, Stadecker MJ, Gause WC. Protective immune mechanisms in helminth infection. *Nat Rev Immunol* (2007) 7:975–87. doi:10.1038/nri2199
50. McKinney W. Data structures for statistical computing in python. In: van der Walt S, Millman J, editors. *Proceedings of the 9th Python in Science Conference*. (Vol. 445), Austin, TX: SciPy (2010). p. 51–6.
51. Pedregosa F, Varoquaux G, Gramfort A, Michel V, Thirion B, Grisel O, et al. Scikit-learn: machine learning in python. *J Mach Learn Res* (2011) 12:2825–30.
52. Seabold S, Perktold J. Statsmodels: econometric and statistical modeling with python. In: van der Walt S, Millman J, editors. *Proceedings of the 9th Python in Science Conference*. Austin, TX: SciPy (2010). p. 57–61.
53. Waskom M, Botvinnik O, O'Kane D, Hobson P, Lukauskas S, Gemperline DC, et al. mwaskom/seaborn: v0.8.1 (September 2017). *Zenodo* (2017). doi:10.5281/zenodo.883859
54. Loeys T, Moerkerke B, De Smet O, Buysse A. The analysis of zero-inflated count data: beyond zero-inflated Poisson regression. *Br J Math Stat Psychol* (2012) 65:163–80. doi:10.1111/j.2044-8317.2011.02031.x
55. Chen T, Guestrin C. XGBoost: a scalable tree boosting system. *arXiv preprint arXiv:160302754. Proceedings of the 22nd ACM SIGKDD International Conference on Knowledge Discovery and Data Mining*. (2016) 785–794.
56. Zou H, Hastie T. Regularization and variable selection via the elastic net. *J R Stat Soc Series B Stat Methodol* (2005) 67:301–20. doi:10.1111/j.1467-9868.2005.00503.x

57. Hämäläinen A, Raharivololona B, Ravoniarimbinina P, Kraus C. Host sex and age influence endoparasite burdens in the gray mouse lemur. *Front Zool* (2015) 12:25. doi:10.1186/s12983-015-0118-9
58. Ferrari N, Rosà R, Pugliese A, Hudson PJ. The role of sex in parasite dynamics: model simulations on transmission of *Heligmosomoides polygyrus* in populations of yellow-necked mice, *Apodemus flavicollis*. *Int J Parasitol* (2007) 37:341–9. doi:10.1016/j.ijpara.2006.10.015
59. Hepworth MR, Hardman MJ, Grencis RK. The role of sex hormones in the development of Th2 immunity in a gender-biased model of *Trichuris muris* infection. *Eur J Immunol* (2010) 40:406–16. doi:10.1002/eji.200939589
60. Bordes F, Ponlet N, de Bellocq JG, Ribas A, Krasnov BR, Morand S. Is there sex-biased resistance and tolerance in Mediterranean wood mouse (*Apodemus sylvaticus*) populations facing multiple helminth infections? *Oecologia* (2012) 170:123–35. doi:10.1007/s00442-012-2300-5
61. Churcher TS, Ferguson NM, Basáñez MG. Density dependence and overdispersion in the transmission of helminth parasites. *Parasitology* (2005) 131:121–32. doi:10.1017/S0031182005007341
62. Bundy DA, Thompson DE, Golden MH, Cooper ES, Anderson RM, Harland PS. Population distribution of *Trichuris trichiura* in a community of Jamaican children. *Trans R Soc Trop Med Hyg* (1985) 79:232–7. doi:10.1016/0035-9203(85)90343-8
63. Barger IA. The statistical distribution of trichostrongylid nematodes in grazing lambs. *Int J Parasitol* (1985) 15:645–9. doi:10.1016/0020-7519(85)90010-4
64. Jia TW, Melville S, Utzinger J, King CH, Zhou XN. Soil-transmitted helminth reinfection after drug treatment: a systematic review and meta-analysis. *PLoS Negl Trop Dis* (2012) 6:e1621. doi:10.1371/journal.pntd.0001621
65. Nunn CL, Altizer S, Jones KE, Sechrest W. Comparative tests of parasite species richness in primates. *Am Nat* (2003) 162:597–614. doi:10.1086/378721
66. Reynolds LA, Filbey KJ, Maizels RM. Immunity to the model intestinal helminth parasite *Heligmosomoides polygyrus*. *Semin Immunopathol* (2012) 34:829–46. doi:10.1007/s00281-012-0347-3
67. Monroy FG, Enriquez FJ. *Heligmosomoides polygyrus*: a model for chronic gastrointestinal helminthiasis. *Parasitol Today* (1992) 8:49–54. doi:10.1016/0169-4758(92)90084-F
68. Pendás AM, Zhou Z, Cadiñanos J, Freije JM, Wang J, Hultenby K, et al. Defective prelamin A processing and muscular and adipocyte alterations in Zmpste24 metalloproteinase-deficient mice. *Nat Genet* (2002) 31:94–9. doi:10.1038/ng871
69. Varga TV, Kurbasic A, Aine M, Eriksson P, Ali A, Hindy G, et al. Novel genetic loci associated with long-term deterioration in blood lipid concentrations and coronary artery disease in European adults. *Int J Epidemiol* (2017) 46:1211–22. doi:10.1093/ije/dyw245
70. Guo T, Yin RX, Huang F, Yao LM, Lin WX, Pan SL. Association between the DOCK7, PCSK9 and GALNT2 gene polymorphisms and serum lipid levels. *Sci Rep* (2016) 6:19079. doi:10.1038/srep19079
71. Ing R, Su Z, Scott ME, Koski KG. Suppressed T helper 2 immunity and prolonged survival of a nematode parasite in protein-malnourished mice. *Proc Natl Acad Sci U S A* (2000) 97:7078–83. doi:10.1073/pnas.97.13.7078
72. Elliott DE, Metwali A, Leung J, Setiawan T, Blum AM, Ince MN, et al. Colonization with *Heligmosomoides polygyrus* suppresses mucosal IL-17 production. *J Immunol* (2008) 181:2414–9. doi:10.4049/jimmunol.181.4.2414
73. Tian BP, Hua W, Xia LX, Jin Y, Lan F, Lee JJ, et al. Exogenous interleukin-17A inhibits eosinophil differentiation and alleviates allergic airway inflammation. *Am J Respir Cell Mol Biol* (2015) 52:459–70. doi:10.1165/rcmb.2014-0097OC
74. Wiesner DL, Smith KD, Kashem SW, Bohjanen PR, Nielsen K. Different lymphocyte populations direct dichotomous eosinophil or neutrophil responses to pulmonary *Cryptococcus* infection. *J Immunol* (2017) 198:1627–37. doi:10.4049/jimmunol.1600821
75. Yang BG, Seoh JY, Jang MH. Regulatory eosinophils in inflammation and metabolic disorders. *Immune Netw* (2017) 17:41–7. doi:10.4110/in.2017.17.1.41
76. Reynolds L, Smith K, Filbey K, Harcus Y, Hewitson J, Redpath S, et al. Commensal-pathogen interactions in the intestinal tract: lactobacilli promote infection with, and are promoted by, helminth parasites. *Gut Microbes* (2014) 5(4):522–32. doi:10.4161/gmic.32155
77. Maurice CF, Knowles SC, Ladau J, Pollard KS, Fenton A, Pedersen AB, et al. Marked seasonal variation in the wild mouse gut microbiota. *ISME J* (2015) 9:2423–34. doi:10.1038/ismej.2015.53
78. Newbold LK, Burthe SJ, Oliver AE, Gweon HS, Barnes CJ, Daunt F, et al. Helminth burden and ecological factors associated with alterations in wild host gastrointestinal microbiota. *ISME J* (2017) 11:663–75. doi:10.1038/ismej.2016.153
79. Takaesu G, Kishida S, Hiyama A, Yamaguchi K, Shibuya H, Irie K, et al. TAB 2, a novel adaptor protein, mediates activation of TAK1 MAPKKK by linking TAK1 to TRAF6 in the IL-1 signal transduction pathway. *Mol Cell* (2000) 5:649–58. doi:10.1016/S1097-2765(00)80244-0
80. Tattoli I, Carneiro LA, Jéhanno M, Magalhaes JG, Shu Y, Philpott DJ, et al. NLRX1 is a mitochondrial NOD-like receptor that amplifies NF-kappaB and JNK pathways by inducing reactive oxygen species production. *EMBO Rep* (2008) 9:293–300. doi:10.1038/sj.embor.7401161
81. McDermott JR, Bartram RE, Knight PA, Miller HR, Garrod DR, Grencis RK. Mast cells disrupt epithelial barrier function during enteric nematode infection. *Proc Natl Acad Sci U S A* (2003) 100:7761–6. doi:10.1073/pnas.1231488100
82. Nibbs RJB, Graham GJ. Immune regulation by atypical chemokine receptors. *Nat Rev Immunol* (2013) 13(11):815–29. doi:10.1038/nri3544
83. Burns JM, Summers BC, Wang Y, Melikian A, Berahovich R, Miao Z, et al. A novel chemokine receptor for SDF-1 and I-TAC involved in cell survival, cell adhesion, and tumor development. *J Exp Med* (2006) 203:2201–13. doi:10.1084/jem.20052144
84. Freitas C, Desnoyer A, Meuris F, Bachelerie F, Balabanian K, Machelon V. The relevance of the chemokine receptor ACKR3/CXCR7 on CXCL12-mediated effects in cancers with a focus on virus-related cancers. *Cytokine Growth Factor Rev* (2014) 25:307–16. doi:10.1016/j.cytogfr.2014.04.006
85. Szpakowska M, Dupuis N, Baragli A, Counson M, Hanson J, Piette J, et al. Human herpesvirus 8-encoded chemokine vCCL2/vMIP-II is an agonist of the atypical chemokine receptor ACKR3/CXCR7. *Biochem Pharmacol* (2016) 114:14–21. doi:10.1016/j.bcp.2016.05.012
86. Beugnet F, Kerboeuf D, Nicolle JC, Soubieux D. Use of free living stages to study the effects of thiabendazole, levamisole, pyrantel and ivermectin on the fine structure of *Haemonchus contortus* and *Heligmosomoides polygyrus*. *Vet Parasitol* (1996) 63:83–94. doi:10.1016/0304-4017(95)00879-9
87. Little TJ, Shuker DM, Colegrave N, Day T, Graham AL. The coevolution of virulence: tolerance in perspective. *PLoS Pathog* (2010) 6:e1001006. doi:10.1371/journal.ppat.1001006
88. Flies AS, Mansfield LS, Flies EJ, Grant CK, Holekamp KE. Socioecological predictors of immune defences in wild spotted hyenas. *Funct Ecol* (2016) 30:1549–57. doi:10.1111/1365-2435.12638
89. Graham AL, Hayward AD, Watt KA, Pilkington JG, Pemberton JM, Nussey DH. Fitness correlates of heritable variation in antibody responsiveness in a wild mammal. *Science* (2010) 330:662–5. doi:10.1126/science.1194878
90. Joyce AR, Palsson BØ. The model organism as a system: integrating 'omics' data sets. *Nat Rev Mol Cell Biol* (2006) 7:198–210. doi:10.1038/nrm1857

Conflict of Interest Statement: The authors declare that the research was conducted in the absence of any commercial or financial relationships that could be construed as a potential conflict of interest.

frontiers in Immunology

ORIGINAL RESEARCH
published: 31 January 2018
doi: 10.3389/fimmu.2018.00105

Investigating Relationships between Reproduction, Immune Defenses, and Cortisol in Dall Sheep

Cynthia J. Downs[1], Brianne V. Boan[2†], Thomas D. Lohuis[3] and Kelley M. Stewart[2]*

[1]Department of Biology, Hamilton College, Clinton, NY, United States, [2]Department of Natural Resources and Environmental Sciences, University of Nevada, Reno, NV, United States, [3]Alaska Department of Fish and Game, Anchorage, AK, United States

Life-history theory is fundamental to understanding how animals allocate resources among survival, development, and reproduction, and among traits within these categories. Immediate trade-offs occur within a short span of time and, therefore, are more easily detected. Trade-offs, however, can also manifest across stages of the life cycle, a phenomenon known as carryover effects. We investigated trade-offs on both time scales in two populations of Dall sheep (*Ovis dalli dalli*) in Southcentral Alaska. Specifically, we (i) tested for glucocorticoid-mediated carryover effects from the breeding season on reproductive success and immune defenses during parturition and (ii) tested for trade-offs between immune defenses and reproduction within a season. We observed no relationship between cortisol during mating and pregnancy success; however, we found marginal support for a negative relationship between maternal cortisol and neonate birth weights. Low birth weights, resulting from high maternal cortisol, may result in low survival or low fecundity for the neonate later in life, which could result in overall population decline. We observed a negative relationship between pregnancy and bacterial killing ability, although we observed no relationship between pregnancy and haptoglobin. Study site affected bactericidal capacity and the inflammatory response, indicating the influence of external factors on immune responses, although we could not test hypotheses about the cause of those differences. This study helps advance our understanding of the plasticity and complexity of the immune system and provides insights into the how individual differences in physiology may mediate differences in fitness.

Keywords: allocation theory, carryover effect, constitutive immunity, glucocorticoids, immune defenses, *Ovis dalli dalli*, reproduction, trade-offs

OPEN ACCESS

Edited by:
Andrew Steven Flies, University of Tasmania, Australia

Reviewed by:
Jorge Contreras-Garduño, Universidad Nacional Autónoma de México, Mexico
Frederic Levy, Institut national de la Recherche Agronomique (INRA), France

****Correspondence:***
Cynthia J. Downs
cdowns@hamilton.edu

†Present address:
Brianne V. Boan, U.S. Forest Service, Sierraville, CA, United States

Specialty section:
This article was submitted to Comparative Immunology, a section of the journal Frontiers in Immunology

Received: *29 August 2017*
Accepted: *12 January 2018*
Published: *31 January 2018*

Citation:
Downs CJ, Boan BV, Lohuis TD and Stewart KM (2018) Investigating Relationships between Reproduction, Immune Defenses, and Cortisol in Dall Sheep. Front. Immunol. 9:105. doi: 10.3389/fimmu.2018.00105

INTRODUCTION

Life-history theory is fundamental to understanding how animals allocate resources among life-history traits including performance traits and physiological functions that contribute to survival (1, 2). Immediate trade-offs occur within a short span of time and, therefore, are more easily detected. Trade-offs, however, can also manifest across multiple stages of the life cycle, a phenomenon known as carryover effects (3). That is, events during one stage of the life cycle may influence allocation decisions of an individual during another stage of the life cycle. For example, capital breeders finance their reproduction from energy stores gained in months prior to the mating season (4, 5). Generally, individuals with larger fat stores upon initiation of reproduction have the greatest reproductive success (6) and those who initiate reproduction with insufficient energy stores pay a fitness cost of

reduced offspring survival (3, 7, 8). Because fat reserves at the time of reproduction depend upon previously acquired resources, events that affect resource acquisition in one season carry over and subsequently affect the energy available for reproduction (9). Similar logic dictates that allocation of resources to physiological functions, such as immune defenses, may be influenced by carryover effects, and physiological mechanisms, such as integrative hormone signaling networks, may mediate these effects across seasons (10, 11).

Survival and reproduction are two key life-history traits, and selection should result in optimal investment in processes that contribute to both (1). Because immune defenses contribute to survival, energetic and nutritional costs of maintaining and mounting immune defenses are included within the optimality equation for life histories (12–14). The effects of collateral damage from immune responses, that is immunopathology, are also included within these optimality equations of life history (15, 16). As a consequence of the expense of immune defenses, individuals are often unable to maintain both a high level of immune function and successfully reproduce when limited resources force a trade-off in allocation between these two physiological processes (14, 15, 17, 18). Nonetheless, life-history strategy may dictate whether an individual reduces investment in reproduction in favor of immune defenses in a given year (16). Many species reduce immune defenses when committed to reproduction (17–22). However, manifestation of these trade-offs may depend on an individual's energetic state and be regulated facultatively, and it may depend on overall life history strategy (16, 17). Large herbivores often exhibit tradeoffs between current and future reproduction, rather than between reproduction and survival (1, 23–25). Thus, individuals from slow-paced species should favor investment in traits that enhance survival, such as immune defenses, when resources are limited (6, 26, 27).

Availability of energetic and nutritional resources mediate trade-offs between immunological and reproductive performance mechanistically through integrative physiological networks and shared signaling molecules (15, 28). Specifically, key integrators in physiological pathways may act as the mechanism by which carryover effects mediate differences among individuals in investment in immune function and reproduction (11, 15, 29). Glucocorticoids are one proposed integrator of carryover effects (30). Glucocorticoids are released to support metabolically demanding activities and, as such, their circulating concentrations change during predictable seasonal and life-cycle events and they increase in response to stressful events (31–34). As part of the signaling pathway that mediates immune defenses and reproduction, acute increase of glucocorticoids facilitates reproduction and stimulate or redistribute immunological defenses (28, 33, 35, 36). However, sustained, elevated concentrations of glucocorticoids that are indicative of chronic stress can suppress immune defenses, prevent pregnancy, and lower juvenile survival by reducing birth weight of neonates (31, 35, 37–39). In brief, glucocorticoids can alter the cost-benefit equation of investment in immune defenses (28).

Changes in glucocorticoid levels during one stage of the life cycle may affect events during another stage (30). Specifically, high levels of glucocorticoids during mating may reduce reproductive success in large ungulates in two ways. First, integrated long-term levels of glucocorticoids may indicate elevated energy expenditure (40, 41), and females with high energy expenditures during the mating season may have fewer resources to invest in reproduction. Alternatively, high levels of glucocorticoids during the mating season may indicate chronic stress unrelated to energetic demands, and high, chronic stress levels can suppress reproduction regardless of energetic constraints (31, 33, 41).

During pelage growth, glucocorticoids from blood are deposited into hair of mammals and evidence suggest that hair glucocorticoids represents systemic-levels of circulating free glucocorticoids (42–44). Thus, glucocorticoid concentrations in pelage represent a non-invasive measure of integrated blood concentrations during pelage growth and provide researchers with the opportunity to study carryover effects by providing information about physiological state during a life event prior to sample collection (41, 45). Briefly, hair glucocorticoid concentrations are sensitive to major prolonged stressors and are correlated with changes in circulating glucocorticoids observed during pregnancy (43, 46, 47). However, single acute events of high glucocorticoids are not reflected in hair glucocorticoid concentrations (48). Thus, measurements of hair glucocorticoids provide a good indicator of energetically demanding or stressful events experienced during pelage growth (43). In most large mammals, pelage growth during the autumn occurs concurrently with the mating season, and thus provides an indicator of an individual's state when allocation decisions about reproduction were made.

We studied two populations of Dall sheep (*Ovis dalli dalli*) in Southcentral Alaska to investigate (i) trade-offs between immune defenses and reproduction within a season and (ii) carryover effects mediated by glucocorticoids on reproduction in a long-lived, slow-paced species. Dall sheep are large ungulates that reside in highly seasonal environments throughout mountainous regions in Alaska and northwestern Canada. They produce a maximum of one offspring per year. We focused on an energy allocation framework because Dall sheep are capital breeders that live in a seasonal environment and, after mating in the fall, undergo gestation during the winter months when food is scarce. They undergo parturition beginning in May and lactate into the early autumn (49). Capital breeders like Dall sheep rely on stored energy reserves for the majority of their energy during the winter, their annual cycles are organized around gaining energy stores in the summer to fuel survival and reproduction in the winter, and their ecology makes energy trade-offs likely (50). We focused on constitutive immunity because these defenses are always present, they represent the first line of physiological defense against an invading pathogen, and they can mediate the outcome of some infections (51, 52). Specifically, we quantified bactericidal capacity and haptoglobin. Bactericidal capacity provides a broad assessment of host immune ability to eliminate bacterial pathogens (53, 54). Haptoglobin is a protein marker that is generally interpreted as a biomarker of an individual's ability to upregulate inflammation (55). The inflammatory response is a cascade involving acute phase proteins that recruit cells and molecules to destroy pathogens (55–57).

Both energy constraints and elevated glucocorticoids can serve as mechanisms that underlie a potential carryover effect from autumn to spring that can reduce pregnancy and constitutive immune function. Thus, we expect that high glucocorticoid levels in the autumn will reduce the probability of parturition in the spring. The timing of our measurements means that our measure of reproduction integrates the probability of becoming pregnant, probability of successful parturition if pregnant, and probability of the neonate surviving until the time of capture. Specifically, we hypothesized (i) that individuals that are non-pregnant in the spring would have had higher glucocorticoid levels during the previous autumn than those that are pregnant in the spring and (ii) that within pregnant individuals, high glucocorticoid levels in the autumn would lead to reduced birth weights of neonates in the spring. Because we expect this slow-paced species to invest in survival (i.e., immune defenses) over reproduction, we did not expect pregnant individuals to reduce constitutive immunity relative to non-pregnant individuals.

MATERIALS AND METHODS

Study Area

We studied two populations of Dall sheep in Southcentral Alaska in the Chugach range. One population was within Alaska Department of Fish and Game's game management unit 14C (GMU 14C) and the other was within game management unit 13D (GMU 13D). The units are approximately 76.5 km apart and separated by a prominent glaciers (**Figure 1**). Dominant vegetation is similar in both study areas and changes with elevation; black spruce (*Picea mariana*) and alder (*Alnus* spp.) occur at lower elevations and short alpine forbs (e.g., mountain avens, *Dryas octopetala*) and grasses (e.g., alpine timothy, *Phleum alpinum*) occur at higher elevations. Most sheep in the study resided between 914 and 1,829 m in elevation.

GMU 14C lies within the Chugach State Park northeast of Anchorage and is comprised of five drainages and their surrounding ridges: Goat Creek, Eklutna, Peters Creek, Eagle River, and Ship Creek. GMU 14C is bordered by Anchorage and the town of Eagle River to the west, the Knik arm and river to the North, and the Turnagain arm to the South. The total study area is approximately 800 km^2. From the weather station closest to GMU 14C, the 30-year (1981–2010) mean annual temperature was about 2.4°C, mean annual snowfall was 189.23 cm, and mean annual precipitation was 41.91 cm (58).

GMU 13D is northeast of GMU 14C and lies between the Matanuska Glacier and Tazlina Lake and is bordered to the north-northwest by the Alaska State Highway 1. GMU 13D is comprised of several mountain groups separated from each other by three prominent glaciers—Powell, Nelchina, and Tazlina—that limit movement within the study unit. The total study area

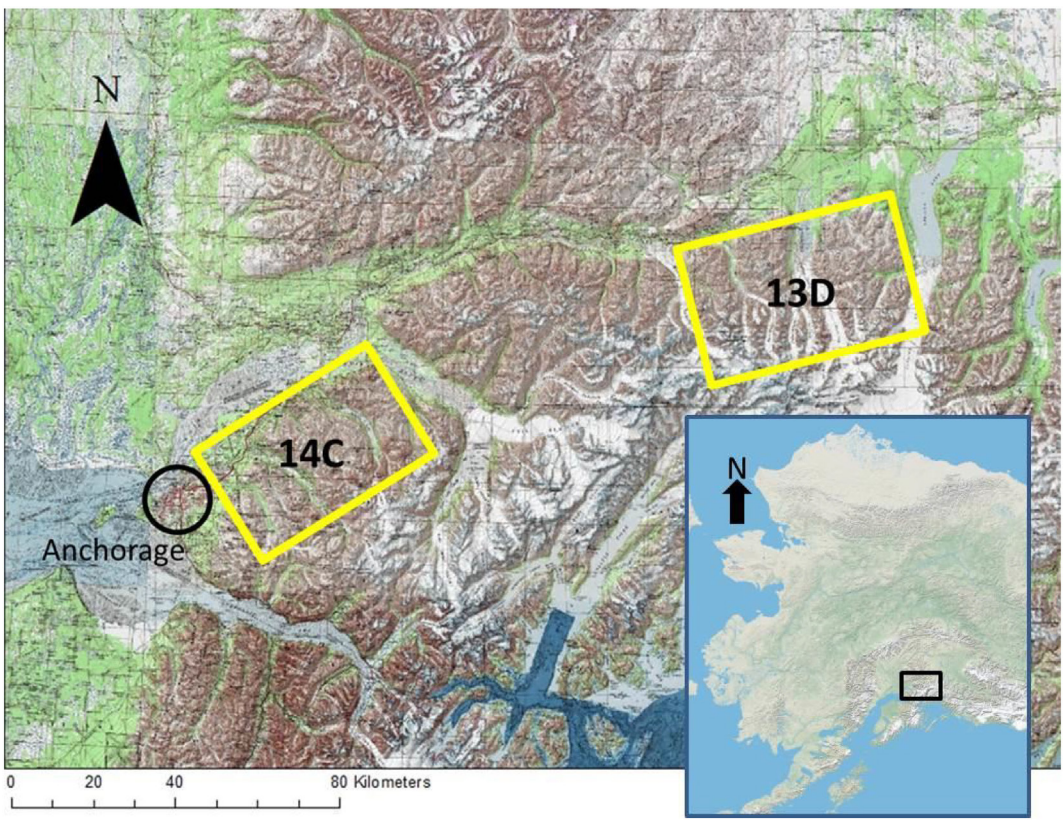

FIGURE 1 | Map of study areas GMU 14C and GMU 13D in the Chugach Range, AK. Anchorage is within the black circle. The map inlay of Alaska shows approximate location of the study units within the state.

is approximately 925 km^2. From the weather stations closest to GMU13D, the 30-year (1981–2010) mean annual temperature was −2.17°C, mean annual snowfall was 167.13 cm, and mean annual precipitation was 41.33 cm (58).

Field Methods

In 2012 and 2013, we captured sheep using standard helicopter and netgun techniques (59), and marked individuals with Telonics VHF radio collars. We attempted to recapture the same individuals each year, however, inaccessible terrain and weather conditions hindered capture efforts of some individuals. During capture, we collected blood samples (2012 and 2013) to determine pregnancy status and to quantify immune defenses, and hair samples (2013 only) to quantify cortisol levels. We determined pregnancy by testing blood serum for the presence of pregnancy specific protein B (BioTracking LLC, Moscow, ID, USA) (25, 60, 61). We determined age using horn growth rings (62). A body condition score was assigned based on the amount of bony structural protrusions felt in the rump, spine, neck, and shoulders (63). Scores ranged from 0 to 5 with 0 representing no subcutaneous fat and five representing individuals with substantial fat reserves (63). All radio-tagged animals were monitored once to twice per week from March to early May when parturition occurred. We attempted to monitor females every day during the parturition season (approximately May 7 to June 10) to detect and capture neonates. Neonates were captured on the ground on foot, collared with Telonics VHF radio collars, weighed (to the nearest 0.1 kg), and sex was determined. Age in days was estimated based on umbilical cord presence and condition, pelage coloration, and mobility. As neonates age, the umbilical cord dries and usually has fallen off by 3 days of age (T. Lohuis, personal observation). At the time of birth, neonate pelage has a gray appearance and lightens with age (T. Lohuis, personal observation). In addition, Dall sheep neonates are precocial and quickly gain stability and mobility with increasing age (64, 65), and we were often limited to capturing neonates between 0 and 5 days old because of this. We did not recapture adult females at the same time that we captured neonates.

Ethical Statement

All aspects of this research were approved by the Institutional Animal Care and Use Committee at the University of Nevada Reno (Protocol #2012-00542) and Alaska Department of Fish and Game (Protocols #2009-13 and #2012-024). All methods were in keeping with protocols adopted by the American Society of Mammalogists for field research involving mammals (66). Use of *Escherichia coli* was approved by the Institutional Biosafety Committee at University of Nevada Reno (B2013-10) and methods were in keeping with recommendations in CDC/NIH Guidelines.

Immune Assays

The bacteria killing ability assay was used to quantify bactericidal capacity of circulating, constitutive components of immune defenses in plasma—complement, acute phase proteins, and natural antibodies (54, 67). We performed assays on serum samples, following Zysling et al. (68) and calibrated for Dall sheep. We used *E. coli* (Epower Microorganisms #0483E7, ATCC8739, MicroBioLogics, St. Cloud, MN, USA) as our ecologically relevant pathogen. Briefly, we mixed 100 µl of a sample with 100 µl of Luria Bertani (LB) broth to make a 1:2 dilution of serum solution and then added 20 µl of our working *E. coli* solution (~5,000 bacteria ml^{-1}). We made two positive controls by mixing 200 µl LB broth with 20 µl of working *E. coli* solution. Samples and controls were vortexed and incubated at 37°C for 30 min. We vortexed samples and controls and plated 50 µl aliquots onto LB agar in petri dishes in triplicate to help ensure reproducibility. One positive control was plated at the beginning and end of each batch. Plates were incubated overnight at 37°C, after which bacteria colonies were counted. We used all six positive control plates (three replicates of two controls) to determine the mean number of control colonies for a particular batch, and samples were compared with the positive controls from their batch. Bactericidal capacity was calculated as percent bacteria killed relative to the positive control. To better ensure reproducibility, we calculated mean intra-control coefficient of variance (CV); it was 8.8%. It was inappropriate to look at CV of number of colony forming units on sample plates because small changes in the number of colonies among plates when there are few colonies results in very high CVs.

We measured haptoglobin concentrations in serum to assess potential for an inflammatory response. Functionally, haptoglobin is an acute phase protein that binds to heme preventing it from serving as a nutrient for pathogens and initiating deleterious oxidation reactions resulting in a rapid inflammatory response (55, 56, 69). Haptoglobin is normally present at low constitutive levels but increases when a pathogen is encountered (70). Because constitutive haptoglobin concentrations are predictive of haptoglobin concentrations after an endotoxin challenge (55), they are indicative of ability to mount an inflammatory response. We assessed haptoglobin presence in raw serum samples (i.e., not diluted) using the Phase Range Haptoglobin Assay Cat. N. TP-801 (Second Generation; Tridelta Development Ltd., Maynooth, Ireland) (55, 71). We followed the manufactures instructions. We ran 16 samples twice to check for reproducibility, the mean CV for these was 13.4%. Mean intra-sample CV was 2%.

Cortisol Assays

We quantified cortisol levels from hair samples collected from 44 individuals in 2013. Cortisol is the dominant glucocorticoid in bighorn sheep (*Ovis canadensis*), another wild sheep species (72). To prepare hair for cortisol extraction, the hair was washed twice in isopropanol, dried, and ground to a powder using a ball mill (SPEX SamplePrep 8000M Mixer/Mill, Metuchen, NJ, USA). Ground hair samples were ~0.05 g and weighed to the nearest 0.0001 g. We then added 1 ml of methanol to each sample, rocked samples for 24 h, and centrifuged them at 2,000 rpm for 1 min. We pipetted 0.6 ml of the supernatant into a vial, evaporated the sample on a heat block at 37°C under nitrogen. The residual cortisol from the sample was reconstituted with 1,040 µl of a 95% assay diluent from the kit and 5% methanol mixture. We quantified cortisol levels using a commercially available kit (Salametrics Salivary Cortisol EIA kit, product #1-3002) (46), following modifications for hair samples suggested by Davenport et al. (46) and Koren et al. (42). Before quantifying samples, we verified that

the kit worked for hair samples from Dall sheep by checking for parallelism between an unknown dilution curve and the standard curve (73). We used a high and low standard provided with the kit as an inter-assay control and we re-quantified all the samples on a plate if these controls were not within the expected range. We re-quantified samples if the coefficient of variation between replicates was greater than 15%.

Statistical Methods

All statistics were performed in SAS (v. 9.3, SAS Inst 2010). We assessed variation in pregnancy rates between years and study sites using the *Z*-test for proportions that allowed sampling with replacement (74). The *Z*-test was appropriate because we attempted to capture the same individuals each year, and no new animals were added to the study after the first year of capture. We used Pearson correlations (Proc CORR) to determine the repeatability of our immune measure across years and to determine the correlation between our immune measures within year. We used untransformed data for all correlations.

We determined the effect of pregnancy status on bactericidal capacity and haptoglobin concentrations using generalized linear models (Proc GLM), with a separate model for each year. We analyzed each year separately because not all individuals were captured in both years. We transformed bactericidal capacity from percent to angular arcsine square root to improve normality of residuals (74). We included study site and body condition score as main effects for both bactericidal capacity and haptoglobin concentration. To account for possible senescence, we included age as a predictor variable of bactericidal capacity and haptoglobin concentrations using linear regression weighted by sample size (74). We did not find a relationship and, therefore, did not include age in further analyses of constitutive immunity.

To determine the effect of cortisol during the autumn on pregnancy status (binomial response: pregnant or not pregnant) the following spring, we used logistic regression (Proc Logistic) and included study site and spring body condition score as dependent variables alongside cortisol. During the preliminary analysis, we also included age as a predictor variable of pregnancy but did not find a relationship and, therefore, did not include age in the final analysis.

To calculate neonate birth weight, we used linear regression to estimate weight gained per day and back calculated birth weight based on age and weight of the neonate at capture. We then determined the effect of cortisol during the autumn on neonate birth weight during the spring with analysis of covariance (Proc GLM). We included maternal age, maternal body condition during the spring, study site, and cortisol concentration as explanatory variables. We also determined the effects of a maternal haptoglobin or bactericidal capacity during pregnancy on birth weights of neonates using separate linear regressions (Proc REG). Significance was determined at $\alpha = 0.05$; however, we consider patterns intriguing at $\alpha = 0.1$ because of our small sample sizes.

RESULTS

The number of adult female sheep and lambs we captured for each GMU during 2012 and 2013 are presented in **Table 1**. Adult female ages ranged from 2 to 11 years and body condition scores ranged from 1.75 to 2.75. Overall pregnancy rates were higher in 2013 (0.833) than in 2012 (0.378) ($Z = 4.31$, $P < 0.0001$), and this pattern held for both GMUs (**Table 1**; **Figure 2**). Pregnancy rates did not differ between study sites in either year (2012: $Z = 0.503$, $P = 0.615$; 2013: $Z = -0.092$, $P = 0.927$, **Figure 2**).

Immune Defenses

We had bactericidal capacity data from 91 samples and haptoglobin data from 87 samples; our samples were spread fairly evenly among sites and years (**Table 2**). Haptoglobin had an 18% repeatability when data were combined across sites, but was not repeatable when only 13D or 14C were examined independently. Bactericidal capacity had a 53% repeatability in GMU 14C, but was not repeatable across years in 13D or when all data were combined (**Table 3**). Haptoglobin levels were not correlated with bactericidal capacity within a year for either site or all the data combined (**Table 3**).

Mean bactericidal capacity was 74.0 ± 27.4% during 2012 and 76.2 ± 27.7% during 2013. In 2012, bactericidal capacity was not associated with pregnancy status ($F_{1,45} = 0.52$, $P = 0.476$), body condition ($F_{3,40} = 0.200$, $P = 0.896$), or study site ($F_{1,45} = 2.41$, $P = 0.128$). Similarly, we observed no relationship between

TABLE 1 | Description of number of adult female and neonate Dall sheep captured in each of the study areas (GMU) for each year in the Chugach Range, AK 2012–2013.

Year	GMU	Adult females captured	Pregnancy rate	Neonates captured
2012	13D	31	0.32	14
	14C	34	0.44	26
2013	13D	26	0.83	26
	14C	22	0.86	11

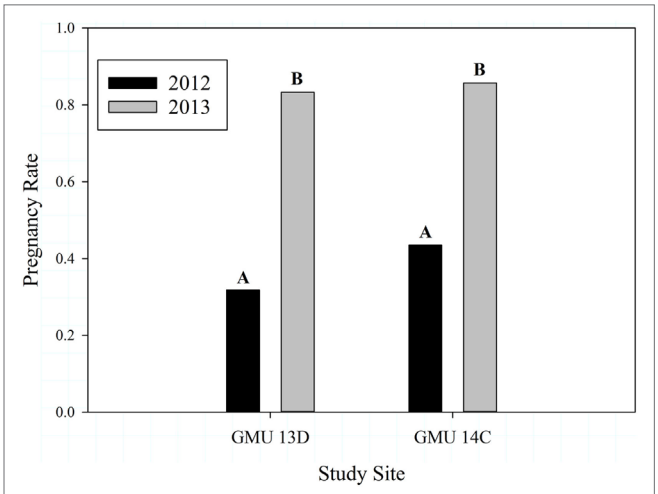

FIGURE 2 | Dall sheep pregnancy rates for years 2012 and 2013 ($Z = 4.31$, $P < 0.0001$) and study sites (2012 $Z = 0.503$, $P = 0.615$; 2013 $Z = -0.092$, $P = 0.927$) in the Chugach Range, AK. Letters over bars indicate results of comparisons following a significant *Z*-test, where different letters are statistically different.

body condition and bactericidal capacity in 2013 ($F_{2,41} = 0.690$, $P = 0.507$). In 2013, however, bactericidal capacity was significantly greater in GMU 14 C than GMU 13D ($F_{1,45} = 5.050$, $P = 0.030$; **Figure 3A**), and there was an intriguing pattern of a negative effect of pregnancy status on bacterial killing ability ($F_{1,45} = 3.19$, $P = 0.081$; **Figure 3B**; overall model $F_{2,45} = 3.99$, $P = 0.026$). Bactericidal capacity was not significantly associated with neonate birth weight ($F_{1,13} = 1.89$, $P = 0.193$, $n = 15$).

TABLE 2 | Samples sizes for immune assays and the cortisol assay by year and site in the Chugach Range, AK 2012–2013.

Site	Year	Bacteria killing assay	Haptoglobin	Cortisol
All data		91	87	44
14C	2012	22	21	N/A[a]
	2013	24	25	22
13D	2012	23	20	N/A
	2013	22	21	22

[a]*We did not quantify cortisol concentrations in 2012.*

TABLE 3 | Repeatability of immune assays between years and correlations between immune traits within years for all data combined and data from each study areas (GMU).

Sites	Variable 1	Variable 2	*r*	*P*-value	*n*
Both GMUs	BKA 2012	BKA 2013	0.258	0.176	29
	Hapt 2012	**Hapt 2013**	**−0.180**	**0.036**	**28**
	BKA 2012	Hapt 2012	−0.015	0.938	28
	BKA 2013	Hapt 2013	−0.062	0.748	29
13D only	BKA 2012	BKA 2013	0.126	0.967	13
	Hapt 2012	Hapt 2013	−0.308	0.263	15
	BKA 2012	Hapt 2012	−0.058	0.845	14
	BKA 2013	Hapt 2013	−0.119	0.687	14
14C only	**BKA 2012**	**BKA 2013**	**0.532**	**0.034**	**16**
	Hapt 2012	Hapt 2013	0.485	0.093	13
	BKA 2012	Hapt 2012	0.213	0.465	14
	BKA 2013	Hapt 2013	0.100	0.724	15

BKA, bactericidal capacity assay; Hapt, haptoglobin.
Bold results indicate significant correlations.

In 2012, haptoglobin did not differ between sites ($F_{1,41} = 0.79$, $P = 0.381$), and was not associated with pregnancy status ($F_{1,45} = 1.16$, $P = 0.287$) or body condition ($F_{2,41} = 0.180$, $P = 0.832$). In 2013, haptoglobin concentration was significantly greater in GMU 13D than 14C ($F_{1,46} = 4.64$, $P = 0.037$, **Figure 4A**); this is the opposite of the pattern observed for bactericidal capacity between sites. In 2013, haptoglobin was not significantly predicted by pregnancy status ($F_{1,41} = 0.45$, $P = 0.506$, **Figure 4B**) or body condition ($F_{3,37} = 0.630$, $P = 0.598$). Haptoglobin levels were not significantly associated with neonate birth ($F_{1,13} = 0.89$, $P = 0.362$, $n = 15$).

Cortisol

We quantified concentrations of cortisol from 44 samples; those samples were evenly distributed between the two study sites (**Table 2**). In 2013, logistic regression was 65.8% concordant and indicated that pregnancy status during the spring was not associated with cortisol during the previous autumn (Wald Chi-Square = 1.275, $P = 0.259$), body condition during the spring (Wald Chi-Square = 1.331, $P = 0.249$), or study site (Wald Chi-Square = 0.008, $P = 0.9298$). There was a marginal negative trend between maternal cortisol during the autumn mating season and neonate birth weight the following spring ($F_{1,11} = 4.79$, $P = 0.057$, **Figure 5**). Adult age ($F_{1,11} = 1.000$, $P = 0.547$), spring body condition ($F_{1,11} = 2.70$, $P = 0.146$), and study site ($F_{1,11} = 1.14$, $P = 0.317$) did not explain birth weight of neonates during spring.

DISCUSSION

We tested for glucocorticoid-mediated carryover effects on reproductive success. We also tested for trade-offs between immune defenses and reproduction within a season. We observed no relationship between maternal cortisol and pregnancy success; however, we found marginal support for a negative relationship between maternal cortisol and neonate birth weights, providing weak evidence of a carryover effect. We observed a weak negative relationship between pregnancy and bacterial killing ability

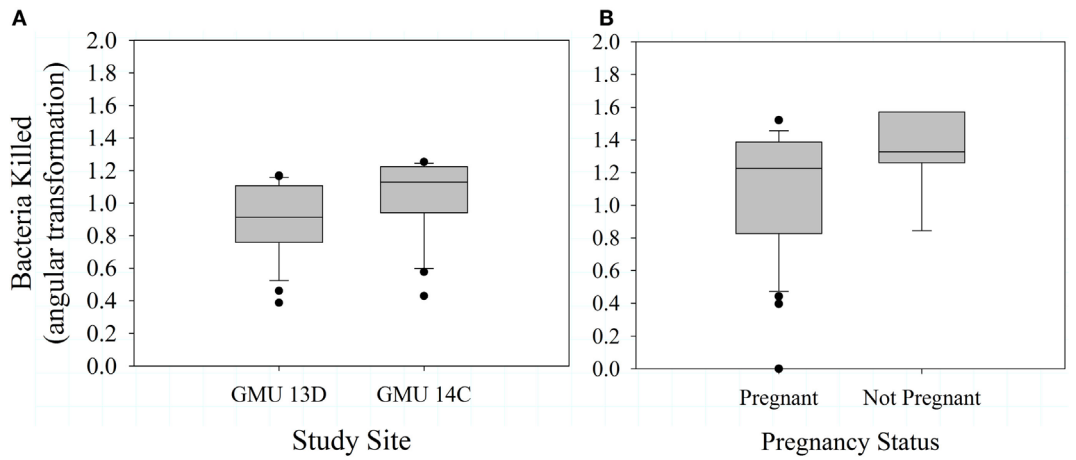

FIGURE 3 | Mean (±SE) bactericidal capacity for female Dall sheep by study sites in the Chugach Range, AK **(A)** and pregnancy status **(B)**. Samples were collected in 2013.

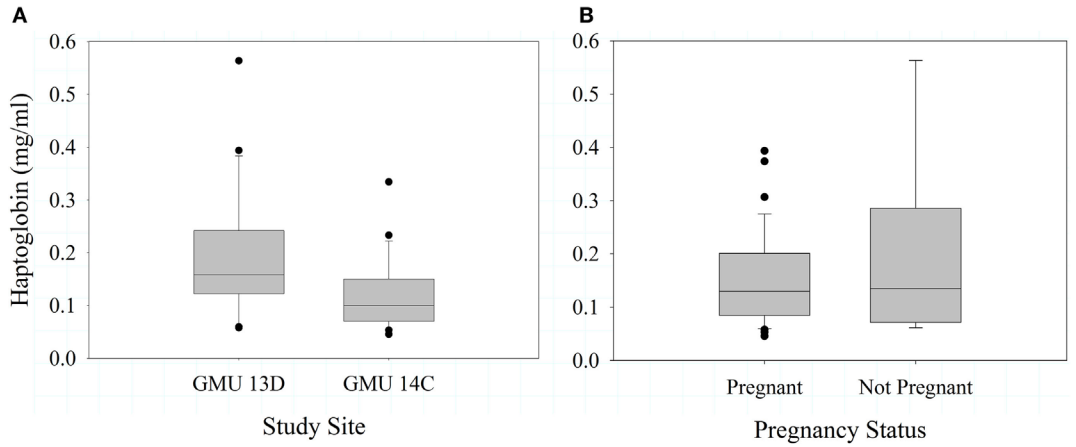

FIGURE 4 | Mean (±SE) haptoglobin concentrations in female Dall sheep by study sites in the Chugach Range, AK **(A)** and pregnancy status **(B)**. Sample were collected 2013.

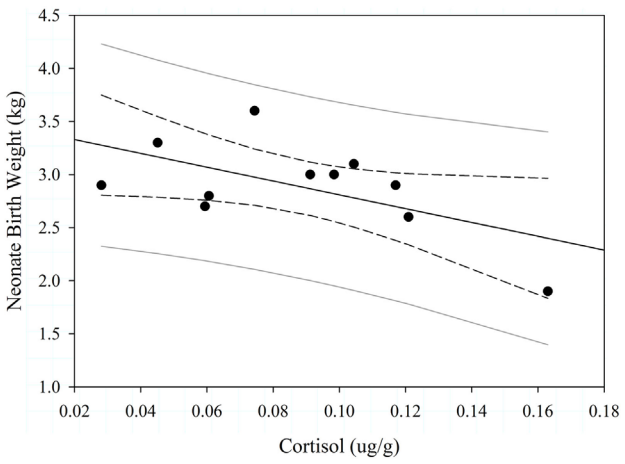

FIGURE 5 | Effect of maternal cortisol levels on Dall sheep neonate birth weight (n = 11) in the Chugach Range, AK, 2013. The dashed lines are the 95% confidence limits and gray solid lines are the 95% prediction limits.

during 1 year of our study providing evidence of a trade-off, although we observed no relationship between pregnancy and haptoglobin. We also found that constitutive immunity differed between sites and years highlighting the plasticity of immune defenses.

Carryover Effects Mediated by Cortisol

We found no evidence of cortisol mediating the ability to become pregnant during the mating season in autumn 2012. Because pregnancy rates were low in the spring of 2012, few sheep underwent the energetically expensive processes of gestation, parturition, and lactation prior to the 2012 autumn mating season. Females in autumn 2012 were likely in better condition going into the mating season because of so few individuals produced offspring the previous year (6, 23). Because females in good nutritional condition are more likely to conceive and maintain pregnancy (6, 23), the low pregnancy rate in 2012 may have led to the high pregnancy rate of spring 2013. If our interpretation is correct, these data would provide evidence of a carryover effect between years, and they corroborate a pattern commonly found in capital breeders with large body sizes (23–25).

Cortisol levels observed during autumn may not have been high enough to affect pregnancy, but we found weak evidence that they were high enough to affect fetal development. Even though we had a small sample of body weights of neonates, we observed that cortisol levels of mothers during autumn were weakly and inversely correlated with birth weights of neonates born the following spring. The effect of maternal cortisol during mating on offspring mass potentially has longer-term implications of reducing success of offspring because low birth weight has been shown to reduce survival of young and lower fecundity during adulthood (75, 76). Furthermore, in highly seasonal environments, like Alaska, young with low birth weight have rarely been observed to catch up in body mass with the larger individuals in their cohorts (77, 78), and larger adults tend to have higher fitness (79). Therefore, the disadvantage of being born small may carry throughout the individual's lifetime.

Pregnancy and Immune Defenses: Evidence of a Carryover Effect?

Parturition in Dall sheep occurs in June. We captured adult female sheep in mid-March, and during that stage of the annual cycles, females are not provisioning offspring (i.e., lactating) from the previous year and because lactation is energetically expensive and most are relying on stored fat for energy because environmental food sources are not readily available (80). Although pregnancy status was not significantly associated with either measure of constitutive immunity in 2012, we observed an interesting trend in 2013, whereby sheep that were pregnant had lower bactericidal capacity than those that were not pregnant ($P < 0.1$). Although our sample sizes were small, the trend suggesting a relationship between pregnancy and bactericidal capacity is worth examining further in future studies.

If generalizable, this trend suggests that Dall sheep approaching parturition invest fewer resources in immune response in favor of reproduction, as has been seen in numerous fast-paced species (17–21). Published results about trade-offs between immune defenses and pregnancy in slow-paced ungulates are ambiguous. Pregnant N'Dama cows maintained under traditional husbandry practices in Gambia had higher rates of Trypanosomiasis than non-pregnant cows (81), indicating a difference in underlying physiology or behavior. Similarly, free-ranging Soay sheep (*Ovis aries*) with higher concentrations of antinuclear antibodies, an indicator of immune defenses, had lower siring probability and lower female breeding probability (82), although this study is not a direct comparison to ours because we instigated how pregnancy affected constitutive immunity rather than investigating how constitutive immunity affected probability of pregnancy. In contrast, pregnancy status did not affect hemolytic-complement activities or bactericidal activity in free-ranging North American elk (*Cervus elaphus*) (26), nor did it affect bactericidal capacity in free-ranging African buffalo (*Syncerus caffer*). These contradictory results suggest that an immune trade-off with reproduction may depend on the immune defense measured, timing of the measurement, and other external variables that regulate traits such as physiological condition and hormone concentrations. Mechanistically, and as previously discussed, the negative trend between pregnancy and immune defenses in 2013 could arise from a carryover effect that is likely mediated by an individual's energy budget.

As pregnancy progresses, some studies show that constitutive immune defense decline (83, 84). Other studies have shown that immunity shifts from humoral to cell-mediated responses as pregnancy progresses (85–87), although those studies focused on adaptive rather than innate immune responses. Our results are consistent with both of those patterns, because we found that humoral measures of constitutive immunity were lower in sheep late in their pregnancy. These shifts in immune strategy might be facilitated by hormones that mediate pregnancy. The physiology mediating pregnancy alone, however, is unlikely to explain our results because we did not find a significant difference in immune defenses between pregnant and non-pregnant sheep in both years. That is, our incontinent results over years may indicate a facultative strategy caused by a reconfiguration of the immune system to increase probability of a successful reproductive event while taking into account other cues such as body condition (17, 28, 87).

Population and Individual-Level Patterns in Immune Defenses

Immune defenses are highly plastic and change between years, seasons, and even weeks (88–90). Immune assays in our study exhibited repeatability across years for only 2 of the 8 analyses we performed, and those repeatabilities suggested an upper limit of additive genetics of only 54 and 18% (**Table 3**). Similarly, a study of captive red knots (*Calidris canutus*) showed that microbiocidal activity for three microbes, white blood cell differentials, hemolytic and hemogglutination activity changed across the annual cycle (88). In addition, T-cell-mediated immunocompetence of free-ranging, nesting tress swallows was influenced by weather within a single nestling season (89).

Constitutive bactericidal capacity and constitutive haptoglobin concentrations of plasma differed between sites during 2013, and interestingly, bactericidal capacity and haptoglobin concentrations showed opposite trends between the two sites. In 2013, sheep from GMU 13D had higher haptoglobin concentrations and lower bactericidal capacity relative to sheep from GMU 14C. These results add to a growing number of studies that have found population-level differences in constitutive immunity. At the same spatial scale of our study, other studies have linked differences in constitutive immunity to group-level differences in mean physiological state (26), parasite prevalence (91), population characteristics such as density (26, 92), habitat quality (92, 93), and weather (89). We cannot distinguish among these alternative possibilities with our data.

Interestingly, neither immune response was related to body condition as measured by body condition scores. These results have two possible explanations. First, body condition scores alone are a coarse measure of body condition and likely are subject to observer bias (94, 95). Therefore, body condition score may not be a precise enough measure to correlate with physiological traits, like immune defenses. Second, we observed little variation in body condition scores. The range of fat scores was 1.75–2.75 on a 6-point scale, and thus the sheep were generally in medium to low nutritional condition, and none were in high condition (63). The range of condition scores is likely related to the season in which we captured individuals. In strongly seasonal environments, as in our study, all individuals lose weight and decline in body condition even when fed *ad libitum* because they use stored fat for energy (96). At the time of capture, sheep were likely in the lowest condition of the annual cycle because we captured at the end of winter (80).

CONCLUSION

Our correlative results suggest extrinsic factors, including study site, play a larger role in mediating immunocompetence than the intrinsic factors studied (reproduction and body condition). This finding corroborates previous work that found local environmental conditions can overwhelm the genetic signature of immune defenses (89). We found weak evidence that high maternal cortisol levels are correlated with low neonate birth weights. Thus, our results have implications for understanding how individual-level differences in chronic glucocorticoids concentrations and individual-differences in immune defenses may affect population dynamics by affecting fitness components (97).

Although interpretation of our results is limited by the complexity of a natural system and the difficulties of studying a natural system in rough terrain and harsh weather conditions, we argue, as others do (98, 99), that studying immunological defenses in free-ranging animals is important for understanding dysfunction of the immune system. Immune defenses and pathologies are the product of genotype by environment interactions and these interactions are hard to replicate in laboratory conditions (100–103). For example, a high level of pathogen exposure causes wild mice (*Mus musculus domesticus*) to have immune systems that are in a highly activated or primed state relative to those of laboratory mice (104). Furthermore, the implications for population dynamics are

hard to extrapolate from laboratory studies. In general, lessons about immunological responses in wild, free-ranging animals will help advance our understanding of the plasticity and complexity of the immune system and enhance our understanding of disease and its effects on population dynamics.

ETHICS STATEMENT

All aspects of this research were approved by the Institutional Animal Care and Use Committee at the University of Nevada Reno (Protocol #2012-00542) and Alaska Department of Fish and Game (Protocols #2009-13 and #2012-024). All methods were in keeping with protocols adopted by the American Society of Mammalogists for field research involving mammals (Sikes, Gannon & Amer Soc 2011). Use of *Escherichia coli* was approved by the Institutional Biosafety Committee at University of Nevada Reno (B2013-10) and methods were in keeping with recommendations in CDC/NIH Guidelines.

AUTHOR CONTRIBUTIONS

TL and KS designed the field component of the study and obtained funding for the project. CD, KS, and BB designed the laboratory portion of the study. BB and TL conducted field work and collected samples for physiological assays. CD and BB calibrated assays for Dall sheep, and BB performed all laboratory assays, CD, BB, and KS analyzed those data and wrote the manuscript. All authors contributed substantially to editing the manuscript and approved the final version.

ACKNOWLEDGMENTS

We thank J. S. Sedinger and T. P. Albright for their editorial input and statistical advice. We thank our pilots, M. Meekins, M. Litzen, T. Levanger, J. Fieldman, T. Cambrier, and B. Silvey, for their excellent flying skills in spotting, tracking, and capturing sheep. We also thank ADFG staff M. Harrington, J. Coltrane, C. Brockman, D. Battle, D. Saalfeld, K. Smith, W. Schock, and C. Stantorf for their speedy assistance in lamb captures. We thank E. Clark for her help in the lab. We thank A. Flies and two anonymous referees for comments on an earlier version of this manuscript.

FUNDING

This study was supported by an Alaska Department of Fish and Game grant, a Hatch grant awarded by Nevada Agriculture Experimental Station, and funding from the University of Nevada Reno awarded to KS.

REFERENCES

1. Stearns SC. *The Evolution of Life Histories*. New York, NY, USA: Oxford University Press (1992). 264 p.
2. Van Noordwijk AJ, De Jong G. Acquisition and allocation of resources: their influence on variation in life-history tactics. *Am Nat* (1986) 128:137–42. doi:10.1086/284547
3. Harrison XA, Blount JD, Inger R, Norris DR, Bearhop S. Carry-over effects as drivers of fitness differences in animals. *J Anim Ecol* (2011) 80:4–18. doi:10.1111/j.1365-2656.2010.01740.x
4. Drent RH, Daan S. The prudent parent: energetic adjustments in avian breeding. *Ardea* (1980) 68:225–52.
5. Houston AI, McNamara JM, Barta Z, Klasing KC. The effect of energy reserves and food availability on optimal immune defence. *Proc Biol Sci* (2007) 274:2835–42. doi:10.1098/rspb.2007.0934
6. Monteith KL, Bleich VC, Stephenson TR, Pierce BM, Conner MM, Kie JG, et al. Life-history characteristics of mule deer: effects of nutrition in a variable environment. *Wildl Monogr* (2014) 186:1–62. doi:10.1002/wmon.1011
7. Ebbinge BS, Spaans B. The importance of body reserves accumulated in spring staging areas in the temperate zone for breeding in dark-bellied brent geese *Branta b. bernicla* in the high Arctic. *J Avian Biol* (1995) 26:105–13. doi:10.2307/3677058
8. Rughetti M, Dematteis A, Meneguz PG, Festa-Bianchet M. Age-specific reproductive success and cost in female Alpine ibex. *Oecologia* (2015) 178:197–205. doi:10.1007/s00442-014-3192-3
9. Festa-Bianchet M. Condition-dependent reproductive success in bighorn ewes. *Ecol Lett* (1998) 1:91–4. doi:10.1046/j.1461-0248.1998.00023.x
10. Flatt T, Heyland A, Stearns SC. What mechanistic insighs can or cannot contribute to life history evolution: an exchange between Stearns, Heyland, and Flatt. In: Flatt T, Heyland A, editors. *Mechanisms of Life History Evolution: The Genetics and Physiology of Life History Traits and Trade-offs*. New York, NY, USA: Oxford University Press (2011). p. 375–9.
11. Cohen AA, Martin LB, Wingfield JC, McWilliams SR, Dunne JA. Physiological regulatory networks: ecological roles and evolutionary constraints. *Trends Ecol Evol* (2012) 27:428–35. doi:10.1016/j.tree.2012.04.008
12. Downs CJ, Stewart KM. A primer in ecoimmunology and immunology for wildlife research and management. *Calif Fish Game* (2014) 100:371–95.
13. Lochmiller RL, Deerenberg C. Trade-offs in evolutionary immunology: just what is the cost of immunity? *Oikos* (2000) 88:87–98. doi:10.1034/j.1600-0706.2000.880110.x
14. Sheldon BC, Verhulst S. Ecological immunology: costly parasite defences and tradeoffs in evolutionary ecology. *Trends Ecol Evol* (1996) 11:317–21. doi:10.1016/0169-5347(96)10039-2
15. Downs CJ, Adelman JS, Demas GE. Mechanisms and methods in ecoimmunology: integrating within-organism and between-organism processes. *Integr Comp Biol* (2014) 54:340–52. doi:10.1093/icb/icu082
16. Lee KA. Linking immune defenses and life history at the levels of the individual and the species. *Integr Comp Biol* (2006) 46:1000–15. doi:10.1093/icb/icl049
17. French SS, DeNardo DF, Moore MC. Trade-offs between the reproductive and immune systems: facultative responses to resources or obligate responses to reproduction? *Am Nat* (2007) 170:79–89. doi:10.1086/518569
18. French SS, Johnston GIH, Moore MC. Immune activity suppresses reproduction in food-limited female tree lizards *Urosaurus ornatus*. *Funct Ecol* (2007) 21:1115–22. doi:10.1111/j.1365-2435.2007.01311.x
19. Ilmonen P, Taarna T, Hasselquist D. Experimentally activated immune defence in female pied flycatchers results in reduced breeding success. *Proc R Soc Lond B Biol Sci* (2000) 267:665–70. doi:10.1098/rspb.2000.1053
20. Cox RM, Parker EU, Cheney DM, Liebl AL, Martin LB, Calsbeek R. Experimental evidence for physiological costs underlying the trade-off between reproduction and survival. *Funct Ecol* (2010) 24:1262–9. doi:10.1111/j.1365-2435.2010.01756.x
21. Råberg L, Nilsson J, Ilmonen P, Stjernman M, Hasselquist D. The cost of an immune response: vaccination reduces parental effort. *Ecol Lett* (2000) 3:382–6. doi:10.1046/j.1461-0248.2000.00154.x
22. Bonneaud C, Mazuc J, Gonzalez G, Haussy C, Chastel O, Faivre B, et al. Assessing the cost of mounting an immune response. *Am Nat* (2003) 161:367–79. doi:10.1086/346134
23. Morano S, Stewart KM, Sedinger JS, Nicolai CA, Vavra M. Life-history strategies of North American elk: trade-offs associated with reproduction and survival. *J Mammal* (2013) 94:162–72. doi:10.1644/12-MAMM-A-074.1
24. Parker KL, Barboza PS, Gillingham MP. Nutrition integrates environmental responses of ungulates. *Funct Ecol* (2009) 23:57–69. doi:10.1111/j.1365-2435.2009.01528.x

25. Stewart KM, Bowyer RT, Dick BL, Johnson BK, Kie JG. Density-dependent effects on physical condition and reproduction in North American elk: an experimental test. *Oecologia* (2005) 143:85–93. doi:10.1007/s00442-004-1785-y
26. Downs CJ, Stewart KM, Dick BL. Investment in constitutive immune function: effects of density-dependent processes. *PLoS One* (2015) 10:e0125586. doi:10.1371/journal.pone.0125586
27. Wobeser GA. *Disease in Wild Animals: Investigation and Management*. 2nd ed. Berlin, Germany: Springer Verlag (2010).
28. Adamo SA. The stress response and immune system share, borrow, and reconfigure their physiological network elements: evidence from the insects. *Horm Behav* (2017) 88:25–30. doi:10.1016/j.yhbeh.2016.10.003
29. Martin LB, Burgan S, Adelman JS, Gervasi SS. Host competence: an organismal trait to integrate immunology and epidemiology. *Integr Comp Biol* (2016) 56:1225–37. doi:10.1093/icb/icw064
30. Schultner J, Moe B, Chastel O, Tartu S, Bech C, Kitaysky AS. Corticosterone mediates carry-over effects between breeding and migration in the kittiwake *Rissa tridactyla*. *Mar Ecol Prog Ser* (2014) 496:125–33. doi:10.3354/meps10603
31. Wingfield JC, Romero LM. Adrenocortical responses to stress and their modulation in free-living vertebrates. In: McEwen BS, editor. *Handbook of Physiology, Section 7: The Endocrine System, Volume 4: Coping with the Environment: Neural and Endocrine Mechanisms*. New York, NY: Oxford University Press (2000). p. 211–36.
32. Romero LM, Romero RC. Corticosterone responses in wild birds: the importance of rapid initial sampling. *Condor* (2002) 104:129–35. doi:10.1650/0010-5422(2002)104[0129:CRIWBT]2.0.CO;2
33. Sapolsky RM, Romero LM, Munck AU. How do glucocorticoids influence stress responses? Integrating permissive, suppressive, stimulatory, and preparative actions. *Endocr Rev* (2000) 21:55–89. doi:10.1210/edrv.21.1.0389
34. Romero LM, Meister CJ, Cyr NE, Kenagy GJ, Wingfield JC. Seasonal glucocorticoid responses to capture in wild free-living mammals. *Am J Physiol Regul Integr Comp Physiol* (2008) 294:R614–22. doi:10.1152/ajpregu.00752.2007
35. Martin LB. Stress and immunity in wild vertebrates: timing is everything. *Gen Comp Endocrinol* (2009) 163:70–6. doi:10.1016/j.ygcen.2009.03.008
36. Dhabhar F, McEwen B. Acute stress enhances while chronic stress suppresses cell-mediated immunity in vivo: a potential role for leukocyte trafficking. *Brain Behav Immun* (1997) 11:286–306. doi:10.1006/brbi.1997.0508
37. Cameron R. Reproductive pauses by female caribou. *J Mammal* (1994) 75:10–3. doi:10.2307/1382230
38. Festa-Bianchet M, Jorgenson J, Luchierini M, Wishart W. Life-history consequences of variation in age of primiparity in bighorn ewes. *Ecology* (1995) 76:871–81. doi:10.2307/1939352
39. Singer F, Harting A, Symonds K, Coughenour M. Density dependence, compensation, and environmental effects on elk calf mortality in Yellowstone National Park. *J Wildl Manage* (1997) 61:12–25. doi:10.2307/3802410
40. Waterhouse MD, Sjodin B, Ray C, Erb L, Wilkening J, Russello MA. Individual-based analysis of hair corticosterone reveals factors influencing chronic stress in the American pika. *Ecol Evol* (2017) 7:4099–108. doi:10.1002/ece3.3009
41. Romero LM, Fairhurst GD. Measuring corticosterone in feathers: strengths, limitations, and suggestions for the future. *Comp Biochem Physiol Part A Mol Integr Physiol* (2016) 202:112–22. doi:10.1016/j.cbpa.2016.05.002
42. Koren L, Mokady O, Karaskov T, Klein J, Koren G, Geffen E. A novel method using hair for determining hormonal levels in wildlife. *Anim Behav* (2002) 63:403–6. doi:10.1006/anbe.2001.1907
43. Russell E, Koren G, Rieder M, Van Uum S. Hair cortisol as a biological marker of chronic stress: current status, future directions and unanswered questions. *Psychoneuroendocrinology* (2012) 37:589–601. doi:10.1016/j.psyneuen.2011.09.009
44. Harkey MR. Anatomy and physiology of hair. *Forensic Sci Int* (1993) 63:9–18. doi:10.1016/0379-0738(93)90255-9
45. Warne RW, Proudfoot GA, Crespi EJ. Biomarkers of animal health: integrating nutritional ecology, endocrine ecophysiology, ecoimmunology, and geospatial ecology. *Ecol Evol* (2015) 5:557–66. doi:10.1002/ece3.1360
46. Davenport M, Tiefenbacher S, Lutz C, Novak M, Meyer J. Analysis of endogenous cortisol concentrations in the hair of rhesus macaques. *Gen Comp Endocrinol* (2006) 147:255–61. doi:10.1016/j.ygcen.2006.01.005
47. Kirschbaum C, Tietze A, Skoluda N, Dettenborn L. Hair as a retrospective calendar of cortisol production—increased cortisol incorporation into hair in the third trimester of pregnancy. *Psychoneuroendocrinology* (2009) 34:32–7. doi:10.1016/j.psyneuen.2008.08.024
48. Ashley N, Barboza P, Macbeth B, Janz D, Cattet M, Booth R, et al. Glucocorticosteroid concentrations in feces and hair of captive caribou and reindeer following adrenocorticotropic hormone challenge. *Gen Comp Endocrinol* (2011) 172:382–91. doi:10.1016/j.ygcen.2011.03.029
49. Festa-Bianchet M. Individual differences, parasites, and the costs of reproduction for bighorn ewes (*Ovis canadensis*). *J Anim Ecol* (1989) 58:785–95. doi:10.2307/5124
50. Festa-Bianchet M, Jorgenson J, King W, Smith K, Wishart W. The development of sexual dimorphism: seasonal and lifetime mass changes in bighorn sheep. *Can J Zool* (1996) 74:330–42. doi:10.1139/z96-041
51. Schmid-Hempel P, Ebert D. On the evolutionary ecology of specific immune defence. *Trends Ecol Evol* (2003) 18:27–32. doi:10.1016/S0169-5347(02)00013-7
52. Millet S, Bennett J, Lee KA, Hau M, Klasing KC. Quantifying and comparing constitutive immunity across avian species. *Dev Comp Immunol* (2007) 31:188–201. doi:10.1016/j.dci.2006.05.013
53. French SS, DeNardo DF, Greives TJ, Strand CR, Demas GE. Human disturbance alters endocrine and immune responses in the Galapagos marine iguana (*Amblyrhynchus cristatus*). *Horm Behav* (2010) 58:792–9. doi:10.1016/j.yhbeh.2010.08.001
54. Demas GE, Zysling DA, Beechler BR, Muehlenbein MP, French SS. Beyond phytohaemagglutinin: assessing vertebrate immune function across ecological contexts. *J Anim Ecol* (2011) 80:710–30. doi:10.1111/j.1365-2656.2011.01813.x
55. Matson KD, Horrocks NP, Versteegh MA, Tieleman BI. Baseline haptoglobin concentrations are repeatable and predictive of certain aspects of a subsequent experimentally-induced inflammatory response. *Comp Biochem Physiol A Mol Integr Physiol* (2012) 162:7–15. doi:10.1016/j.cbpa.2012.01.010
56. Dobryszycka W. Biological functions of haptoglobin – new pieces to an old puzzle. *Eur J Clin Chem Clin Biochem* (1997) 35:647–54.
57. Murphy KP, Travers P, Walport M. *Janeway's Immunobiology*. Garland Science (2007). 928 p.
58. Alaska Climate Research Center. *Climate Normal.* (2017).
59. Krausman P, Hervet J, Ordway L. Capturing deer and mountain sheep with a net-gun. *Wildl Soc Bull* (1985) 13:71–3.
60. Noyes JH, Sasser RG, Johnson BK, Bryant LD, Alexander B. Accuracy of pregnancy detection by serum protein (PSPB) in elk. *Wildl Soc Bull* (1997) 25:695–8.
61. Keech MA, Bowyer RT, Ver Hoef JM, Boertje RD, Dale BW, Stephenson TR. Life-history consequences of maternal condition in Alaskan moose. *J Wildl Manag* (2000) 64:450–62. doi:10.2307/3803243
62. Geist V. Validity of horn segment counts in aging bighorn sheep. *J Wildl Manag* (1966) 30:634–5. doi:10.2307/3798763
63. Stephenson TR, Bleich VC, Pierce BM, Mulcahy GP. Validation of mule deer body composition using in vivo and post-mortem indices of nutritional condition. *Wildl Soc Bull* (2002) 30:557–64.
64. Bowyer RT, Leslie DMJ, Rachlow JL. Dall's and Stone's sheep. In: Demaris S, Krausman PR, editors. *In Ecology and Management of Large Mammals in North America*. Upper Saddle River, New Jersey: Prentice-Hall Press (2000). p. 491–516.
65. Pitzman M. *Birth Behavior and Lamb Survival in Mountain Sheep in Alaska*. Ph.D. thesis, University of Alaska Fairbanks, Fairbanks, Alaska (1970).
66. Sikes RS, Gannon WL, Amer Soc M. Guidelines of the American Society of Mammalogists for the use of wild mammals in research. *J Mammal* (2011) 92:235–53. doi:10.1644/10-MAMM-F-355.1
67. Tieleman IB, Williams JB, Ricklefs RE, Klasing KC. Constitutive innate immunity is a component of the pace-of-life syndrome in tropical birds. *Proc R Soc Lond B Biol Sci* (2005) 272:1715–20. doi:10.1098/rspb.2005.3155
68. Zysling DA, Garst AD, Demas GE. Photoperiod and food restriction differentially affect reproductive and immune responses in Siberian hamsters *Phodopus sungorus*. *Funct Ecol* (2009) 23:979–88. doi:10.1111/j.1365-2435.2009.01572.x
69. Matson KD, Cohen AA, Klasing KC, Ricklefs RE, Scheuerlein A. No simple answers for ecological immunology: relationships among immune indices at the individual level break down at the species level in waterfowl. *Proc R Soc Lond B Biol Sci* (2006) 273:815–22. doi:10.1098/rspb.2005.3376
70. Delers F, Strecker G, Engler R. Glycosylation of chicken haptoglobin: isolation and characterization of three molecular variants and studies of their distribution in hen plasma before and after turpentine-induced inflammation. *Biochem Cell Biol* (1988) 66:208–17. doi:10.1139/o88-028

71. Versteegh MA, Schwabl I, Jaquier S, Tieleman BI. Do immunological, endocrine and metabolic traits fall on a single Pace-of-Life axis? *J Evol Biol* (2012) 25:1864–76. doi:10.1111/j.1420-9101.2012.02574.x
72. Koren L, Whiteside D, Fahlman Å, Ruckstuhl K, Kutz S, Checkley S, et al. Cortisol and corticosterone independence in cortisol-dominant wildlife. *Gen Comp Endocrinol* (2012) 177:113–9. doi:10.1016/j.ygcen.2012.02.020
73. Buchanan K, Goldsmith A. Noninvasive endocrine data for behavioural studies: the importance of validation. *Anim Behav* (2004) 67:183–5. doi:10.1016/j.anbehav.2003.09.002
74. Zar JH. *Biostatistical Analysis*. Upper Saddle River, NJ, USA: Prentice-Hall Press (2010).
75. Gaillard JM, Festa-Bianchet M, Yoccoz NG, Loison A, Toigo C. Temporal variation in fitness components and population dynamics of large herbivores. *Annu Rev Ecol Syst* (2000) 31:367–93. doi:10.1146/annurev.ecolsys.31.1.367
76. Hurley MA, Unsworth JW, Zager P, Hebblewhite M, Garton EO, Montgomery DM, et al. Demographic response of mule deer to experimental reduction of coyotes and mountain lions in southeastern Idaho. *Wildl Monogr* (2011) 178:1–33. doi:10.1002/wmon.4
77. Hamel S, Gaillard J, Festa-Bianchet M, Cote SD. Individual quality, early-life conditions, and reproductive success in contrasted populations of large herbivores. *Ecology* (2009) 90:1981–95. doi:10.1890/08-0596.1
78. Monteith KL, Schmitz LE, Jenks JA, Delger JA, Bowyer RT. Growth of male white-tailed deer: consequences of maternal effects. *J Mammal* (2009) 90:651–60. doi:10.1644/08-MAMM-A-191R1.1
79. Festa-Bianchet M, Jorgenson JT, Réale D. Early development, adult mass, and reproductive success in bighorn sheep. *Behav Ecol* (2000) 11:633–9. doi:10.1093/beheco/11.6.633
80. Barboza PS, Parker KL, Hume ID. *Integrative Wildlife Nutrition*. Berlin, Germany: Springer Berlin Heidelberg (2009). 342 p.
81. Agyemang K, Dwinger R, Little D, Leperre P, Grieve A. Interaction between physiological status in N'Dama cows and trypanosome infections and its effect on health and productivity of cattle in Gambia. *Acta Trop* (1991) 50:91–9. doi:10.1016/0001-706X(91)90001-Z
82. Graham AL, Hayward AD, Watt KA, Pilkington JG, Pemberton JM, Nussey DH. Fitness correlates of heritable variation in antibody responsiveness in a wild mammal. *Science* (2010) 330:662–5. doi:10.1126/science.1194878
83. Robinson DP, Klein SL. Pregnancy and pregnancy-associated hormones alter immune responses and disease pathogenesis. *Horm Behav* (2012) 62:263–71. doi:10.1016/j.yhbeh.2012.02.023
84. Coe CL. Immunity in primates within a psychobiological perspective. In: Demas GE, Nelson RJ, editors. *Ecoimmunology*. New York, USA: Oxford University Press (2012). p. 144–64.
85. Baker M, Schountz T, Wang L. Antiviral immune responses of bats: a review. *Zoonoses Public Health* (2013) 60:104–16. doi:10.1111/j.1863-2378.2012.01528.x
86. Christe P, Arlettaz R, Vogel P. Variation in intensity of a parasitic mite (*Spinturnix myoti*) in relation to the reproductive cycle and immunocompetence of its bat host (*Myotis myotis*). *Ecol Lett* (2000) 3:207–12. doi:10.1046/j.1461-0248.2000.00142.x
87. Szekeres-Bartho J. Immunological relationship between the mother and the fetus. *Int Rev Immunol* (2002) 21:471–95. doi:10.1080/08830180215017
88. Buehler DM, Piersma T, Matson KD, Tieleman BI. Seasonal redistribution of immune function in a migrant shorebird: annual-cycle effects override adjustments to thermal regime. *Am Nat* (2008) 172:783–96. doi:10.1086/592865
89. Lifjeld JT, Dunn PO, Whittingham LA. Short-term fluctuations in cellular immunity of tree swallows feeding nestlings. *Oecologia* (2002) 130:185–90. doi:10.1007/s004420100798
90. De Coster G, De Neve L, Martin-Galvez D, Therry L, Lens L. Variation in innate immunity in relation to ectoparasite load, age and season: a field experiment in great tits (*Parus major*). *J Exp Biol* (2010) 213:3012–8. doi:10.1242/jeb.042721
91. Horrocks NP, Hegemann A, Ostrowski S, Ndithia H, Shobrak M, Williams JB, et al. Environmental proxies of antigen exposure explain variation in immune investment better than indices of pace of life. *Oecologia* (2015) 177:281–90. doi:10.1007/s00442-014-3136-y
92. Ortego J, Espada F. Ecological factors influencing disease risk in eagle owls *Bubo bubo*. *Ibis* (2007) 149:386–95. doi:10.1111/j.1474-919X.2007.00656.x
93. Schmitt C, Garant D, Bélisle M, Pelletier F. Agricultural intensification is linked to constitutive innate immune function in a wild bird population. *Physiol Biochem Zool* (2017) 90:201–9. doi:10.1086/689679
94. Cook RC, Stephenson TR, Myers WL, Cook JG, Shipley LA. Validating predictive models of nutritional condition for mule deer. *J Wildl Manag* (2007) 71:1934–43. doi:10.2193/2006-262
95. Cook RC, Cook JG, Stephenson TR, Myers WL, McCorquodale SM, Vales DJ, et al. Revisions of rump fat and body scoring indices for deer, elk, and moose. *J Wildl Manag* (2010) 74:880–96. doi:10.2193/2009-031
96. Schwartz CC, Hubbert ME, Franzmann AW. Energy requirements of adult moose for winter maintenance. *J Wildl Manag* (1988) 52:26–33. doi:10.2307/3801052
97. Smith GD, French SS. Physiological trade-offs in lizards: costs for individuals and populations. *Integr Comp Biol* (2017) 57:344–51. doi:10.1093/icb/icx062
98. Pedersen AB, Babayan SA. Wild immunology. *Mol Ecol* (2011) 20:872–80. doi:10.1111/j.1365-294X.2010.04938.x
99. Jolles AE, Beechler BR, Dolan BP. Beyond mice and men: environmental change, immunity and infections in wild ungulates. *Parasite Immunol* (2015) 37:255–66. doi:10.1111/pim.12153
100. Adamo SA. How should behavioural ecologists interpret measurements of immunity? *Anim Behav* (2004) 68:1443–9. doi:10.1016/j.anbehav.2004.05.005
101. Buehler DM, Piersma T, Irene Tieleman B. Captive and free-living red knots *Calidris canutus* exhibit differences in non-induced immunity that suggest different immune strategies in different environments. *J Avian Biol* (2008) 39:560–6. doi:10.1111/j.0908-8857.2008.04408.x
102. Viney M, Lazarou L, Abolins S. The laboratory mouse and wild immunology. *Parasite Immunol* (2015) 37:267–73. doi:10.1111/pim.12150
103. Owen-Ashley NT, Turner M, Hahn TP, Wingfield JC. Hormonal, behavioral, and thermoregulatory responses to bacterial lipopolysaccharide in captive and free-living white-crowned sparrows (*Zonotrichia leucophrys* gambelii). *Horm Behav* (2006) 49:15–29. doi:10.1016/j.yhbeh.2005.04.009
104. Abolins S, King EC, Lazarou L, Weldon L, Hughes L, Drescher P, et al. The comparative immunology of wild and laboratory mice, *Mus musculus domesticus*. *Nat Commun* (2017) 8:1–14. doi:10.1038/ncomms14811

Conflict of Interest Statement: The authors declare that the research was conducted in the absence of any commercial or financial relationships that could be construed as a potential conflict of interest.

frontiers in Immunology

ORIGINAL RESEARCH
published: 22 January 2018
doi: 10.3389/fimmu.2018.00013

Differing House Finch Cytokine Expression Responses to Original and Evolved Isolates of *Mycoplasma gallisepticum*

Michal Vinkler[1], Ariel E. Leon[2], Laila Kirkpatrick[2], Rami A. Dalloul[3] and Dana M. Hawley[2]*

[1] Faculty of Science, Department of Zoology, Charles University, Prague, Czechia, [2] Department of Biological Sciences, Virginia Tech, Blacksburg, VA, United States, [3] Avian Immunobiology Laboratory, Department of Animal and Poultry Sciences, Virginia Tech, Blacksburg, VA, United States

The recent emergence of the poultry bacterial pathogen *Mycoplasma gallisepticum* (MG) in free-living house finches (*Haemorhous mexicanus*), which causes mycoplasmal conjunctivitis in this passerine bird species, resulted in a rapid coevolutionary arms-race between MG and its novel avian host. Despite extensive research on the ecological and evolutionary dynamics of this host–pathogen system over the past two decades, the immunological responses of house finches to MG infection remain poorly understood. We developed seven new probe-based one-step quantitative reverse transcription polymerase chain reaction assays to investigate mRNA expression of house finch cytokine genes (*IL1B*, *IL6*, *IL10*, *IL18*, *TGFB2*, *TNFSF15*, and *CXCLi2*, syn. *IL8L*). These assays were then used to describe cytokine transcription profiles in a panel of 15 house finch tissues collected at three distinct time points during MG infection. Based on initial screening that indicated strong pro-inflammatory cytokine expression during MG infection at the periorbital sites in particular, we selected two key house finch tissues for further characterization: the nictitating membrane, i.e., the internal eyelid in direct contact with MG, and the Harderian gland, the secondary lymphoid tissue responsible for regulation of periorbital immunity. We characterized cytokine responses in these two tissues for 60 house finches experimentally inoculated either with media alone (sham) or one of two MG isolates: the earliest known pathogen isolate from house finches (VA1994) or an evolutionarily more derived isolate collected in 2006 (NC2006), which is known to be more virulent. We show that the more derived and virulent isolate NC2006, relative to VA1994, triggers stronger local inflammatory cytokine signaling, with peak cytokine expression generally occurring 3–6 days following MG inoculation. We also found that the extent of pro-inflammatory interleukin 1 beta signaling was correlated with conjunctival MG loads and the extent of clinical signs of conjunctivitis, the main pathological effect of MG in house finches. These results suggest that the pathogenicity caused by MG infection in house finches is largely mediated by host pro-inflammatory immune responses, with important implications for the dynamics of host–pathogen coevolution.

Keywords: avian pathogen, bird cytokine signalling, disease ecology, emerging infectious diseases, evolution of virulence, host–parasite interaction, periocular inflammation, wild immunology

OPEN ACCESS

Edited by:
Andrew Steven Flies, University of Tasmania, Australia

Reviewed by:
Jeanne Marie Fair, Los Alamos National Laboratory (DOE), United States
Magdalena Chadzińska, Jagiellonian University, Poland

****Correspondence:***
Michal Vinkler
michal.vinkler@natur.cuni.cz

Specialty section:
This article was submitted to Comparative Immunology, a section of the journal Frontiers in Immunology

Received: *28 September 2017*
Accepted: *04 January 2018*
Published: *22 January 2018*

Citation:
Vinkler M, Leon AE, Kirkpatrick L, Dalloul RA and Hawley DM (2018) Differing House Finch Cytokine Expression Responses to Original and Evolved Isolates of Mycoplasma gallisepticum. Front. Immunol. 9:13. doi: 10.3389/fimmu.2018.00013

INTRODUCTION

Emerging infectious diseases apply novel and powerful selection pressures on wildlife host immune responses. There is a growing list of examples of wildlife hosts that have rapidly evolved resistance or tolerance to recently emerged infectious diseases [e.g., rabbits and myxoma virus (1); amphibians and chytridiomycosis (2); bats and white-nose syndrome (3); and house finches and mycoplasmal conjunctivitis (4)]. However, due to a historical dearth of techniques available for characterizing immune responses in non-model systems (5), we still know relatively little about the immune responses of natural wildlife hosts to well-studied emerging diseases, particularly for non-mammalian hosts (6, 7). Furthermore, there have been few opportunities to experimentally characterize how pathogen evolution following initial disease emergence has altered the immune responses of natural wildlife hosts to infection (8, 9).

Here, we use a well-studied and recently emerged wildlife disease system—the bacterium *Mycoplasma gallisepticum* (MG) and its novel songbird host, the house finch—to characterize cytokine responses during *in vivo* infection, and to understand how cytokine responses differ for birds inoculated with an original versus evolved pathogen isolate. MG is an economically significant pathogen of poultry, where it largely causes a chronic respiratory disease (10). In the early to mid-1990s, a novel clade of this pathogen emerged in house finches (11), causing severe conjunctivitis (12), and resulting in significant decreases (up to 60%) in the size of free-living house finch populations (13). Since its initial detection in 1994, MG spread rapidly across the United States (14) and evolved both genotypically (15, 16) and phenotypically (17), with rapid increases in virulence and pathogenicity observed following MG's establishment on each coast of the United States (18). Thus, while original isolates (e.g., VA1994) produce moderately severe but often self-healing disease in captivity, evolutionarily derived isolates (e.g., NC2006) are more likely to cause severe and/or chronic infection and disease (9, 19).

The house finch–MG interaction has become an important natural model of coevolution between a host and an emerging pathogen, facilitating insights into fundamental issues in disease ecology and evolutionary biology (18, 20, 21). However, we still have only a limited understanding of the key immunological features of the house finch response to MG. Several studies show that house finch immune responses to MG are associated with hematological changes (22, 23) and antigen-specific antibody production in both lachrymal fluid and blood (9, 24). Nevertheless, the protective effects of humoral immunity remain unclear (19). Studies of house finch gene expression in the spleen using suppression subtractive hybridization and cDNA microarrays identified several immune response genes differentially expressed 14 days after experimental inoculation with MG (25), with upregulation of many immune response genes in birds from a resistant population relative to a susceptible population (4). Differential expression of immunity genes was also detected in house finch spleens on day 3 postinoculation (26), with population differences at that time point suggesting that differences in innate immunity might be important for host resistance. However, the role of cytokines, shown to be upregulated early in poultry infection with MG at the infection site (27), could not be elucidated in this study. Using the ratio of interleukin (IL)-1β (*IL1B*) to *IL10* mRNA expression in whole blood 24 h after experimental inoculation with MG, Adelman et al. (28) provided evidence for a potential association between early inflammatory cytokine responses and the degree of inflammation caused by a given load of MG. Thus, inflammatory immune responses may play an important role in host defense to this disease, but these responses have not yet been well examined during MG infection in house finches. Furthermore, despite the existence of archived MG isolates that span the course of this emerging disease (29), no studies to date have examined how inflammatory immune responses differ for hosts inoculated with an early, less virulent isolate of MG versus a more derived, virulent isolate (18).

Inflammation is one of the most important mechanisms of pathogen clearance in vertebrate immunity (30). As a self-damaging immunological process, inflammation is carefully regulated by highly coordinated cytokine signaling. In birds, pro-inflammatory cytokines such as IL1B, IL6, IL18, tumor necrosis factor superfamily members (TNFSF), and various chemokines (e.g., IL8 homologs including avian CXCLi2), together with anti-inflammatory cytokines including IL10 and transforming growth factor-β (TGFB), guide the immune response to avoid severe host damage associated with immunopathology (31, 32). Initial variation in the balance between these cytokines in different tissues may be responsible for the difference between successful and unsuccessful pathogen elimination. Here, using quantitative reverse transcription polymerase chain reaction (RT-qPCR), we investigate the temporal dynamics and mechanisms of MG-induced inflammation in the house finch. Furthermore, we examine whether differences in cytokine signaling are linked to the higher virulence associated with more recently evolved isolates of MG (18). To provide a comprehensive view, we described the house finch immune response to MG in a panel of 15 house finch tissues. We then examined a subset of tissues that showed strongest responses to MG infection at three time points over the course of MG infection with two distinct MG isolates. We identify differences between an original and evolutionary-derived MG isolate in their capacity to trigger expression of key inflammatory cytokine genes (*IL1B*, *IL6*, *IL10*, *IL18*, *TGFB2*, *CXCLi2*, and *TNFSF15*) leading to signaling that may be crucial for the development of MG-induced immunopathology.

MATERIALS AND METHODS

Animals

Sixty house finches of mixed sex (34 males, 26 females) were trapped in June–July 2015 (31 hatch-year individuals) and December 2015 (29 individuals of unknown age) *via* mist net or cage traps placed around feeders at sites located in Montgomery County, VA, USA or within the city of Radford, VA, USA (all capture sites were within 25 km of each other). House finches can only be accurately aged by plumage before completion of the pre-basic molt in September–October, and thus birds captured in December were of unknown age. Immediately following capture, birds were housed individually or in pairs in wire-mesh

cages (76 cm × 46 cm × 46 cm) in a Biosafety Level 1 animal facility with constant daylength (12L:12D) and temperature (21–22°C) and provided with drinking water and pelleted diet *ad libitum* (Daily Maintenance Diet, Roudybush Inc., Woodland, CA, USA). All birds underwent a 2-week quarantine following capture to ensure they had no exposure to MG before capture. In brief, birds were captured and assessed every 3–4 days for the presence of visible eye lesions (see methods below). On day 14 following capture (to account for time for development of antibodies if exposure to MG occurred on the day of capture), all birds were tested for MG-specific antibodies using an Idexx FlockCheck MG antibody ELISA kit (IDEXX, Westbrook, ME, USA) with modifications described in Ref. (33). Only individuals that were seronegative, never showed clinical signs, and were never housed with a cagemate that showed clinical signs were used in this experiment. Because their immune systems were still maturing at the time of capture, animals caught in July–August were treated preventatively with Cankarex and sulfadimethoxine (see Supplementary Material) in their drinking water to prevent overgrowth of *Trichomonas* and coccidial parasites, respectively. Following quarantine, mass and tarsus length (estimate of size) were measured in all birds used in this experiment, and the birds were moved to individual cages, but all other housing conditions remained unchanged. Animal capture was approved by federal (USFWS permit MB158404-1) and state (VDGIF permit 050352) agencies, and procedures for animal care and use were approved by Virginia Tech's Institutional Animal Care and Use Committees.

MG Isolates

Expansions of MG field isolates were acquired from the Mycoplasma Diagnostic and Research Laboratory at the NC State University College of Veterinary Medicine [ADRL NCSU CVM (29)]. For our study, we selected two MG isolates: (1) isolate VA1994 that is an expansion of the earliest collected MG isolate from a free-living house finch with conjunctivitis, collected in Virginia in 1994 shortly after MG first emerged in house finches [(34); ADRL NCSU CVM Accession No. 7994-1 (7P) 2/12/09] and (2) isolate NC2006 that is an expansion of a more evolutionarily derived isolate collected from a house finch in North Carolina with conjunctivitis in 2006 [ADRL NCSU CVM Accession No. 2006.080-5-4P 7/26/12]. Upon thawing, isolates were diluted in Frey's media with 15% swine serum (FMS) to match the suspension concentration of 2×10^4 color changing units/mL.

Experimental Design and Timeline

To quantify house finch cytokine responses to an original and more evolved isolate of MG, we used three treatment groups (**Table 1**): (1) sham-inoculated controls ($n = 12$), (2) NC2006-inoculated experimental group ($n = 24$), and (3) VA1994-inoculated experimental group ($n = 24$). To capture the temporal dynamics of cytokine expression, birds were further divided within each group into three equally sized time-point batches ($n = 4$ per time point in the case of controls and $n = 8$ per time point in the case of experimental groups). All groups were designed to contain approximately equal proportions of males and females, and hatch-year birds and individuals of unknown age (Table S1 in Supplementary Material), but otherwise assignments to treatments were random. We tested for pretreatment differences in size or mass and no significant differences in these traits were present (all $P > 0.05$).

TABLE 1 | Design of *Mycoplasma gallisepticum* (MG) inoculation experiment.

Treatment	Day 3 PI	Day 6 PI	Day 13 PI
Control	$N = 4$	$N = 4$	$N = 4$
VA1994	$N = 8$	$N = 8$	$N = 8$
NC2006	$N = 8$	$N = 8$	$N = 8$

House finches were inoculated with sham treatment (media alone) or one of two MG isolates (VA1994 or NC2006) on day 0. Equal sample sizes from each treatment group were euthanized on one of each of the three post inoculation (PI) time points.

The experiment was conducted in January–February 2016. On day 0, the mass of all individuals was measured, and conjunctiva was swabbed for qPCR to ensure that no birds harbored baseline loads of MG (see below for details). Thereafter, all birds were treated with the respective inoculum: experimental birds were inoculated with 35 μL of MG suspended in FMS (either isolate NC2006 or VA1994) administered directly into the palpebral conjunctiva of each eye *via* micropipette (70 μL in total), while sham control individuals were given the same volume of FMS alone. Afterward, birds were held in individual paper lunchbags for approximately 5 min to allow full absorption of inoculum, and then released back into their home cages and left undisturbed. On day 3 post inoculation (DPI 3), birds assigned to the first time point batch were eye scored (see below), conjunctival swabs were collected (see below), and the birds were euthanized *via* rapid decapitation to collect fresh tissue samples and prevent confounding effects of chemical inhalants on gene expression. The same procedure was performed with birds assigned to the second time point batch on DPI 6 and to the third time point batch on DPI 13. All manipulation with experimental animals (including euthanasia) was performed in the quickest and most humane way possible to minimize pain and distress. Latex gloves were changed between manipulations with each individual to prevent any inadvertent MG transmission. Because MG requires direct contact between individuals or contact with a highly contaminated surface (35), this measure is sufficient to prevent transmission between experimental birds.

Eye Lesion Scoring and Conjunctival Swabbing

Eye lesions characteristic of mycoplasmal conjunctivitis were visually scored on a 0–3 scale as previously described (36). Briefly, no visible clinical signs were scored as 0, minor swelling and discoloration around the eye was scored as 1, moderate swelling with occasional conjunctival eversion was scored as 2, and moderate to severe swelling, conjunctival eversion, and noticeable exudate was scored as 3. Scores from each eye were combined within time points to give a total eye score ranging from 0 to 6 for each individual.

To quantify MG load, conjunctivae were gently swabbed for 5 s with a sterile cotton swab pre-dipped in sterile tryptose phosphate broth (TPB). Swabs were swirled in 300 μL of sterile TPB and then wrung out into the sample collection tube. Samples from

both eyes were pooled within sampling date for a given individual and frozen at −20°C until further processing. Genomic DNA was extracted with Qiagen DNeasy 96 Blood and Tissue kits (Qiagen, Valencia, CA, USA). Extracted DNA was used to measure overall numbers of MG in the conjunctivae using a qPCR assay targeting the *mgc2* gene of MG using primers and a probe previously described (37) and qPCR methods previously outlined (18).

Samples Used for Gene Expression Analysis

Immediately after decapitation, blood from the disconnected carotids was collected from each bird into a microcentrifuge tube containing RLT lysis buffer (Qiagen, Cat No. 79216). Then, the following tissues were collected separately into RNA*later* (Ambion, cat. No. AM7021): conjunctiva (lower external eyelid), nictitating membrane (internal eyelid), Harderian gland (HG), upper respiratory tract and choana, brain, bone marrow, liver, spleen, trachea, lungs, kidney, pancreas, duodenum, and ileum (small intestine *ca.* 1 cm proximal from the caeca). Dissection and sample collection were performed simultaneously by three persons, and all tissues were collected within 15 min after euthanasia. The collected tissue samples were stored at −80°C until total RNA extraction. RNA extraction was performed using High Pure RNA Tissue Kit v. 09 (Roche, Cat. No. 12033674001) according to the manufacturer's instructions. The total RNA concentration in each extracted sample was then measured using NanoDrop 2000 (Thermo Scientific): range 2.7–1,335.8 ng/μL, average 197.6 ng/μL. We checked for the quality of the RNA extracted from different tissues in different batches using TapeStation (Agilent) as a service of the Genomics Research Laboratory, Biocomplexity Institute, Virginia Tech. In most tissue samples, the RNA quality was good [RNA integrity number (RIN) generally ranged between 8.4 and 9.5]. RIN was <8.0 in some lung, liver, and tracheal samples, and these tissues were thus excluded from further analysis.

RT-qPCR Assays for Assessment of Target and Reference Gene Expression

In this study, we focused on a set of 7 selected pro-inflammatory and anti-inflammatory cytokine genes: *IL1B*, *IL6*, *IL10*, *IL18*, *TGFB2*, *CXCLi2* (*IL8L*), and *TNFSF15*. Pro-inflammatory *IL1B* and anti-inflammatory *IL10* were selected as key target genes based on the results of previous studies (28, 38). To be able to normalize the RT-qPCR data, we had to select an appropriate reference (house-keeping) gene to serve as an endogenous control in the analysis. We tested three reference genes: beta-actin (*ACTB*), glyceraldehyde 3-phosphate dehydrogenase (*GAPDH*), and *28S rRNA*.

Because allelic variation in primer/probe-annealing regions would importantly bias the accuracy of our RT-qPCR data, we first evaluated the sequence variation in the genes of interest in a sample of six individuals (three control and three MG infected) with spleen and liver RNA-seq data available (sequences obtained through Illumina HiSeq 2500) to check for common SNPs. The reads were filtered for hits to the genes of interest using blast with Atlantic canary (*Serinus canaria*) sequences (XM_009086347.1, XM_009091807.1, XM_009093631.1, XM_009096394.1, XM_009097367.1, XM_009097655.1, XM_009098024.1, XM_009098521.1, and XM_009102634.1) as references. The filtered reads were then quality trimmed and mapped to reference using Geneious v. 9.1.8-implemented tools. While this approach yielded good data on sequence variation for the reference genes (full-length mean coverage 600–7,000, 8,000–150,000 reads per individual and tissue), the sequence data were scarce for several cytokine genes (full-length mean coverage 0–35, 0–850 reads per individual and tissue). Therefore, to improve our information on the sequence variation in our genes of interest, we Sanger-sequenced the partial coding regions in mRNA of the cytokines in seven additional individuals and of *ACTB* and *GAPDH* in two additional individuals (sequences uploaded to NCBI GenBank under accession numbers MG587727–MG587771; for description of the PCR protocol see Table S2 in Supplementary Material).

Based on the sequence information on the genes of interest in the canary and the house finch, including the common house finch sequence variation, we designed the primers and probes for RT-qPCR that were located across exon–exon borders, avoided any interspecifically and intraspecifically variable positions and selecting primers that shared basic features for the RT-qPCR with annealing temperature standardized to 60°C (see the list in Table S3 in Supplementary Material). PCR with these primers was tested using cDNA (electrophoresis and Sanger-sequencing of amplicons was performed for assay specificity verification). Next, qPCR with synthesized standard DNA sequences (IDT, gBlocks Gene Fragments; Table S4 in Supplementary Material) was done using the iTaq™ Universal Probes One-Step Kit (BioRad, Cat. No. 172-5140) with cycling conditions following manufacturer's instructions. Once the assay efficiency was estimated, all further RT-qPCR were performed with the same kit (iTaq™ Universal Probes One-Step Kit) and set up: final primer concentration 0.6 μM, final probe concentration 0.125 μM and mixed RNA template diluted in carrier tRNA (Qiagen, Cat. No. 1068337) enriched molecular water 1:5 (or 1:500 for *28S rRNA* qPCR); cycling conditions (1) 50°C 10 min, (2) 95°C 3 min, (3) (95°C 15 s, 60°C 60 s) × 40. All assays were performed with a template-free negative control and gBlock positive controls (Table S4 in Supplementary Material) in a freshly prepared dilution series. Calibrator samples were included in all assays to check for inter-plate RT-qPCR variation. Based on the results of GeNorm and RefFinder analyses (39, 40), *28S rRNA* was selected as a reference gene for the RT-qPCR assays (see Supplementary Material).

RT-qPCR Data Analysis

Before data analysis, any technical replicates with Cq values highly deviating from the other two measurements in the triplicate (difference greater than 1.5, indicating error in PCR) were excluded from the calculation of Cq means. To select candidate tissues of interest, we first performed an initial screening of the qPCR data on *IL1B* and *TGFB2* across all 15 tissues in two controls and two NC2006-infected individuals at DPI 6 by using the relative quantification method described by Pfaffl (41). Here, the relative expression ratio (R) is calculated as $R = (E_T)\Delta^{CqT}/(E_R)\Delta^{CqR}$, where E_T is the mean amplification efficiency of the particular assay for a target gene (cytokine), E_R is the mean amplification efficiency of the particular assay for a reference gene (*28S rRNA*),

the ΔCq*T* is the difference in Cq values between control mean and the treatment mean in the target gene (cytokine), and ΔCq*R* is the difference in Cq values between control mean and the treatment mean in the reference gene (*28S rRNA*). Then, for the purpose of statistical testing of the differences in cytokine expression between controls and treatments in the selected tissues, we calculated the relative RNA quantities (Q) as $Q = E\Delta^{Cq}$, where E is the mean amplification efficiency of the particular assay and ΔCq is the difference between an arbitrary Cq value chosen for the gene (in our case the lowest Cq value in the data set) and the sample Cq (42, 43). The level of *28S rRNA* expression was used as a normalization factor to standardize RNA quantities for each target gene, providing standardized expression quantity, $stQ = Q_{TARGET}/Q_{28S\ rRNA}$. Absolute quantity (aQ) was calculated as number of target gene copies per nanogram of the total extracted RNA. Target gene copy number was estimated based on the average standard curve equation obtained from a dilution series of a calibrated synthetic standard (gBlock sequences of known DNA copy number in the solution).

Finally, to compare the cytokine expression profiles of the response to VA1994 and NC2006 MG isolates in the data set of all experimental individuals, we again used the relative quantification based on relative expression ratio R (41), where, this time, ΔCqT was obtained as the difference in Cq values between control mean for the particular sampling time point and the treatment mean in the target gene (cytokine), and ΔCqR was the difference in Cq values between control mean for the particular sampling time point and the treatment mean in the reference gene (*28S rRNA*). Similarly, absolute quantification ratio was calculated as $A = (CN_T/CN_R)_{Treatment}/(CN_T/CN_R)_{Control}$, where CN_T is target gene copy number, CN_R is reference gene (*28S rRNA*) copy number; in controls we used mean copy number values for the particular sampling time point. Log base 2 values of R and A were used. A general overview of the gene expression data analysis procedure is shown in **Figure 1**.

Statistics

All statistical analysis was performed using R software v. 3.4.0 (44) with a significance level of $P = 0.05$. Because cytokine expression data (both absolute and relative) often deviate from a normal distribution (tested using the Shapiro–Wilk normality test), we used Spearman's rank correlation tests to reveal correlations between relative (stQ) and absolute (A) expression data. As the relative and aQ data were highly correlated (for all cytokine genes studied $P = 0.001$ and $r_S > 0.84$), we show only the results obtained for the relative expression data in the main text of the article and report analogous results obtained using absolute quantification in the Supplementary Material to provide quantification method-independent confirmation to our main results.

We used the non-parametric Wilcoxon rank sum test to test for differential gene expression (stQ or aQ) between control and NC2006-infected individuals screened across 7 tissues selected for further investigation after the initial cursory screening of 15 tissues in 2 individuals per treatment. To indicate consistency in the expression of the cytokine genes, principal component analysis (PCA) was done for the stQ and aQ data after $\log_2$-transformation. The first three principal component scores were added to a correlation matrix prepared using Pearson's correlations with Holm's adjusted P-values. A heatmap showing variation in cytokine gene expression was constructed based on $\log_2$-transformed stQ and

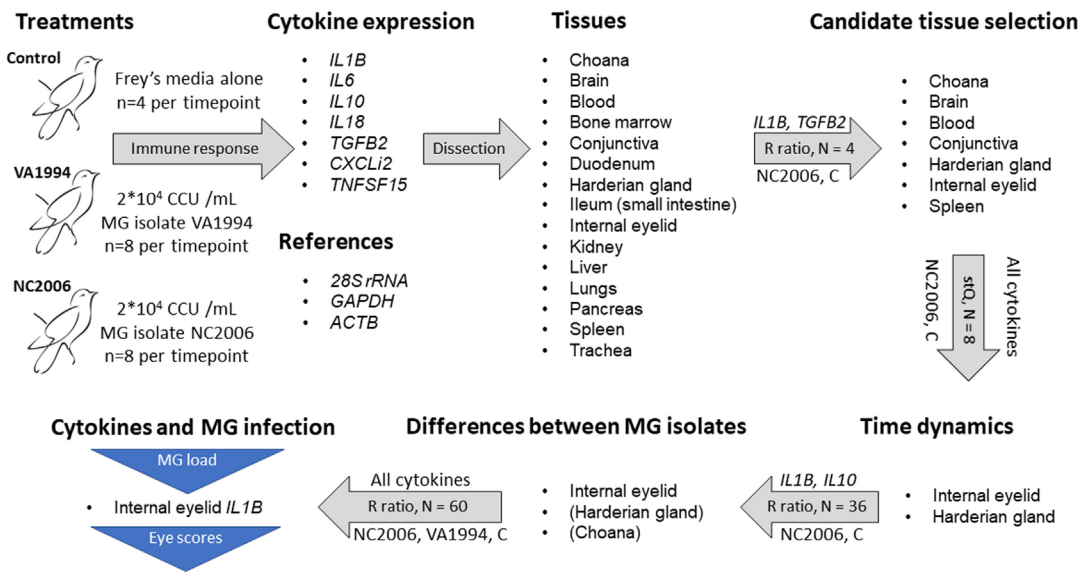

FIGURE 1 | Design of the experiment and qPCR analysis. Successive steps are linked with gray arrows indicating procedures being done. The text above the arrows indicates the specific cytokine genes used for each step, and the text below the arrows indicates the treatment group(s) used for that step [control (C)]. The text inside the arrows indicates the sample size per tissue and the metric of gene expression used [relative expression (*R*) ratio (41) calculation and standardized expression quantity (stQ) (42, 43)]. The stQ quantification was used for analyses where statistical comparisons between treatments and controls were necessary, as this is not possible using the *R* ratio. Blue triangles indicate traits for which associations to cytokine expression were tested. For isolate differences in cytokine expression in Harderian gland and choana, only a subset of cytokines was examined, and thus those two tissues are in parentheses.

aQ quantities in R software using the "heatmap" function of the "stats" library, with the Unweighted Pair Group Method with Arithmetic Mean selected as the clustering algorithm.

After this second and more in-depth round of screening of seven house finch tissues, we focused on a subset of two selected tissues (internal eyelid and HG) to examine the temporal dynamics of cytokine expression responses to MG and the differences between MG isolates. We used generalized linear models (GLMs) with cytokine expression ratio *R* or *A* as the response variable. For these GLMs, the non-Gaussian response variables were $\log_2$-transformed to achieve residual normality and tested against selected factors as explanatory variables: tissue or MG isolate (depending on analysis), time point, sex, and all two-way interactions. Because there was little variability in size and mass and the treatment groups and time point groups did not show any significant differences with respect to size or mass or mass change over the experiment (all $P > 0.05$), these variables were excluded from the full models tested in this study. We tested the significances of the explanatory variables both in full models and in minimum adequate models (MAMs; i.e., models with all terms either significant, $P \leq 0.05$, or marginally non-significant, $P < 0.10$) that were obtained by backward eliminations of particular terms from the full model. Candidate models were compared based on the change in deviance with an accompanied change in degrees of freedom (ANOVA) using *F* statistics. Tukey's *post hoc* tests were used to test for differences between individual time points or MG isolates.

A two-sample *t*-test was used to compare relative *IL1B* and *IL10* expression ($\log_2 R$) induced by the two MG isolates in upper respiratory tract at DPI 6. Relative *IL1B* and *IL10* expression ($\log_2 R$) comparisons between upper respiratory tract, internal eyelid and HG were done using linear mixed-effects models (LMMs), where $\log_2 R$ data (response variable) were tested against MG isolate, tissue type, sex and all two-way interactions (explanatory variables with fixed effects). Individual identity was included into the models as a random effect and we used backward elimination of fixed effects to obtain the minimum adequate models.

For testing the association between *IL1B* expression and conjunctival MG loads, *IL1B* $\log_2 R$ data were used as the response variable in a GLM containing endpoint MG quantities ($\log_{10}$MG), MG isolate, sampling time point (DPI), sex, and two-way interactions of the factors as explanatory variables. In an analogous GLM, we tested for an association between total eye scores and *IL1B* expression using the quasipoisson residual distribution. Here, the endpoint total eye scores were used as the response variable, and we included *IL1B* $\log_2 R$ data, MG isolate, sampling time point (DPI), sex and two-way interactions of the factors as explanatory variables in the model. Again, we used a backward elimination method (as described earlier) to obtain the minimum adequate models.

RESULTS

Tissue-Specific Variation in Cytokine Expression Response to MG

To identify candidate tissues for further research, we first compared the relative expression ratios *R* based on two NC2006-infected and two control individuals for two selected genes (*IL1B* and *TGFB2*) across the whole panel of 15 tissues. Our results (Figure S1 in Supplementary Material) show highest *R* in at least one of these genes in blood, brain, conjunctiva, HG, choana and internal lid; we thus selected these six tissues for further analysis. Spleen was also included in further analysis as a standardly investigated lymphatic tissue for the purpose of comparison.

For these seven selected tissues, we analyzed the expression of all seven investigated cytokine genes in four control individuals and four NC2006-infected individuals at DPI 6 to identify the genes differentially expressed in individual tissues during MG infection. The cytokine standardized relative quantity data (stQ) show significant differential expression of *IL1B* in brain, conjunctiva, HG and internal eyelid, of *IL6* in conjunctiva and internal eyelid, of *IL10* in conjunctiva, HG and internal eyelid, and of *CXCLi2* and *TNFSF15* in conjunctiva and internal eyelid (**Figure 2**; see Figure S2 and Tables S5 and S6 in Supplementary Material for analogous results obtained based on aQ data, *A*). No differential expression was indicated for spleen and only marginally non-significant changes in inflammatory cytokine expression were revealed in blood and upper respiratory tract. No differential expression was revealed for *IL18* or *TGFB2* in any tissue. While there was low consistency in the cytokine expression patterns across distinct tissues (except for conjunctiva and internal eyelid; **Figure 3**; Figure S3 in Supplementary Material), the expression of different cytokine genes was highly correlated within individual tissue samples (Table S7 in Supplementary Material; PCA: cumulative proportion of variance explained by PC1–PC3 = 0.898). Based on these results and prior work in this system (28), we selected pro-inflammatory *IL1B* and anti-inflammatory *IL10* as the candidate genes, and internal eyelid and HG as the target tissues, for investigation of the temporal dynamics of cytokine expression.

Temporal Dynamics of the Cytokine Expression Response to MG

To initially compare temporal patterns of cytokine expression in internal eyelid and HG in MG infected birds, we compared *IL1B* and *IL10* expression changes in NC2006 isolate-inoculated birds. Our results show significant effects of both tissue type and DPI for both genes (relative quantification: **Figure 4**; Table S8 in Supplementary Material; for absolute quantification, see Supplementary Material). Although in both genes there is apparent peak of the response at DPI 6 in both tissues, Tukey's *post hoc* tests showed significant differences between the sampling time points in internal eyelid only in *IL10* (DPI 6–DPI 13: $P = 0.023$), while in HG, DPI 6 was significantly different from the other sampling time points for both genes (*IL1B*: DPI 6–DPI 3: $P = 0.018$, DPI 6–DPI 13: $P = 0.030$; *IL10*: DPI 6–DPI 3: $P = 0.001$, and DPI 6–DPI 13: $P < 0.001$).

Differences between Cytokine Expression Responses to Original and Evolved MG Isolate

To compare the immune responses triggered by distinct MG isolates (VA1994 and NC2006), we selected the internal eyelid

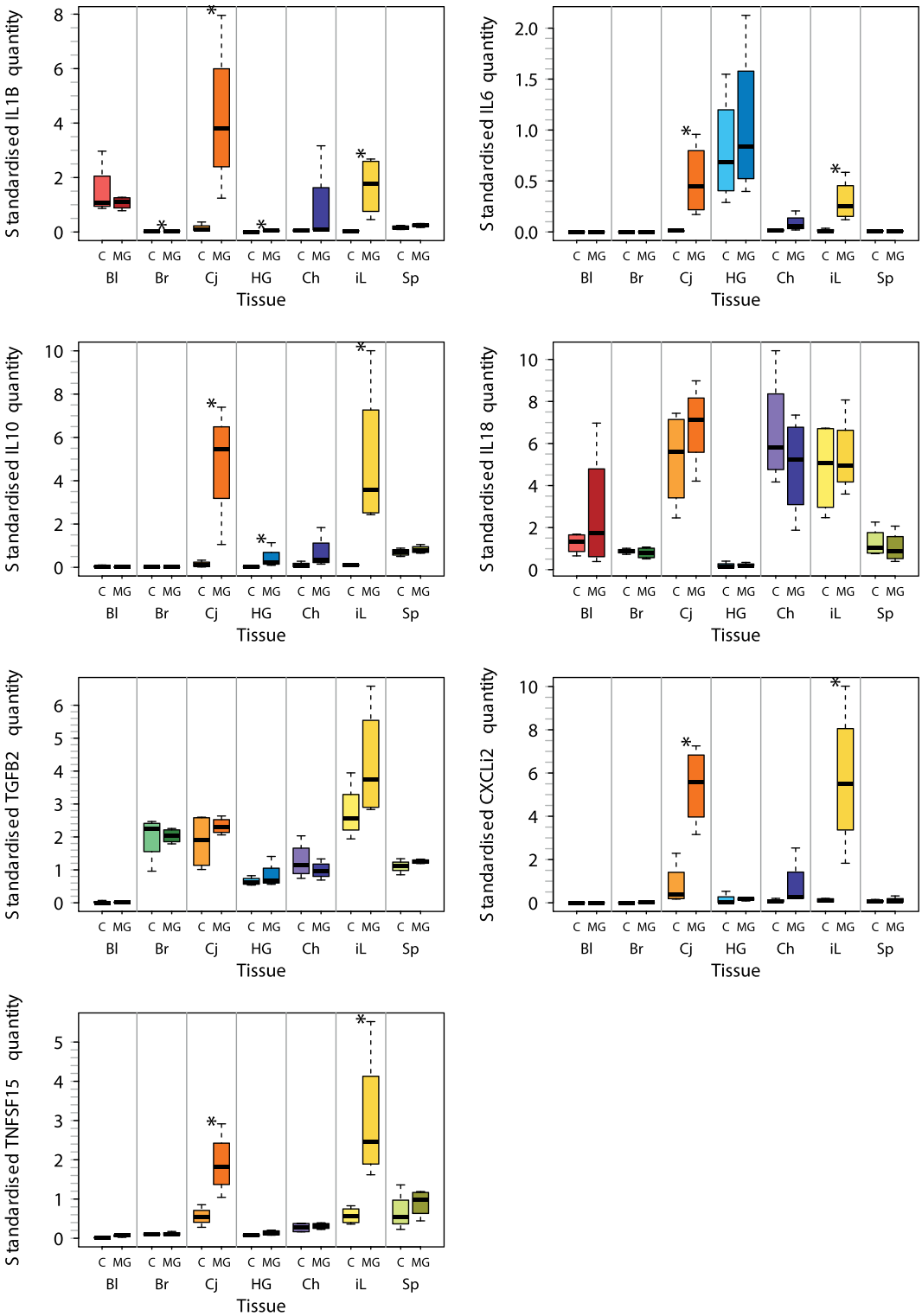

FIGURE 2 | Tissue-specific differential cytokine gene expression in *Mycoplasma gallisepticum* (MG)-infected house finches versus uninfected control (C) on day 6 postinoculation (DPI 6). The boxplots show the median (line), the upper and lower quartiles (the box), and the range (dotted lines) of relative cytokine quantity standardized on *28S rRNA* expression (stQ). Tissue types are shown on the *x* axis highlighted with color: red—blood (Bl), green—brain (Br), orange—conjunctiva (Cj), blue—Harderian gland (HG), purple—choana and upper respiratory tract (Ch), yellow—nictitating membrane = internal eyelid (iL), light green—spleen (SP). Treatment type: C, control (light colors); MG, inoculation with MG isolate NC2006 (dark colors). Asterisks indicate significant difference in gene expression in the tissue (Wilcoxon test, $P < 0.050$).

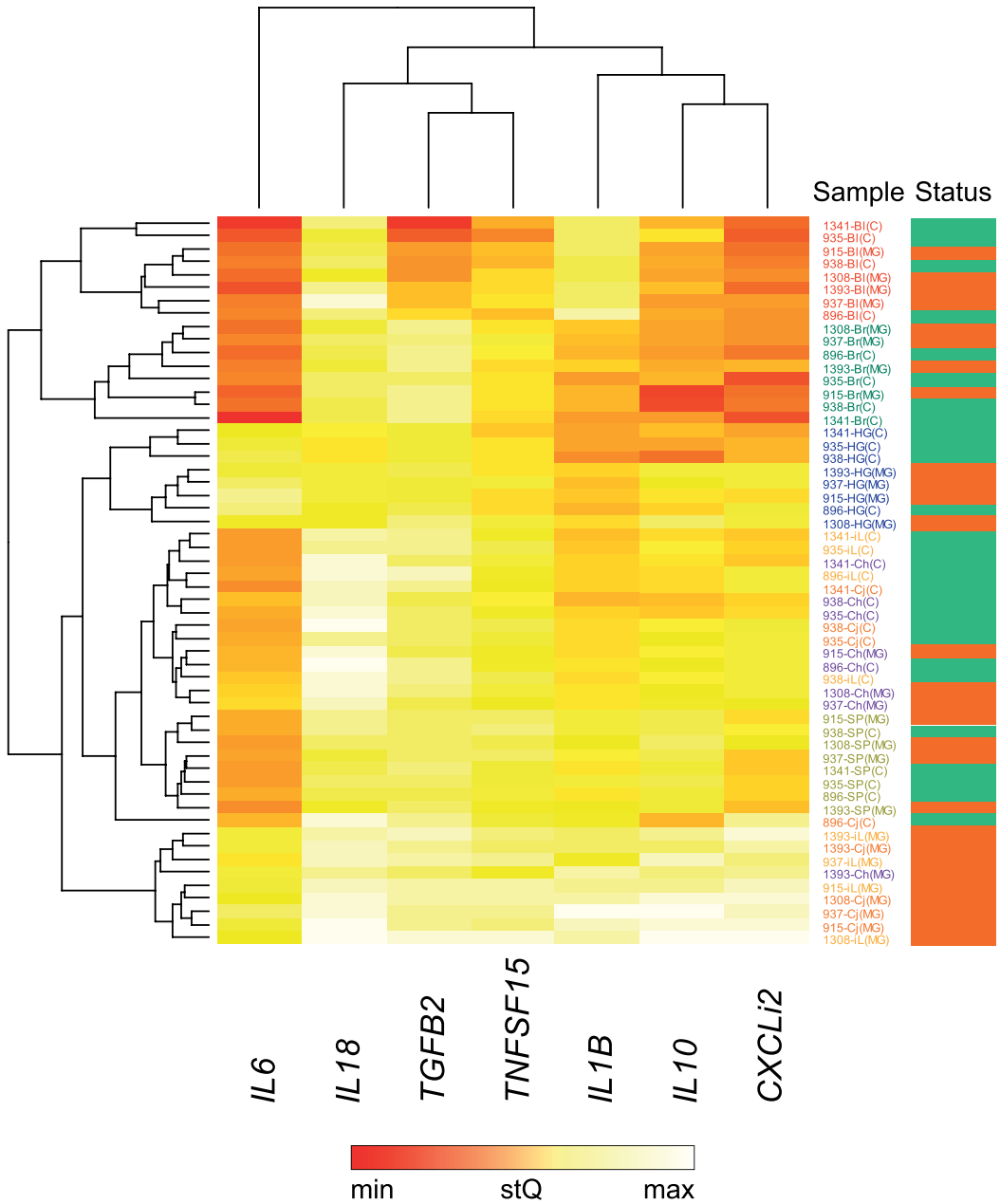

FIGURE 3 | Heatmap of differential cytokine gene expression in *Mycoplasma gallisepticum* (MG)-infected (red bar, far right) and control (green bar, far right) house finches on day 6 postinoculation (DPI 6). For this analysis, all MG-infected birds received the NC2006 isolate. The heatmap is based on relative cytokine quantity standardized on *28S rRNA* expression (stQ). Gene names are shown at the bottom of the chart. Low gene expression is indicated in red; high gene expression in white. Tissue type is highlighted with color of the sample label: red—blood (Bl), green—brain (Br), orange—conjunctiva (Cj), purple—choana and upper respiratory tract (Ch), blue—Harderian gland (HG), light orange—nictitating membrane = internal eyelid (iL), light green—spleen (SP). Dendrograms showing the clustering of the cytokine expression patterns were constructed using Unweighted Pair Group Method with Arithmetic Mean method.

as a primary model tissue, because here the strength of cytokine expression relative to controls was most prominent. In *IL1B*, *IL10*, *IL6*, *CXCLi2*, and *TNFSF15*, we found significant effects of MG isolate on cytokine expression quantified using both relative (**Table 2**; **Figure 5**) and absolute approaches (Supplementary Material). Generally, the evolved NC2006 isolate triggered stronger cytokine responses than the original VA1994 isolate, though the *post hoc* significance of isolate differences varied across genes and time points, with the strongest differences between isolates generally occurring earlier in infection (**Figure 4**). In most cases, we also detected significant effects of sampling time point. However, there was no significant effect of MG isolate or

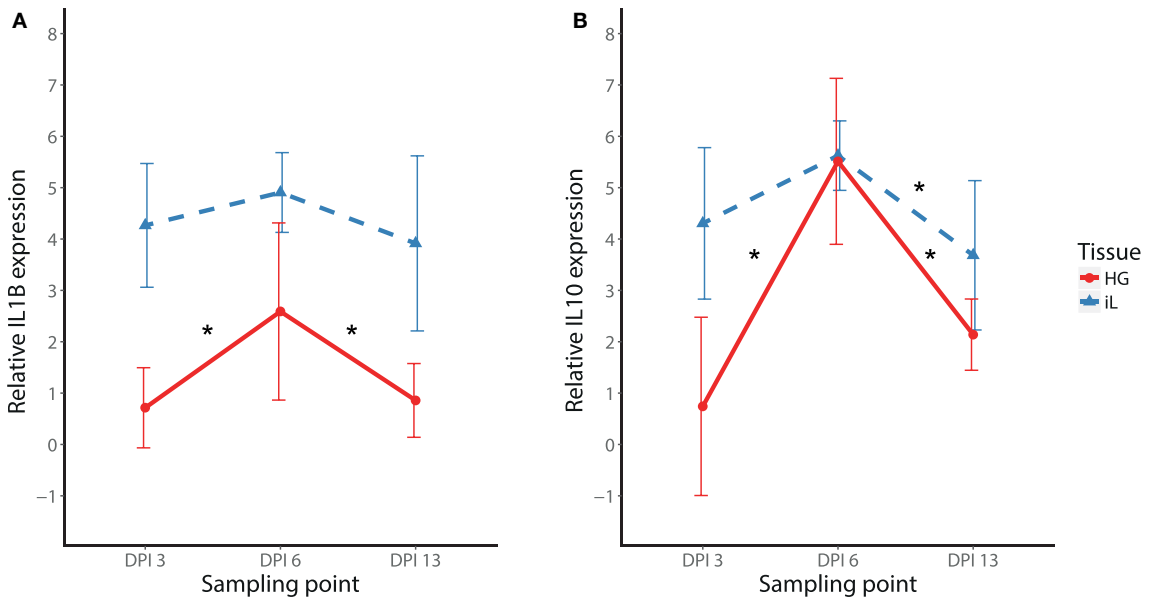

FIGURE 4 | Temporal dynamics of *IL1B* **(A)** and *IL10* **(B)** expression in response to MG-NC2006 infection in selected tissues across three different time points. The data are shown as relative expression ratio (*R*; i.e., *28S rRNA*- and control-normalized relative expression quantities) mean ± SD. Red circles represent values in Harderian gland, and blue triangles indicate values in internal eyelid. Abbreviation: DPI, day postinoculation. Asterisks mark significant differences between DPI in the respective tissues (Tukey's *post hoc* test $P_{adj} < 0.050$).

TABLE 2 | Minimum adequate models (MAMs) for effects of infection with *Mycoplasma gallisepticum* isolates VA1994 and NC2006 on house finch expression of cytokines *IL1B*, *IL6*, *IL10*, *CXCLi2*, and *TNFSF15* in internal eyelid (nictitating membrane) across three different time points.

MAM/variable	Df	*F*	*P*
Log_2R(IL1B) ~ treatment	1/46	17.88	<0.001
Log_2R(IL6) ~ treatment + DPI	3/44	5.63	0.002
Treatment	1/44	6.70	0.013
DPI	2/44	5.09	0.010
Log_2R(IL10) ~ treatment + DPI	3/44	8.50	<0.001
Treatment	1/44	9.33	0.004
DPI	2/44	8.09	0.001
Log_2R(CXCLi2) ~ treatment + DPI	3/44	12.41	=0.001
Treatment	1/44	16.21	<0.001
DPI	2/44	10.51	<0.001
Log_2R(TNFSF15) ~ treatment + DPI	5/42	4.55	0.002
Treatment	3/42	6.87	0.001
DPI	4/42	2.35	0.070
Treatment: DPI	2/42	3.63	0.035

Based on the relative expression ratio (R) data (i.e., 28S rRNA- and control-normalized relative expression quantities).
Treatment, inoculation with VA1994 or NC2006; DPI, days postinoculation; IL, interleukin; TNFSF, tumor necrosis factor superfamily members.

sampling time point on expression of *IL18* and *TGFB2* in internal eyelid in house finches (relative and absolute quantification data; all terms $P > 0.05$).

We also compared isolate-specific patterns of expression (original VA1994 versus evolved NC2006) for a subset of cytokines (*IL1B* and *IL10*) in HG. Similar to the results from internal eyelid, the NC2006 isolate triggered stronger *IL1B* responses than the original VA1994 isolate in HG (MG isolate $F_{1/44} = 7.03$, $P = 0.011$; stp $F_{2/44} = 10.33$, $P < 0.001$; MAM: $F_{3/44} = 9.23$, $P = 0.001$; **Figure 6A**). However, for the anti-inflammatory cytokine *IL10*, expression in HG was dependent only on sampling time point (MAM: $F_{2/45} = 29.78$, $P = 0.001$; **Figure 6B**) and not the MG isolate.

Because MG infection in chickens induces cytokine responses in the upper respiratory tract (27), we also checked for isolate-specific differences in *IL1B* and *IL10* stimulation in the upper respiratory tract at the time of the peak cytokine expression response (DPI 6) and compared the cytokine expression in this tissue with cytokine expression in HG and internal eyelid. Although we found significant effects of both tissue and MG isolate on *IL1B* and *IL10* expression across the three tissues (LMM analysis; Table S12 in Supplementary Material), we did not detect any significant differences between the MG isolates in either *IL1B* or *IL10* in the upper respiratory tract in particular (two-sample *t*-test, in both cases $P > 0.05$; **Figure 7**). Thus, isolates VA1994 and NC2006 activate similar pro-inflammatory cytokine expression responses in the upper respiratory tract, but as shown earlier, NC2006 triggers significantly stronger immune activation in internal eyelid and HG (for *IL1B* alone) than VA1994 (**Figure 7A**). When analyzed as tissue-specific differences within individuals, there is no difference in *IL1B* and *IL10* expression between upper respiratory tract, HG and internal eyelid for VA1994 (Tukey's test, in all cases $F_{adj} > 0.05$); however, in the case of NC2006, cytokine expression responses are significantly stronger in internal eyelid/HG compared with the upper respiratory tract (Tukey's *post hoc* test, *IL1B*: Ch-HG $P_{adj} > 0.05$, iL-HG $P_{adj} = 0.023$, iL-Ch $P_{adj} = 0.005$, *IL10*: Ch-HG $P_{adj} < 0.001$, iL-HG $P_{adj} > 0.05$, iL-Ch $P_{adj} < 0.001$).

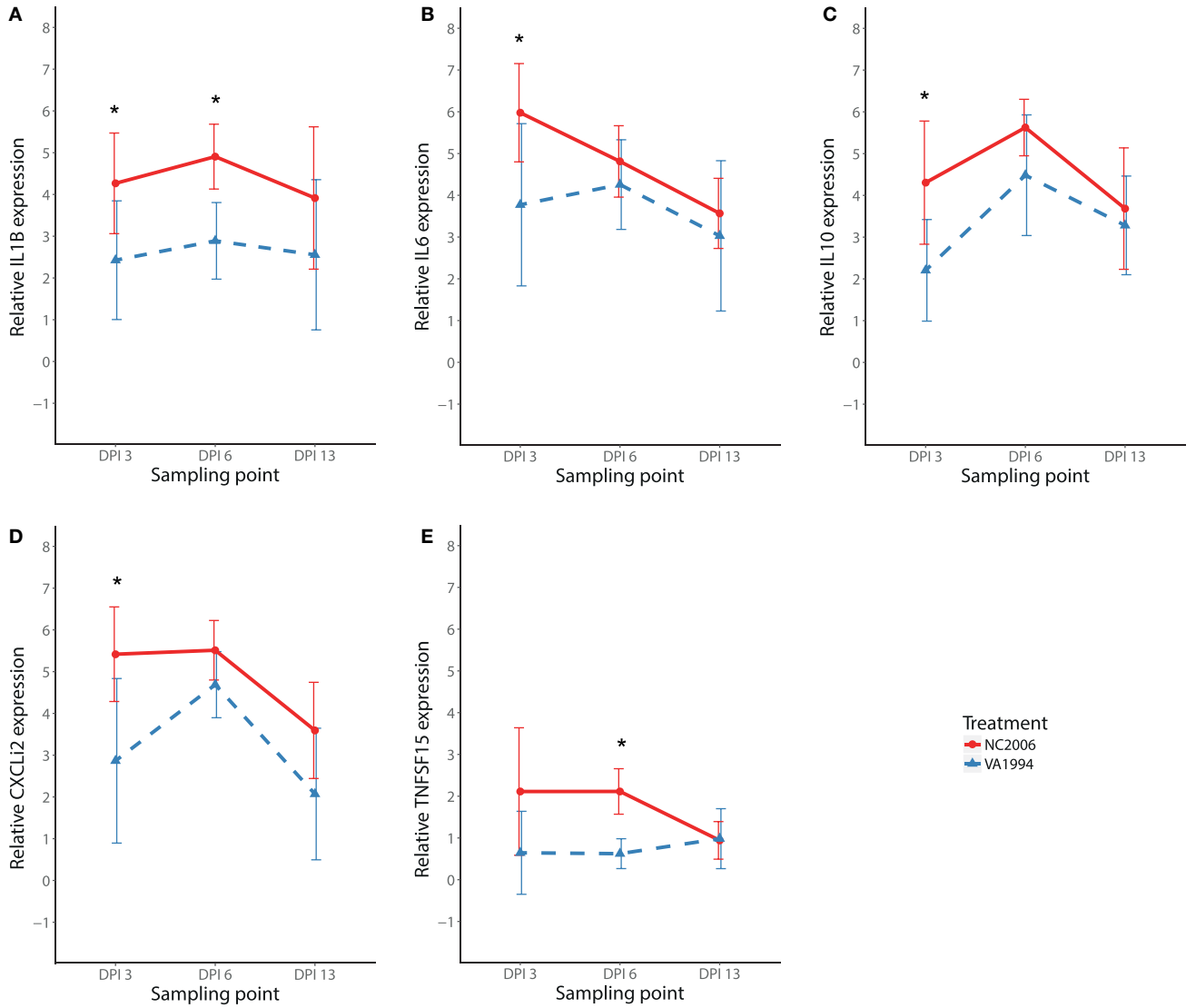

FIGURE 5 | Effects of experimental infection with *Mycoplasma gallisepticum* isolates VA1994 and NC2006 on *IL1B* **(A)**, *IL6* **(B)**, *IL10* **(C)**, *CXCLi2* **(D)**, and *TNFSF15* **(E)** expression in internal eyelid (nictitating membrane) across three different time points. The data are shown as *28S rRNA*- and control-normalized mean ± SD relative expression quantities. Blue triangles indicate VA1994 isolate data, and red circles represent NC2006 isolate data. Asterisks indicate significant difference in gene expression between isolates at that time point (Tukey's *post hoc* test, $P < 0.050$). Sampling points: DPI 3, 3 days post inoculation; DPI 6, 6 days post inoculation; DPI 13, 13 days post inoculation.

Relationship between Cytokine Expression and Intensity of MG Infection

To examine the association between MG infection intensity (MG loads in the conjunctiva at the time of sampling, which differed by batch) and cytokine expression in periorbital tissues, we focused on *IL1B* as the cytokine that showed the most consistent differences between isolates. We found strong effects of conjunctival MG load on internal eyelid *IL1B* relative expression ($F_{1/45} = 69.37$, $P = 0.001$), with higher *IL1B* relative expression in birds with higher conjunctival MG burdens (**Figure 7**). We also found notable effect of MG isolate ($F_{1/45} = 18.53$, $P = 0.001$), with higher average pathogen loads in birds inoculated with NC2006 (MAM: $F_{2/45} = 56.90$, $P = 0.001$; **Figure 8**).

Finally, to examine the relationship between pro-inflammatory cytokine expression in internal eyelid and MG pathogenicity, we analyzed the interaction between *IL1B* and total eye scores (representing the visible pathological effects of MG infection) at the time of sampling. Our results show significant associations between *IL1B* expression ($F_{1/44} = 13.32$, $P < 0.001$), sampling time point ($F_{2/44} = 12.37$, $P = 0.001$), and total eye scores (MAM: $F_{3/44} = 12.66$, $P = 0.001$; **Figure 9**), such that birds with higher *IL1B* expression had significantly higher total eye scores.

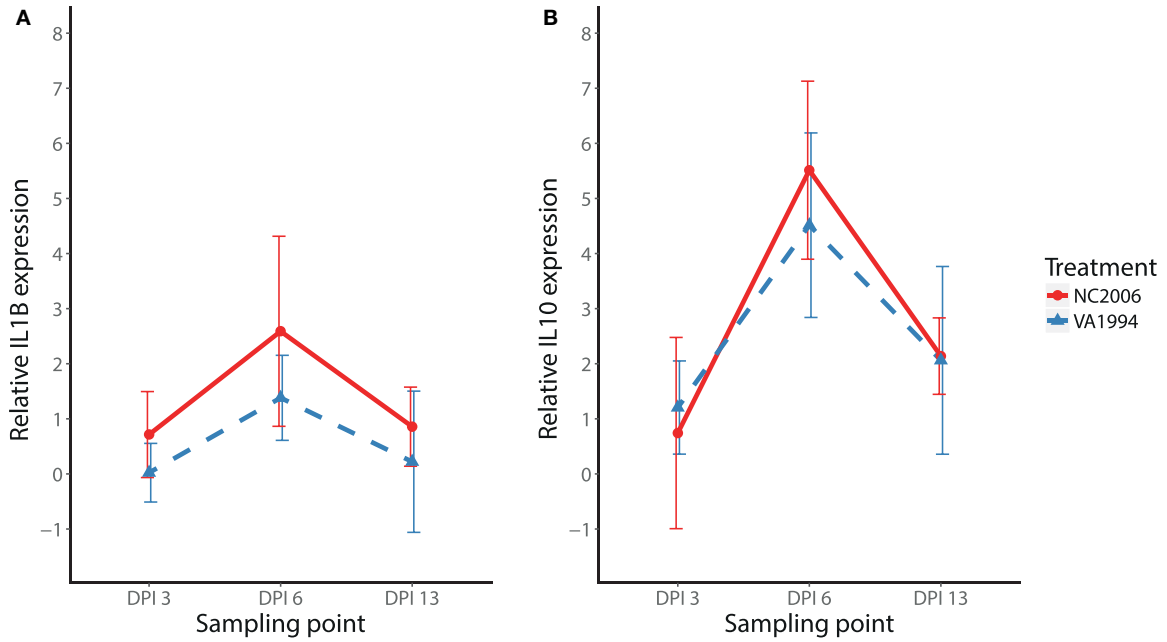

FIGURE 6 | Effects of experimental infection with *Mycoplasma gallisepticum* isolates VA1994 and NC2006 on *IL1B* **(A)** and *IL10* **(B)** expression in Harderian gland across three different time points. The data are shown as *28S rRNA*- and control-normalized mean ± SD relative expression quantities. Blue triangles indicate birds inoculated with VA1994 isolate, and red circles indicate birds inoculated with NC2006. Sampling points: DPI 3, 3 days post inoculation; DPI 6, 6 days post inoculation; DPI 13, 13 days post inoculation.

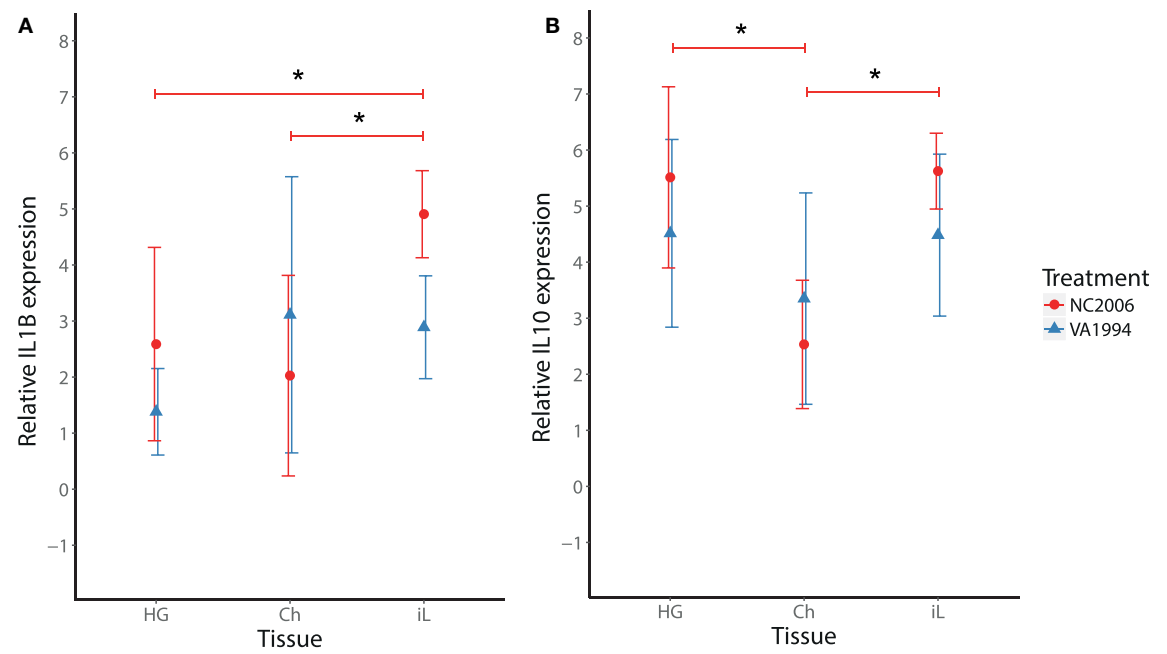

FIGURE 7 | Effects of experimental infection with *Mycoplasma gallisepticum* isolates VA1994 and NC2006 on *IL1B* **(A)** and *IL10* **(B)** expression in selected tissues at the time of peak cytokine expression [day 6 post inoculation (DPI 6)]. The data are shown as *28S rRNA*- and control-normalized mean ± SD relative expression quantities. Blue triangles indicate VA1994 isolate data, and red circles represent NC2006 isolate data. Asterisks above connecting lines indicate significant difference in gene expression between tissues (Tukey's *post hoc* test, $P < 0.050$). Tissues: HG, Harderian gland; Ch, upper respiratory tract and choana; iL, internal eyelid (nictitating membrane).

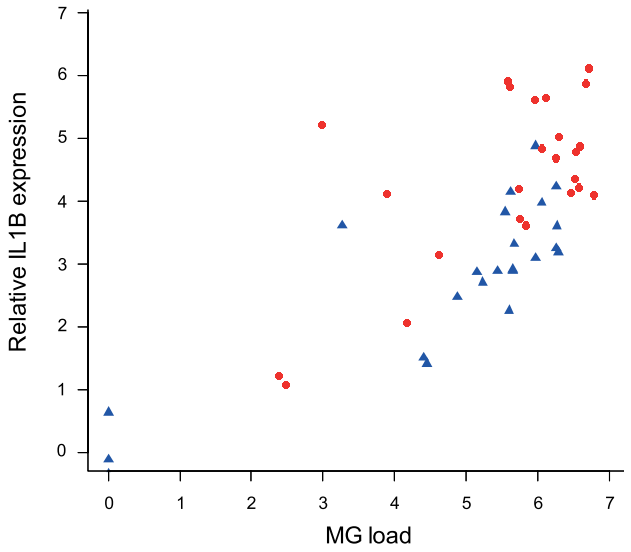

FIGURE 8 | Association between conjunctival MG loads at the time of examination (which varied for each batch collected at one of three sampling time points) and *IL1B* expression in internal eyelid. The data on *IL1B* expression are shown as *28S rRNA*- and control-normalized relative expression quantities ($\log_2 R$). Because isolate was significant in the statistical model, points are labeled by MG isolate (blue circles = VA1994 and red triangles = NC2006).

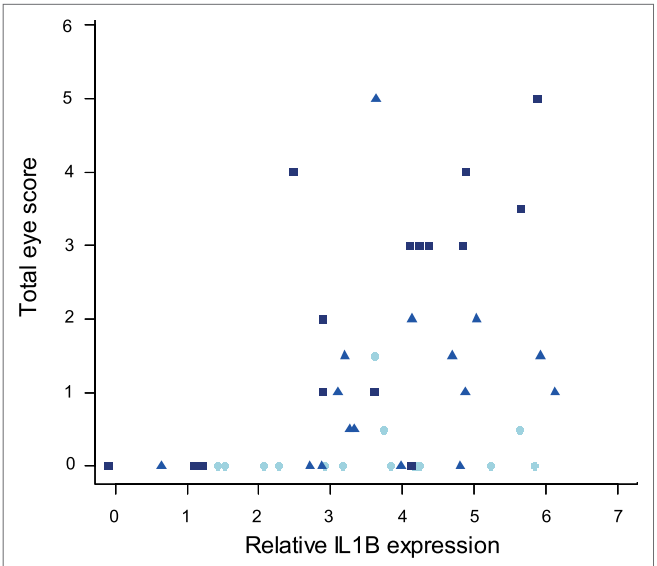

FIGURE 9 | Relationship between *IL1B* expression in internal eyelid and total eye scores (index of MG pathogenicity) at the time of sampling (which varied for each batch collected at one of three sampling time points). The data on *IL1B* expression (explanatory variable) are shown as *28S rRNA*- and control-normalized relative expression quantities ($\log_2 R$). Because sampling time point was significant in the minimum adequate model, points are labeled by sample date (light blue = DPI 3, blue = DPI 6, and dark blue = DPI 13).

DISCUSSION

Mycoplasma gallisepticum-infected house finches show several systemic changes in immunological traits, including alterations in blood leukocyte profiles (22) and antibody production (24). In this study, we characterized the tissue distribution and temporal dynamics of cytokine responses to MG infection, showing that cytokine expression changes are strongest in periocular tissues, and peak between days 3 and 6 postinoculation (PI). Furthermore, we showed that cytokine responses are significantly stronger following inoculation with an evolutionarily derived lineage of MG, and that the load of MG infection among individuals directly predicts the degree of *IL1B* expression, which is associated with the severity of mycoplasmal conjunctivitis (an index of MG pathogenicity).

The capacity of MG to trigger expression of pro-inflammatory cytokines has been previously shown in both poultry (27, 45, 46) and human (47) cells and tissues. Here, we first used a subset of individuals to characterize the tissue distribution of cytokine expression on day 6 postinoculation in house finches. For this analysis, we chose to only examine the most virulent isolate of MG to maximize our likelihood of detecting differential expression. We detected significant upregulation of five (*IL1B*, *IL10*, *IL6*, *CXCLi2*, and *TNFSF15*) of the seven examined cytokines in conjunctiva and nictitating membrane (internal eyelid), and significant upregulation of *IL1B* and *IL10* in HG. In birds, the conjunctiva and the HG are parts of the eye-associated secondary lymphoid tissue (48). Being colonized with large number of T cells and B cells, the HG plays an important role in the regulation of ocular immunity, including antibody and inflammatory responses to conjunctival pathogens. The nictitating membrane, on the other hand, is primarily a non-lymphoid tissue, that is, however, rapidly infiltrated with leukocytes upon MG infection.

While upregulation of key cytokines in the periocular tissues during MG infection is not surprising, we also observed significant upregulation of *IL1B* expression in the brain. IL1B experimentally administrated to the brain as well as released in the periphery during infection can elicit vertebrate sickness behaviors and impair memory (49, 50). Our results support the view that, like in mammals (51), IL1B may act in the avian brain as an important mediator of the acute phase response, which in house finches leads to fever and severe lethargy associated with MG infection (12, 28). The mechanism behind this relationship, however, awaits verification in the house finch–MG system.

There was only low consistency in the cytokine expression patterns across distinct tissues, and we found no evidence for significant differential cytokine expression in any other tissues aside from the brain and periocular tissues, including spleen, upper respiratory tract, or blood. Although this result could be affected by the limited sample size used for the investigation of the tissue distribution of cytokine expression ($n = 4$ per treatment), overall, our results clearly indicate that differential cytokine expression responses during MG infection are strongest in periorbital tissues (conjunctiva, internal eyelid, and HG). Finally, although the expression of most inflammatory cytokine genes was highly correlated within individual tissues, we did not detect differential expression of *IL18* or *TGFB2* in any tissue examined, suggesting that these cytokines do not respond to MG infection. This pattern is consistent with house finch cytokine regulation toward a type 1 adaptive immune response that is mediated by non-specific inflammation leading to induction of Th1 cell activation.

After determining which genes and tissues would be most relevant for further study, we examined the temporal dynamics of cytokine expression in internal eyelid and HG (two distinct periorbital immune tissues), focusing on pro-inflammatory *IL1B* and anti-inflammatory *IL10*. For both of these cytokines, responses peaked at day 6 postinoculation, but this peak was only significant in both genes for HG, where overall expression was generally lower than in internal eyelid. In poultry, *IL1B* expression responses to MG inoculation appear to be strongest between day 4 and day 8 PI (27). This is consistent with our further findings on the temporal dynamics in most other pro-inflammatory cytokines (*IL6*, *CXCLi2*, and *TNFSF15*), where the expression in internal eyelid exhibits similar patterns of early upregulation (DPI 3–6) followed by a decline in cytokine expression at our latest sampling point examined (DPI 13). Nevertheless, our multiple-isolate analysis showed that the temporal dynamics of responses varied to some extent with the strain of MG used. Future work with higher temporal sampling resolution and larger sample sizes will help to shed further light on strain-specific temporal dynamics of cytokine expression in house finches.

A primary goal of our study was to examine how pathogen evolution affects cytokine expression responses in its host. Various MG strains, including those from the house finch–MG clade, differ in their surface antigens, which may cause variation in their interaction with the immune system of the host (16, 52). Because MG has evolved to become significantly more virulent since its initial emergence in house finches (18), we characterized cytokine responses to an original field isolate (VA1994) collected the year that MG was first detected in house finches, and a more evolved isolate (NC2006) shown to be significantly more virulent in house finches. These two isolates are closely related (11) but show notable genomic differences (19) and produce markedly distinct host responses and epidemiological parameters, with NC2006 producing significantly higher conjunctival pathogen loads and disease severity (18), stronger IgG and IgA responses (9), and faster rates of transmission than that of VA1994 (53). For all five of the cytokine genes differentially expressed on day 6 post-MG inoculation in periocular tissues (*IL1B*, *IL6*, *IL10*, *CXCLi2*, and *TNFSF15*), we found significantly stronger cytokine responses in birds inoculated with NC2006 relative to those inoculated with VA1994 in internal eyelid (and for *IL1B* in HG). These results are consistent with the stronger stimulation of humoral responses by the NC2006 isolate relative to the VA1994 isolate detected in prior work (9). We did not detect any significant changes in cytokine expression in response to MG infection in the upper respiratory tract, and we did not detect any differences between the MG isolates in either *IL1B* or *IL10* expression in this tissue. Hence, our results suggest that the house finch–MG strains have evolved in their capacity to specifically elicit pro-inflammatory cytokine expression in periorbital tissues and not in other tissues, such as the upper respiratory tract. MG was previously shown to adapt to its passerine host, resulting in milder virulence for more evolved house finch–MG isolates in the original poultry host (54, 55), but increased virulence in the novel house finch host, where the disease has become established (18, 56). Although our results are strongly suggestive of an evolutionary change in cytokine expression linked with increased virulence, multiple evolved (and virulent) isolates are needed to definitively link strain-level changes in virulence with host cytokine expression responses.

We also leveraged individual variation in the degree of pathogenicity (eye lesion score) and infection intensity (conjunctival pathogen load) at the time of euthanasia to further link host immune responsiveness to virulence, as has been done in prior studies with humoral responses (9). We show that birds with higher expression of *IL1B* also had significantly higher eye lesion scores and conjunctival pathogen loads. Together, these results suggest that prolonged house finch pro-inflammatory cytokine responses are likely not protective during MG infection, but instead may underlie the degree of pathology experienced by hosts. Thus, although evolution of a protective immune response to MG has been reported in house finches (4, 26, 57), mycoplasmal conjunctivitis *per se* appears to be largely immunopathological in house finches, with important implication for host–pathogen coevolution (58). Experimental manipulations of pro-inflammatory cytokine signaling in the house finch–MG system are, nonetheless, needed to confirm the causality underlying the detected associations.

There are several documented examples of animal diseases where overactivation of immune cytokine signaling is responsible for immunopathology (59–61). In poultry, overly strong inflammation is likely a cause of some of the pathologies associated with mycoplasmosis (62). Although much of the recent knowledge on cytokine regulation of inflammation comes from mammalian studies (63), present evidence from birds, mainly from the domestic chicken (31), suggests that (although equipped with slightly different sets of cytokines) the basic functions of the most essential cytokines may be conserved within amniotes. In house finches, this has been confirmed for IL1B, where its conserved function was demonstrated in splenocytes (38). Our results, combined with prior research (28), suggest that the degree of inflammation is a key trait underlying house finch responses to this disease. Thus, any factors that suppress inflammation, such as anti-inflammatory cytokines, Treg cells or circulating immunosuppressing stress hormones levels, may be key in limiting the severity of disease, and thus, the fitness effects on house finches. In fact, Love et al. (64) showed that preinfection glucocorticoid (in this case, corticosterone) concentrations in male house finches were associated with reduced inflammation and pathogen load, suggesting that dampened inflammation may be a key mechanism of resistance or tolerance in this system.

Pathogens have been shown to use many different means to manipulate host immunity for the purpose of increasing their transmission rate (65, 66). This manipulation may include down-regulation, as well as upregulation of host inflammatory immunity that may be used by the pathogen to increase permeability of host tissues and facilitate transmission. While Ganapathy and Bradbury (67) previously reported temporary T-cell suppression at 2 weeks post MG infection in chickens, it is possible that in house finches, MG manipulates its host toward more intense and/or prolonged pro-inflammatory gene expression in the periocular tissues. In house finches experimentally inoculated with MG, enhanced pathology (i.e., higher eye scores) leads to a higher proportion of conjunctival MG deposited onto bird feeders (68),

likely due to exudate or swelling enhancing pathogen deposition into the environment. Thus, prolonged or enhanced expression of pro-inflammatory cytokines may have important fitness benefits for MG by enhancing host pathologies that contribute to transmission. However, experiments directly manipulating cytokine levels are needed to causally test this hypothesis.

Altogether, our results show that increased virulence of an evolutionarily derived MG isolate is associated with increased periocular expression of pro-inflammatory cytokines. Although our experiment cannot confirm the direction of causality underling this association, immunopathology induced by this inflammation might explain the mechanism of maladaptation of house finch immunity to MG. Given the demonstrated fitness costs of conjunctivitis for free-living house finches (69), future research should examine whether house finch populations with distinct coevolutionary histories with MG differ in their inflammatory cytokine responses to this pathogen, which would suggest that host evolution is also influencing house finch cytokine responses. Overall, future studies that simultaneously examine evolutionary variation in both host and pathogen will be critical to dissecting the distinct contributions of each coevolutionary player to house finch pro-inflammatory cytokine responses during MG infection.

ETHICS STATEMENT

This study was carried out in accordance with the recommendations of federal (USFWS permit MB158404-1) and state (VDGIF permit 050352) agencies. The protocol was approved by the Virginia Tech's Institutional Animal Care and Use Committees.

AUTHOR CONTRIBUTIONS

MV and DH designed the research; MV, AL, LK, and DH performed the research procedures; RD provided RNA-seq data; MV and DH analyzed the data; and MV, RD, and DH prepared the manuscript. All the authors contributed with their comments to the conception of the work and final version of the manuscript.

ACKNOWLEDGMENTS

The authors are grateful to Prof. David Ley and his team of the Mycoplasma Diagnostic and Research Laboratory at the NC State University College of Veterinary Medicine for MG isolates used in this experiment, to Robert E. Settlage for his help with NGS data analysis, to Myeongseon Park for her laboratory assistance, to Matthew Aberle, Sarah Taylor, Eddie Schuler, Natalie Bale, Courtney Thomason, Courtney Youngbar, and Sahnzi C. Moyers for their help with field procedures and data collection and to Zuzana Świderská for her assistance with figure design. The authors are also thankful to the subject editors and two anonymous reviewers for their valuable comments on earlier versions of the manuscript.

FUNDING

This experiment was supported by NIH grant 5R01GM105245 to DH from the joint NIH-NSF-USDA Ecology and Evolution of Infectious Diseases Program. MV was supported by grant No. 2015-21-04 from the Fulbright Commission in the Czech Republic and grant No. PRIMUS/17/SCI/12 from the Charles University.

SUPPLEMENTARY MATERIAL

The Supplementary Material for this article can be found online at http://www.frontiersin.org/articles/10.3389/fimmu.2018.00013/full#supplementary-material.

REFERENCES

1. Kerr PJ. Myxomatosis in Australia and Europe: a model for emerging infectious diseases. *Antiviral Res* (2012) 93:387–415. doi:10.1016/j.antiviral.2012.01.009
2. Savage AE, Zamudio KR. Adaptive tolerance to a pathogenic fungus drives major histocompatibility complex evolution in natural amphibian populations. *Proc Biol Sci* (2016) 283:20153115. doi:10.1098/rspb.2015.3115
3. Langwig KE, Hoyt JR, Parise KL, Frick WF, Foster JT, Kilpatrick AM. Resistance in persisting bat populations after white-nose syndrome invasion. *Philos Trans R Soc Lond B Biol Sci* (2017) 372:20160044. doi:10.1098/rstb.2016.0044
4. Bonneaud C, Balenger SL, Russell AF, Zhang JW, Hill GE, Edwards SV. Rapid evolution of disease resistance is accompanied by functional changes in gene expression in a wild bird. *Proc Natl Acad Sci U S A* (2011) 108:7866–71. doi:10.1073/pnas.1018580108
5. Fassbinder-Orth CA. Methods for quantifying gene expression in ecoimmunology: from qPCR to RNA-Seq. *Integr Comp Biol* (2014) 54:396–406. doi:10.1093/icb/icu023
6. Ellison AR, Savage AE, DiRenzo GV, Langhammer P, Lips KR, Zamudio KR. Fighting a losing battle: vigorous immune response countered by pathogen suppression of host defenses in the chytridiomycosis-susceptible frog *Atelopus zeteki*. *G3 (Bethesda)* (2014) 4:1275–89. doi:10.1534/g3.114.010744
7. Staley M, Bonneaud C. Immune responses of wild birds to emerging infectious diseases. *Parasite Immunol* (2015) 37:242–54. doi:10.1111/pim.12191
8. Duggal NK, Bosco-Lauth A, Bowen RA, Wheeler SS, Reisen WK, Felix TA, et al. Evidence for co-evolution of West Nile virus and house sparrows in North America. *PLoS Negl Trop Dis* (2014) 8:e3262. doi:10.1371/journal.pntd.0003262
9. Grodio JL, Hawley DM, Osnas EE, Ley DH, Dhondt KV, Dhondt AA, et al. Pathogenicity and immunogenicity of three *Mycoplasma gallisepticum* isolates in house finches (*Carpodacus mexicanus*). *Vet Microbiol* (2012) 155:53–61. doi:10.1016/j.vetmic.2011.08.003
10. Ley DH. *Mycoplasma gallisepticum* infection. In: Saif YM, editor. *Diseases of Poultry*. Ames, IA: Blackwell Publishing. (2008). p. 807–34.
11. Hochachka WM, Dhondt AA, Dobson A, Hawley DM, Ley DH, Lovette IJ. Multiple host transfers, but only one successful lineage in a continent-spanning emergent pathogen. *Proc Biol Sci* (2013) 280:20131068. doi:10.1098/rspb.2013.1068
12. Kollias GV, Sydenstricker KV, Kollias HW, Ley DH, Hosseini PR, Connolly V, et al. Experimental infection of house finches with *Mycoplasma gallisepticum*. *J Wildl Dis* (2004) 40:79–86. doi:10.7589/0090-3558-40.1.79
13. Hochachka WM, Dhondt AA. Density-dependent decline of host abundance resulting from a new infectious disease. *Proc Natl Acad Sci U S A* (2000) 97:5303–6. doi:10.1073/pnas.080551197
14. Dhondt AA, Altizer S, Cooch EG, Davis AK, Dobson A, Driscoll MJL, et al. Dynamics of a novel pathogen in an avian host: mycoplasmal conjunctivitis in house finches. *Acta Trop* (2005) 94:77–93. doi:10.1016/j.actatropica.2005.01.009
15. Delaney NF, Balenger S, Bonneaud C, Marx CJ, Hill GE, Ferguson-Noel N, et al. Ultrafast evolution and loss of CRISPRs following a host shift in a novel wildlife pathogen, *Mycoplasma gallisepticum*. *PLoS Genet* (2012) 8:e1002511. doi:10.1371/journal.pgen.1002511

16. Tulman ER, Liao X, Szczepanek SM, Ley DH, Kutish GF, Geary SJ. Extensive variation in surface lipoprotein gene content and genomic changes associated with virulence during evolution of a novel North American house finch epizootic strain of *Mycoplasma gallisepticum*. *Microbiology* (2012) 158:2073–88. doi:10.1099/mic.0.058560-0
17. Hawley DM, Dhondt KV, Dobson AP, Grodio JL, Hochachka WM, Ley DH, et al. Common garden experiment reveals pathogen isolate but no host genetic diversity effect on the dynamics of an emerging wildlife disease. *J Evol Biol* (2010) 23:1680–8. doi:10.1111/j.1420-9101.2010.02035.x
18. Hawley DM, Osnas EE, Dobson AP, Hochachka WM, Ley DH, Dhondt AA. Parallel patterns of increased virulence in a recently emerged wildlife pathogen. *PLoS Biol* (2013) 11:e1001570. doi:10.1371/journal.pbio.1001570
19. Grodio JL, Ley DH, Schat KA, Hawley DM. Chronic *Mycoplasma* conjunctivitis in house finches: host antibody response and *M. gallisepticum* VlhA expression. *Vet Immunol Immunopathol* (2013) 154:129–37. doi:10.1016/j.vetimm.2013.05.010
20. Hill GE, Farmer KL. Carotenoid-based plumage coloration predicts resistance to a novel parasite in the house finch. *Naturwissenschaften* (2005) 92:30–4. doi:10.1007/s00114-004-0582-0
21. Hosseini PR, Dhondt AA, Dobson A. Seasonality and wildlife disease: how seasonal birth, aggregation and variation in immunity affect the dynamics of *Mycoplasma gallisepticum* in house finches. *Proc Biol Sci* (2004) 271:2569–77. doi:10.1098/rspb.2004.2938
22. Davis AK, Cook KC, Altizer S. Leukocyte profiles in wild house finches with and without mycoplasmal conjunctivitis, a recently emerged bacterial disease. *Ecohealth* (2004) 1:362–73. doi:10.1007/s10393-004-0134-2
23. Fratto M, Ezenwa VO, Davis AK. Infection with *Mycoplasma gallisepticum* buffers the effects of acute stress on innate immunity in house finches. *Physiol Biochem Zool* (2014) 87:257–64. doi:10.1086/674320
24. Grodio JL, Buckles EL, Schat KA. Production of house finch (Carpodacus mexicanus) IgA specific anti-sera and its application in immunohistochemistry and in ELISA for detection of *Mycoplasma gallisepticum*-specific IgA. *Vet Immunol Immunopathol* (2009) 132:288–94. doi:10.1016/j.vetimm.2009.06.006
25. Wang ZS, Farmer K, Hill GE, Edwards SV. A cDNA macroarray approach to parasite-induced gene expression changes in a songbird host: genetic response of house finches to experimental infection by *Mycoplasma gallisepticum*. *Mol Ecol* (2006) 15:1263–73. doi:10.1111/j.1365-294X.2005.02753.x
26. Bonneaud C, Balenger SL, Zhang JW, Edwards SV, Hill GE. Innate immunity and the evolution of resistance to an emerging infectious disease in a wild bird. *Mol Ecol* (2012) 21:2628–39. doi:10.1111/j.1365-294X.2012.05551.x
27. Mohammed J, Frasca S, Cecchini K, Rood D, Nyaoke AC, Geary SJ, et al. Chemokine and cytokine gene expression profiles in chickens inoculated with *Mycoplasma gallisepticum* strains R-low or GT5. *Vaccine* (2007) 25:8611–21. doi:10.1016/j.vaccine.2007.09.057
28. Adelman JS, Kirkpatrick L, Grodio JL, Hawley DM. House finch populations differ in early inflammatory signaling and pathogen tolerance at the peak of *Mycoplasma gallisepticum* infection. *Am Nat* (2013) 181:674–89. doi:10.1086/670024
29. Ley DH, Hawley DM, Geary SJ, Dhondt AA. House finch (*Haemorhous mexicanus*) conjunctivitis, and *Mycoplasma* spp. isolated from North American wild birds, 1994–2015. *J Wildl Dis* (2016) 52:669–73. doi:10.7589/2015-09-244
30. Ashley NT, Weil ZM, Nelson RJ. Inflammation: mechanisms, costs, and natural variation. In: Futuyma DJ, editor. *Annual Review of Ecology, Evolution, and Systematics*. (Vol. 43), Palo Alto: Annual Reviews (2012). p. 385–406.
31. Kaiser P, Stäheli P. Avian cytokines and chemokines. *Avian Immunology*. London: Academic Press (2014). p. 189–204.
32. Vinkler M, Svobodova J, Gabrielova B, Bainova H, Bryjova A. Cytokine expression in phytohaemagglutinin-induced skin inflammation in a galliform bird. *J Avian Biol* (2014) 45:43–50. doi:10.1111/j.1600-048X.2011.05860.x
33. Hawley DM, Grodio J, Frasca S, Kirkpatrick L, Ley DH. Experimental infection of domestic canaries (*Serinus canaria domestica*) with *Mycoplasma gallisepticum*: a new model system for a wildlife disease. *Avian Pathol* (2011) 40:321–7. doi:10.1080/03079457.2011.571660
34. Ley DH, Berkhoff JE, McLaren JM. *Mycoplasma gallisepticum* isolated from house finches (*Carpodacus mexicanus*) with conjunctivitis. *Avian Dis* (1996) 40:480–3. doi:10.2307/1592250
35. Dhondt AA, Dhondt KV, Hawley DM, Jennelle CS. Experimental evidence for transmission of *Mycoplasma gallisepticum* in house finches by fomites. *Avian Pathol* (2007) 36:205–8. doi:10.1080/03079450701286277
36. Sydenstricker KV, Dhondt AA, Hawley DM, Jennelle CS, Kollias HW, Kollias GV. Characterization of experimental *Mycoplasma gallisepticum* infection in captive house finch flocks. *Avian Dis* (2006) 50:39–44. doi:10.1637/7403-062805R.1
37. Grodio JL, Dhondt KV, O'Connell PH, Schat KA. Detection and quantification of *Mycoplasma gallisepticum* genome load in conjunctival samples of experimentally infected house finches (*Carpodacus mexicanus*) using real-time polymerase chain reaction. *Avian Pathol* (2008) 37:385–91. doi:10.1080/03079450802216629
38. Park M, Kim S, Adelman JS, Leon AE, Hawley DM, Dalloul RA. Identification and functional characterization of the house finch interleukin-1 beta. *Dev Comp Immunol* (2017) 69:41–50. doi:10.1016/j.dci.2016.12.004
39. Vandesompele J, De Preter K, Pattyn F, Poppe B, Van Roy N, De Paepe A, et al. Accurate normalization of real-time quantitative RT-PCR data by geometric averaging of multiple internal control genes. *Genome Biol* (2002) 3:RESEARCH0034. doi:10.1186/gb-2002-3-7-research0034
40. Xie F, Xiao P, Chen D, Xu L, Zhang B. miRDeepFinder: a miRNA analysis tool for deep sequencing of plant small RNAs. *Plant Mol Biol* (2012) 80:75–84. doi:10.1007/s11103-012-9885-2
41. Pfaffl MW. A new mathematical model for relative quantification in real-time RT-PCR. *Nucleic Acids Res* (2001) 29:e45. doi:10.1093/nar/29.9.e45
42. Kennedy SA, van Diepen AC, van den Hurk CM, Coates LC, Lee TW, Ostrovsky LL, et al. Expression of the serine protease inhibitor neuroserpin in cells of the human myeloid lineage. *Thromb Haemost* (2007) 97:394–9. doi:10.1160/TH06–09–0543
43. Bergkvist A, Rusnakova V, Sindelka R, Garda JMA, Sjögreen B, Lindh D, et al. Gene expression profiling – clusters of possibilities. *Methods* (2010) 50:323–35. doi:10.1016/j.ymeth.2010.01.009
44. R Core Team. *A Language and Environment for Statistical Computing*. (2017). Available from: https://www.R-project.org/
45. Lam KM. *Mycoplasma gallisepticum*-induced alterations in cytokine genes in chicken cells and embryos. *Avian Dis* (2004) 48:215–9. doi:10.1637/7081
46. Majumder S, Silbart LK. Interaction of *Mycoplasma gallisepticum* with chicken tracheal epithelial cells contributes to macrophage chemotaxis and activation. *Infect Immun* (2016) 84:266–74. doi:10.1128/IAI.01113-15
47. Kita M, Ohmoto Y, Hirai Y, Yamaguchi N, Imanishi J. Induction of cytokines in human peripheral-blood mononuclear-cells by mycoplasmas. *Microbiol Immunol* (1992) 36:507–16. doi:10.1111/j.1348-0421.1992.tb02048.x
48. Oláh I, Nagy N, Vervelde L. Structure of the avian lymphoid system. In: Schat KA, Kaspers B, Kaiser P, editors. *Avian Immunology*. London: Academic Press (2014). p. 11–44.
49. Rothwell NJ, Hopkins SJ. Cytokines and the nervous system II: actions and mechanisms of action. *Trends Neurosci* (1995) 18:130–6. doi:10.1016/0166-2236(95)93890-A
50. Yirmiya R, Goshen I. Immune modulation of learning, memory, neural plasticity and neurogenesis. *Brain Behav Immun* (2011) 25:181–213. doi:10.1016/j.bbi.2010.10.015
51. Goshen I, Yirmiya R. Interleukin-1 (IL-1): a central regulator of stress responses. *Front Neuroendocrinol* (2009) 30:30–45. doi:10.1016/j.yfrne.2008.10.001
52. Garcia M, Elfaki MG, Kleven SH. Analysis of the variability in expression of *Mycoplasma gallisepticum* surface antigens. *Vet Microbiol* (1994) 42:147–58. doi:10.1016/0378-1135(94)90014-0
53. Williams PD, Dobson AP, Dhondt KV, Hawley DM, Dhondt AA. Evidence of trade-offs shaping virulence evolution in an emerging wildlife pathogen. *J Evol Biol* (2014) 27:1271–8. doi:10.1111/jeb.12379
54. O'Connor RJ, Turner KS, Sander JE, Kleven SH, Brown TP, Gomez L, et al. Pathogenic effects on domestic poultry of a *Mycoplasma gallisepticum* strain isolated from a wild house finch. *Avian Dis* (1999) 43:640–8. doi:10.2307/1592732
55. Pflaum K, Tulman ER, Beaudet J, Liao X, Dhondt KV, Dhondt AA, et al. Attenuated phenotype of a recent house finch-associated *Mycoplasma gallisepticum* isolate for domestic poultry. *Infect Immun* (2017) 85:e00185–17. doi:10.1128/iai.00185-17
56. Osnas EE, Hurtado PJ, Dobson AP. Evolution of pathogen virulence across space during an epidemic. *Am Nat* (2015) 185:332–42. doi:10.1086/679734
57. Bonneaud C, Balenger SL, Hill GE, Russell AF. Experimental evidence for distinct costs of pathogenesis and immunity against a natural pathogen in a wild bird. *Mol Ecol* (2012) 21:4787–96. doi:10.1111/j.1365-294X.2012.05736.x

58. Graham AL, Allen JE, Read AF. Evolutionary causes and consequences of immunopathology. *Annu Rev Ecol Evol Syst* (2005) 36:373–97. doi:10.1146/annurev.ecolsys.36.102003.152622
59. Hussell T, Pennycook A, Openshaw PJM. Inhibition of tumor necrosis factor reduces the severity of virus-specific lung immunopathology. *Eur J Immunol* (2001) 31:2566–73. doi:10.1002/1521-4141(200109)31:9<2566:aid-immu2566>3.0.co;2-l
60. Lilley TM, Prokkola JM, Johnson JS, Rogers EJ, Gronsky S, Kurta A, et al. Immune responses in hibernating little brown myotis (*Myotis lucifugus*) with white-nose syndrome. *Proc Biol Sci* (2017) 284:20162232. doi:10.1098/rspb.2016.2232
61. Long GH, Chan BHK, Allen JE, Read AF, Graham AL. Experimental manipulation of immune-mediated disease and its fitness costs for rodent malaria parasites. *BMC Evol Biol* (2008) 8:128. doi:10.1186/1471-2148-8-128
62. Bradbury JM. Poultry mycoplasmas: sophisticated pathogens in simple guise. *Br Poult Sci* (2005) 46:125–36. doi:10.1080/00071660500066282
63. Thomson AW, Lotze MT. *The Cytokine Handbook*. London: Academic Press (2003).
64. Love AC, Foltz SL, Adelman JS, Moore IT, Hawley DM. Changes in corticosterone concentrations and behavior during *Mycoplasma gallisepticum* infection in house finches (*Haemorhous mexicanus*). *Gen Comp Endocrinol* (2016) 235:70–7. doi:10.1016/j.ygcen.2016.06.008
65. Hornef MW, Wick MJ, Rhen M, Normark S. Bacterial strategies for overcoming host innate and adaptive immune responses. *Nat Immunol* (2002) 3:1033–40. doi:10.1038/ni1102-1033
66. Schmid-Hempel P. Immune defence, parasite evasion strategies and their relevance for "macroscopic phenomena" such as virulence. *Philos Trans R Soc Lond B Biol Sci* (2009) 364:85–98. doi:10.1098/rstb.2008.0157
67. Ganapathy K, Bradbury JM. Effects of cyclosporin A on the immune responses and pathogenesis of a virulent strain of *Mycoplasma gallisepticum* in chickens. *Avian Pathol* (2003) 32:495–502. doi:10.1080/0307945031000154099
68. Adelman JS, Carter AW, Hopkins WA, Hawley DM. Deposition of pathogenic *Mycoplasma gallisepticum* onto bird feeders: host pathology is more important than temperature-driven increases in food intake. *Biol Lett* (2013) 9:20130594. doi:10.1098/rsbl.2013.0594
69. Faustino CR, Jennelle CS, Connolly V, Davis AK, Swarthout EC, Dhondt AA, et al. *Mycoplasma gallisepticum* infection dynamics in a house finch population: seasonal variation in survival, encounter and transmission rate. *J Anim Ecol* (2004) 73:651–69. doi:10.1111/j.0021-8790.2004.00840.x

Conflict of Interest Statement: The authors declare that the research was conducted in the absence of any commercial or financial relationships that could be construed as a potential conflict of interest.

frontiers in Immunology

ORIGINAL RESEARCH
published: 14 December 2017
doi: 10.3389/fimmu.2017.01814

Detection of Signal Regulatory Protein α in *Saimiri sciureus* (Squirrel Monkey) by Anti-Human Monoclonal Antibody

*Hugo Amorim dos Santos de Souza[1†], Edmar Henrique Costa-Correa[1†], Cesare Bianco-Junior[1], Márcia Cristina Ribeiro Andrade[2], Josué da Costa Lima-Junior[3], Lilian Rose Pratt-Riccio[1], Cláudio Tadeu Daniel-Ribeiro[1] and Paulo Renato Rivas Totino[1]**

[1] Laboratory for Malaria Research, Instituto Oswaldo Cruz (IOC), Fundação Oswaldo Cruz (Fiocruz), Rio de Janeiro, Brazil, [2] Service of Primatology, Instituto de Ciência e Tecnologia em Biomodelos, Fiocruz, Rio de Janeiro, Brazil, [3] Laboratory of Immunoparasitology, Instituto Oswaldo Cruz (IOC), Fiocruz, Rio de Janeiro, Brazil

OPEN ACCESS

Edited by:
Greg Woods,
University of Tasmania, Australia

Reviewed by:
Annalisa Pinsino,
Istituto di biomedicina e di immunologia molecolare Alberto Monroy (CNR), Italy
Hao-Ching Wang,
Taipei Medical University, Taiwan

***Correspondence:**
Paulo Renato Rivas Totino
prtotino@ioc.fiocruz.br

[†]These authors have contributed equally to this work.

Specialty section:
This article was submitted to Comparative Immunology, a section of the journal Frontiers in Immunology

Received: 31 August 2017
Accepted: 01 December 2017
Published: 14 December 2017

Citation:
Souza HAS, Costa-Correa EH, Bianco-Junior C, Andrade MCR, Lima-Junior JC, Pratt-Riccio LR, Daniel-Ribeiro CT and Totino PRR (2017) Detection of Signal Regulatory Protein α in Saimiri sciureus (Squirrel Monkey) by Anti-Human Monoclonal Antibody. Front. Immunol. 8:1814. doi: 10.3389/fimmu.2017.01814

Non-human primates (NHP) are suitable models for studying different aspects of the human system, including pathogenesis and protective immunity to many diseases. However, the lack of specific immunological reagents for neo-tropical monkeys, such as *Saimiri sciureus*, is still a major factor limiting studies in these models. An alternative strategy to circumvent this obstacle has been the selection of immunological reagents directed to humans, which present cross-reactivity with NHP molecules. In this context and considering the key role of inhibitory immunoreceptors—such as the signal regulatory protein α (SIRPα)—in the regulation of immune responses, in the present study, we attempted to evaluate the ability of anti-human SIRPα monoclonal antibodies to recognize SIRPα in antigen-presenting *S. sciureus* peripheral blood mononuclear cells (PBMC). As shown by flow cytometry analysis, the profile of anti-SIRPα staining as well as the levels of SIRPα-positive cells in PBMC from *S. sciureus* were similar to those observed in human PBMC. Furthermore, using anti-SIRPα monoclonal antibody, it was possible to detect a decrease of the SIRPα levels on surface of *S. sciureus* cells after *in vitro* stimulation with lipopolysaccharides. Finally, using computed-based analysis, we observed a high degree of conservation of SIRPα across six species of primates and the presence of shared epitopes in the extracellular domain between humans and *Saimiri* genus that could be targeted by antibodies. In conclusion, we have identified a commercially available anti-human monoclonal antibody that is able to detect SIRPα of *S. sciureus* monkeys and that, therefore, can facilitate the study of the immunomodulatory role of SIRPα when *S. sciureus* is used as a model.

Keywords: non-human primates, *Saimiri sciureus*, immune response, signal regulatory protein α, flow cytometry

INTRODUCTION

Saimiri sciureus, also known as squirrel monkey, is a small species of non-human primate natively found in the tropical rainforests of South America (1, 2). As many other non-human primates (NHP), *S. sciureus* is used in diverse areas of biomedical research and, although its full genome has not yet been sequenced, the well-known close phylogenetic relationship of NHP to humans

renders this model an accurate system to study biological, immunological, and pharmacologycal phenomena of medical importance (2). Indeed, *S. sciureus* has been shown to be susceptible to several human pathogens and, in this way, has been proposed as model for study the pathogenesis of malaria (3), measles (4), HTLV-associated diseases (5), BK virus infection (6), and vaginal trichomoniasis (7). Moreover, *S. sciureus* has been studied in the context of Parkinson's disease therapy (8) and, as recommended by the World Health Organization (9), malaria vaccine candidates have been frequently tested in preclinical trials using *S. sciureus* in the last three decades (10, 11). However, the lack of specific immunological tools to assess immune response of *S. sciureus* represents a major factor limiting vaccinology and immunopathology studies using this model.

An alternative strategy to circumvent this limitation is the identification of immunological reagents directed to molecules of human immune system that also present reactivity with *S. sciureus*. In fact, a variety of anti-human monoclonal antibodies commercially available are able to satisfactorily detect surface molecules of immune cells as well as cytokines of *S. sciureus* (12–14) and other non-human primate models, such as common marmoset (*Callithrix jacchus*), rhesus macaque (*Macaca mulatta*), and chimpanzee (*Pan troglodytes*) (15–17). To the best of our knowledge, however, there is no evaluation concerning the signal regulatory protein α (SIRPα) in NHP.

Signal regulatory protein α is a transmembrane protein present in leukocytes of the myeloid lineage, including monocytes and dendritic cells (DC), which is implicated in inhibitory signaling of innate immune functions, such as phagocytosis, proinflammatory cytokine production, and DC maturation (18–20), as well as induction of programmed cell death (21). Comprehensively, SIRPα is believed to play a relevant role in the regulation of immune responses, impacting the pathogenesis of etiologically distinct diseases as well as vaccination (22–24). Nevertheless, SIRPα has not been investigated in non-human primate models. Thus, attempting to support further studies related to involvement of SIRPα in immune responses, in the present work, we evaluated by flow cytometry if monoclonal antibody directed to human SIRPα cross-reacts with peripheral blood mononuclear cells (PBMC) from *S. sciureus*.

MATERIALS AND METHODS

Animals and Blood Samples

Seven clinically healthy *S. sciureus* monkeys from the breeding colony at the Department of Primatology of the Instituto de Ciência e Tecnologia em Biomodelos/Fiocruz, Rio de Janeiro, Brazil, were studied. Animals were male adults, aged 3–10 years, housed in accordance with the guidelines of the institutional ethical committee for animal use. For blood sample collection, animals were anesthetized with a combination of 0.1 mL midazolan and 0.4 mL ketamine and, then, 4 mL heparinized venous blood were drawn *via* femoral venipuncture. All animal experimentation was performed in compliance with the protocol reviewed and approved by the Fiocruz ethical committee (LW-9/14). Peripheral blood samples (4 mL) from five healthy human donors were also obtained by venipuncture in heparinized tubes, as approved by the Fiocruz Research Ethic Committee (46084015.1.0000.5248).

PBMC Isolation and Antigenic Stimulation

Peripheral blood mononuclear cells were isolated from *S. sciureus* whole blood through density gradient centrifugation using Histopaque-1077 (Sigma). Cells were washed twice in RPMI-1640 medium (Sigma) containing 2.05 mM L-glutamine, 25 mM Hepes, and 2.0 g/L sodium bicarbonate and, then, resuspended in RPMI medium supplemented with 200 U/mL penicillin (Gibco), 200 mg/mL streptomycin (Gibco), and 10% inactivated fetal calf serum (Gibco). Cells (2.5×10^5) were assayed *ex vivo* or after 24 h stimulation with *Escherichia coli* lipopolysaccharides (LPS, 5 μg/mL, Sigma) in 96-well culture plates (Falcon) at 37°C in 5% CO_2.

Flow Cytometry Assay

Detection of SIRPα in *S. sciureus* PBMC was assayed by flow cytometry using allophycocyanin (APC)-conjugated anti-human SIRPα monoclonal antibody purchased from eBioscience (isotype: mouse/IgG2a, clone: 15-414). Cells (2.5×10^5) were washed in phosphate saline buffer (PBS) and, subsequently, incubated at 4°C for 30 min in PBS containing 10% fetal bovine serum (FBS) to reduce non-specific staining. After incubation, cells were stained with 2.0 μL anti-SIRPα monoclonal antibody or APC-conjugated isotype control (eBioscience) at 4°C for 40 min in 100 μL PBS containing 1% FBS. Cells were washed twice and, finally, analyzed by a FACSVerse flow cytometer (Becton Dickinson). In parallel, anti-SIRPα monoclonal antibody was tested *ex vivo* with PBMC obtained from blood human samples, as described in Section "PBMC Isolation and Antigenic Stimulation."

Computer-Assisted Analysis of Sequence Alignment and Potential B-Cell Epitopes

To detect SIRPα protein homology among several primate species, protein BLAST were done and protein sequences of *Homo sapiens* (AAH26692.1), *P. troglodytes* (JAA44167.1), *C. jacchus* (JAB51896.1), *Macaca fascicularis* (XP_015313155.1), *Gorilla gorilla* (XP_004061735.2), and *Saimiri boliviensis* (XP_010350139.1) were analyzed. Multiple alignment CLUSTAL OMEGA, distance matrix, and the phylogenetic tree were done using the Megalign Pro 15 (Lasergene DNASTAR) program and the circular map of protein alignment was generated using the software GenVision 15 (Lasergene DNASTAR). The prediction of linear B-cell epitopes was carried out using the web server BepiPred. For each input FASTA sequence of extracellular domain of SIRPα, the server outputs a epitope prediction score for each amino acid. The recommended cutoff of 0.35 was used to determine potential B-cell linear epitopes, ensuring sensibility of 49% and specificity of 75%. Linear B-cell epitopes of SIRPα extracellular domain of *H. sapiens* and *S. boliviensis* were predicted to be located at the residues with the highest scores in at least nine consecutive amino acids.

RESULTS AND DISCUSSION

Signal regulatory protein α has been studied by flow cytometric analysis in both human (25, 26) and animal models, i.e., mice, rats, and cattle (27–29), but the frequency and distribution of SIRPα-positive cells in peripheral blood has not been reported. Thus, to investigate the reactivity of anti-human SIRPα monoclonal antibody with *S. sciureus* PBMC by flow cytometry; we first evaluated anti-SIRPα staining profile in PBMC obtained from five normal healthy human donors.

Signal regulatory protein α is known as an immune inhibitory receptor present in leukocytes of the myeloid lineage and, therefore, it is expected that SIRPα in PBMC population is mainly detected on surface of cells showing monocyte morphology by size and granularity analysis in flow cytometry using forward scatter and sideward scatter parameters (30). Indeed, an elevated percentage (95.55 ± 1.16%) of SIRPα-positive cells was observed in the human monocyte population, while only 3.27 ± 3.38% cells presented SIRPα in the lymphocyte population (**Figures 1A** and **2**). Moreover, SIRPα-positive cells corresponded to 18.98 ± 3.12% of total PBMC, agreeing with the frequency of total myeloid innate immune cells found in human PBMC samples, which manly comprises monocytes and DC (31, 32).

Subsequently, anti-human SIRPα monoclonal antibody was tested against *S. sciureus* cells. Previous reports demonstrated that different immune cell surface receptors as well as cytokines of *S. sciureus* can be detected by a range of antibodies directed to human (12–14) and, in the same way, we observed that anti-human SIRPα antibody cross-reacted with cell surface of *S. sciureus* PBMC. As shown in **Figure 1B**, the profile of anti-SIRPα staining in PBMC from *S. sciureus* was similar to that observed in human samples. SIRPα-positive *S. sciureus* cells corresponded to 8.92 ± 3.65% of total PBMC and 1.59 ± 1.03% of the lymphocyte population, while an increased frequency of SIRPα-presenting cells (85.27 ± 1.41%) was observed in monocytes population (**Figure 2**). These data suggest that anti-human SIRPα antibody recognizes a specific antigen present on surface of *S. sciureus* innate immune cells, possibly the cognate of human SIRPα in *S. sciureus*.

Although the cross-reactivity of antibodies cannot indicate *per se* the degree of homology between proteins across phyla, an increased similarity (>90%) has been shown through molecular approaches between human, *S. sciureus*, and other NHP concerning nucleotide sequence of genes coding for many cytokines (33, 34) as well as dopamine transport (35) and, therefore, it was already possible to quantify gene expression of 12 *S. sciureus* cytokines (IL-1A, IL-2, IL-4, IL-5, IL-6, IL-10, IL-12B, IL-17, IFN-β, IFN-γ, LTA, and TNF) by commercially available real-time PCR assays using predesigned human gene-specific primers and probes (14). Moreover, genomic studies demonstrate the presence of SIRPα gene in a vast group of animals, from cats to NHP, supporting that SIRPα is a ubiquitous molecule of innate immune system of mammalians (36, 37). In the case of *S. sciureus* SIRPα, however, there are no molecular data available, i.e., neither genome nor SIRPα gene was reported yet, limiting

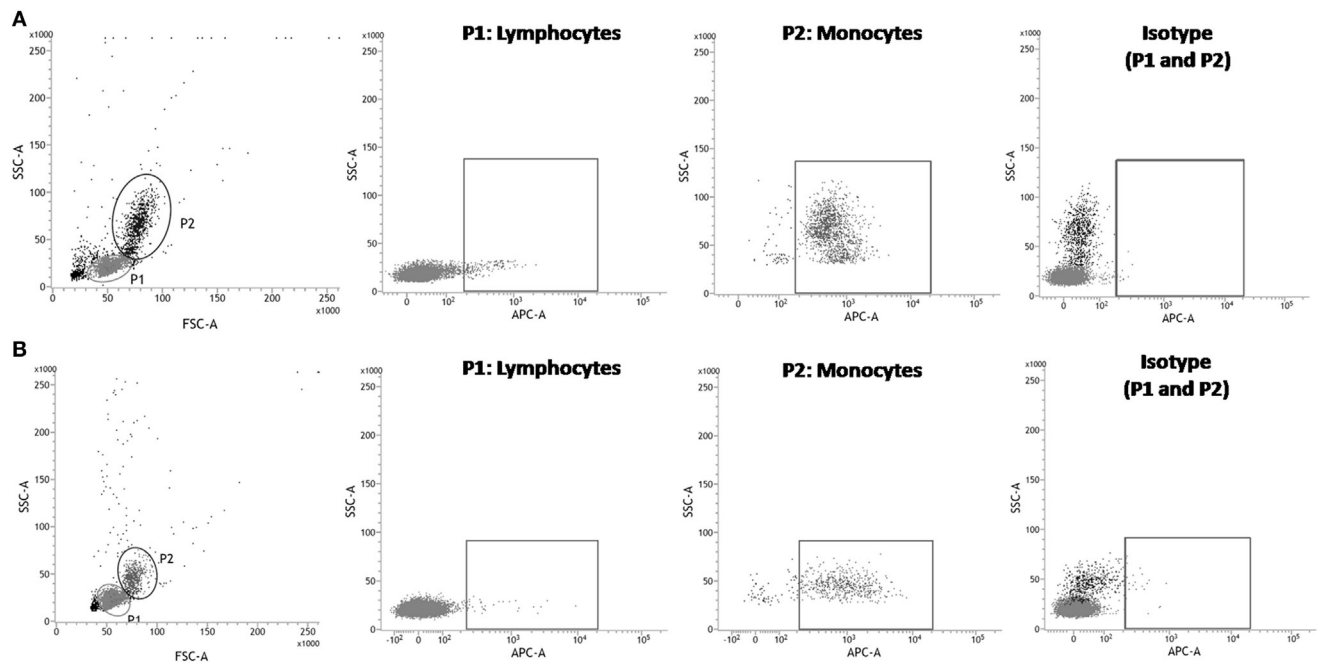

FIGURE 1 | Flow cytometry analysis of anti-human signal regulatory protein α (SIRPα) monoclonal antibody cross-reactivity with *Saimiri sciureus* cells. Peripheral blood mononuclear cells (PBMC) were isolated from human or *S. sciureus* whole blood, stained with anti-SIRPα monoclonal antibody or isotype control and, then, analyzed by flow cytometry. Reactivity of anti-SIRPα antibodies [allophycocyanin (APC)] with human **(A)** and *S. sciureus* **(B)** PBMC was evaluated gating lymphocytes (P1) or monocytes populations, as defined by forward scatter (FSC) and sideward scatter (SSC) parameters.

the analysis of *S. sciureus* SIRPα homology with their cognates in other primates.

In this scenario, to confirm that the cross-reactivity herein detected was a natural consequence of the similarity of SIRPα protein across primates, we aligned the amino acid sequences of SIRPα from six different primate species including *Saimiri* and *Homo sapiens* (**Figure 3**). As expected, a significant degree of identity was observed across the primates, which showed a complete matching in 72% of all sequences analyzed (**Figure 3A**). The homology rate ranged from 87% (*M. Fascicularis* vs. *S. boliviensis*) to 99% (*P. troglodites* vs. *G. gorilla*) and human SIRPα showed a high identity with its orthologs, ranging from 88% in *S. boliviensis* to 98% in *G. gorilla,* despite the deletion of 58 amino acid present in *S. boliviensis* sequence, which was determinant to reduce the homology rate (**Figures 3A,B**). Since the amino acid sequence to which the commercial anti-human SIRPα monoclonal binds is not available, we also checked if the deletion in *S. boliviensis*, which is taxonomically the closest to *S. sciureus* among the NHP species studied herein, could potentially influence the antibody recognition. In this way, we verified the potential epitopes shared between the *H. sapiens* and *S. boliviensis* through analysis of linear B-cell epitopes in SIRPα extracellular domain and we observed at least 10 B-cell epitopes that can be targeted by antibodies (**Figure 4**). Importantly, all of these regions were shared by both species, indicating that anti-human SIRPα antibodies can target SIRPα of *Saimiri* monkeys in a similar way to its orthologous in human.

Thus, to better study the capacity of anti-human antibodies to detect *S. sciureus* SIRPα, we additionally evaluated the levels of this immune receptor on surface of PBMC after stimulation with LPS. It has been described that pathogen-associated molecular patterns present modulatory effects on SIRPα levels in macrophages and DC and, in this context, LPS was recognized as a negative modulator (24, 38, 39). Indeed, analyzing monocytes population by flow cytometry, which mainly includes innate immune cells present in PBMC, we found that the anti-human SIRPα monoclonal antibody was able to identify a significant

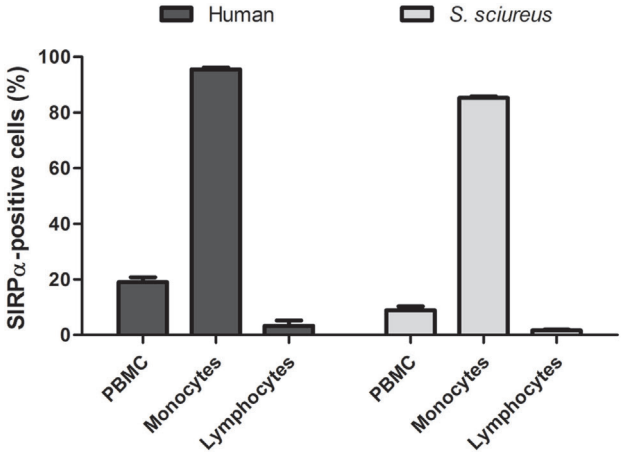

FIGURE 2 | Frequency of signal regulatory protein α (SIRPα)-positive cells in peripheral blood mononuclear cells (PBMC) samples from humans and *Saimiri sciureus* monkeys. PBMC were isolated from whole blood, stained with anti-human SIRPα monoclonal antibody and, then, analyzed by flow cytometry. Cells presenting SIRPα were quantified considering three main cells populations by morphological criteria: total PBMC, monocytes, and lymphocytes, as shown in **Figure 1**. Data represent mean ± SEM for five humans and seven monkeys.

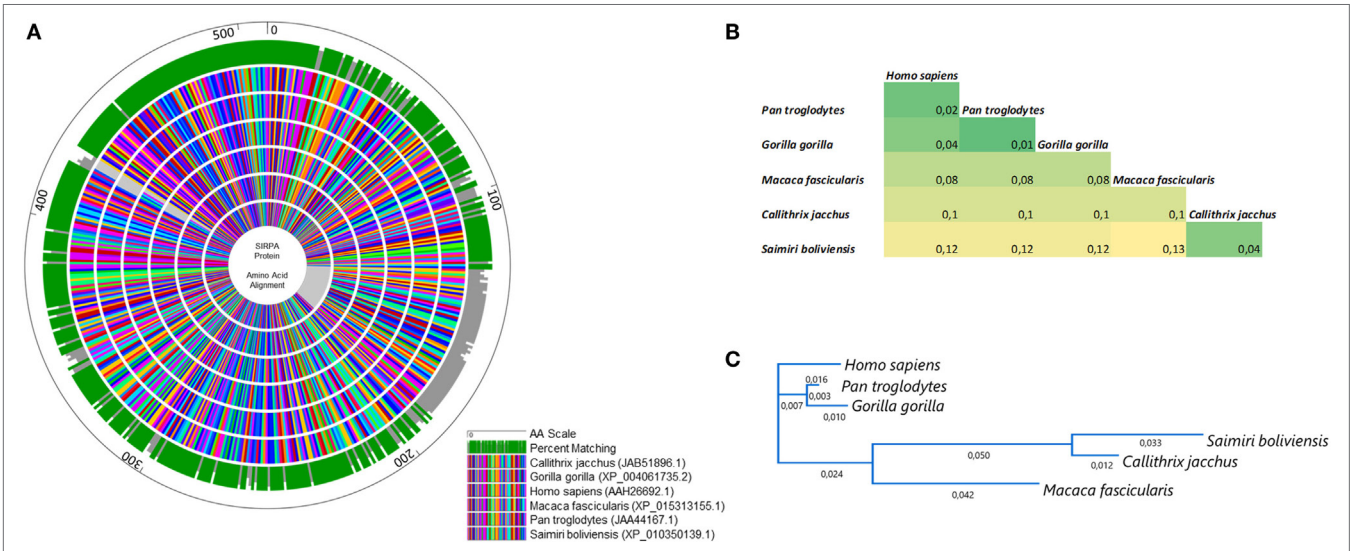

FIGURE 3 | Homology analysis of signal regulatory protein α (SIRPα) across primates. **(A)** Circular alignment of amino acid sequences of SIRPα protein in human and five non-human primates (*Pan troglodytes*, *Gorilla gorilla*, *Macaca fascicularis*, *Callithrix jacchus*, *Saimiri boliviensis*). The outer circle shows the amino acid scale. Green and gray bars on the second circle show the percent matching among all sequences used in the analysis. Inner circles show the sequence alignment in which each amino acid was represented by a different color. **(B)** Pairwise distance among all primates studied and **(C)** phylogenetic tree based on SIRPα protein alignments.

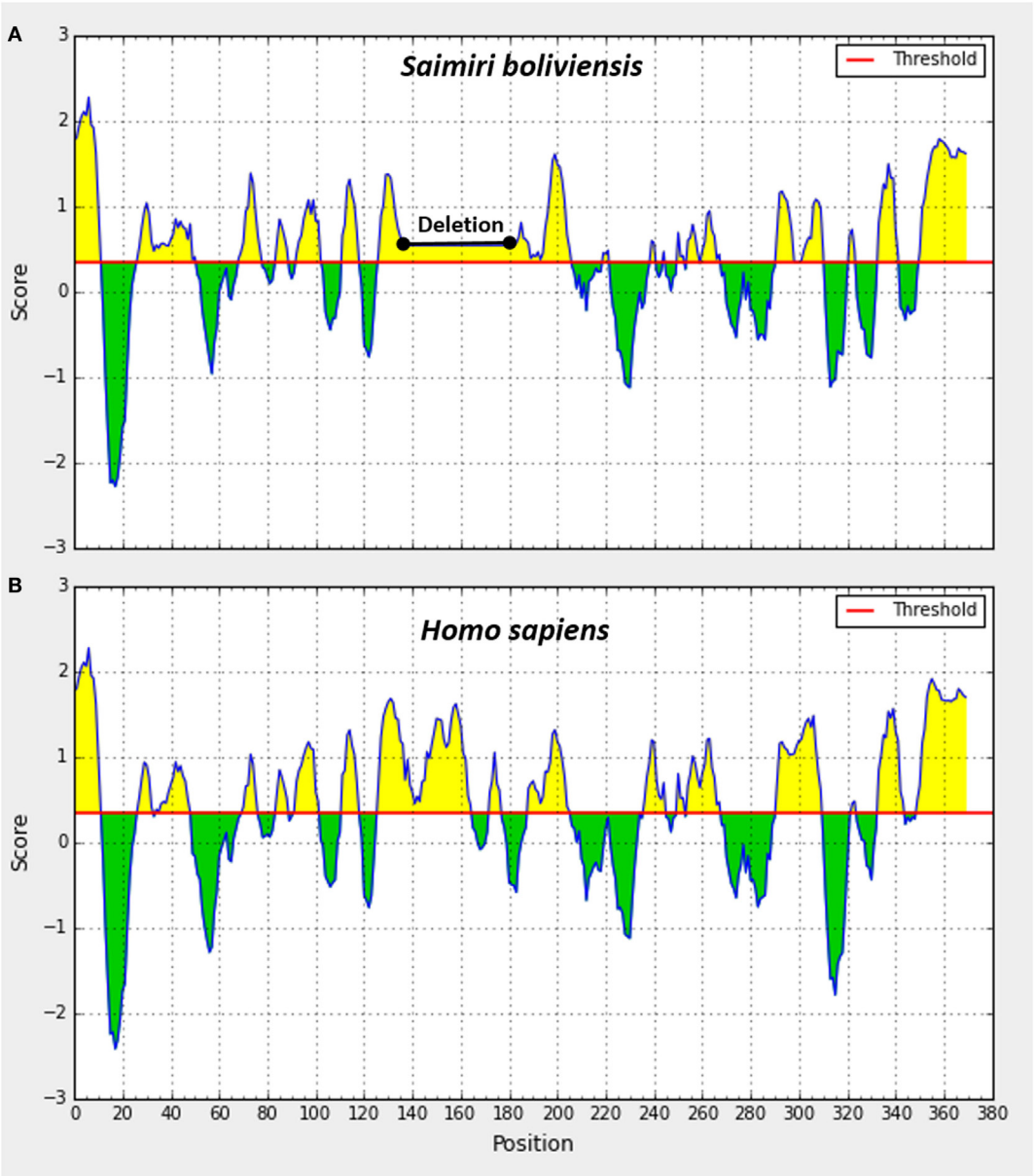

FIGURE 4 | Prediction of linear B-cell epitopes in extracellular domain of signal regulatory protein α protein in *Saimiri* **(A)** and *Homo sapiens* **(B)**. Linear B-cell epitopes were predicted to be located at the residues with the scores above 0.35 (yellow) and regions not predicted to be B-cell epitopes are under the threshold (green). The epitope score represents the average of the scores of least nine consecutive amino acids above the cut-off, and the sequences with higher mean values were detected as potential linear epitopes.

reduction not only in the frequency of SIRPα-positive cells but also in the levels of SIRPα present on the surface of these cells after LPS stimulation (**Figure 5**). Despite LPS-mediated regulation of SIRPα expression has not been investigated in human or NHP PBMC, decreased levels of SIRPα on the surface of peripheral blood monocytes were found in LPS-treated pigs and it was already reported a downregulation of SIRPα gene expression in cultured primary mouse microglia following LPS-stimulation (40, 41), agreeing with our data on PBMC and, consequently, supporting that anti-human SIRPα antibodies can recognize SIRPα of *S. sciureus*, whose levels were downmodulated by LPS in monocyte population.

Collectively, the flow cytometry assays showing that SIRPα-positive cells are similarly present and distributed in PBMC of human and *S. sciureus*, together with observation by computed-based analysis that SIRPα has a high degree of conservation across primates, with the presence of conserved B-cell epitopes in the extracellular domain between humans and the *Saimiri* genus, strongly indicate that anti-SIRPα antibodies directed to humans can detect SIRPα of *S. sciureus*. Take into account the role of SIRPα

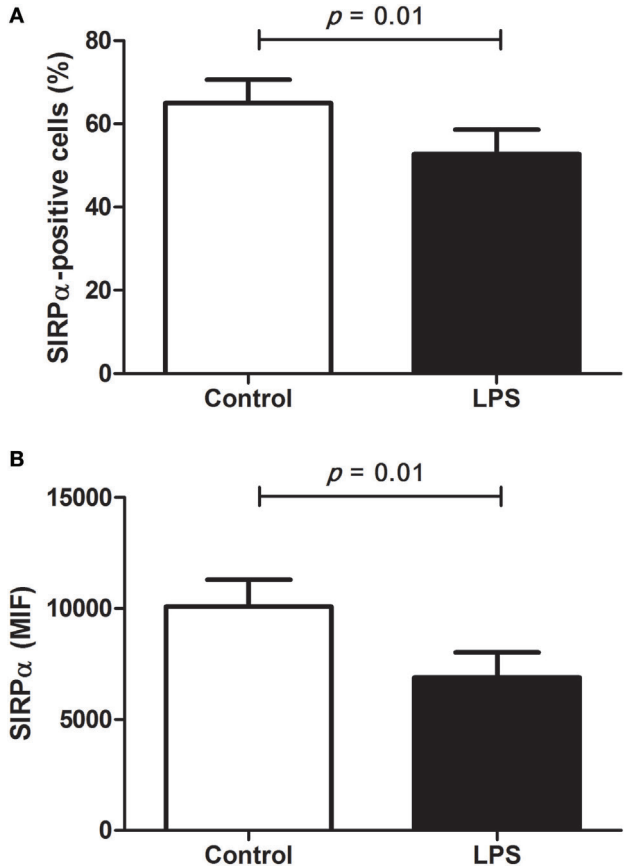

FIGURE 5 | Modulation of signal regulatory protein α (SIRPα) levels by lipopolysaccharides (LPS) in *Saimiri sciureus* cells. Peripheral blood mononuclear cells (PBMC) of *S. sciureus* monkeys ($n = 7$) were incubated for 24 h in presence or absence (control) of LPS and, then, SIRPα was detected in monocytes population by flow cytometry using anti-human monoclonal antibody. **(A)** Frequency of SIRPα-positive cells in PBMC and **(B)** levels of SIRPα present on cell surface of SIRPα-positive cells (monocytes), as measured by mean fluorescence intensity. Data (mean ± SEM) are representative of two separate experiments. Statistical difference was tested by paired *t*-test in GraphPad Prism 5.0 software and $p < 0.05$ was considered significant.

in the negative regulation of immune responses, we believe that further studies in *S. sciureus* or other non-human primate models, exploring SIRPα signaling with anti-human antibodies, may help the understanding of the immunopathogenesis of diseases, such as cancer, neurodegenerative disorders, and infectious diseases, and, consequently, contribute to the development of therapeutic and vaccinal strategies that mitigate their impact in public health.

ETHICS STATEMENT

This study was carried out in accordance with the recommendations and approved by the Fiocruz Ethics Committee on Animal Use (CEUA Licence LW-9/14).

AUTHOR CONTRIBUTIONS

HS and EC-C performed the experiments and helped PT in drafting the manuscript. CB-J and MA carried out animal manipulation and helped in the experiments. LP-R performed the experiments and helped in the computed-based analysis. JL-J performed the computed-based analyses and reviewed the manuscript. CD-R reviewed the manuscript. PT performed data analysis and reviewed the manuscript.

ACKNOWLEDGMENTS

This study was supported through funding from the Programa de Desenvolvimento Tecnológico em Insumos para Saúde (PDTIS/Fiocruz), the Programa de Apoio a Núcleos de Excelência (Pronex) [Departamento de Ciência e Tecnologia (DECIT) do Ministério da Saúde do Brasil, Conselho Nacional de Desenvolvimento Científico e Tecnológico (CNPq, Brazil) and Fundação de Amparo à Pesquisa do Estado do Rio de Janeiro (FAPERJ)], the Neglected Disease Program from FAPERJ, and the Instituto Oswaldo Cruz (Fiocruz, Brazil) POM grants. CTDR is recipient of a Research Productivity Fellowship from the CNPq and CTDR and JCLJ received grants from FAPERJ as "Cientista do Nosso Estado" and "Jovem Cientista do Nosso Estado", respectively.

REFERENCES

1. Lynch Alfaro JW, Boubli JP, Paim FP, Ribas CC, Silva MN, Messias MR, et al. Biogeography of squirrel monkeys (genus *Saimiri*): south-central Amazon origin and rapid pan-Amazonian diversification of a lowland primate. *Mol Phylogenet Evol* (2015) 82 Pt B:436–54. doi:10.1016/j.ympev.2014.09.004
2. Phillips KA, Bales KL, Capitanio JP, Conley A, Czoty PW, 't Hart BA, et al. Why primate models matter. *Am J Primatol* (2014) 76:801–27. doi:10.1002/ajp.22281
3. Contamin H, Behr C, Mercereau-Puijalon O, Michel J. *Plasmodium falciparum* in the squirrel monkey (*Saimiri sciureus*): infection of non-splenectomised animals as a model for exploring clinical manifestations of malaria. *Microbes Infect* (2000) 2:945–54. doi:10.1016/S1286-4579(00)00401-9
4. Delpeut S, Sawatsky B, Wong XX, Frenzke M, Cattaneo R, von Messling V. Nectin-4 interactions govern measles virus virulence in a new model of pathogenesis, the squirrel monkey (*Saimiri sciureus*). *J Virol* (2017) 91:e02490–16. doi:10.1128/JVI.02490-16
5. Kazanji M. HTLV type 1 infection in squirrel monkeys (*Saimiri sciureus*): a promising animal model for HTLV type 1 human infection. *AIDS Res Hum Retroviruses* (2000) 16:1741–6. doi:10.1089/08892220050193245
6. Zaragoza C, Li RM, Fahle GA, Fischer SH, Raffeld M, Lewis AM, et al. Squirrel monkeys support replication of BK virus more efficiently than simian virus 40: an animal model for human BK virus infection. *J Virol* (2005) 79:1320–6. doi:10.1128/JVI.79.2.1320-1326.2005
7. Gardner WA, Culberson DE, Scimeca JM, Brady AG, Pindak FF, Abee CR. Experimental genital trichomoniasis in the squirrel monkey (*Saimiri sciureus*). *Genitourin Med* (1987) 63:188–91.
8. Quik M, Mallela A, Ly J, Zhang D. Nicotine reduces established levodopa-induced dyskinesias in a monkey model of Parkinson's disease. *Mov Disord* (2013) 28:1398–406. doi:10.1002/mds.25594
9. World Health Organization. Role of non-human primates in malaria vaccine development: memorandum from a WHO meeting. *Bull World Health Organ* (1988) 66:719–28.
10. James MA, Kakoma I, Ristic M, Cagnard M. Induction of protective immunity to *Plasmodium falciparum* in *Saimiri sciureus* monkeys with partially purified exoantigens. *Infect Immun* (1985) 49:476–80.

11. Carvalho LJ, Alves FA, Bianco C, Oliveira SG, Zanini GM, Soe S, et al. Immunization of *Saimiri sciureus* monkeys with a recombinant hybrid protein derived from the *Plasmodium falciparum* antigen glutamate-rich protein and merozoite surface protein 3 can induce partial protection with Freund and Montanide ISA720 adjuvants. *Clin Diagn Lab Immunol* (2005) 12:242–8. doi:10.1128/CDLI.12.2.242-248.2005
12. Contamin H, Loizon S, Bourreau E, Michel JC, Garraud O, Mercereau-Puijalon O, et al. Flow cytometry identification and characterization of mononuclear cells subsets in the neotropical primate *Saimiri sciureus* (squirrel monkey). *J Immunol Methods* (2005) 297:61–71. doi:10.1016/j.jim.2004.11.019
13. Carville A, Evans TI, Reeves RK. Characterization of circulating natural killer cells in neotropical primates. *PLoS One* (2013) 8:e78793. doi:10.1371/journal.pone.0078793
14. Riccio EK, Pratt-Riccio LR, Bianco-Júnior C, Sanchez V, Totino PR, Carvalho LJ, et al. Molecular and immunological tools for the evaluation of the cellular immune response in the neotropical monkey *Saimiri sciureus*, a non-human primate model for malaria research. *Malar J* (2015) 14:166. doi:10.1186/s12936-015-0688-1
15. Ozwara H, Niphuis H, Buijs L, Jonker M, Heeney JL, Bambra CS, et al. Flow cytometric analysis on reactivity of human T lymphocyte-specific and cytokine-receptor-specific antibodies with peripheral blood mononuclear cells of chimpanzee (*Pan troglodytes*), rhesus macaque (*Macaca mulatta*), and squirrel monkey (*Saimiri sciureus*). *J Med Primatol* (1997) 26:164–71. doi:10.1111/j.1600-0684.1997.tb00048.x
16. Kireta S, Zola H, Gilchrist RB, Coates PT. Cross-reactivity of anti-human chemokine receptor and anti-TNF family antibodies with common marmoset (*Callithrix jacchus*) leukocytes. *Cell Immunol* (2005) 236:115–22. doi:10.1016/j.cellimm.2005.08.017
17. Rodriguez AR, Hodara V, Murthy K, Morrow L, Sanchez M, Bienvenu AE, et al. T cell interleukin-15 surface expression in chimpanzees infected with human immunodeficiency virus. *Cell Immunol* (2014) 288:24–30. doi:10.1016/j.cellimm.2014.01.009
18. Latour S, Tanaka H, Demeure C, Mateo V, Rubio M, Brown EJ, et al. Bidirectional negative regulation of human T and dendritic cells by CD47 and its cognate receptor signal-regulator protein-alpha: down-regulation of IL-12 responsiveness and inhibition of dendritic cell activation. *J Immunol* (2001) 167:2547–54. doi:10.4049/jimmunol.167.5.2547
19. Smith RE, Patel V, Seatter SD, Deehan MR, Brown MH, Brooke GP, et al. A novel MyD-1 (SIRP-1alpha) signaling pathway that inhibits LPS-induced TNFalpha production by monocytes. *Blood* (2003) 102:2532–40. doi:10.1182/blood-2002-11-3596
20. Janssen WJ, McPhillips KA, Dickinson MG, Linderman DJ, Morimoto K, Xiao YQ, et al. Surfactant proteins A and D suppress alveolar macrophage phagocytosis via interaction with SIRP alpha. *Am J Respir Crit Care Med* (2008) 178:158–67. doi:10.1164/rccm.200711-1661OC
21. Irandoust M, Alvarez Zarate J, Hubeek I, van Beek EM, Schornagel K, Broekhuizen AJ, et al. Engagement of SIRPa inhibits growth and induces programmed cell death in acute myeloid leukemia cells. *PLoS One* (2013) 8:e52143. doi:10.1371/journal.pone.0052143
22. Barclay AN, Van den Berg TK. The interaction between signal regulatory protein alpha (SIRPα) and CD47: structure, function, and therapeutic target. *Annu Rev Immunol* (2014) 32:25–50. doi:10.1146/annurev-immunol-032713-120142
23. Yi T, Li J, Chen H, Wu J, An J, Xu Y, et al. Splenic dendritic cells survey red blood cells for missing self-CD47 to trigger adaptive immune responses. *Immunity* (2015) 43:764–75. doi:10.1016/j.immuni.2015.08.021
24. Liu Q, Wen W, Tang L, Qin CJ, Lin Y, Zhang HL, et al. Inhibition of SIRPα in dendritic cells potentiates potent antitumor immunity. *Oncoimmunology* (2016) 5:e1183850. doi:10.1080/2162402X.2016.1183850
25. Barros MM, Yamamoto M, Figueiredo MS, Cançado R, Kimura EY, Langhi DM Jr, et al. Expression levels of CD47, CD35, CD55, and CD59 on red blood cells and signal-regulatory protein-alpha,beta on monocytes from patients with warm autoimmune hemolytic anemia. *Transfusion* (2009) 49:154–60. doi:10.1111/j.1537-2995.2008.01936.x
26. Han Y, Wang H, Shao Z. Monocyte-derived macrophages are impaired in myelodysplastic syndrome. *J Immunol Res* (2016) 2016:5479013. doi:10.1155/2016/5479013
27. Stephens SA, Howard CJ. Infection and transformation of dendritic cells from bovine afferent lymph by *Theileria annulata*. *Parasitology* (2002) 124:485–93. doi:10.1017/S003118200200152X
28. Baba T, Nakamoto Y, Mukaida N. Crucial contribution of thymic Sirp alpha+ conventional dendritic cells to central tolerance against blood-borne antigens in a CCR2-dependent manner. *J Immunol* (2009) 183:3053–63. doi:10.4049/jimmunol.0900438
29. Signarovitz AL, Ray HJ, Yu JJ, Guentzel MN, Chambers JP, Klose KE, et al. Mucosal immunization with live attenuated *Francisella novicida* U112ΔiglB protects against pulmonary *F. tularensis* SCHU S4 in the Fischer 344 rat model. *PLoS One* (2012) 7:e47639. doi:10.1371/journal.pone.0047639
30. Autissier P, Soulas C, Burdo TH, Williams KC. Evaluation of a 12-color flow cytometry panel to study lymphocyte, monocyte, and dendritic cell subsets in humans. *Cytometry A* (2010) 77:410–9. doi:10.1002/cyto.a.20859
31. Hoffmann TK, Müller-Berghaus J, Ferris RL, Johnson JT, Storkus WJ, Whiteside TL. Alterations in the frequency of dendritic cell subsets in the peripheral circulation of patients with squamous cell carcinomas of the head and neck. *Clin Cancer Res* (2002) 8:1787–93.
32. Mortezagholi S, Babaloo Z, Rahimzadeh P, Ghaedi M, Namdari H, Assar S, et al. Evaluation of PBMC distribution and TLR9 expression in patients with systemic lupus erythematosus. *Iran J Allergy Asthma Immunol* (2016) 15:229–36.
33. Heraud JM, Lavergne A, Kazanji M. Molecular cloning, characterization, and quantification of squirrel monkey (Saimiri sciureus) Th1 and Th2 cytokines. *Immunogenetics* (2002) 54:20–9. doi:10.1007/s00251-002-0443-y
34. Alves FA1, Souza MT, Gonçalves EC, Schneider MP, Marinho AM, Muniz JA, et al. DNA sequencing of 13 cytokine gene fragments of Aotus infulatus and Saimiri sciureus, two non-human primate models for malaria. *Cytokine* (2010) 52:151–5. doi:10.1016/j.cyto.2010.09.004
35. Miller GM, Yatin SM, De La Garza R, Goulet M, Madras BK. Cloning of dopamine, norepinephrine and serotonin transporters from monkey brain: relevance to cocaine sensitivity. *Mol Brain Res* (2001) 87:124–43. doi:10.1016/S0169-328X(00)00288-6
36. van Beek EM, Cochrane F, Barclay AN, van den Berg TK. Signal regulatory proteins in the immune system. *J Immunol* (2005) 175:7781–7. doi:10.4049/jimmunol.175.12.7781
37. Flies AS, Blackburn NB, Lyons AB, Hayball JD, Woods GM. Comparative analysis of immune checkpoint molecules and their potential role in the transmissible tasmanian devil facial tumor disease. *Front Immunol* (2017) 8:513. doi:10.3389/fimmu.2017.00513
38. Kong XN, Yan HX, Chen L, Dong LW, Yang W, Liu Q, et al. LPS-induced down-regulation of signal regulatory protein α contributes to innate immune activation in macrophages. *J Exp Med* (2007) 204:2719–31. doi:10.1084/jem.20062611
39. Dong LW, Kong XN, Yan HX, Yu LX, Chen L, Yang W, et al. Signal regulatory protein α negatively regulates both TLR3 and cytoplasmic pathways in type I interferon induction. *Mol Immunol* (2008) 45:3025–35. doi:10.1016/j.molimm.2008.03.012
40. Ebdrup L, Krog J, Granfeldt A, Tønnesen E, Hokland M. Dynamic expression of the signal regulatory protein alpha and CD18 on porcine PBMC during acute endotoxaemia. *Scand J Immunol* (2008) 68:430–7. doi:10.1111/j.1365-3083.2008.02157.x
41. Nuvolone M, Paolucci M, Sorce S, Kana V, Moos R, Matozaki T, et al. Prion pathogenesis is unaltered in the absence of SIRPα-mediated "don't-eat-me" signaling. *PLoS One* (2017) 12:e0177876. doi:10.1371/journal.pone.0177876

Conflict of Interest Statement: The authors declare that the research was conducted in the absence of any commercial or financial relationships that could be construed as a potential conflict of interest.

Advantages of publishing in Frontiers

OPEN ACCESS
Articles are free to read for greatest visibility and readership

FAST PUBLICATION
Around 90 days from submission to decision

HIGH QUALITY PEER-REVIEW
Rigorous, collaborative, and constructive peer-review

TRANSPARENT PEER-REVIEW
Editors and reviewers acknowledged by name on published articles

Frontiers
Avenue du Tribunal-Fédéral 34
1005 Lausanne | Switzerland

Visit us: www.frontiersin.org
Contact us: info@frontiersin.org | +41 21 510 17 00

REPRODUCIBILITY OF RESEARCH
Support open data and methods to enhance research reproducibility

DIGITAL PUBLISHING
Articles designed for optimal readership across devices

FOLLOW US
@frontiersin

IMPACT METRICS
Advanced article metrics track visibility across digital media

EXTENSIVE PROMOTION
Marketing and promotion of impactful research

LOOP RESEARCH NETWORK
Our network increases your article's readership